

HART ISAACS, JR.

Tumors of the Fetus and Infant

An Atlas

Second Edition

Tumors of the Fetus and Infant

Hart Isaacs, Jr

Tumors of the Fetus and Infant

An Atlas

Second Edition

 Springer

Hart Isaacs, Jr
Department of Pathology
Rady Childrens Hospital San Diego
University of California San Diego
School of Medicine
San Diego, CA
USA

ISBN 978-3-642-31619-7 ISBN 978-3-642-31620-3 (eBook)
DOI 10.1007/978-3-642-31620-3
Springer Heidelberg New York Dordrecht London

Library of Congress Control Number: 2013936091

© Springer-Verlag Berlin Heidelberg 2013

This work is subject to copyright. All rights are reserved by the Publisher, whether the whole or part of the material is concerned, specifically the rights of translation, reprinting, reuse of illustrations, recitation, broadcasting, reproduction on microfilms or in any other physical way, and transmission or information storage and retrieval, electronic adaptation, computer software, or by similar or dissimilar methodology now known or hereafter developed. Exempted from this legal reservation are brief excerpts in connection with reviews or scholarly analysis or material supplied specifically for the purpose of being entered and executed on a computer system, for exclusive use by the purchaser of the work. Duplication of this publication or parts thereof is permitted only under the provisions of the Copyright Law of the Publisher's location, in its current version, and permission for use must always be obtained from Springer. Permissions for use may be obtained through RightsLink at the Copyright Clearance Center. Violations are liable to prosecution under the respective Copyright Law.

The use of general descriptive names, registered names, trademarks, service marks, etc. in this publication does not imply, even in the absence of a specific statement, that such names are exempt from the relevant protective laws and regulations and therefore free for general use.

While the advice and information in this book are believed to be true and accurate at the date of publication, neither the authors nor the editors nor the publisher can accept any legal responsibility for any errors or omissions that may be made. The publisher makes no warranty, express or implied, with respect to the material contained herein.

Printed on acid-free paper

Springer is part of Springer Science+Business Media (www.springer.com)

*The new-born infant brings with it into the world, not the tumour,
but merely the superabundant cell-material, and from the latter,
if circumstances be favorable, a tumour may grow later on.*

London, 1889

Julius Cohnheim

*To my family,
without whose support
this atlas would not
have been possible.*

Preface to the Second Edition

In the near decade since the first edition, there has been a great increase in basic studies on fetal and infant pathology. Newer diagnostic methods especially in imaging and molecular biology have led to the diagnosis of an increasing number of tumors in this age group. This revised, abundantly illustrated second edition of *Tumors of the Fetus and Infant: An Atlas* presents an up-to-date account of the clinical and pathological features of neoplastic disease and tumor-like conditions in the fetus and infant and discusses tumor studies and cases from the international literature. The full range of tumors is covered, with each chapter reviewing the incidence, clinical findings, cytogenetics, pathology, radiology, treatment, and prognosis. The ultimate goal is to enable pathologists and clinicians to gain a clear understanding of these lesions so that a correct diagnosis can be achieved and appropriate treatment initiated.

Preface to the First Edition

The atlas attempts to bring together in a simple and clear fashion the wealth of information that is presently available concerning neoplasia in the young. The purpose of the atlas is to present a concise account of the clinical and pathological features of neoplastic disease and tumor-like conditions in the fetus and infant. It is not meant to be an encyclopedic work but instead a survey of the field supplemented by plentiful illustrative material. The incorporation of a generous bibliography is intended to help those who are interested in extended reading and who would like to have an easy access to the references of the original sources.

Most of the material on which the Atlas is based is largely a product of the author's experience as a pediatric pathologist for over four decades. Throughout I have used my own material as fully as possible and have introduced accounts of personally studied cases supplemented by ones from other colleagues illustrative of the subjects under discussion. For the same reason, the author has made frequent reference to his own published articles and to his earlier publications, *Tumors of the Fetus and Newborn*, the chapter "Tumors" in *Potter's Pathology of the Fetus and Infant* and *Tumors of the Fetus and Infant: An Atlas*, First edition (Refs. 1–4 of Chap. 1), the contents of which in many ways supplement that of the present work. Most illustrations and tables have been produced from personally studied material while others were taken, by permission, from various articles appearing in the literature.

The Atlas is addressed primarily to pathologists, but I am not without hope that clinicians, residents, and medical students in both pathology and other medical specialties may find it useful and beneficial as a concise, easy to use, quick ready reference source and a valuable teaching aid.

Acknowledgments

My grateful thanks are due to my colleagues and friends who have assisted me in various ways during the preparation of this book. To all who have allowed me to use illustrations from their published work and the publishers of journals and books from which they have been produced. Particular thanks are due to Drs. Henry Krous, Robert Newbury, and Eric Breisch for their continual encouragement and support. The help given me by Ann Peters with the electron photomicrographs has been invaluable. I want also to acknowledge my publishers for their helpfulness in the preparation and production of this atlas.

Hart Isaacs, Jr, M.D.

Contents

1	General Survey	1
1.1	General Survey	1
1.2	Incidence.....	2
1.3	Tumors Occurring in Patients with Congenital Malformations and Syndromes.....	3
	References.....	3
2	Germ Cell Tumors	5
2.1	Introduction.....	5
2.2	Cytogenetics	7
2.3	Teratoma	7
2.3.1	Clinical Findings	13
2.3.2	Pathology.....	13
2.4	Fetus-in-Fetu.....	19
2.4.1	Prognosis	21
2.5	Yolk Sac Tumor	22
2.6	Gonadoblastoma	24
2.7	Embryonal Carcinoma.....	26
2.8	Polyembryoma.....	27
2.9	Dysgerminoma and Choriocarcinoma	27
	References.....	28
3	Non-Germ-Cell Gonadal Tumors	31
3.1	Introduction.....	31
3.2	Leukemic Infiltration of the Infant Testis	32
3.3	Follicular Cysts of the Ovary.....	33
3.4	Juvenile Granulosa Cell Tumor	33
3.5	Sertoli-Leydig Cell Tumors	34
	References.....	35
4	Soft Tissue Tumors	37
4.1	Introduction.....	37
4.2	Vascular Conditions	40
4.2.1	Hemangioma	40
4.2.2	Capillary Hemangioma	40
4.2.3	Cavernous Hemangioma	41
4.2.4	Infantile Kaposiform Hemangioendothelioma.....	42
4.2.5	Tufted Angioma	43
4.2.6	Malignant Vascular Tumors	43
4.2.7	Lymphangioma.....	44
4.2.8	Vascular Malformations	45

4.3	Fibrous Connective Tissue (Myofibroblastic) Tumors	46
4.3.1	Fibromatosis.....	47
4.3.2	Gardner Fibroma.....	48
4.3.3	Digital Fibromatosis (Recurring Digital Fibroma)	49
4.3.4	Torticollis	49
4.3.5	Myofibromatosis	49
4.3.6	Granular Cell Tumor	50
4.3.7	Fibrous Hamartoma of Infancy	52
4.3.8	Giant-Cell Fibroblastoma.....	53
4.3.9	Infantile (Congenital) Fibrosarcoma.....	53
4.3.10	Nodular (Proliferative) Fasciitis.....	60
4.3.11	Cranial Fasciitis.....	62
4.3.12	Inflammatory Myofibroblastic Tumor.....	62
4.4	Fibrohistiocytic Tumors.....	63
4.4.1	Fibrous Histiocytoma	65
4.4.2	Angiomatoid Fibrous Histiocytoma.....	65
4.4.3	Juvenile Xanthogranuloma.....	65
4.5	Skeletal Muscle Tumors	72
4.5.1	Rhabdomyoma	72
4.5.2	Rhabdomyosarcoma.....	72
4.6	Rhabdoid Tumor	73
4.7	Adipose Tissue Tumors	74
4.7.1	Lipoblastoma.....	74
4.8	Peripheral Nervous System Tumors	76
4.8.1	Neurofibroma	76
4.9	Primitive Neuroectodermal Tumor (PNET)	78
4.9.1	Melanotic Neuroectodermal Tumor of Infancy.....	80
4.10	Miscellaneous Soft Tissue Tumors	80
4.10.1	Triton Tumor	80
4.10.2	Polyphenotypic Small Cell Tumor.....	82
	References.....	83
5	Tumors and Tumor-Like Conditions of the Skin	87
5.1	Introduction.....	87
5.2	Vascular Conditions	90
5.2.1	Hemangioma	90
5.2.2	Macular Stains.....	92
5.2.3	Syndromes Associated with Vascular Conditions.....	92
5.2.4	Hemangioma Variants	93
5.2.5	Lymphangioma.....	94
5.3	Epidermal Birthmarks.....	94
5.3.1	Epidermal Nevus	94
5.3.2	Becker's Nevus (Becker's Melanosis).....	95
5.3.3	Sebaceous Nevus.....	95
5.4	Cutaneous Hamartomas	96
5.4.1	Smooth Muscle Hamartoma.....	96
5.4.2	Nevus Lipomatosus	96
5.5	Melanocytic Nevi.....	96
5.5.1	Pigmented Nevus.....	96
5.5.2	Giant Congenital Melanocytic Nevi.....	97
5.5.3	Malignant Melanoma	99
5.5.4	Neurocutaneous Melanosis	100

5.6	Neurofibromatosis.....	101
5.7	Tuberous Sclerosis.....	101
5.7.1	Infantile Digital Fibromatosis.....	102
5.7.2	Fibrous Hamartoma of Infancy.....	102
5.7.3	Papilloma.....	102
5.8	Tumors and Tumor-Like Infiltrations of the Skin.....	102
5.8.1	Leukemia.....	102
5.8.2	Neuroblastoma.....	102
5.8.3	Langerhans Cell Histiocytosis.....	104
5.8.4	Juvenile Xanthogranuloma.....	104
5.8.5	Rhabdomyosarcoma.....	106
5.8.6	Rhabdoid Tumor.....	107
5.8.7	Urticaria Pigmentosa (Mast Cell Disease).....	108
	References.....	108
6	Neuroblastoma	111
6.1	Introduction.....	111
6.2	Incidence.....	111
6.3	Clinical Findings.....	111
6.4	Diagnostic Tests.....	121
6.5	Genetic Factors.....	121
6.6	Pathology.....	122
6.7	Spontaneous Regression.....	127
6.8	Neuroblastoma In Situ.....	127
6.9	Ganglioneuroma.....	128
6.10	Prognosis.....	128
	References.....	129
7	Leukemia	131
7.1	Introduction.....	131
7.2	Incidence.....	131
7.3	Hematopoiesis.....	131
7.4	Clinical Features.....	132
7.5	Leukemia Occurring in Infants with Chromosomal Anomalies, Syndromes, and Malformations.....	133
7.6	Differential Diagnosis.....	135
7.7	Diagnosis of Leukemia.....	139
7.8	Pathology.....	142
7.9	Prognosis.....	146
	References.....	146
8	Histiocytoses	149
8.1	Introduction.....	149
8.2	Ontogeny of the Monophagocytic System.....	150
8.3	Classification of Histiocytoses.....	151
8.4	Dendritic Cell Disorders.....	151
8.4.1	Langerhans Cell Histiocytosis.....	151
8.4.2	Juvenile Xanthogranuloma.....	155
8.5	Macrophage-Related Disorders.....	155
8.5.1	Hemophagocytic Syndromes.....	155
8.5.2	Sinus Histiocytosis with Massive Lymphadenopathy.....	158
8.6	Malignant-Related Disorders.....	159
8.6.1	Malignant Histiocytoses.....	159
8.6.2	Acute Monocytic Leukemia.....	159

8.7	Prognosis.....	160
	References.....	160
9	Brain Tumors.....	163
9.1	Introduction.....	163
9.1.1	Incidence	163
9.1.2	Association of Brain Tumors with Heritable Disorders and Other Conditions	164
9.1.3	Clinical Findings	165
9.1.4	Pathology.....	165
9.1.5	Cytogenetics.....	166
9.2	Teratoma	166
9.3	Astrocytoma.....	168
9.4	Primitive Neuroectodermal Tumors.....	172
9.5	Medulloblastoma	177
9.6	Cerebral PNET.....	177
9.7	Gangliocytoma.....	178
9.8	Ganglioglioma	178
9.9	Infantile Desmoplastic Ganglioglioma	178
9.10	Ependymoma	180
9.11	Choroid Plexus Papilloma	182
9.12	Choroid Plexus Carcinoma	185
9.13	Oligodendroglioma	186
9.14	Craniopharyngioma	187
9.15	Atypical Teratoid/Rhabdoid Tumor.....	188
9.16	Medulloepithelioma.....	188
9.17	Meningioma.....	189
9.18	Vascular Malformations of the Brain.....	189
9.19	Prognosis for Infants with Brain Tumors.....	192
9.20	Miscellaneous Craniofacial Anomalies	193
	References.....	193
10	Tumors of the Eye	197
10.1	Retinoblastoma	197
10.1.1	Cytogenetics.....	197
10.1.2	Clinical Findings	197
10.1.3	Differential Diagnosis	198
10.1.4	Spontaneous Regression.....	198
10.1.5	Pathology.....	199
10.1.6	Prognosis.....	203
10.2	Trilateral Retinoblastoma	203
10.3	Medulloepithelioma.....	204
10.4	Astrocytic Tumors of the Retina.....	204
10.5	Neurofibromatosis.....	205
10.6	Optic Glioma	206
10.7	Orbital Tumors.....	206
	References.....	207
11	Renal Tumors	209
11.1	Introduction.....	209
11.2	Wilms' Tumor.....	216
11.2.1	Pathology.....	216
11.3	Nephrogenic Rests and Nephroblastomatosis	221
11.4	Congenital Mesoblastic Nephroma.....	222
11.4.1	Pathology.....	222

11.5 Rhabdoid Tumor of the Kidney	228
11.5.1 Pathology.....	228
11.6 Clear Cell Sarcoma of the Kidney	229
11.6.1 Pathology.....	229
11.7 Cystic Conditions of the Kidney.....	230
11.8 Ossifying Renal Tumor of Infancy	233
References.....	234
12 Liver Tumors	237
12.1 Introduction.....	237
12.2 Hemangioma.....	238
12.3 Mesenchymal Hamartoma	241
12.4 Hepatoblastoma	244
12.5 Primary Sarcomas of the Liver	250
12.6 Germ Cell Tumors	252
12.7 Liver Cell Adenoma and Focal Nodular Hyperplasia.....	252
12.8 Miscellaneous Tumors and Tumorlike Conditions	253
References.....	256
13 Adrenocortical Tumors	259
13.1 Introduction.....	259
13.2 Incidence.....	259
13.3 Clinical Findings.....	260
13.4 Adrenal Cortical Adenoma	261
13.5 Adrenocortical Carcinoma.....	265
13.6 Adrenal Cortical Hyperplasia	266
13.6.1 Congenital Adrenal Cortical Hyperplasia Associated with Adrenogenital Syndrome	267
13.6.2 Clinical Findings	267
13.6.3 Pathology.....	268
13.6.4 Adrenocortical Hyperplasia Associated with Cushing's Syndrome	269
13.6.5 Clinical Findings	269
13.6.6 Pathological Findings.....	269
13.7 Adrenal Cortical Cytomegaly	269
13.8 Adrenal Cyst	270
References.....	270
14 Pancreatic Tumors	273
14.1 Introduction.....	273
14.2 Endocrine Tumors and Tumorlike Conditions of the Pancreas	273
14.2.1 Hypertrophy and Hyperplasia of the Islets of Langerhans.....	273
14.2.2 Nesidioblastosis, Nesidioblastoma.....	273
14.2.3 Persistent Hyperinsulinemic Hypoglycemia of Infancy.....	275
14.2.4 Islet Cell Adenoma.....	276
14.3 Exocrine Tumors and Tumorlike Conditions of the Pancreas	277
14.3.1 Adenoma and Cystadenoma.....	277
14.3.2 Adenocarcinoma	278
14.3.3 Pancreatoblastoma.....	278
14.4 Miscellaneous Tumors and Tumorlike Conditions	280
References.....	280
15 Cardiac Tumors	283
15.1 Introduction.....	283
15.2 Cardiac Rhabdomyoma	285

15.3	Pericardial and Cardiac Teratoma.....	287
15.4	Cardiac Fibroma	289
15.5	Cardiac Myxoma	289
15.6	Vascular Tumors	289
15.7	Oncocytic (“Histiocytoid”) Cardiomyopathy	290
15.8	Miscellaneous Conditions.....	290
	References.....	291
16	Salivary Gland Tumors.....	293
16.1	Introduction.....	293
16.2	Sialoblastoma.....	295
16.3	Congenital Pleomorphic Adenoma (Salivary Gland Anlage Tumor).....	296
16.4	Miscellaneous Salivary Gland Tumors and Tumorlike Conditions	296
	References.....	300
17	Lung Tumors and Tumor-like Conditions	301
17.1	Introduction.....	301
17.2	Inflammatory Pseudotumor	306
17.3	Fibromatoses (Myofibromatoses)	307
17.4	Vascular Conditions	307
17.5	Congenital Pulmonary Cystic Diseases.....	307
17.5.1	Congenital Cystic Adenomatoid Malformation	307
17.6	Laryngotracheal Papilloma.....	308
17.7	Congenital Pulmonary Myofibroblastic Tumor.....	309
17.8	Pleuropulmonary Blastoma	310
17.9	Skeletal Muscle Tumors	310
17.10	Peripheral Neuroectodermal Tumor of Thoracopulmonary Origin.....	311
	References.....	312
18	Tumors and Tumor-Like Conditions of Bones	315
18.1	Introduction.....	315
18.2	Chest Wall Hamartoma.....	317
18.3	Nasal Chondromesenchymal Hamartoma	319
18.4	Fibrous Dysplasia of Bone.....	321
18.5	Enchondromatosis (Ollier’s Disease)	321
18.6	Congenital Generalized Fibromatosis (Infantile Myofibromatosis).....	323
18.7	Congenital Fibrosarcoma.....	323
18.8	Ewing’s Sarcoma	323
18.9	Miscellaneous Conditions.....	324
	References.....	326
Index	327

1.1 General Survey

Although tumors and tumorlike conditions of the fetus and infant occur infrequently, they present challenging diagnostic and treatment problems [1–13]. There is considerable drama and terrible parental apprehension when dealing with a tumor in an infant or unborn child. Unfamiliarity with these conditions may lead to an erroneous diagnosis and unnecessarily aggressive treatment. Neoplasms and tumorlike conditions occurring during early life are not entirely the same as those observed in the adolescent or adult for the types, incidence, clinical features, their behavior, and response to treatment are different [7–17] (Tables 1.1 and 1.2). Although some are unique, most childhood tumors have been described at some time or another in this older age group [6].

No tumor of the adult grows as rapidly as does the normal embryo. In the early stages of development, normal embryonic cells may have some of the characteristics of neoplastic cells. Generally, it is accepted by pathologists that the diagnosis of malignancy depends on certain microscopic criteria, but they are not always helpful or valid in a young child. Normal developing organs and tissues display significant mitotic activity and contain immature or embryonic-appearing structures which may simulate malignancy. It is often only from knowledge of the postnatal course of a tumor that definite proof can be obtained of its malignancy [1–4].

Tumors that are not histologically malignant may cause death in utero or shortly after birth because of their location,

for example, a large lymphangioma, mature teratoma, or fibromatosis involving vital structures [1–4].

Moreover, tumors occurring in the fetus and newborn differ markedly in their presenting clinical signs and symptoms as compared to those found in older individuals [7–13, 17] (Table 1.2). Maternal *dystocia* (difficult delivery) may be the first sign of a large space occupying congenital tumor such as a giant intracranial or sacrococcygeal teratoma.

Fetal circulation may determine the pattern of metastasis observed at birth [2, 6]. *Fetal hydrops* is another unique manifestation [18, 19]. *Rupture* of a large tumor, for example, a neuroblastoma or hepatoblastoma, during delivery with fatal exsanguination of the fetus is another unusual presentation [1–4].

Antenatal imaging diagnosis of fetal neoplasms allows an understanding of the prenatal natural history and pathophysiology of these tumors [10, 13, 16, 20]. Advances in this field, particularly ultrasonography and rapid magnetic resonance imaging, are responsible for making an early diagnosis possible. Tumors most often diagnosed by antenatal imaging are teratomas, mesoblastic nephroma, liver tumors, and neuroblastoma [3, 4, 10, 20].

The initial sign of a congenital tumor in pregnancy is frequently *polyhydramnios* (excessive amniotic fluid) which is attributed to difficulties in the fetal-swallowing mechanism resulting in decreased absorption of amniotic fluid from the gastrointestinal tract [3] (Table 1.2). For example, intracranial teratomas affecting the neural control of swallowing or epignathi (palatal teratomas) producing mechanical obstruction

Table 1.1 Comparison of five surveys consisting of 597 fetal and neonatal tumors

Institution						
Tumor	CCRG	HSC	CHB	CHLA	CHSD	Total tumors
Neuroblastoma	27 (26.7) ^a	48 (47.0)	31 (18)	36 (21.6)	16 (19.3)	158 (26)
Teratoma	16 (15.8)	–	49 (29)	62 (37.1) ^c	15 (30.1) ^d	142 (25)
Leukemia	17 (16.8)	8 (7.8)	21 (12)	18 (10.8)	10 (12.1)	74 (12.2)
Brain tumors	12 (11.9)	9 (8.8)	14 (8)	15 (9.0)	13 (5.7)	63 (10.4)
Sarcoma	13 (12.9)	12 (11.8)	17 (10)	8(4.8)	8 (9.6)	58 (9.6)
Renal tumors	8 (7.9)	4 (3.9)	8 (5)	6 (3.6)	4 (4.8)	30 (4.9)
Liver tumors	3 (3.0)	1 (1)	8 (5)	18 (10.8)	7 (8.4)	37 (6.1)
Retinoblastoma	–	17 (6.7)	14 (8)	4 (2.4)	–	35 (5.8)
Total ^e	96	99	162	167	73	597 (100)

Reprinted from Isaacs H Jr [1]. With kind permission of © W.B. Saunders, 1997

Abbreviations for institutions and references: CCRG Childhood Cancer Research Group, Oxford [9], HB Children's Hospital, Birmingham, UK [8], CHLA Children's Hospital Los Angeles [2], CHSD Children's Hospital San Diego [2]

^aIsaacs [4]. © Springer-Verlag, 2002

^b() = percent of total cases in study for that institution

^c2 of 62 with yolk sac tumor

^d2 of 25 with yolk sac tumor

^eThis figure represents the total for cases recorded in the study reported and not the total of the columns in the table

Table 1.2 Unusual clinical presentations of fetal and neonatal tumors

<i>Maternal dystocia</i>
Teratoma
Neuroblastoma
Congenital mesoblastic nephroma
Astrocytoma
Ependymoma
Sialoblastoma
<i>Fetal hydrops</i>
Teratoma
Neuroblastoma
Congenital mesoblastic nephroma
Wilms' tumor
Hepatoblastoma
Cardiac rhabdomyoma
Astrocytoma (glioblastoma multiforme)
Primitive neuroectodermal tumor
Lymphangioma
Hemangioma
Neurofibroma
<i>Rupture of tumor during delivery with fatal exsanguination</i>
Teratoma
Neuroblastoma
Hepatoblastoma
Hepatic Hemangioma
<i>Congestive heart failure shortly after birth</i>
Arteriovenous malformation
Cavernous hemangioma
Teratoma
Congenital mesoblastic nephroma
Astrocytoma
Cardiac rhabdomyoma
Cardiac myxoma

Table 1.2 (continued)

Cardiac fibroma
<i>Polyhydramnios</i>
Teratoma
Hemangioma
Congenital mesoblastic nephroma
Wilms' tumor
Astrocytoma
Myofibroblastic tumor

Unusual clinical presentations. Reprinted from Arceci and Weinstein [17]. With kind permission of © JB Lippincott, 1994; Reprinted from Isaacs H Jr [1]. With kind permission of © W.B. Saunders, 1997

can be responsible for this problem [3, 4]. Polyhydramnios is often accompanied by fetal hydrops, which can occur with several different kinds of tumors and other nonneoplastic conditions [18, 19] (Table 1.2).

1.2 Incidence

Tumors of the newborn are uncommon with an incidence of 7.2/100,000 live births in the UK, 1960–1989 [8]. Most fetal and newborn tumors are benign rather than malignant with cancer estimated to occur in 3.65/100,000 live births in the USA (1969–1971) [21] and 223/1,000,000 in infants overall in the USA in a later study (1973–1992) [22]. Several series show that the *most common malignancies noted at birth are neuroblastoma, leukemia, brain tumors, and sarcomas* in that order [3, 4, 7–10, 21, 23] (Table 1.1). Almost all tumors occurring during the first year of life are essentially the same histologically as those found later on, but the

order of frequency of the neoplasms in the two age groups is different. Leukemia-lymphoma, brain tumors, neuroblastoma, and soft tissue sarcomas, in decreasing order of occurrence, are the more common neoplasms found in older children and adolescents less than 15 years of age [21–23].

1.3 Tumors Occurring in Patients with Congenital Malformations and Syndromes

An important relationship exists between certain *congenital malformations and syndromes and the development of neoplasms* [3–5, 24–29] (Table 1.4). In this setting, the tumor occurs after birth or later in life in individuals with specific inherited diseases, congenital anomalies, or malformation syndromes, many of whom probably have an underlying chromosomal defect (Table 1.4).

Hereditary conditions such as the neurocutaneous syndromes, also known as “*phakomatoses*,” are characterized by a high incidence of neoplasia. For example, tuberous sclerosis and neurofibromatosis, which are autosomal dominant, predispose the individual to the development of gliomas and other tumors [3, 28, 29]. Examples of pediatric neoplasms associated with recognized recessive chromosomal aberrations include the 11p13 deletion anomaly observed with Wilms’ tumor and the 13q14 deletion in patients with retinoblastoma and osteosarcoma [26, 27] (Tables 1.1, 1.2, 1.3, and 1.4).

Table 1.3 Chromosomal anomalies associated with childhood tumors

Chromosomal defect	Childhood tumor
1p del, 1p-32-p36 del, double minutes	Neuroblastoma
11p13 del, trisomy 18	Wilms’ tumor
13q14 del	Retinoblastoma Osteosarcoma
Trisomy 21 (Down syndrome)	Leukemia
Monosomy 7	Leukemia Myelodysplasia syndrome
t(11q23), t(1;22), t(9;11)	Leukemia
t(1;22) (p13;q13)	Leukemia
Gonadal dysgenesis (46,XY; 45X/46,XY)	Gonadoblastoma Germinoma
Klinefelter syndrome (XXY)	Teratoma
t(11;22)(q24;q12), t(21;22)	Ewing’s sarcoma PNET
t(11;22) (p13;q12) t(21;)	Desmoplastic small round cell tumor
t(1;13) t(2;13)	Alveolar rhabdomyosarcoma
Del 1p	Astrocytoma
22q11 del ^a	Rhabdoid tumor

Reprinted from Isaacs [4]. © Springer-Verlag, 2002; Reprinted from Isaacs [2]. With kind permission of © Mosby, 1997

^aAssociated with hSNF5/INI1 gene mutations

Table 1.4 Syndromes and congenital malformations associated with childhood tumors

Malformation or syndrome	Tumor
Beckwith-Wiedemann syndrome, hemihypertrophy	Wilms’ tumor Adrenocortical adenoma Adrenocortical carcinoma Hepatoblastoma Pancreatoblastoma
Aniridia	Wilms’ tumor
Genitourinary system anomalies, Perlman and Drash syndromes	Wilms’ tumor Nephroblastomatosis
Hirschsprung disease	Neuroblastoma
Tuberous sclerosis	Cardiac rhabdomyoma Astrocytoma Angiomyolipoma
Neurofibromatosis I	Astrocytoma
Multiple endocrine neoplasia (MEN-2)	Thyroid medullary carcinoma Pheochromocytoma Submucosal neuromas
Nevoid basal cell carcinoma (Gorlin syndrome)	Basal cell carcinoma Medulloblastoma Ovarian fibroma Cardiac fibroma
Wiskott-Aldrich syndrome	Lymphoma
Bloom’s syndrome	Leukemia
Down syndrome	Leukemia
Poland syndrome	Leukemia

Reprinted from Bolande [5]. With kind permission of © Mosby-Year Book, 1976; Reprinted from Isaacs [4]. © Springer-Verlag, 2002; Gilbert-Barness and Debich-Spicer [16]. With kind permission of © Cambridge University Press

References

- Isaacs H Jr (1997) Etiology and incidence. In: Tumors of the fetus and newborn, vol. 35 in the Series major problems in pathology. W.B. Saunders, Philadelphia
- Isaacs H Jr (1997) Tumors. In: Gilbert-Barness E (ed) Potter’s pathology of the fetus and infant, vol 2. Mosby, St. Louis, pp 1242–1339
- Isaacs H Jr (2007) Tumors. In: Gilbert-Barness E (ed) Potter’s pathology of the fetus, infant and child, vol 2, 3rd edn. Mosby, St. Louis, pp 1677–1709
- Isaacs H Jr (2002) General survey. In: Tumors of the fetus and infant: an atlas. Springer, New York, p 434
- Bolande RP (1976) Neoplasia of early life and its relationships to teratogenesis. In: Rosenberg HS, Bolande RP (eds) Perspectives in pediatric pathology, vol 3. Year Book, Chicago
- Dehner LP (1981) Neoplasms of the fetus and neonate. In: Naeye RL, Kissane JM, Kaufman N (eds) Perinatal diseases. International Academy of Pathology, monograph no. 22. Williams and Wilkins, Baltimore, p 286–345
- Campbell AN, Chan HSL, O’Brien A et al (1987) Malignant tumours in the neonate. Arch Dis Child 62:19–23
- Parkes SE, Muir KR, Southern L et al (1994) Neonatal tumours: a thirty-year population-based study. Med Pediatr Oncol 22:309–317
- Broadbent VA (1992) Malignant disease in the neonate. In: Robertson NRC (ed) Textbook of neonatology, 2nd edn. Churchill Livingstone, Edinburgh, pp 879–888

10. Gallagher PG, Lampkin BC (1999) Neonatal tumors. *Semin Perinatol* 23:261–262
11. Arceci RJ, Weinstein HJ (1999) Neoplasia. In: Avery GB, Fletcher MA, MacDonald MG (eds) *Neonatology: pathophysiology and management in the newborn*, 4th edn. J.B. Lippincott, Philadelphia, pp 1301–1322
12. Reaman GH, Bleyer WA (2002) Infants and adolescents with cancer. In: Pizzo PA, Poplack DG (eds) *Principles and practice of pediatric oncology*, 4th edn. Lippincott Williams and Wilkins, Philadelphia, pp 409–427
13. Garmel SH, Crombleholme TM, Semple JP et al (1994) Prenatal diagnosis and management of fetal tumors. *Semin Perinatol* 18:350–365
14. Willis RA (1962) *The borderland of embryology and pathology*, 2nd edn. Butterworths, London
15. Werb P, Scurry J, Ostr A et al (1992) Survey of congenital tumors in perinatal necropsies. *Pathology* 24:247–253
16. Gilbert-Barness E, Debich-Spicer D (2004) *Embryo and fetal pathology: color atlas with ultrasound correlation*. Cambridge University Press, Cambridge, pp 546–578
17. Arceci RJ, Weinstein HJ (1994) Neoplasia. In: *Neonatology: pathophysiology and management in the newborn*, 4th edn. JB Lippincott, Philadelphia, p 1211
18. Keeling JW (2001) Fetal hydrops. In: Keeling JW (ed) *Fetal and neonatal pathology*, 3rd edn. Springer, London, pp 261–284
19. Isaacs HJR (2008) Fetal hydrops associated with tumors. *Am J Perinatol* 25:43–68
20. Wienk MA, Van Geijn HP, Copray FJA et al (1990) Prenatal diagnosis of fetal tumors by ultrasonography. *Obstet Gynecol Surv* 45:639–653
21. Bader JL, Miller RW (1979) U.S. cancer incidence and mortality in the first year of life. *Am J Dis Child* 133:157–159
22. Gurney JG, Ross JA, Wall DA et al (1997) Infant cancer in the U.S.: histology-specific incidence and trends, 1973 to 1992. *J Pediatr Hematol Oncol* 19:428–432
23. Young JL, Miller RW (1975) Incidence of malignant tumors in U.S. children. *J Pediatr* 86:254–258
24. Narod SA, Hawkins MM, Robertson CM et al (1997) Congenital anomalies and childhood cancer in Great Britain. *Am J Hum Genet* 60:474–485
25. Koufos A, Grundy P, Morgan K (1989) Familial Wiedemann-Beckwith syndrome and a second Wilms tumor locus both map to 11p15.5. *Am J Hum Genet* 44:711–719
26. Murphree AL (1998) Retinoblastoma. In: Traboulsi EI (ed) *Genetic diseases of the eye*. Oxford monographs on medical genetics, no. 36. Oxford University Press, Oxford, p 813
27. Li FP (1986) Genetic and familial cancer: opportunities for prevention and early detection. *Cancer Detect Prev* 9:41–45
28. Isaacs HJR (2009) Perinatal (fetal and neonatal) tuberous sclerosis: a review. *Am J Perinatol* 26:755–760
29. Isaacs H Jr (2009) Perinatal neurofibromatosis: two case reports and review of the literature. *Am J Perinatol* 27:285–292

2.1 Introduction

Germ cell tumors are a varied group of benign and malignant neoplasms derived from primordial germ cells [1–10, 11–15] (Table 2.1 and Fig. 2.1). They occur in a variety of sites, both gonadal and extragonadal, the latter in midline locations as the sacrococcygeal, retroperitoneal, mediastinal, cervical, and pineal regions (Tables 2.2 and 2.3). *Teratoma* is the leading fetal and neonatal neoplasm in several reviews [9, 10, 12, 14, 16, 17] (Table 1.1). Most germ cell tumors of the fetus and infant are histologically benign and are diagnosed as either mature or immature teratomas (Table 2.2). *Yolk sac tumor*, second in frequency, occurs alone or in combination with a teratoma. Although yolk sac tumor of the cervix or vagina is the subject of a few case reports, yolk sac tumor of the infant testis is more prevalent and is the most common germ cell tumor arising from this organ [2, 4, 8, 20]. To my knowledge, neither yolk sac tumor nor teratoma of the ovary has been reported during the first year of life [7, 14].

The *World Health Organization (WHO) classification of germ cell tumors* is the basis for most contemporary classifications [2, 6, 10] (Table 2.1). According to this classification, germ cell neoplasms are divided into eight histologic types: *dysgerminoma*, *yolk sac tumor*, *embryonal carcinoma*, *polyembryoma*, *choriocarcinoma*, *teratoma*, *gonadoblastoma*, and *germ cell sex cord tumor* [6]. Moreover, *gonadoblastoma*, a neoplasm typically occurring in dysgenetic gonads, is included in this category of germ cell tumors, although granulosa and Sertoli cells are found in addition to germ cells [2, 5, 6, 19] (Fig. 2.30).

Table 2.1 WHO classification of germ cell tumors

1. Dysgerminoma
Variant – with syncytiotrophoblast cells
2. Yolk Sac Tumor (Endodermal Sinus Tumor)
Variants
Polyvesicular vitelline tumor
Hepatoid
Glandular (“endometrioid”)
3. Embryonal Carcinoma
4. Polyembryoma
5. Choriocarcinoma
6. Teratomas
(a) Immature
(b) Mature
Solid
Cystic (dermoid cyst)
With secondary tumor (specify type)
Fetiform
(c) Monodermal
Struma ovarii
Carcinoid
Mucinous carcinoid
Neuroectodermal tumors (specify type)
Sebaceous tumors
Others
Mixed (specify types) ^a
7. Gonadoblastoma
Variant – with dysgerminoma or other germ cell tumor
8. Germ Cell Sex Cord, Stromal Tumor
Variant – with dysgerminoma or other germ cell tumor

Reprinted from Scully et al. [6]. With kind permission of © Armed Forces Institute of Pathology, 1998

^aFor example, immature teratoma + yolk sac tumor

Fig. 2.1 Origin of germ cell tumors; *indicates inclusion of dysgerminoma and seminoma (Reprinted from Teilum [5]. With kind permission of © Lippincott, 1976; From Isaacs [10, 15], with permission)

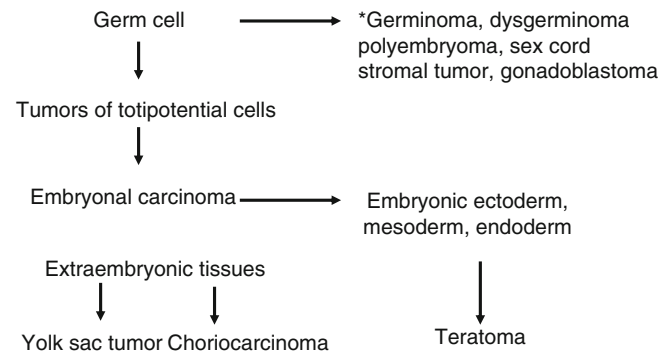


Table 2.2 Fetal and neonatal teratomas ($n=534$)

Location	Number	Sex histology	Survival (%)	Female	Male	NS	M I	NS	YST ^a
Sacrococcygeal	214 (40.1) ^b	134	40	40	106	108	–	22	67
Intracranial	71 (13.3)	32	34	5	6	56	7	2	11
Cervical	70 (13.1)	34	35	1	26	43	–	–	66
Palatal and nasopharyngeal	41 (7.7)	18	17	1	27	12	–	2	56
Cardiac	40 (7.5)	18	15	6	8	15	–	2	75
Fetus-in-fetu ^c	25 (4.5)	11	14	7	21	3	–	1	96
Gastric	14 (2.6)	3	11	–	7	7	–	–	100
Orbital	13 (2.4)	10	3	–	8	4	–	1	85
Mediastinal	13 (2.4)	7	5	–	4	9	–	–	69
Facial	8 (1.5)	6	2	1	7	1	–	–	87
Placenta	8 (1.5)	4	4	–	6	2	–	–	75
Miscellaneous ^d	17 (3.2)	7	10	–	11	6	–	1	76
<i>Overall survival</i>	335 (63 %)								

Reprinted from Isaacs [14]. With kind permission of © Elsevier, 2004

Abbreviations: I immature teratoma, M mature teratoma, NS not specified, YST yolk sac tumor

^aOverall incidence of yolk sac tumor 6 %; survival of fetuses and neonates with yolk sac tumor 39 %

^b() = percent

^cFetus-in-fetu: retroperitoneum 18 (72 %); hard palate 2 (20 %); 1 each undescended testis, scrotal sac, intrahepatic, attached to ovary, sacrococcygeal

^dMiscellaneous: tongue, tonsil, retroperitoneum, eye, mesentery, ileum, testis, vulva, anorectal area

Table 2.3 Clinicopathological features of fetal and infant germ cell tumors

Tumor	Clinical findings	Pathological findings
Teratoma	Mass at site of origin, e.g., sacrococcygeal and cervical areas	Mature: tissues derived from the 3 germ layers; Immature: immature tissues mostly neuroglial and neuroepithelial elements: GFAP +, NSE +, S-100 +
Fetus-in-fetu	Fetiform mass occurs most often in retroperitoneal area	Mature tissues; vertebral axis and long bones present; heart and brain absent
Yolk sac tumor	Mass at site of origin, testis and sacrococcygeal areas main sites; ±association with a teratoma	Six histologic patterns; reticular and papillary most common ones in infants, netlike and papillary formations, perivascular Schiller-Duval bodies; PAS+ hyaline droplets; α-FP+ cytoplasm
Gonadoblastoma	Gonadal dysgenesis, 46XY or 45X0/46XY karyotypes; flecks of calcification on imaging studies	Malformed gonad(s), e.g., streak ovary, with small, tan calcified nodules; large germ cells encircled by smaller round, darkly staining Sertoli and/or granulosa cells forming microfollicles with hyaline bodies and foci of calcification
Embryonal carcinoma ²	Mass; usually not associated with a teratoma in infants	Poorly differentiated, malignant tumor with large primitive embryonal-appearing epithelial cells with vesicular nuclei and characteristic large nucleoli; solid, papillary, and glandular patterns; cytokeratin +, NSE +, placental alkaline phosphatase and NSE +; HCG, and α-FP variable staining
Polyembryoma	Gonadal or sacrococcygeal mass; found in combination with yolk sac tumor	Tiny embryoid bodies with 2 cavities separated by a 2–3 cell layer embryonic disc; α-FP, hCG +, and α1-antitrypsin +
Choriocarcinoma	Mass (s), widespread metastases on imaging studies; severe bleeding tendencies; increased serum and urinary hCG	Soft, hemorrhagic, necrotic mass(es); cytotrophoblasts and giant syncytiotrophoblasts with cells intermediate between the two; hCG+, cytokeratin +, α-FP

Reprinted from Scully et al. [6]. With kind permission of © Armed Forces Institute of Pathology, 1998; Reprinted from Isaacs [15]. © Springer Verlag, 2002

Abbreviations: α-FP alpha-fetoprotein, GFAP glial fibrillary acidic protein, hCG human chorionic gonadotropin, NSE neuron-specific enolase, PAS periodic acid-Schiff reaction

2.2 Cytogenetics

Nonrandom structural aberrations most often involving chromosomes 1 and 12 have been described in germ cell tumors [21]. The chromosomal patterns of malignant ovarian and testicular germ cell tumors are alike, and thus, these tumors are similar and may have the same origin and pathogenesis. The cytogenetic anomalies described are a hypertriploid/hypotetraploid chromosome number, presence of $i(12p)$, and overrepresentation of chromosomes [3, 21–23]. Investigations in extragonadal and testicular germ cell tumors show that they arise mitotically from either a somatic or a germ cell [22, 23].

Transcription factors GATA-4 and GATA-6 are expressed in pediatric yolk sac tumors and in teratomas [22, 23]. They play critical roles in mammalian yolk sac differentiation and function. GATA-6 is expressed not only in most yolk sac tumors but also in nonmalignant tissues including gut and respiratory epithelium, sebaceous cells, and neuroepithelium in mature and immature teratomas. GATA-6 can be used to identify yolk sac components in pediatric germ cell tumors. In addition, it is expressed in specific tissues in teratomas [22, 23].

2.3 Teratoma

Teratoma is defined as a true tumor composed of multiple tissues foreign to, and capable of growth in excess of, those characteristic of the part from which it is derived [10].

However, it is sometimes difficult to make a distinction between teratomas and structures that result from abortive attempts at twinning. An even progression can be traced from normal twins to conjoined twins, parasitic twins, fetus-in-fetu, and teratoma [10]. Careful studies reveal a break in the progression from an oriented, longitudinal, partially symmetrical structure of a twin to the jumbled, disordered, irregular growth of a teratoma in which one, two, or three tissues predominate [10]. Despite the apparent progression from twins to fetus-in-fetu to teratomas, some investigators feel that this relationship does not exist. The distinction is based primarily on the fact that teratomas are capable of independent growth, whereas structures included under malformations are limited in their potentiality for growth to a rate similar to the part of the body they resemble [10].

Teratomas are observed in several locations at birth, but the most common ones are the sacrococcygeal, cervical, and retroperitoneal areas [1–4, 7, 12, 14, 15, 17] (Table 2.2) (Figs. 2.2, 2.3, 2.4, and 2.10). Other locations are the brain, anterior mediastinum, stomach, heart and pleura, pharynx, base of the skull, upper jaw, gonads pelvis, liver, and subcutaneous tissue [3, 4, 7, 10, 15, 24–28] (Figs. 2.5, 2.6, 2.8, 2.9, 2.10, 2.11, and 2.12). Intracranial teratomas are not uncommon in the fetus and newborn [14, 27]. The types of tissues found in fetal and infant teratomas are practically the same regardless of the site of origin [10, 15].

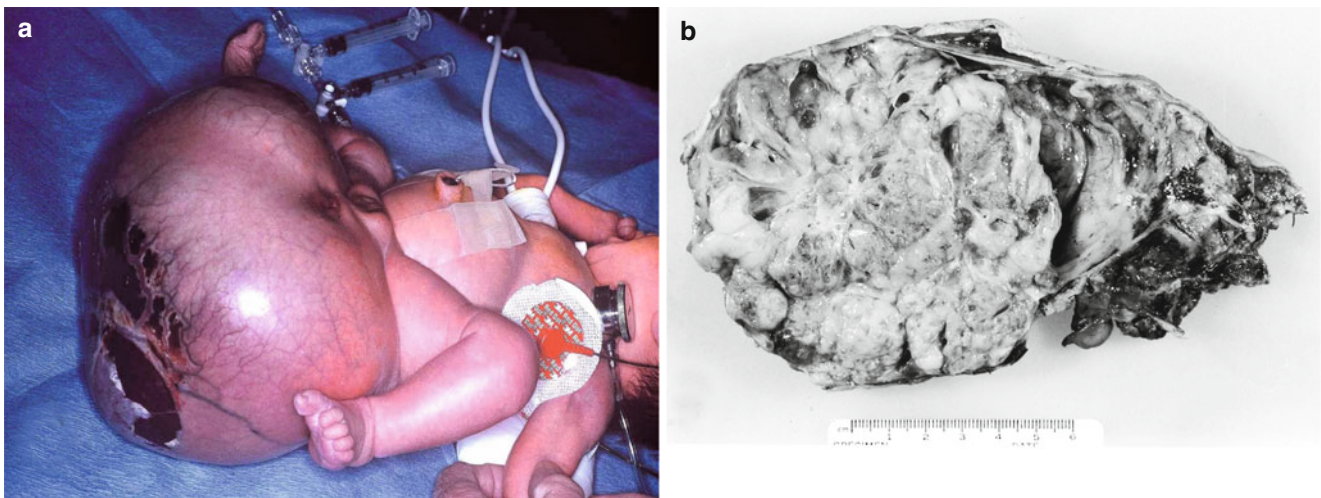


Fig. 2.2 Solid sacrococcygeal teratoma. Sonography at 30 weeks gestation revealed a large abnormality in the sacral region. Shortly before delivery, fetal distress was noted and a cesarean section was performed. (a) The 4.4-kg female was born at 37 weeks gestation with a huge sacrococcygeal tumor. (b) The tumor excised at 1 day of age weighed 1.5 kg (1/3rd the baby's birth weight) and measured 15 × 13 × 10 cm.

The bisected tumor with a variegated solid and cystic appearance. Skin partially covers the periphery of the specimen. Microscopically, the tumor consists of immature neuroglial elements in addition to a variety of mature tissues typically found in these teratomas (see Figs. 2.13, 2.14, 2.15, 2.16, 2.17, 2.18, 2.19, 2.20, 2.21, and 2.22) (Reprinted from Isaacs [15], with kind permission of © Springer-Verlag, 2002)

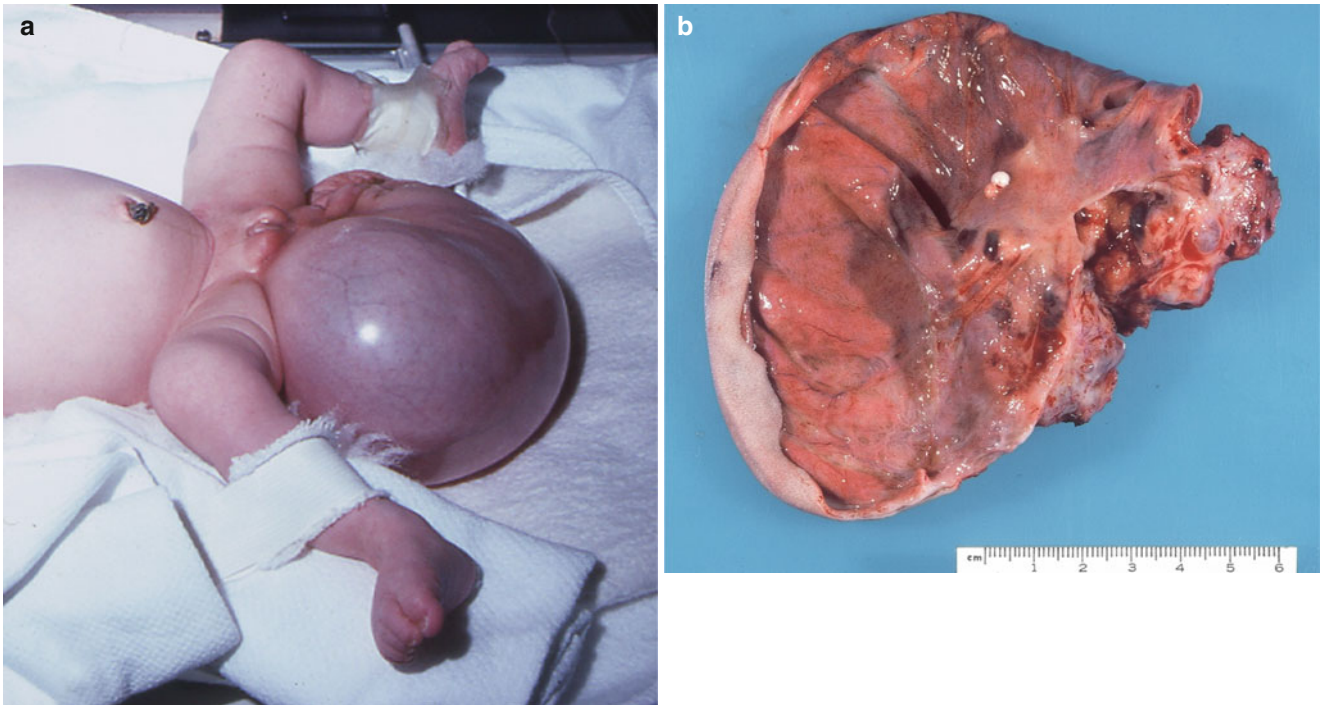


Fig. 2.3 Cystic sacrococcygeal teratoma. (a) 12-day-old, 4.5-kg female, product of a full-term gestation, was delivered by cesarian section because of dystocia. The external genitalia and anus are displaced anteriorly by the mass. (b) Gross specimen, 1,090 g, 18.5×12.4×9.8 cm,

consisted mostly of a large cyst partially covered by skin. The cyst was filled with 900 ml of clear fluid which was drained prior to removal. Microscopically, the teratoma consisted of both mature and immature tissues (Reprinted from Isaacs [15]. © Springer-Verlag, 2002)

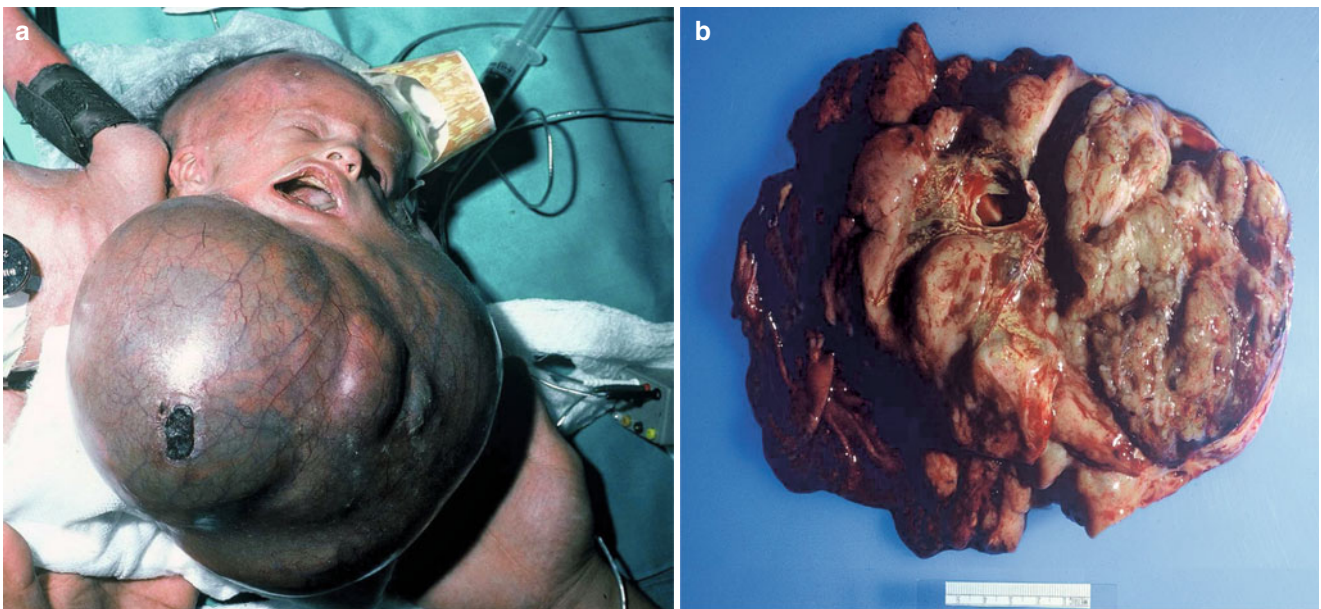


Fig. 2.4 Thyrocervical teratoma. (a) 2-week-old male with a gigantic teratoma arising from the neck producing maternal dystocia. (b) The specimen weighed 1,184 g, measured 24×15×8 cm, and consisted of

both mature and immature neural tissue in addition to cartilage, respiratory, and gastrointestinal epithelium (Reprinted from Tumors Isaacs [15]. © Springer-Verlag, 2002)

Fig. 2.5 Pharyngeal teratoma with great distortion of the facial region. **(a)** Lateral view of the body surface. **(b)** Sagittal section through the midline showing the extent of the tumor (Reprinted from Isaacs [15]. © Springer-Verlag, 2002)

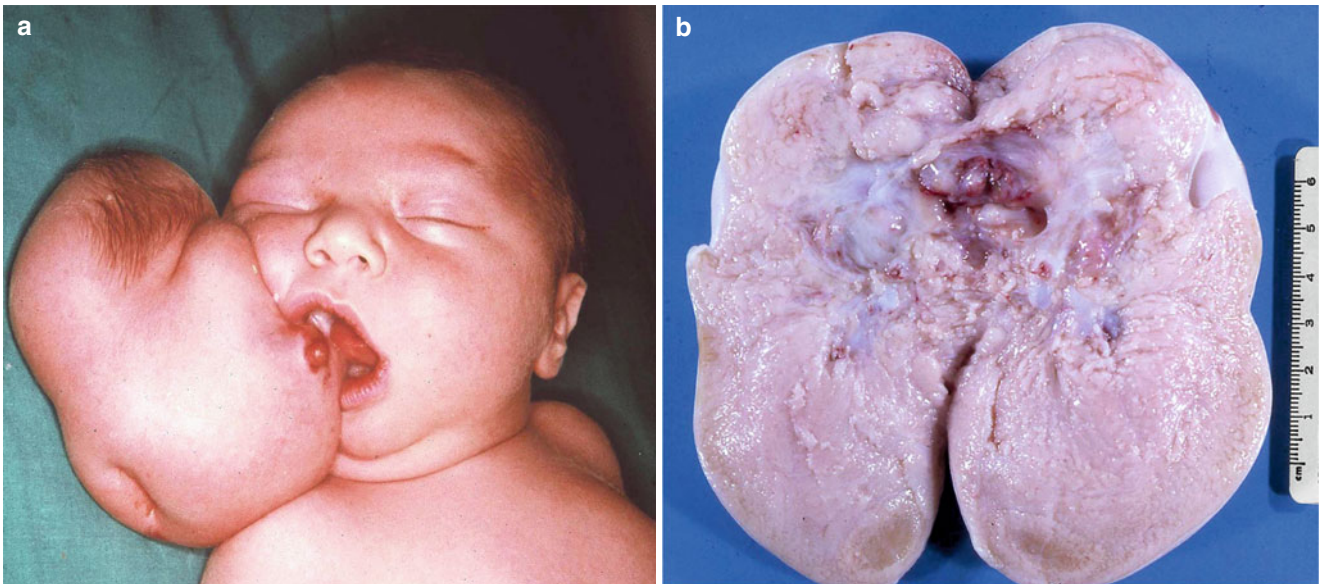
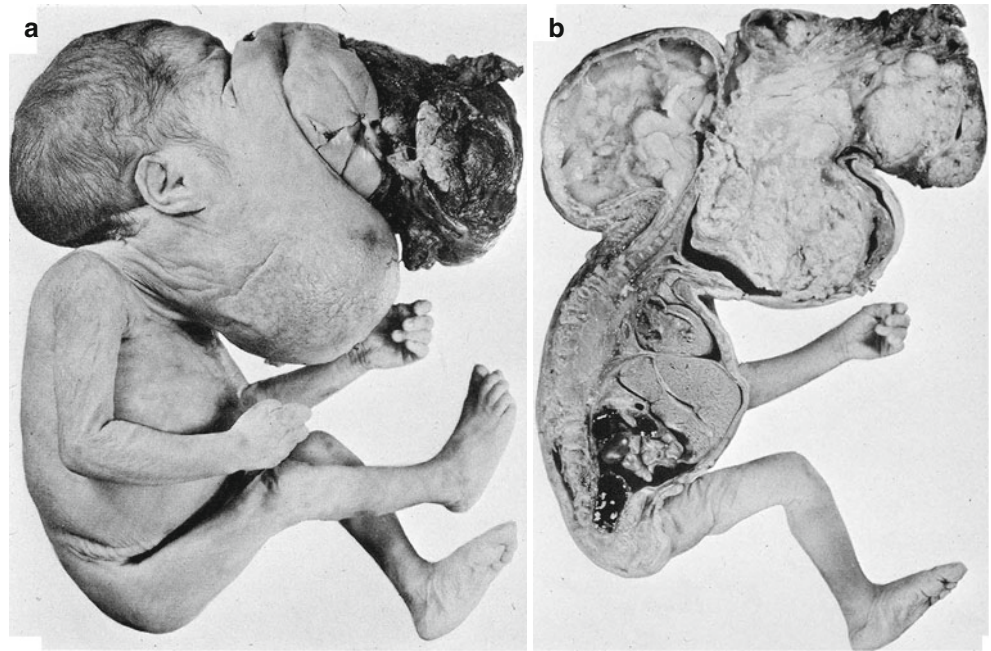


Fig. 2.6 Epignathus. **(a)** 4-day-old, full-term male infant with a solid teratoma attached to the right side of the hard palate. **(b)** The specimen consists mostly of fat. There is an appendage-like protrusion sticking out on the left side. The central nodular area is composed of mature tissues consisting of brain, gastrointestinal tract, and bone. Although

the tumor is suggestive of “fetus-in-fetu” microscopically, neither a well-defined vertebra nor structural organization of the tissue components were found (Reprinted from Isaacs [15]. © Springer-Verlag, 2002)



Fig. 2.7 Nasopharyngeal dermoid (“hairy polyp”). Intermittent respiratory distress related to positioning of the infant was noted shortly after birth. Laryngoscopy revealed a fingerlike projection protruding from and obstructing the nasopharynx. (a) Radiograph shows a bright white mass within the nasopharynx and oropharynx with signal

characteristics of fat. (b) The polyp consists only of skin with hair follicles, fat, and cartilage, which is not shown. (c) Histologically the polyp consists only of skin with hair follicles, fat and cartilage, not shown in this field. (Reprinted from Isaacs [15]. © Springer-Verlag, 2002)

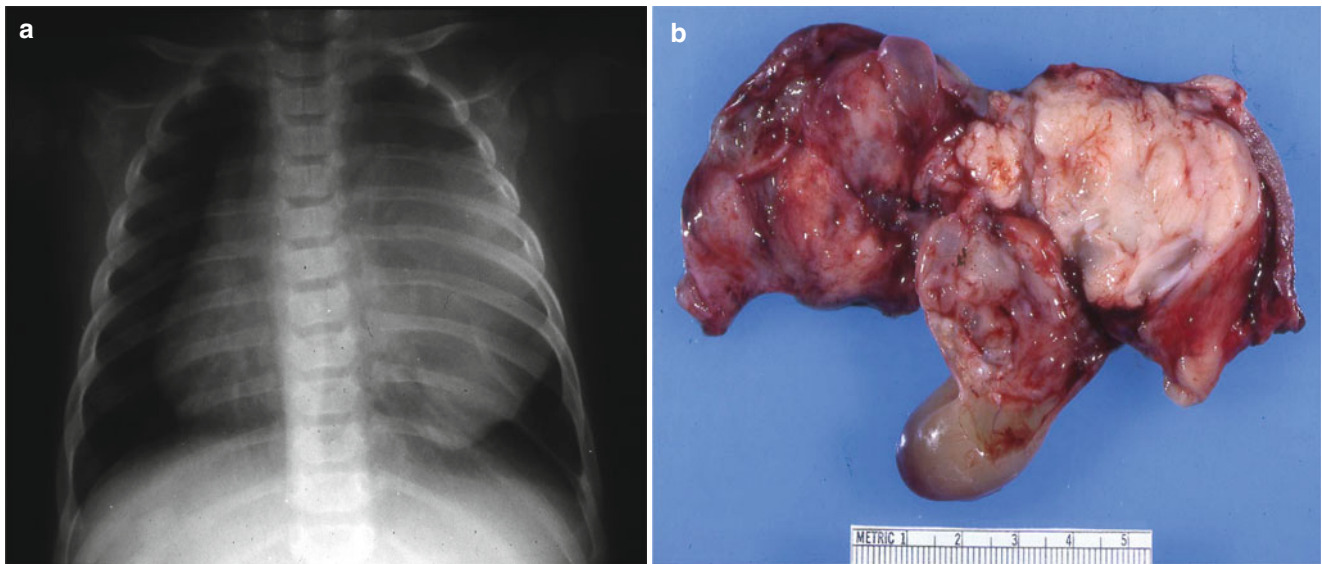


Fig. 2.8 Mediastinal teratoma. 4-month-old male was evaluated for an upper respiratory infection. A mediastinal mass was discovered on a chest radiograph. **(a)** Chest radiograph shows the mass occupying the

right thoracic cavity. **(b)** The teratoma is attached to the thymus and consists of both mature and immature tissues (Reprinted from Isaacs [15]. © Springer-Verlag, 2002)

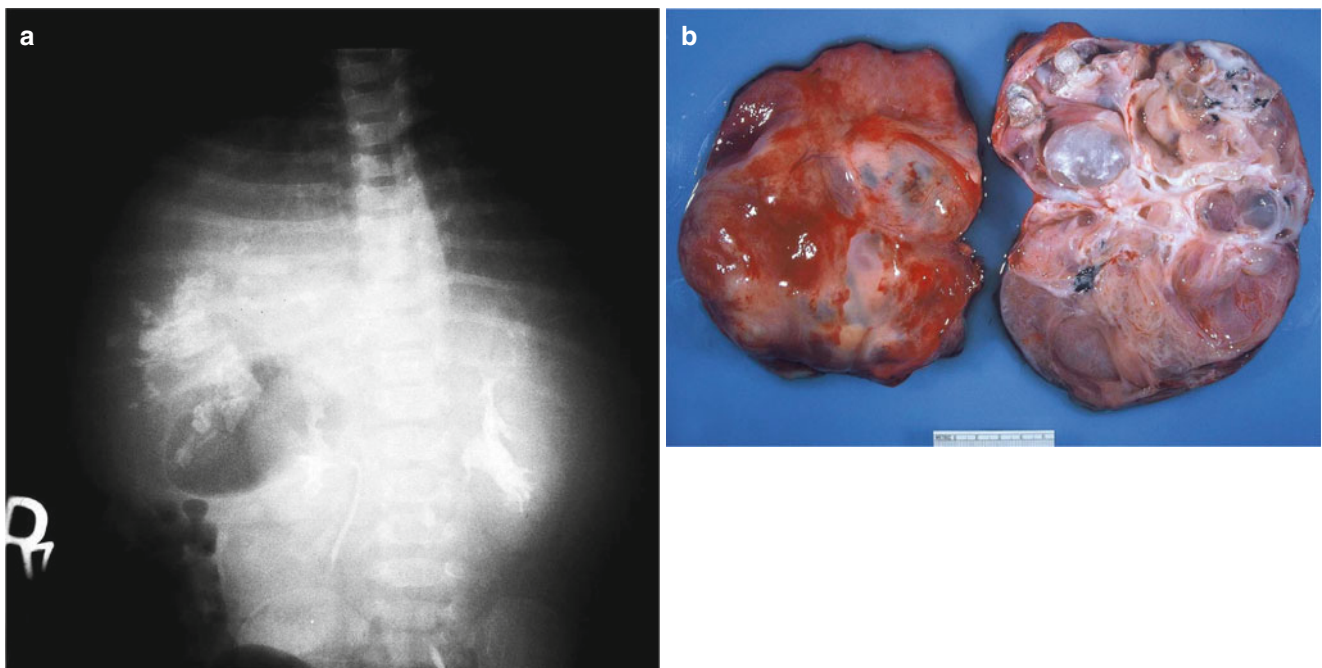


Fig. 2.9 Gastric teratoma. 4-month-old male with a history of constipation, progressive abdominal distension vomiting, feeding problems, and an abdominal mass. **(a)** Intravenous pyelogram reveals a tumor arising from the lesser curvature of the body of the stomach. **(b)** The cystic and

solid tumor measures 16×14 cm and contains immature neuroglial tissue, skin, choroid plexus, gastrointestinal and respiratory epithelium, and cartilage (Reprinted from Isaacs [15], © Springer-Verlag, 2002)

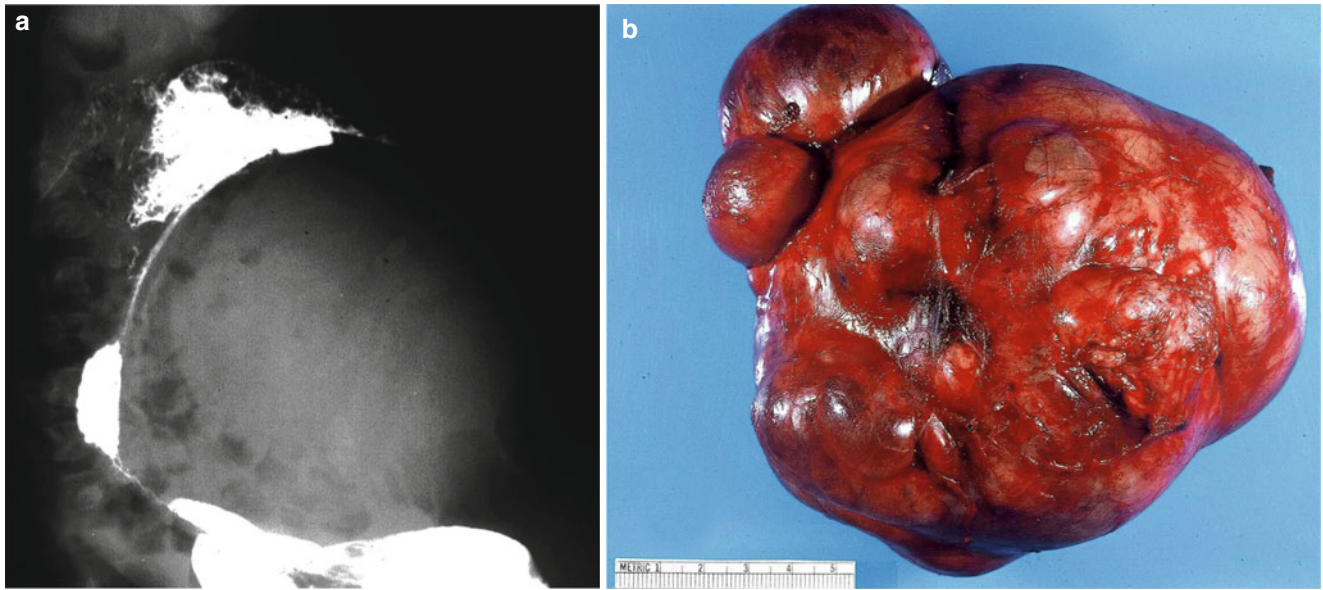


Fig. 2.10 Retroperitoneal teratoma. The patient was a 2-month-old male with a history of constipation, progressive abdominal distension and an enlarging abdominal mass since birth. **(a)** Abdominal imaging reveals compression of the intestine by a large retroperitoneal mass

situated anterior to the spine. **(b)** The specimen, 799 g, 15×15×6 cm, consists of solid and cystic areas. Both mature and immature tissue elements are present histologically (Reprinted from Isaacs [15]. © Springer-Verlag, 2002)

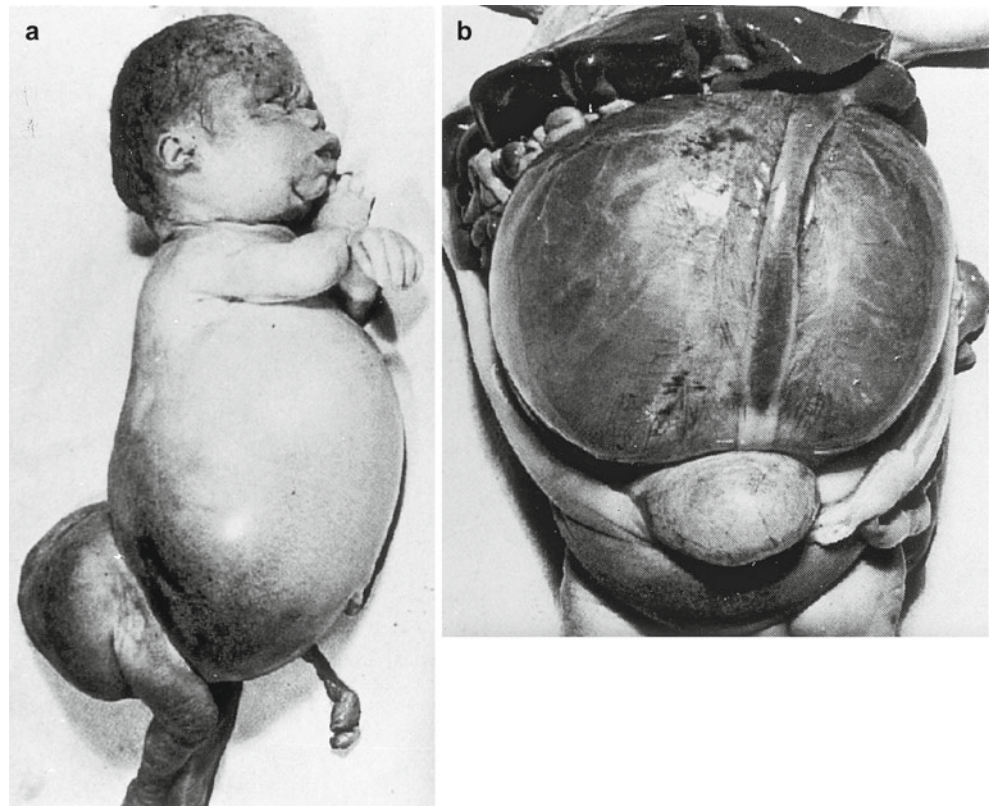


Fig. 2.11 Newborn female infant with combined pelvic and retroperitoneal immature teratoma. **(a)** External appearance. **(b)** Large tumor with overlying sigmoid colon. The bladder is distended as a result of urethral obstruction. The teratoma consists of both mature and immature neuroglial elements (Reprinted from Isaacs [15]. © Springer-Verlag, 2002)

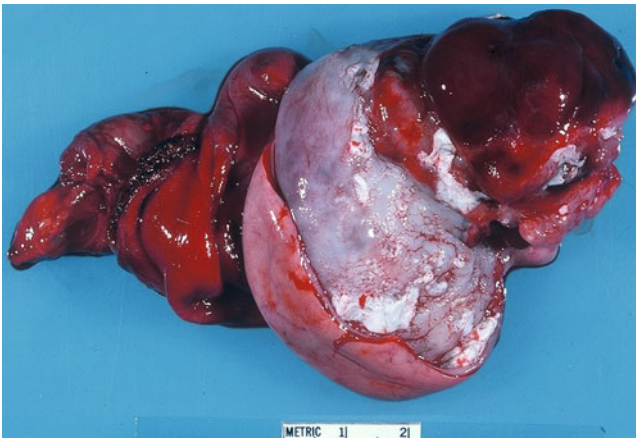


Fig. 2.12 Immature teratoma of the testis. The patient is a 1-year-old male operated on because of bilateral inguinal hernias and what was thought to be a left-sided hydrocele. Instead, an enlarged testis was found that measures 7.5×5×3.5 cm. The cut surface of the testis reveals a tumor composed of skin, sebaceous material, hair, and multiple cysts. In addition to skin, bone, and gastrointestinal tract epithelium, immature neuroglial elements are present histologically (Reprinted from Isaacs [15]. © Springer-Verlag, 2002)

2.3.1 Clinical Findings

Teratoma is the leading germ cell tumor of the fetus and infant typically presenting as an obvious mass with signs and symptoms referable to the location of origin [10, 12, 14, 15] (Table 2.3). Half of childhood teratomas are congenital, and in some series, they are the most common tumor overall [4, 7, 10, 13, 16–18] (Table 1.1). They are discovered as unexpected or incidental findings on routine prenatal or neonatal imaging studies, in a stillborn, as a mass during a newborn physical examination or later on during a routine follow-up visit or for some other unrelated clinical problem. Although a teratoma is defined as benign histologically, it may cause death if vital structures are involved or if the airway is compromised [7, 10, 15, 24, 25, 28] (Fig. 2.6).

Significant congenital anomalies are associated with certain types of teratomas [10, 15, 28, 29]. They depend on the site of the primary tumor and vary considerably in their appearance and extent. For example, single or combined malformations of the genitourinary tract, rectum and anus, and vertebra and caudal spinal cord are found in some patients with sacrococcygeal teratomas [10, 29]. Large, disfiguring cleft palate defects occur in newborns with extensive cranial, palatal, and nasopharyngeal neoplasms [4, 10, 28].

Several unique clinical presentations associated with large space-occupying congenital teratomas are described. They include nonimmune fetal hydrops; respiratory distress and/or hemoptysis resulting from a mediastinal teratoma compressing or eroding into the airway; polyhydramnios occurring with epignathus and cervical tumors because the fetus cannot swallow amniotic fluid; stillbirths resulting

from intracranial teratomas and maternal dystocia (difficult delivery) caused by large intracranial, pharyngeal, cervical, and sacrococcygeal teratomas; and gigantic exophthalmos and massive hydrocephalus secondary to orbital and cranial teratomas, respectively [10, 12, 15] (Table 1.2). Failure to establish respirations due to airway obstruction or compression may be the initial finding in a newborn with a nasopharyngeal, tonsillar, palatal, cervical, or mediastinal teratoma [10, 15, 25, 28] (Figs. 2.4, 2.5, and 2.6). Some palatal (epignathic), thyrocervical, and nasopharyngeal teratomas are so large that they are not resectable and cause death by asphyxia at birth [10, 15, 28] (Fig. 2.6).

2.3.2 Pathology

Teratomas are composed of tissues representing each of the three layers derived from the embryonic disc [1, 2, 4, 6, 10] (Table 2.3 and Figs. 2.12, 2.13, 2.14, 2.15, 2.16, 2.17, 2.18, and 2.19). Endodermal components are the least common, but at times, intestinal or gastric mucosa is remarkably well developed and may be surrounded by muscle layers. Ectodermal components, especially brain tissue, make up a large portion of most teratomas that are present at birth and are more prominent in these than in such tumors discovered later in life. This is particularly true of the sacrococcygeal group. The tissue of these tumors for the most part resembles neuroglia (Figs. 2.14 and 2.15), although ganglion cells and cavities lined by cells simulating ependyma and choroid plexus are not uncommon [10, 15] (Figs. 2.13, 2.20, 2.21, and 2.22).

The *immature teratoma* consists primarily of embryonic-appearing neuroglial or neuroepithelial components, which may coexist with mature tissues. They may display a worrisome histologic appearance because of their hypercellularity, nuclear atypia, and increased mitotic activity (Figs. 2.21, 2.22, 2.23, 2.24, and 2.25). In most instances, immature teratomas, high grade or otherwise, occurring in the fetus and infant are considered benign and associated with a favorable prognosis [10, 15, 30]. The presence of microscopic foci of yolk sac tumor rather than the grade of immature teratoma, per se, is the only valid predictor of recurrence in pediatric immature teratomas at any site [10, 15] (Fig. 2.26). Therefore, grading of immature teratomas in the young child is not required at any site [10, 15, 30].

The neuroectodermal components of a teratoma are variably immunoreactive for one or more neural markers including GFAP, NSE, S-100, neurofilament protein, synaptophysin, nerve growth factor receptor, glial filament protein, myelin basic protein, and polysialic acid [10] alpha-fetoprotein (α -FP) (Fig. 2.28e); immunoreactivity in immature teratomas is generally confined to hepatic tissue, intestinal type epithelium, and yolk sac tumor, if present [10]. DNA ploidy,

Fig. 2.13 Mature teratoma with skin, neuroglial tissue, and choroid plexus. Most teratomas contain these tissues, which were found in tumors described in Figs. 2.2, 2.3, 2.4, 2.5, 2.6, 2.8, 2.9, 2.10, 2.11, and 2.12 (Reprinted from Isaacs [15]. © Springer-Verlag, 2002)

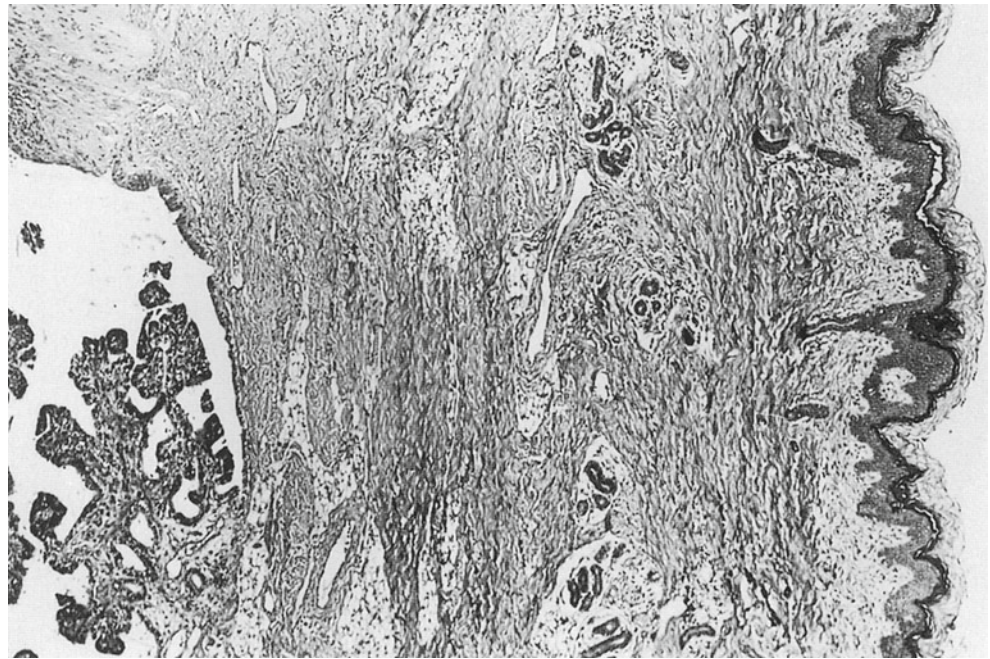
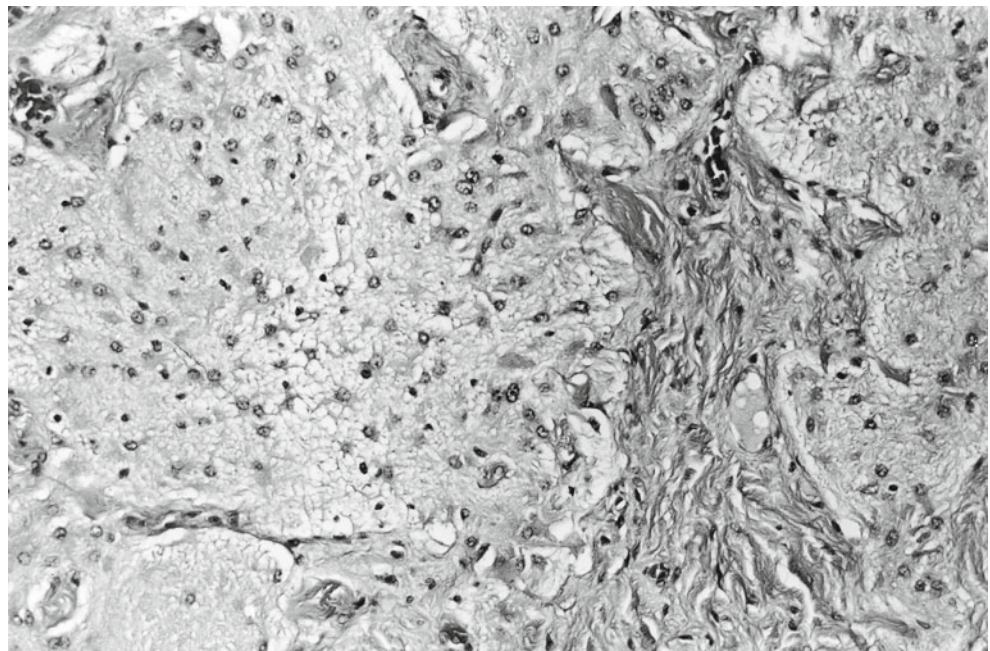


Fig. 2.14 Neuroglial tissue is found often in both mature and immature teratomas. Section taken from a mature teratoma of the testis (Reprinted from Isaacs [15]. © Springer-Verlag, 2002)



p53 and ret expression in teratomas are discussed by Herrmann et al. [31]. Occasionally, tissues other than neural in origin such as nodular renal blastema are found in the immature teratoma [4, 10] (Fig. 2.20).

Epidermis and dermal structures including hairs and sebaceous and sweat glands and fairly well-developed teeth are generally present (Figs. 2.13 and 2.17). Varieties of epithelium

include columnar, pseudostratified, stratified, ciliated and nonciliated, secretory and nonsecretory. Glands in addition to those derived from the skin include salivary, thyroid, pancreas, adrenal, and others. Tissues resembling kidney, liver, and lung are uncommon. Mesodermal components as fat, cartilage, bone, and muscle are present in almost all congenital teratomas [10, 15] (Figs. 2.13, 2.15, and 2.16).

Fig. 2.15 Photomicrograph of a mediastinal teratoma composed of neuroglial tissue with cysts lined by a variety of epithelium in addition to cartilage and salivary gland (Reprinted from Isaacs [15]. © Springer-Verlag, 2002)

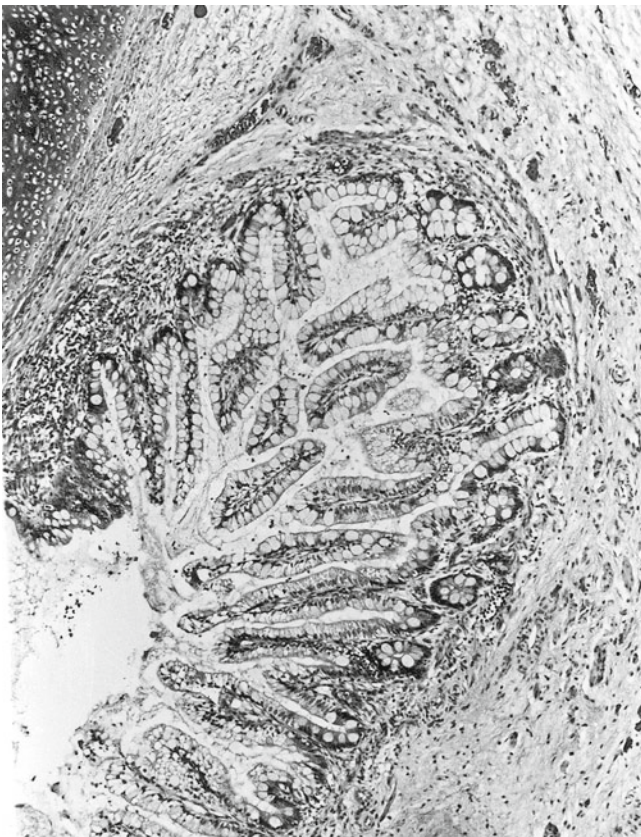
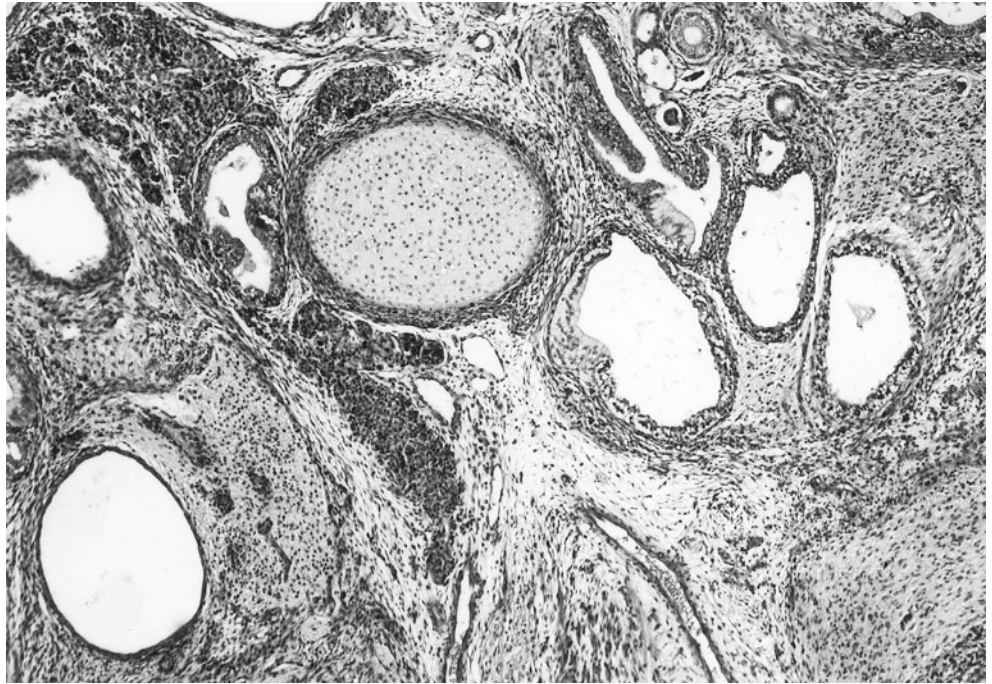


Fig. 2.16 Mature sacrococcygeal teratoma with small intestine and cartilage components (Reprinted from Isaacs [15]. © Springer-Verlag, 2002)

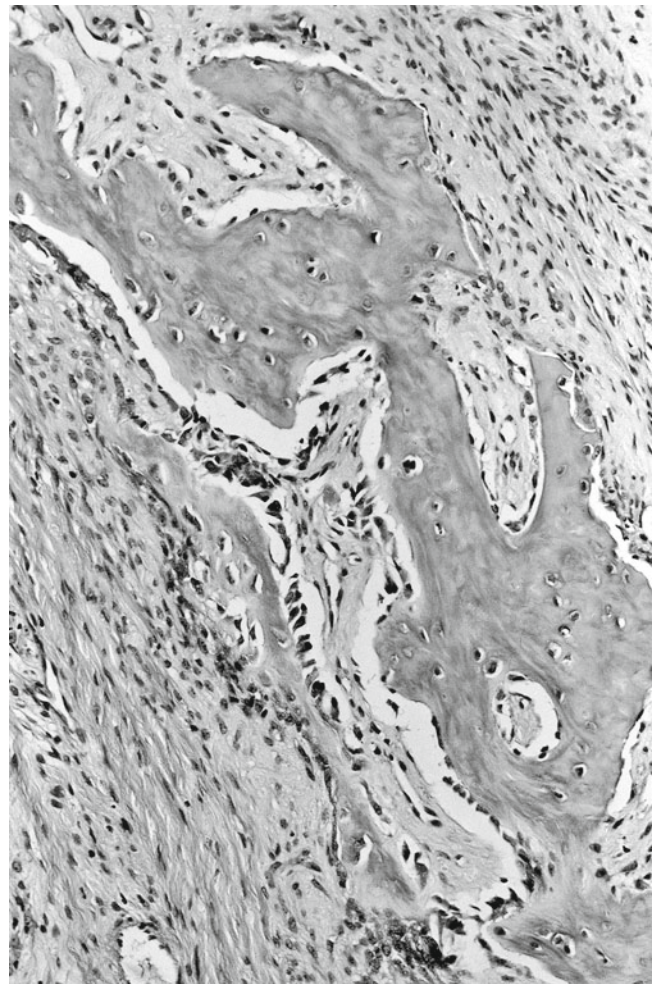


Fig. 2.17 Bone from a testicular teratoma. Bone is present frequently in mature teratomas (Reprinted from Isaacs [15]. © Springer-Verlag, 2002)

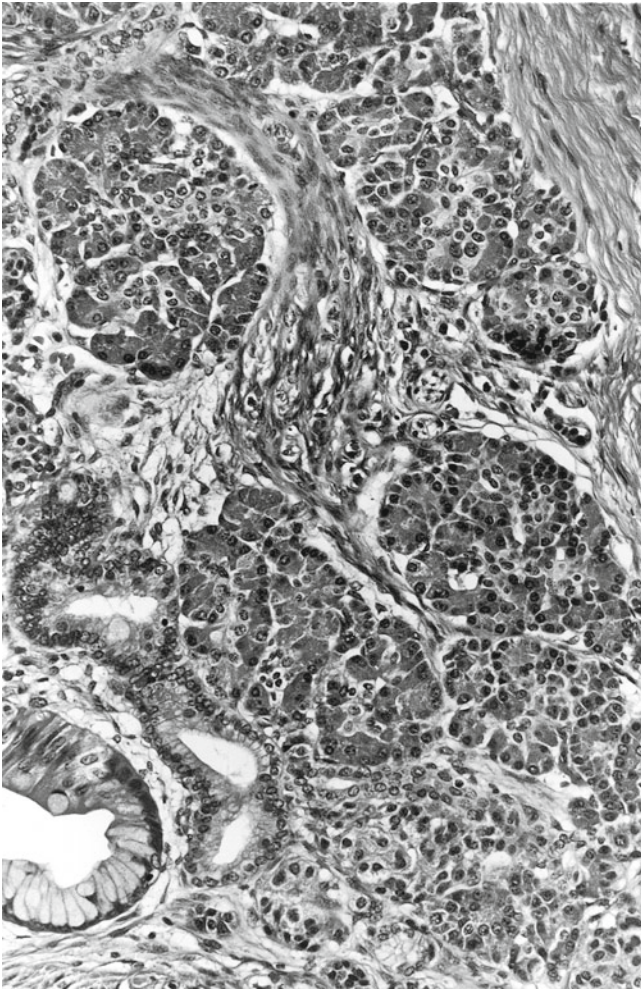


Fig. 2.18 Mature sacrococcygeal teratoma with pancreas (Reprinted from Isaacs [15]. © Springer-Verlag, 2002)

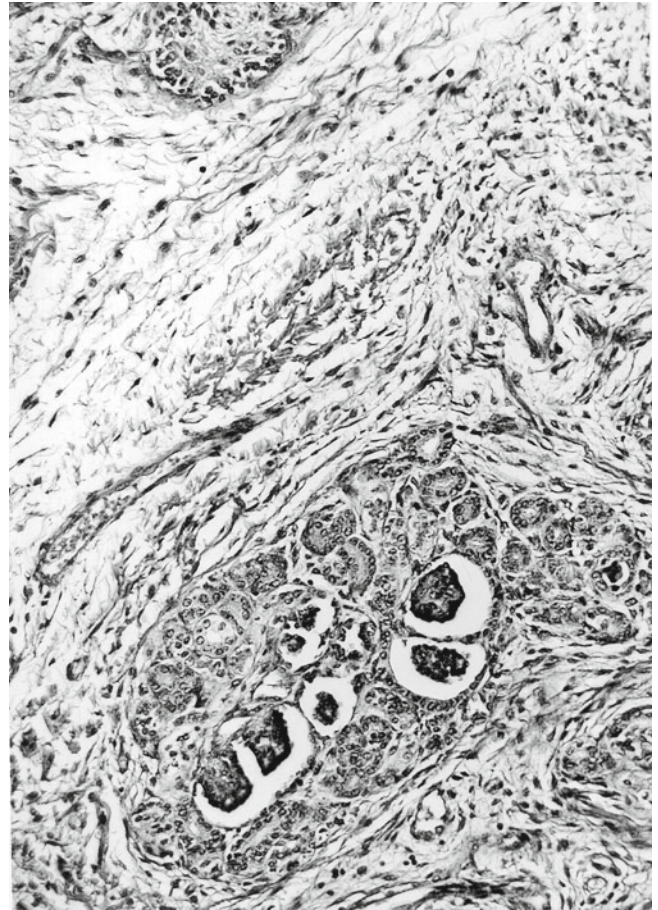


Fig. 2.20 Nephrogenic tissue is an uncommon component of teratomas; section taken from an immature mediastinal teratoma (Reprinted from Isaacs [15]. © Springer-Verlag, 2002)

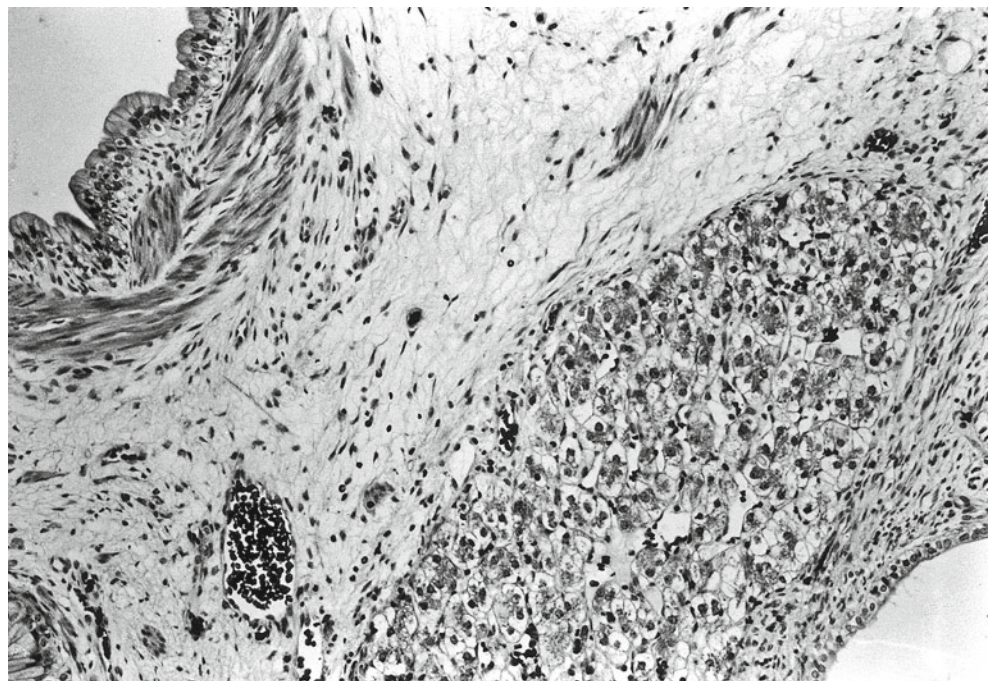


Fig. 2.19 Mature sacrococcygeal teratoma with liver and primitive gut (Reprinted from Isaacs [15]. © Springer-Verlag, 2002)

Fig. 2.21 Immature cerebellar teratoma with ependymal rosette neuroglial elements. The main component of immature teratomas regardless of location are neuroglial elements, which may be derived from brain germinal matrix, ependyma, choroid plexus, or retina. The presence of immature neuroglial elements in a fetal or infant teratoma is not considered malignant in contrast to adult teratomas (Reprinted from Isaacs [15]. © Springer-Verlag, 2002)

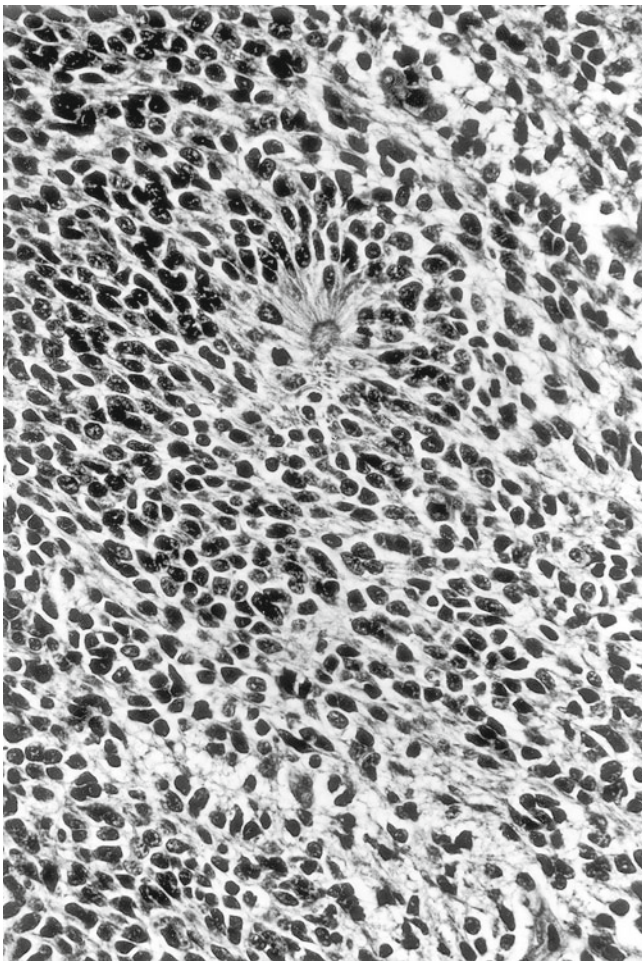
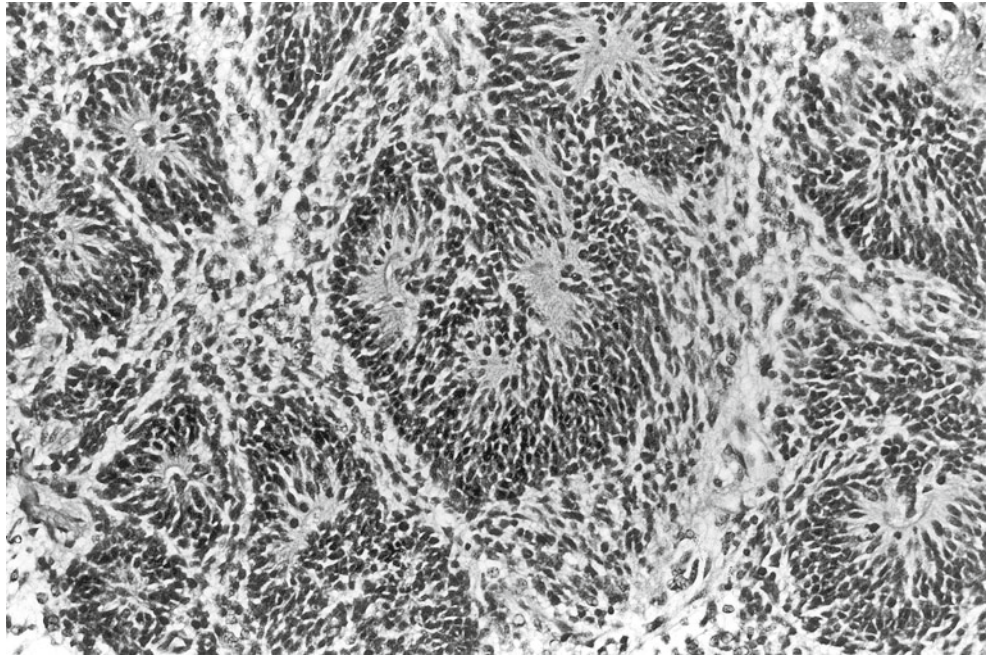


Fig. 2.22 Higher magnification of an ependymal rosette showing foot processes (Reprinted from Isaacs [15]. © Springer-Verlag, 2002)



Fig. 2.23 Immature cervical teratoma with neuroepithelial elements forming primitive ependymal-like canals, which are present also in other immature teratomas, for example, Figs. 2.8 and 2.9, respectively (Reprinted from Isaacs [15]. © Springer-Verlag, 2002)

Fig. 2.24 Immature cerebellar teratoma with germinal matrix-like cells having the appearance of a small cell malignant tumor. In addition, the hypercellular, small dark round cells resemble those of PNETs, neuroblastoma, and medulloblastoma. Immature neuroglial elements blend imperceptively with adjacent mature neural tissues which are helpful in distinguishing them from malignant cells (Reprinted from Isaacs [15]. © Springer-Verlag, 2002)

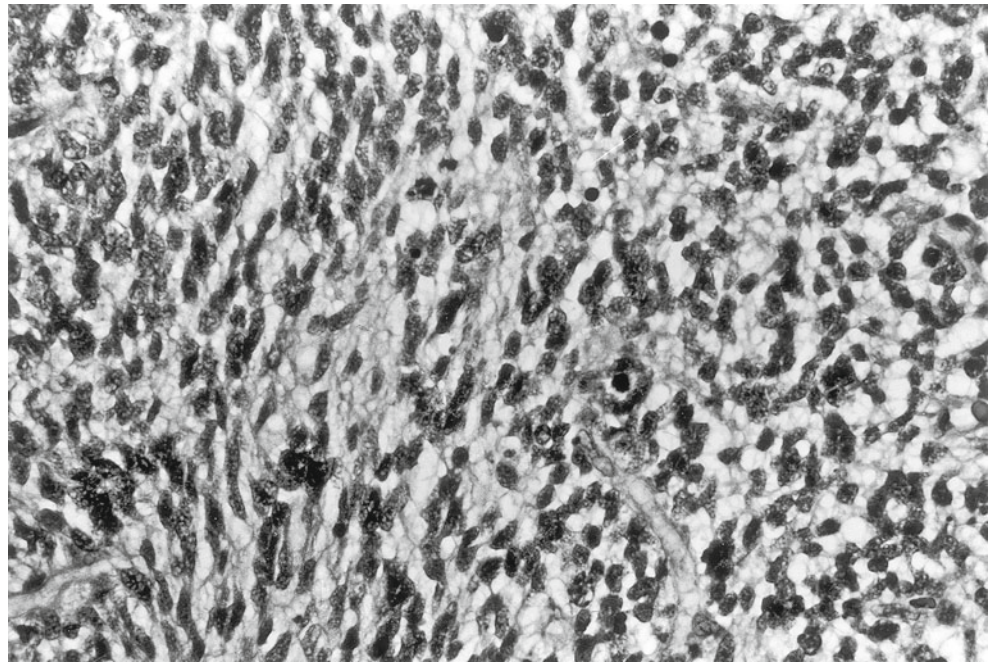


Fig. 2.25 Immature cerebellar teratoma with a pigmented structure suggestive of an optic cup. Heavily pigmented epithelium, resembling retina, is present along the *right* margin of the vesicle (Reprinted from Isaacs [15]. © Springer-Verlag, 2002)

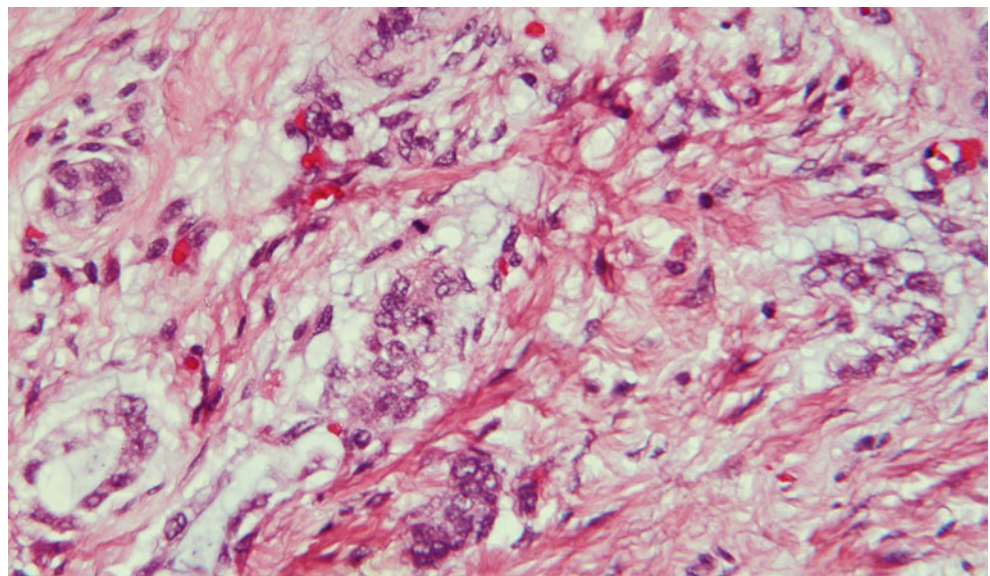


Fig. 2.26 Subtle yolk sac tumor components in an immature sacrococcygeal teratoma removed from a 6-day-old male. Small clusters of bubbly yolk sac tumor cells are scattered throughout. If not diligently searched for, these small foci of malignant cells can be missed easily. The tumor cells stain positively for α -fetoprotein (Reprinted from Isaacs [15]. © Springer-Verlag, 2002)



2.4 Fetus-in-Fetu

Fetus-in-fetu is a strange congenital condition in which a fetiform mass with an axial skeleton and vertebral column is enclosed within the body of its host [10, 15, 32, 33] (Fig. 2.27). Most occur within the retroperitoneum as a single fetiform mass. Less common locations are the pelvis, mesentery, cranial cavity, scrotum, undescended testis, oral cavity, and sacrum. Both fetus-in-fetu and teratoma may coexist in the same individual, and a family history of twinning, as high as 18 %, is present in some patients with both entities [10, 14, 32, 33].

Fetus-in-fetu is detected readily on routine prenatal sonograms. Diagnosis is established on imaging studies by demonstrating a diminutive vertebral column and other parts of a skeleton [10, 14, 33]. The most common imaging and clinical finding is an abdominal retroperitoneal mass (Fig. 2.27). Other

presenting signs in the patient are abdominal distension, feeding difficulty, vomiting dyspnea, and rarely jaundice [10, 14].

The fetiform mass is anencephalic, acardiac, and showing various degrees of organ system differentiation and deformity. Well-formed limbs, vertebra, gut, and various other organs are noted on gross dissection and on prior imaging studies [10, 32, 33] (Fig. 2.27). Microscopic examination shows recognizable organs in various stages of development, mostly mature and sometimes immature tissues (e.g., neuroglial and renal) derived from the three germinal layers. Reported cases of fetus-in-fetu in the neonate thus far have been shown to be histologically benign initially [10].

Treatment of the fetus-in-fetu is surgical resection, which results in cure. There are case reports of patients who had yolk sac tumor recurrences several years after the original surgery [14].

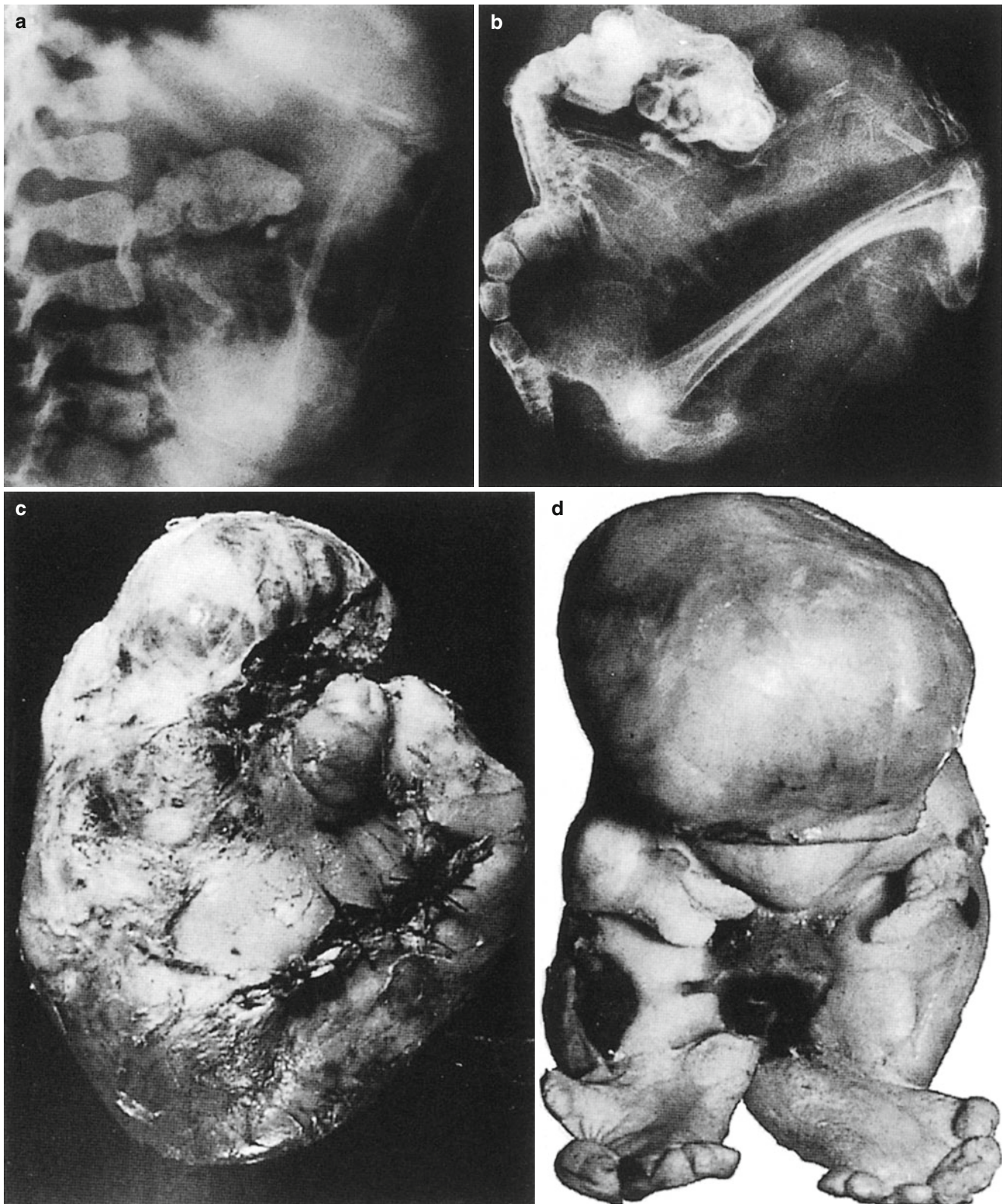


Fig. 2.27 Fetus-in-fetu. Radiographs of a retroperitoneal mass resembling a fetus in a 1-year-old child. (a) Before removal from the abdomen. (b) After removal. (c) External surface of the mass shown in (a). (d) Before removal of the outer covering. (e) After removal of outer covering. (f) Sagittal section shows well-developed vertebra, spinal nerves, base of skull, and cystic replacement of the brain. The large

black convoluted structure is intestine filled with blood. Heart was not identified. (f) Cross section of intestine showing the presence of all muscle layers. Auerbach's plexus appears identical with that of normal intestines (Reprinted from Isaacs [10]. © Mosby, 1997. With kind permission)

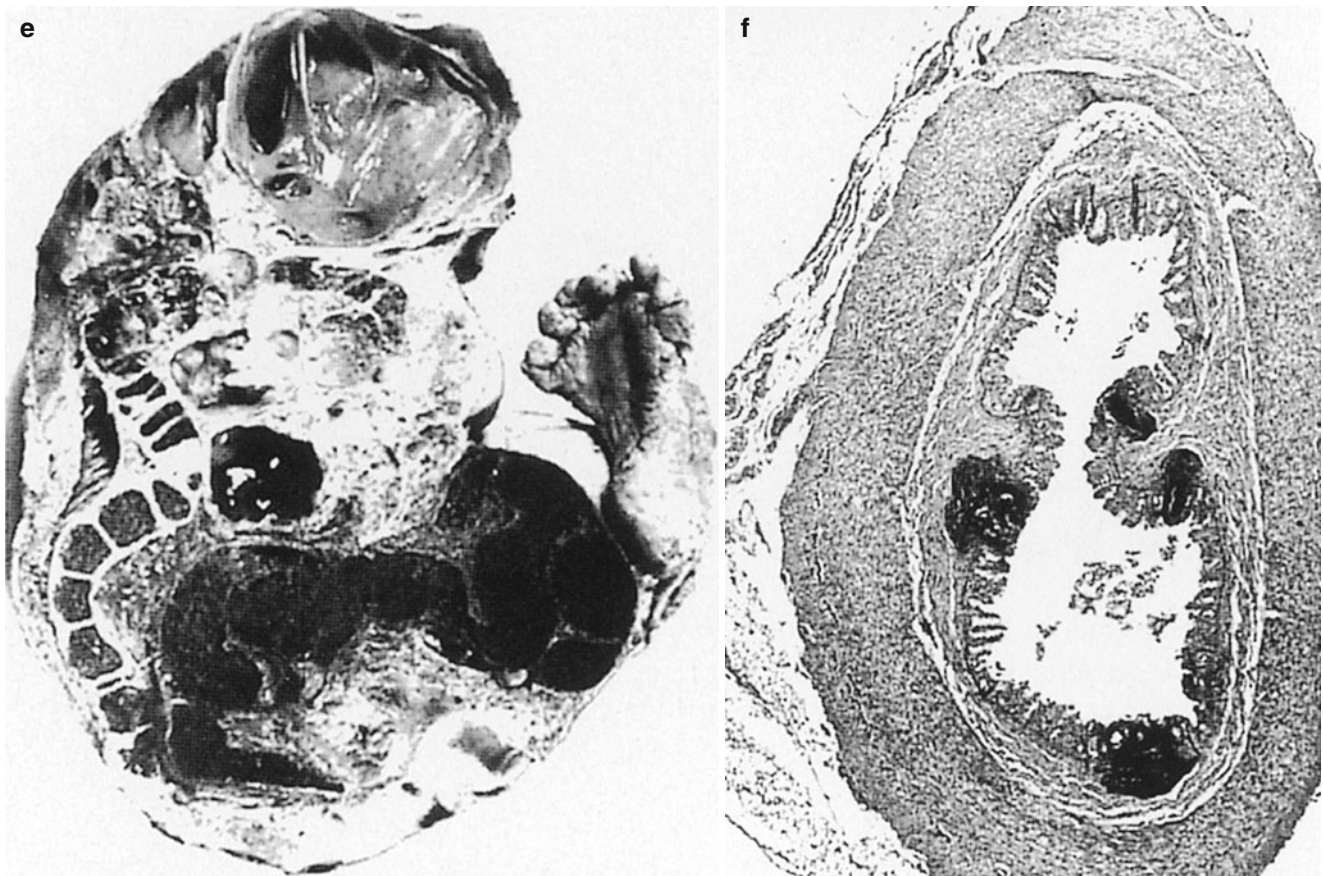


Fig. 2.27 (continued)

2.4.1 Prognosis

Most teratomas diagnosed in infants are classified microscopically as mature [10, 14]. The immature teratoma, with or without a mature component, is second in frequency [7, 10, 14]. In the fetus and neonate teratomas, mature and immature tissues occur about equally depending on the gestational age [10, 14]. The sacrococcygeal area is associated with the highest incidence of malignancy, in the form of yolk sac tumor [1, 7, 14, 15] (Table 2.4). The frequency of yolk sac tumor in sacrococcygeal teratomas is approximately 10 %; however, the values range from as low as 2.5 to 20 % [10, 12, 14, 15]. The presence of immature neuroglial elements in infant and fetal teratomas has no bearing on prognosis [10, 12, 14, 15].

Table 2.4 Location and patient survival with various types of teratomas ($n=534$)

Location	Survival
Sacrococcygeal	44/214 (67) ^a
Cervical	46/70 (66 %)
Intracranial	8/71 (11)
Oro-nasopharyngeal	23/41 (56)
Cardiac ^b	30/40 (75)
Gastric	11/14 (79)
Mediastinal ^c	9/13 (69)
Facial	7/8 (87.5)
Fetus-in-fetu	24/25 (96)
Teratoma recurrence rate	29/534 (5)
<i>Overall survival</i>	<i>335/534 = 63 %</i>

Reprinted from Isaacs [14]. With kind permission of © Elsevier, 2004

^aPercent

^bMost cardiac teratomas were situated in the pericardium

^cMediastinal teratomas outside of the heart and pericardium

2.5 Yolk Sac Tumor

Yolk sac tumor (endodermal sinus tumor) is the leading malignant germ cell tumor in infants and children [2, 8, 10, 14, 15] (Tables 2.2 and 2.3). More arise from the sacrococcygeal area than from any other location during the first year of life where it adversely affects the prognosis [14]. Less common primary sites in this age group are the testis, pelvic retroperitoneum, and vagina but, practically, never the ovary [2, 10].

Yolk sac tumors have a slimy, pale tan-yellow gross appearance with grayish-red foci of necrosis and small cyst

formations. Generally, they are very soft and mushy falling apart upon removal [10, 15]. When the testis is involved, most of it is replaced by tumor, leaving a barely recognizable light tan, thin rim of parenchyma (Fig. 2.28).

Six or more histologic patterns are recognized [2, 4–6, 10]. The *papillary* form consists of papillary projections with or without the perivascular endodermal sinus structures (Schiller-Duval bodies) (Figs. 2.28b and c). The *reticular* pattern shows tumor cells arranged in a network situated about spaces containing vacuolated pink-staining material (Fig. 2.28d). The *solid* pattern shows mostly solid nests of cells. The rare

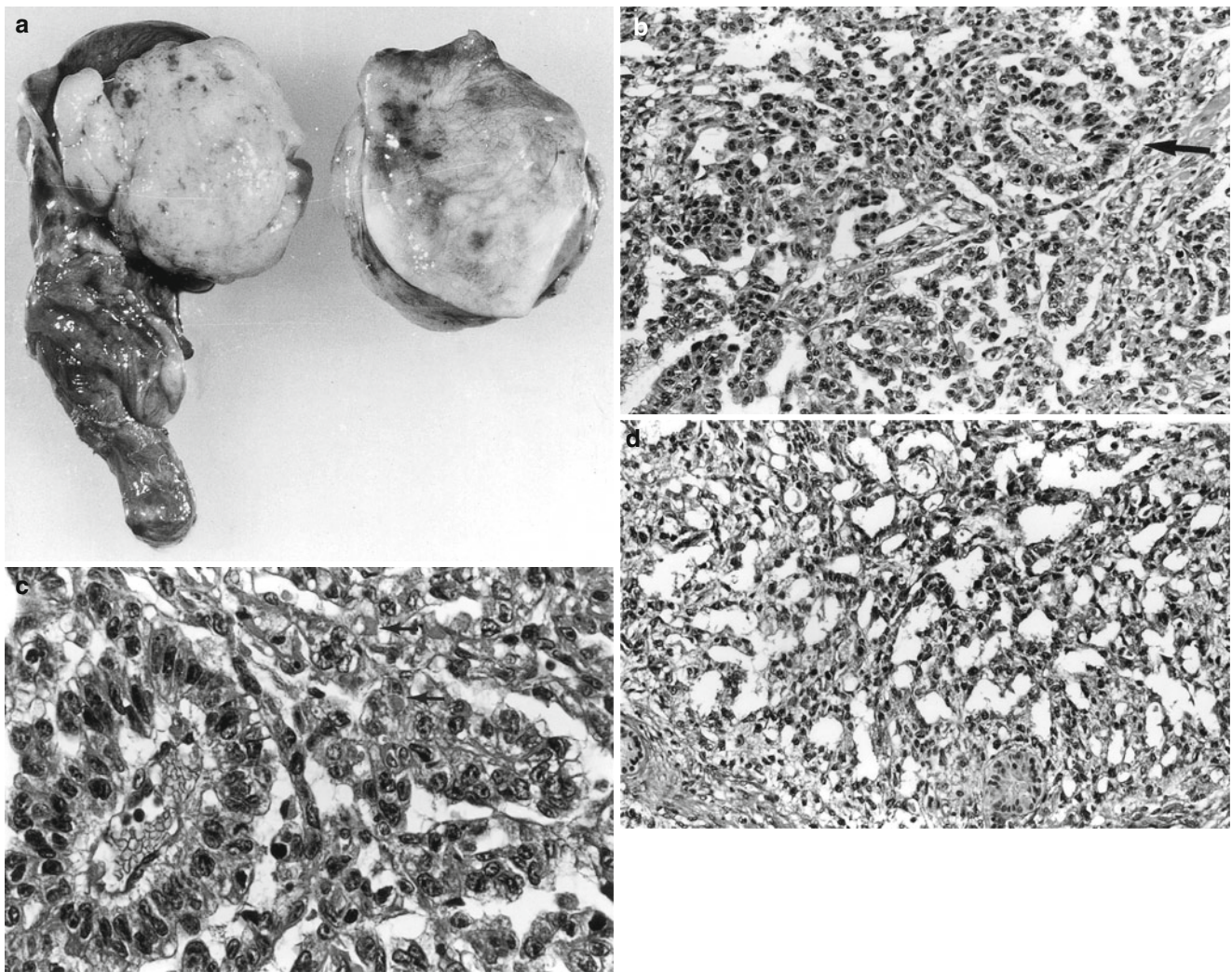


Fig. 2.28 Yolk sac tumor of the testis. (a) 11-month-old male with a scrotal mass. The bisected testicular tumor and attached spermatic cord. (b) Photomicrograph reveals the characteristic papillary pattern of yolk sac tumor with perivascular endodermal sinus structures (Schiller-Duval bodies) (*arrow*) in a solid pattern background. (c) Higher magnification of one of the endodermal sinus structures showing the relationship of the central blood vessel with surrounding tumor cell. Droplets of hyaline staining material representing α -fetoprotein are present (*arrows*). (d) Histological section showing the reticular (*netlike*)

pattern. Two small, testicular tubules are present near the lower margin of the photograph. Tumor cells react with α -fetoprotein. (e) Embryoid body of the polyembryoma variant. 1-year-old male with a yolk sac tumor of the testis. The embryoid body, upper right corner, resembles a tiny embryo consisting of two vesicles resembling yolk sac and amniotic cavities separated by a 2–3 cell layer embryonic disc. (f) Yolk sac tumor hepatoid variant consisting of fetal-like liver cells (Reprinted from Isaacs [15]; With kind permission of © Springer-Verlag, 2002)

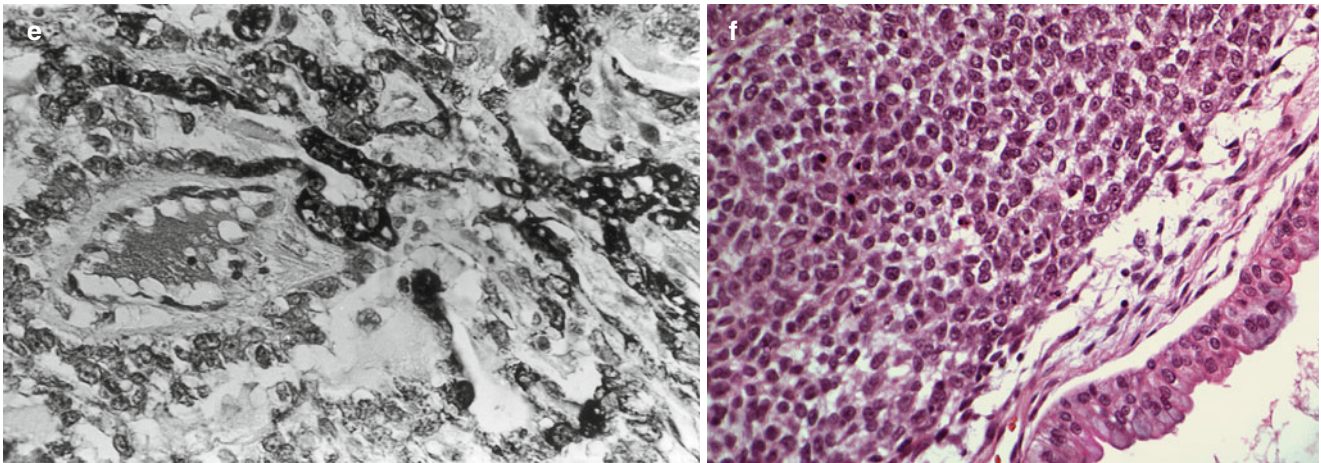


Fig. 2.28 (continued)

Table 2.5 Average normal serum alpha-fetoprotein levels in the newborn and infant

Age	Mean \pm SD (ng/ml)
Premature	134,734 \pm 41,444
Newborn	48,406 \pm 37,718
Newborn 2 weeks	33,113 \pm 32,503
Newborn 1 month	9,452 \pm 12,610
2 weeks 1 month	2,654 \pm 3,080
2 months	323 \pm 278
3 months	88 \pm 87
4 months	74 \pm 56

Wu et al. [33]. With kind permission of © Nature Publishing Group, 1981

polyvesicular vitelline variant displays hourglass-like vesicles with constrictions (blastocyst yolk sac vesicles with constrictions described by Teilum) embedded in a cellular mesenchymal background [5]. A unique variation of the solid pattern is the *hepatoid* pattern, which derives its name from the

histologic observation that the cells resemble fetal liver cells, suggesting hepatocellular differentiation by the tumor [6, 8] (Fig. 2.28f). The *endometrioid-like* variant occurs in the ovary in girls over 11 years of age and is characterized by gland-like formations lined by tall clear cells similar to the early secretory endometrium [34]. There is also a more primitive *glandular* form [34].

Intra- and extracellular hyaline droplets are present in most yolk sac tumors. The droplets are periodic acid-Schiff (PAS) positive, diastase resistant, and variably reactive with α -FP, which is a useful biologic marker present in the serum of these patients [2, 6, 10, 14, 15] (Fig. 2.28e). α -FP can be used also to monitor for the presence of recurrence and/or metastases and the effect of chemotherapy [10, 14, 15]. It is important to note that normally, serum α -FP levels are markedly elevated in the newborn attaining normal levels around 4 months of age [35] (Table 2.5).

The main sites of yolk sac tumor metastases are the lungs and liver (Fig. 2.29a–c).

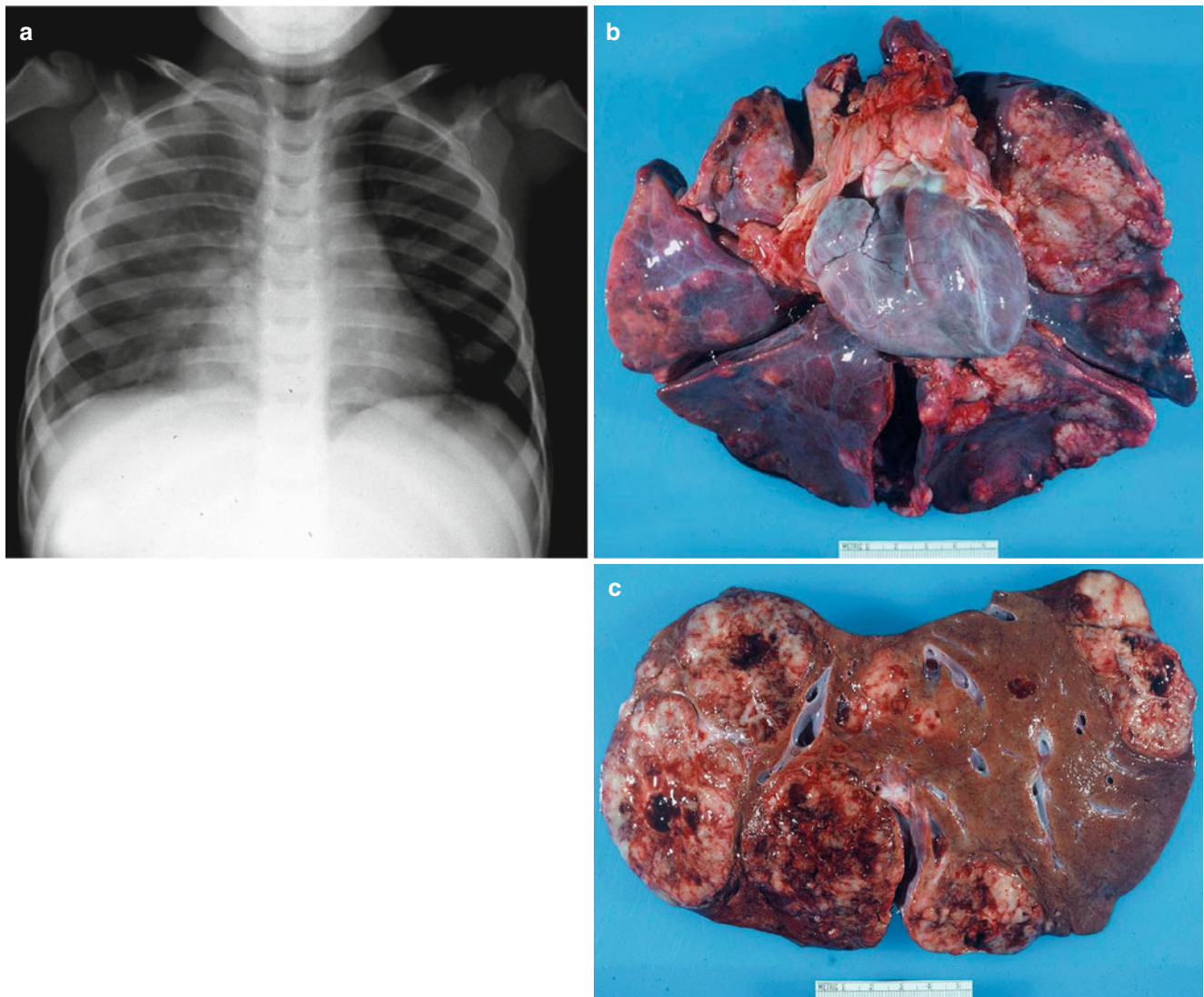


Fig. 2.29 Sacrococcygeal teratoma with yolk sac tumor metastases. Yolk sac tumor is the primary malignant component of sacrococcygeal teratomas; the malignancy occurs in approximately 5–10 % of sacro-

coccygeal tumors. (a, b) Lung metastases. (c) Liver metastases (Reprinted from Isaacs [15]. © Springer-Verlag, 2002)

2.6 Gonadoblastoma

Gonadoblastoma usually arises from within a dysgenetic gonad, but there are a few case reports of this tumor occurring in apparently normal testes or streak ovary [4–6, 10, 15, 36–38] (Table 2.3) (Figs. 2.30a, b and 2.31). Grossly, the tumor consists of one or more small, firm, tan nodules, which may be single or multiple, characteristically containing flecks of calcification visible on imaging studies. Gonadoblastoma has a distinctive appearance consisting of large germ cells surrounded by smaller immature cells of darkly staining, immature cells of sex cord derivation (Fig. 2.31a, b). The latter are round, darkly

staining Sertoli cells or granulosa cells forming microfollicles and containing hyaline bodies and calcium deposits [4, 6, 10, 15, 36–38]. In addition stromal Leydig or lutein cells may be present around the follicles. Gonadoblastoma practically always occurs in individuals having a karyotype with a Y chromosome [10, 37, 38].

It is regarded as an in situ malignancy from which germinoma and other malignant germ cell tumors arise [2, 8, 10, 37, 38]. It is neither locally invasive nor does it metastasize. Gonadectomy is recommended for young children with mixed gonadal dysgenesis because of not only the increased risk of gonadoblastoma and germinoma but also the virilizing effects of residual testicular tissue [3, 10, 15].

Fig. 2.30 Gonadoblastoma arising from a dysgenetic gonad. The patient was a 7-year-old, 45X0/46XY child with ambiguous genitalia. **(a)** The *left side* of the field beneath the tunica albuginea shows the morphologic features of a “streak gonad,” that is, ovarian stroma without either oocytes or developing follicles. Several tumor microfollicles with focal calcifications are present. **(b)** Higher magnification reveals microfollicles composed of nests of large clear germ cells and smaller, *dark round to oval* Sertoli cells. Some cell nests contain round spaces filled with hyaline staining material. According to Teilum, gonadoblastoma recapitulates the structure of the fetal gonad [5]. Calcifications form in the microfollicles which can be appreciated grossly by a gritty sensation on section and also on imaging studies (Courtesy of Rob Newbury, M.D., Department of Pathology, Rady Children’s Hospital, San Diego; Reprinted from Isaacs [15]. © Springer-Verlag, 2002)

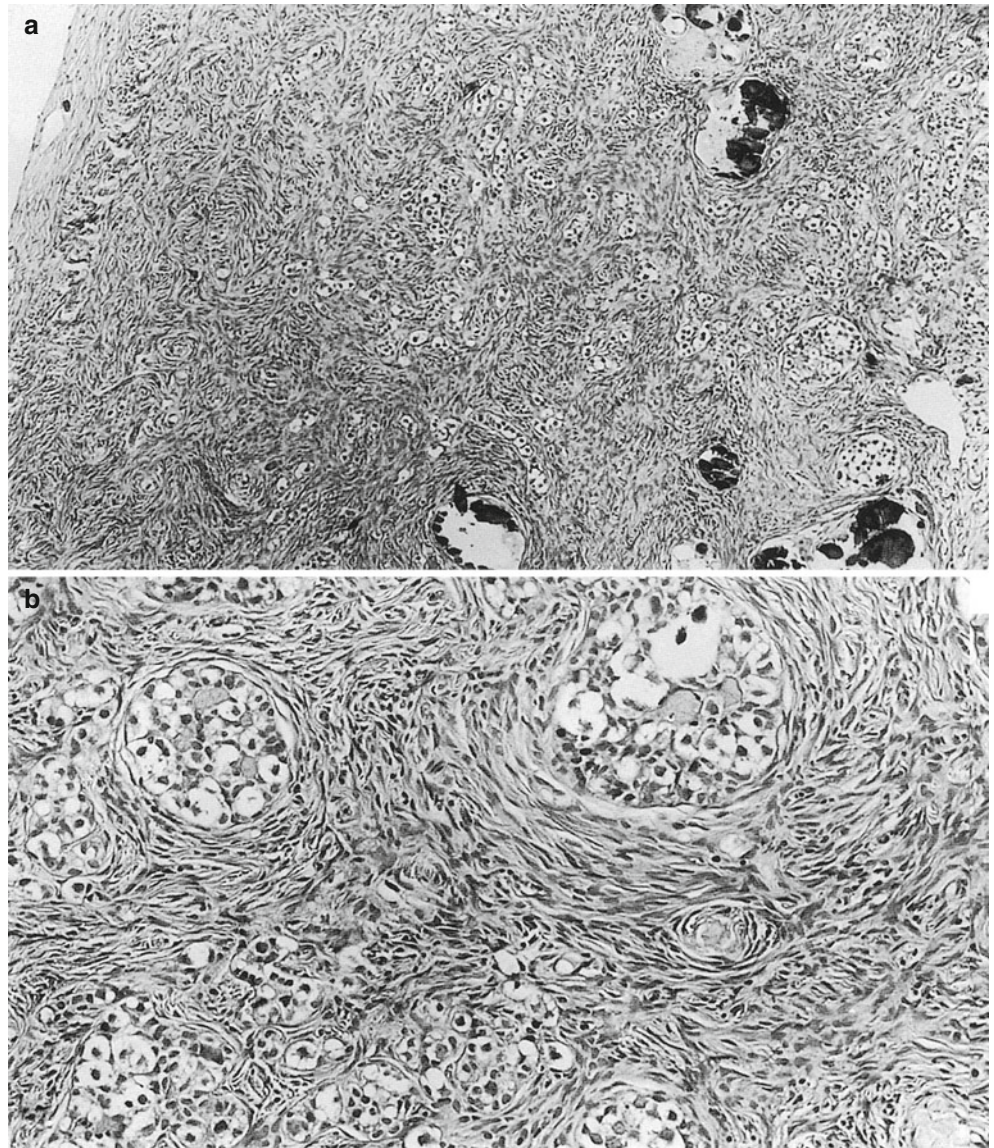
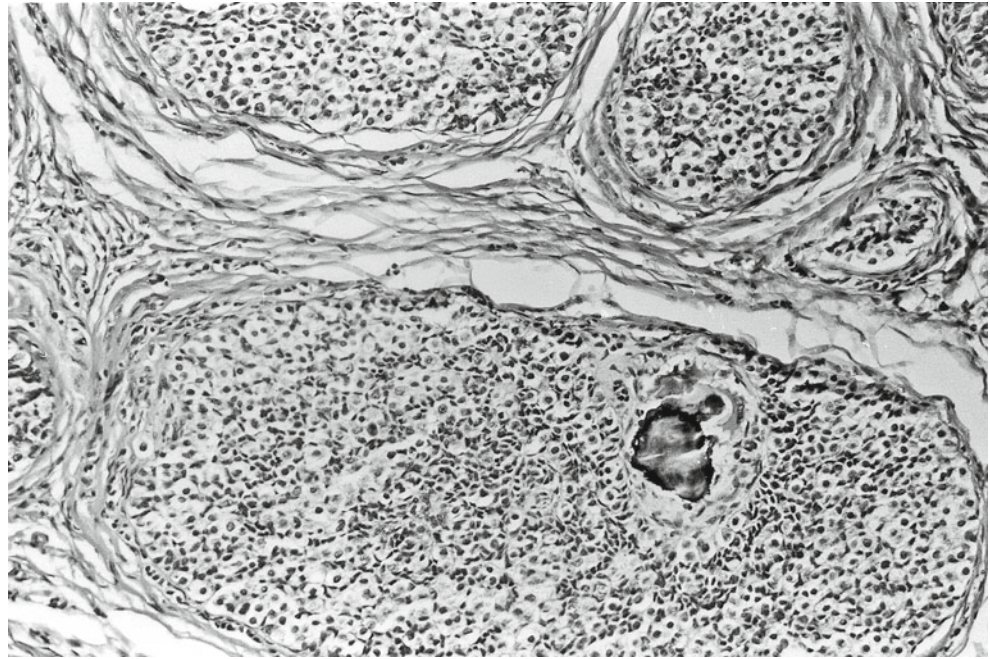


Fig. 2.31 Gonadoblastoma arising from a dysgenetic gonad. The patient was a dysmorphic 4-month-old child with tetralogy of Fallot, ambiguous genitalia, and a karyotype of 45XO/46XY. During a bilateral herniorrhaphy, an undescended “streak” gonad, measuring 2 × 1.3 cm, was found on the right side and an undescended immature testis, 1.5 × 1.5 cm, was noted on the left. Tumor was present only in the streak gonad. The photomicrograph shows an early stage of gonadoblastoma consisting of nests of large germ cells and smaller, dark round to oval Sertoli cells situated in lobules surrounded by fibrous ovarian stroma. A focus of calcification is present (Reprinted from Isaacs [15]. © Springer-Verlag, 2002)



2.7 Embryonal Carcinoma

Embryonal carcinoma is extremely rare in infants [8, 10, 15, 39] (Tables 2.2 and 2.3). It is far less common occurring alone or in association with a teratoma than yolk sac tumor. In the past, many yolk sac tumors were called embryonal carcinomas which resulted in the confusion in the terminology of these two tumors [10]. Grossly, embryonal carcinoma has a variegated cut surface with white tan-gray to yellow soft areas with extensive hemorrhage and necrosis.

Microscopically, embryonal carcinoma consists of a poorly differentiated tumor composed of large, primitive, embryonal-appearing epithelial cells, resembling those of the embryonic disc, with characteristic large nucleoli growing in solid, papillary, and glandular patterns [4, 6, 8, 10, 15, 39] (Fig. 2.32). Tumor cells are immunoreactive with cytokeratin, placental alkaline phosphatase, and NSE and usually negative for EMA [6]. Human chorionic gonadotropin (HCG) and α -feto-protein staining are variable [6]. Electron microscopy is not helpful for the diagnosis.

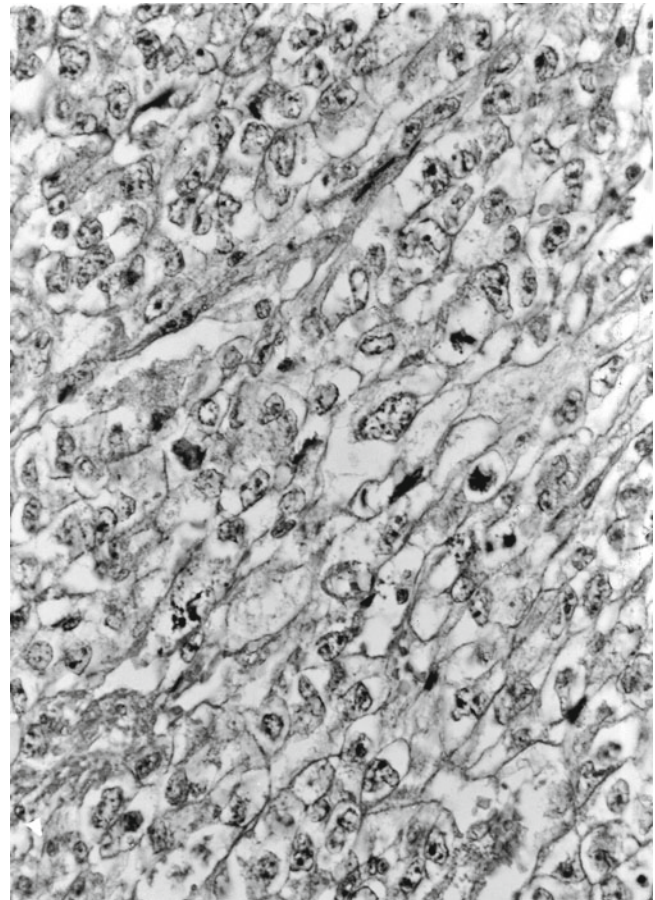


Fig. 2.32 Presacral teratoma with embryonal carcinoma and yolk sac tumor. The patient was a 1-year-old female with a large presacral mass. Microscopically, the tumor contained neuroglial tissue, cysts lined by squamous and respiratory epithelium, and nodules of cartilage. In addition, there was a malignant germ cell tumor component composed of both yolk sac tumor (mainly) and focal embryonal carcinoma. The latter consists of sheets of large, pleomorphic, anaplastic, epithelial cells with vesicular nuclei and prominent nucleoli (Reprinted from Isaacs [15]. © Springer-Verlag, 2002)

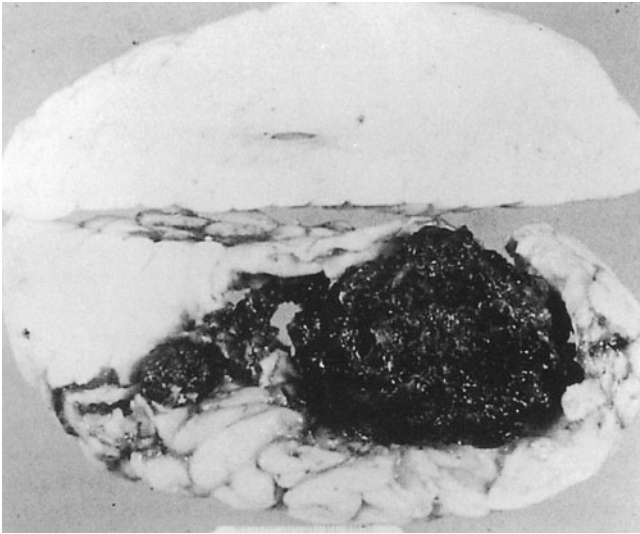


Fig. 2.33 Choriocarcinoma in the brain of a newborn, presumably a metastasis presumably from a placental primary. A large hemorrhagic tumor mass occupies half of one cerebral hemisphere (Reprinted from Isaacs [15]. © Springer-Verlag, 2002)

2.8 Polyembryoma

Polyembryoma is a very uncommon, unusual germ cell tumor of the gonads characterized by the presence of embryoid bodies, which resemble developing presomite embryos [5, 6, 10, 15] (Table 2.3). Microscopically, the embryoid bodies are similar to tiny embryos composed of two vesicles resembling yolk sac and amniotic cavities separated by a two or three cell layer embryonic disc (Fig. 2.33). The yolk sac and hepatic elements of the embryoid body are immunoreactive for α -FP and α -1-antitrypsin and the syn-

cytotrophoblastic component with HCG [6]. In the Children's Hospital Los Angeles review, two infants had yolk sac tumors of the testis with minor polyembryoma components [10, 12, 15].

2.9 Dysgerminoma and Choriocarcinoma

Primary dysgerminoma (germinoma) has not been described in infants either alone or in combination with a teratoma [2, 10, 12, 14, 15]. *Choriocarcinoma*, however, can present in the first year of life either as metastases secondary to a placenta choriocarcinoma [10, 14, 40–43] (Figs. 2.33 and 2.34a–c) or as a primary tumor arising in a variety of locations such as liver, lung, brain, kidney, and maxilla [10, 40–43] (Table 2.3). Choriocarcinoma practically never occurs in association with a teratoma during the first year of life [10].

Infantile choriocarcinoma becomes symptomatic at a mean age of 1 month [42]. Symptoms with decreasing frequency are anemia, failure to thrive, hepatomegaly, hemoptysis, or respiratory failure. Signs of precocious puberty may be present. HCG levels are diagnostically markedly elevated in all patients tested. The most common extraplacental site is the liver followed by the lung, brain, and skin [42, 43]. Maternal choriocarcinoma develops in slightly more than half the women; since 1989, practically all have survived following chemotherapy. Without appropriate treatment, the disease in the infant is rapidly fatal and death occurs on average within 3 weeks from first presentation [40–42]. However, in a recent study, 18 % of patients achieved a sustained remission after multiagent cisplatinum-based chemotherapy and delayed or primary tumor resection [42].

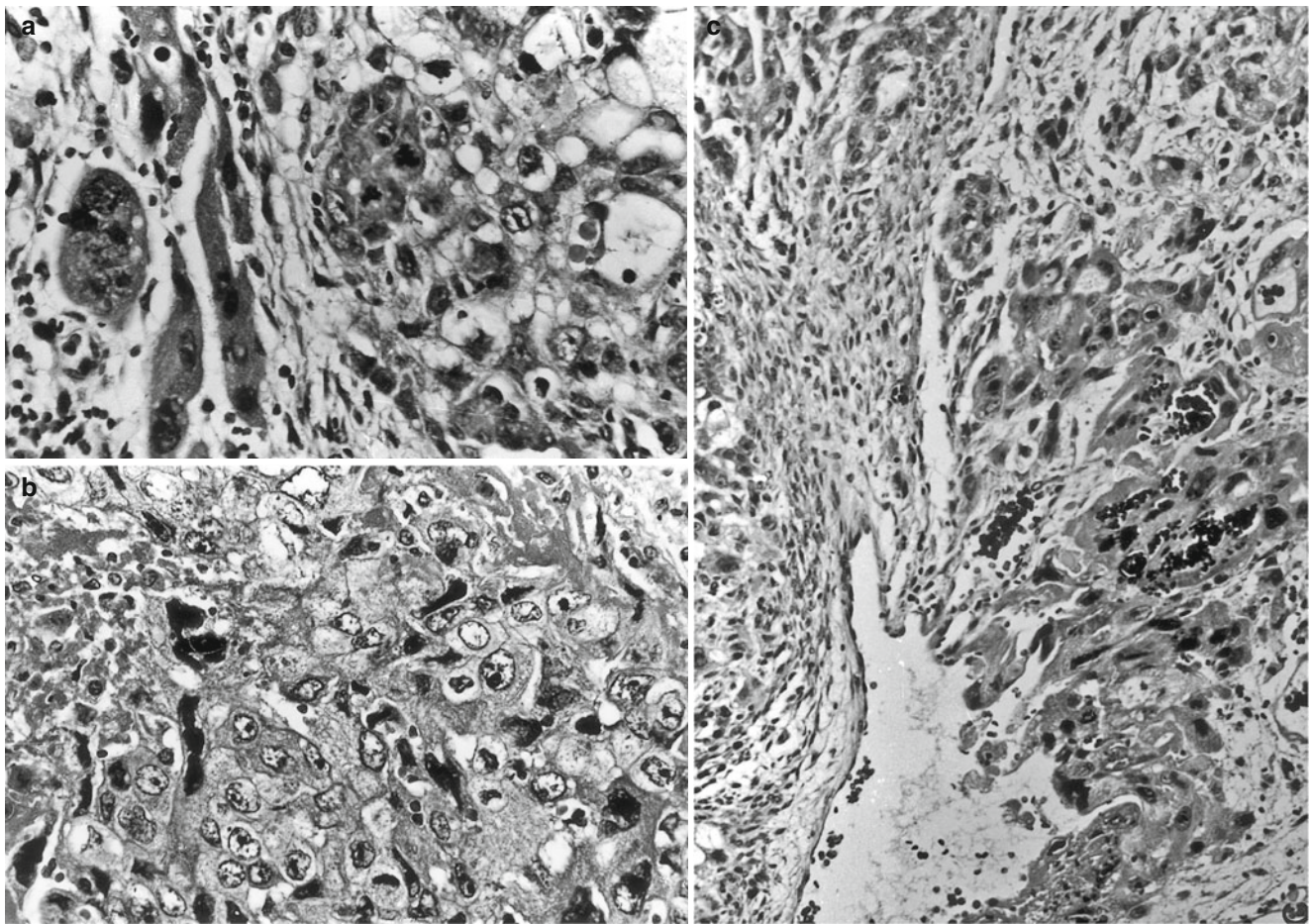


Fig. 2.34 Choriocarcinoma. (a) Cytotrophoblasts occupy the left half of the field; giant, elongated, multinucleated syncytial trophoblasts are situated on the right. (b) Cytotrophoblasts with large vesicular nuclei, prominent nucleoli, and vacuolated to granular cytoplasm. Necrosis is

present. (c) Tumor cells invading and lining up along vascular channels. Foci of necrosis and vascular invasion are characteristic features of choriocarcinoma (Reprinted from Isaacs [15]. © Springer-Verlag, 2002)

References

- Dehner LP (1981) Neoplasms of the fetus and neonate. In: Naeye RL, Kissane JM, Kaufman, N (eds), Perinatal diseases, International Academy of Pathology, monograph no. 22. Williams and Wilkins, Baltimore pp 286–345
- Dehner LP (1983) Gonadal and extragonadal germ cell neoplasia in childhood. *Hum Pathol* 14:493–511
- Dehner LP, Mills A, Talerma A et al (1990) Germ cell neoplasms of head and neck soft tissues: a pathologic spectrum of teratomatous and endodermal sinus tumors. *Hum Pathol* 21:309–318
- Gonzalez-Crussi F (1982) Extragonadal teratomas. In: Atlas of tumor pathology, 2nd series, Fascicle 18. Armed Forces Institute of Pathology, Washington, D.C.
- Teilmann G (1976) Special tumors of ovary and testis and related extragonadal lesions: comparative pathology and histological identification, 2nd edn. J.B. Lippincott, Philadelphia
- Scully RE, Young RH, Clement PB (1998) Tumors of the ovary, maldeveloped gonads, fallopian tube, and broad ligament. In: Atlas of tumor pathology, 3rd series, Fascicle 23. Armed Forces Institute of Pathology, Washington, D.C.
- Tapner D, Lack EE (1983) Teratomas in infancy and childhood: a 54 year experience at the Children's Hospital Medical Center. *Ann Surg* 198:398–410
- Hawkins EP (1990) Pathology of germ cell tumors in children. *Crit Rev Oncol Hematol* 10:165–179
- Heerema-McKenney A, Harrison MR, Bratton B et al (2005) Congenital teratoma: a clinicopathologic study of 22 fetal and neonatal tumors. *Am J Surg Pathol* 29:29–38
- Isaacs H Jr (1997) Tumors. In: Gilbert-Barnes E (ed), Potter's pathology of the fetus and infant, vol 2. Mosby, St. Louis, pp 1242–1339
- Isaacs H Jr (2007) Tumors. In: Gilbert-Barnes E (ed) Potter's pathology of the fetus, infant and child, 2nd edn, vol 2. Mosby Elsevier, Philadelphia, pp 1677–1708
- Isaacs H Jr (1997) Germ cell tumors. In: Tumors of the fetus and newborn. Series Major problems in pathology, vol. 35. W.B. Saunders, Philadelphia, pp 15–38
- Isaacs H Jr (1985) Perinatal (congenital and neonatal) neoplasms: a report of 110 cases. *Pediatr Pathol* 3:165–216
- Isaacs H Jr (2004) Perinatal (fetal and neonatal) germ cell tumors. *J Pediatr Surg* 39:1003–1013
- Isaacs H Jr (2002) Germ cell tumors. In: Tumors of the fetus and infant: an atlas. Springer, New York, pp 5–36
- Isaacs H Jr (1987) Congenital and neonatal malignant tumors: a 28 year experience at Children's Hospital of Los Angeles. *Am J Pediatr Hematol Oncol* 9:121–129
- Werb P, Scurry J, Ostor A et al (1992) Survey of congenital tumors in perinatal necropsies. *Pathology* 24:247–253

18. Parkes SE, Muir KR, Southern L et al (1994) Neonatal tumours: a thirty-year population-based study. *Med Pediatr Oncol* 22:309–317
19. Scully RE, Gilbert-Barness E (2007) Intersex disorders. In: Gilbert-Barness E (ed) *Potter's pathology of the fetus, infant and child*, vol 2, 2nd edn. Mosby Elsevier, Philadelphia, pp 1431–1452
20. Robboy SJ, Miller T, Donahoe PK et al (1982) Dysgenesis of testicular and streak gonads in the syndrome of mixed gonadal dysgenesis: perspective derived from a clinicopathologic analysis of twenty-one cases. *Hum Pathol* 13:700–716
21. van Echten J, van Doorn LC, van der Linden HC et al (1998) Cytogenetics of a malignant ovarian germ-cell tumor. *Int J Cancer* 77:217–218
22. Hoffner L, Deka R, Chakravarti A et al (1994) Cytogenetics and origins of pediatric germ cell tumors. *Cancer Genet Cytogenet* 74:54–58
23. Siltanen S, Heikkilä P, Bielinska M et al (2003) Transcription factor GATA-6 is expressed in malignant endoderm of pediatric yolk sac tumors and in teratomas. *Pediatr Res* 54:542–546
24. Berlin AJ, Rich LS, Hahn JF (1983) Congenital orbital teratoma. *Childs Brain* 10:208–216
25. Lack EE, Weinstein HJ, Welch KJ (1985) Mediastinal germ cell tumors in childhood. A clinical and pathological study of 21 cases. *J Thorac Cardiovasc Surg* 89:826–835
26. Lakhoo K, Boyle M, Drake DP (1993) Mediastinal teratomas: review of 15 pediatric cases. *J Pediatr Surg* 28:1161–1164
27. Isaacs H Jr (2002) I. Perinatal brain tumors: a review of 250 cases. *Pediatr Neurol* 27:249–261
28. Byard RW, Jimenez CL, Carpenter BF et al (1990) Congenital teratomas of the neck and nasopharynx: a clinical and pathological study of 18 cases. *J Paediatr Child Health* 26:12–16
29. Bale PM (1984) Sacrococcygeal developmental abnormalities and tumors in children. *Perspect Pediatr Pathol* 1:9–56
30. Heifetz SA, Cushing B, Giller R et al (1998) Immature teratomas in children: pathologic considerations: a report from the combined Pediatric Oncology Group/Children's Cancer Group. *Am J Surg Pathol* 22:1115–1124
31. Herrmann ME, Thompson K, Wojcik EM et al (2000) Congenital sacrococcygeal teratomas: effect of gestational age on size, morphologic pattern, ploidy, p53, and ret expression. *Pediatr Dev Pathol* 3:240–248
32. Heifetz SA, Alrabeeah A, Brown BS et al (1988) Fetus-in-fetu: a fetiform teratoma. *Pediatr Pathol* 8:215–226
33. Wu JT, Book L, Sudar K (1981) Serum alpha-fetoprotein levels in normal infants. *Pediatr Res* 15:50
34. Fink AM, Cuckow PM, Scott R (1995) Case report: fetus-in-fetu – imaging, surgical and pathological findings. *Clin Radiol* 50:274–275
35. Clement PB, Young RH, Scully RE (1987) Endometrioid-like variant of ovarian yolk sac tumor. A clinicopathological analysis of eight cases. *Am J Surg Pathol* 11:767–778
36. Luisiri A, Vogler C, Steinhardt G et al (1991) Neonatal cystic testicular gonadoblastoma. Sonographic and pathologic findings. *J Ultrasound Med* 10:59–61
37. Tsuchiya K, Reijo R, Page DC et al (1995) Gonadoblastoma: molecular definition of the susceptibility region on the Y chromosome. *Am J Hum Genet* 57:1400–1407
38. Scully RE (1970) Gonadoblastoma: a review of 74 cases. *Cancer* 25:1340–1356
39. Rodriguez SL, Kostick DA, Hered RW et al (2005) Primary embryonal carcinoma of the orbit in a 10-month-old female: a seven-year follow-up. *Am J Ophthalmol* 139:380–381
40. Witzleben CL, Bruninga G (1968) Infantile choriocarcinoma: a characteristic syndrome. *J Pediatr* 73:374–378
41. Chandra SA, Gilbert EF, Viseskul C et al (1990) Neonatal intracranial choriocarcinoma. *Arch Pathol Lab Med* 114:1079–1082
42. Blohm ME, Gobel U (2004) Unexplained anaemia and failure to thrive as initial symptoms of infantile choriocarcinoma: a review. *Eur J Pediatr* 163:1–6
43. Isaacs H Jr (2011) Cutaneous metastases in neonates. A review. *Pediatr Dermatol* 28:85–93

3.1 Introduction

Non-germ-cell gonadal tumors are uncommon in the fetus and infant [1–6]. Approximately 6 % of childhood testicular tumors occur in the first month of life [2]. Most primary tumors of the testis in older children are of germ cell origin,

namely, teratoma and yolk sac tumor, and occasionally gonadoblastoma [2–5] (Tables 3.1 and 3.2).

Ovarian cysts are by far more common than ovarian tumors in the female fetus and infant; *juvenile granulosa cell tumor* is the main ovarian neoplasm in this age group [4] (Fig. 3.1).

Table 3.1 Classification of tumors and tumorlike conditions of the fetal and infant testis

Germ cell tumors
Teratoma
Yolk sac tumor
Gonadoblastoma
Sex cord-stromal tumors
Juvenile granulosa cell tumor
Sertoli cell tumor
Leydig cell tumor
Undifferentiated stromal tumors
Vascular conditions
Hemangioma
Lymphangioma
Non-germ cell tumors
Leukemia
Paratesticular tumors
Rhabdomyosarcoma
Wilms' tumor
Neuroblastoma
Rhabdoid tumor
Cysts
Dermoid cyst
Cystic dysplasia of the rete testis
Simple cyst of testis
Hydrocele
Cystic change following testicular torsion

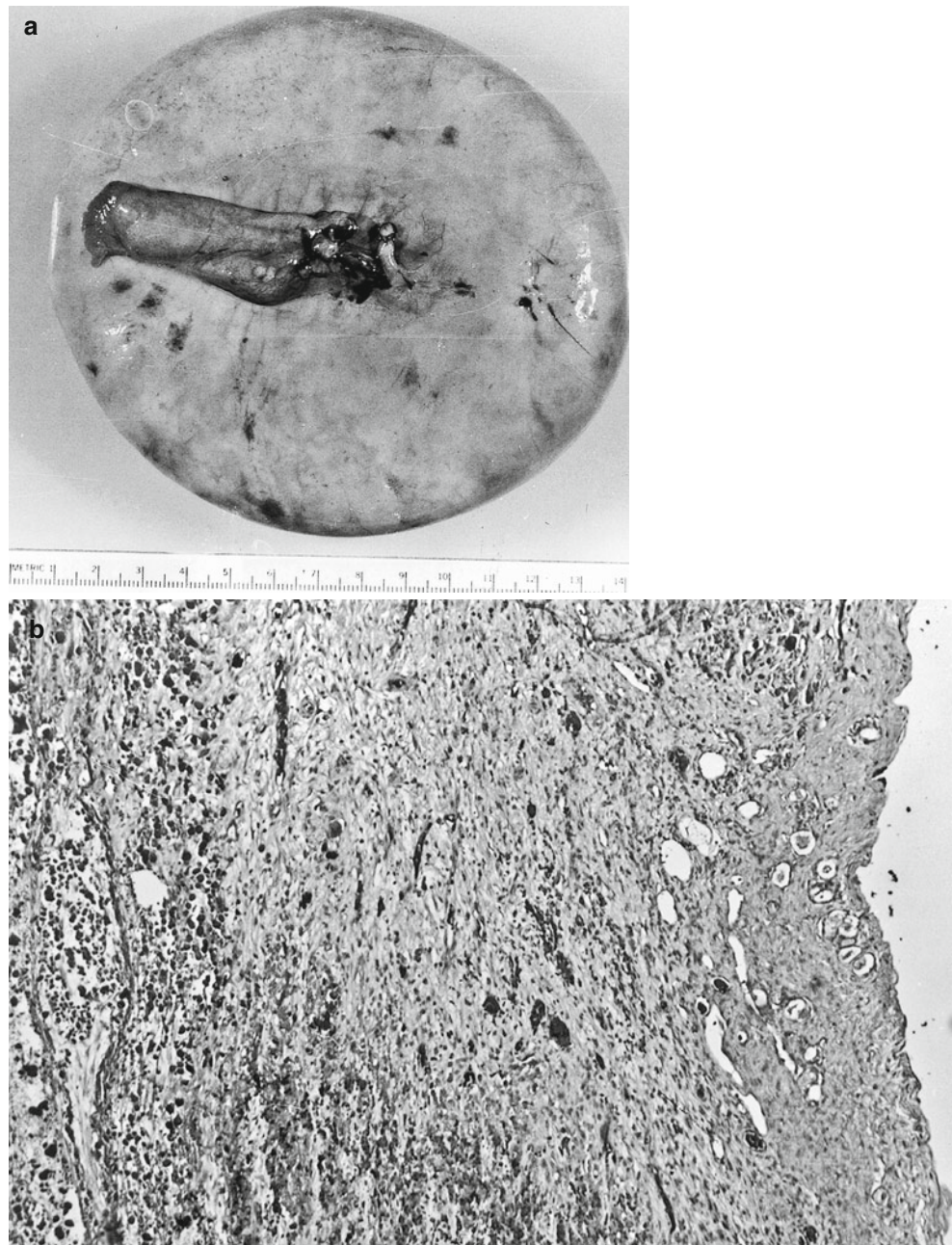
Reprinted from Isaacs [6]; © Springer-Verlag, 2002; Reprinted from Isaacs [4]. With kind permission of © Mosby, 2007

Table 3.2 Twenty-two neonatal testis tumors recorded in the Prepubertal Testis Tumor Registry

Tumor	Number of cases
Yolk sac tumor	6
Teratoma	1
Gonadal stromal tumor	6
Juvenile granulosa cell tumor	6
Gonadoblastoma	2
Hamartoma	1
Total	22

Levy et al. [2]. With kind permission of © Elsevier, 1994

Fig. 3.1 Follicular cyst of the ovary. Three-week-old female with an abdominal mass. (a) The left ovary is replaced by a 6×4.5 cm, 40 g cyst containing brown cloudy fluid and old blood clot. (b) Atrophic ovary and cyst wall with foci of necrosis, calcification, old hemorrhage, and fibrosis. The findings are consistent with old torsion (probably in utero) of a large follicular cyst followed by infarction (Reprinted from Isaacs [6]. © Springer-Verlag, 2002)

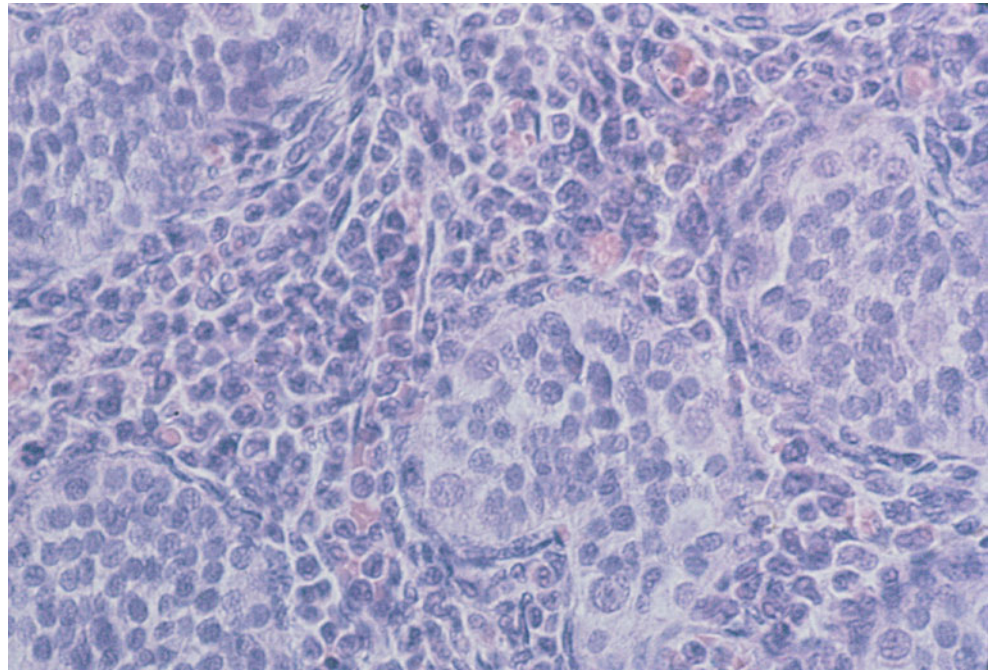


3.2 Leukemic Infiltration of the Infant Testis

Infants with *acute leukemia*, either lymphocytic or myelocytic, typically present with an anemia, high peripheral leukocyte counts, thrombocytopenia, bone marrow, and skin involvement [7]. In the course of their disease, males may develop enlarged testes due to leukemic infiltration [3, 5, 6].

The gonads and central nervous system are sanctuaries for residual leukemic cells even after treatment. Patients undergoing chemotherapy may develop a testicular mass as the first sign of relapse. Testis biopsy is important to confirm the diagnosis of leukemia especially when the hematologic findings are nonspecific [3, 5]. The involved testis shows interstitial leukemic cell infiltrates varying in intensity (Fig. 3.2).

Fig. 3.2 Leukemic infiltration of testis. Biopsy showing extensive infiltration of testicular interstitium by leukemic cells (Reprinted from Isaacs [6]; With kind permission of © Springer-Verlag, 2002)



3.3 Follicular Cysts of the Ovary

Although ovarian enlargement due to nonneoplastic *follicular cysts* is relatively common, true tumors of the ovary occur infrequently in the first year of life [4, 6, 8–10] (Fig. 3.1). During the third trimester, primordial follicles can develop further [4]. Some ova enlarge as they do in the postpubertal female, and as a result, the peripheral layer of cells proliferates into a thick layer of granulosa cells and the follicles develop central cavities of varying size. The ovarian cysts formed are either follicular or luteinizing cysts [6, 8–10]. The presence of small follicular cysts is a normal, common finding at postmortem examination. Rarely, follicles are so numerous that the ovary is conspicuously enlarged. Occasionally, single follicles may contain more than the usual amount of fluid, measure up to 20 cm or more in diameter, and produce an abdominal mass [4]. Etiology of perinatal follicular cysts is unclear [8, 9].

3.4 Juvenile Granulosa Cell Tumor

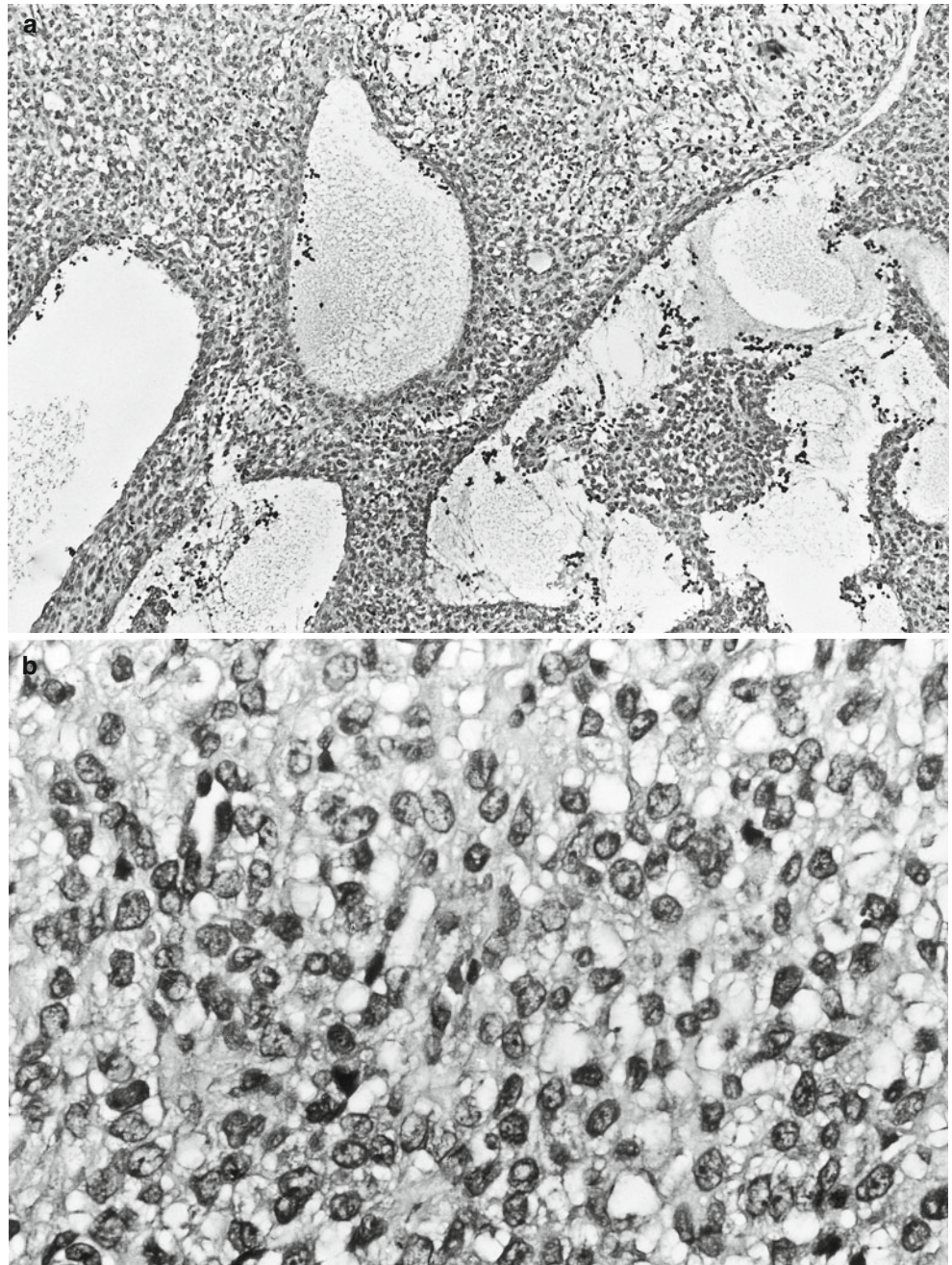
Sex cord-stromal tumors are composed of cells resembling those of *sex cord derivation* (*granulosa and Sertoli cells*) and of *stromal origin* (*theca cells, fibroblasts, and Leydig cells*) [10]. The *granulosa cell tumor* that occurs in the first three decades of life is designated “juvenile” (JGCT). It is the main sex cord tumor involving both the ovary and testis in the fetus and young infant [11–22]. Approximately 2–5 % of JGCTs are bilateral [18, 19]. In a series by Zaloudek and

Norris (1982), there were 32 girls less than 16 years of age all with unilateral JGCTs; 6 of 32 (19 %) were less than age 1 year and 2 (6 %) were congenital consisting of 1 stillborn and 1 neonate [16].

The presenting clinical findings in infants with JGCTs are an abdominal mass which may appear cystic on sonography, abdominal pain, and ascites [16, 17, 20]. Breast enlargement is the most common manifestation of isosexual precocity. Some patients with JGCTs, mostly bilateral, have congenital dysmorphic features such as micrognathia, facial asymmetry, and low-set ears; Potter sequence (oligohydramnios secondary to renal agenesis, dysplasia, or cystic disease) and leprechaunism are other associated conditions [3, 13, 18, 20].

Testicular and ovarian JGCTs have essentially the same gross and microscopic findings. Both have a variety of gross appearances, ranging from a thin-walled cyst to multiple cysts (“Swiss cheese” appearance) to a solid tumor, which may be uniformly yellow or show areas of necrosis and hemorrhage [11, 12, 14–17, 19–22] (Fig. 3.3). Microscopically, JGCT is composed of a diffuse or nodular growth of granulosa cells, forming follicles of varying size and shape containing mucicarmine-positive fluid. Cysts are lined by stratified granulosa cells having a clear or vacuolated cytoplasm. Nuclei are small and round resembling those of a developing follicle while others are variably hyperchromatic. Few have a grooved appearance. Marked nuclear atypia with 5–7 mitoses /10 high-power field are present [12, 13, 16]. Variable numbers of theca cells and fibroblasts are noted within the adjacent stroma.

Fig. 3.3 Juvenile granulosa cell tumor of the testis, 5-month-old male. Grossly, the tumor had a multicystic, “Swiss cheese”-like appearance. **(a)** Diffuse infiltrates of granulosa cells separated by large cystic follicles filled with pale staining material. **(b)** Higher magnification shows bubbly tumor cells with mild nuclear atypia and occasional nuclear infolding. Few mitotic figures are present (Reprinted from Isaacs [6]. © Springer-Verlag, 2002)



Tumor cells and normal granulosa cells are immunoreactive with cytokeratin and vimentin [10]. The spindle cells and theca externa cells react with vimentin, actin, and focally with desmin. In addition, granulosa cells show membrane expression of α -inhibin and CD99 (Ewing’s sarcoma antibody) which are helpful in establishing the diagnosis [22]. Immunostains for α -fetoprotein and HCG are characteristically negative.

Most JGCTs are confined to the ovary and testis and almost always are curable by surgical excision; salpingo-oophorectomy is the procedure of choice [17]. The goal of bilateral ovarian JGCTs treatment is designed to conserve as

much ovarian tissue which is compatible with an adequate resection [17]. Generally, infants with JGCT have a favorable prognosis [16]. However, there are instances of recurrences [17].

3.5 Sertoli-Leydig Cell Tumors

The *Sertoli-Leydig cell tumor* is much less common compared with JGCT and germ cell tumors. The neoplasm has a nonspecific-appearing cut surface containing both solid and cystic areas. It has a variety of histological patterns.

Some resemble the Leydig (interstitial) cells of the testis. The intermediate pattern is the most common one in neonates and infants consisting of immature Sertoli cells and Leydig cells, which resemble those of the developing testis [4, 10]. The tumor is composed of ill-defined groups of Sertoli cells with scanty cytoplasm separated by Leydig cells having an abundant eosinophilic cytoplasm. Those with the rarer retiform pattern are more common in older patients. Sertoli-Leydig cell tumors tend to be virilizing, but occasionally, they are estrogenic. Prognosis is correlated with the degree of differentiation and mitotic activity of the cells [17].

Thecomas are very rare in young children. *Fibromas* are somewhat more common, particularly when they occur in association with the basal cell nevus Gorlin syndrome where they typically are bilateral, multi-nodular, and calcified [4, 6]. Vascular tumors and sarcomas are not mentioned very often [4, 6].

References

- Dehner LP (1981) Neoplasms of the fetus and neonate. In: Naeye RL, Kissane JM, Kaufman N (eds), Perinatal diseases. International Academy of Pathology, monograph no. 22. Williams and Wilkins, Baltimore, pp 286–345
- Levy DA, Kay R, Elder JS (1994) Neonatal testis tumors: a review of the Prepubertal Testis Tumor Registry. *J Urol* 151:715–717
- Isaacs H Jr (1997) Tumors of the fetus and newborn. Series major problems in pathology, vol 35. W.B. Saunders, Philadelphia
- Isaacs H Jr (2007) Tumors. Of the female reproductive system. In: Gilbert-Barness E (ed) *Potter's pathology of the fetus, infant and child*, vol 2, 3rd edn. Mosby, St. Louis, pp 1405–1413
- Isaacs H Jr (2007) Tumors. Of the male reproductive system. In: Gilbert-Barness E (ed) *Potter's pathology of the fetus, infant and child*, vol 2, 3rd edn. Mosby, St. Louis, pp 1427–1431
- Isaacs H Jr (2002) Germ cell tumors. In: *Tumors of the fetus and infant: An Atlas*. Springer, New York, pp 5–36
- Isaacs H Jr (2003) Fetal and neonatal leukemia. *J Pediatr Hematol Oncol* 25:348–361
- DeSa DJ (1975) Follicular ovarian cysts in stillbirths and neonates. *Arch Dis Child* 50:45–50
- Bower R, Dehner LP, Ternberg JL (1974) Bilateral ovarian cysts in the newborn: a triad of neonatal abdominal masses, polyhydramnios, and maternal diabetes mellitus. *Am J Dis Child* 128:731–733
- Scully RE, Young RH, Clement PB (1998) Tumors of the ovary, maldeveloped gonads, fallopian tube, and broad ligament. In: *Atlas of tumor pathology*, 3rd series, fascicle 23. Armed Forces Institute of Pathology, Washington, D.C.
- Bryan DE, Cain MP, Casale AJ (2003) Juvenile granulosa-theca cell (sex cord-stromal) tumor of the infant testis. *J Urol* 169:1497–1498
- Lawrence WD, Young RH, Scully RE (1985) Juvenile granulosa cell tumor of the infantile testis. A report of 14 cases. *Am J Surg Pathol* 9:87–94
- Young RH, Lawrence WD, Scully RE (1985) Juvenile granulosa cell tumor – another neoplasm associated with abnormal chromosomes and ambiguous genitalia. A report of three cases. *Am J Surg Pathol* 9:87–94
- Harms D, Kock LR (1997) Testicular juvenile granulosa cell and Sertoli cell tumours: a clinicopathological study of 29 cases from the Kiel Paediatric Tumour Registry. *Virchows Arch* 430:301–309
- Schwentner C, Oswald J, Rogatsch H et al (2003) Stromal testis tumors in infants. A report of two cases. *Urology* 62:1121
- Zaloudek C, Norris HJ (1982) Granulosa tumors of the ovary in children: a clinical and pathologic study of 32 cases. *Am J Surg Pathol* 6:503–512
- Bouffet E, Basset T, Chetail N et al (1997) Juvenile granulosa cell tumor of the ovary in infants: a clinicopathologic study of three cases and review of the literature. *J Pediatr Surg* 32:762–765
- Pysher TJ, Hitch DC, Krous HF (1981) Bilateral juvenile granulosa cell tumors in a 4-month-old dysmorphic infant. A clinical, histologic, and ultrastructural study. *Am J Surg Pathol* 5:789–794
- Yikilmaz A, Lee EY (2007) MRI findings of bilateral juvenile granulosa cell tumor of the testis in a newborn presenting as intraabdominal masses. *Pediatr Radiol* 37:1031–1034
- Brisigotti M, Fabbretti G, Pesce F et al (1993) Congenital bilateral juvenile granulosa cell tumor of the ovary in leprechaunism: a case report. *Pediatr Pathol* 13(5):549–558
- Peterson C, Skoog S (2008) Prenatal diagnosis of juvenile granulosa cell tumor of the testis. *J Pediatr Urol* 4:472–474
- Kommoss F, Oliva E, Bhan AK et al (1998) Inhibin expression in ovarian tumors and tumor-like lesions: an immunohistochemical study. *Mod Pathol* 11:656–664

4.1 Introduction

Soft tissue tumors are relatively common in the first year of life and are the source of a wide variety of neoplasms and tumorlike conditions often presenting as a palpable mass [1–17] (Tables 4.1 and 4.2). Excluding hemangiomas and lymphangiomas, they are the leading group of tumors in infants overall and are second in frequency to teratoma in the newborn [1]. Neoplasms of fibrous connective tissue (myofibroblastic) origin are the most prevalent [6–9, 12–15]. Approximately one third of all neonatal and infant soft tissue tumors are classified histologically as malignant. The major malignancies are fibrosarcoma, rhabdomyosarcoma, primitive neuroectodermal tumor (PNET), and rhabdoid tumor [3, 6, 8, 13, 15, 17] (Tables 4.1 and 4.2).

In the normal developing fetus and newborn, cells appear immature making the distinction between some benign and malignant tumors difficult or sometimes impossible, particularly in the interpretation of soft tissue tumors, for which the diagnosis of sarcoma must be made with caution [8, 12, 13, 15] (Fig. 4.1). Congenital mesenchymal tumors are seldom malignant in spite of their large size or microscopic resemblance to soft tissue sarcomas in adults. Although a soft tissue lesion, such as hemangioma or fibromatosis, is called benign microscopically, it may cause death as the result of involvement of a vital structure, for example, in the neck or thorax. In spite of this, most soft tissue neoplasms diagnosed in the first year of life, including some of the sarcomas, deserve a conservative therapeutic approach and generally have a favorable outcome [6, 8, 12, 13, 15].

Table 4.1 Fetal and infant soft tissue tumors and tumorlike conditions

Vascular
Infantile hemangioma
Capillary Hemangioma
Cavernous hemangioma
Kaposiform hemangioendothelioma
Tufted angioma
Lymphangioma
Vascular malformation
Fibroblastic
Fibromatosis
Infantile fibrosarcoma
Digital fibroma
Gardner fibroma
Fibrous hamartoma of infancy
Lipofibroma
Torticollis ^a
Myofibroblastic
Myofibromatosis
Inflammatory myofibroblastic tumor
Nodular fasciitis
Cranial fasciitis
? Congenital granular cell tumor
Fibrohistiocytic
Fibrous histiocytoma
Juvenile xanthogranuloma
Angiomatoid fibrous histiocytoma
Giant cell fibroblastoma
Myogenic
Cardiac rhabdomyoma
Fetal rhabdomyoma
Rhabdomyosarcoma
Embryonal
Botryoid
Spindle cell
Alveolar
Ectomesenchymoma

(continued)

Table 4.1 (continued)

Neural
Neurofibroma
Plexiform
Diffuse
Schwannoma
Malignant peripheral nerve sheath tumor
Melanotic neuroectodermal tumor
Ewing sarcoma/primitive neuroectodermal tumor
Adipose
Lipoma
Lipoblastoma
Lipoblastomatosis
Other
Rhabdoid tumor
Synovial sarcoma
Polyphenotypic small cell tumor

Reprinted from Isaacs [15]. © Springer-Verlag, 2002; Reprinted from Coffin [9]. With kind permission of © Elsevier, 2007

^aBelieved to be a reaction to injury

Table 4.2 Soft tissue tumors and tumorlike conditions of the fetus and infant: distinguishing features

Tumor	Gross findings	Histological findings
Capillary hemangioma	Tan-red nodule resembling lymph node; skin most common site	Lobules of proliferating capillaries; Glut1+
Cavernous hemangioma	Prominent, blood-filled vascular channels; thrombi common	Dilated vascular channels lined by regular endothelial cells and filled with blood
Lymphangioma	Hygroma: large single cyst filled with lymph; dilated lymphatic channels filled with lymph	Single large cyst or many cystically dilated lymphatics lined focally by flat endothelial cells and containing pale, pink-staining lymph
Angiomatoid fibrous histiocytoma	Red-brown mass; some resemble a lymph node with a hemorrhagic center	Vascular channels lined by atypical histiocytes and fibroblasts; few mitoses; peripheral lymphoid nodules; Des+; actin+; desmin; CD68+; CD 99+
Fibromatosis	Firm, light tan-gray to white, whorled, bulging cut surface; no necrosis or hemorrhage.	Regular, spindle-shaped fibroblastic cells with herringbone and storiform growth patterns; no nuclear atypia; few or no mitoses. Vim +, DES –
Digital fibromatosis	Firm, light tan-gray nodule (s) on fingers or toes	Regular, spindle-shaped fibroblastic cells with herringbone and storiform growth patterns; no nuclear atypia; ± red paranuclear intermediate filament inclusions
Torticollis	Firm, fibrous lump in sternocleidomastoid muscle; ± wry neck	Time dependent: early lesion resembles fibromatosis; late: fibrosis with muscle fiber loss and atrophy
Myofibromatosis	Rubbery, tan nodule with central congestion, necrosis; single or multiple	Regular spindle cells resembling smooth muscle cells and fibroblasts; central blood vessels, necrosis, hemorrhage, and calcification; Vim +; smooth muscle actin +
Fibrous hamartoma of infancy	Round to oval bulging mass with firm, gray-white tissue and fat	Myxoid areas with small spindle cells; fibrous areas with tendon-like fibrous trabeculae; fat; Vim+, Des +
Juvenile xanthogranuloma	Firm tan-gray to tan-yellow nodules	Less well-differentiated histiocytes with eosinophilic or foamy cytoplasm and vesicular nuclei; fibroblasts; eosinophils prominent; multinucleated Touton giant cells ±; Vim +; actin ±; CD68 +; CD1a +; Factor VIIIa +; EM: immature fibroblasts and histiocytes
Botryoid embryonal rhabdomyosarcoma	Grapelike masses protruding from a mucosal lined site of origin	Polypoid projections covered by mucosa of site of origin; submucosal mantle layer with rind of tiny rhabdomyoblasts; pale myxoid stroma; Vim +; Des +; actin; myogenin +; EM: myofilaments
Embryonal rhabdomyosarcoma	Soft, pale-tan-gray, gelatinous, friable tissue	Spindle- and tadpole-shaped cells, eosinophilic giant cells; foci of necrosis and hemorrhage; cytoplasmic cross striations; dark cellular areas alternating with pale myxoid areas; muscle markers ± (see above); EM: myofilaments; 11p del

Table 4.2 (continued)

Tumor	Gross findings	Histological findings
Alveolar rhabdomyosarcoma	Soft, pale-tan-gray, gelatinous; foci of necrosis and hemorrhage	Small blue cell malignant tumor with alveolar pattern; muscle markers ± (see above); EM: myofilaments; [t(2;13) (q35;q14)]
Spindle-cell rhabdomyosarcoma	Soft, pale-tan-gray, gelatinous; necrosis and hemorrhage ±	Uniform spindle-shaped rhabdomyoblasts; interdigitating growth pattern; muscle markers +; EM; myofilaments
Lipoma	Soft, light-yellow circumscribed lobules of fat; single or multiple sites	Lobules of mature fat cells surrounded by delicate fibrous septa
Lipoblastoma	Light-gray to yellow lobules of fat firmer than lipoma; single or multiple sites	Lobules of immature fat cells; vacuolated lipoblasts in gray myxoid areas; S-100 +; EM: developing white fat cells (lipoblasts)
Diffuse neurofibroma	Firm pale, homogeneous, light-gray-white tissue	Small round to oval Schwann cells, wavy neurites, pale, gray, myxoid stroma; S-100 +; Leu-7+; myelin basic protein +
Plexiform neurofibroma	Shiny, pale, gray-white wormlike nodules	Tortuous, pale myxoid, enlarged nerve fibers with proliferation of nerve fibers and Schwann cells; S-100 +; myelin basic protein +
Primitive neuroectodermal tumor (PNET); Ewing's sarcoma	Soft, friable, pale-tan-gray tissue fragments; foci of necrosis and hemorrhage	Small blue cell tumor with indistinct cytoplasm, round or oval nuclei, fine or clumped chromatin, small nucleoli; many mitoses; rosettes +; vim+, HBA7 +, S-100 +, NSE +; CD 99 +; synaptophysin + EM: small primitive cells ± neurosecretory granules and neurofilaments; t(11;22) (q24; q11-12)
Melanotic neuroectodermal tumor	Tumor in craniofacial bones or soft tissues; tan, firm with black streaks or irregular pigmented areas	Irregular cystic spaces with small, round, dark neuroblasts and larger pigmented melanocytes; NSE +; synaptophysin +, HMB45 +. Dopamine-β-hydroxylase+; neuroblasts with neurosecretory granules and melanocytes with melanosomes
Ectomesenchymoma (gangliorhabdomyosarcoma)	Light tan-gray to white, bulging cut surface; gelatinous areas	Embryonal rhabdomyosarcoma cells; ganglioneuroma and/or neuroblastoma cells; Schwann cells; rhabdomyosarcoma cells: muscle markers +; Schwann cells S-100 +; ganglion cells and neuroblasts NSE +; EM: rhabdomyosarcoma: myofilaments +; neuroblastoma: neurofilaments and neurosecretory granules +
Granular cell tumor (gingival and soft tissues)	Mucosal covered tan nodules; soft tissue ill-defined tan-gray infiltrates	Polygonal cells with PAS ± granules; regular, round purple nuclei; prominent cell membranes; Vim +; S-100 -; muscle markers -; EM: membrane-bound, pleomorphic cytoplasmic granules, cell membranes
Rhabdoid tumor	Gray-white, soft; foci of necrosis and hemorrhage	Variable histology: cellular tumor with round to oval cells with pink cytoplasm, large vesicular nucleus, single nucleolus and paranuclear eosinophilic inclusions ("rhabdoid cells"); appearance of small blue cell tumor +; EM: inclusions composed of intermediate filaments; Vim +; EMA +; cytoker +; actin; NSE +; S-100 +; variable immunoreactions. 22q11 del; INI1 gene mutations
Proliferative myositis and fasciitis; inflammatory myofibroblastic tumor	Soft to firm gray-white nodule	Fibroblasts, histiocytes, giant cells resembling ganglion cells, pale myxoid stroma, many mitoses; Vim +; actin +; Des +; CD 68+; EM: cells with fibroblastic, myofibroblastic, and histiocytic differentiation; inflammatory cells

Reprinted from Isaacs [15]. © Springer-Verlag, 2002; Reprinted from Coffin [9]. Infantile soft tissue tumors. With kind permission of © Elsevier, 2007; Reprinted from Weiss and Goldblum [16]. With kind permission of © CV Mosby, 2001

Abbreviations: EM electron microscopy, Cytoker cytokeratin, Des desmin, Vim vimentin, NSE neuron -specific enolase, PAS periodic acid Schiff reagent; Glut1 Glucose transporter protein

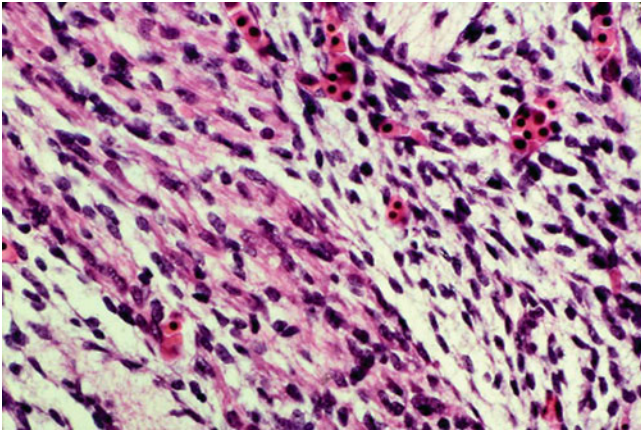


Fig. 4.1 Developing limb bud from a fetus of 3 months gestation (Reprinted from Isaacs [12] © W.B. Saunders, 1997)

4.2 Vascular Conditions

Vascular lesions comprise over two thirds of all cases of soft tissue tumors and tumorlike conditions in infants and children [13, 15, 18, 19]. Of these, *hemangioma* and *lymphangioma* make up the majority during the first year of life. The vascular malignancies Kaposi sarcoma and angiosarcoma are uncommon in this age group [12, 15, 18, 19].

4.2.1 Hemangioma

Infantile hemangiomas are single or multiple and extremely variable in extent [13, 15, 18–21]. After birth, they may remain the original size, grow with the body, or grow more rapidly. Many of those in the skin are not noticed until the child is a few weeks old and are typically located on the head and neck (60 %), trunk (25 %), or extremities (15 %) [22]. Many regress after a limited period of growth and most disappear by the end of the second year. Although at times they are very cellular, for example, the solid, cellular capillary hemangioma (hemangioendothelioma, infantile hemangioma), and show little formation of recognizable vascular structures, those present at birth generally have a favorable prognosis [19]. The skin is the most common site of hemangiomas, although they may be found in mucous membranes, deep connective tissue, or internal organs such as the liver, heart, and brain [15, 16]. Cutaneous hemangiomas are occasionally associated with extensive similar lesions in the brain, liver, and other organs, and the term “diffuse hemangiomatosis” is applied to this often fatal condition [13, 15, 18, 21].

Hemangiomas in the region of the distribution of the trigeminal nerve may be associated with vascular anomalies of the choroid of the eye, meninges covering of the brain, and

the brain itself in the area directly beneath the involved skin. Known as the Sturge-Weber syndrome, this condition is associated with other findings as congenital glaucoma and buphthalmos, local thickening of the skull, atrophy of the body on the side opposite the cutaneous hemangioma, paralysis, aphasia, epilepsy, and mental retardation [13] (see Chaps. 5 and 9). The hemangiomas associated with Von Hippel-Lindau disease (cerebellar-retinal hemangiomatosis) may be present in early life, but symptoms are rarely recognizable until the second decade [13].

4.2.2 Capillary Hemangioma

The *capillary hemangioma* consists of anastomosing capillaries with lumens lined by a single layer of endothelial cells. A thin sheet of such anastomosing vessels lying in the dermis produces a pink to purple, noncompressible area on the skin surface and forms no tumor mass [13] (Fig. 4.2). Such is the nevus flammeus (Fig. 5.1) or port wine stain (nevus venosus) often seen on the face or nape of the neck. When such a proliferation involves a solid organ, the shape of the organ is not changed although it may be enlarged. Capillary hemangiomas consist of lobules and masses of immature endothelial cells, some lining patent blood-containing spaces and some forming solid sheets (Fig. 4.2), with little variation among the cells although mitoses may be found. The cells and constituent vessels are distributed closely among normal muscle, subcutaneous tissue, or parenchymal elements of the part involved. Most of the endothelial cells are intimately associated with reticulum fibers although little or no connective tissue is present in most cellular portions of the tumor [13, 15]. The term *hemangioendothelioma* is used to describe the cellular, solid form of capillary hemangioma; currently, both are included under the general category of “infantile hemangioma” [15].

During the proliferative and early involuting phases, the capillary hemangioma becomes more lobular with large feeding and draining vessels located within fibrous septa adjacent to the lobules [12, 15, 20]. Glucose transporter protein (GLUT1) is expressed during this stage [9]. The hemangioma variants, for example, the *rapidly involuting hemangioma* and *non-involuting congenital hemangioma*, are nonreactive with antibodies to GLUT1 [9]. The involuting phase, defined clinically as ages 1–7 years, is manifested histologically by decreasing cellular proliferation and a progressive increase in perivascular and interlobular fibrous tissue [15]. Apoptosis is characteristic of the involuting phase, which begins before age 1 year, reaching its peak at 2 years and gradually diminishing from then on [9, 19, 20, 22]. With continued involution, the endothelial cells flatten, the vascular channels become more dilated, and fibrofatty tissue increases in amount both within and between the lobules. At

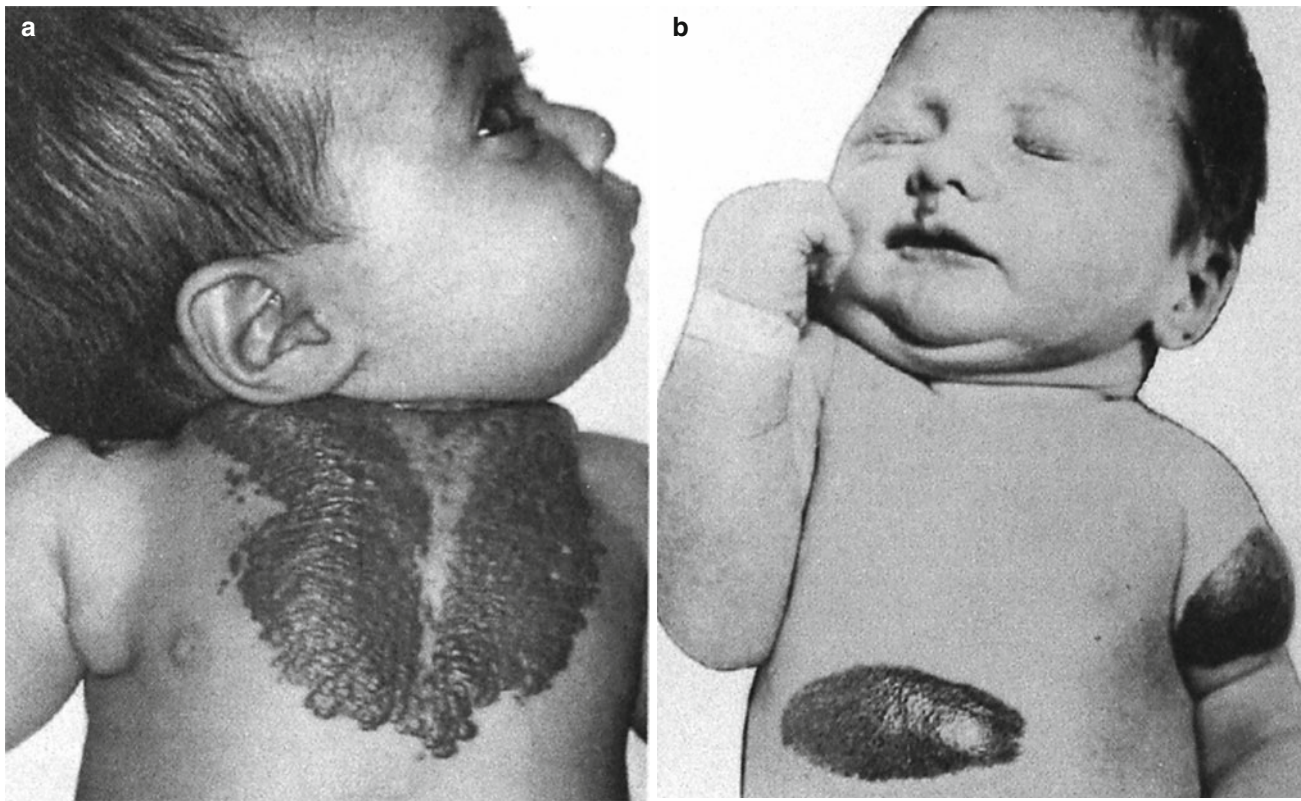


Fig. 4.2 Infantile hemangioma. (a) Raised hemangioma with multiple small excrescences involving the anterior chest wall. (b) Multiple hemangiomas having smooth, cushion-like surfaces (Reprinted from Isaacs [13]. With kind permission of © Mosby, 1997)

the end of the involuting phase, histological findings consist only of a few tiny vessels that are lined by flattened endothelial cells surrounded by fibrofatty tissue (Fig. 4.3).

Clinical complications that arise from hemangiomas result from the size, location, and physiology [14, 15]. They may impair vision by encroaching upon the eye; produce respiratory distress by tracheal compression; cause high-output congestive cardiac failure associated with nonimmune fetal hydrops and polyhydramnios; produce central nervous system or gastrointestinal hemorrhage; or are responsible for a consumptive coagulopathy from platelet and fibrinogen trapping as in the Kasabach-Merritt syndrome [19, 20, 22].

In *diffuse neonatal (infantile) hemangiomatosis*, multiple hemangiomas of the skin and viscera involve at least three organ systems to fulfill this definition [13, 15, 21]. Bloody amniotic fluid and hydrops may be the initial manifestations of in utero diffuse hemangiomatosis. Even though the hemangiomas are benign histologically, most infants and newborns with this condition die during the first few months of life. Death occurs as the result of high-output cardiac failure secondary to arteriovenous shunting through the hemangioma, massive hemorrhage from fragile vessels, thrombocytopenia, or involvement of the central nervous system [9, 13]. The organs most often affected by the hemangiomas, excluding the skin (100%), are the liver

(64%), brain (52%), gastrointestinal tract (52%), lungs (52%), oral cavity (44%), and eyes (32%) [12, 13]. The hemangiomas vary in size from 0.2 to 2 cm and range in number from 50 to 500. The female to male ratio is 2:1. So far no genetic factor has been implicated [13].

Cellular hemangiomas of infancy (infantile hemangioendotheliomas, infantile hemangiomas) are benign tumors whose cellularity may lead to confusion with soft tissue sarcoma. Pericytes and endothelial cells predominate as well as fibroblasts and mast cells. An interstitial cell that expresses factor XIIIa and a macrophage marker is present [9]. The natural evolution of the tumors is to grow, to become stable, and finally to involute.

4.2.3 Cavernous Hemangioma

Cavernous hemangiomas, which are part of the “infantile hemangioma” group, have larger vascular spaces than the capillary hemangiomas and are compressible because of the large amounts of blood they contain [9, 14, 15]. Those involving the skin are raised above the general skin level and often have a warty, red granular surface (Fig. 4.4). Raised cutaneous vascular nevi such as the strawberry nevi contain mixtures of cavernous and capillary

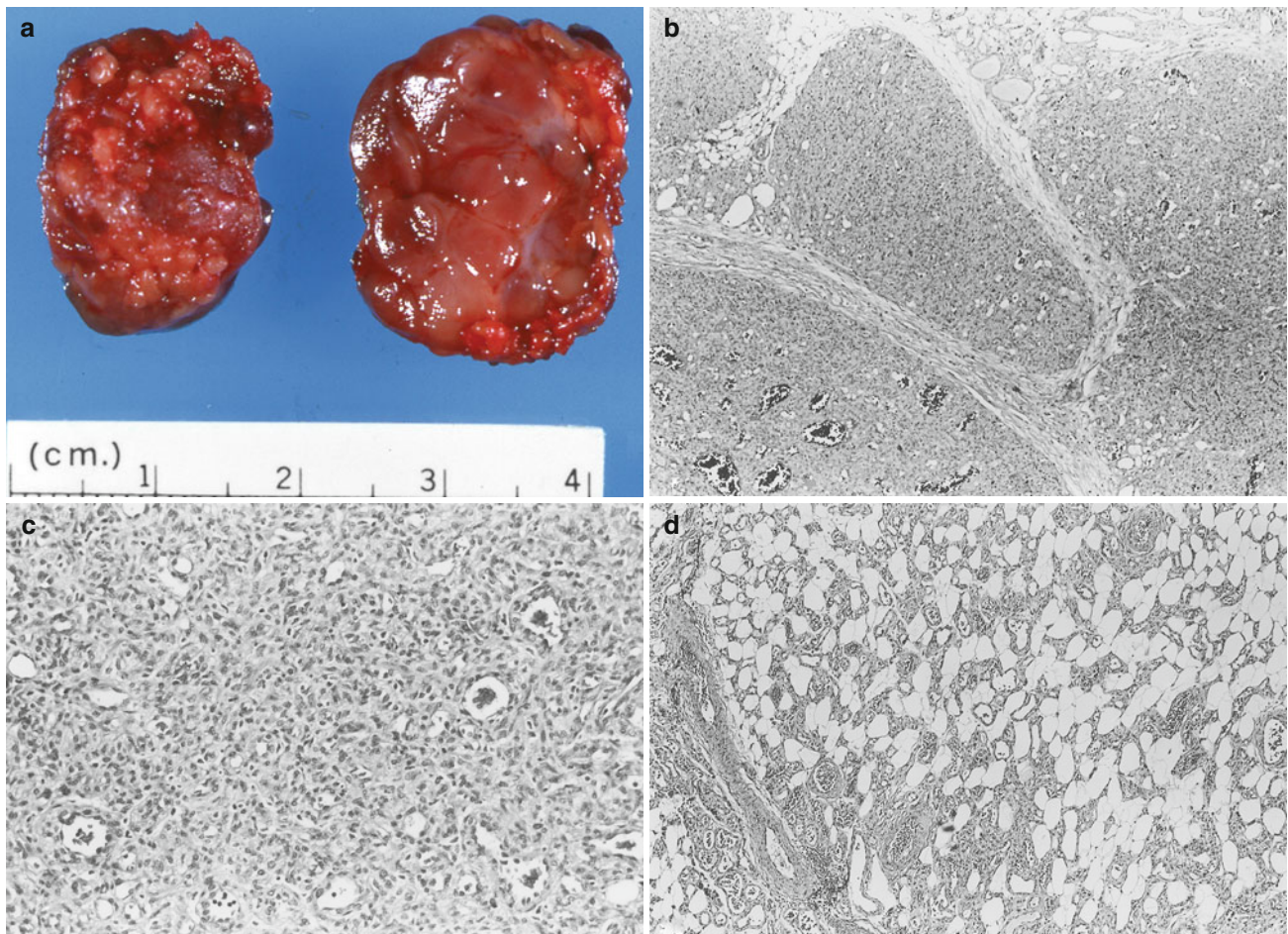


Fig. 4.3 Capillary hemangioma. (a) 2.5 × 1.5 cm mass removed from the neck of a 3-month-old male. The lesion was brownish-red and nodular resembling a mat of lymph nodes. (b) Low-power view displaying the lobular architecture corresponding to the gross appearance. (c) The “open and closed hemangioma pattern” consisting of dense clusters of endothelial cells with a few capillary lumens. (d) An involuting capillary

hemangioma taken from a 6-month-old female, showing abundant fat in the lobule separating residual nests of capillaries. Enlarged “feeding” vessels situated along the left side of the picture are noted at the periphery of the lobules (Reprinted from Isaacs [13]. With kind permission of © Mosby, 1997)

components (Fig. 5.3). The vascular channels vary greatly in size and extent and occasionally may involve large parts of the body

In infants, the liver is the internal organ most often the site of a cavernous hemangioma [15] (see Chap. 12). The extent of involvement may vary from a few millimeters to several centimeters. If superficial, trauma may cause rupture of some of the outermost channels within the liver. Fatal intra-abdominal hemorrhage from a hepatic cavernous hemangioma may result during delivery. If it is situated deep in the liver, the tumor may never be discovered except as an incidental finding at imaging or at necropsy.

Microscopically, the cavernous hemangioma consists of anastomosing thin-walled vascular channels lined by endothelial cells larger than those found in the capillary hemangioma (Fig. 4.5). Vascular thrombi with calcifications are not uncommon in these lesions. Often they are components of large vascular malformations [15].

4.2.4 Infantile Kaposiform Hemangioendothelioma

Most are present at birth or develop shortly thereafter typically as a red or purple cutaneous patch that rapidly enlarges eventually becoming an indurated deep soft tissue mass [9, 20, 22, 23]. *Kaposiform hemangioendothelioma* is a distinctive form of hemangioma often associated with the Kasabach-Merritt syndrome [9]. Some but not all investigators feel strongly that the Kasabach-Merritt phenomenon does not occur with the common hemangioma and that the previously reported cases of lesions associated with this phenomenon probably represented kaposiform hemangioendotheliomas rather than capillary or cavernous hemangiomas [19, 23].

Kaposiform hemangioendothelioma differs from the common infantile hemangioma in that the sexes are affected about equally, and the former occurs more often on the trunk, in the retroperitoneum, and the proximal portion of the

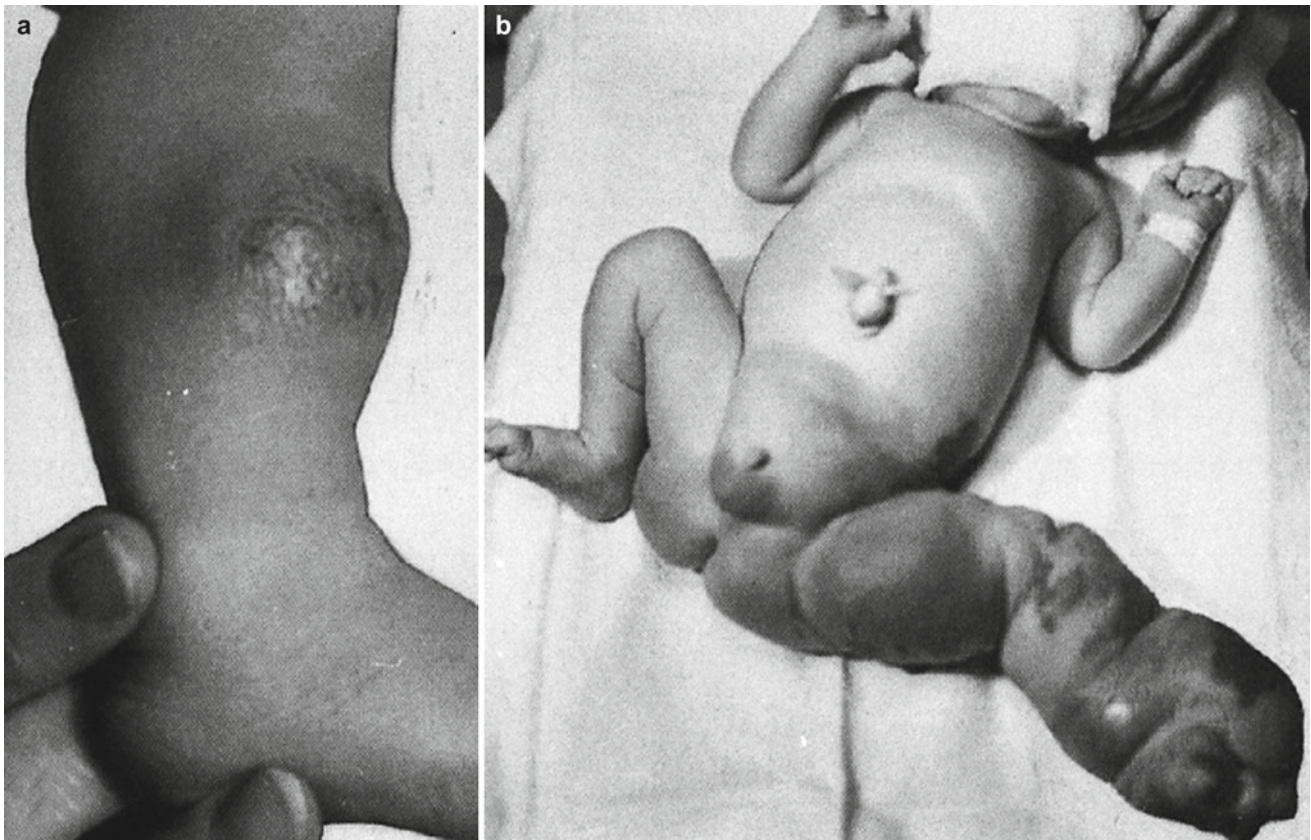


Fig. 4.4 Deep-seated cavernous hemangioma. (a) Localized lesion on the right leg. (b) Generalized hemangioma involving the left leg, buttocks, and lower abdomen composed of greatly dilated vascular spaces

extremities and less frequently in the cervicofacial region. The most common locations are the retroperitoneum and upper extremities [9, 18]. Their large size and infiltrative nature result in complications of hemorrhage, obstruction, or respiratory compromise making complete surgical excision sometimes difficult [23, 24].

Two histological patterns, angiomatous and kaposiform, are described [9]. The former consists of rounded or dilated vascular spaces lined by flattened endothelial cells and the latter infiltrating fascicles, sheets, or nodules of spindled cells lining compressed (slit-like) or crescentic vascular channels surrounded by fibrosis. Mitoses are noted infrequently. Microthrombi and hemosiderin deposits are variably present. It is the kaposiform pattern that differentiates this lesion from the common cellular hemangioma. Endothelial markers are present in the angiomatous areas but are variably expressed in the spindled cells [9].

4.2.5 Tufted Angioma

Tufted angioma is a benign vascular lesion regarded as another form of hemangioma which occurs in the newborn and early

and responsible for local gigantism. The findings are consistent with the Klippel-Trenaunay-Weber syndrome. Death occurred at 10 days (Reprinted from Isaacs [13]. With kind permission of © Mosby, 1997)

childhood [9, 15]. The angioma is characterized by slow growth and the tendency to cover large areas of the trunk and neck. Other sites of involvement are the head and extremities. Patients with tufted angiomas may present with Kasabach-Merritt syndrome [9, 22–24]. Histologically, the tumor consists of small lobules or vascular tufts scattered in a multiple “cannon ball-like” distribution in the dermis and subcutis (see Chap. 5). The endothelial cells are reactive for Ulex lectin I and factor VIII, and the spindle cells between the vascular spaces are reactive with actin; GLUT 1 is not expressed [9]. Endothelial cells and pericytes are noted by EM.

Composite hemangioendothelioma, *endovascular papillary angioendothelioma*, and *giant cell angioblastoma* are further examples of intermediate vascular tumors having a tendency to recur locally or occasionally metastasize [9]. They are seldom found in infants.

4.2.6 Malignant Vascular Tumors

Malignant forms of endothelial vascular tumors, while uncommon in infancy, occur in the liver and soft tissues. The tumor cells have large, variable nuclei, less cytoplasm than

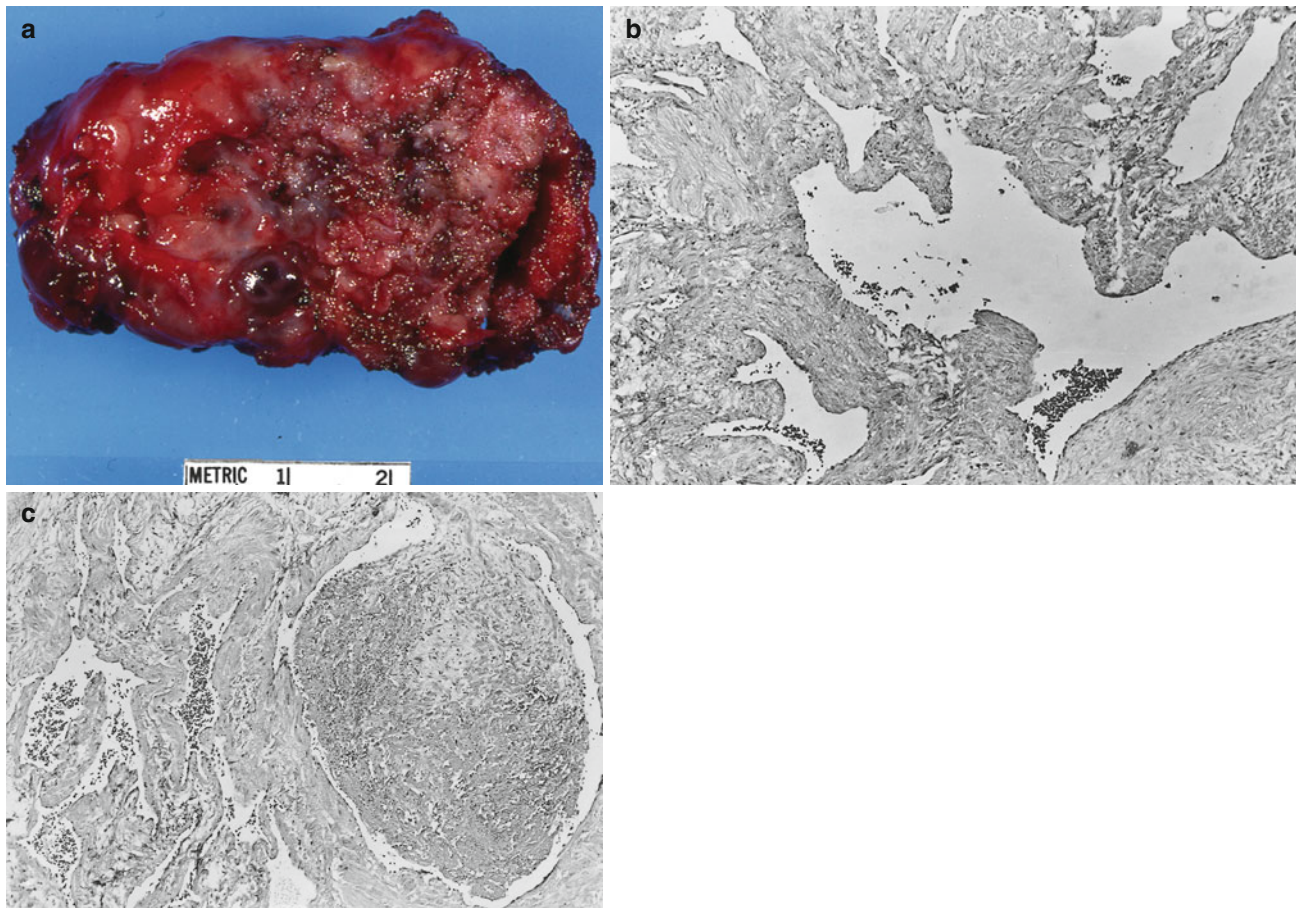


Fig. 4.5 (a) Cavernous hemangioma. 6×4 cm red-brown, nodular mass consisting of many dilated blood vessels was removed from the forearm of a male infant. (b) Large irregular vascular channels are lined

by endothelium containing collections of erythrocytes. (c) Organizing thrombi are not uncommon in cavernous hemangiomas (Reprinted from Isaacs [12]. © W.B. Saunders, 1997)

infantile hemangiomas, and show increased mitotic activity [9, 18]. *Kaposi sarcoma* (malignant hemangioendothelioma) is a variable malignant tumor involving the skin and liver characterized by proliferation of both capillary and connective tissue. With onset of the AIDS era, the number of pediatric cases appears to be increasing [14].

4.2.7 Lymphangioma

Lymphangioma is a benign, nonneoplastic, vascular malformation composed of cystically dilated lymphatics. Many cystic lymphangiomas (hygromas) and diffuse or cavernous lymphangiomas are present at birth [13, 15, 25, 26] (Figs. 4.6, 4.7, 4.8, 4.9, and 4.10). They are second to hemangioma as a cause of a soft tissue mass in the newborn and infant [11, 14, 15]. The incidence of cystic hygroma is estimated at 1 in 6,000 pregnancies [15, 26].

Lymphangiomas range in size from small, barely visible subepidermal skin or mucosal blebs (*lymphangioma circumscriptum*) to massively dilated cystic masses (*hygromas*).

They occur in almost any location, including the viscera and bones. The soft tissues of the neck, axilla, thorax, and the lower extremities are the major sites [13, 15] (Figs. 4.6, 4.7, 4.8, 4.9, and 4.10).

The use of the terms “cystic” and “cavernous” lymphangioma varies, with little reason to distinguish between the two conditions since they both result from a congenital defect where failure of communication and obstruction of lymphatics occurs. However, the term cystic lymphangioma, or hygroma, has been applied especially to large single or slightly multilocular [13, 15] (Figs. 4.6, 4.7, and 4.8). Occasionally, they are multiple and may be found in other locations. Typically, cystic hygromas develop late in the first trimester to early in the second one, becoming less common as pregnancy progresses. Fluid accumulation in dilated lymphatics and surrounding connective tissue leads to progressive lymphedema and in some instances fetal hydrops from congestive heart failure [13, 15].

The prognosis of a fetus with cervical cystic hygroma is poor when detected early prenatally, especially before 30 weeks gestation; whereas when the hygroma is diagnosed

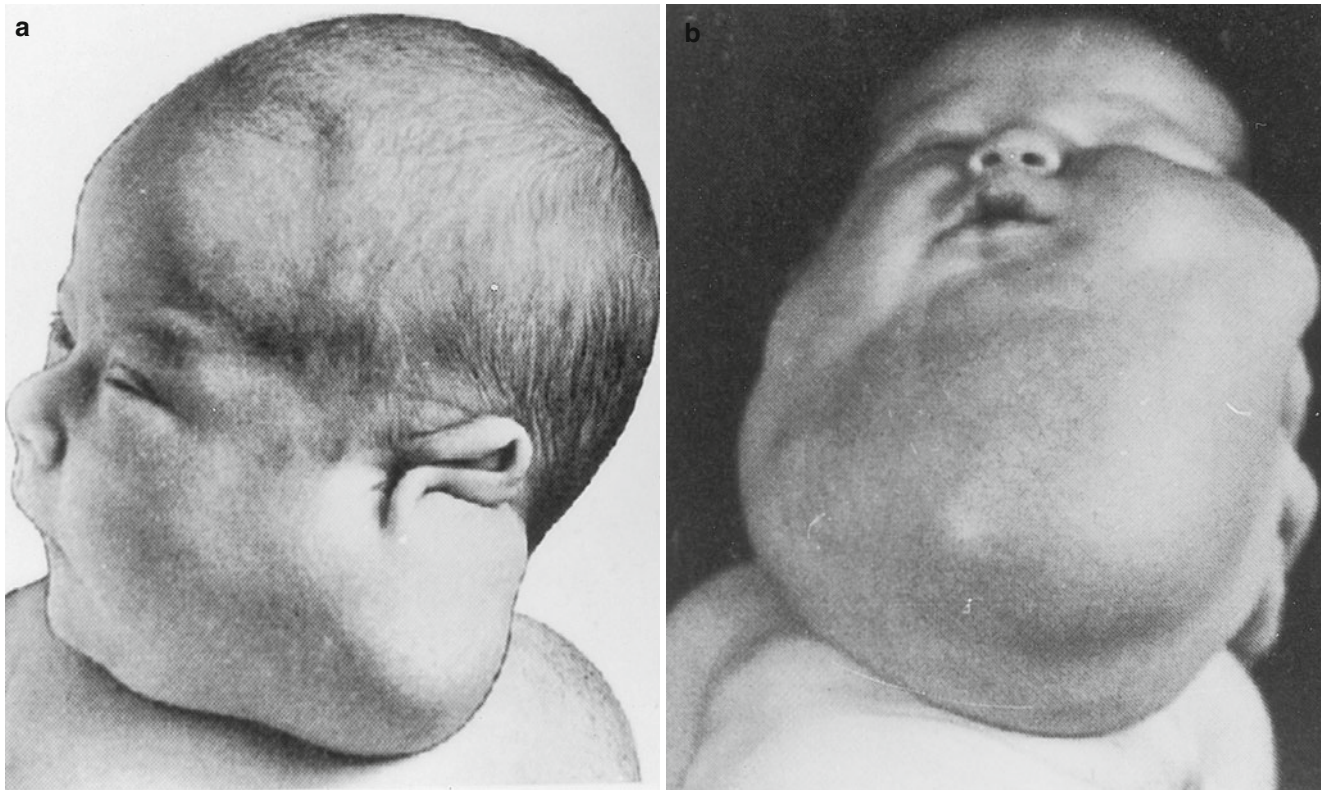


Fig. 4.6 Cystic lymphangiomas (hygroma). (a) Unilocular tumor of the left side of the neck in an infant aged 4 days. (b) Multilocular tumor involving both sides and anterior part of the neck in an infant aged 4 weeks (Reprinted from Isaacs [13]. With kind permission of © Mosby, 1997)

after birth, the outcome is generally more favorable [13, 24, 25]. Bilateral hygromas of the neck with widespread lymphangiectasis are not uncommon in aborted fetuses [13–15] (Fig. 4.9). Lymphangiomas discovered in utero by sonography are associated with a variety of syndromes and birth defects [13, 15]. Turner syndrome is the major one which is noted in approximately 50–70 % of cases [13]. Turner syndrome occurs in 1 of 5,000 to 10,000 births and usually is the result a 45,X karyotype arising from chromosomal nondisjunction. Fetuses with cystic hygroma and Turner syndrome may have coexistent anomalies of cardiac development as aortic valve defects, aortic arch hypoplasia, anomalous origin of the aortic arch vessels, and septal defects [13]. In utero fetal demise occurs frequently in 45,X fetuses [13]. Over 95 % of non-mosaic 45,X fetuses are spontaneously aborted. Other abnormalities associated with cystic hygroma are fetal hydrops, oligohydramnios, single-vessel umbilical cord, Noonan syndrome, fetal alcohol syndrome, diaphragmatic hernia (with Fryns syndrome), and trisomies 13,18, and 21; the lesion is described also in normal individuals [13, 15].

Microscopically, lymphangiomas are thin-walled, filled with clear straw-colored fluid, lined by a single layer of flat endothelial cells and surrounded by varying amounts of connective tissue and smooth muscle (Figs. 4.8, 4.10, and 4.11). They are not compressible and are not visibly connected to

large lymphatic channels. Often the endothelial lining is missing. The endothelial-lined dilated lymphatic channels react positively with factor VIII, CD31, CD34, smooth muscle actin, and particularly CD34, which shows the most uniform pattern of endothelial reactivity [9]. Lymphangiomas do not show the proliferative and involutonal growth phases of hemangiomas despite their propensity for recurrence [9, 13]. They may become larger after birth because of increased secretion of fluid and expansion. The hygromas with Turner syndrome are composed of single cavities whereas isolated cystic hygromas tend to be multiloculated [13]. At birth, larger lymphangiomas appear to have destroyed or prevented the development of muscles and other structures in the involved areas. Evacuation of the fluid gives only temporary relief, and unless the wall is completely excised, the fluid will reappear. Lymphangiomas are almost never encapsulated, and thus, surgical removal may be difficult or even impossible [9, 15].

4.2.8 Vascular Malformations

Vascular malformations are developmental errors consisting of dysplastic vessels lined by inactive appearing endothelium. By definition, they are present at birth, but

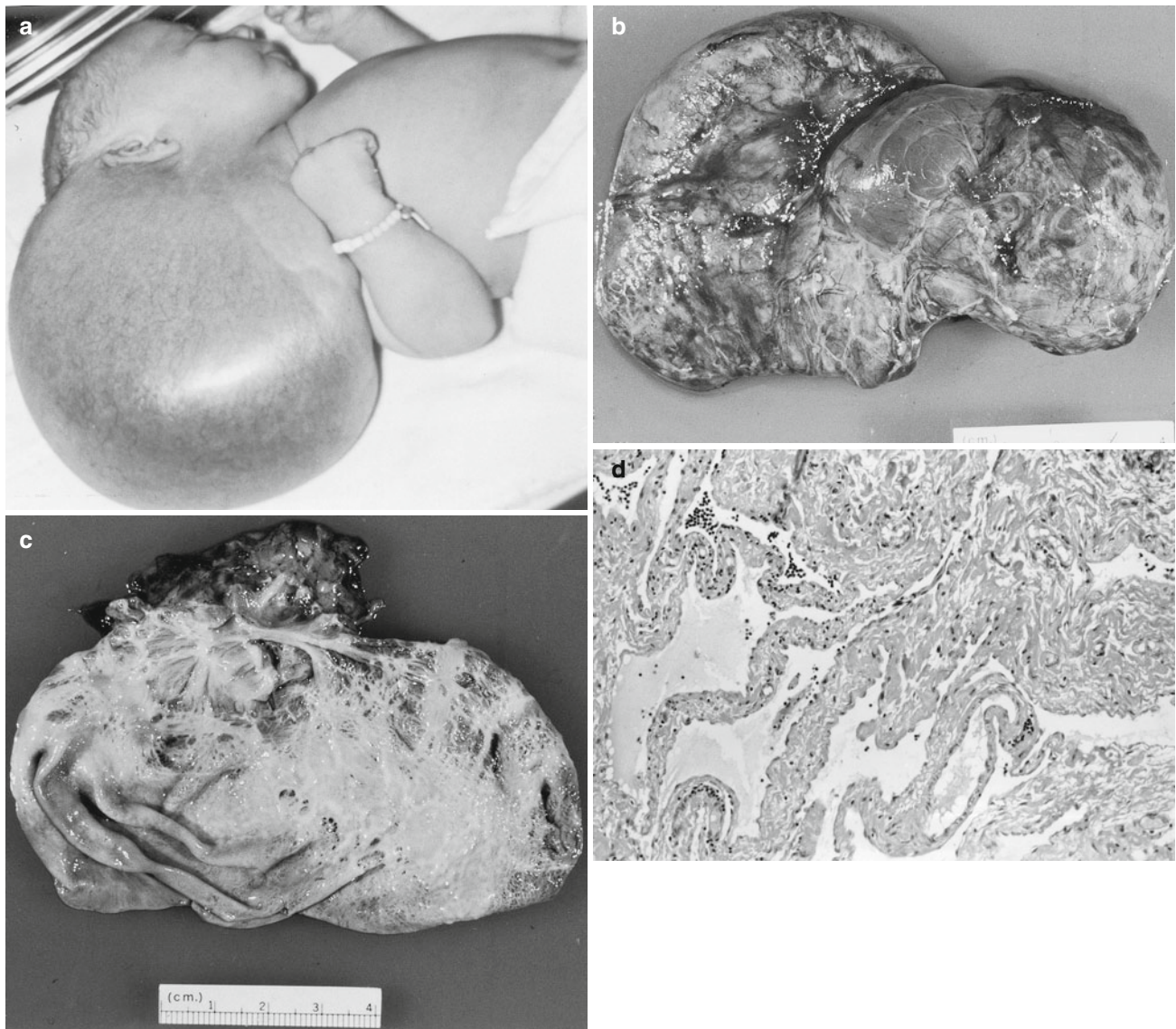


Fig. 4.7 Cystic lymphangioma (hygroma) of the neck. (a) Newborn with a large, unilocular, fluid-filled, cystic mass arising from the back of the neck and shoulder. (b) Unopened specimen taken from another infant with a similar but smaller hygroma, measuring 10×7 cm. (c) The opened specimen shows one large cyst and a smaller solid microcystic component situated at the *top* of the photograph. The cyst was filled

with clear lymph fluid. (d) Several large vascular channels are lined by single rows of endothelial cells and filled with pale proteinaceous material. Lymphangiomas in Figs. 4.6, 4.7, 4.8, 4.9, 4.10, 4.11, 4.12, and 4.13 show similar histological findings (Reprinted from Isaacs [12]. © W.B. Saunders, 1997)

they may become clinically evident any time during life (Fig. 4.6). Vascular malformations are composed of large endothelial-lined channels with varying amounts of smooth muscle within their walls. They may involve a large body area as an extremity producing gigantism of that part. Venous angiomas are regarded as a form of vascular malformation. Generally, arterial malformations, including arteriovenous anomalies, are diagnosed in late infancy or later in childhood [7, 13, 15, 23].

Usually, vascular malformations practically never regress but often undergo progressive expansion resulting in clinical problems. In contrast to hemangiomas, they do not express

certain cellular markers as proliferating cell nuclear antigen, vascular endothelial growth factor, type IV collagenase, and basic fibroblast growth factor (GLUT 1) [7, 15].

4.3 Fibrous Connective Tissue (Myofibroblastic) Tumors

The so-called fibrous connective tissue tumors are the largest category of nonvascular soft tissue neoplasms found in the fetus and infant. The major members of this group include the *fibromatoses* (desmoid type), the most common entity,

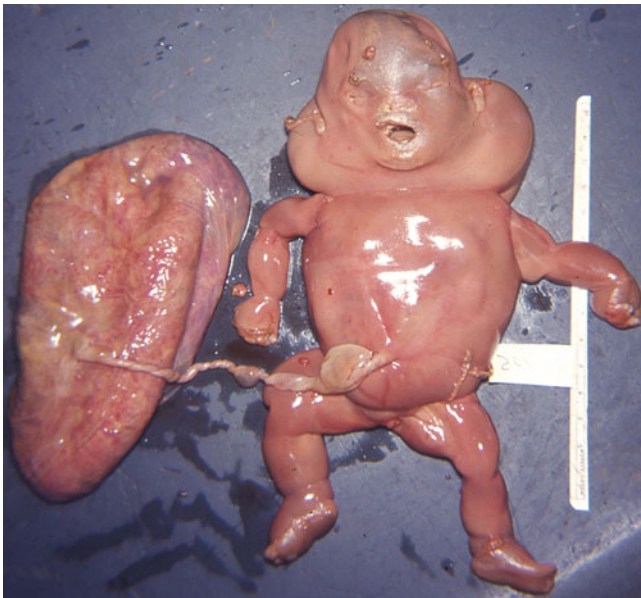


Fig. 4.8 Fetus with bilateral cystic lymphangiomas (hygromas) of the neck and generalized lymphangiectasis of subcutaneous tissue. There is a high incidence of Turner's syndrome (45, X0) and other chromosomal anomalies, for example, trisomy 21, associated with bilateral cervical hygromas (Reprinted from Isaacs [12]. © W.B. Saunders, 1997)

myofibromatosis, infantile fibrosarcoma, digital fibromatosis, and fibrous hamartoma of infancy [5, 6, 8–13, 15, 27] (Figs. 4.12, 4.13, 4.14, 4.15, 4.16, 4.17, 4.18, 4.19, 4.20, 4.21, 4.22, 4.23, 4.24, 4.25, 4.26, and 4.27). More than half involve the extremities and approximately one third are malignant [3, 8, 15, 27] (Table 4.1). *Fibrosarcoma* is the leading malignant soft tissue tumor in most fetal and infant series [3, 8, 10, 11, 27, 30].

Immunohistochemical and EM studies show that the fibrous connective tissue tumors are composed primarily of myofibroblasts and fibroblasts [8, 9, 12, 15, 27]. Although these tumors have the same clinical presentation, namely, a palpable mass, and possibly a similar histogenesis, they show a variety of distinct gross and microscopic appearances. Overall, this group is associated with a favorable prognosis and deserves a conservative treatment approach [9, 12, 15].

4.3.1 Fibromatosis

Fibromatosis (juvenile or infantile desmoid fibromatosis) is a benign tumor presenting as a mass in the fascia, skeletal muscle, or periosteum [8, 9, 15, 27, 31]. The most frequent sites in newborns and infants are the extremities

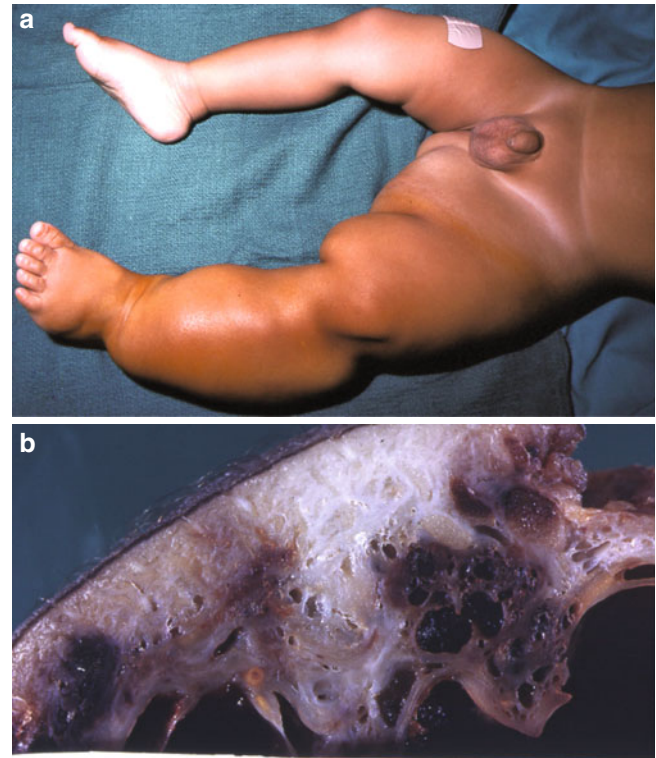
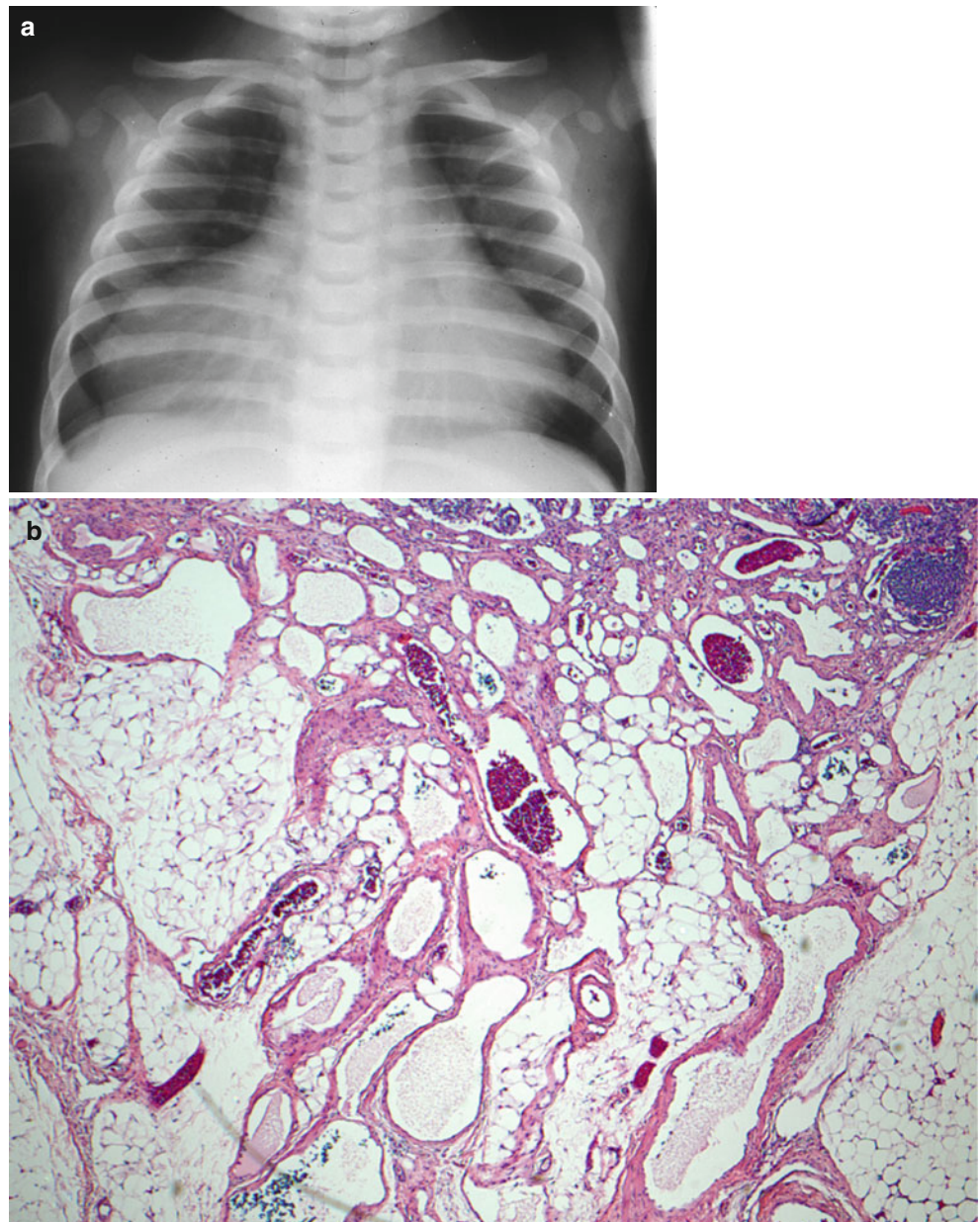


Fig. 4.9 Cavernous lymphangioma producing focal gigantism of an extremity. (a) 1-year-old male was born with a left lower extremity much larger than the right. (b) The subcutaneous tissue is replaced by cystically dilated lymphatics of various sizes. Some are filled with blood (probably related to surgical artifact) (Reprinted from Isaacs [12]. © W.B. Saunders, 1997)

and the head and neck region; it occurs more often in males than in females [8, 10, 15, 27, 31] (Figs. 4.12, 4.13, 4.14, and 4.15). Sometimes, it is difficult to distinguish between a cellular fibromatosis and a low-grade fibrosarcoma histologically [12, 15]. Although the two tumors are aggressive locally and often recur, generally they do not metastasize [6, 8, 15].

Fibromatosis consists of a firm light-gray or white mass having a rubbery, whorled cut surface (Figs. 4.13 and 4.14). Often it appears encapsulated but usually the tumor invades imperceptively or blends into the adjacent soft tissues. Fibrosarcoma shows similar gross features but tends to be considerably softer, friable, and more myxoid or gelatinous appearing than fibromatosis [6, 8, 15] (Fig. 4.24). Fibromatoses tend to be smaller than fibrosarcomas, the former averaging 2 cm in greatest dimension and the latter 15 cm or more. However, size is not always a reliable criterion for diagnosis.

Fig. 4.10 Lymphangioma of the mediastinum. **(a)** Chest X-ray of a large mediastinal mass with radiating vessels in a 5-month male with a history of increasing respiratory distress. **(b)** Biopsy reveals numerous cystically dilated lymphatics and blood vessels. Lymphoid nodules within the lymphangioma are characteristic features (Reprinted from Isaacs [12]. © W.B. Saunders, 1997)



Fibromatoses are basically spindle-cell neoplasms with moderate variation in the cellularity and the amount of intercellular collagen (Figs. 4.12, 4.13, 4.14, and 4.15). Some are hypocellular with abundant collagen resembling scar tissue while others are more cellular with an occasional mitosis and a prominent pale-staining myxoid background [11, 15, 27]. These histological differences can be seen in the same tumor, especially if it is large. Sampling error plays an important role in the diagnosis. The tumors stain positively with vimentin immunoperoxidase and negatively with actin and desmin. EM studies show that the tumor cells are composed of fibroblasts and myofibroblasts [15].

Surgical excision is the treatment of choice. The tumor recurs if not completely excised and will cause fatal complications if a vital structure is involved [15, 27, 31].

4.3.2 Gardner Fibroma

Gardner fibroma is a benign, soft tissue, fibrous tumor that is intimately associated with fibromatosis and familial adenomatous polyposis coli [9]. The lesion presents as an irregular fibrous plaque typically on the back and chest wall, also other areas, during the first year of life. Microscopically the fibroma consists of sheets of dense, coarse collagen fibers separated by



Fig. 4.11 Arteriovenous malformation. Newborn with a large arteriovenous malformation of the right forearm that functioned as an arteriovenous shunt producing high-output congestive heart failure. Ligation of the artery to the blood supply of the malformation was required to control the life-threatening effect of the shunt (Reprinted from Isaacs [12]. © W.B. Saunders, 1997)

irregular clear spaces (“cracks”). Barely visible, spindle-shaped cells, immunoreactive with CD 34, are present within the fibers. Coffin warns that practically every patient with Gardner fibroma will eventually develop adenomatous polyposis complicated by adenocarcinoma. The parents should be advised of this [9].

4.3.3 Digital Fibromatosis (Recurring Digital Fibroma)

Infantile digital fibromatosis characteristically involves the lateral aspects of the distal phalanges of the fingers and toes. Almost half are discovered within the first month and the majority by the first year of life; most recur after simple excision [6, 8, 15, 27]. The tumors are single or multiple and are composed of white firm nodules with a broad base and shiny surfaces (Fig. 4.15).

Histological examination reveals the usual picture of a fibromatosis in this age group: small, regular spindle-shaped cells showing an interlacing bundle or “herringbone” growth pattern with little or no mitotic activity, embedded in a collagenous matrix invading the dermis and subcutaneous tissue [6, 8, 9, 15, 27, 32] (Fig. 4.15). Variably the trichrome stain shows red paranuclear intracytoplasmic inclusions, which by EM consist of packets of actin filaments [32]. Like the other

fibromatoses of infancy, the cells of origin are myofibroblasts and fibroblasts [9, 15, 27]. Digital fibromatoses invade locally, frequently recur; many eventually spontaneously regress and disappear after adolescence [13, 15, 27]. Conservative surgical excision is recommended if necessary.

4.3.4 Torticollis

Torticollis is a tumorlike condition that presents as a firm, palpable nodule in the sternocleidomastoid muscle. It usually appears within the first 2 weeks of life and frequently causes a deformity called “wry neck.” Torticollis is observed in less than 1 % of newborns [15]. In about half the patients, there is a history of complicated delivery, for example, a breech or forceps extraction.

Although other names applied to this condition are fibromatosis colli and sternocleidomastoid tumor, studies indicate that the lesion most likely represents a reactive, reparative process rather than a true neoplastic one [14, 15, 33, 34].

The histological features of torticollis are time dependent. During the first few months of life, they are similar to those of fibromatosis. However, a few years later biopsy shows acellular fibrosis accompanied by skeletal muscle fiber atrophy and loss (Fig. 4.16).

4.3.5 Myofibromatosis

Myofibromatosis is an unusual soft tissue neoplasm found primarily in the first year of life presenting as one or more nodular lesions involving the soft tissues and occasionally the bones and the viscera. Almost two thirds of the cases are discovered at birth [9, 13, 15, 27, 35].

Solitary myofibromas are more common than multiple ones [13, 15, 35, 36] (Figs. 4.17, 4.18, and 4.19). The solitary tumor involves primarily the soft tissues of the head, neck, and trunk whereas the multicentric ones not only arise from the soft tissues situated over various parts of the body but also from the muscles, bones, and viscera [15, 31, 35, 36]. Congenital generalized fibromatosis is classified into two main types: type I involves the skin, subcutaneous tissue, muscle, and bone whereas type II primarily affects the viscera [35, 36]. Tumors may occur in the brain and spinal cord of patients with congenital visceral myofibromatosis [15, 35, 36]. Moreover, solitary congenital myofibromatosis of the small or large intestine is responsible for an abdominal mass and neonatal bowel obstruction [15]. Some erroneously have been called sarcomas.

Although fibromatosis and myofibromatosis share several features in common such as the distribution of solitary lesions and the presence of fibroblasts and myofibroblasts by light and EM, the findings of central necrosis, calcification, and a

Fig. 4.12 Congenital fibromatosis involving the forearm of a 3-month-old male. (a) Left forearm is diffusely enlarged by a firm, hard mass. There are barely visible café-au-lait spots on the patient's chest and axilla. (b) Uniform, spindle-shaped cells invading fat and surrounding blood vessels (Reprinted from Isaacs [12]. © W.B. Saunders, 1997)



prominent vascular pattern in the myofibromatosis are helpful diagnostic criteria used to distinguish the two [15, 31, 35]. Moreover, the tumor cells often resemble smooth muscle cells (Fig. 4.17b). They are positively stained with PTAH, are immunoreactive with smooth muscle actin and vimentin, and are variably reactive with desmin [15, 27].

Myofibromatosis and congenital hemangiopericytoma are now considered to be the same entity although some myofibromas have a prominent hemangiopericytoma-like vascular pattern [9, 37].

When there is extensive involvement of multiple viscera, and especially the heart and lungs, the patients with type 2

multicentric myofibromatosis have a poor prognosis [15, 35, 36]. The recurrence rate of single lesions is 7% after primary excision, but cure is usually achieved after re-excision. Some appear to spontaneously regress [13, 15, 36].

4.3.6 Granular Cell Tumor

Granular cell tumor (congenital epulis) is a neoplasm of controversial histogenesis occurring primarily in the gingiva of newborns and infants [9, 13, 15, 38]. Two forms of granular cell tumor have been described: one is the classical

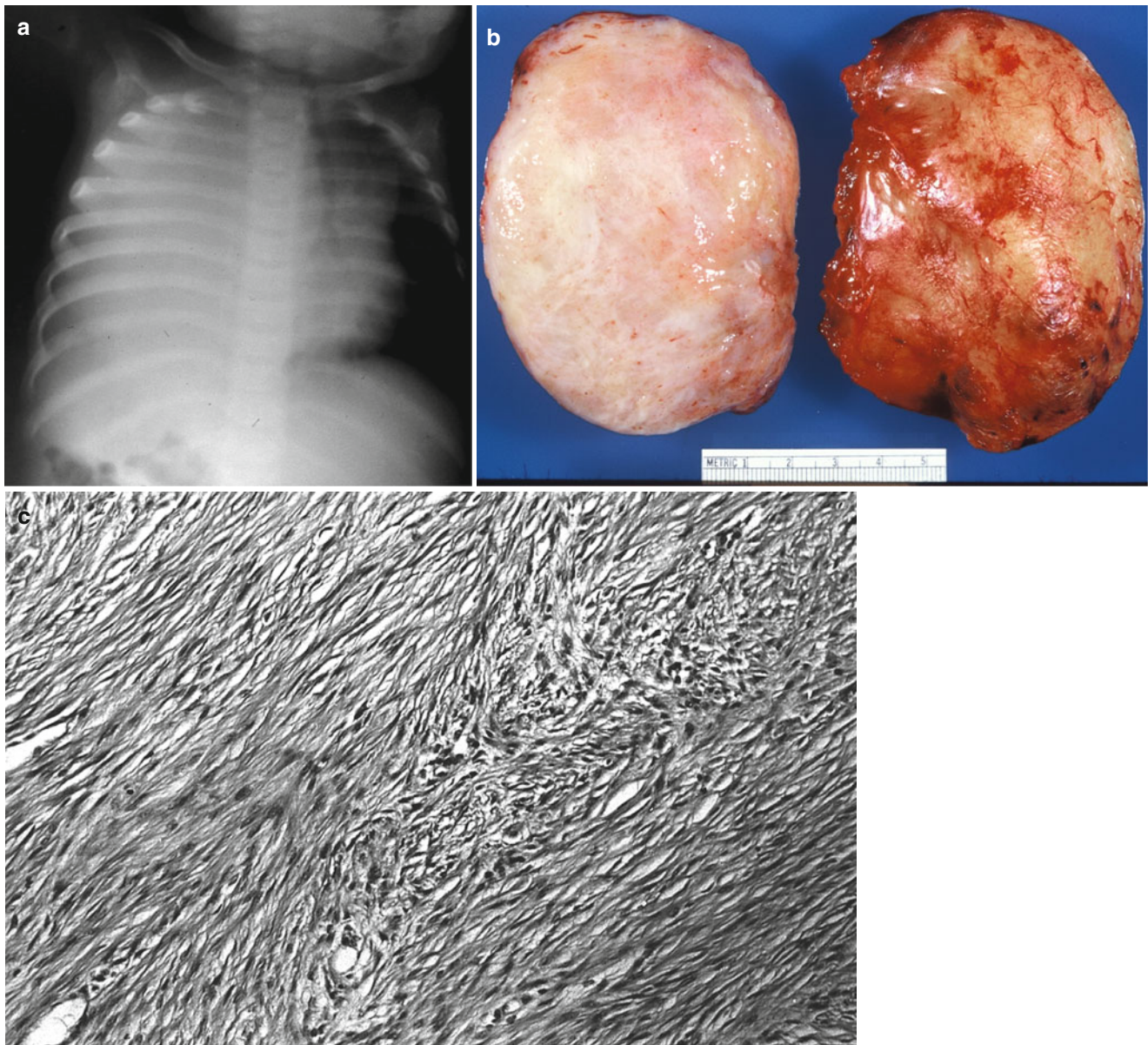


Fig. 4.13 Fibromatosis of the mediastinum and supraclavicular area. Seven-month-old female presented with a mass in the shoulder and chest. (a) Chest radiograph shows a large mediastinal mass occupying much of the left thorax displacing the mediastinal structures to the right. (b) Excised gross specimen, 10.5×8 cm, divided in half with the cut surface on the left of the picture and the external surface on the right.

The tumor has a pale, gray appearance without hemorrhage or necrosis. (c) Interdigitating (“herringbone”) and fan-like storiform growth patterns (middle of the field) are typical for this group of soft tissue tumors. The spindle-shaped cells resemble tissue culture-like fibroblasts (Reprinted from Isaacs [12]. © W.B. Saunders, 1997)

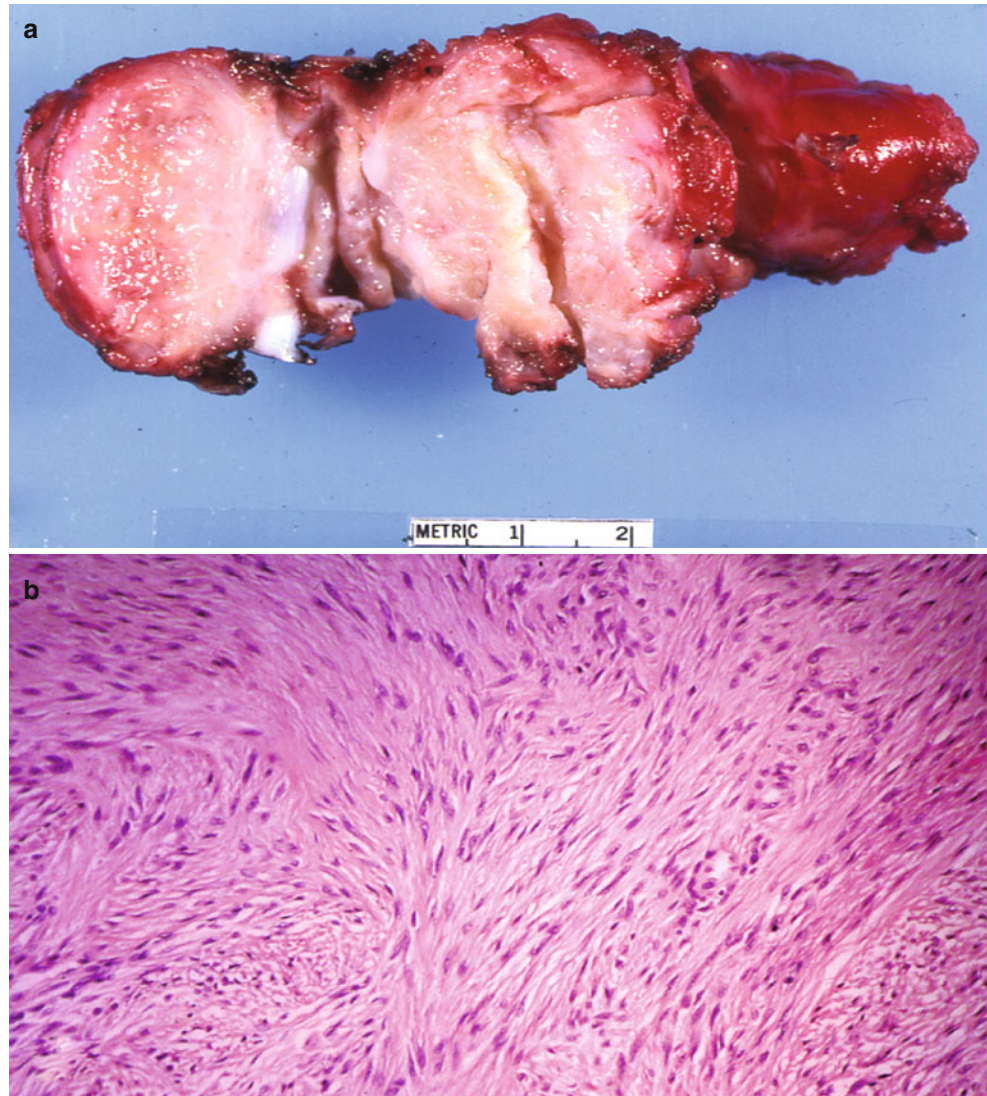
congenital epulis involving the gums, and the other occurs in the skin, the mucosa of the respiratory, gastrointestinal, and genitourinary tracts, and the various sites throughout the body in older individuals [15, 38]. Immunohistochemical and EM studies suggest that the myofibroblast is the cell of origin of the congenital form, but an ongoing debate continues regarding its exact histogenesis [38].

In the newborn and infant, the granular cell tumor typically arises as one or more mucosal-covered nodules from the gingiva of the anterior alveolar ridge of either the mandible or the maxilla and occurs predominately in

females. Occasionally, the tongue and palate are involved. The tumor may present as a big mass arising from the mucosa of the upper jaw causing airway obstruction and feeding problems like that of a teratoma (epignathus) [14, 15] (Fig. 4.20).

Granular cell tumors are composed of polygonal cells with pink, PAS positive granular cytoplasm and regular, round dark basophilic staining nuclei (Fig. 4.20c, d). Immunostaining is reactive with vimentin but unreactive with S-100, muscle, and histiocytic markers; EM features include membrane-bound, pleomorphic cytoplasmic granules, cell

Fig. 4.14 Congenital fibromatosis of the sternum. Six-month-old male had repeated resections and recurrences of his tumor since birth. (a) The sternum is replaced by a firm, whitish-gray mass extending into adjacent intercostal muscles. (b) The tumor consists of regular, small spindle-shaped cells separated by loose fibrous connective tissue (Reprinted from Isaacs [15]. © Springer-Verlag, 2002)



membranes, and intermediate filaments with fusiform electron densities suggestive of myofibroblasts [27, 38]. The granular cell tumor is cured by simple excision. However, spontaneous regression has been documented even after incomplete removal or without surgery [38]

4.3.7 Fibrous Hamartoma of Infancy

Fibrous hamartoma is a moderately common soft tissue neoplasm observed primarily within the first year of life; about 20 % are congenital [8, 15, 27, 35, 39]. The tumor presents as a palpable mass most often in the axilla, arm, thigh, shoulder, and back arising from the lower dermis or subcutaneous tissue [8, 15, 27, 35]. Unusual primary sites reported in infants are the hand and genital areas. Underlying skeletal muscle and nerves may be involved. Rarely, more

than one lesion is found in the same patient. Usually, the tumors do not recur after complete excision [15]. The lesion does not regress.

The fibrous hamartoma consists of a round, bulging mass with firm glistening, gray-white tissue and yellow nodules of fat (Fig. 4.21). It rarely exceeds 8 cm in greatest diameter. Some appear well circumscribed while others blend imperceptively with the surrounding subcutaneous fat [8, 9, 15, 27, 35] (Fig. 4.22).

Microscopic examination shows three main tissue components: nests of immature-looking spindle-shaped cells embedded in a myxoid background, interlacing dense fibrous trabeculae resembling tendon, and lobules of mature adipose tissue situated between the other two components [8, 9, 15, 27, 35] (Fig. 4.22). Blood vessels are prominent in the myxoid areas. Tumor cells in the myxoid and fascicular fibroblastic areas react with vimentin and desmin [39]. The

adipose tissue component is S-100 positive. By EM, the spindle cells consist of both fibroblasts and myofibroblasts [35, 39].

4.3.8 Giant-Cell Fibroblastoma

Giant-cell fibroblastoma is an unusual fibroblastic neoplasm found predominately in males under 10 years of age [9, 13]. Less than 50 cases are reported, the youngest on record being in an infant 4 months of age. Typically, the tumor is superficial, occurring mostly on the trunk, but it is also found in the inguinal region, scrotum, thigh, or neck [9, 13]. Giant-cell fibroblastoma consists grossly of a gray, rubbery, or gelatinous mass with infiltrative borders. Histological findings include moderately cellular, solid areas, dilated spaces resembling lymphatics, and areas of dense collagen having a gray, myxoid background containing entrapped fat. Fibroblasts and floret-type giant cells are required for the

diagnosis. The tumor is immunoreactive with vimentin, smooth muscle actin, and CD 34. Like other benign fibroblastic tumors of infancy, it recurs if not completely excised and has a good prognosis.

4.3.9 Infantile (Congenital) Fibrosarcoma

Fibrosarcoma is a relatively uncommon soft tissue sarcoma that has two peaks of incidence in children: one in fetuses and infants (congenital or infantile fibrosarcoma) and another in older individuals (“adult type” fibrosarcoma) [40]. Congenital or infantile fibrosarcoma occurs less often than the adult type [8, 9, 11, 15, 27, 30, 35, 40–44]. Although the rate of local recurrence is significant, 50 % or more, metastases seldom occur [5, 9–11, 15, 35, 43, 44]. Cytogenetic studies reveal chromosome 11, 20, and several other trisomies [44]. Moreover, infantile fibrosarcoma and congenital cellular mesoblastic nephroma share similar histological appear-



Fig. 4.15 Digital fibromatosis. One-year-old male with nodules present on the lateral aspects of the distal phalanges of the fourth fingers since birth. The nodules were excised but each time recurred; they eventually disappeared during late adolescence. (a) Mirror image distribution of the nodular lesions. (b) The tumor is moderately cellular consisting of small, regular spindle-shaped cells involving the dermis and

subcutaneous tissue. The tumor displays an interdigitating or “herringbone” growth pattern. The epidermis is not involved. (c) Intracytoplasmic hyaline inclusions (arrows). (d) The intracytoplasmic inclusions are composed of actin-like filaments, which are situated beneath the nucleus (EM Courtesy of Ann Peters, Rady Childrens Hospital San Diego; Reprinted from Isaacs [12]. © W.B. Saunders, 1997)

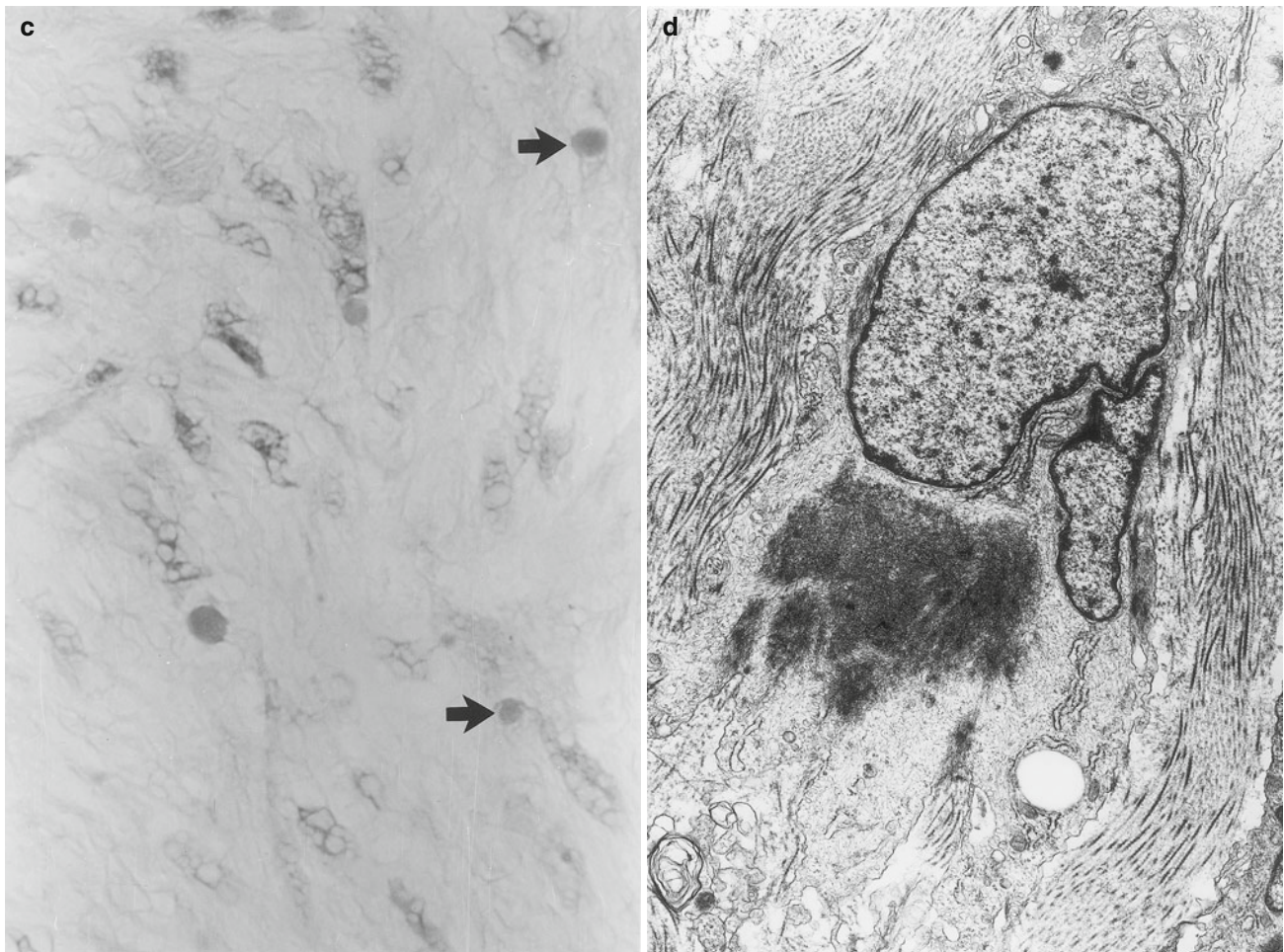
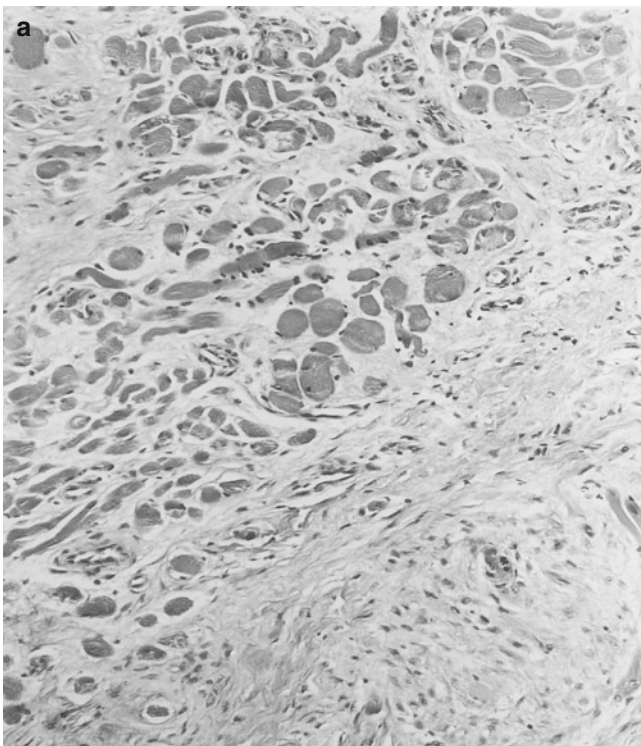


Fig. 4.15 (continued)



ances and a trisomy 11 karyotype suggesting that the two may be histogenetically related [15, 44].

Typically, the newborn or infant with a fibrosarcoma presents with an impressive soft tissue mass varying in size from a few centimeters to as large as 20 cm or more often involving an extremity, the trunk, head, or neck [6, 9, 15, 27, 41, 42] (Figs. 4.23 and 4.24). The abdominal wall, retroperitoneum, inguinal area, and thoracic cavity are less common primary sites [15, 42].

The tumor consists of firm, light-gray, occasionally gelatinous tissue partially surrounded by a fibrous capsule. Some

←

Fig. 4.16 Torticollis (fibromatosis colli). The histological findings of this lesion are age dependent. (a) Photomicrograph of a portion of sternocleidomastoid muscle removed from a 6-week-old male with torticollis. There are skeletal muscle fibrosis and atrophy. At this early stage, the appearance of interstitial fibrosis may resemble fibromatosis. (b) Section taken from the sternocleidomastoid muscle of a 7-year-old boy with torticollis. In contrast to the previous micrograph above (a), this one shows much more skeletal muscle fiber atrophy and loss; the interstitial fibrosis appears bland and hypocellular that of a scar (Reprinted from Isaacs [12]. © W.B. Saunders, 1997)

Fig. 4.16 (continued)

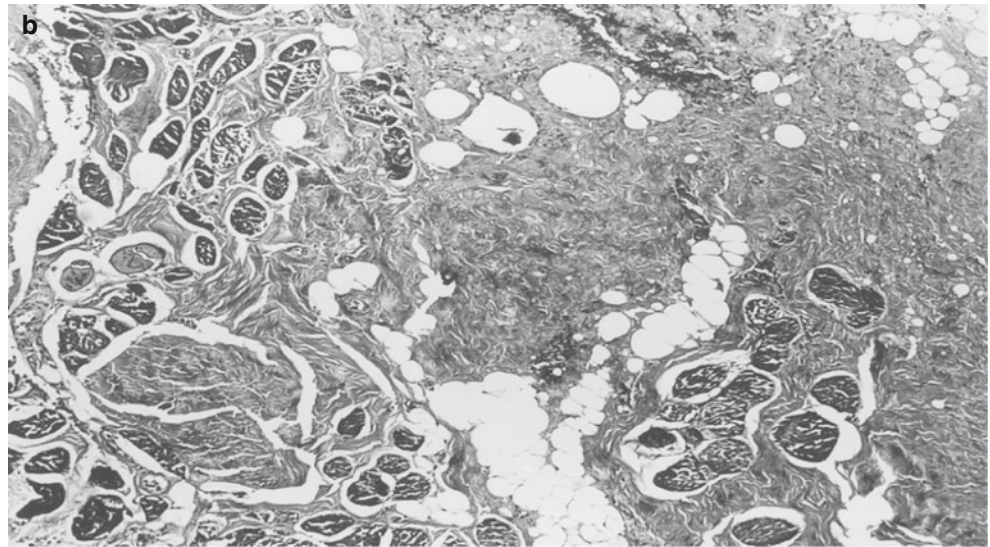
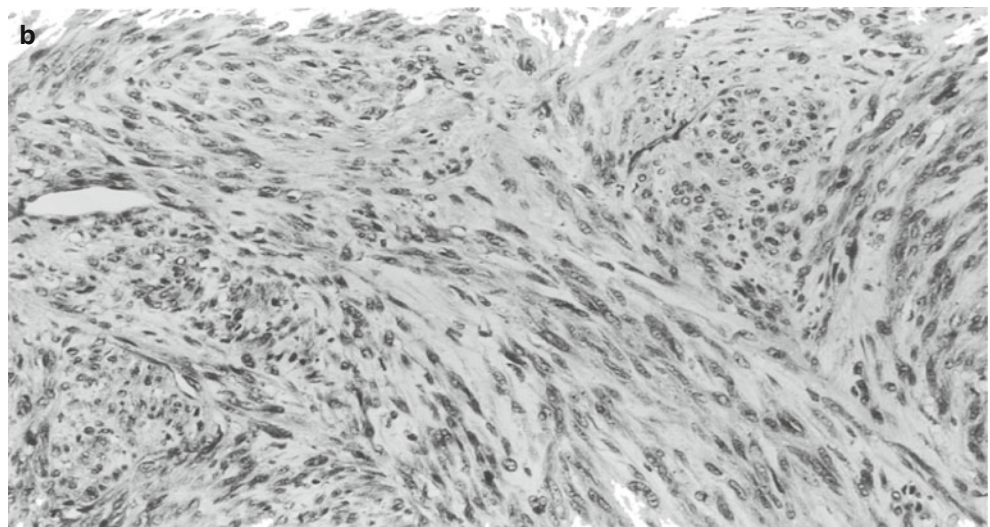


Fig. 4.17 Infantile myofibromatosis. Facial soft tissue mass from a 4-month-old female. (a) CT scan reveals a fairly well-circumscribed, nonhomogeneous, enhancing solid and cystic mass in the soft tissues of the left side of the face. The mass is adjacent to the left maxilla and orbit which show slight erosive bony changes. (b) Biopsy reveals bundles of regular spindle-shaped fibromuscular cells situated in a pale myxoid background. Within the center, there is an area of cellular degeneration and focal necrosis. Immunohistochemistry results: vimentin immunoreactive; actin and desmin focally positive (Reprinted from Isaacs [12]. © W.B. Saunders, 1997)



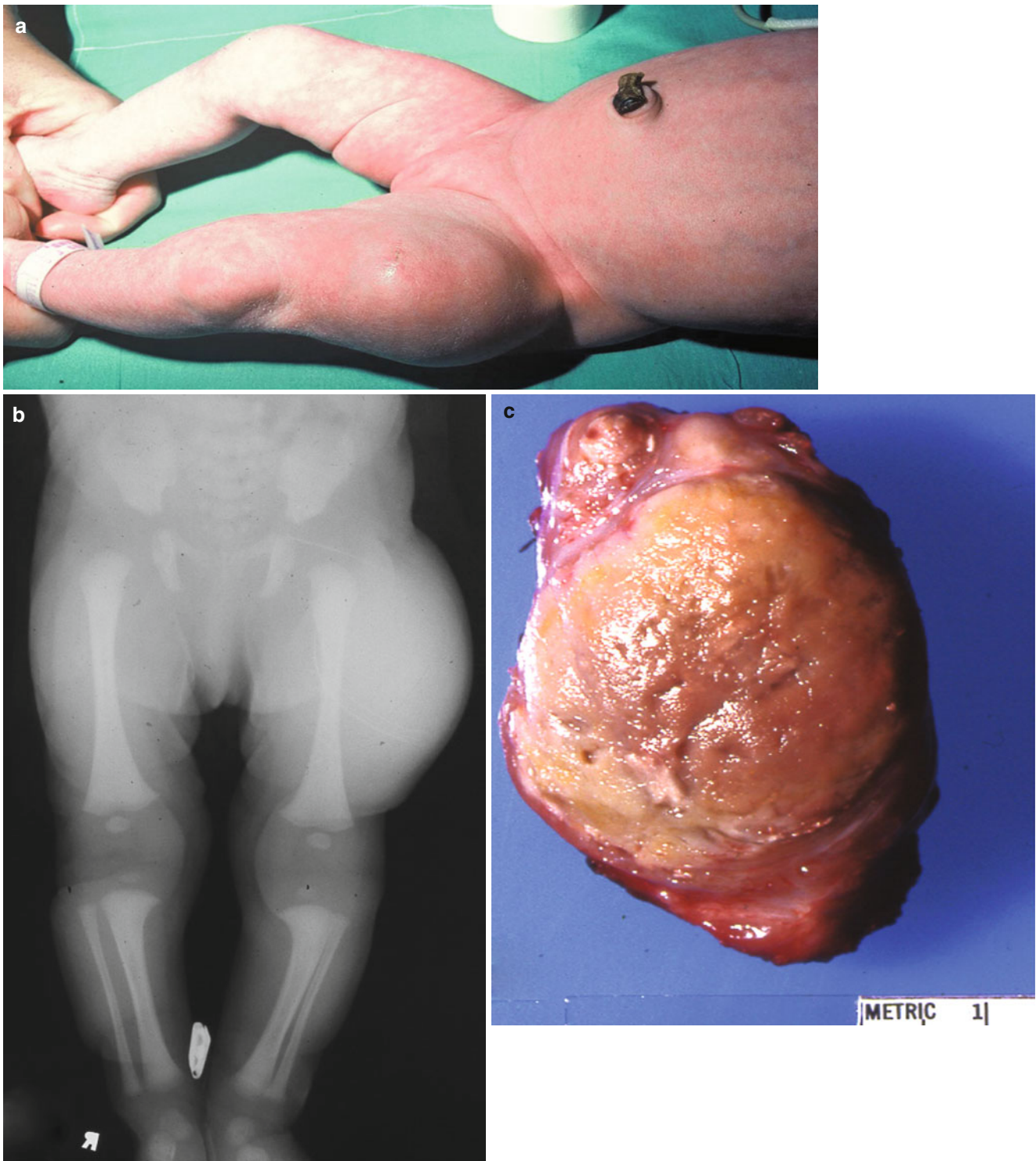
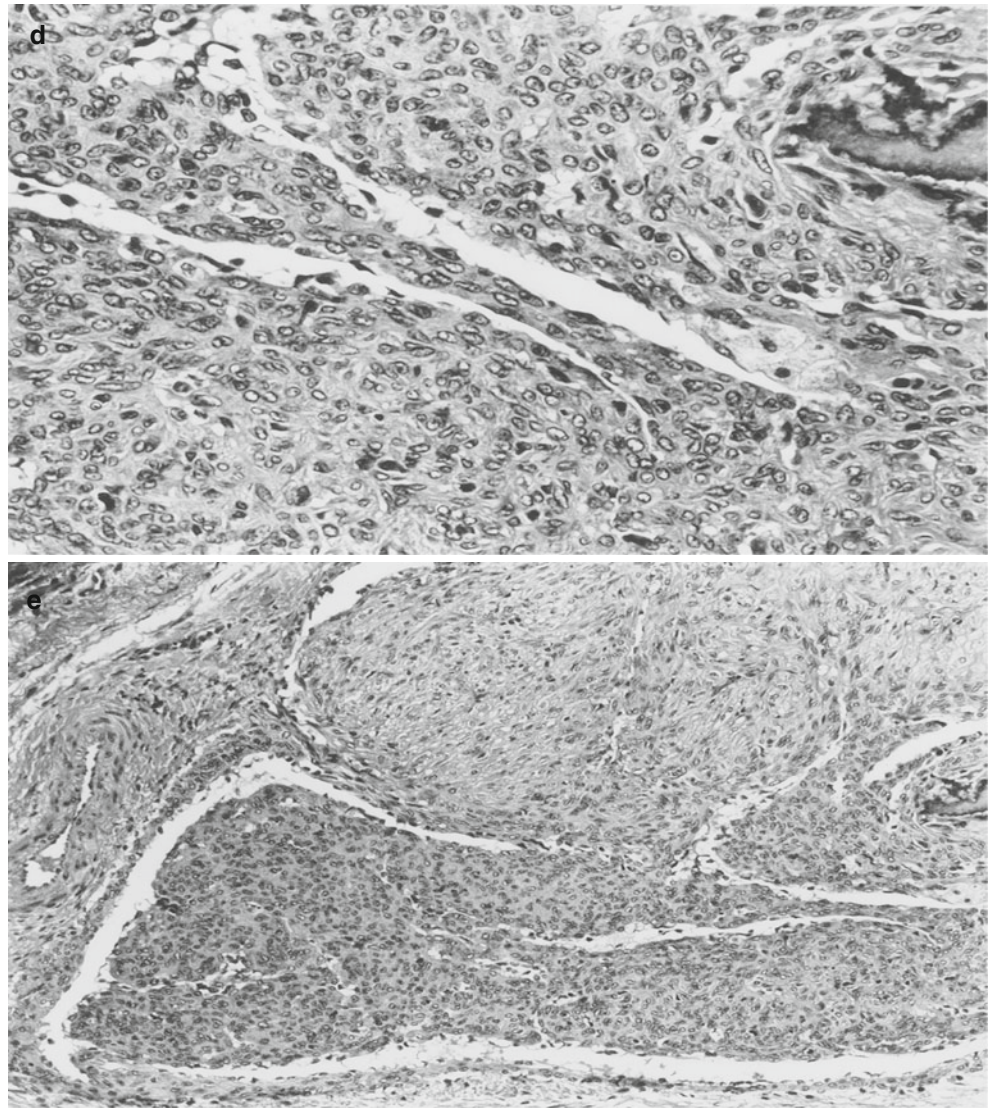


Fig. 4.18 Infantile myofibromatosis. (a) 1-month-old female with a left thigh mass present at birth. (b) X-ray reveals a uniform soft tissue mass occupying the outer aspect of the left thigh. (c) The tumor weighed 43.6 gm and measured 5.5 × 4.5 cm. The cut surface is lobular, bulging, and tan-gray to yellow-brown with areas of necrosis. (d) Low-power view displaying the lobular architecture of the tumor. The lobules are

rimmed peripherally by slit-like vascular spaces (“staghorn appearance”) which is a characteristic feature. (e) The tumor consists of cells with regular round to oval vesicular nuclei and inconspicuous nucleoli. A focus of calcification is present at the lower left corner (Reprinted from Isaacs [12]. © W.B. Saunders, 1997)

Fig. 4.18 (continued)

larger tumors show areas of hemorrhage, necrosis, and small cystic formations (Fig. 4.24). The gross appearance may be deceptive because extensions of tumor blend in subtly with the adjacent soft tissues of the affected part so that just “shelling it out” leaves residual tumor behind. Therefore, a wide local excision is recommended at the initial surgery, if this is technically feasible [14, 40].

The tumor is composed of small, spindle-shaped cells separated by variable amounts of pale-gray staining stroma often myxoid in appearance (Figs. 4.23, 4.24 and 4.25). Differing amounts of eosinophilic staining collagen depend on the degree of differentiation. Histologically, fibrosarcoma may be almost identical to fibromatosis except that the former displays more cellularity, nuclear atypia, increased mitotic activ-

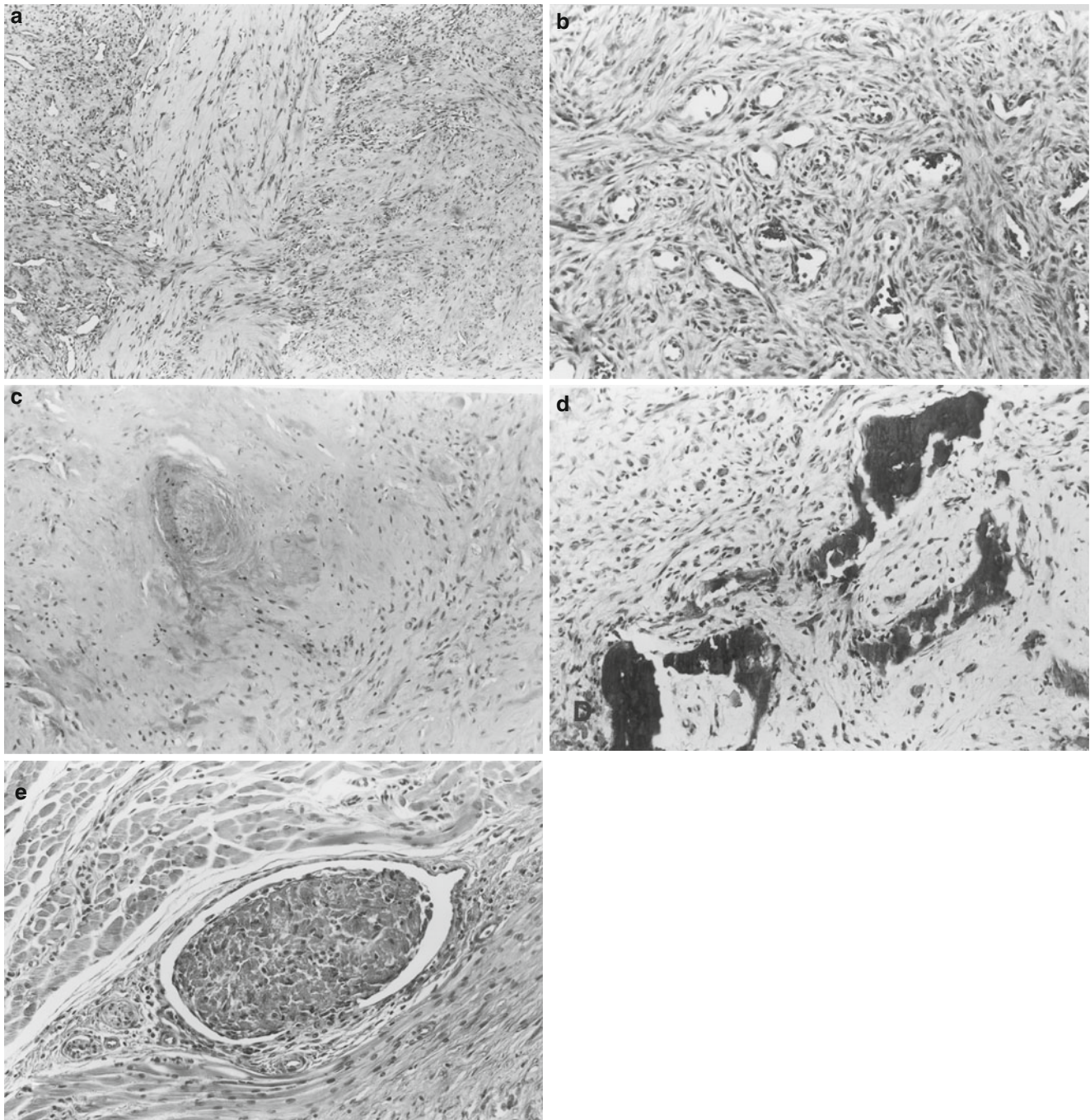


Fig. 4.19 Infantile myofibromatosis, histological features. The tumors may be single or multiple involving subcutaneous tissue, muscle, viscera, or bones. **(a)** Photomicrograph of a solitary tannish-pink, 2×1.8 cm, subcutaneous nodule removed from a 2-month-old male. The tumor shows regular spindle-shaped myofibroblastic cells with a

fibrous background and a focal vascular pattern. **(b)** Some tumors have a prominent vascular component suggestive of hemangioma or heman-giopericytoma. **(c)** Areas of degeneration and necrosis. **(d)** Foci of dystrophic calcification. **(e)** Intravascular tumor thrombus within skeletal muscle (Reprinted from Isaacs [12]. © W.B. Saunders, 1997)

ity, and areas of necrosis than the latter [15]. “Herringbone” and storiform growth patterns are present in both tumors. Congenital fibrosarcoma cells are morphologically similar to those of the older child and adult, but they tend to be smaller and less mature [16]. The less common, small cell “diffuse” fibrosarcoma variant consists of tiny round to oval cells

embedded in an abundant pale-staining myxoid stroma accompanied by mild cellular atypia and a low mitotic rate [16].

Fibrosarcomas are immunoreactive with vimentin and type IV collagen but not with cytokeratin, epithelial membrane antigen, neurofilament, S-100, actin, and desmin immunoperoxidase antibodies [27, 42]. EM studies reveal

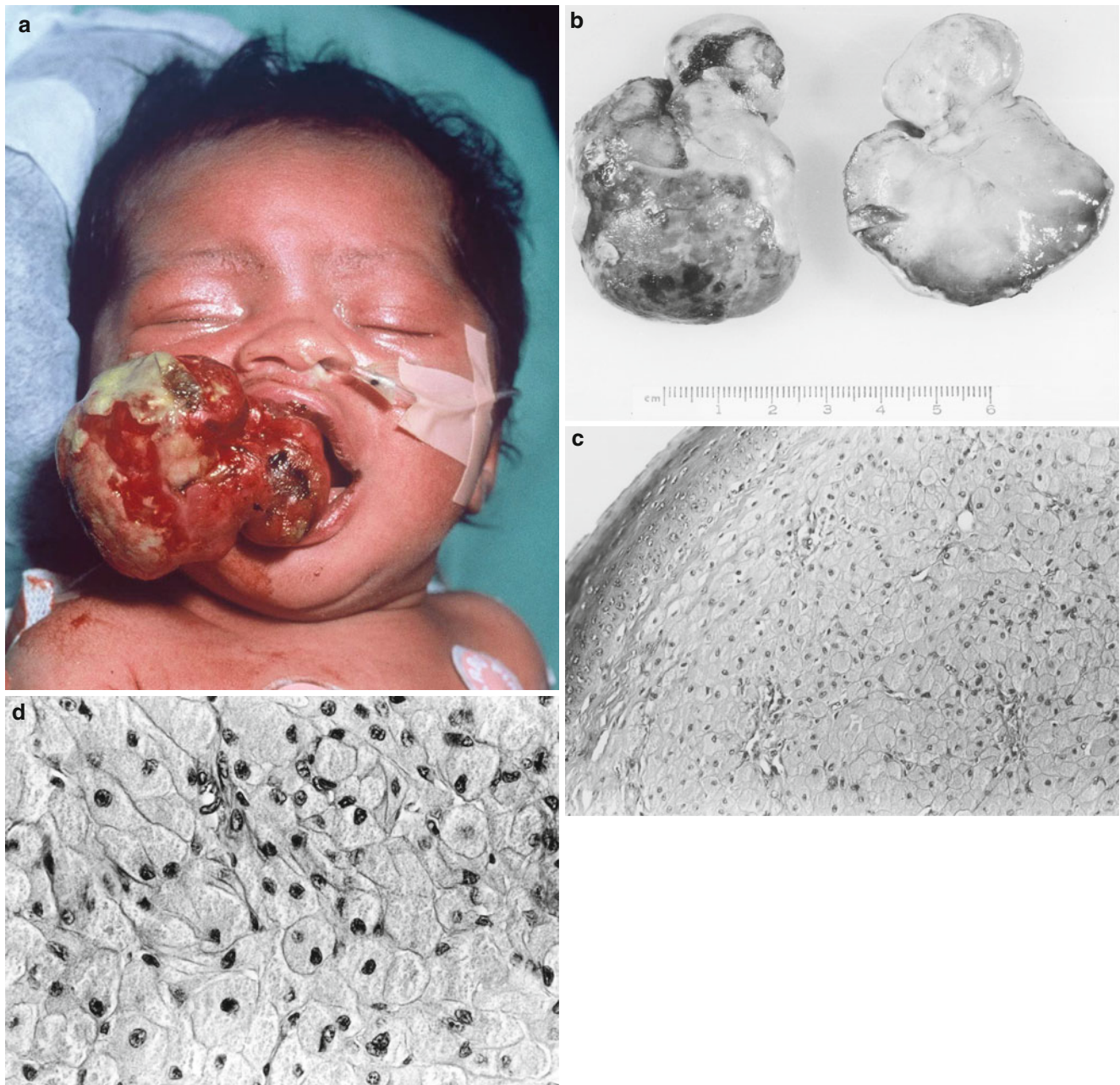


Fig. 4.20 Congenital gingival granular cell tumor (gingival epulis). Five-day-old, full-term female delivered by cesarean section born with a mass arising from the upper midline gingiva and alveolar ridge. Teratoma was the main diagnostic consideration. (a) The mass originates from the gingiva and adjacent palate and obstructs the oral cavity. (b) The tumor, 6×5.5 cm, 39 g, has a uniform, gelatinous, and *tan-gray*

to yellow cut surface. (c) Closely packed, polygonal granular cells with prominent cell membranes are situated beneath the mucosa. (d) Tumor cells have characteristic cytoplasmic granules and regular round nuclei with inconspicuous nucleoli. The granules are PAS positive. Otherwise, immunoperoxidase findings were nonspecific (Reprinted from Isaacs [12]. © W.B. Saunders, 1997)

primarily immature fibroblasts and myofibroblasts [27, 42] (Fig. 4.25d). There is no definite relationship between the histological findings and either recurrence or metastases [15, 27, 41]. The incidence of metastases is low, ranging from 0 to 8 % [11, 15, 41]. The presence of the trisomy 11 karyotype can be used to distinguish fibrosarcoma from other childhood sarcomas [27, 44] (Fig. 4.25e).

Management of this tumor is of prime concern because of its aggressive behavior and the functional impairment which may result from local treatment. Wide excision at the initial surgery is the treatment of choice with amputation, as a last resort, if the tumor has caused a dysfunctional extremity [15]. Adjuvant therapy is recommended for those patients with axial and proximal extremity unresectable lesions [40,



Fig. 4.21 Fibrous hamartoma of infancy. Gross appearance of a 30 g, 7.4×3.6 cm² subcutaneous mass removed from the lateral aspect, upper right arm, of a 4-month-old female. The tumor was present since birth. The specimen consists mostly of adipose tissue that blends in with adjacent subcutaneous fat. The overlying skin is stretched but intact. The gross appearance resembles a lipoma (Reprinted from Isaacs [12]. © W.B. Saunders, 1997)

[41]. Chemotherapy has been used following limb salvage surgery with some success. The majority of patients do well following surgical resection with or without chemotherapy [9, 40]. Infants with fibrosarcoma have a much better prognosis than older individuals with this tumor [40].

4.3.10 Nodular (Proliferative) Fasciitis

Nodular (proliferative) fasciitis is a nonneoplastic, reparative lesion infrequently encountered in the newborn and infant. Nevertheless, they should be considered in the differential diagnosis of a soft tissue mass [16]. Microscopically, they are characterized by marked cellularity, a brisk mitotic rate, nuclear atypia, and a myxoid background. The lesions are thought to be derived from myofibroblasts and histiocytes; they are more common in adults and older children [9, 15, 16, 45, 46]. Mistakenly, they have been called sarcomas

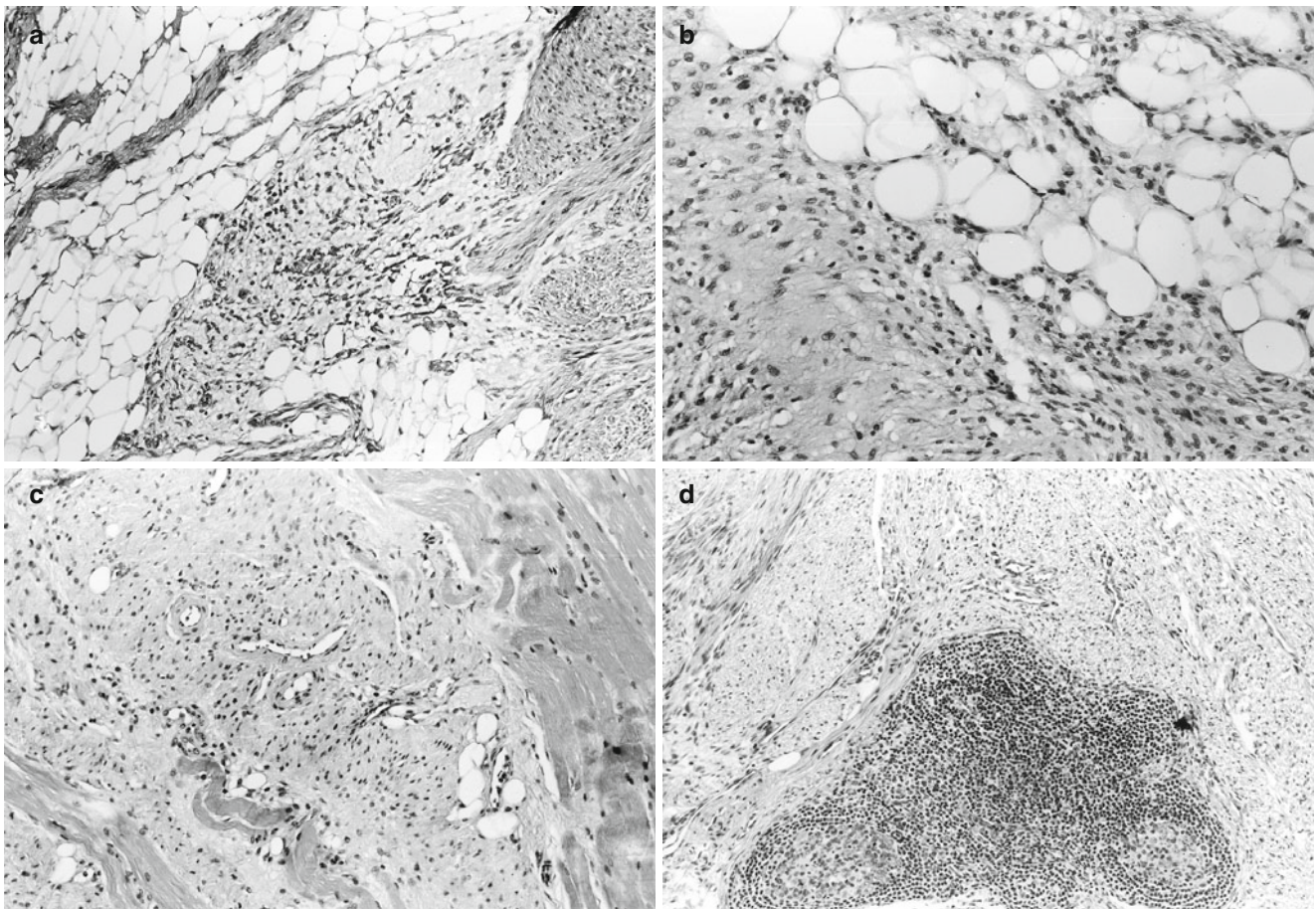


Fig. 4.22 Fibrous hamartoma of infancy. Histological findings, (a) fibroblastic areas on the right side of the photomicrograph, myxoid (gray) areas with small, spindle-shaped cells in the center, cord-like fibrous bands traversing the upper left hand corner, and fat.

(b) Higher magnification of the immature spindle cells. (c) Tumor infiltrating skeletal muscle. (d) Lymph node surrounded by tumor (Reprinted from Isaacs [12]. © W.B. Saunders, 1997)

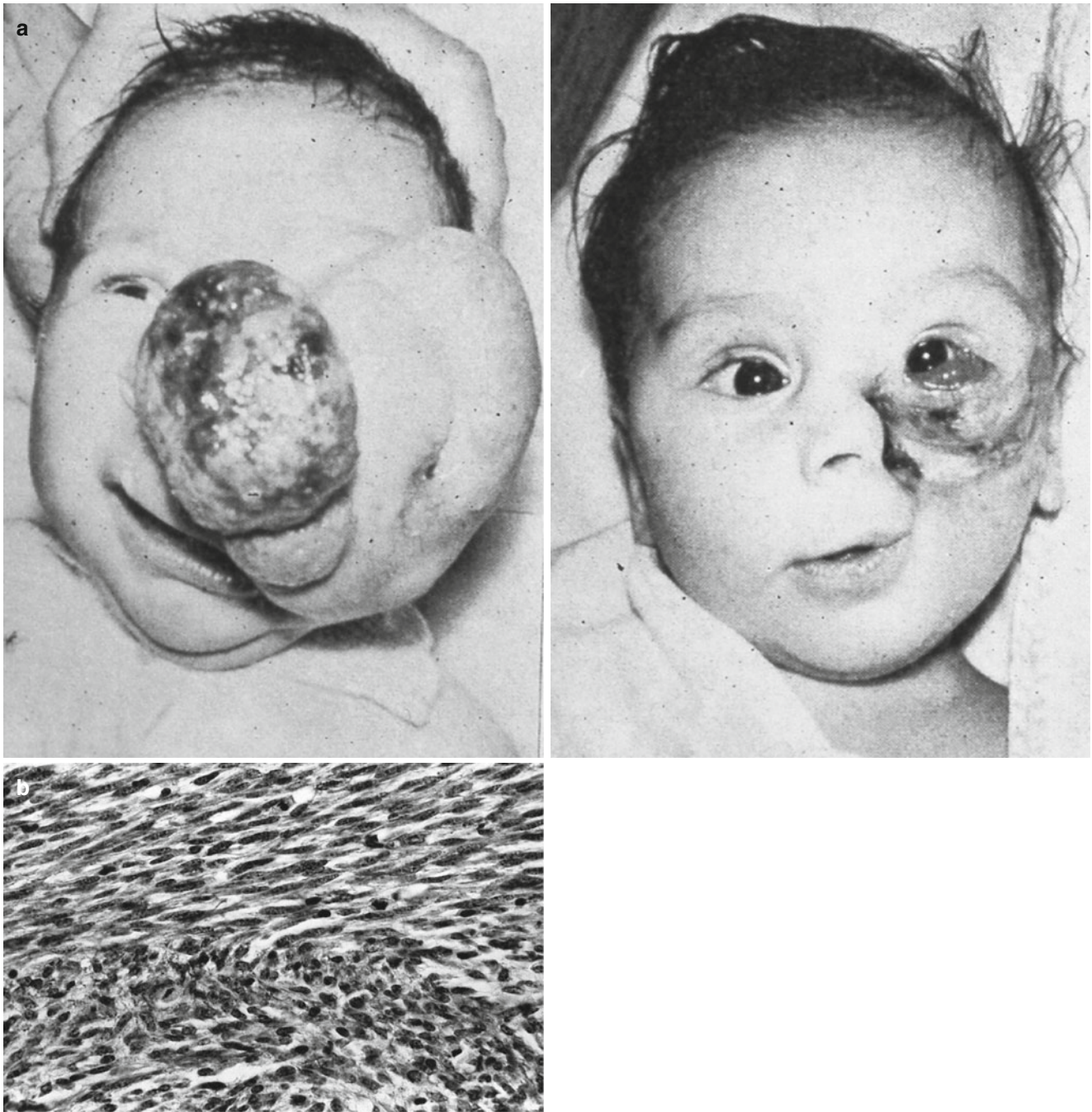


Fig. 4.23 Congenital fibrosarcoma. (a) Three-day-old female with a large, fungating tumor, $16 \times 16 \times 10$ cm, involving the face, nose, and maxillary sinus. The patient was cured by a wide local excision followed by grafting. (b) Hypercellular tumor composed of irregular,

hyperchromatic spindle-shaped, fibroblastic cells with moderate nuclear atypia and prominent mitotic activity. (Reprinted from Hays et al. [28]. With kind permission of © Elsevier, 1970)

(or “pseudosarcomas”) because of their ominous microscopic features [7, 15, 45, 46]. They are found in the neck, chest wall, back, and extremities. The lesions tend to be small, usually less than 5 cm in diameter, and not well circumscribed [45, 46]. Microscopically, they are composed of fibroblasts and giant cells with vesicular nuclei, prominent nucleoli, and basophilic cytoplasm resembling ganglion

cells, which are diagnostic features [15, 16, 46] (Fig. 4.26). The ganglion-like cells stain positively for vimentin and actin and focally positive with CD68 antigen, which is consistent with myofibroblastic and histiocytic properties, respectively [46]. Keratin, desmin, and S-100 immunoperoxidase are not reactive. EM shows cells with fibroblastic, myofibroblastic, and histiocytic differentiation. The prognosis

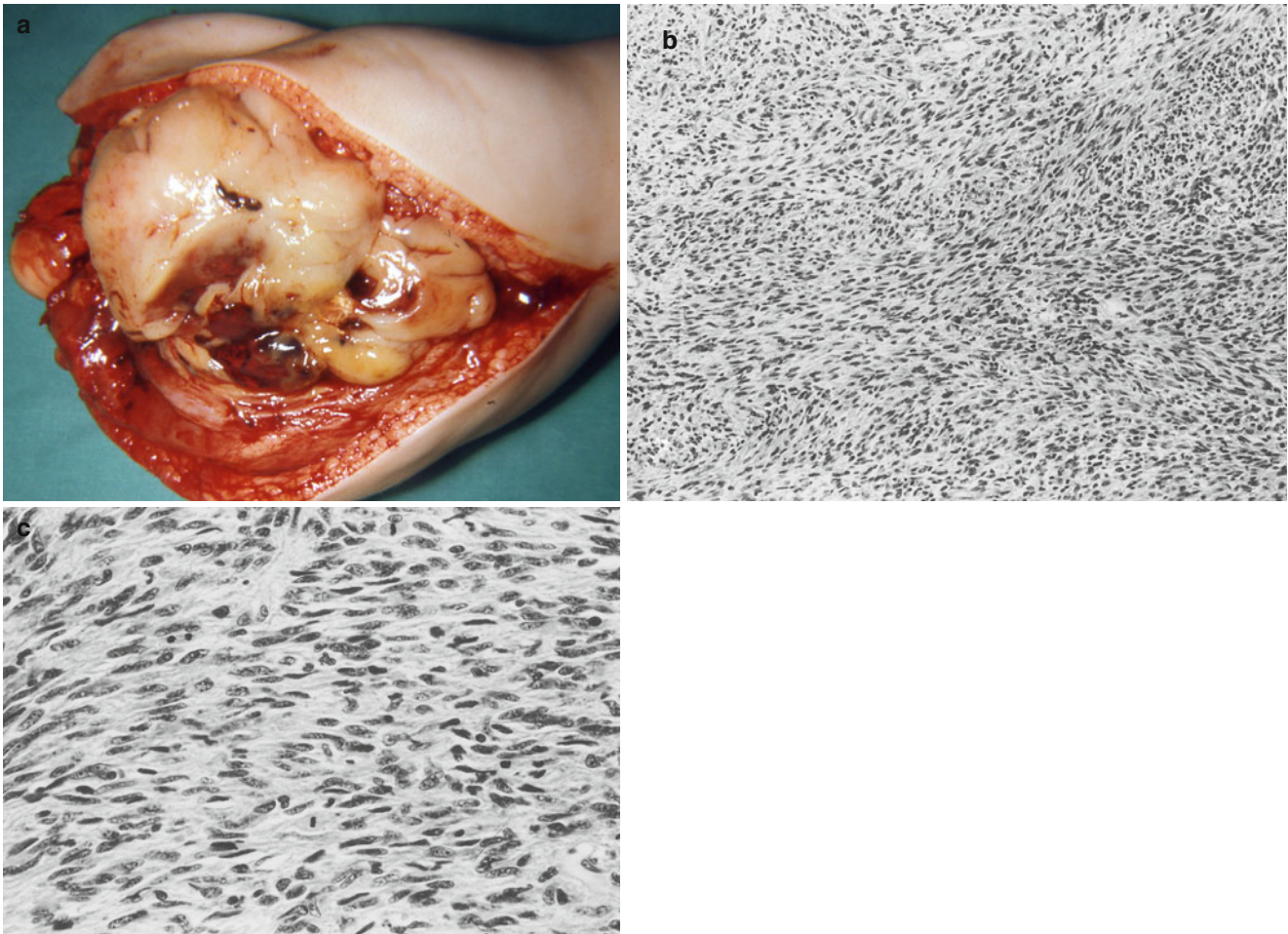


Fig. 4.24 Congenital fibrosarcoma. Five-month-old male with a rapidly growing mass in the right thigh discovered at 1 week of age. (a) Amputation specimen consists of a large soft, gelatinous tumor occupying most of the thigh. The head of the femur is visible on the medial aspect. (b) Photomicrograph showing the interdigitating, fascicular

growth pattern of the tumor. (c) The hypercellular spindle-cell neoplasm displays moderate nuclear atypia, three or four mitoses per high-power field and in the background of scant interstitial collagen (Reprinted from Isaacs [12]. © W.B. Saunders, 1997)

is excellent following local excision. If the lesion is incompletely removed, it may recur very rapidly, faster than a tumor would be expected. Unnecessary aggressive treatment should be avoided [46].

4.3.11 Cranial Fasciitis

Cranial fasciitis occurs in infants ranging in age from birth to 2 years and sometimes in older children [6, 15, 16, 29, 47] (Fig. 4.27). Typically, the lesion begins as a rapidly growing firm soft tissue scalp mass which may or may not be painful [29, 47]. Imaging studies reveal an irregular, lytic lesion with a sclerotic rim, varying in size from 1.5 to 9 cm situated most commonly in the temporal and parietal areas of the cranium accompanied by an overlying soft tissue mass [29] (Fig. 4.27a). Usually, it involves only the outer table of the skull with preservation of the inner table forming a saucer-like defect seen on tangential views [29, 47]. Sometimes, the lesion extends through the inner table into the underlying

dura. Cranial fasciitis is seldom bilateral [47]. The lesion clinically and on imaging studies may be confused with Langerhans cell histiocytosis [29].

Grossly, cranial fasciitis consists of firm, gray-white, dense fibrous connective tissue. If small spicules of bone are present, they may have a gritty sensation on section. Histological examination reveals small islands of cranial bone surrounded by spindle-shaped cells embedded in loose myxoid-appearing connective tissue stroma. Areas of dense fibrosis are present (Fig. 4.27b). Low mitotic activity, a storiform growth pattern, and mild chronic inflammation are other findings [47]. Although excisional biopsy and curettage are curative, the lesion will recur if not adequately excised. The etiology is unknown.

4.3.12 Inflammatory Myofibroblastic Tumor

Inflammatory myofibroblastic tumor, a controversial lesion composed myofibroblastic spindle cells and chronic inflammatory

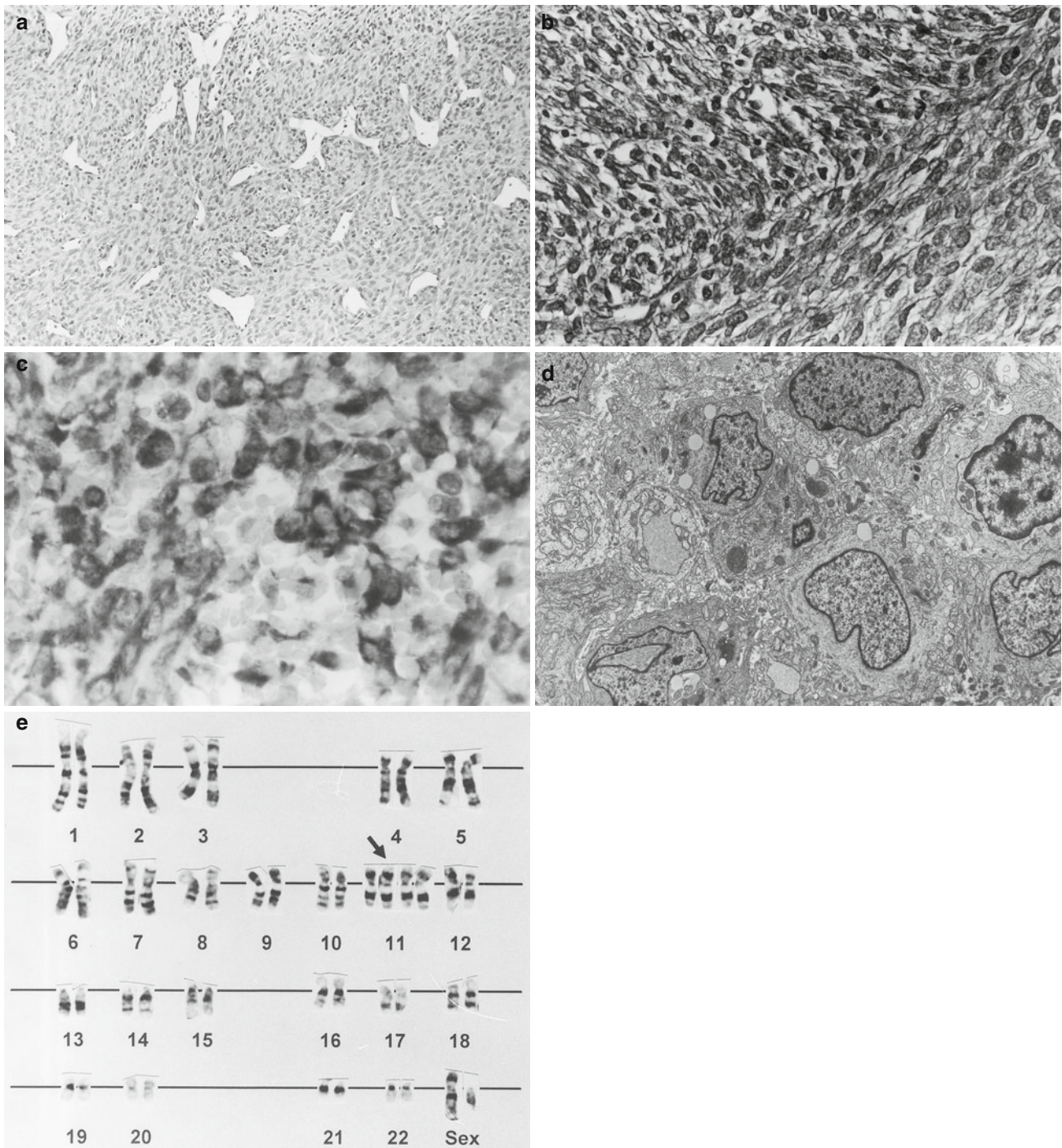


Fig. 4.25 Congenital fibrosarcoma. Two-month-old male with a shoulder mass. (a) Prominent vascular pattern which may be confused with hemangiopericytoma. (b) Reticulin fibers separating tumor cells. (c) The tumor cells are reactive with vimentin but not with actin, desmin, or neuron-specific enolase. (d) EM shows oval cells with slightly irregular, smooth cytoplasmic contours. The irregular nuclei have evenly

spaced chromatin. Scattered small filaments are present within the cytoplasm. Focal intercellular collagen fibrils are noted. (e) Karyotype of the tumor shows a trisomy 11 ((d) Courtesy of Ann Peters; (e) Courtesy of James Mascarello, Ph.D. Children's Hospital San Diego; Reprinted from Isaacs [15]. © Springer-Verlag, 2002)

cells, rarely occurs in infants [9]. Microscopically, it may resemble a variety of conditions such as granulation tissue, nodular fasciitis, scar, or fibromatosis infiltrated by lymphocytes, plasma cells, and eosinophils. Some regard it as a tumor of intermediate malignancy with a tendency to locally occur but rarely metastasize [9].

4.4 Fibrohistiocytic Tumors

Fibrohistiocytic tumors include a wide variety of both benign and malignant conditions composed of histiocytes and fibroblasts which involve primarily the skin and soft tissues.

Fig. 4.26 Nodular (proliferative) fasciitis. Three-month-old female with a subcutaneous mass in the lower leg. (a) Gross specimen consists of large, bulging nodules of dense fibrous connective tissue. (b) Biopsy reveals fibroblasts and ganglion-like giant cells with vesicular nuclei, prominent nucleoli, and basophilic cytoplasm. There are a few scattered lymphocytes. (c) Higher magnification showing the ganglion-like cells in more detail. A trichrome stain demonstrates abundant blue-staining fibrosis (Courtesy of D.R. Dickson, M.D., Santa Barbara Cottage Hospital, Santa Barbara, CA; Reprinted from Isaacs [12]. © W.B. Saunders, 1997)

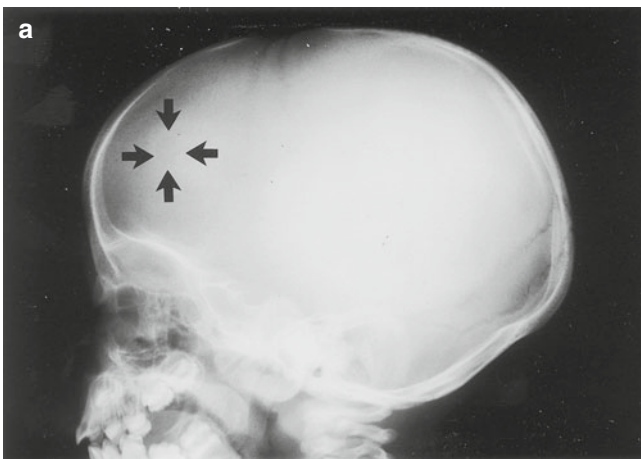
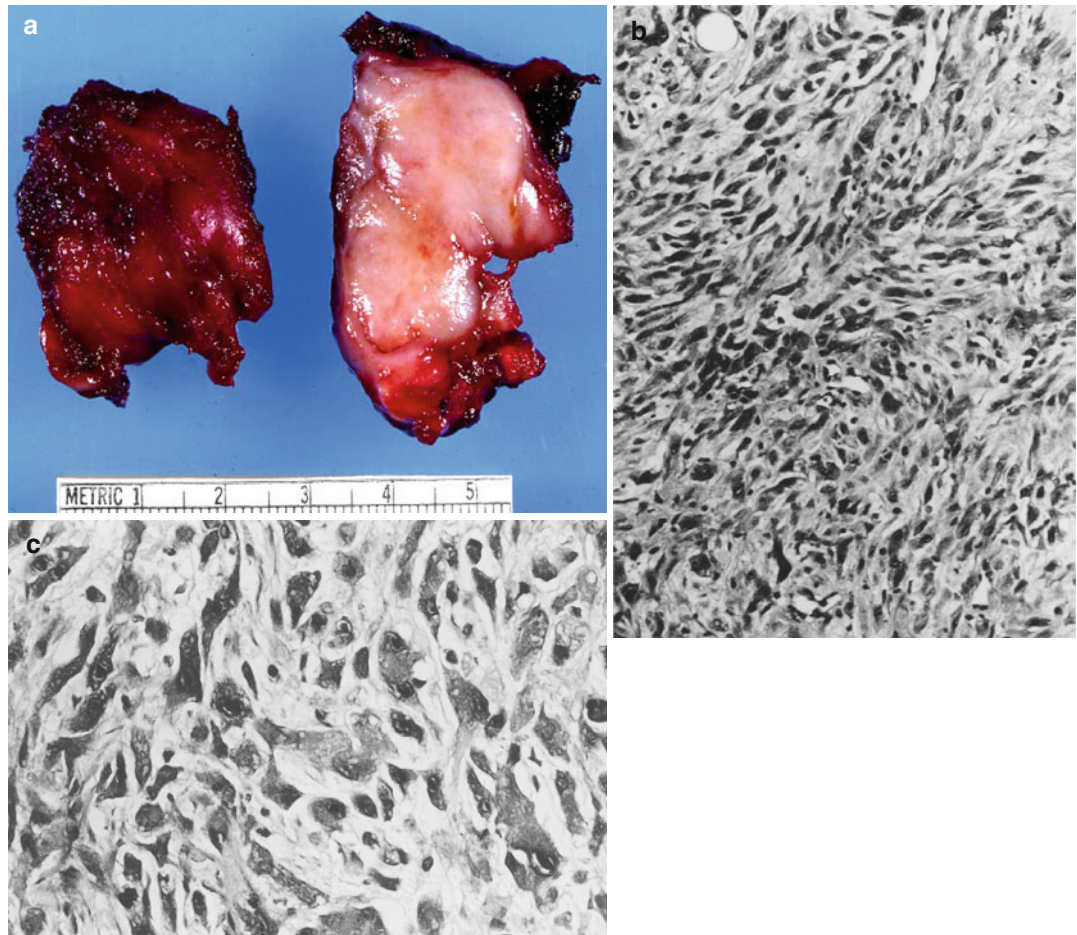
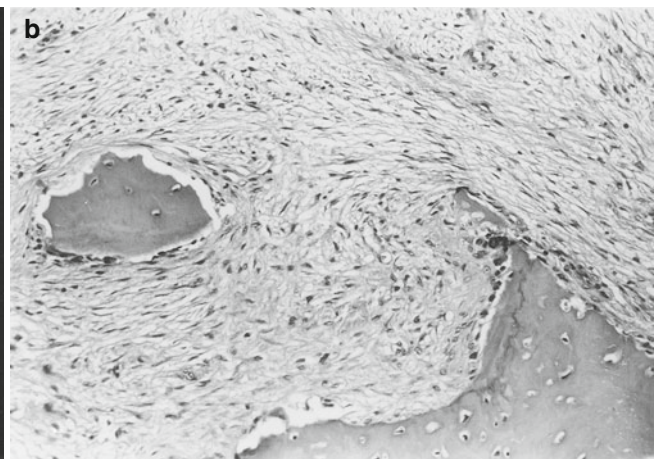


Fig. 4.27 Cranial fasciitis. (a) Skull X-ray of a 1.5-year-old male with bilateral scalp masses depicts an irregular punched-out lesion (arrows) in the left frontal bone. Langerhans cell histiocytosis, which is one of the main considerations in the radiological differential diagnosis here,



has a similar X-ray appearance. Osteomyelitis and neuroblastoma are other considerations in the differential diagnosis. (b) Biopsy with fibroblastic reaction surrounding irregular bone spicules (Reprinted from Adler and Wong [29]. With kind permission of © Elsevier, 1986)

Not all members of this group are seen in the newborn and infant. The majority are found as subcutaneous nodules or soft tissue masses. The principal fibrohistiocytic lesions are *juvenile xanthogranuloma (JXG)*, *fibrous histiocytoma*, and

angiomatoid fibrous histiocytoma [8, 9, 15, 16, 48–56] (Figs. 4.29, 4.30, and 4.31). During the first year of life, *juvenile xanthogranuloma (JXG)* is the leading condition in this broad category. Both benign and malignant forms of *fibrous*

histiocytoma occur in infants, but most are benign [8, 9, 15, 16]. Neonates with *JXG* limited to the skin and/or subcutaneous tissue generally do well with or without treatment. Although most systemic lesions undergo spontaneous involution, ocular and CNS involvement result in significant morbidity and sometimes mortality [53–55]. The *angiomatoid fibrous histiocytoma* is the least common of the group and considered to be of low to intermediate malignancy [9, 15, 16].

4.4.1 Fibrous Histiocytoma

Like most soft tissue tumors of the young, the *fibrous histiocytoma* presents as a palpable mass. The benign fibrous histiocytoma consists of a firm, well-circumscribed or encapsulated tan-gray to yellow, 2–3 cm nodule. Microscopic examination reveals a moderately cellular tumor composed of a mixture of spindle-shaped fibroblastic cells and smaller numbers of round or oval vacuolated histiocytes [15, 16, 48–50] (Fig. 4.28). A few multinucleated giant cells may be present but not the typical Touton giant cells of *JXG*. The interdigitating or “herringbone” and storiform growth patterns are evident in some fields. The mitotic rate in the benign fibrous histiocytoma does not exceed 1 or 2 mitoses per high-power field. Vimentin, α -1-antitrypsin, and factor VIIIa are variably positive [15, 16]. EM studies show spindle-shaped fibroblasts with a prominent rough endoplasmic reticulum, larger, rounder histiocytic cells with variable numbers of lysosomes, and fibrohistiocytes composed of both endoplasmic reticulum and lysosomes. Both the fibrous and histiocytic components are more immature than their mature soft tissue counterparts and show little or no evidence of phagocytosis or production of typical collagen fibers. Most fibrous

histiocytomas found in infants are benign, but they will recur if not completely removed [15, 16].

4.4.2 Angiomatoid Fibrous Histiocytoma

The *angiomatoid fibrous histiocytoma* may have the gross appearance of a large soft tissue hematoma, a hemorrhagic hemangioma, or a severely congested lymph node [8, 15, 16, 51, 52] (Figs. 4.29 and 4.30). The characteristic light microscopic findings consist of central, cystically dilated vascular spaces lined by atypical appearing fibroblasts and histiocytes with pleomorphic and hyperchromatic nuclei and moderate numbers of mitoses (instead of single rows of regular endothelial cells lining the vessels) (Fig. 4.29d, e). About the periphery, lymphoid follicles surround the central hemorrhagic zone giving the tumor the appearance of a lymph node with a hemorrhagic center under low magnification. Because of these inflammatory changes and hemorrhage, the diagnosis may be missed. The myofibroblastic phenotype of this tumor is supported by the reactive vimentin and desmin staining and variable actin, calponin; CD68 and CD99 expression is present in about half [9, 13, 16].

Low recurrence rates and metastases reported in a few patients suggest that angiomatoid fibrous histiocytoma is a tumor of low to intermediate malignancy [15, 16].

4.4.3 Juvenile Xanthogranuloma

Juvenile xanthogranuloma (JXG) is a fibrohistiocytic proliferation of dendritic cell derivation found most often in newborns and infants characterized by one or more cutaneous

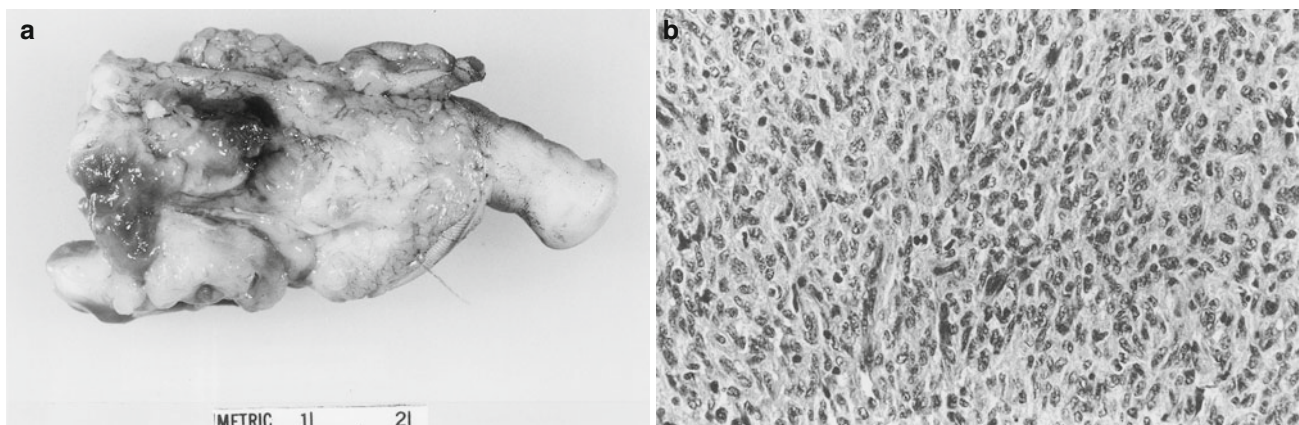


Fig. 4.28 Fibrous histiocytoma. Six-month-old female had an excisional biopsy of a mass on the dorsum of her left foot at 1 month of age. (a) Recurrent tumor consists of a brownish-yellow mass situated within the interosseous muscles and fat. On the left, a toe is attached to the

tumor. (b) Photomicrograph reveals histiocytes and fibroblasts showing noticeable mitotic activity and mild to moderate nuclear atypia (Reprinted from Isaacs [12]. © W.B. Saunders, 1997)

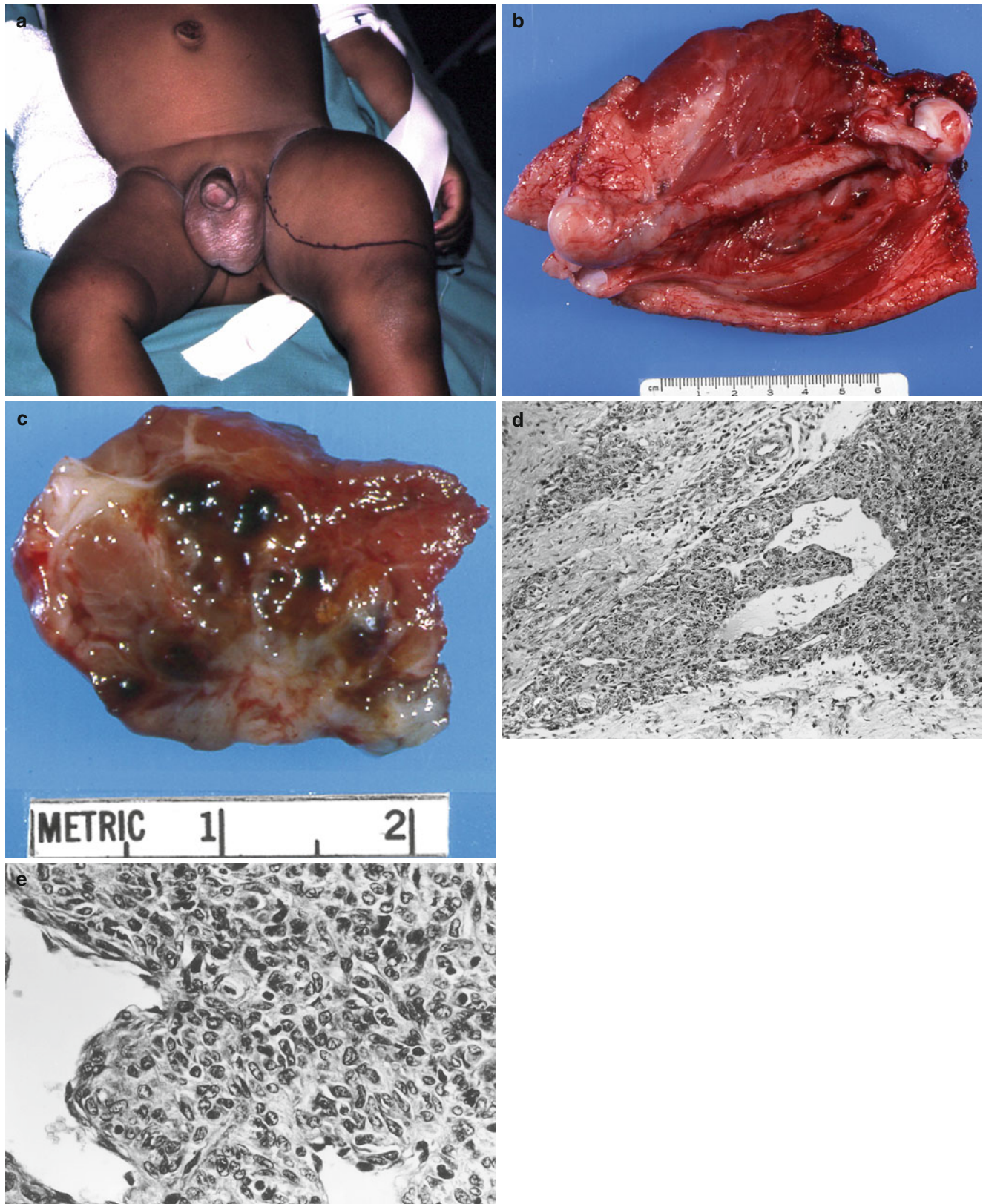


Fig. 4.29 Angiomatoid fibrous histiocytoma. (a) Three-month-old male with a left thigh mass, which gradually increased in size. (b) Amputation specimen showing a dark hemorrhagic mass situated beneath the proximal femur in the belly of the vastus medialis muscle. The head of the femur is situated on the right-hand side of the photograph, and the femoral condyles are on the left. (c) Close-up view of the

involved muscle with tumor, which is composed of several, dark, hemorrhagic sponglike cavities. (d) Vascular channels are bordered by atypical histiocytes and fibroblastic cells. (e) Tumor cells line the vascular channels instead of endothelial cells. Trichrome, (d) and (e) (Reprinted from Isaacs [12]. © W.B. Saunders, 1997)

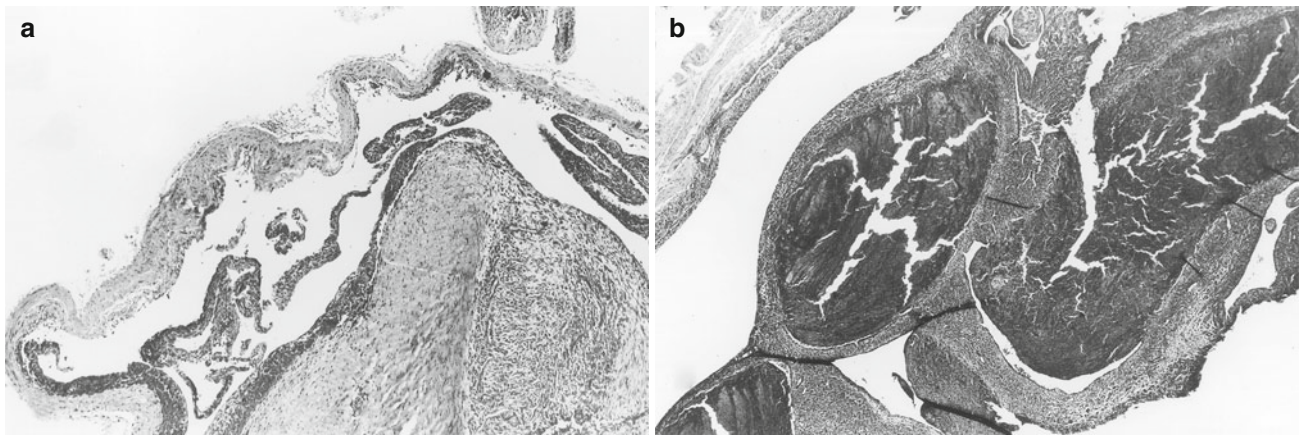


Fig. 4.30 Angiomatoid fibrous histiocytoma of the neck from a 3-month-old male. (a) The partially cystic tumor mass surrounded by a dense fibrous pseudocapsule. (b) The prominent vascular component is shown (Reprinted from Isaacs [12]. © W.B. Saunders, 1997)

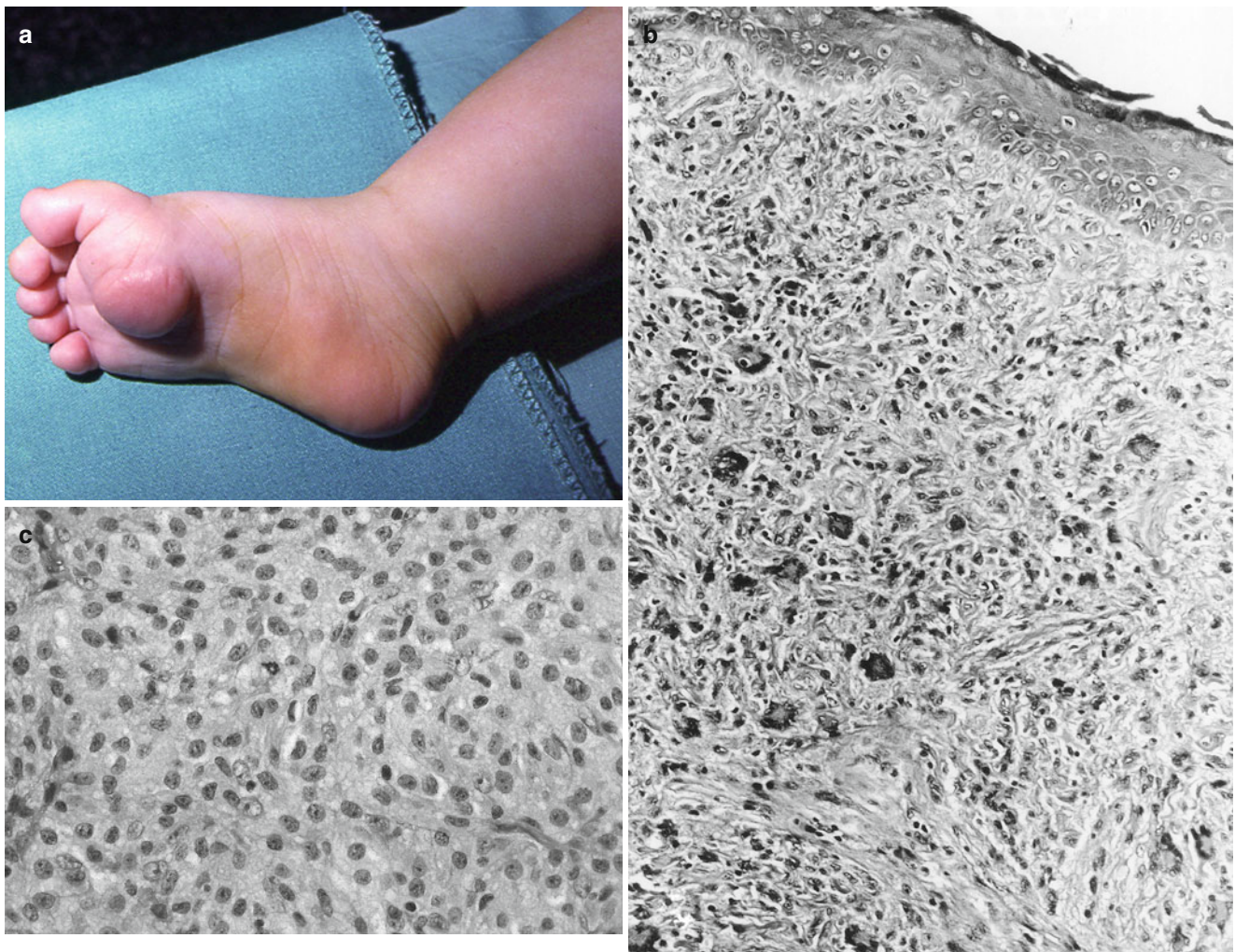


Fig. 4.31 Juvenile xanthogranuloma. (a) Five-month-old male with a mass on the plantar aspect of the right foot present since birth. The specimen measures 3 cm in diameter and has a uniform, smooth tan-yellow cut surface. (b) There is a mixed cellular infiltrate involving the dermis and subcutaneous tissue composed of round to oval histiocytes,

spindle-shaped fibroblasts, and scattered Touton multinucleated giant cells. Some histiocytes appear vacuolated. Fibrosis is present. The epidermis is not invaded. (c) The early phase consists of collections of foamy histiocytes with small foci of lymphocytes (Reprinted from Isaacs [12]. © W.B. Saunders, 1997)

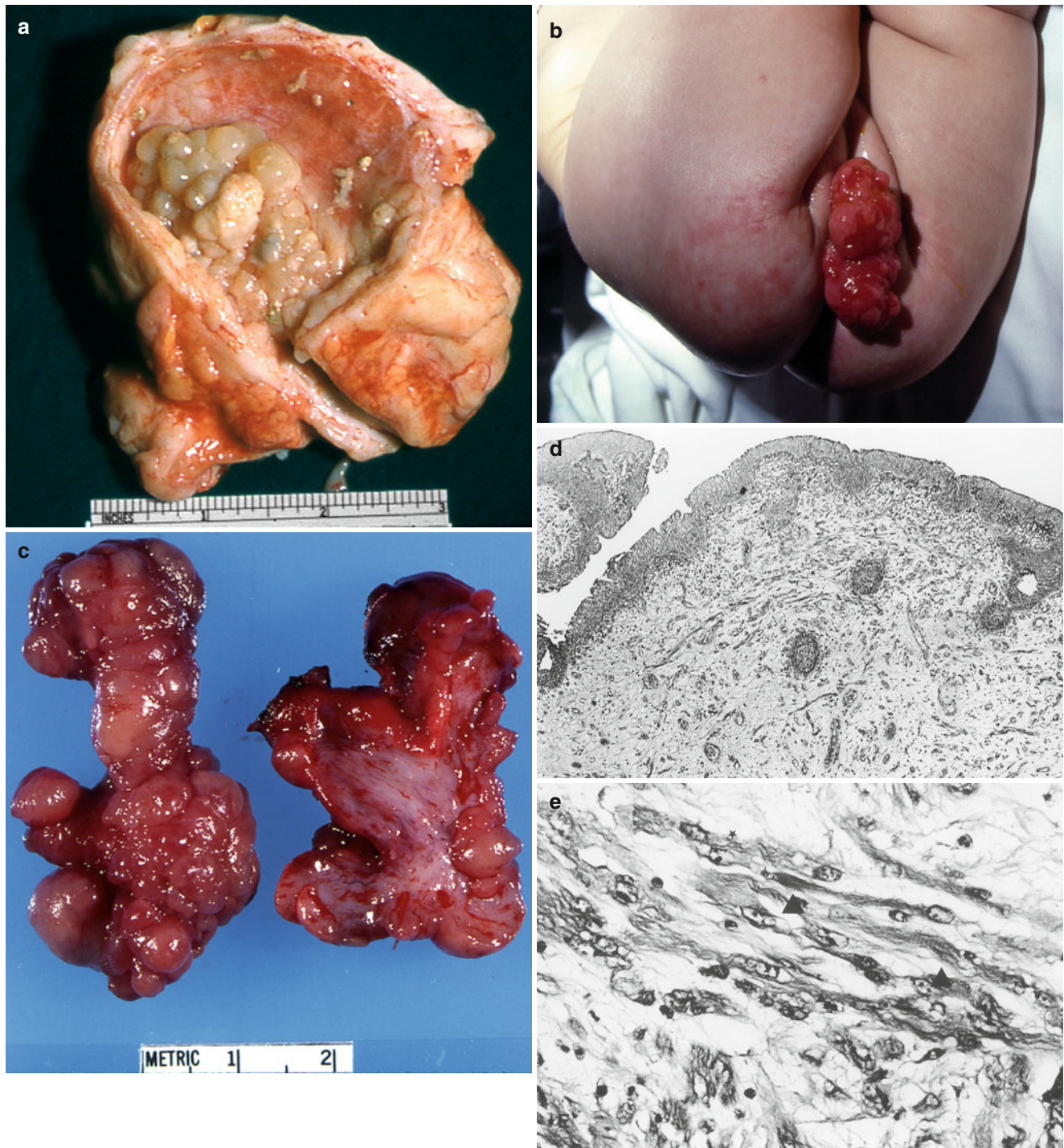


Fig. 4.32 Botryoid embryonal rhabdomyosarcoma. (a) One-year-old male with grapelike tumor masses invading the trigone and posterior wall of the urinary bladder. (b) Seven-month-old female with similar appearing polypoid lesions protruding from the vagina. (c) Gross specimen of (b) showing grapelike masses resting on a pale, gray fibrovascular

stroma. (d) Low-power view of submucosal tumor cells. Directly beneath the vaginal mucosa, there is a cellular rind or mantle composed of tiny rhabdomyoblasts. (e) Rhabdomyoblasts are shown in more detail. Some cells exhibit suggestive cytoplasmic cross striations (*arrowhead*) (Reprinted from Isaacs [12]. © W.B. Saunders, 1997)

nodules or less frequently by lesions in the deep soft tissues or organs [8, 15, 53–56] (Chap. 8) (Fig. 4.31a). Most infants with cutaneous JXG have solitary rather than multiple nod-

ules, 78 % versus 22 % in one newborn study [55]. The cutaneous JXGs occur as red to yellow-brown papules distributed on the head, neck, and extremities which usually regress

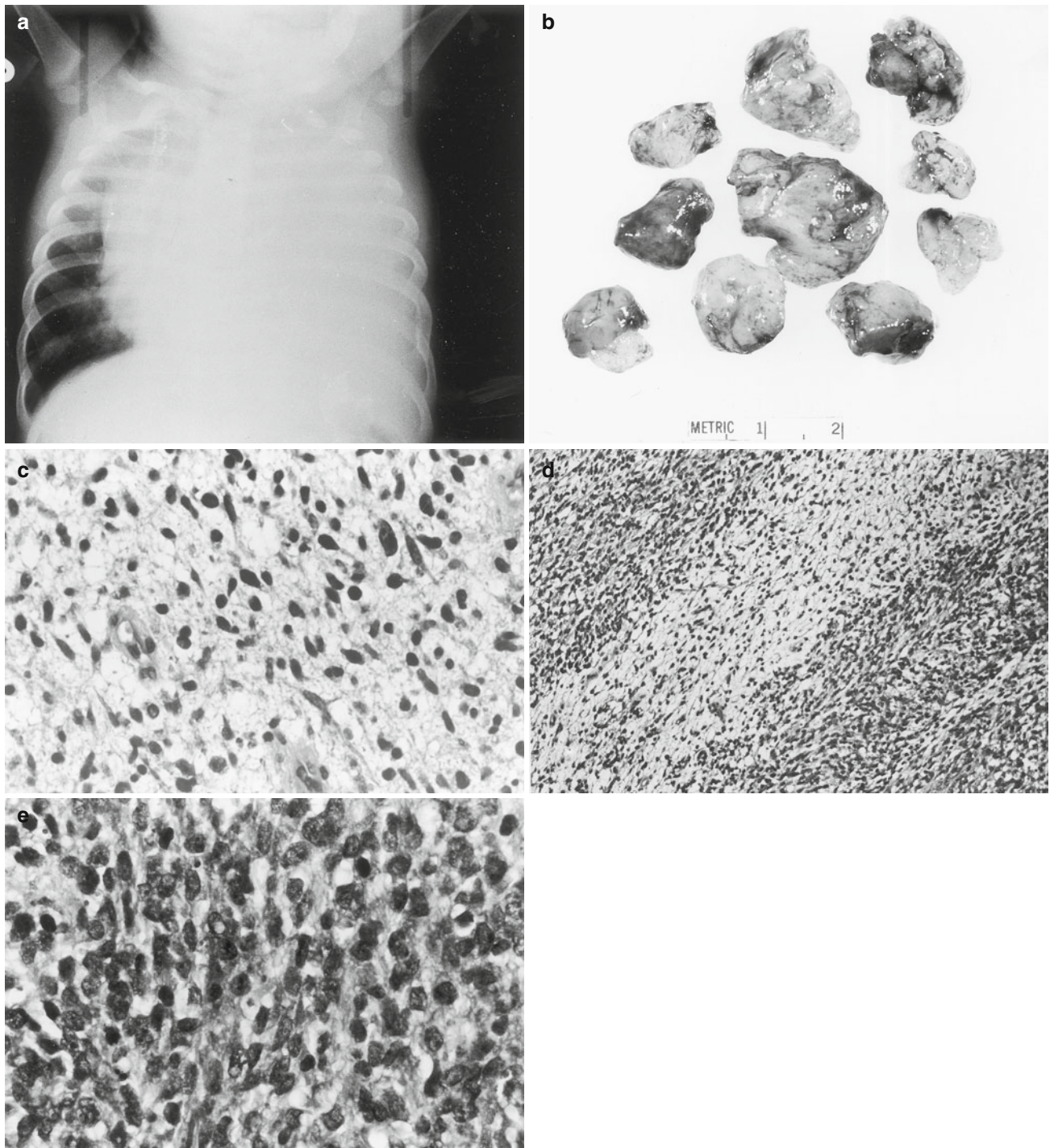


Fig. 4.33 Embryonal rhabdomyosarcoma of the mediastinum. (a) Chest X-ray of an 8-month-old male with a 1-week history of a cough and progressive respiratory distress. Imaging reveals consolidation of the left thorax with displacement of the mediastinum to the left. In the differential diagnosis of a thoracic “white out” consolidation in an infant, the main following neoplastic conditions should be considered: pleuropulmonary blastoma, pleuropulmonary PNET (“Askin tumor”), and rhabdomyosarcoma. Malignant lymphoma is very rare in infants. (b) Biopsy material obtained from the mediastinal mass showing a soft

gray gelatinous appearance. (c) The tumor consists of small, darkly staining rhabdomyoblasts situated in a myxoid (pale-gray staining) background. The cells are round, tadpole shaped or elongated. Cytoplasm is slightly vacuolated. (d) Myxoid areas alternating with hypercellular areas are characteristic of this tumor. (e) Cellular area composed small, poorly differentiated cells. Tumor cells were immunoreactive only with desmin, actin, and vimentin and nonreactive with NSE and LCA (Reprinted from Isaacs [12]. © W.B. Saunders, 1997)

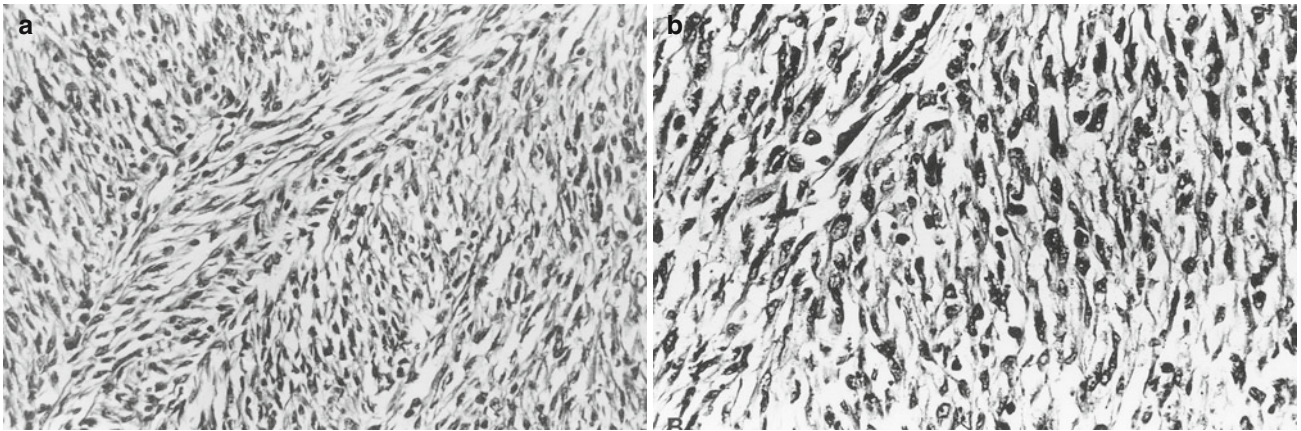


Fig. 4.34 Embryonal rhabdomyosarcoma, spindle cell type. Biopsy of a large, unresectable pelvic mass arising from the prostate and urinary bladder in a 6-month-old male. (a) The tumor consists of small spindle-shaped rhabdomyoblasts displaying an interdigitating (“herringbone”)

growth pattern. (b) Higher power view depicting elongated spindle-shaped rhabdomyoblasts. Tiny tadpole-shaped cells are present. Vimentin and muscle markers were positive (Reprinted from Isaacs [12]. © W.B. Saunders, 1997)

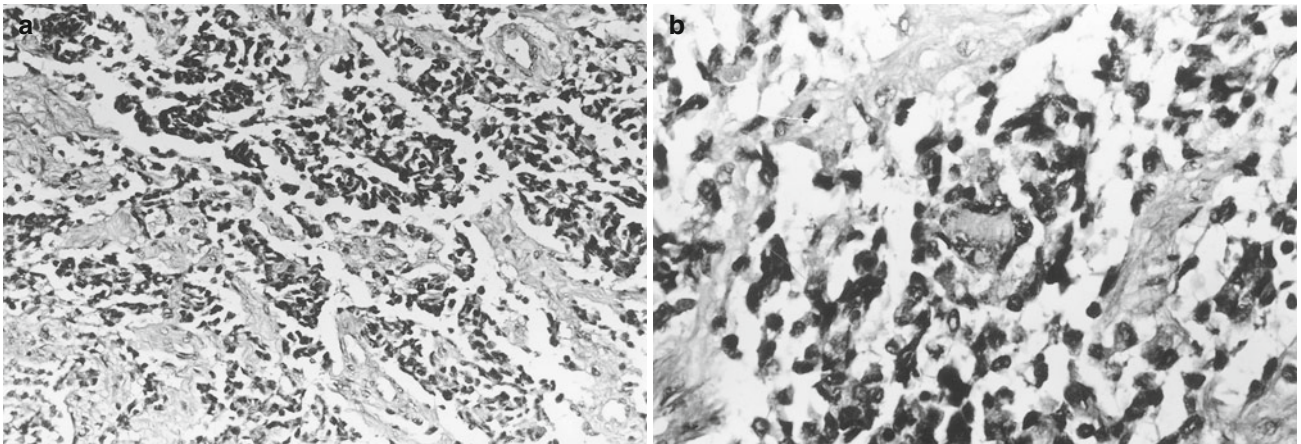


Fig. 4.35 Alveolar rhabdomyosarcoma. Seven-month-old male with a thigh mass and metastases to the lip and cervical lymph nodes. (a) Small darkly staining tumor cells are situated in alveolar-like spaces separated by slightly vascular fibrous septae. (b) Higher magnification depicting the variable morphology of the tumor cells. There is a tumor

giant cell in the center of the field. (c) Tumor cells stained positively only for skeletal muscle markers desmin and vimentin. (d) EM showing diagnostic cytoplasmic myofilaments (Electron photomicrograph courtesy of Darkin Chan, Children’s Hospital Los Angeles; Reprinted from Isaacs [12]. © W.B. Saunders, 1997)

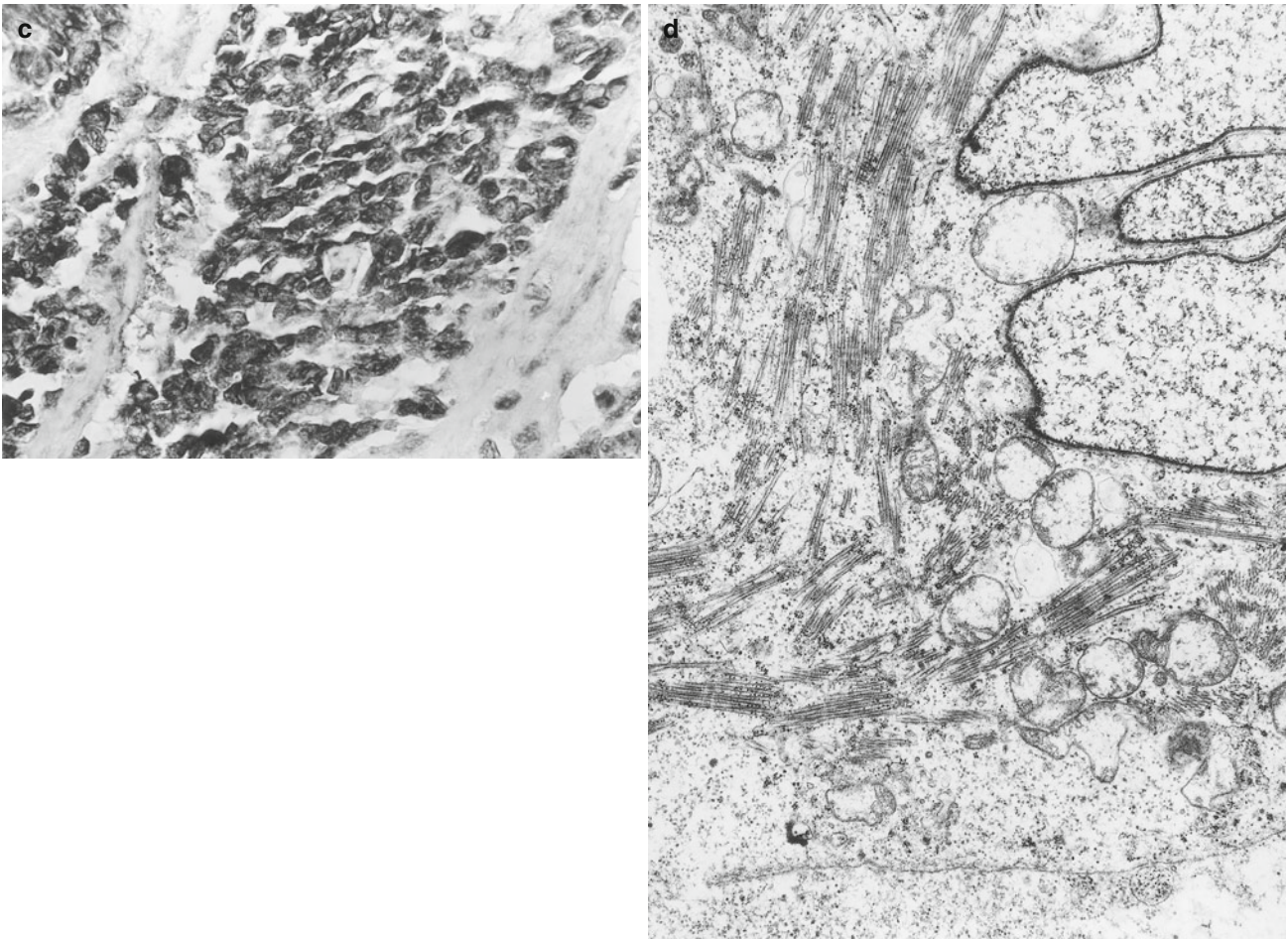


Fig. 4.35 (continued)

within 2 years of diagnosis [53–55]. The tumors occur in other sites as the eye, heart, lung, and deep soft tissues which may or may not be present with cutaneous lesions [53–56].

Systemic involvement is rare but associated with significant morbidity and occasional deaths [53–55]. Symptoms are usually referable to bulky or infiltrative disease. The most frequent extracutaneous locations are the subcutaneous soft tissue, central nervous system, liver, spleen, lung, eye/orbit, oropharynx, and muscle—in that order [55]. Deep-seated JXGs occur as firm nodules averaging 2–4 cm in size varying from tan-gray to tan-yellow on cross section [15, 16, 53–55]. The extracutaneous JXGs have essentially the same histological features as the cutaneous ones consisting of sheets of well-differentiated histiocytes with eosinophilic or foamy cytoplasm and vesicular nuclei (Fig. 4.31b). There are multinucleated Touton giant cells characterized by peripheral wreaths of nuclei. Eosinophils about the periphery of the tumor are a prominent feature [54]. Variable numbers of lymphocytes and plasma cells are present as well.

The histiocytic nature of the tumor cells is confirmed by EM. The cells are composed of pseudopodia, lysosomes, and lipid droplets [15, 16]. Racket-shaped Birbeck granules characteristic of Langerhans cells are notably absent [54, 55]. JXG immunohistochemical studies show reactivity for CD68 and factor X111a and no reactivity for CD1a and S-100 [54].

Touton giant cells, which are requisite for establishing the diagnosis, may not be present in the early active proliferative phase, especially in extracutaneous locations. In older lesions, foci of fibrosis may have the storiform and herringbone growth patterns seen in fibrous histiocytoma, the fibromatoses, and fibrosarcoma [16, 54, 56]. There is no correlation between histology with clinical findings or outcome [55].

Practically, all infants with JXG limited to the skin and/or subcutaneous tissue survive with or without treatment, but ocular and CNS involvement are associated with a less favorable outcome. Newborn mortality rate can be as high as 25 % [55].

4.5 Skeletal Muscle Tumors

Tumors of skeletal muscle are of two main types, *rhabdomyoma* and *rhabdomyosarcoma*. The former is a rare, benign skeletal muscle lesion comprising less than 2 % of all striated muscle tumors whereas the latter is the most common soft tissue sarcoma in childhood [6, 8, 15]. Rhabdomyoma is subclassified further into fetal and adult types [57]. Generally, *fetal rhabdomyomas* are found in infants, and they more closely resemble developing skeletal muscle than the adult form, which is typically noted in later life [57–59]. Rhabdomyomas of the female genital tract are regarded as a special form of fetal rhabdomyoma. *Cardiac rhabdomyoma* is a distinct lesion, probably hamartomatous, found primarily in cardiac muscle and is associated with tuberous sclerosis [9, 60, 61] (see Chap. 15).

4.5.1 Rhabdomyoma

The most common site of the extracardiac *fetal rhabdomyoma* is the subcutaneous tissue of the head and neck region [15, 16, 57–59]. Rhabdomyomas present as slowly growing solitary masses within the soft tissue or submucosa, most often in the pre- and postauricular areas followed in frequency by the neck, nasopharynx, and tongue. The abdominal wall and the retroperitoneal area are other locations [57].

Grossly, fetal rhabdomyomas are circumscribed but not encapsulated, light-gray to tan-pink nodules, averaging 3 cm in size. Microscopically, they show haphazardly arranged, fetal-appearing, slender skeletal muscle cells with cross striations separated by a pale-staining myxoid stroma containing small oval to spindle-shaped undifferentiated cells [16, 57–59]. Mitoses are essentially absent, and nucleoli are small. The immunoperoxidase skeletal muscle markers are reactive, and EM findings are consistent with skeletal myocytes in different stages of development [57–59]. Local recurrence rate is low, less than 10 %.

The diagnosis of rhabdomyoma in a young child should be made with caution, since the tumor is so rare. On the other hand, recognition of fetal rhabdomyoma is important to prevent unnecessary treatment and morbidity [15].

4.5.2 Rhabdomyosarcoma

Rhabdomyosarcoma (RMS) is primarily a neoplasm of children and adolescents comprising over half of all sarcomas in this age group. RMS occurs less often than fibrosarcoma in fetuses and infants than in older individuals [11, 12, 15, 16, 62, 63]. Traditionally, the tumor is considered a sarcoma derived from the embryonic skeletal muscle cell, the rhabdomyoblast [12, 15, 16]. RMS is a highly malignant

neoplasm accounting for most soft tissue malignancies in infants and second or third in frequency in the newborn [11, 62, 63].

There are associations between RMS and hereditary diseases and congenital malformations [14, 64, 65]. Postmortem studies performed on 115 children enrolled in the Intergroup Rhabdomyosarcoma Study revealed that 37 (32 %) had congenital malformations and over half of these involved the central nervous system [64]. An increased frequency of breast carcinoma and brain tumors is noted in families of patients with this sarcoma: the so-called family cancer syndrome [65]. RMS is one of the malignancies occurring in patients with neurofibromatosis I [9, 66].

Cytogenetic studies reveal karyotypic differences between *embryonal* and *alveolar rhabdomyosarcomas* [9, 16]. The former shows a loss of heterozygosity of one of the short arms of chromosome 11 whereas the latter a translocation between chromosomes 2 and 13 [t(2;13) (q35;q14)].

RMS seldom occurs at birth; approximately 3 % of the pediatric age group with this neoplasm are diagnosed in the first month of life, and 10 % are found in patients less than 1 year of age [1, 5, 15, 62, 63]. The tumor is detected on prenatal ultrasound examination [15]. The head and neck region and the genitourinary tract are the leading primary sites in the newborn and infant [6, 7, 15].

RMSs can be subclassified according to the International Classification of Rhabdomyosarcoma: *embryonal*, *botryoid*, *alveolar*, *spindle cell*, and *undifferentiated* [9, 67] (Tables 4.1 and 4.2). As in the older child and adolescent, most RMSs diagnosed in the first year of life are of the embryonal and botryoid types [15]. Patients with the alveolar form, ranking third, may present with metastatic disease. The RMS subtypes with the most favorable prognosis are the botryoid and spindle cell types; embryonal RMS has an intermediate prognosis and alveolar RMS the worst [9, 15].

The *botryoid form of embryonal rhabdomyosarcoma* arises from mucosal lined body cavities, for example, the vagina, urinary bladder, oral cavity, middle ear, and biliary system. Typically, it forms lobulated, grapelike, polypoid projections with pale-gray gelatinous cut surfaces (Fig. 4.32). Microscopic examination reveals tiny, round to spindle-shaped rhabdomyoblasts situated directly beneath the epithelium located in a submucosal cellular rind or mantle (Fig. 4.32d, e). Well-defined cytoplasmic cross striations are often difficult to find. Desmin and actin immunoperoxidase stains are helpful in identifying the small cells as rhabdomyoblasts. The remainder of the polyp consists of pale-staining myxoid-appearing connective tissue and blood vessels. The botryoid form has the most favorable prognosis of all the histological types [15, 67]. *Embryonal and alveolar rhabdomyosarcomas* consist of a gray-white, myxoid-appearing infiltrative mass, seldom encapsulated, with more extensive necrosis and hemorrhage than that observed in the botryoid

Table 4.3 Clinical group stage system used in intergroup rhabdomyosarcoma studies [I–III]

I. Localized disease, completely resected
II. Total gross resection with evidence of regional spread
A. Grossly resected tumor with microscopic residual disease
B. Regional disease with involved nodes, completely resected with no microscopic residual disease
C. Regional disease with involved nodes, grossly resected but with evidence of microscopic residual disease and/or histological involvement of the most distal regional node (from the primary site) in the dissection specimen
III. Incomplete resection with gross residual disease
IV. Distant metastatic disease present at onset

Reprinted from Huh and Skapek [71]. With kind permission of © Springer, 2010

type. *Embryonal rhabdomyosarcoma* shows considerable variation in morphology, showing cellular areas alternating with pale myxoid areas [16] (Fig. 4.33). The more differentiated tumors show round to oval, sometimes tadpole or racket-shaped cells, giant cells with irregular nuclei and eosinophilic staining cytoplasm, and occasionally, cytoplasmic cross striations.

Some poorly differentiated embryonal and alveolar RMSs have the same nondescript, histological appearance as the other “small blue cell malignant tumors” of infancy and childhood; therefore, immunohistochemical and EM studies are required to definitely establish their diagnosis [15]. Table (Fig. 4.2) lists the histological differential diagnoses of the small blue cell malignant tumors of infancy.

Spindle-cell rhabdomyosarcoma is a “prognostically favorable variant” of embryonal RMS [6, 8, 15, 68]. The paratesticular area and urinary bladder are the most common sites. Microscopically, the tumor consists of uniform spindle-shaped rhabdomyoblasts displaying an interdigitating (“herringbone”) growth pattern (Fig. 4.34). The tumor cells react with vimentin and with the skeletal muscle markers, actin and desmin [15, 68].

Alveolar rhabdomyosarcoma has a characteristic microscopic picture consisting of small round to spindle-shaped cells forming irregular cyst-like spaces mimicking pulmonary alveoli (Fig. 4.35). In some instances, with adequate preservation, the rhabdomyoblasts attached to the lining of the fibrovascular septae appear to “spin off” into the lumen. Although well-defined cross striations are difficult or sometimes impossible to find, the positive vimentin and desmin immunoperoxidase staining, Z-band material and/or thick and thin filaments observed in the tumor cells by EM and the t(2;13) translocation confirm the diagnosis (Fig. 4.35d). In addition, there is a less well-differentiated form called “*solid*” *alveolar rhabdomyosarcoma* [69]. This variant is composed of sheets of small cells with round nuclei but without fibrous septa and alveolar-like spaces. Moreover, the t(2;13)

(q35;q14) chromosomal anomaly, characteristic of alveolar rhabdomyosarcoma, is present.

The prognosis of patients with RMS depends on three main factors: the location, stage (extent of disease), and histological type [6, 15, 62, 63, 67]. A poorer outcome is reported for infants with RMS compared with older children [62, 63, 70] (Table 4.3).

4.6 Rhabdoid Tumor

Rhabdoid tumor of the kidney was identified as a neoplasm different from that of Wilms’ tumor in the 1970s [72]. The tumor was given the name “rhabdoid” because microscopically, it resembles a rhabdomyosarcoma although it does not show skeletal muscle components either by immunoperoxidase studies or by EM. This highly malignant neoplasm, characterized clinically by early metastases and a high mortality rate, occurs in the fetus, infant, and occasionally in older age groups (see also Chaps. 5, 7, and 8). The most common primary sites in the fetus and infant are the skin and soft tissues followed by the kidney and CNS [9, 15, 17, 72–75]. The main extrarenal locations are the skin, soft tissues of the chest wall, orbit, face, and neck [17]. Rhabdoid tumor may appear as one or more metastatic cutaneous nodules prior to the discovery of the primary tumor [74–75]. Moreover, it may present as widespread metastases without a definite primary and prove to be rapidly fatal [17, 74, 75]. Metastases are found at the time of diagnosis in most patients, 70 % in one review [17]. The tumor spreads to multiple sites such as the skin, placenta, skeleton, kidney, brain, lungs, and liver. Cytogenetic analysis shows deletions of chromosome 22q11 and mutations of the INI1 gene resulting in loss of the hSNF5/INI1 protein, which is helpful in the diagnosis [9, 17, 74]. The histogenesis of this neoplasm is unknown [17, 74].

Rhabdoid tumors of soft tissue are similar histologically to those arising in the kidney and brain. The rhabdoid cells are round to oval with large vesicular nuclei typically having one big, round nucleolus. Pink-staining cytoplasm contain red inclusions composed of intermediate filaments demonstrated by EM and immunohistochemistry [9, 15, 17, 73–75] (Fig. 11.21). Some rhabdoid tumors have the appearance of a malignant small blue cell tumor containing only a few scattered rhabdoid cells. Tumor cells are immunoreactive with both vimentin and keratin and variably with EMA, actin, NSE, and S-100 protein [9, 15, 73–75]. The presence of rhabdoid cells and absence of the hSNF5/INI1 protein by immunochemistry are considered diagnostic [9].

Prognosis for young patients with rhabdoid tumor is dismal [73–75], for example, it was less than 10 % in one infant study [17].

4.7 Adipose Tissue Tumors

Tumors of fatty tissue origin are not as common in infants as in adults, in whom they comprise most of the soft tissue neoplasms [15, 16, 76–78]. There are two main types of adipose tissue: white and brown fat [16]. Generally, white fat is located in the subcutaneous tissue, abdomen, retroperitoneum, and mediastinum. The back, neck, mediastinum, axilla, and retroperitoneum are the main locations for brown fat, which is found more often in infants and children [15, 16] (Fig. 4.36).

Both the clinical features and the pathological appearance of a *lipoma* are essentially the same as in older individuals [15, 16, 76]. Most present as a slowly growing, painless, soft subcutaneous mass (Fig. 4.37). Less than a third are noted at birth.

Benign adipose tissue tumors are classified into several categories: *lipoma*—single, multiple, superficial, and deep; variants of lipoma, namely, *lipoblastoma* and *angiomyolipoma*; heterotopic lipoma, for example, intra- and *intramuscular lipoma* and *neural fibrolipoma*; infiltrating proliferations of mature fat cells—*lipomatosis*; and *hibernoma*, a benign neoplasm of brown fat [15, 16]. Neural fibrolipomas are present in newborns as a component of a spinal dysraphic malformation, for example, myelomeningoceles.

4.7.1 Lipoblastoma

Lipoblastoma is a benign tumor related to embryonic white fat having the property for differentiation over a period of time [15, 16, 76–78]. It occurs primarily during the first 3 years of life. *Lipoblastoma* is defined as the circumscribed form and *lipoblastomatosis* as the diffuse form of this tumor [16]. The diffuse form usually arises in deep soft tissue, has an infiltrative, lobular growth pattern and an increased tendency to recur. The upper and lower extremities are the most common sites where the tumor presents as a painless mass [15, 16, 78]. Trunk and retroperitoneum are less frequent locations. The neoplasm may compress or impair function of adjacent structures because of its size and location [76, 77].

Lipoblastoma grows slightly more rapidly than a lipoma and has a much firmer consistency. On cross section, they are paler and more grayish (myxoid) in appearance than a typical lipoma (Fig. 4.38a). The tumors range in size from 2 cm to over 14 cm in greatest diameter [16, 76, 77]. Microscopic examination shows immature fat cells with varying degrees of differentiation separated by connective tissue septa and loose myxoid areas. The presence of lipoblasts with a bubbly, vacuolated cytoplasm is requisite for the diagnosis. Usually, mitoses are not observed. The underlying skeletal muscle may be involved. Over half the tumors consist of mature fat cells and thus in some areas have the appearance of a lipoma (Fig. 4.38b). Lipid vacuoles stain positively with

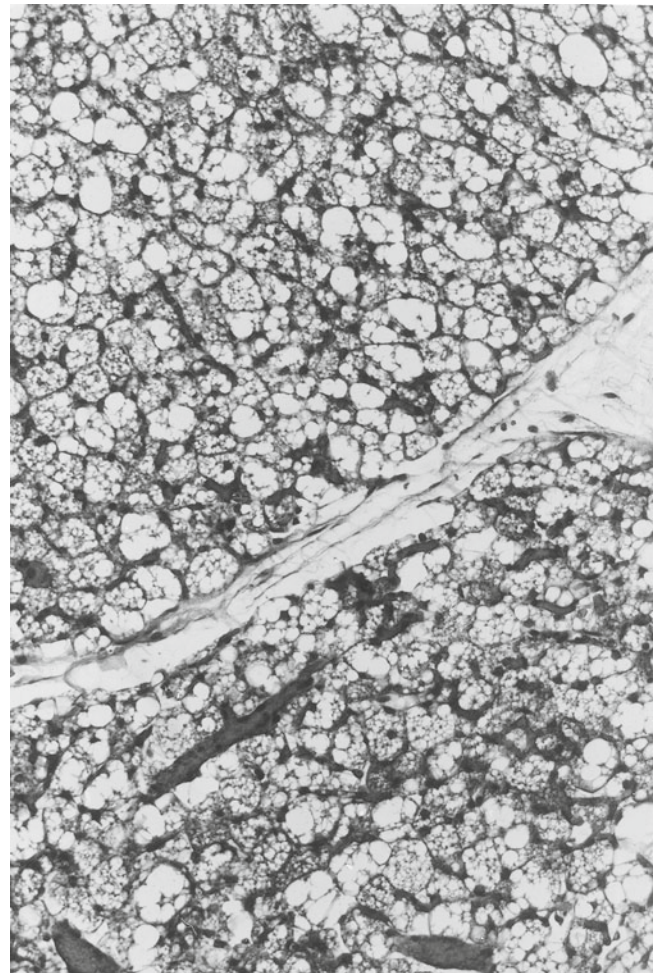


Fig. 4.36 Brown fat. The specimen was removed incidentally from a 7-week-old male as part of the thymus during a thoracotomy for correction of a congenital heart defect. The adipocytes are arranged in lobules and are composed of finely vacuolated or granular cytoplasm. Nuclei are small and round and tend to be centrally located. Transitions between brown and clear white fat cells are present (Reprinted from Isaacs [12]. © W.B. Saunders, 1997)

oil red O. Immunoperoxidase studies performed on lipoblastoma reveal that the tumor cells are S-100 positive and non-reactive with vimentin, actin, Leu-7, and factor VIII [76, 77]. The EM findings of lipoblastoma resemble developing white fat and show lipoblasts in various stages of maturation [15].

Lipoblastomas and lipoma are cured by complete excision of the mass, and patients with these tumors usually have a favorable outcome [15, 16, 76–78]. Chung and Enzinger quoted a low recurrence rate of 14 %, which they attributed to incomplete removal of the lipoblastoma [78]. Sequential biopsies have shown that lipoblastomas tend to spontaneously mature to lipomas or fibrolipomas, which conceivably accounts for their good prognosis despite an inadequate excision [15, 16, 76, 77].

Liposarcoma in infants is extremely rare and the subject of an isolated case report [15].

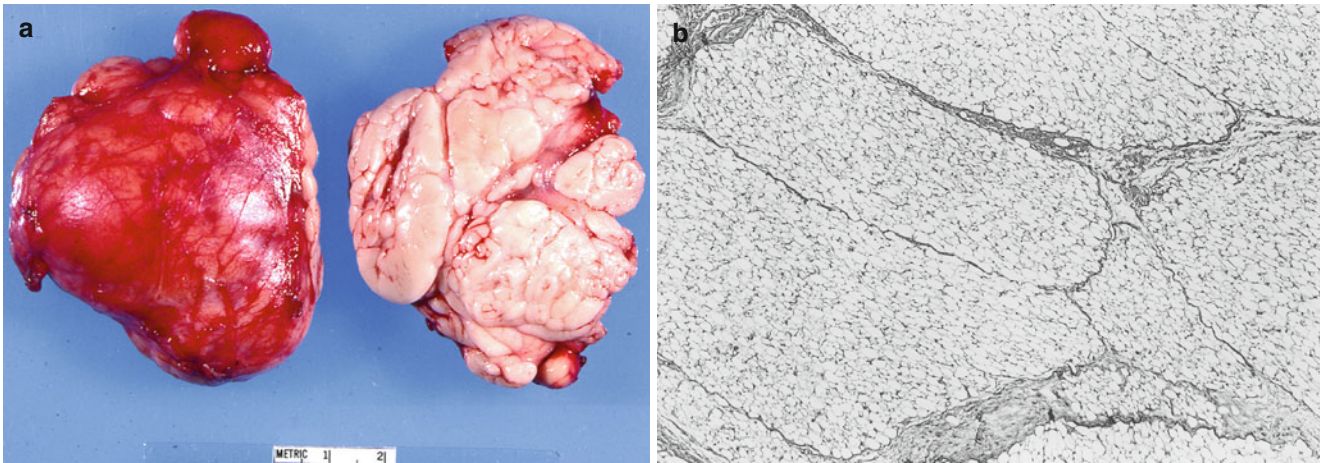


Fig. 4.37 Lipoma. (a) 6×5.5 cm mass present for several months was removed from the right side of the neck of 6-month-old male. The cut surface demonstrates the typical lobular pattern typical of lipomas.

(b) Low-power view shows the lobular pattern and the uniform, mature fat cells (Reprinted from Isaacs [12]. © W.B. Saunders, 1997)

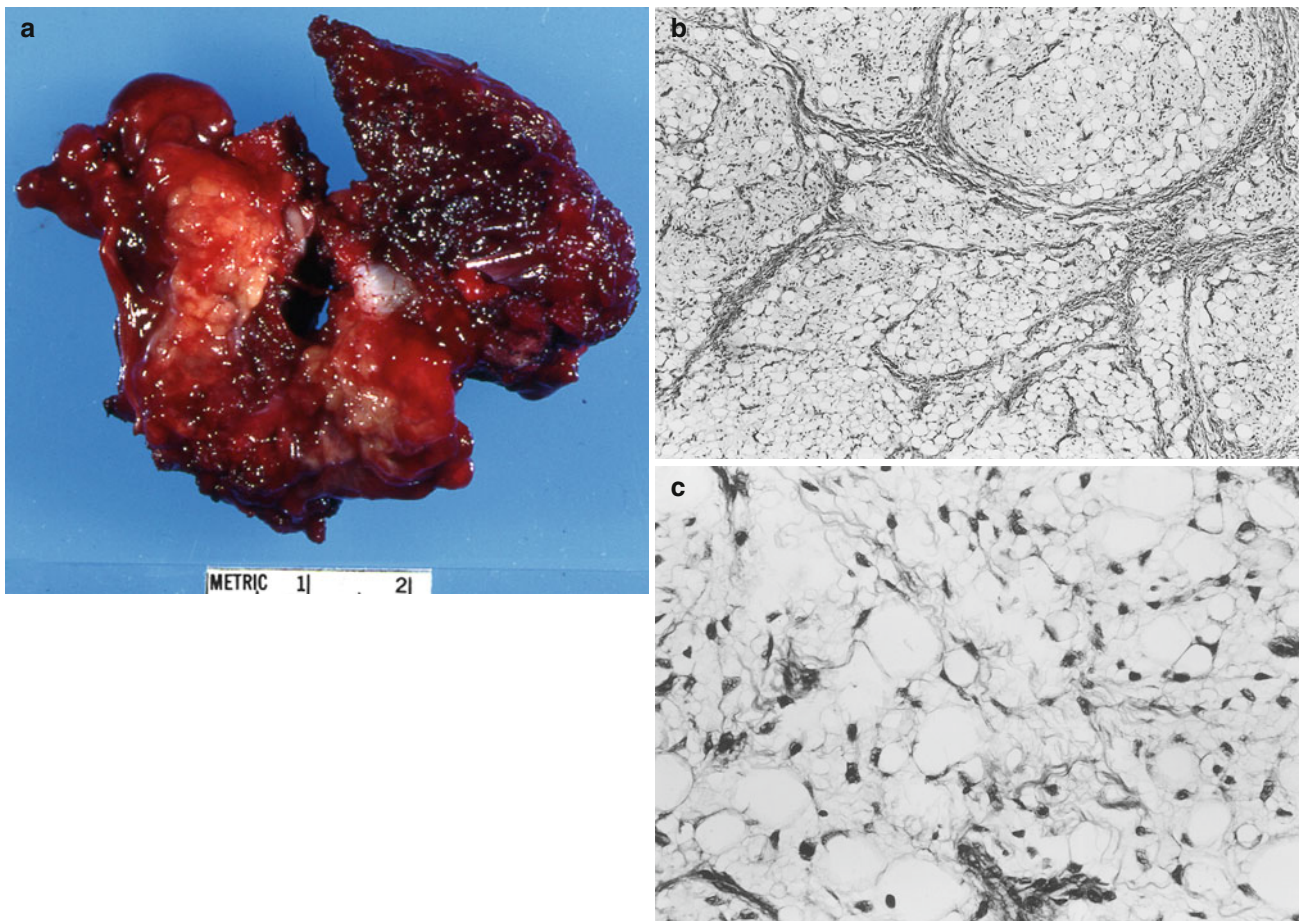


Fig. 4.38 Lipoblastoma. (a) 4×2 cm mass removed from the back of a 1-year-old female. The tumor has a tan to yellow nodular cut surface. Lobules are less well defined compared to the lipoma above. (b) The tumor shows an infiltrative pattern consisting of immature fat cells and

myxoid areas separated by fibrous septae. (c) Vacuolated lipoblasts are situated in myxoid areas and infiltrate skeletal muscle (Reprinted from Isaacs [12]. © W.B. Saunders, 1997)

4.8 Peripheral Nervous System Tumors

Peripheral nervous system tumors are considered neural crest in origin and include a wide variety of benign and malignant conditions [9, 12, 15, 79–86]. Not all members of this group occur in the fetus and infant. However, the mundane *neurofibroma* and the more exotic entities *primitive neuroectodermal tumor (PNET)*, *melanotic PNET*, *ectomesenchymoma*, and *malignant “triton” tumor* are reported in the first year of life [9, 12, 79–86] (Figs. 4.39, 4.40, and 4.41). However, a few examples of congenital malignant peripheral nerve sheath tumors are mentioned [86].

4.8.1 Neurofibroma

Neurofibroma occurs either as a single dermal or soft tissue mass or as multiple tumors in association with cafe-au-lait spots and neurofibromatosis type 1 (Von Recklinghausen disease), which is an autosomal dominant disorder. Some neurofibromas are detected on imaging before or after birth while others are not observed until later on in childhood, adolescence, or adulthood [12, 13, 87]. There is a strongly positive family history associated with perinatal neurofibromatosis, as high as 70 % [87]. In the fetus and infant, neurofibromatosis may manifest clinically in a variety

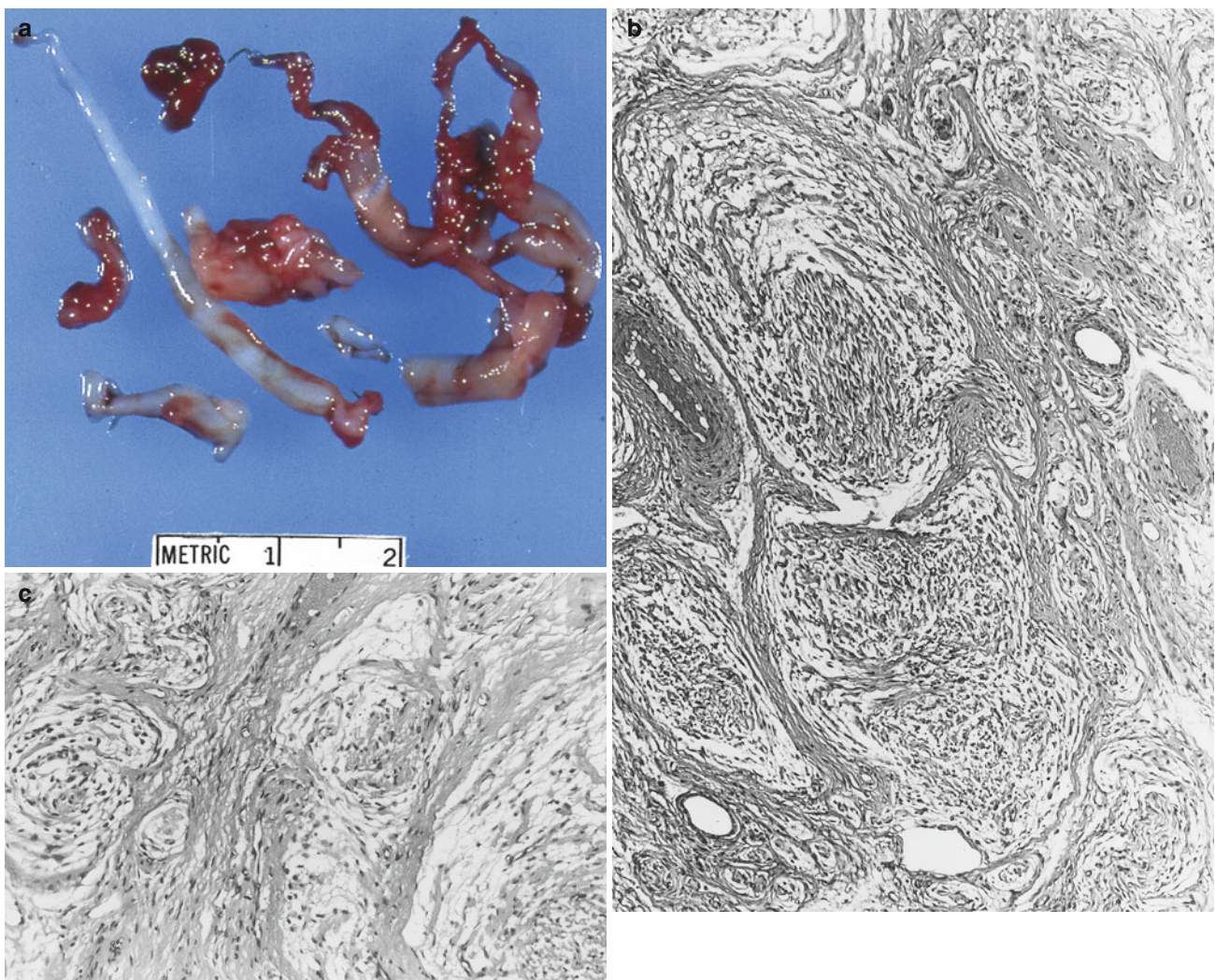


Fig. 4.39 Plexiform neurofibroma. One-year-old male with neurofibromatosis I and a disfiguring facial mass since birth. (a) The excised specimen consists of several, elongated, white, and shiny worm-like pieces of tissue. (b) Tumor is composed of enlarged, myxoid-appearing nerve trunks with proliferations of neurites and Schwann

cells. (c) Higher power view showing the expanded nerve trunks with neurites and Schwann cells situated in a pale-staining stroma. The facial area is one of the most common sites for neurofibromatosis I in young children (Reprinted from Isaacs [12]. © W.B. Saunders, 1997)

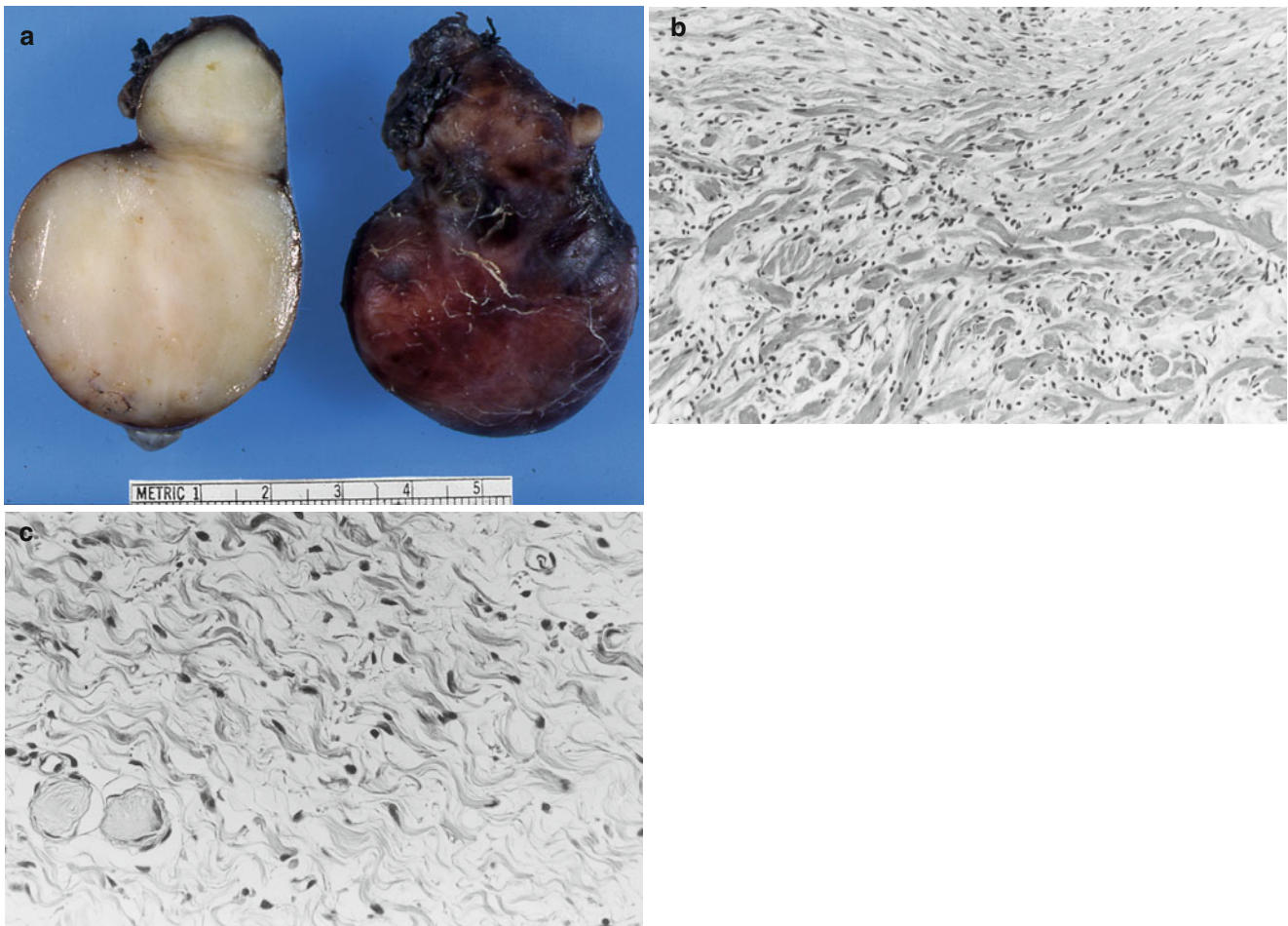


Fig. 4.40 Diffuse neurofibroma. (a) The cut surface is light gray, smooth, and bulging. (b) Microscopic examination reveals interlacing bundles of elongated cells with wavy, darkly staining nuclei. Wirelike strands of collagen and pale-staining mucoid material are present. (c) Another area of the tumor displays irregular, thick bundles of collagen

and scattered Schwann cells separated by pale mucoid matrix. Structures consistent with Pacinian corpuscles are present in the lower left corner of the photograph (Reprinted from Isaacs [15]. © Springer-Verlag, 2002)

of ways [13, 15, 87]. The leading presenting findings in the fetus are hydrops, macrocephaly, and thickened soft tissues and those in the neonate café-au-lait macules, skin nodules, and buphthalmos [87]. Survivors eventually develop serious sequelae such as progressive growth of neurofibromas within the oral cavity, neck, and mediastinum leading to increasing airway obstruction; an enlarging, proptotic glaucomatous eye; and occurrence of brain and malignant nerve sheath tumors. Congenital generalized (disseminated) neurofibromatosis is associated with a poor prognosis and a mortality rate as high as 92 % [87].

Neurofibromas are grouped into three main histological types: solitary, plexiform, and diffuse [16]. Microscopically, the *solitary* type consists of neurites, Schwann cells, and collagen bundles surrounded by a pale-staining myxoid stroma. *Plexiform neurofibroma*, the hallmark of neurofibromatosis type I, grossly resembles a bunch of pale-white worms and microscopically shows expansion of nerve fibers by irregu-

lar, tortuous, haphazardly arranged proliferations of Schwann cells, neurites, and collagen fibers within a pale-staining stroma (Fig. 4.39). *Diffuse neurofibroma* occurs in children with or without neurofibromatosis and in association with congenital melanocytic nevi having neural differentiation (see Chap. 5). The tumor subtly infiltrates the lower dermis and subcutaneous tissue as firm, homogeneous white tissue consisting of tiny round to oval Schwann cells, wavy neurites embedded within a pale-staining connective tissue stroma [16] (Fig. 4.40). Neurofibromas are immunoreactive with S-100, Leu-7, and vimentin [9].

Skeletal malformations are noted in almost half the patients with neurofibromatosis type I [13, 16, 87]. Spinal deformities including vertebral dysplasia and kyphoscoliosis are the main ones; congenital tibial pseudoarthrosis is next in frequency [13, 87].

Several other neoplasms, both benign and malignant, occur in association with neurofibromatosis such as gangli-

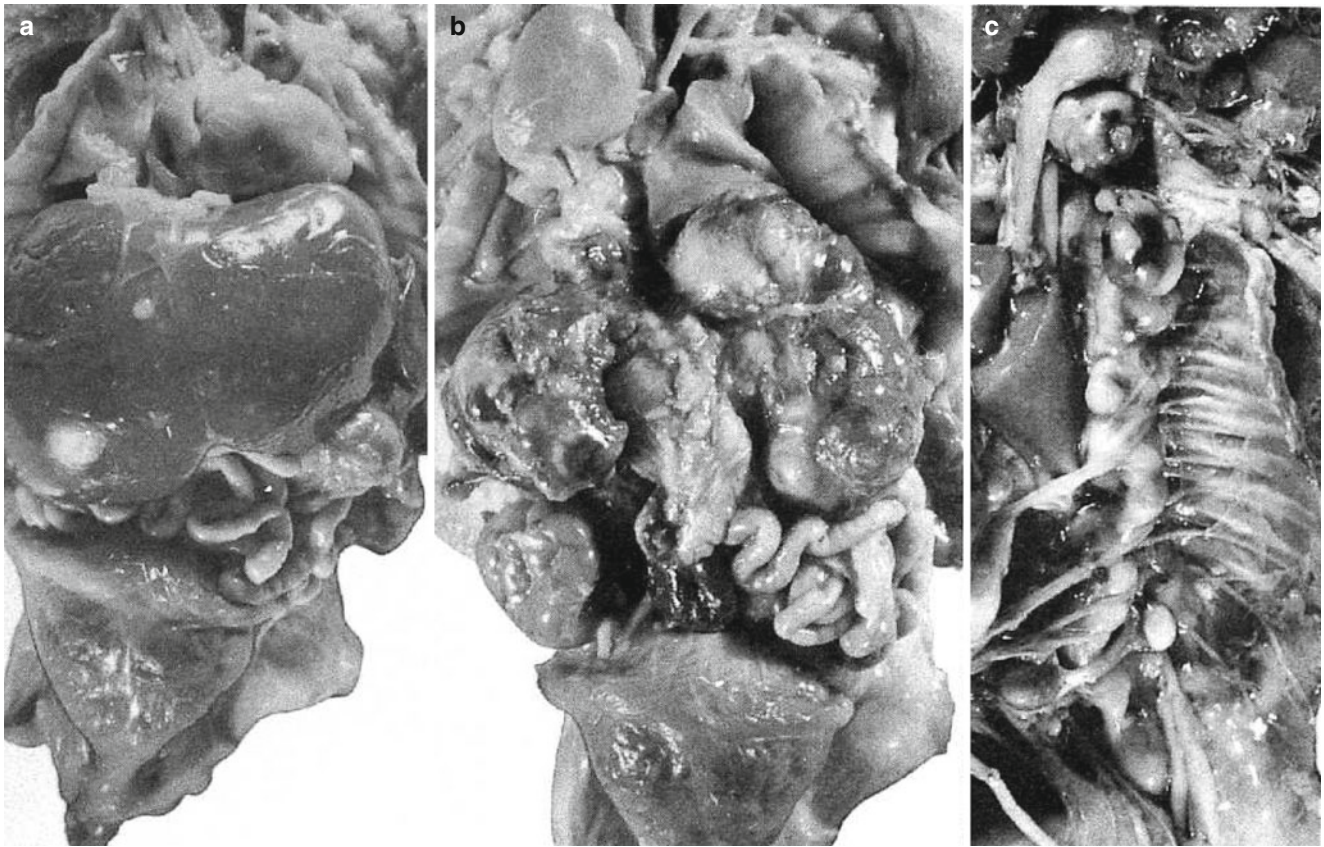


Fig. 4.41 Disseminated neurofibromatosis I. Neuroblastoma, gangli-
oneuroma, pheochromocytoma, schwannoma, malignant
nerve sheath tumor, rhabdomyosarcoma, Wilms' tumor, and
leukemia [12, 13, 82, 86, 87].

upper abdomen. (c) Massive involvement of nerve trunks and sympa-
thetic ganglia (Reprinted from Isaacs [13]. With kind permission of ©
Mosby, 1997)

oneuroma, pheochromocytoma, schwannoma, malignant
nerve sheath tumor, rhabdomyosarcoma, Wilms' tumor, and
leukemia [12, 13, 82, 86, 87].

4.9 Primitive Neuroectodermal Tumor (PNET)

Primitive neuroectodermal tumors (PNETs) are a group of malignant neoplasms arising from the central and peripheral nervous systems and soft tissues [12, 16, 88–92]. They are believed to be of neural crest origin. The PNET category contains a wide variety of neoplasms including medulloblastoma, retinoblastoma, neuroblastoma, Askin thoracopulmonary tumor, Ewing's sarcoma, melanotic PNET of the jaw, and peripheral neuroepithelioma of the soft tissues [13, 88–92].

Studies show that Ewing's sarcoma (both osseous and extra-osseous), PNET of bone, small cell malignant tumor of the thoracopulmonary region (Askin tumor), and peripheral neuroepithelioma are probably histogenetically related.

Neuronal differentiation manifested by the presence of neurosecretory granules and neurofilaments is observed by EM. PAS staining is variably positive. Immunohistochemical findings include reactivity with vimentin, neuron-specific enolase (NSE), HBA71, S-100 protein, and sometimes epithelial markers; cytogenetic findings, namely, $t(11;22)(q24;q11-12)$ chromosomal translocations, are identical [13, 16, 88, 89].

The chest wall, extremities, and face are the main primary sites [12, 88–91]. PNETs show a variable gross appearance consisting of soft, friable, white to pale-tan-gray tissue fragments with mucoid and cystic areas, foci of necrosis, and hemorrhage. Histologically, they are the small blue cell tumors forming nests and lobules of cells having round or oval nuclei, coarse or clumped chromatin, small nucleoli and indistinct or scant cytoplasm. Many mitoses are present (see Chap. 17). Homer-Wright rosettes similar to those observed in neuroblastomas are noted in a few tumors [16, 88–90].

The prognosis is poor [12, 91, 92]. Patients with tumors arising from all sites characteristically show early development of widespread metastases and a rapidly fatal outcome.

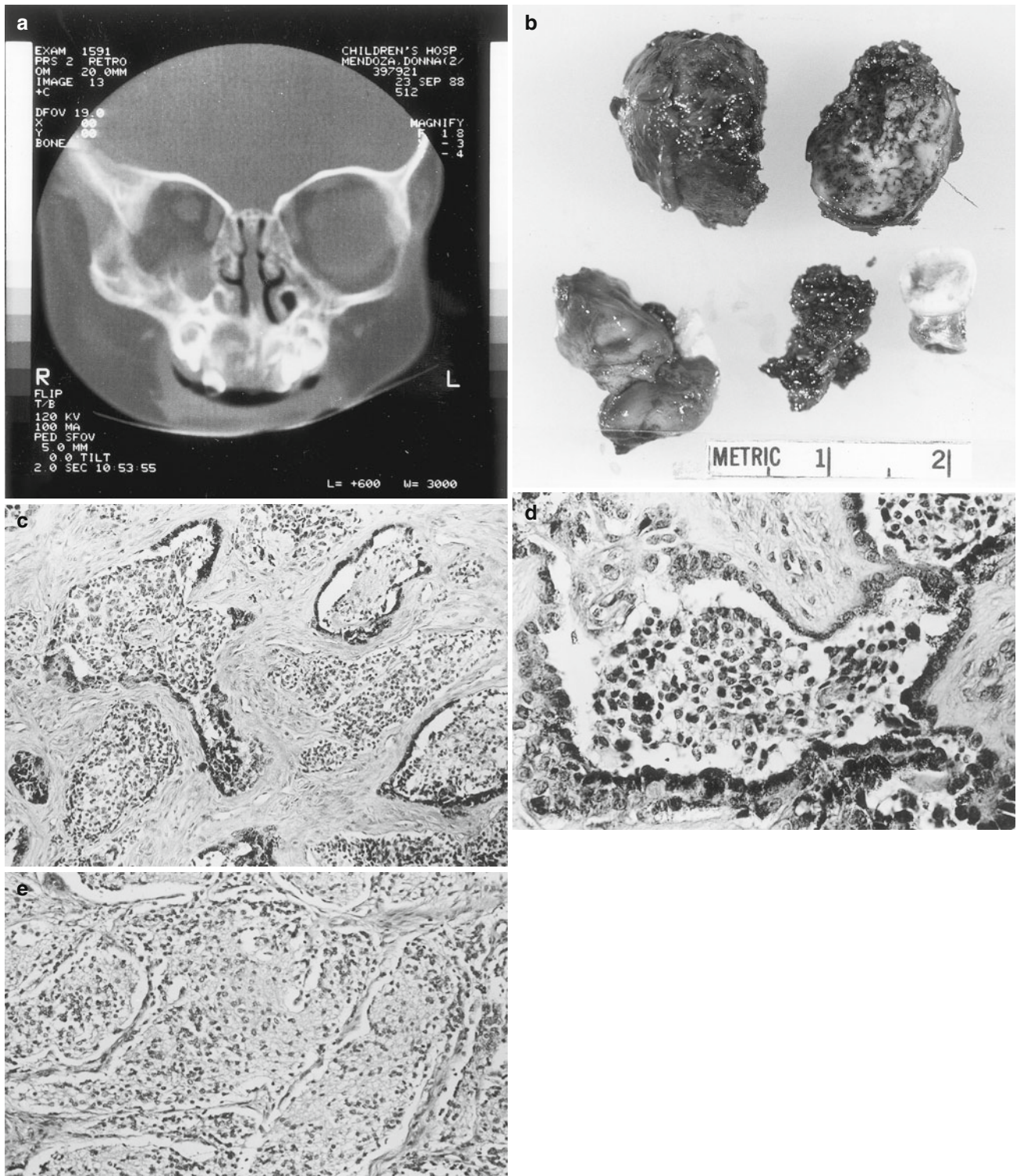


Fig. 4.42 Pigmented (melanotic) primitive neuroectodermal tumor. (a) Cranial MRI of a 6-month-old female with a history of a mass in the hard palate for 2 months duration. The imaging study shows a lytic lesion in the right maxilla and hard palate, erosion of the wall of the inferior orbit, and displacement of teeth. (b) Bone fragments contain tumor which is tan, firm with irregular black pigmented areas. A tooth is part of the specimen. (c) Low-power view showing irregular cystic

spaces containing nests of small darkly staining cells consistent with neuroblasts and larger pigmented melanocytes lining the microcysts. (d) Higher magnification demonstrating the neuroblasts and melanocytes in more detail. (e) Neuroblastoma component consisting of a lobular pattern, collections of small darkly staining cells and fine fibrillar material (Reprinted from Isaacs [12]. © W.B. Saunders, 1997)

4.9.1 Melanotic Neuroectodermal Tumor of Infancy

Several names have been applied to the peculiar neoplasm known as melanotic neuroectodermal tumor of infancy, including *melanotic progonoma*, *retinal anlage tumor*, *melanotic adamantinoma*, *pigmented neuroectodermal tumor*, and *pigmented congenital epulis* [14–16, 93, 94]. Neural crest origin has been proposed for this tumor; however, its relationship to other small cell tumors with neuroectodermal features as neuroblastoma, Ewing's tumor, and PNET remains unclear [95–98]. Studies suggest that *melanotic neuroectodermal tumor (melanotic PNET)* is a dysembryogenetic neoplasm that recapitulates early embryonic retinal development; the tumor cells resemble those derived from retinal pigmented epithelium, and the pigment is essentially the same as that seen in the normal retina [94]. However, ongoing debate remains regarding its exact histogenesis [15, 16, 95, 96, 98].

Melanotic PNET is found at birth or during the first year of life presenting as a rapidly growing mass most often arising from the anterior maxilla and less frequently from the mandible, brain, fontanelle, skull, and orbit [12, 14, 93]. In addition, it occurs in the oropharynx or outside the head in soft tissues and epididymis [16, 97, 98]. Serum α -fetoprotein and urinary VMA levels are inconsistently elevated [15, 93, 98].

The tumor varies in color from gray to black depending upon the amount of melanin pigment content (Fig. 4.42). One or more deciduous teeth may be found as part of the specimen when the tumor involves the alveolar process of either the maxilla or mandible [15].

Histologically, melanotic PNET consists of two types of cells situated in irregular microcystic spaces: one a small, dark, round cell resembling a neuroblast and the other a slightly larger, paler cell containing melanin pigment (Fig. 4.42c, d). The tumor insidiously infiltrates bone and soft tissues and provokes an exuberant fibrotic and/or gliotic response depending on location. EM studies show that the small dark round cells represent neuroblasts since they contain neurosecretory granules and neurofilaments and the larger, paler cells resemble melanocytes since cytoplasmic melanosomes are present in their cytoplasm [93, 94].

Immunohistochemical studies reveal neural, melanocytic, and epithelial elements [16, 95, 96, 98]. The small neuroblastic cells are reactive with NSE and synaptophysin whereas the larger melanocytic cells react with HMB45, dopamine- β -hydroxylase, and focally with vimentin and cytokeratin [95, 98].

The prognosis of patients with melanotic PNET is relatively good providing that the tumor has been *completely* resected [14, 15, 95, 97, 98]. The recurrence rate is approximately 15 % and overt malignant behavior noted in approxi-

mately 5 % [93, 98]. At present, there are no reliable clinical or histological findings that can be used to predict outcome.

4.10 Miscellaneous Soft Tissue Tumors

Ectomesenchymoma is an unusual malignant neoplasm thought to be derived from remnants of migratory pluripotential neural crest cells, the so-called ectomesenchyme, formed of both neuroectodermal and mesenchymal elements [15, 16, 81, 84, 85, 99]. The former component consists of ganglioneuroma and/or neuroblastoma and Schwann cells and the latter rhabdomyosarcoma [16, 81, 84]. Because of this biphasic pattern, it has been termed *gangliorhabdomyosarcoma* also [81]. Ectomesenchymomas occur mainly in infants, comprising 33–77 % of the cases reported [99]. They occur in the head and neck but most are intra-abdominal involving the genitourinary system, perineum, retroperitoneum, and abdominal wall [15, 81, 84, 99] (Fig. 4.43).

The tumor is multilobate, often encapsulated with a pale tan to gray, bulging cut surface (Fig. 4.43a). Foci of necrosis and hemorrhage are present. The tumors vary in size from 3 to 18 cm in greatest dimension [84, 99]. Microscopically, the rhabdomyosarcoma component may be either embryonal and/or alveolar type [15, 81, 84, 85, 99]. Over half the tumors contain mature ganglion cells with or without neuroblasts (Fig. 4.41c).

Immunohistochemical studies show that the rhabdomyoblasts are reactive with desmin and muscle-specific actin antibodies and variably positive for myoglobin; the Schwann cells are reactive with S-100 protein; the ganglion cells and neuroblasts are reactive with NSE and synaptophysin antibodies [81, 84]. EM studies confirm the biphasic immunohistochemical findings [15, 81].

Patients whose tumors are localized and resectable have the best prognosis whereas those with inoperable ones or metastases generally have a fatal outcome [98].

4.10.1 Triton Tumor

Triton tumor is another neoplasm with more than one line of differentiation. It is characterized by the coexistence of nerve sheath tumor and skeletal muscle components [16, 85, 100]. Both benign and malignant forms are described. The name triton was derived from the genus of salamander in which the growth of both neural and muscular elements was induced by nerve transplantation experiments [101]. Neurofibromatosis 1 is common in patients with this tumor [9, 16, 87]. Two examples of fatal, congenital triton tumor (malignant peripheral nerve sheath tumor with rhabdomyoblastic differentiation) occurring in the retroperitoneal area are described [15].

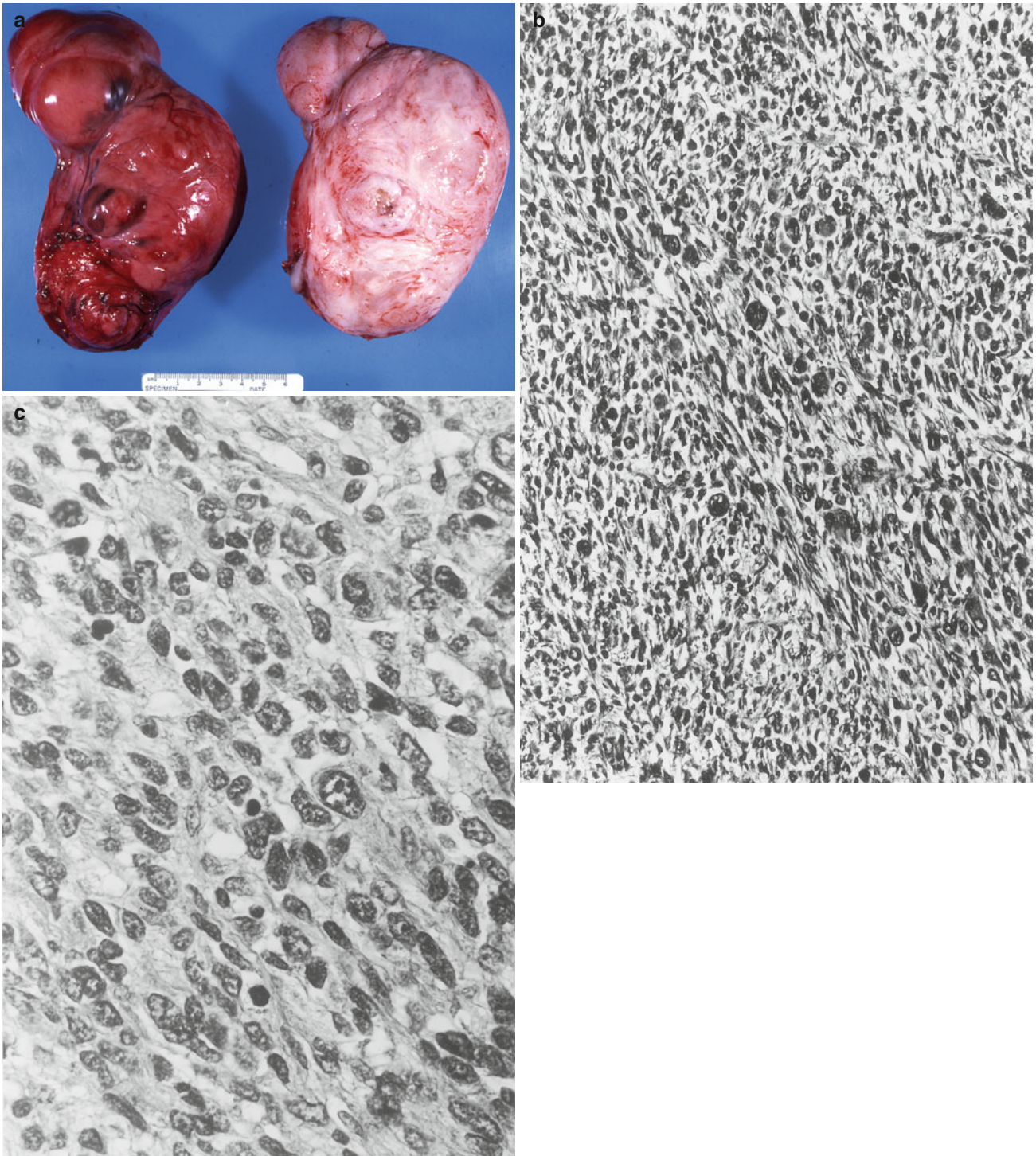


Fig. 4.43 Ectomesenchymoma (gangliorhabdomyosarcoma). Six-month-old male with an abdominal mass noted by his parents 2 months prior to hospitalization. (a) The tumor, 940 g, 18 × 11 cm, attached to the internal inguinal ring, has a white, bulging, whorled, lobular-appearing

cut surface. (b) The tumor consists of spindle-shaped rhabdomyoblasts and larger, rounder ganglion cells. (c) Higher magnification of the rhabdomyoblasts and ganglion cells (Reprinted from Isaacs [12]. © W.B. Saunders, 1997)

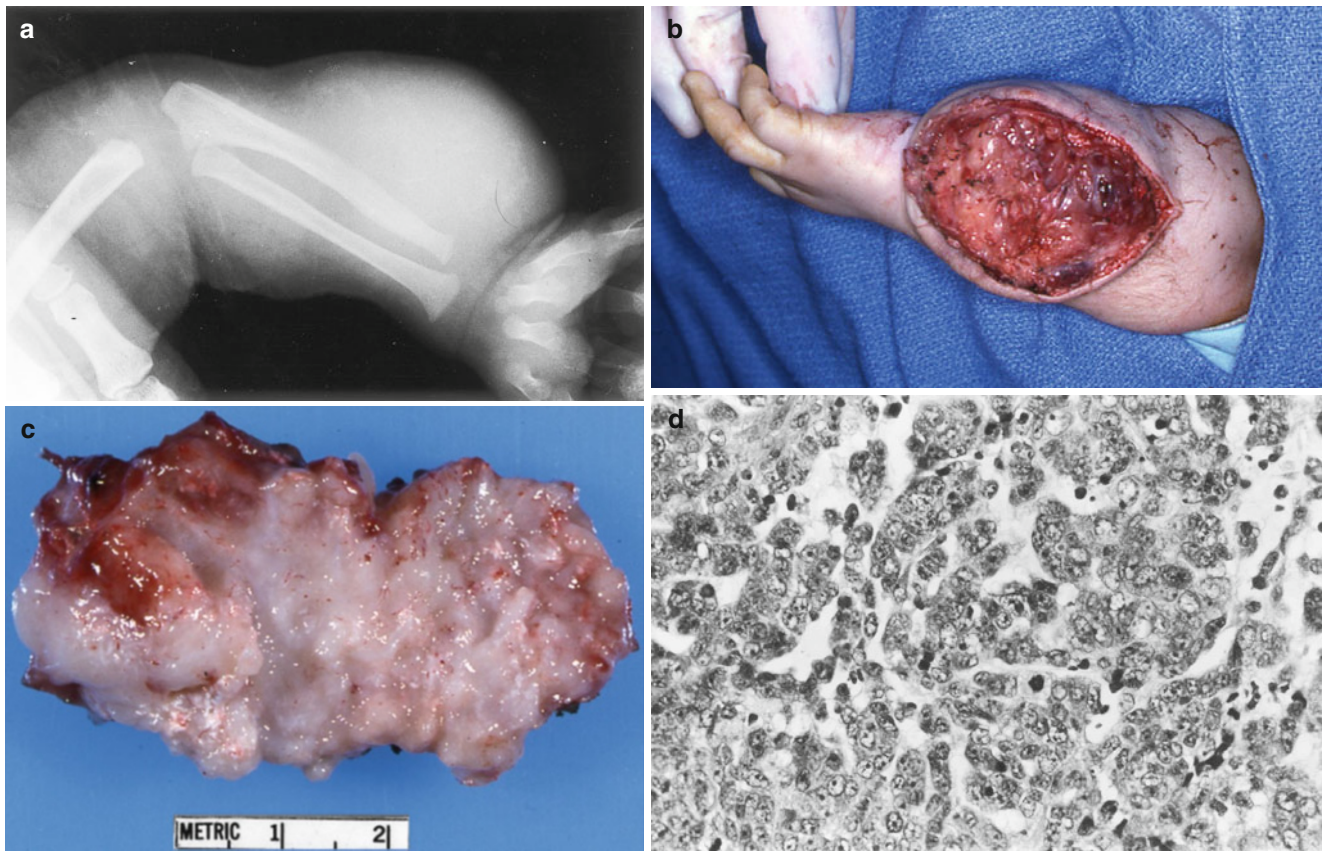


Fig. 4.44 Polyphenotypic small cell tumor. Two-month-old male with a rapidly growing neoplasm of the forearm which was present since birth. (a) X-ray depicting a large soft tissue mass. (b) Tumor is exposed in situ at surgery. (c) Grossly, the tumor has a soft gelatinous appear-

ance. (d) Tumor forms nests and cords of primitive appearing epithelial-like cells. Immunoperoxidase staining was weakly positive for neuron-specific enolase, vimentin, cytokeratin, and actin (Reprinted from Isaacs [12]. © W.B. Saunders, 1997)

The diagnosis of malignant triton tumor depends on identifying both malignant peripheral nerve sheath tumor and rhabdomyosarcoma components [16, 84, 100]. The former consist of spindle- or comma-shaped cells with a scanty cytoplasm and elongated nuclei, which form alternating bundles, Antoni type A and microcystic tissue, which are reactive with S-100 protein antibody. The skeletal muscle component has embryonal or alveolar rhabdomyoblasts immunoreactive with myoglobin, desmin, and actin. Neither site nor age of the child apparently affects the outcome, for the prognosis for patients with malignant triton tumor is dismal [84, 100]. Recurrence and metastases are the rule.

4.10.2 Polyphenotypic Small Cell Tumor

Complex phenotypic tumors with neural, rhabdoid, skeletal muscle and epithelial components occur. They include the *intra-abdominal small cell desmoplastic tumor* usually found in older children [102, 103] and the *congenital facial tumor* with PNET, glial, and epithelial elements [91]. The orbit and soft tissues of the forearm are examples of other primary sites [12, 15, 102, 103, 104] (Fig. 4.43). These small blue cell tumors are immunoreactive with vimentin and cytokeratin, in addition to neuron-specific enolase and muscle-specific actin. With few exceptions, most patients die from their malignancy within 2 years of diagnosis (Fig. 4.44).

References

1. Bader JL, Miller RW (1979) U.S. cancer incidence and mortality in the first year of life. *Am J Dis Child* 133:157–159
2. Barson AJ (1978) Congenital neoplasia: the Society's experience, abstracted. *Arch Dis Child* 53:436
3. Parkes SE, Muir KR, Southern L et al (1994) Neonatal tumours: a thirty-year population-based study. *Med Pediatr Oncol* 22:309–317
4. Campbell AN, Chan HSL, O'Brien A et al (1987) Malignant tumours in the neonate. *Arch Dis Child* 62:19–23
5. Dehner LP (1981) Neoplasms of the fetus and neonate. In: Naeye RL, Kissane JM, Kaufman N (eds) *Perinatal diseases*. International Academy of Pathology, monograph no. 22. Williams and Wilkins, Baltimore, p 286–345
6. Dehner LP (1997) Some general considerations about the clinicopathologic aspects of soft tissue tumors. In: Coffin CM, Dehner LP, O'Shea PA (eds) *Pediatric soft tissue tumors: a clinical, pathological, and therapeutic approach*. Williams and Wilkins, Baltimore, p 1
7. Coffin CM, Dehner LP (1992) Congenital Tumors. In: Stocker JT, Dehner LP (eds) *Pediatric pathology*, vol I. JB Lippincott, Philadelphia, p 325
8. Coffin CM, Dehner LP (1990) Soft tissue tumors in the first year of life. A report of 190 cases. *Pediatr Pathol* 10:509–526
9. Coffin CM (2007) Infantile soft tissue tumors. In: Gilbert-Barness E (ed) *Potter's pathology of the fetus, infant and child*, vol 2, 2nd edn. Mosby Elsevier, Philadelphia, pp 1709–1742
10. Isaacs H Jr (1983) Neoplasms in infants: a report of 265 cases. *Pathol Annu* 18:165–214
11. Isaacs H Jr (1985) Perinatal (congenital and neonatal) neoplasms: a report of 110 cases. *Pediatr Pathol* 3:165–216
12. Isaacs H Jr (1997) Soft tissue tumors. In: *Tumors of the fetus and newborn*, vol 35, Major problems in pathology. W.B. Saunders, Philadelphia, pp 43–108
13. Isaacs H Jr (1997) Tumors. In: Gilbert-Barness E (ed) *Potter's pathology of the fetus and infant*, vol 2. Mosby, St. Louis, pp 1242–1339
14. Isaacs H Jr (2007) Tumors. In: Gilbert-Barness E (ed) *Potter's pathology of the fetus, infant and child*, vol 2, 2nd edn. Mosby Elsevier, Philadelphia, pp 1677–1742
15. Isaacs H Jr (2002) *Tumors of the fetus and infant: an atlas*. Springer, New York, 434 pages
16. Weiss SW, Goldblum JR (eds) (2001) *Enzinger and Weiss's soft tissue tumors*, 4th edn. CV Mosby, St. Louis, 1622 pages
17. Isaacs H Jr (2010) Fetal and neonatal rhabdoid tumor. *J Pediatr Surg* 45:619–626
18. Coffin CM, Dehner LP (1993) Vascular tumors in children and adolescents: a clinicopathologic study of 228 tumors in 222 patients. *Pathol Annu* 28(Pt 1):97–120
19. Mulliken JB, Enjolras O (2004) Congenital hemangiomas and infantile hemangioma: missing links. *J Am Acad Dermatol* 50:875–882
20. Boon LM, Enjolras O, Mulliken JB (1996) Congenital hemangioma: evidence of accelerated involution. *J Pediatr* 128:329–335
21. Byard RW, Burrows PE, Izakawa T et al (1991) Diffuse infantile haemangiomas: clinicopathological features and management problems in five fatal cases. *Eur J Pediatr* 150:224–227
22. Enjolras O (1997) Classification and management of the various superficial vascular anomalies: hemangiomas and vascular malformations. *J Dermatol* 24:701–710
23. Currie BG, Schell D, Bowring AC (1991) Giant hemangioma of the arm associated with cardiac failure and the Kasabach-Merritt syndrome in a neonate. *J Pediatr Surg* 26:734–737
24. Sarkar M, Mulliken JB, Kozakewich HP et al (1997) Thrombocytopenic coagulopathy (Kasabach-Merritt phenomenon) is associated with Kaposiform hemangioendothelioma and not with common infantile hemangioma. *Plast Reconstr Surg* 100:1377–1386
25. Gallagher PG, Mahoney MJ, Gosche JR (1999) Cystic hygroma in the fetus and newborn. *Semin Perinatol* 23:341–356
26. Chervenak FA, Isaacson G, Tortora M (1985) A sonographic study of fetal cystic hygromas. *J Clin Ultrasound* 13:311–315
27. Coffin CM (1997) Fibroblastic-Myofibroblastic tumors. In: Coffin CM, Dehner LP, O'Shea PA (eds) *Pediatric soft tissue tumors: a clinical, pathological, and approach*. Williams and Wilkins, Baltimore, p 133
28. Hays DM, Mirabal VQ, Karlan MS et al (1970) Fibrosarcomas in infants and children. *J Pediatr Surg* 5:176
29. Adler R, Wong CA (1986) Cranial fasciitis simulating histiocytosis. *J Pediatr* 109:85–88
30. Isaacs H Jr (1987) Congenital and neonatal malignant tumors. A 28-year experience at Children's Hospital of Los Angeles. *Am J Pediatr Hematol Oncol* 9:121–129
31. Baerg J, Murphy JJ, Magee JF (1999) Fibromatoses: clinical and pathological features suggestive of recurrence. *J Pediatr Surg* 34:1112–1114
32. Mukai M, Torikata C, Iri H et al (1992) Immunohistochemical identification of aggregated actin filaments in formalin-fixed, paraffin-embedded sections. I. A study of infantile digital fibromatosis by a new pretreatment. *Am J Surg Pathol* 16:110–115
33. Davids JR, Wenger DR, Mubarak SJ (1993) Congenital muscular torticollis: sequelae of intrauterine or perinatal compartment syndrome. *J Pediatr Orthop* 13:141–147
34. Cheng JC, Tang SP, Chen TM (1999) Sternocleidomastoid pseudo-tumor and congenital muscular torticollis in infants: a prospective study of 510 cases. *J Pediatr* 134:712–716
35. Rosenberg HS, Stenback WA, Spjut HJ (1978) The fibromatoses of infancy and childhood. *Perspect Pediatr Pathol* 4:269–348
36. Chung EB, Enzinger FM (1981) Infantile myofibromatosis. *Cancer* 15(48):1807–1818
37. Mentzel T, Calonje E, Nascimento AG et al (1994) Infantile heman-gio-pericytoma versus infantile myofibromatosis. Study of a series suggesting a continuous spectrum of infantile myofibroblastic lesions. *Am J Surg Pathol* 18:922–930
38. Lack EE, Worsham GF, Callihan MD et al (1981) Gingival granular cell tumors of the newborn (congenital "epulis"): a clinical and pathologic study of 21 patients. *Am J Surg Pathol* 5:37–46
39. Dickey GE, Sotelo-Avila C (1999) Fibrous hamartoma of infancy: current review. *Pediatr Dev Pathol* 2:236–243
40. Cecchetto G, Carli M, Alaggio R et al (2001) Fibrosarcoma in pediatric patients: results of the Italian Cooperative Group studies (1979–1995). *J Surg Oncol* 78:225–231
41. Kodet R, Stejskal J, Pilt D et al (1996) Congenital-infantile fibrosarcoma: a clinicopathological study of five patients entered on the Prague children's tumor registry. *Pathol Res Pract* 192:845–853
42. Chung EB, Enzinger FM (1976) Infantile fibrosarcoma. *Cancer* 38:729–739
43. Soule EH, Pritchard DJ (1977) Fibrosarcoma in infants and children: a review of 110 cases. *Cancer* 40:1711–1721
44. Knezevich SR, Garnett MJ, Pysher TJ et al (1998) ETV6-NTRK3 gene fusions and trisomy 11 establish a histogenetic link between mesoblastic nephroma and congenital fibrosarcoma. *Cancer Res* 58:5046–5048
45. Pasquel P, Salazar M, Marvan E (1988) Proliferative myositis in an infant: report of a case with electron microscopic observations. *Pediatr Pathol* 8:545–551
46. Meis JM, Enzinger FM (1992) Proliferative fasciitis and myositis of childhood. *Am J Surg Pathol* 16:364–372
47. Lauer DH, Enzinger FM (1980) Cranial fasciitis of childhood. *Cancer* 45:401–406
48. Zuppan CW, Mierau GW, Wilson HL (1987) Malignant fibrous histiocytoma in childhood: a report of two cases and review of the literature. *Pediatr Pathol* 7:303–318

49. Daw NC, Billups CA, Pappo AS et al (2003) Malignant fibrous histiocytoma and other fibrohistiocytic tumors in pediatric patients: the St. Jude Children's Research Hospital experience. *Cancer* 97:2839–2847
50. Fletcher CD (1990) Benign fibrous histiocytoma of subcutaneous and deep soft tissue: a clinicopathologic analysis of 21 cases. *Am J Surg Pathol* 14:801–809
51. Enzinger FM (1979) Angiomatoid malignant fibrous histiocytoma: a distinct fibrohistiocytic tumor of children and young adults simulating a vascular neoplasm. *Cancer* 44:2147–2157
52. Costa MJ, Weiss SW (1990) Angiomatoid malignant fibrous histiocytoma. A follow-up study of 108 cases with evaluation of possible histologic predictors of outcome. *Am J Surg Pathol* 14:1126–1132
53. Freyer DR, Kennedy R, Bostrom BC et al (1996) Juvenile xanthogranuloma: forms of systemic disease and their clinical implications. *J Pediatr* 129:227–237
54. Dehner LP (2003) Juvenile xanthogranulomas in the first two decades of life: a clinicopathologic study of 174 cases with cutaneous and extracutaneous manifestations. *Am J Surg Pathol* 27: 579–593
55. Isaacs H Jr (2006) Fetal and neonatal histiocytoses. *Pediatr Blood Cancer* 47:123–129
56. Janney CG, Hurt MA, Santa Cruz DJ (1991) Deep juvenile xanthogranuloma. Subcutaneous and intramuscular forms. *Am J Surg Pathol* 15:150–159
57. Dehner LP, Enzinger FM, Font RL (1972) Fetal rhabdomyoma. An analysis of nine cases. *Cancer* 30:160–166
58. Kapadia SB, Meis JM, Frisman DM et al (1993) Fetal rhabdomyoma of the head and neck: a clinicopathologic and immunophenotypic study of 24 cases. *Hum Pathol* 24:754–765
59. Bozic C (1986) Fetal rhabdomyoma of the parotid gland in an infant: histological, immunohistochemical, and ultrastructural features. *Pediatr Pathol* 6:139–144
60. Beghetti M, Gow RM, Haney I et al (1997) Pediatric primary benign cardiac tumors: a 15-year review. *Am Heart J* 134: 1107–1114
61. Isaacs H Jr (2004) Fetal and neonatal cardiac tumors. *Pediatr Cardiol* 25:252–273
62. Ragab AH, Heyn R, Tefft M et al (1986) Infants younger than 1 year of age with rhabdomyosarcoma. *Cancer* 58:2606–2610
63. Lobe TE, Wiener ES, Hays DM et al (1994) Neonatal rhabdomyosarcoma: the IRS experience. *J Pediatr Surg* 29:1167–1170
64. Ruymann FB, Maddux HR, Ragab A et al (1988) Congenital anomalies associated with rhabdomyosarcoma: an autopsy study of 115 cases. A report from the Intergroup Rhabdomyosarcoma Study Committee (representing the Children's Cancer Study Group, the Pediatric Oncology Group, the United Kingdom Children's Cancer Study Group, and the Pediatric Intergroup Statistical Center). *Med Pediatr Oncol* 16:33–39
65. Li FP, Fraumeni JF (1969) Rhabdomyosarcoma in children: epidemiologic study and identification of a familial cancer syndrome. *J Natl Cancer Inst* 43:1365–1373
66. McKeen EA, Bodurtha J, Meadows AT et al (1978) Rhabdomyosarcoma complicating multiple neurofibromatosis. *J Pediatr* 93:992–993
67. Newton WA, Gehan EA, Webber BL et al (1995) Classification of rhabdomyosarcomas and related sarcomas. Pathologic aspects and proposal for a new classification—an Intergroup Rhabdomyosarcoma Study. *Cancer* 76:1073–1085
68. Leuschner I, Newton WA, Schmidt D et al (1993) Spindle cell variants of embryonal rhabdomyosarcoma in the paratesticular region. A report of the Intergroup Rhabdomyosarcoma Study. *Am J Surg Pathol* 17:221–230
69. Parham DM, Shapiro DN, Downing JR et al (1994) Solid alveolar rhabdomyosarcomas with the t(2;13). Report of two cases with diagnostic implications. *Am J Surg Pathol* 18:474–478
70. Malempati S, Rodeberg DA, Donaldson S et al (2011) Rhabdomyosarcoma in infants younger than 1 year: a report from the Children's Oncology Group. *Cancer* 117(15):3493–3501
71. Huh WW, Skapek SX (2010) Childhood rhabdomyosarcoma: a new insight on biology and treatment. *Curr Oncol Rep* 12:402–410
72. Weeks DA, Beckwith JB, Mierau GW et al (1989) Rhabdoid tumor of kidney. A report of 111 cases from the National Wilms' Tumor Study Pathology Center. *Am J Surg Pathol* 13:439–458
73. Parham DM, Weeks DA, Beckwith JB (1994) The clinicopathologic spectrum of putative extrarenal rhabdoid tumors. An analysis of 42 cases studied with immunohistochemistry or electron microscopy. *Am J Surg Pathol* 18:1010–1029
74. White FV, Dehner LP, Belchis DA et al (1999) Congenital disseminated malignant rhabdoid tumor: a distinct clinicopathologic entity demonstrating abnormalities of chromosome 22q11. *Am J Surg Pathol* 23:249–256
75. Kodet R, Newton WA Jr, Sachs N et al (1991) Rhabdoid tumors of soft tissues: a clinicopathologic study of 26 cases enrolled on the Intergroup Rhabdomyosarcoma Study. *Hum Pathol* 22(7): 674–684
76. Coffin CM (1994) Lipoblastoma: an embryonal tumor of soft tissue related to organogenesis. *Semin Diagn Pathol* 11:98–103
77. Collins MH, Chatten J (1997) Lipoblastoma/lipoblastomatosis: a clinicopathologic study of 25 tumors. *Am J Surg Pathol* 21: 1131–1137
78. Chung EB, Enzinger FM (1973) Benign lipoblastomatosis. An analysis of 35 cases. *Cancer* 32:482–492
79. Dehner LP (1986) Peripheral and central primitive neuroectodermal tumors. A nosologic concept seeking a consensus. *Arch Pathol Lab Med* 110:997–1005
80. Hendrickson MR, Ross JC (1981) Neoplasms arising in congenital giant nevi: morphologic study of seven cases and a review of the literature. *Am J Surg Pathol* 5:109–135
81. Karcioğlu Z, Someren A, Mathes SJ (1977) Ectomesenchymoma. A malignant tumor of migratory neural crest (ectomesenchyme) remnants showing ganglionic, schwannian, melanocytic and rhabdomyoblastic differentiation. *Cancer* 39:2486–2496
82. Qualman SJ, Green WR, Brovall C et al (1986) Neurofibromatosis and associated neuroectodermal tumors: a congenital neurocristopathy. *Pediatr Pathol* 1986(5):65–78
83. Coffin CM, Dehner LP (1989) Peripheral neurogenic tumors of the soft tissues in children and adolescents: a clinicopathologic study of 139 cases. *Pediatr Pathol* 9:387–407
84. Kodet R, Kasthuri N, Marsden HB et al (1986) Gangliorhabdomyosarcoma: a histopathological and immunohistochemical study of three cases. *Histopathology* 10:181–193
85. Brooks JS, Freeman M, Enterline HT (1985) Malignant 'Triton' tumors. Natural history and immunohistochemistry of nine new cases with literature review. *Cancer* 55:2543–2549
86. Meis JM, Enzinger FM, Martz KL et al (1992) Malignant peripheral nerve sheath tumors (malignant schwannomas) in children. *Am J Surg Pathol* 16:1992
87. Isaacs H Jr (2010) Perinatal neurofibromatosis: two case reports and review of the literature. *Am J Perinatol* 27:285–292
88. Tsokos M (1992) Peripheral primitive neuroectodermal tumors. Diagnosis, classification, and prognosis. *Perspect Pediatr Pathol* 16:27–98
89. Schmidt D, Harms D, Burdach S (1985) Malignant peripheral neuroectodermal tumours of childhood and adolescence. *Virchows Arch A Pathol Anat Histopathol* 406:351–365
90. Askin FB, Rosai J, Sibley RK et al (1979) Malignant small cell tumor of the thoracopulmonary region in childhood: a distinctive clinicopathologic entity of uncertain histogenesis. *Cancer* 43:2438–2451
91. Hachitanda Y, Tsuneyoshi M, Enjoji M et al (1990) Congenital primitive neuroectodermal tumor with epithelial and glial differentiation. An ultrastructural and immunohistochemical study. *Arch Pathol Lab Med* 114:101–105
92. Chan GC, Nicholls JM, Lee AC et al (1996) Malignant peripheral neuroectodermal tumor in an infant with neurofibromatosis type 1. *Med Pediatr Oncol* 26:215–219

93. Dehner LP, Sibley RK, Sauk JJ Jr et al (1979) Malignant melanotic neuroectodermal tumor of infancy: a clinical, pathologic, ultrastructural and tissue culture study. *Cancer* 43:1389–1410
94. Lamping KA, Albert DM, Lack E et al (1985) Melanotic neuroectodermal tumor of infancy (retinal anlage tumor). *Ophthalmology* 92:143–149
95. Pettinato G, Manivel JC, d'Amore ES et al (1991) Melanotic neuroectodermal tumor of infancy. A reexamination of a histogenetic problem based on immunohistochemical, flow cytometric, and ultrastructural study of 10 cases. *Am J Surg Pathol* 15:233–245
96. Khoddami M, Squire J, Zielenska M et al (1998) Melanotic neuroectodermal tumor of infancy: a molecular genetic study. *Pediatr Dev Pathol* 1:295–299
97. Ricketts RR, Majmudarr B (1985) Epididymal melanotic neuroectodermal tumor of infancy. *Hum Pathol* 16:416–420
98. Kapadia SB, Frisman DM, Hitchcock CL et al (1993) Melanotic neuroectodermal tumor of infancy. Clinicopathological, immunohistochemical, and flow cytometric study. *Am J Surg Pathol* 17:566–573
99. Boué DR, Parham DM, Webber B et al (2000) Clinicopathologic study of ectomesenchymomas from Intergroup Rhabdomyosarcoma Study Groups III and IV. *Pediatr Dev Pathol* 3:290–300
100. Daimaru Y, Hashimoto H, Enjoji M (1984) Malignant “Triton” tumors: a clinicopathologic and immunohistochemical study of nine cases. *Hum Pathol* 15:768–778
101. Woodruff JM, Chernik NL, Smith MC et al (1973) Peripheral nerve tumors with rhabdomyosarcomatous differentiation (malignant “Triton” tumors). *Cancer* 32:426–439
102. Gonzalez-Crussi F, Crawford SE, Sun CC (1990) Intraabdominal desmoplastic small-cell tumors with divergent differentiation. Observations on three cases of childhood. *Am J Surg Pathol* 14:633–642
103. Ordóñez NG, el-Naggat AK, Ro JY et al (1993) Intra-abdominal desmoplastic small cell tumor: a light microscopic, immunocytochemical, ultrastructural, and flow cytometric study. *Hum Pathol* 24:850–865
104. Lyon DB, Dortzbach RK, Gilbert-Barnes E (1993) Polyphenotypic small-cell orbitocranial tumor. *Arch Ophthalmol* 111:1402–1408

5.1 Introduction

Tumors and tumor-like conditions of the skin are not uncommon in the fetus and infant and include a wide variety of entities (Table 5.1). Vascular lesions, hemangioma and lymphangioma, are by far the most prevalent, but other conditions such as congenital melanocytic nevi, cutaneous hamartomas, and neoplastic-like infiltrations occur as well [1–8].

Hamartoma is defined as an overgrowth of mature cells normally present in the tissue of origin. The term *nevus* includes any abnormal growth in the skin

(a “birthmark”) or more specifically to tumors containing nevus cells [6].

Malignant neoplasms may appear in the fetus and infant as *cutaneous metastases* which may be the first manifestation of the tumor [1, 7–10]. Neuroblastoma and leukemia are the major malignancies metastasizing to the skin [1, 8, 9] (Table 5.2). Rhabdomyosarcoma and rhabdoid tumor are examples of others that spread to the skin forming cutaneous nodules [8] (Table 5.3). Some nonneoplastic conditions may be mistaken for tumors. For example, subcutaneous fat necrosis of the newborn may appear several days after a difficult delivery as skin nodules [1] (Fig. 5.1).

Table 5.1 Tumors and tumor-like conditions of the skin in the fetus and infant

Hemangioma
Capillary hemangioma
Port-wine stain and nevus flammeus
Cavernous hemangioma
Blue rubber bleb nevus
Lobular capillary hemangioma (pyogenic granuloma)
Kaposiform hemangioendothelioma
Tufted angioma
Kaposi sarcoma
Lymphangioma
Neurofibroma
Digital fibromatosis
Myofibromatosis
Fibrous hamartoma of infancy
Facial angiofibroma ^a
Shagreen patch ^a
Leaf-shaped areas of hypopigmentation ^a
Smooth muscle hamartoma
Nevus lipomatosis
Granular cell tumor
Melanocytic nevus
Malignant melanoma
Blue nevus
Epidermal nevus
Becker's nevus
Sebaceous nevus
Papilloma
Langerhans cell histiocytosis
Urticaria pigmentosa (mast cell disease)
Juvenile xanthogranuloma
Dermal extramedullary erythropoiesis
Subcutaneous fat necrosis of the newborn
Tumors metastatic to the skin
Neuroblastoma
Leukemia
Rhabdomyosarcoma
Rhabdoid tumor
Adrenocortical carcinoma
Choriocarcinoma

Reprinted from Isaacs [1]. © Springer-Verlag, 2002

^aSkin lesions of tuberous sclerosis

Table 5.2 Differential diagnosis of the “blueberry muffin baby” (cutaneous blue nodules)

Dermal extramedullary erythropoiesis
Congenital infection
Rubella
Cytomegalovirus
Toxoplasmosis
Hemolytic disease of the newborn
Twin–twin transfusion syndrome
Hereditary spherocytosis
Blue rubber bleb nevus syndrome
Neoplastic infiltrations of the skin
Leukemia
Langerhans cell histiocytosis
Neuroblastoma
Rhabdoid tumor
Rhabdomyosarcoma
Primitive neuroectodermal tumor
Choriocarcinoma
Adrenocortical carcinoma

Reprinted from Gottesfeld et al. [11]. With kind permission of © American Academy of Dermatology, 1989; Reprinted from Isaacs [1]. © Springer-Verlag, 2002

Table 5.3 Skin manifestations of tuberous sclerosis in the infant

Lesion	Gross appearance	Histology
Angiofibroma	Red, smooth papules symmetrically distributed on nasolabial folds, cheeks, and chin	Dermal fibrosis, capillary dilatation
Fibroma	Raised, soft brown nodules on face, scalp, and beneath nails	Thick collagen bundles concentrically arranged around atrophic skin appendages; fibrosis
Shagreen patch	Raised and thickened areas of skin	Dense scar-like collagen in dermis resembling scleroderma; interwoven bundles of collagen and reduction of elastic fibers
Hypopigmentation	White, leaf-shaped hypopigmented areas of skin	Decreased pigmentation of melanocytes and keratinocytes

Elder et al. [4]. With kind permission of © Lippincott-Raven, 1997; Reprinted from Isaacs [1]. © Springer-Verlag, 2002

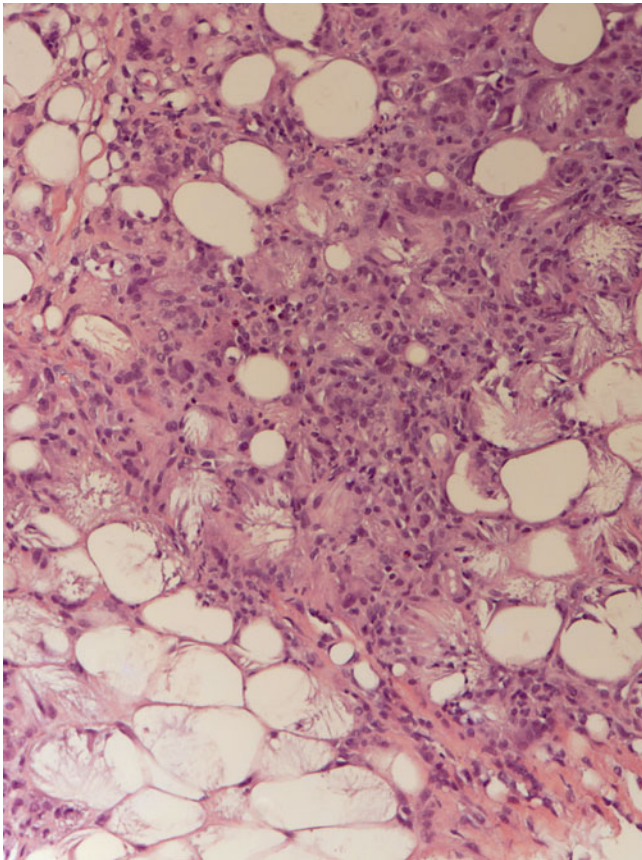


Fig. 5.1 Subcutaneous fat necrosis of the newborn. 3-week-old female with progressive firm nodule formation on both upper arms and left thigh. There was a history of a difficult delivery. The skin “punch biopsy” shows the distribution of the fat necrosis in the subcutis. The fat is infiltrated by lymphocytes, macrophages, and foreign body type giant cells. Macrophages and multinucleated giant cells contain radial crystalline arrays of fat (Reprinted from Isaacs [5]. © W.B. Saunders, 1997)

5.2 Vascular Conditions

Hemangioma and *lymphangioma* are the main vascular conditions involving the skin of fetuses and infants [1, 12, 13]. The borderline between vascular malformations and hemangiomas is not always well defined [13]. It is open to question whether hemangiomas represent malformations or true neoplasms. They occur more often than lymphangiomas. Most hemangiomas regress or disappear spontaneously by adolescence [4, 7, 12–15]. On the other hand, lymphangioma is considered a benign vascular malformation rather than a tumor; it is composed of cystically dilated lymphatics resulting from failure of communication and ongoing obstruction [1, 5].

5.2.1 Hemangioma

Hemangioma is the leading vascular condition and birthmark of the newborn and infant. It is found on any part of

the skin, most often on the neck and face, as one or sometimes multiple lesions [2, 3, 12–19]. Hemangiomas are observed in 10 % of infants as compared to only 2–4 % of newborns since many are not apparent at birth [2, 5, 15]. Females are affected more often than males (3:1). Of the various vascular lesions, the *capillary hemangioma* and the *port-wine nevus* are the ones observed most often during the first year of life [7, 16].

The common infantile hemangioma can be divided into two main histological categories, *capillary* and *cavernous*, on the basis of the caliber of the blood vessels involved [1, 2, 7] (Figs. 5.2 and 5.3) (see Chap. 4 for further discussion). The terms “strawberry hemangioma” or “strawberry nevus” are applied to raised, verrucous, cutaneous vascular lesions with a reddish-purple color (Fig. 5.4). They are typically mixed hemangiomas composed of both capillary and cavernous components [7, 12]. By age 7 years, at least 70 % of the strawberry hemangiomas regress or disappear completely [15]. Therefore, conservative management is warranted.



Fig. 5.2 Macular stains. (a) Nevus flammeus involving the left eyelid and forehead in an infant aged 3 days. (b) Port-wine stain (nevus venosus) involving the left cheek and forehead in an infant aged 2 days.

Hemangiomas in this location are often associated with hemangiomas of the underlying meninges and brain (Reprinted from Isaacs [6]. With kind permission of © Mosby, 1997)

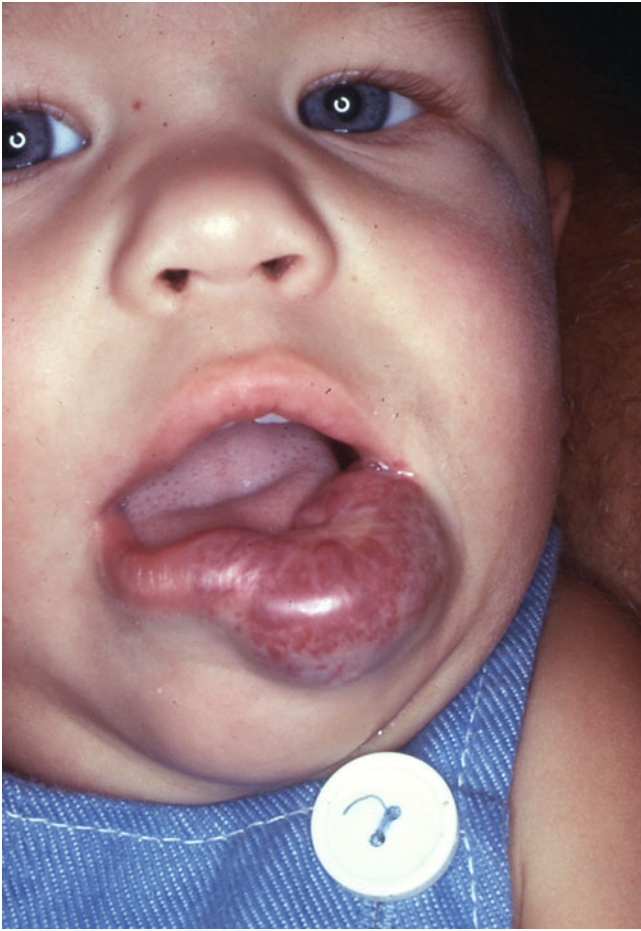


Fig. 5.3 1-year-old-male with a cutaneous capillary hemangioma presenting as a raised nodule on the lip (Reprinted from Isaacs [1]. © Springer-Verlag, 2002)

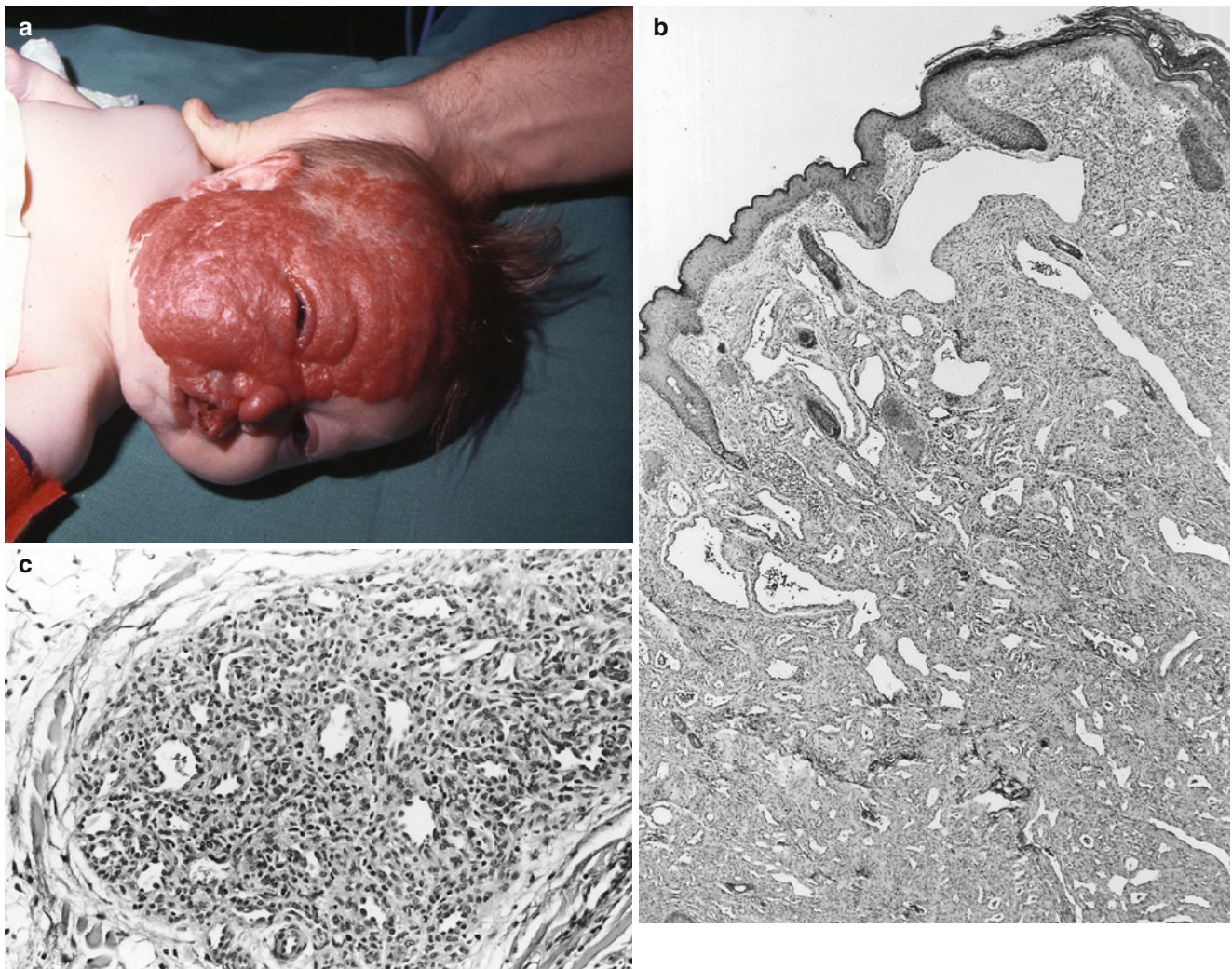


Fig. 5.4 Strawberry hemangioma. (a) Newborn with an extensive capillary and cavernous (“strawberry”) hemangioma distributed over the scalp, face, and neck. In addition, the baby had a hemangioma of the larynx which was causing respiratory distress. (b) Low-power view of a strawberry

hemangioma showing the cavernous component within the dermis and the capillary component in the subcutaneous tissue. (c) The lobular pattern of the capillary hemangioma component within the deeper part of the tumor is shown (Reprinted from Isaacs [5]. © W.B. Saunders, 1997)

5.2.2 Macular Stains

Both *port-wine stain* and *nevus flammeus* are present usually at birth and are situated most often on the face and neck [6, 7, 15–18] (Fig. 5.2). They occur in approximately 3 births/1,000 [16]. Initially, they exhibit a pink appearance, but with age, the port-wine stain develops a bluish-red to purple tone while becoming darker, irregular, thickened, and nodular. In contrast to the port-wine stain, the nevus flammeus resolves with time, but some may remain and become lighter. Microscopic findings consist essentially of dilated capillaries in the dermis or no recognizable abnormality at all [2, 6, 7, 15]. Individuals who have port-wine stains of the eyelids, bilateral lesions, or unilateral port-wine stains involving all three branches of the trigeminal nerve should be screened for glaucoma and have appropriate testing for central nervous system involvement [6, 16, 18].

5.2.3 Syndromes Associated with Vascular Conditions

Cutaneous vascular lesions particularly macular stains and vascular malformations may be an indication of a more serious underlying condition. This depends on the location of the birthmark and on whether or not structures beneath are affected [5, 7, 15, 16, 18, 19]. Most vascular conditions described in syndromic newborns are not hemangiomas but instead are macular stains and vascular malformations (cavernous, venous, arterial, lymphatic, or combinations thereof) [16, 18]. On the other hand, hemangioma is found only incidentally with dysmorphic syndromes but has been noted in association with midline sternal and abdominal clefting, right-sided aortic arch coarctation, and sacral and genitourinary defects [15, 16]. In the Sturge-Weber syndrome, there is involvement of the forehead and upper eyelid by a vascular

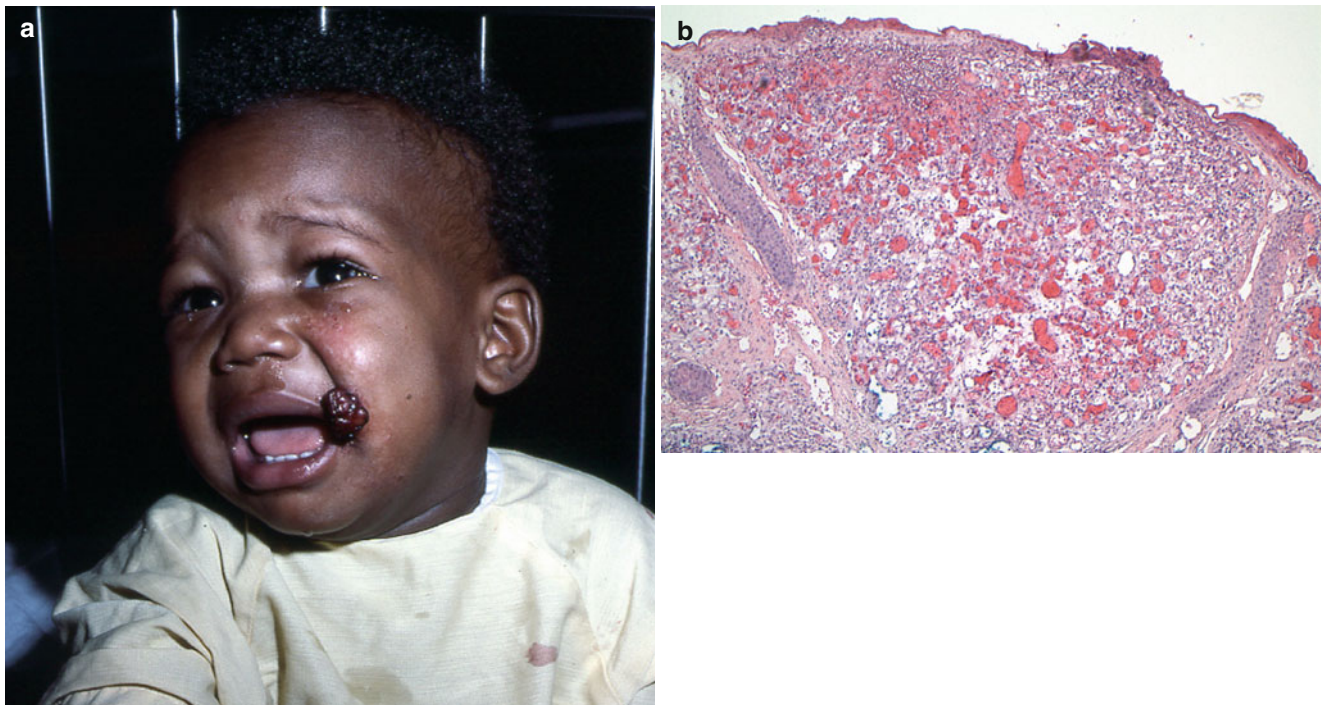


Fig. 5.5 Lobular capillary hemangioma (“pyogenic granuloma”). (a) 1-year-old male with a rapidly growing, polypoid mass on the left side of the cheek. The excised specimen measured 1.5×1.5 cm and had a red, fleshy appearing cut surface. (b) Lobules of capillaries are separated by fibrous connective tissue. There is a notch in the skin suggestive of

an epithelial collarette situated in the *lower right corner* of the photograph. Notice the similarity between the histological features of the pyogenic granuloma to those of the capillary hemangioma depicted in Fig. 3.1. H&E. **b** $\times 120$) (From Isaacs [22]. Mosby Year Book, 1991. Used by permission)

lesion in the distribution of the first branch of the trigeminal (fifth) nerve involving the meninges and brain beneath. The associated leptomeningeal hemangiomatosis is manifested clinically in at least half the infants with this syndrome by a constellation of findings consisting of mental retardation, seizures, and hemiplegia with or without cerebral calcification [2, 7, 15] (see Chap. 9, Fig. 9.21). Glaucoma is another important complication of the disease. When an individual has a hemangioma and/or a port-wine stain present on an extremity accompanied by focal gigantism of the affected part and often a bony deformity, the diagnosis of Klippel-Trenaunay-Weber syndrome should be considered [6, 7, 13, 15, 16] (Fig. 4.4).

5.2.4 Hemangioma Variants

5.2.4.1 Pyogenic Granuloma (Lobular Capillary Hemangioma)

Pyogenic granuloma (lobular capillary hemangioma) is a common acquired vascular lesion of the skin and mucous membranes in the pediatric age group [1, 4, 20, 21]. It occurs during the first year of life and in the older individual typically as a single polypoid nodule that bleeds easily on palpation (Fig. 5.5). The face and lip are the main sites in the infant. In a retrospective analysis of 178 patients, 12 % of lesions occurred during the first year of life; however, the median age

of appearance was age 6 years [21]. Although the pyogenic granuloma appears in areas of trauma or infection, currently it is believed that this condition represents a form of capillary hemangioma since it is practically indistinguishable from this entity microscopically [20, 21]. The lesion consists of lobules of proliferating capillaries and fibroblasts often resembling granulation tissue. Often there is an epithelial collarette at the base of the nodule which is a helpful diagnostic feature setting the lesion apart from some of the other vascular conditions described above. In contrast to the common capillary hemangioma, pyogenic granuloma, which is not an infectious process, rarely heals spontaneously and usually requires curettage or surgical excision [12, 20, 21].

5.2.4.2 Blue Rubber Bleb Nevus Syndrome

This rare condition, also known as the *Bean syndrome* named after the individual who first described it, is characterized by distinctive vascular malformations of the skin, gastrointestinal tract, and less often in other organs, leading to intestinal bleeding and chronic anemia [1, 4, 23, 24]. The vascular lesions are present at birth or early infancy tending to increase in size and in number with age. Generally, they are inherited as an autosomal dominant trait but sporadic cases do occur. There is no sex predilection. Although the tumors can appear throughout the body, they are found more often on the upper limbs, trunk, and perineum. The syndrome may be

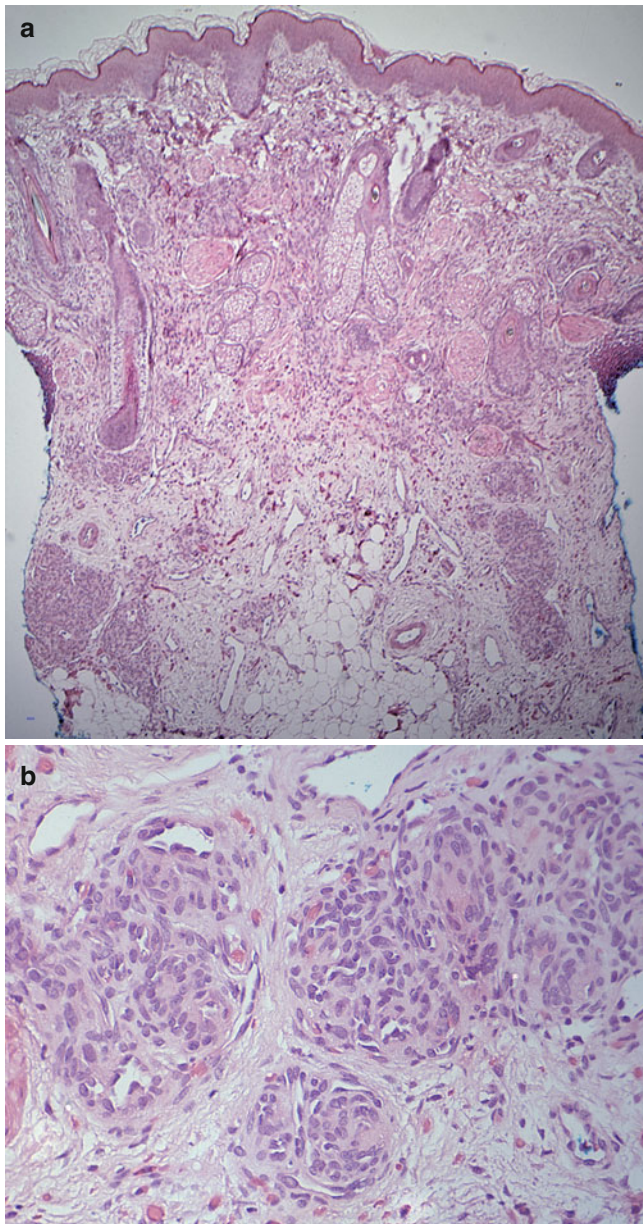


Fig. 5.6 Tufted angioma. 13-day-old female with a reddish-purple, slightly indurated area over the cheek. **(a)** Scattered small lobules of vascular tufts are distributed throughout the dermis. **(b)** The lobules are composed of empty capillaries surrounded by dilated crescent-shaped vascular channels (Reprinted from Isaacs [1]. © Springer-Verlag, 2002)

complicated by gastrointestinal bleeding and bony abnormalities as hemarthroses, pathologic fractures, and skeletal bowing [24]. The lesions vary in size from a few millimeters to over 2 cm in diameter. They are soft dark-blue bulge from the skin surface and are compressible. They may have the appearance of the so-called blueberry muffin baby (Table 5.2). Microscopically, they show features of a cavernous hemangioma consisting of markedly dilated and congested vascular spaces lined by regular endothelial cells.

Kaposiform hemangioendothelioma, *tufted angioma*, and *Kaposi sarcoma* are discussed in Chap. 4 (Fig. 5.6).

5.2.5 Lymphangioma

Lymphangiomas occur as superficial cutaneous and deep-seated soft tissue lesions and regardless of their location consist histologically of cystically dilated lymphatic channels lined by a single layer of regular endothelial cells [1, 4, 7, 13, 14]. The superficial ones, namely, lymphangioma circumscriptum, composed of one or more small cutaneous vesicles, are seldom seen in the neonatal period but are noted more often later in infancy and childhood. The deeply situated cavernous lymphangiomas present clinically as rubbery, skin-colored nodules that may enlarge rapidly producing a palpable mass in an extremity or form a large lymph fluid-filled sac, for example, in the neck, axilla, or mesentery, called a *cystic hygroma* [6] (Figs. 4.7, 4.8, 4.9, 4.10, and 4.11) (see Chap. 4).

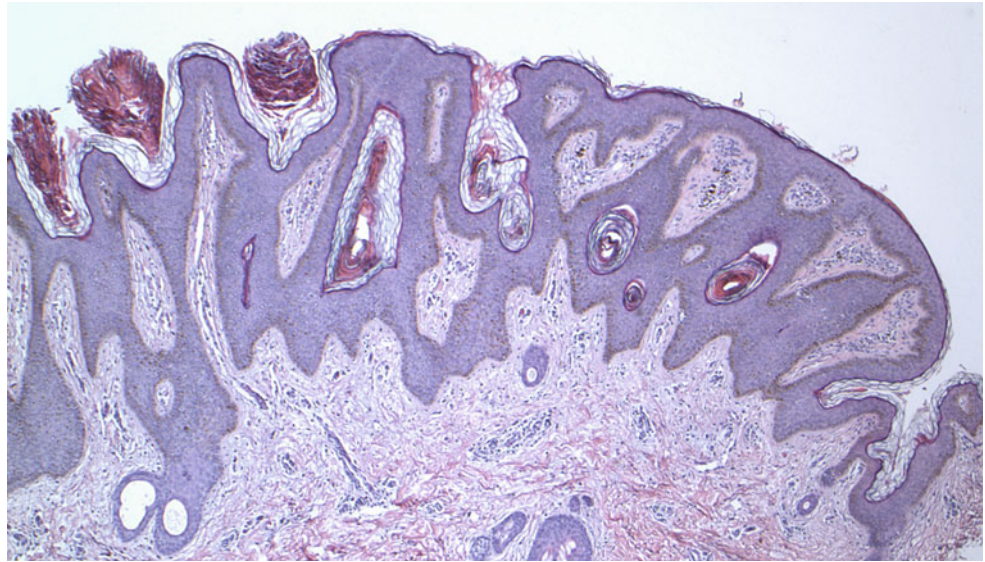
5.3 Epidermal Birthmarks

The two main epidermal birthmarks are the *epidermal nevus* (*linear or verrucous epidermal nevus*) and the *sebaceous nevus*, each of which have an incidence of about 0.2 % [1, 3, 25–27]. The Becker nevus is a more uncommon member of this group. Linear epidermal nevus and nevus sebaceous syndromes are rare neurocutaneous syndromes characterized by epidermal nevi, epilepsy, and mental retardation [6, 25]. Tuberous sclerosis, Sturge-Weber syndrome, and neurofibromatosis I are examples of other neurocutaneous syndromes [1, 27, 28].

5.3.1 Epidermal Nevus

The *epidermal nevus* occurs as local or systemic lesions noted at birth or developing later on in childhood. They present as flesh-colored to yellow-brown, verrucous, oval, or linear plaques that continue to enlarge and spread until puberty. Microscopically, they have the appearance of a papilloma, that is, they display papillomatosis, hyperkeratosis, and acanthosis [1, 3, 4, 6] (Fig. 5.7). The epidermal nevus is associated not only with benign and malignant tumors that arise from within the nevus but also with an increased incidence of non-cutaneous malformations within the central nervous system, eye, and skeleton. The *epidermal nevus syndrome* is characterized by the triad of large epidermal nevi, mental retardation, and epilepsy [1, 3, 7]. Skeletal anomalies, vascular malformations, and eye defects have been described also.

Fig. 5.7 Giant linear epidermal nevus. This 3-year-old boy had multiple, large congenital epidermal nevi on the head, trunk, and extremities. The lesions involved the right side of the body, stopping abruptly at the midline, and did not increase in size after birth. No other congenital anomalies were present. The epidermal nevus has a verrucous appearance and appears darker than the surrounding skin. There is papillomatosis, hyperkeratosis, and acanthosis, features of a papillomatous process (Reprinted from Isaacs [5]. © W.B. Saunders, 1997)



5.3.2 Becker's Nevus (Becker's Melanosis)

This pigmented variant of epidermal nevus usually appears in childhood or adolescence, but it may be found at birth [4, 29]. Clinically, the lesion presents as a pigmented macule containing many hairs, and microscopically, it shows acanthosis and diffuse, heavy pigmentation of epidermal cells. Moreover, Becker's nevus has been described in association with smooth muscle hamartoma and neurofibroma [1, 4, 26].

5.3.3 Sebaceous Nevus

Sebaceous nevus occurs in infants as flat or slightly raised yellow-brown to pink, hairless plaques distributed

over the scalp or forehead. The nevus tends to regress after birth only to enlarge again at puberty. Biopsy of the lesion in the first year of life may show no definite diagnostic abnormality, but later on, the skin appendages appear malformed and irregular, and the sebaceous glands are increased in number [4, 6, 7, 25, 30] (Fig. 5.8). Older individuals with nevus sebaceous are at risk for developing basal cell carcinoma and adnexal tumors arising from the lesion, and therefore, removal is indicated. Moreover, some patients with nevus sebaceous have central nervous system and other anomalies in common with both the epidermal nevus syndrome and tuberous sclerosis [3, 6, 7, 25]. *Optic glioma (pilocytic astrocytoma)* and abnormal neuronal migration have been described with the linear sebaceous nevus syndrome [30].

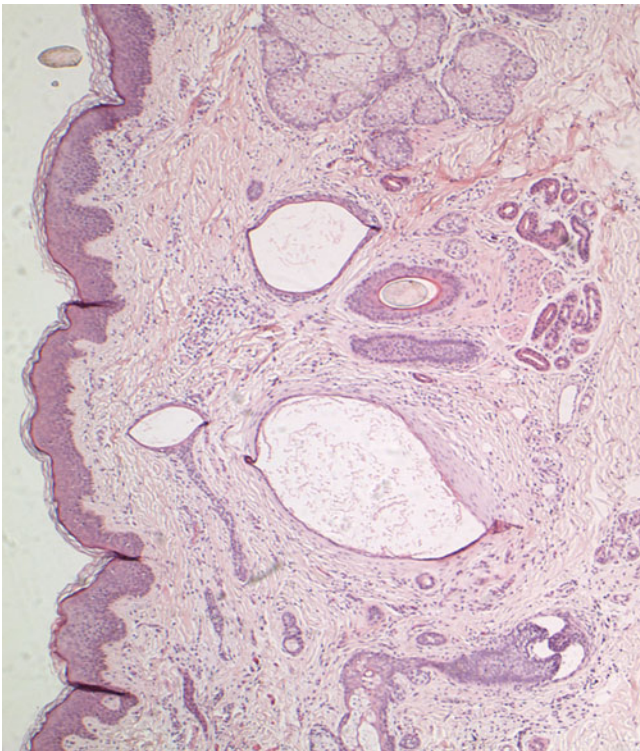


Fig. 5.8 Nevus sebaceus. Typically, the lesion presents at birth as a flat yellowish, hairless plaque on the scalp, forehead, or neck. Hyperkeratosis, irregular papillomatosis, and acanthosis are noted. Skin appendages are malformed consisting of sebaceous glands without hair follicles (Reprinted from Isaacs [5]. © W.B. Saunders, 1997)

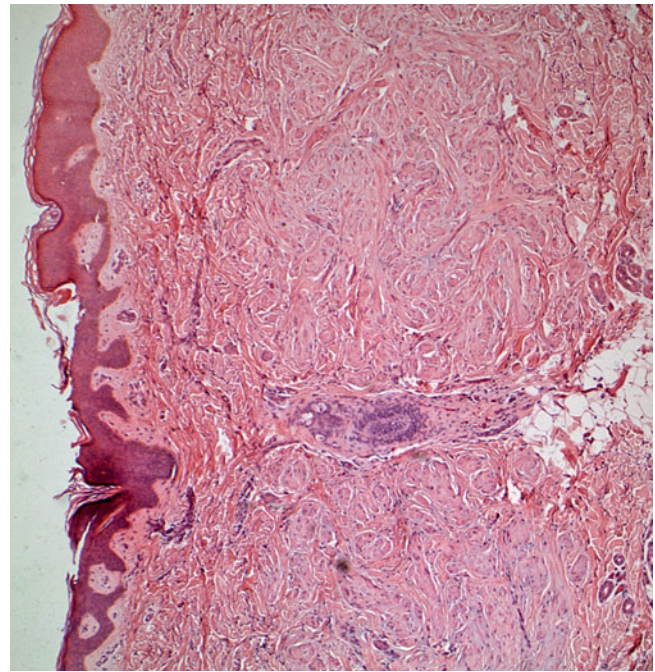


Fig. 5.9 Smooth muscle hamartoma. The lesion most likely represents overgrowths of arrector pili smooth muscle; typically, it occurs in the lumbosacral region. Prominent bundles of smooth muscle are noted within the dermis (Reprinted from Isaacs [5]. © W.B. Saunders, 1997)

5.4 Cutaneous Hamartomas

5.4.1 Smooth Muscle Hamartoma

Smooth muscle hamartoma is usually noted at birth manifesting as an irregular elevated patch with hypertrichosis and mild hyperpigmentation [1, 4, 26]. The incidence of the lesion is about 1:2,600. It is located primarily over the lumbar area. Microscopically, the main finding is a haphazard proliferation of smooth muscle bundles within the lower dermis (Fig. 5.9). When hypertrichosis is present, prominent hair follicles are attached to the smooth muscle bundles. An association with Becker's melanosis has been suggested [4, 29].

5.4.2 Nevus Lipomatosus

Nevus lipomatosus is a rare, often congenital, hamartoma of adipose tissue characterized by excessive amounts of adipose tissue in the dermis [4, 31]. Clinical features include large irregular papules and nodules situated most often in the skin of the hip and gluteal region. The infant may have generalized folding of the skin giving it the appearance of the "Michelin-tire baby." The folding gradually decreases as the child becomes older [4, 31].

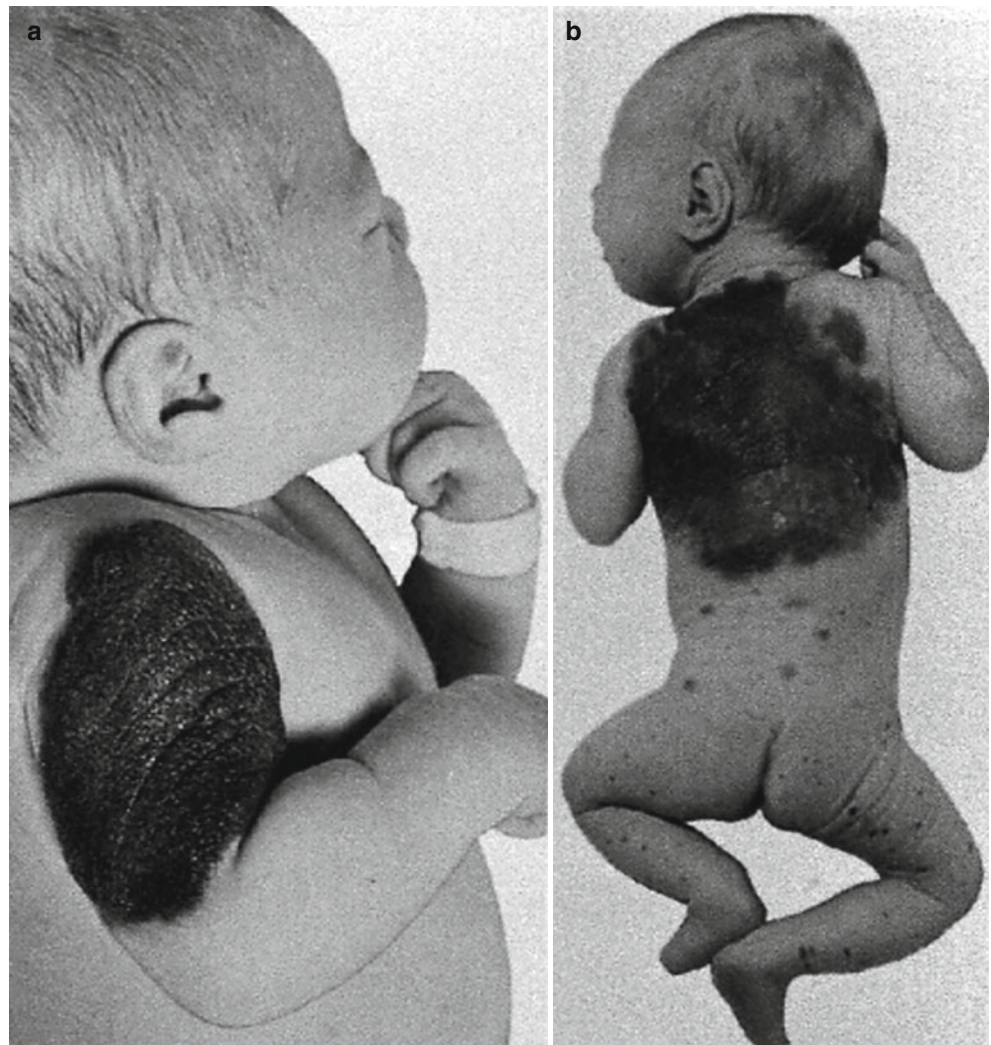
Other types of "mesenchymal" hamartoma have been described in the newborn and infant skin. *Connective tissue, neural* composed of Schwann cells, and *facial rhabdomyomatous mesenchymal hamartomas* consisting of mature skeletal muscle and fat are examples [4, 32–34].

5.5 Melanocytic Nevi

5.5.1 Pigmented Nevus

The term *nevus*, mentioned above, is used in a broad sense to include all abnormal growths in the skin but in a more restricted sense is limited to tumors containing nevus cells [6, 7]. Pigmented nevi also are called *melanocytic or nevocellular nevi*. Since most nevus cells contain melanin, the majority of true nevi are pigmented, the color varying from light brown to black. It has been estimated that they are present in the skin of at least 90 % of the adult population [6, 7]. Although melanocytic nevi are common among adults, they are not often visible at birth. Roughly 1 % of melanocytic nevi are congenital [6, 7]. Nevi less than 2 cm in greatest dimension are by far more common than the giant pigmented nevi, which are noted in less than 1 in 20,000 newborns [35, 36].

Fig. 5.10 Congenital verrucous, hairy pigmented nevi. (a) Lesion localized to the upper arm. (b) Large lesion on the upper back with small, flat, pigmented nevi over the rest of the body (Reprinted from Isaacs [6]. With kind permission of © Mosby, 1997)



5.5.2 Giant Congenital Melanocytic Nevi

Giant pigmented nevi are cutaneous developmental anomalies of the neural crest since they often contain both melanocytic (nevus cells) and neural elements, similar to those observed in association with neurofibromatosis [37–44]. Nevi may be located on the face, trunk, or extremities and involve extensive areas of the skin affecting an entire segment of the body [1, 6, 7, 45–49] (Figs. 5.10 and 5.11). Giant pigmented nevi have a variable gross appearance ranging from flat to nodular to rough and verrucous. The amount of pigmentation and hair present differ as well with each lesion and with the age of the patient. Generally, the color is dark-brown or black. When present on the trunk, countless other small non-elevated nevi are usually scattered over the surrounding skin. Lesions on the extremities are more often single.

The histological features of congenital melanocytic nevi, either giant or otherwise, are different in some respects from those of acquired nevi [1, 6, 7, 35–49]. In the neonate, most congenital nevi are classified histologically as com-

pound, that is, nevus cells are situated in the epidermis, epidermal–dermal junction, and dermis, but later on in childhood, the nevus cells tend to be more intradermal in location [1, 6, 7]. The main finding observed in the congenital melanocytic nevus that distinguishes it from the acquired nevus is that nevus cells extend deeply into the dermis and subcutaneous fat and connective tissue and surround skin appendages, blood, and lymphatic vessels in an infiltrative fashion (Fig. 5.11). The cells, which are triangular or polyhedral, are arranged in small groups isolated by narrow connective tissue fascicles. The nevus cells are reactive with S-100 protein and HMB-45. Some cells contain melanin. The amount of melanin both in normal skin and in nevi increases after birth and causes deepening of the color of the nevi or makes them visible for the first time. Maturation of nevus cells, that is, they become smaller and rounder as they migrate deeper into the dermis, is an important histological feature of benign nevi. In addition to the melanocytic component mentioned above, the congenital nevus may contain blue nevus and neural elements, the



Fig. 5.11 Giant congenital melanocytic nevus. (a) 3-month-old male with a huge pigmented nevus involving most of the back, thorax, and abdomen. In addition, there are multiple other pigmented nevi located on the extremities and scalp. (b) Biopsy reveals nests of pigmented and nonpigmented nevus cells situated in the dermis and deep in the subcutaneous tissue surrounding skin appendages which is a characteristic

feature of congenital melanocytic nevi. (c) The cut surface of a large nodule, 3 cm in diameter, on the right side of the back has a pale white gelatinous cystic appearance. (d) Sections of the nodule show palisades of spindle-shaped cells of a neuroid component (Reprinted from Isaacs [5]. © W.B. Saunders, 1997)

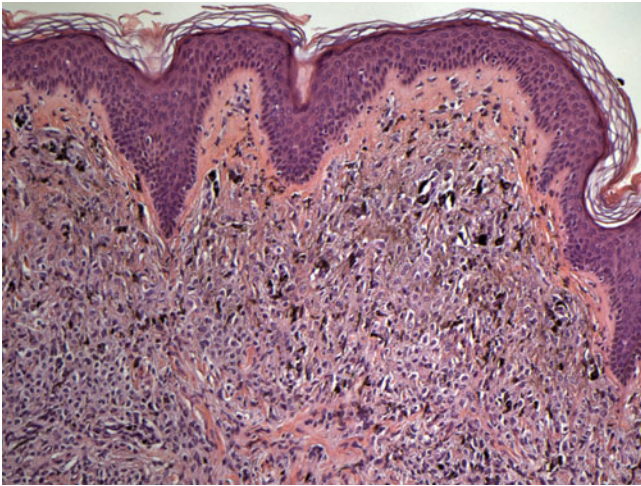


Fig. 5.12 Blue nevus within a congenital melanocytic nevus. In addition to clusters of round to oval nevus cells within the epidermal–dermal junction, dermis, and subcutis, collections of darkly staining spindle cells are present. Congenital melanocytic nevi may contain three different types of tissues: pigmented nevus cells, neurocytic elements resembling neurofibroma, and blue nevus cells (Reprinted from Isaacs [5]. © W.B. Saunders, 1997)

latter in the form of Schwann cells, Meissner's corpuscles, Verocay bodies, neurofibroma, and ganglioneuroma [4, 36, 38, 41] (Fig. 5.12). An extra chromosome 7 (trisomy 7), described in malignant melanoma, has been found in congenital pigmented nevi as well [41].

Nevus cell aggregates occur in placentas and lymph nodes of newborns with giant pigmented nevi [42–44]. The interstitium of placental villi is infiltrated by collections of nevus cells. Melanin pigment is present within both nevus cells and in the interstitium. Neither the umbilical cord nor the fetal membranes are affected usually. An aberrant migration of neural crest elements is suggested as an explanation for this unusual placental finding [42, 43]. Nevus cell aggregates resulting from lymphatic spread are noted also in lymph nodes of patients with giant congenital nevi [44]. In this setting, both ordinary and “atypical” nevus cells are found in the lymph nodes which are S-100 and variably HMB-45 positive and display melanosomes and other ultrastructural features of melanocytes [44].

5.5.3 Malignant Melanoma

Nearly all nevi seen at birth are benign and grow only as the body grows, but a few have been described that were considered to have been malignant even before birth [6, 7, 45–53].

The exact incidence of malignant melanoma arising from a giant pigmented nevus is difficult to determine from the literature with published figures ranging from 3 to 12 % [35, 36, 45–48].

Congenital malignant melanoma can be divided into 4 main categories: (1) transplacentally acquired from the mother, (2) primary malignant melanoma developing antenatally de novo, (3) melanoma originating from a giant melanocytic nevus, and (4) melanoma arising from neurocutaneous melanosis [5–7, 36, 45, 46, 50]. Transmission of melanoma to the mother from the affected fetus via the placenta has not been documented.

In the first category, the fetus develops malignant melanoma as a result of advanced maternal disease and transplacental metastases. The affected mothers are usually primiparous, conceive within 4 years of their diagnosis and treatment, and have a high rate of recurrence and a 100 % mortality [5, 50–53]. The involved placentas have a mottled brownish-black appearance varying in size from normal to enlarged [46]. Tumor cells are present within the intervillous space and rarely in the chorionic villi per se. Fetal melanoma is not usually apparent at birth but becomes manifest several weeks or months post partum. Occasionally, there are exceptions where tumor cells are found in the cord blood and cutaneous lesions appear in the neonatal period [51]. Of 6 infants reported with transplacental congenital melanoma, 5 died within 11 months and 1 survived [5].

In the second category, melanoma may arise de novo from smaller pigmented nevi in the fetus during gestation and metastasize [46, 50, 53–57]. Primary cutaneous melanoma typically presents as a small, 1–3 cm, fast-growing black tumor with a tendency to ulcerate and bleed. The most common sites are the head and extremities [6, 7]. Their behavior even in the presence of metastases is unpredictable [45]. Williams and Pennella reported an overall mortality rate of 40 % from their analysis of 13 childhood surveys [48]. Cutaneous malignant melanoma associated with a giant pigmented nevus falls into the third category; the malignancy has been detected by antenatal sonography [1, 7, 46]. Patients with melanomas arising from giant pigmented nevi have an intermediately poor outcome compared to those with transplacental metastatic disease and those with primary melanomas. The mortality rate for six patients in one series was 67 % [5]. Of the six patients, two survived and were the only ones treated, that is, by surgical resection. Metastases were documented in three, all of whom died in the neonatal period (Fig. 5.13).



Fig. 5.13 Malignant melanoma. (a) Widespread metastases were present over the body with tumor arising from the anal and genital region. Tumor cells were found also in the brain and liver. (b) Skin from older child with superficial spreading melanoma, which is one of the main forms of melanoma arising from congenital melanocytic

nevi. Clusters of melanoma cells are present within the epidermal junction with extension into the epidermis and dermis. The dermis beneath the tumor shows a chronic inflammatory infiltrate intermingled with pigmented melanophages (Reprinted from Isaacs [5]. © W.B. Saunders, 1997)

5.5.4 Neurocutaneous Melanosis

Neurocutaneous melanosis (melanocytosis, Touraine's syndrome) is a rare congenital disorder where giant or multiple congenital melanocytic nevi occur in association with benign or malignant melanocytic tumors of the leptomeninges [5, 7, 36, 39, 40, 45, 58]. This disorder comprises the fourth category in which congenital malignant melanoma occurs. Normally, melanin-containing cells are present in the leptomeninges of individuals particularly over the brain stem [39]. Dandy-Walker malformation and the Sturge-Weber syndrome are reported in patients with this disease [40]. Cytological examination of the cerebrospinal fluid in patients

with neurocutaneous melanosis is an important diagnostic procedure which reveals pigmented nevus cells with atypical hyperchromatic nuclei and cytoplasmic projections [58].

Touraine's syndrome is the clinical manifestation of neurocutaneous melanosis and is characterized by increased intracranial pressure, seizures, developmental delay, and generally a poor prognosis [48, 58]. Patients with neurocutaneous melanosis become symptomatic before 2 years of age. Eventually, half of the children develop leptomeningeal melanoma. Leptomeningeal melanoma infiltrates the leptomeninges and forms multiple nodules in the brain [58]. When this occurs, frankly malignant-appearing pigmented cells appear in the cerebrospinal fluid.

When a *melanoma* originates from a congenital nevus, it generally occurs at the epidermal–dermal junction and has the features of the ordinary form of malignant melanoma, specifically the superficial spreading type [4] (Fig. 5.13b). Sometimes, the melanoma in a giant pigmented nevus arises deep in the dermis which is different from almost all other cutaneous melanomas [4, 39]. In this setting, the melanoma consists mostly of small undifferentiated “blastic cells” resembling lymphoblasts or neuroblasts and containing little or no melanin [4, 39].

There are several different types of malignant neoplasms arising from congenital nevi other than melanoma [1, 4, 38, 59–61]. *Liposarcoma*, *rhabdomyosarcoma*, *malignant blue nevus*, *malignant peripheral nerve sheath tumor*, and other undifferentiated spindle-cell tumors presumably of neural origin are examples [59–61]. It is important to note that peculiar differentiation is to be expected in neoplasms arising in congenital nevi and that alarming cellular tumors may not behave aggressively [4, 38, 41]. Therefore, pathology does not always predict the outcome in the young infant [4].

Cellular proliferative nodules arising from dermal components of congenital pigmented nevi usually do not behave in a clinically aggressive fashion. According to Elder et al., indications of a likely benign behavior in such nodules are the following: a low mitotic rate, absence of necrosis, lack of high-grade nuclear atypia, and evidence of maturation in the form of “blending” or transitional forms between the cells in the nodule and the adjacent nevus cells [4].

The complex treatment and management of congenital melanoma is beyond the scope of this atlas, and readers are referred elsewhere (e.g., PubMed.gov, PubMed U.S. National Library of Medicine National Institutes of Health).

5.6 Neurofibromatosis

Neurofibromatosis (NF) includes several entities, most of which are transmitted as an autosomal dominant trait [28, 62–64]. The main forms of neurofibromatosis recognized at birth are NF-1, which is the classic form or Von Recklinghausen’s disease and is responsible for most of the cases, and less commonly NF-2 which is associated with bilateral acoustic neuromas.

The gene locus for NF-1 has been localized to chromosome 17q11.2 and encodes the protein gene product neurofibromin [28]. The frequency of neurofibromatosis is approximately 1 in 3,000 live births [63].

Skin findings in the newborn with types 1 and 2 consist only of a few cafe-au-lait spots, which increase in number as the child grows older [1, 7, 62] (Table 5.3). One or more cutaneous neurofibromas may be present at birth particularly with NF-1. There is a strong family history in newborns with

congenital NF-1, 70 % in one study [28]. The tumors are almost always *plexiform neurofibromas* [1, 7, 62] (Fig. 5.11). The earlier the appearance of the plexiform neurofibromas the more likely there will be serious neurologic and other problems later on [28, 64]. Congenital generalized (disseminated) neurofibromatosis is associated with a poor prognosis with mortality rates as high as 92 % [28]. Pathological findings are discussed in Chap. 4.

5.7 Tuberous Sclerosis

Tuberous sclerosis (TSC) is an autosomal dominant disorder that presents with highly variable clinical manifestations including seizures, mental retardation, skin lesions, and hamartomas affecting multiple organ systems such as the heart, brain, eye, and kidney [1, 7, 27]. Obvious signs may be present in the perinatal period. Cardiac rhabdomyoma(s) detected on routine antenatal sonography, arrhythmias, cerebral lesions, hydrops, and stillbirth are the major presenting findings in the fetus whereas respiratory distress, arrhythmias, murmurs, and cardiomegaly are the main ones initially in the infant. Skin lesions and retinal hamartomas are noted rarely at birth [27]. When TSC manifests in the perinatal period, it is associated with a high incidence of morbidity and mortality [27].

Facial angiofibroma and *fibroma*, *shagreen patch*, and leaf-shaped *areas of hypopigmentation* are the four main cutaneous lesions occurring in patients with TSC [4, 7] (Table 5.4). The earliest cutaneous manifestation of the disease is the maple leaf-shaped area of white hypopigmentation which may be present at birth [4, 7]. Later in childhood when mental deficiency and seizures become apparent, the characteristic facial angiofibromas and other hamartomatous lesions begin to appear. Central nervous system, eye, and cardiac lesions of tuberous sclerosis are discussed in Chaps. 9, 10, and 15, respectively.

Table 5.4 Skin lesions of the fetus and infant associated with neurofibromatosis

Cafe-au-lait patches
Hyperpigmentation
Hypopigmentation
Axillary freckling
Neurofibroma
Hemangioma
Melanocytic nevi
Juvenile xanthogranuloma

Reprinted from Elder et al. [4]. With kind permission of © Lippincott-Raven, 1997; Reprinted from Riccardi [62]. With kind permission of © Elsevier, 1992; Reprinted from Isaacs [1]. © Springer-Verlag, 2002

5.7.1 Infantile Digital Fibromatosis

Digital fibromatosis presents clinically as one or more nodular swellings on the sides or dorsal surfaces of the distal or middle aspects of the fingers or toes [1, 7, 14]. The tumor occurs almost exclusively in neonates and infants. Most eventually resolve at puberty although there is an increased incidence of recurrence after inadequate excision [1, 6, 14] (Fig. 4.15).

5.7.2 Fibrous Hamartoma of Infancy

Under this term, Enzinger described poorly circumscribed, rapidly infiltrating tumors of the dermis and subcutaneous tissue present at birth or appearing in the first year of life (average age 51/2 months), which occurred almost exclusively in males [14, 66]. Most frequent in the region of the shoulder, axilla, and upper arm, they consist of loosely arranged myxoid-appearing cellular connective tissue, tendon-like bands of fibrous connective tissue and fat (Figs. 4.21 and 4.22). Some lesions spread or recur locally following removal, but distant metastases do not occur. Fibrous hamartoma histological findings are discussed in more detail in Chap. 4.

5.7.3 Papilloma

Papillomas may be found at birth as localized outgrowths of skin and connective tissue [6, 7]. They may be present on any part of the body but are most common on the side of the face in front of the ear, where they arise by anomalous growth of tissue surrounding the first branchial cleft. The ear may be abnormal also in shape. Papillomas may result from adhesions attaching the skin to the amniotic sac, for example, with an omphalocele [6, 7].

5.8 Tumors and Tumor-Like Infiltrations of the Skin

Malignant neoplasms may appear in the infant as *cutaneous metastases* which may be the first manifestation of the tumor (Table 5.5). Generally, this finding portends a poor prognosis for the affected child [3, 6–10]. The tendency for infants to present with skin nodules is one of the significant differences between cancers in the young and the same malignancy in the older individuals [8]. The differential diagnosis of bluish skin nodules producing the so-called blueberry muffin baby is divided roughly into two main groups: neoplastic and non-neoplastic [1, 11] (Table 5.5). The nonneoplastic group consists of infections (“TORCH” infectious agents) and blood dyscrasias such as hemolytic disease of the newborn and

Table 5.5 Cutaneous metastases in the neonate: distribution of cutaneous metastases in the neonate ($n=208$)

Tumor	Incidence (n/%)	Survival (%)
Leukemia	80 (38.5) ^a	30/80 (37.5)
Multisystem LCH	43 (20.7)	23/43 (53.5)
Neuroblastoma	36 (17.3)	21/36 (58.3)
Rhabdoid tumor	24 (11.5)	1/24 (4.2)
Rhabdomyosarcoma	13 (6.3)	2/13 (15)
PNET	5 (2.4)	1/5 (20)
Choriocarcinoma	4 (1.9)	1/4 (25)
Adrenocortical carcinoma	3 (1.4)	2/3 (67)
Overall survival		81/208 (39)

Isaacs [8]. With kind permission of © Wiley, 2011

^aPercent

twin–twin transfusion. The neoplastic category includes leukemia and other malignancies which manifest in the formation of cutaneous malignant tumor nodules [1, 11]. Malignancies most often associated with cutaneous metastases in the newborn, in order of rank, are leukemia, multisystem Langerhans histiocytosis, neuroblastoma, rhabdoid tumor, rhabdomyosarcoma, PNET, choriocarcinoma, and adrenocortical carcinoma [8].

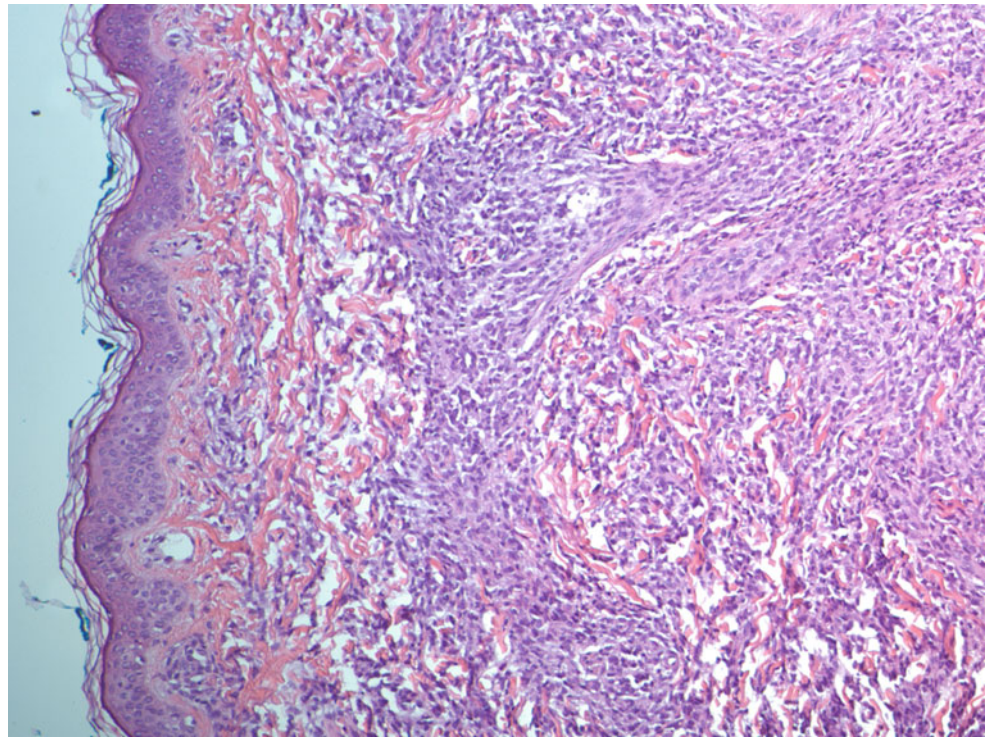
5.8.1 Leukemia

Leukemia cutis occurs in more than half of infants born with leukemia and is often associated with a high leukocyte count and hepatosplenomegaly [5, 8, 9, 11, 67] (see Chap. 7). When extensively involved, the skin may have a nodular, indurated appearance (Figs. 7.2 and 7.7). Skin biopsy reveals infiltrates of immature lymphoid, monocytic, or myeloid cells, depending on the type of leukemia, within the dermis and subcutaneous tissues (Fig. 5.14). Acute monocytic leukemia is the most common form of acute non-lymphoblastic leukemia (ANLL) and the main cytological type associated with infant leukemia cutis [1, 67]. EM and immunocytochemical studies may be required to rule out other conditions which present in a similar way. Bone marrow examination is not always helpful in resolving the issue. The infant’s leukemia and leukemia cutis may spontaneously resolve [5, 9, 11] (Fig. 7.7). Survival rate of infants with leukemia cutis in one study was 37.5 %; 30 of the 80 patients were alive in remission [8].

5.8.2 Neuroblastoma

Neuroblastoma is the leading malignant tumor of the newborn and infant [1, 6–8, 68, 69]. The tumor is unique because of its distinctive biologic behavior and many different clinical manifestations. Multiple bluish cutaneous nodules producing

Fig. 5.14 Leukemia cutis. 1-month-old female with acute myeloid leukemia had a peripheral leukocyte count of 118,000 and several raised purplish nodules on the scalp. Biopsy of a scalp nodules reveals a dense cellular infiltrate composed of small round tumor cells in the dermis and subcutaneous tissue. The cells consist of round, oval, or indented nuclei some with prominent nucleoli. Myeloid markers were positive (From Isaacs [8], with permission)



the “blueberry muffin baby” appearance occur in over a third of patients under 1 year of age, and it may be the initial presentation of metastatic neuroblastoma [8, 68, 69] (Fig. 5.15). Most infants with cutaneous metastases are classified as stage IV-S. In addition to their skin lesions, typically IV-S patients have a small tumor situated in the adrenal with multiple metastases to the liver and bone marrow which tend to spontaneously resolve [68, 69]. Histological examination of the cutaneous nodule reveals a uniform small cell malignant

tumor with or without Homer-Wright pseudorosette formation. The tumor cells show neuron-specific enolase and synaptophysin reactivity and neurosecretory (dense core granules) and neurotubules by EM [1, 7, 69].

The adrenal is the most common primary site of neuroblastoma in infants with cutaneous metastases [1, 7, 69]. The interval between appearance of skin lesions and diagnosis is often the same. More than half, 21/36 (58%), of infants with skin metastases in one study survived [8].

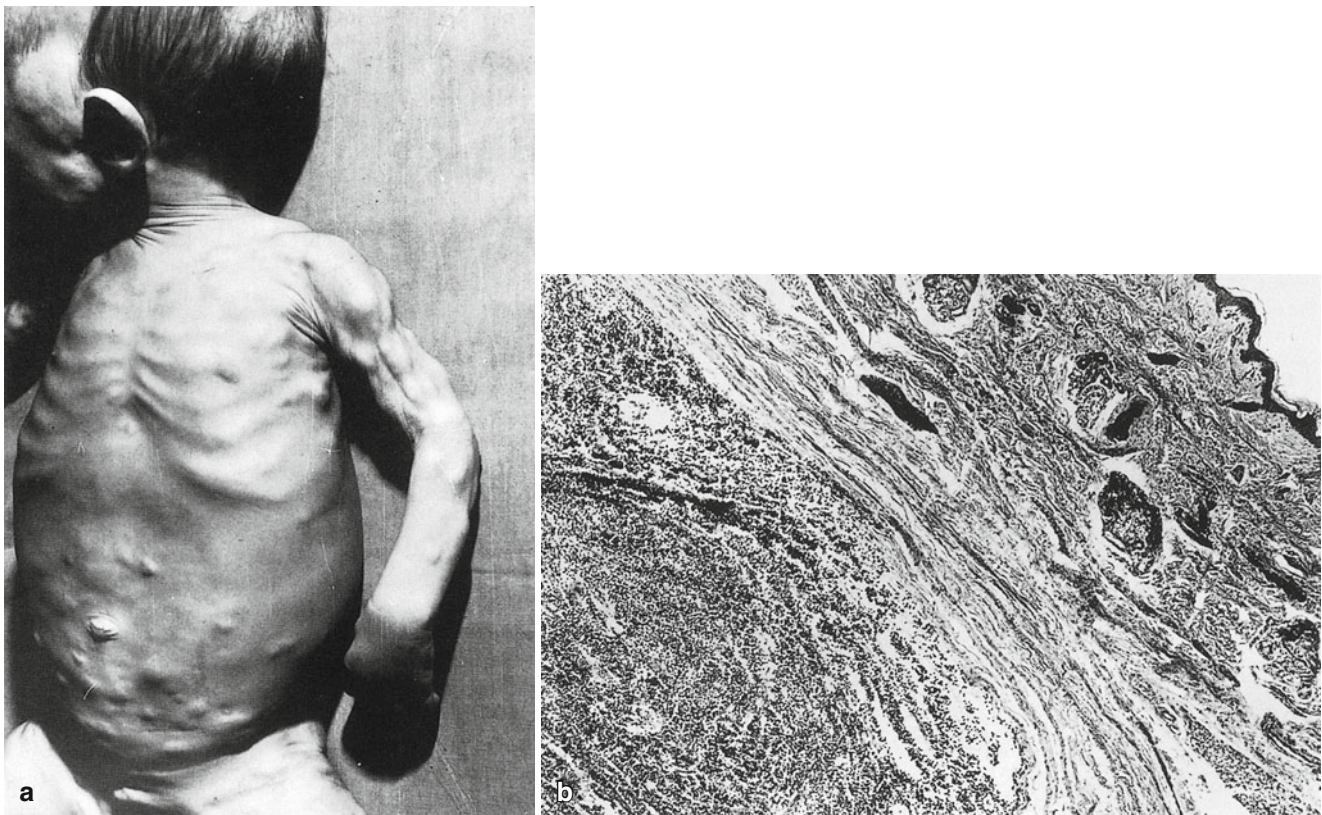


Fig. 5.15 Skin nodules as the initial manifestation of congenital neuroblastoma (“blueberry muffin baby”). (a) 3-month-old male with IV-S neuroblastoma and multiple cutaneous nodules distributed over the

body. (b) Subcutaneous nodule showing a partially autolyzed small cell malignant tumor (Reprinted from Isaacs [5]. © W.B. Saunders, 1997)

5.8.3 Langerhans Cell Histiocytosis

Skin lesions are an important manifestation of *Langerhans cell histiocytosis (LCH)* in the fetus and infant [8, 65, 70]. Typically, patients with disseminated disease present with a salmon-colored macular papular rash, refractory to therapy accompanied by anemia, thrombocytopenia, hepatosplenomegaly, lymphadenopathy, and generally failure to thrive [5, 7, 65, 70, 71] (Fig. 5.16a).

The disease is considered as a proliferation of Langerhans cells that normally reside in small numbers in the skin and other organs. A generalized polymorphous eruption is more common initially than cutaneous blue nodules in infants with multisystem LCH. Approximately half of infants with multisystem LCH die within a year of diagnosis [8].

Diagnosis of LCH is established following a skin biopsy of a representative lesion which microscopically shows variable numbers of Langerhans histiocytes infiltrating the subcutaneous tissue, dermis, and extending through the epidermis into the stratum corneum, which are helpful diagnostic features [1] (Fig. 5.16b). The Langerhans cell has a characteristic coffee bean-shaped, infolded nucleus, a small nucleolus, and a eosinophilic cytoplasm. EM studies reveal the presence of hard to find diagnostic tennis

racket-shaped Birbeck granules in the cytoplasm; Langerhans cells are S-100 protein and CD1a thymocyte antigen positive [1, 7, 65, 71]. Survival of infants with disseminated LCH associated with cutaneous lesions is approximately 50 % [8, 70].

5.8.4 Juvenile Xanthogranuloma

Juvenile xanthogranuloma (JXG) is another disorder of histiocytes occurring more often in the newborn and infant than in the older child and adolescent [4, 14, 70, 72–75]. One fifth of all infants with JXG are affected at birth, and two thirds have onset of lesions prior to age 3 months [72]. Clinically, JXG presents as one or more yellow to reddish-brown cutaneous nodules usually less than 1 cm in diameter. Most occur on the head and neck area and extremities; many spontaneously regress within 2 years or less after diagnosis [1, 4, 8, 70, 72] (Fig. 5.17a). Sometimes, cutaneous JXG is associated with similar lesions in other sites such as the eye, lung, and deep soft tissues [4, 14, 70, 72, 75]. Ocular involvement is one of the most serious complications. The iris, ciliary body, sclera, or the entire orbit may become infiltrated by Langerhans cell histiocytes [75].

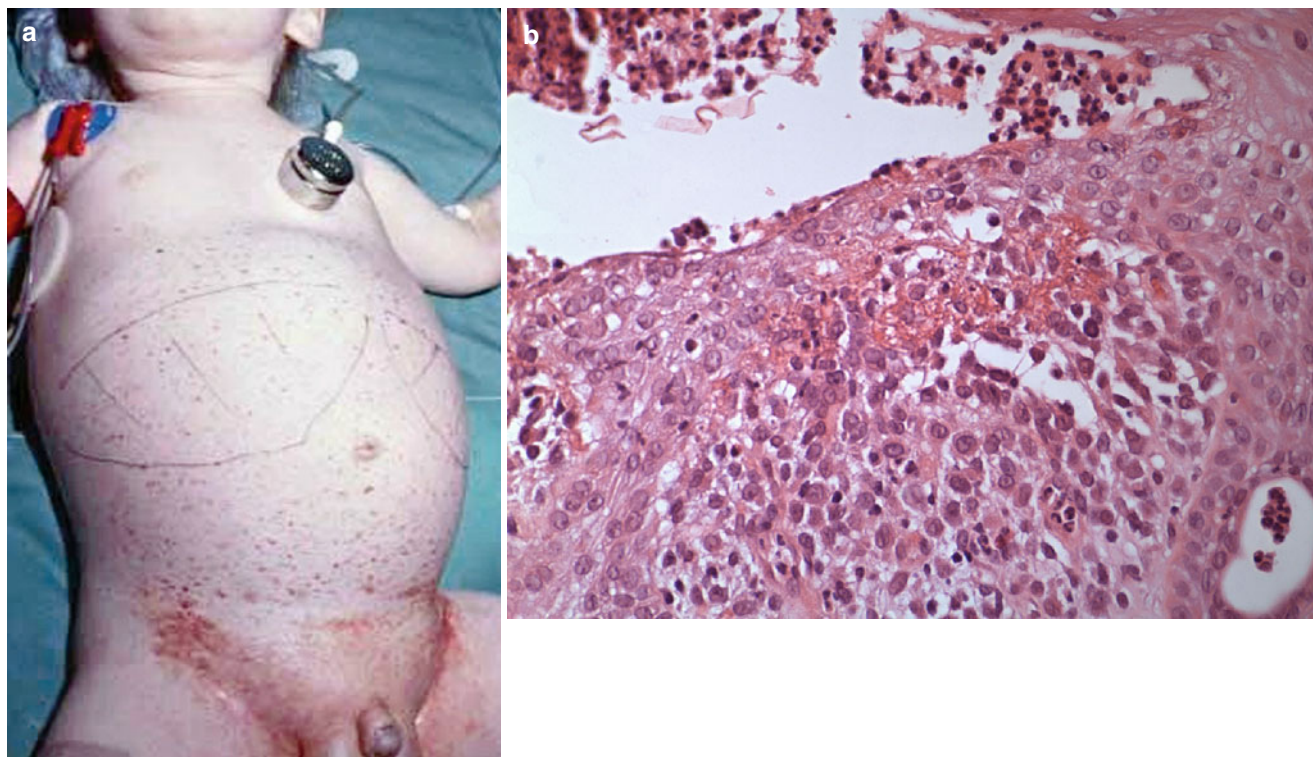


Fig. 5.16 Disseminated Langerhans cell histiocytosis (Letterer-Siwe disease). 11-month-old male with a salmon-colored maculopapular rash, anemia, thrombocytopenia, and hepatosplenomegaly. (a) The maculopapular rash is particularly prominent over the diaper area. The enlarged liver and spleen are outlined on the abdomen. (b) Biopsy of one of the skin lesions showing a dense cellular infiltrate composed of Langerhans histiocytes with characteristic “coffee bean,” folded nuclei

and prominent eosinophilic cytoplasm. The histiocytes typically extend into the epidermis as compared to urticaria pigmentosa and juvenile xanthogranuloma where the infiltrates stop abruptly at the epidermal junction. Langerhans histiocytes are S-100 and T6 thymocyte antigen positive and contain Birbeck granules with electron microscopy in comparison to the other entities mentioned above (Reprinted from Isaacs [5]. © W.B. Saunders, 1997)

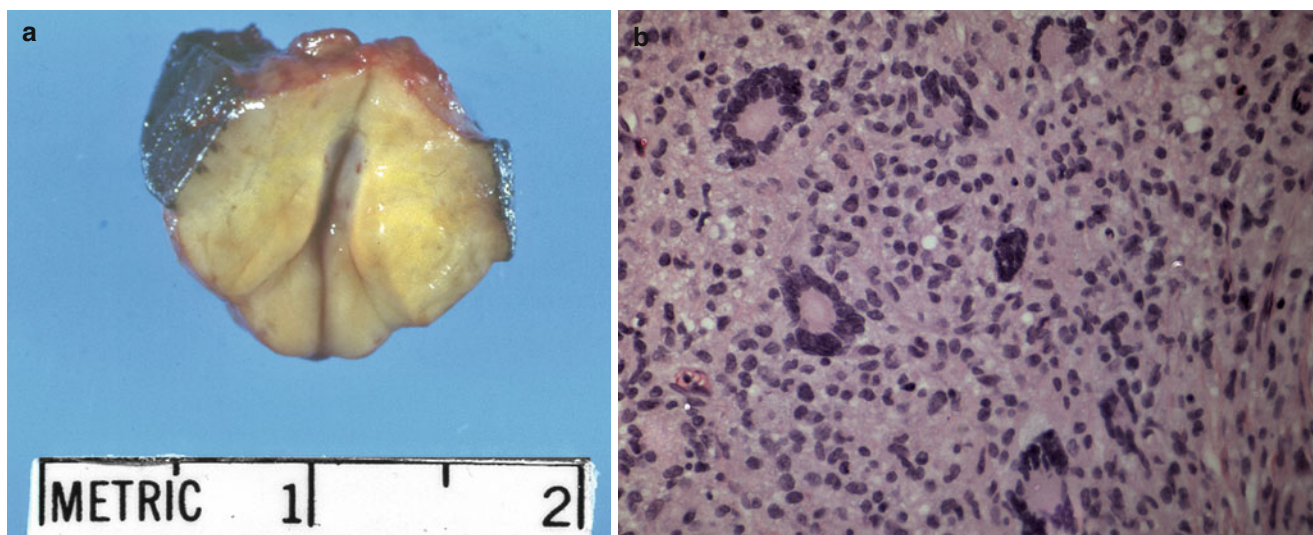


Fig. 5.17 Juvenile xanthogranuloma, later “classic” lesion. Biopsy of a scalp nodule removed from an 8-month-old male. The section shows an intact epidermis without cellular infiltrates. The dermis is infiltrated by mature appearing, vacuolated histiocytes with regular nuclei. In addition,

there are several multinucleated Touton giant cells with rows of nuclei situated at the periphery of the cell in a wreath-like fashion (Reprinted from Isaacs[5]. © W.B. Saunders, 1997)

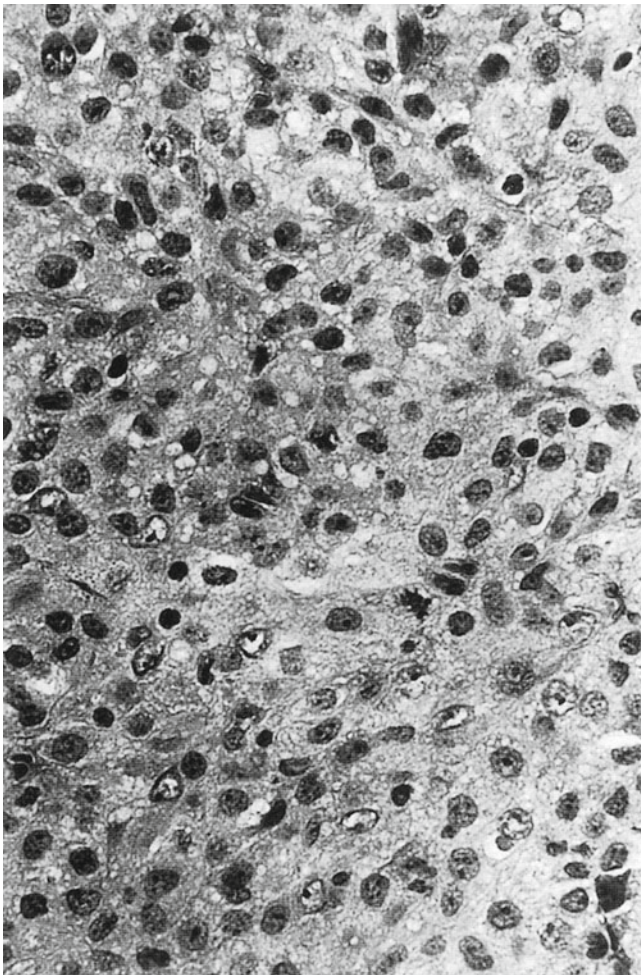


Fig. 5.18 Juvenile xanthogranuloma, early cellular variant. 4-month-old male presented with a small nodule in the posterior auricular area noted for several months. (a) Gross specimen divided in half consists of a 1.2 × 1 cm yellow nodule. (b) Histology shows uniform histiocytes with round to oval nuclei and vacuolated cytoplasm. Early lesions may not show “classic” Touton giant cells. The presence of eosinophils in the periphery of the infiltrate is a diagnostic aid. (c) Reticulin stain reveals a prominent black reticulin network surrounding histiocytes and fibroblasts (Reprinted from Isaacs [1]. © Springer-Verlag, 2002)

Microscopic examination reveals a subcutaneous nodule composed chiefly of proliferating histiocytes, often vacuolated, and fibroblasts accompanied by a lesser component of eosinophils and lymphocytes (Fig. 5.17b). The presence of multinucleated Touton giant cells is a helpful diagnostic finding which distinguishes the lesion from LCH, mastocytosis, and other cutaneous infiltrative processes [1]. However, early cellular lesions such as those found in the newborn may not contain Touton giant cells initially (Fig. 5.18). EM and immunohistochemical studies reveal that the cells are of histiocytic origin but different from the Langerhans cell. Xanthogranuloma cells are immunoreactive with CD 68, factor 3a, and vimentin but are unreactive with S-100; Birbeck granules are not found by EM [1, 73, 74].

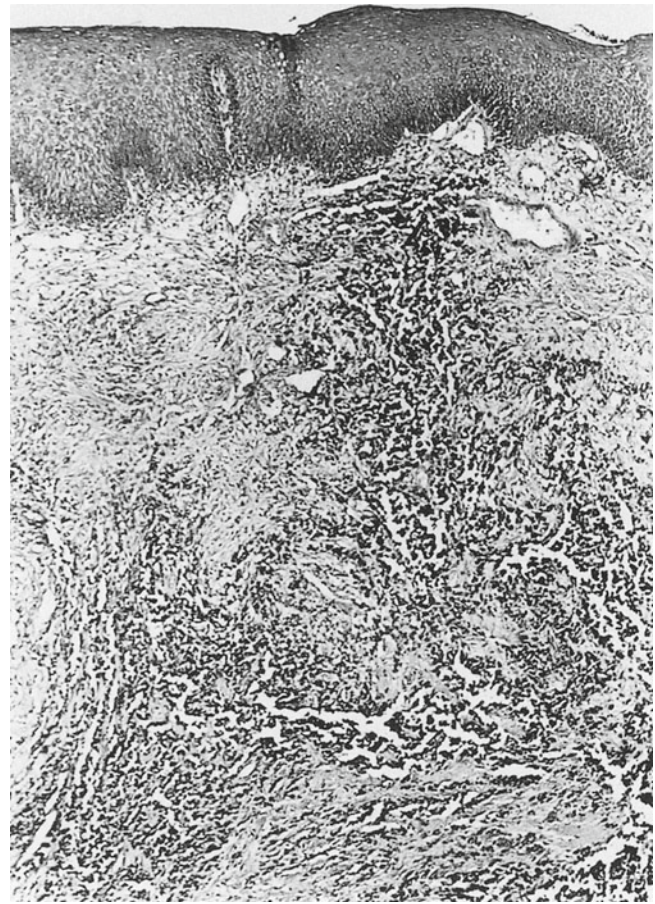


Fig. 5.19 Rhabdomyosarcoma presenting as a skin metastasis. 7-month-old male had a biopsy of what was thought to be a pyogenic granuloma of the lip. The excised specimen measured 2.5 cm in diameter and had a pale tan-gray cut surface. The biopsy shows dense infiltrates of small darkly staining neoplastic cells in the submucosa and underlying soft tissue. The tumor has a suggestive alveolar pattern (Reprinted from Isaacs [5]. © W.B. Saunders, 1997)

5.8.5 Rhabdomyosarcoma

Both primary and metastatic *rhabdomyosarcoma* (RMS) of the skin are uncommon [1, 7, 8, 61]. Alveolar RMS, the main type of RMS metastasizing to the skin, consists of small to medium-sized, darkly staining cells with rounded nuclei and scant cytoplasm arranged in an alveolar (“lung-like”) pattern (Figs. 5.19 and 5.20). The tumor is immunoreactive with vimentin, desmin, myogenin, and muscle actin [1] (Table 3.2). RMS metastasizes to the skin forming bluish cutaneous nodules similar to those found in the “blue berry muffin baby” with neuroblastoma, dermal erythropoiesis in Rh hemolytic disease of the newborn, and congenital leukemia [1, 7, 11, 68, 69] (Table 5.3). Clinically, the tumor may resemble

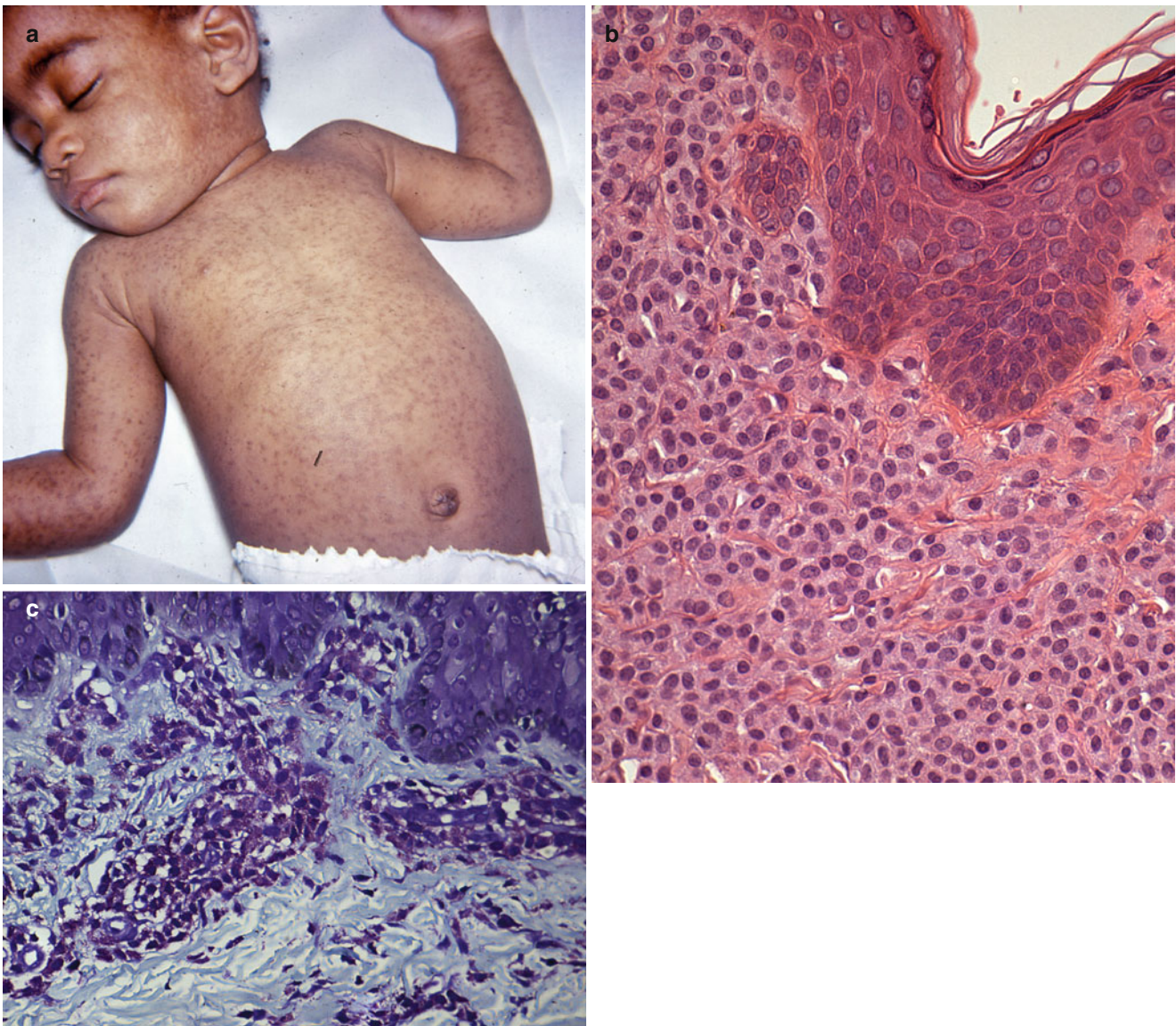


Fig. 5.20 Urticaria pigmentosa (mast cell disease). (a) 1-year-old male infant with a generalized brown, maculopapular rash that urticated (formed wheals) on stroking. (b) Skin biopsy showing a dermal infiltrate composed of rather uniform, round cells with regular small, round to

oval nuclei. (c) Giemsa-stained section demonstrating the metachromatic mast cell granules which cannot be identified on ordinary H&E stained sections (Reprinted from Isaacs [5]. © W.B. Saunders, 1997)

leukemia presenting with widespread metastases of a small blue cell tumor, which may present initially in the bone marrow aspirate.

5.8.6 Rhabdoid Tumor

In the newborn and infant, this highly malignant neoplasm is characterized by rapid growth, early metastases, and a high mortality rate. *Rhabdoid tumor* may occur in the skin, particularly in the head and neck areas, as a solitary primary tumor or as one or more metastatic blue skin nodules [8, 10, 76, 77]. Metastatic disease is noted in more

than half of fetuses and infants at the time of diagnosis [8, 77]. Concomitant brain tumors are present in almost one third with this malignancy [77]. The histological appearance is similar to the rhabdoid tumors occurring in the kidney, soft tissues, and brain (see Chaps. 4, 9, and 11, respectively). The rhabdoid cells are round to oval having a prominent eosinophilic cytoplasm, a large round, vesicular nucleus, and a single, big nucleolus. The cytoplasm contains characteristic eosinophilic inclusions composed of intermediate filaments demonstrated by EM [1, 76, 77] (see Table 3.2).

Rhabdoid tumor has the lowest survival rate, less than 5%, of all malignancies spreading to the skin [8].

5.8.7 Urticaria Pigmentosa (Mast Cell Disease)

In this condition, bullous or nodular lesions associated with focal nodular or diffuse infiltration of mast cells in the skin appear in infants, usually before 6 months of age and sometimes at birth [1, 4, 78, 79] (Fig. 5.20). Mast cell proliferations may be preceded by a pink macular rash and fever; later plaques may develop in the dermis. The solitary mast cell tumor is the most common form present at birth, and the maculopapular and nodular eruptions appear later in infancy. Development of systemic disease is considerably less common than in adult mastocytosis [4, 78, 79].

Skin lesions consist of infiltrates of mast cells within the upper dermis (Fig. 5.20b). The overlying epidermis is essentially normal except for increased melanin in the basal layers. Mast cells are round to spindle shaped with round regular nuclei by the H&E stain. They cannot be identified definitely without special stains or EM. Giemsa or toluidine blue staining demonstrates cytoplasmic purple metachromatic granules (Fig. 5.20c) and the Leder stain (naphthol chloroacetate esterase) characteristic red granules [1, 4]. When discrete, the lesions usually disappear in childhood. When diffuse, the disease may persist throughout life and become generalized involving the liver, spleen, and bone marrow, and patients rarely develop mast cell leukemia [4, 78, 79]. The prognosis in infants is generally good.

References

- Isaacs H Jr (2002) Tumors of the fetus and infant an atlas. Springer, New York
- Alper JC, Holmes LB (1983) The incidence and significance of birthmarks in a cohort of 4,641 newborns. *Pediatr Dermatol* 1:58–68
- Jacobs AH, Walton RG (1976) The incidence of birthmarks in the neonate. *Pediatrics* 58:218–222
- Elder D, Elenitsas R, Jaworsky C, Johnson BJ (eds) (1997) *Lever's Histopathology of the skin*, 8th edn. Lippincott-Raven, Philadelphia
- Isaacs H Jr (1997) Tumors and tumor-like conditions of the skin. In: *Tumors of the fetus and newborn*, vol. 35 in the series *Major problems in pathology*. W.B. Saunders, Philadelphia
- Isaacs H Jr (1997) Tumors. In: *Gilbert-Barness E (ed) Potter's Pathology of the fetus and infant*, vol 2. Mosby, St. Louis
- Isaacs H Jr (2007) Skin diseases. In: *Gilbert-Barness E (ed) Potter's Pathology of the fetus, infant and child*, vol 2. Mosby-Elsevier, Philadelphia
- Isaacs H Jr (2011) Cutaneous metastases in neonates. *Pediatr Dermatol* 28:85–93
- Resnik KS, Brod BB (1993) Leukemia cutis in congenital leukemia. *Arch Dermatol* 129:1301–1306
- Dominey A, Paller AS, Gonzalez-Crussi F (1990) Congenital rhabdoid sarcoma with cutaneous metastases. *J Am Acad Dermatol* 22:969–974
- Gottesfeld E, Silverman RA, Coccia PF et al (1989) Transient blueberry muffin appearance of a newborn with congenital monoblastic leukemia. *J Am Acad Dermatol* 21:347–351
- Greene AK, Liu AS, Mulliken JB et al (2011) Vascular anomalies in 5,621 patients: guidelines for referral. *J Pediatr Surg* 46:1784–1789
- Coffin CM, Dehner LP (1993) Vascular tumors in children and adolescents: a clinico-pathologic study of 228 tumors in 222 patients. *Pathol Annu* 28(1):97–120
- Weiss SW, Goldblum JR (1995) *Enzinger and Weiss's soft tissue tumors*, 4th edn. CV Mosby, St. Louis
- Jacobs AH (1983) Vascular nevi. *Pediatr Clin North Am* 30:465–482
- Burns AJ, Kaplan LC, Mulliken JB (1991) Is there an association between hemangioma and syndromes with dysmorphic features? *Pediatrics* 88:1257–1267
- Karvonen S-J, Vaajalahti P, Marenk M et al (1992) Birthmarks in 4346 Finnish newborns. *Acta Derm Venereol* 72:55–57
- Tallman B, Tan OT, Morelli JG et al (1991) Location of port-wine stains and likelihood of ophthalmic and/or central nervous system complications. *Pediatrics* 87:323–327
- Enjolras O, Wassef M, Mazoyer E et al (1997) Infants with Kasabach-Merritt syndrome do not have true hemangiomas. *J Pediatr* 130:631–640
- Mills SE, Cooper PH, Fechner RE (1980) Lobular capillary hemangioma: the underlying lesion of pyogenic granuloma. A study of 73 cases from the oral and nasal mucous membranes. *Am J Surg Pathol* 4:470–479
- Patrice SJ, Wiss K, Mulliken JB (1991) Pyogenic granuloma (lobular capillary hemangioma): a clinicopathologic study of 178 cases. *Pediatr Dermatol* 8:267–276
- Isaacs H Jr (1991) *Tumors of the newborn and infant*. Mosby Year Book, St. Louis
- Munkvad M (1983) Blue rubber nevus syndrome. *Dermatologica* 167:307–309
- Boente MC, Cordisco MR, Frontini MV et al (1999) Blue rubber bleb nevus (Bean syndrome): evolution of four cases and clinical response to agents. *Pediatr Dermatol* 16:222–227
- Prayson RA, Kotagal P, Wyllie E et al (1999) Linear epidermal nevus and nevus sebaceous syndromes: a clinicopathologic study of 3 patients. *Arch Pathol Lab Med* 123:301–305
- Zvulunov A, Rotem A, Merlob P (1990) Congenital smooth muscle hamartoma: prevalence, clinical findings and follow-up in 15 patients. *Am J Dis Child* 144:782–784
- Isaacs H Jr (2009) Perinatal (fetal and neonatal) tuberous sclerosis: a review. *Am J Perinatol* 26:755–760
- Isaacs HJR (2010) Perinatal neurofibromatosis: two case reports and review of the literature. *Am J Perinatol* 27:285–292
- Chapel TA, Tavafoghi V, Mehregan AH et al (1981) Becker's melanosis: an organoid hamartoma. *Cutis* 27:405–406
- Sato K, Kubota T, Kitai R (1994) Linear sebaceous nevus syndrome (sebaceous nevus of Jadassohn) associated with abnormal neuronal migration and optic glioma: case report. *Neurosurgery* 35:318–320
- Hendricks WM, Limber GK (1982) Nevus lipomatosus cutaneous superficialis. *Cutis* 29:183–185
- Mills AE (1989) Rhabdomyomatous mesenchymal hamartoma of skin. *Am J Dermatopathol* 11:58–63
- Argenyi ZB, Goodenberger ME (1990) Congenital neural hamartoma ("fascicular schwannoma"). A light microscopic, immunohistochemical, and ultrastructural study. *Am J Dermatopathol* 12:283–293
- Uitto J, Santa Cruz DJ, Eisen AZ (1980) Connective tissue nevi of the skin. Clinical, genetic, and histopathologic classification of hamartomas of the collagen, elastin, and proteoglycan type. *J Am Acad Dermatol* 3:441–461
- Ceballos PI, Ruiz Maldonado R, Mihm MC (1995) Melanoma in children. *N Engl J Med* 332:656–662
- Spatz A, Avril MF (1998) Melanoma in childhood: review and perspectives. *Pediatr Dev Pathol* 1:463–474

37. Cramer SF (1991) The origin of epidermal melanocytes Implications for the histogenesis of nevi and melanomas. *Arch Pathol Lab Med* 115:115–119
38. Hendrickson MR, Ross JC (1981) Neoplasms arising in congenital giant nevi: morphologic study of seven cases and a review of the literature. *Am J Surg Pathol* 5:109–135
39. Reed WB, Becker SW Sr, Becker SW Jr et al (1965) Giant pigmented nevi, melanoma, and leptomeningeal melanocytosis. *Arch Dermatol* 91:100–119
40. Kadonaga JN, Barkovich AJ, Edwards MS et al (1992) Neurocutaneous melanosis in association with the Dandy-Walker complex. *Pediatr Dermatol* 9:37–43
41. Drut R, Drut RM, Cohen M (1999) Adnexal-centered giant congenital melanocyte nevus with extensive ganglioneuromatous component and trisomy 7. *Pediatr Dev Pathol* 2:473–477
42. Demian SD, Donnelly WH, Frias JL et al (1974) Placental lesions in congenital giant pigmented nevi. *Am J Clin Pathol* 61:438–442
43. Antaya R, Keller RA, Wilkerson JA (1995) Placental nevus cells associated with giant congenital pigmented nevi. *Pediatr Dermatol* 12:260–262
44. Hara K (1993) Melanocytic lesions in lymph nodes associated with congenital nevus. *Histopathology* 23:445–451
45. Ruiz Maldonado R, Orozco Covarrubias ML (1997) Malignant melanoma in children. A review. *Arch Dermatol* 133:363–371
46. Campbell WA, Storlazzi E, Vintzileos AM et al (1987) Fetal malignant melanoma: ultrasound presentation and review of the literature. *Obstet Gynecol* 70:434–439
47. Rhodes AR, Melski JW (1982) Small congenital nevocellular nevi and the risk of cutaneous melanoma. *J Pediatr* 100:219–224
48. Williams ML, Pennella R (1994) Melanoma, melanocytic nevi, and other melanoma risk factors in children. *J Pediatr* 124:833–845
49. Marghoob AA, Schoenbach SP, Kopf AW et al (1996) Large congenital melanocytic nevi and the risk for the development of malignant melanoma. A prospective study. *Arch Dermatol* 132:170–175
50. Broadway D, Lang S, Harper J et al (1991) Congenital malignant melanoma of the eye. *Cancer* 67:2642–2652
51. Brodsky I, Baren M, Kahn SB et al (1965) Metastatic malignant melanoma from mother to fetus. *Cancer* 18:1048–1054
52. Cavell B (1963) Transplacental metastasis of malignant melanoma. Report of a case. *Acta Paediatr Suppl* 146(Suppl):37–40
53. Schneiderman H, Wu AYY, Campbell WA et al (1987) Congenital melanoma with multiple prenatal metastases. *Cancer* 60:1371–1377
54. Hayes FA, Green AA (1984) Malignant melanoma in childhood: clinical course and response to therapy. *J Clin Oncol* 2:1229–1234
55. Ishii N, Ichiyama S, Saito S et al (1991) Congenital malignant melanoma. *Br J Dermatol* 124:492–494
56. Pratt CB, Palmer MK, Thatcher N et al (1981) Malignant melanoma in children and adolescents. *Cancer* 47:392–397
57. Prose NS, Laude TA, Heilman ER et al (1987) Congenital malignant melanoma. *Pediatrics* 79:967–970
58. Reyes-Mugica M, Chou P, Byrd S et al (1993) Nevomelanocytic proliferations in the central nervous system of children. *Cancer* 72:2277–2285
59. Roth MJ, Medeiros LJ, Kapur S et al (1993) Malignant schwannoma with Melanocytic and neuroepithelial differentiation in an infant with congenital giant melanocytic nevus: a complex neuro-rhistopathy. *Hum Pathol* 24:1371–1375
60. Weidner N, Flanders DJ, Jochimsen PR et al (1985) Neurosarcomatous malignant melanoma arising in a neuroid giant congenital melanocytic nevus. *Arch Dermatol* 121:1302–1306
61. Schmitt FC, Bittencourt A, Mendonca N (1992) Rhabdomyosarcoma in a congenital pigmented nevus. *Pediatr Pathol* 12:93–98
62. Riccardi VM (1992) Type 1 neurofibromatosis and the pediatric patient. *Curr Probl Pediatr* 22:66–106
63. Friedman JM (2002) Neurofibromatosis 1: clinical manifestations and diagnostic criteria. *J Child Neurol* 17:548–554
64. Stewart H, Bowker C, Edees S et al (2008) Congenital disseminated neurofibromatosis type 1: a clinical and molecular case report. *Am J Med Genet* 146A:1444–1452
65. Dehner LP, Bamford JT, McDonald EC (1983) Spontaneous regression of congenital cutaneous histiocytosis X: report of a case with discussion of nosology pathogenesis. *Pediatr Pathol* 1:99–106
66. Enzinger FM (1965) Fibrous hamartoma of infancy. *Cancer* 18:241–248
67. Isaacs H Jr (2003) Fetal and neonatal leukemia. *J Pediatr Hematol Oncol* 25:348–361
68. Evans AE, Chatten J, D'Angio JG et al (1980) A review of 17 IV-S neuroblastoma patients at the Children's Hospital of Philadelphia. *Cancer* 45:833–839
69. Isaacs H (2007) Fetal and neonatal neuroblastoma: retrospective review of 271 cases. *Fetal Pediatr Pathol* 26:177–184
70. Isaacs H (2006) Fetal and neonatal histiocytoses. *Pediatr Blood Cancer* 47:123–129
71. Favara BE, Feller AC, Pauli M et al (1997) Contemporary classification of histiocytic disorders. The WHO Committee On Histiocytic/Reticulum Cell Proliferations. Reclassification Working Group of the Histiocyte Society. *Med Pediatr Oncol* 29:157–166
72. Cohen BA, Hood A (1989) Xanthogranuloma: report on clinical and histologic findings in 64 patients. *Pediatr Dermatol* 6:262–266
73. Freyer DR, Kennedy R, Bostrom BC et al (1996) Juvenile xanthogranuloma: forms of systemic disease and their clinical implications. *J Pediatr* 129:227–237
74. Sonoda T, Hashimoto H, Enjoji M (1985) Juvenile xanthogranuloma: clinicopathologic analysis and immunohistochemical study of 57 patients. *Cancer* 56:2280–2286
75. Chang MW, Frieden IJ, Good W (1996) The risk intraocular juvenile xanthogranuloma: survey of current practices and assessment of risk. *J Am Acad Dermatol* 34:445–449
76. Hsueh C, Kuo TT (1998) Congenital malignant rhabdoid tumor presenting as a cutaneous nodule: report of 2 cases with review of the literature. *Arch Pathol Lab Med* 122:1099–1102
77. Isaacs H (2010) Fetal and neonatal rhabdoid tumor. *J Pediatr Surg* 45:619–626
78. Azana JM, Torrelo A, Mediero IG et al (1994) Urticaria pigmentosa: a review of 67 pediatric cases. *Pediatr Dermatol* 11:102–106
79. Kettelhut BV, Metcalfe DD (1991) Pediatric mastocytosis. *J Invest Dermatol* 96(3 Suppl):15S–18S

6.1 Introduction

Neuroblastomas are derived from neuroblasts that arise in the neural crest and normally migrate downward to form ganglion cells and chromaffin tissue [1]. Historically, these neoplasms have been called poorly differentiated neuroblastoma, neuroblastoma, differentiating neuroblastoma, ganglioneuroblastoma, and ganglioneuroma, depending on the variety and degree of differentiation of the cells composing the tumors [2].

6.2 Incidence

Neuroblastoma is the most common malignant tumor of the fetus and infant [2–9] (Table 1.1). The Third United States National Cancer Survey (1969–1971) recorded an incidence rate of 19.7 neuroblastoma cases per million live births per year in the neonate as compared to a rate of 4.7 for both leukemia and renal tumors [2]. Neuroblastoma comprised 21 (54 %) of the 39 malignancies recorded in the survey for neonates and 67 (34 %) of 196 malignant tumors for infants.

6.3 Clinical Findings

Familial neuroblastoma, an autosomal dominant transmitted condition, occurs among siblings and identical twins and is associated with multiple primary tumors [10, 11]. Most familial cases present in the first 18 months of life at ages that fall within 1 year of the age at diagnosis of the other affected sibling. The occurrence of neuroblastoma with von Recklinghausen disease [12, 13], severe hypoglycemia in the neonate secondary to nesidioblastosis [14], central hypoventilation (Ondine's curse) [15], and Hirschsprung disease [16] suggests that the tumor is part of a complex neurocristopathy, that is, a maldevelopment of the neural crest tissues [1]. In addition, neuroblastoma has been described in association

with other apparently nonneural crest-related syndromes such as the *Beckwith-Wiedemann syndrome* (macroglossia, macrosomia, omphalocele, hypoglycemia) [17], the *CHARGE association* (choanal atresia, heart defects, growth retardation, mental deficiency, hypogonadism, ear anomalies) [2], *DiGeorge anomaly* (defect in development of fourth branchial arch and derivatives of third and fourth pharyngeal pouches-thymus, parathyroid, and aortic arch anomalies) [18], and the *fetal hydantoin* and *fetal alcohol syndromes* [19]. A wide variety of developmental defects without a specific pattern occur in association with neuroblastoma [20, 26] (Table 6.1).

Neuroblastoma exhibits many different, unusual clinical manifestations in the fetus and infant [6, 8, 9, 21] (Table 6.2). The tumor is an unsuspected finding in the fetus on prenatal sonograms. On imaging studies, the tumor appears as a cystic and/or solid mass above upper pole of the kidney with or without hydrops and hydramnios [22–26]. Metastatic disease in the fetus without an identifiable primary tumor is detected by sonography [23–25].

Fetal hydrops with extensive *placental metastases* may be evident at birth [8, 27–39] (Fig. 6.1). Congenital neuroblastoma may present with a picture similar to that of hemolytic disease of the newborn (erythroblastosis fetalis), including hydrops, anemia, hepatosplenomegaly, jaundice, and increased numbers of nucleated erythrocytes on the peripheral blood smear [28, 29]. Disseminated neuroblastoma causes intrauterine death and stillbirth [9, 29]. Placentas show neuroblasts situated almost entirely within blood vessels, particularly in the villous capillaries [9, 29, 30] (Fig. 6.1c). The placentas are histologically immature and greatly enlarged. Their gross appearances are similar to erythroblastosis due to Rh incompatibility as they tend to weigh over a 1,000 g and have a bulky edematous appearance. Many organs including the liver, spleen, and brain are infiltrated by tumor cells [9, 29] (Fig. 6.1b, d and e).

Neuroblastoma is the malignant tumor most often found at birth clinically presenting as an abdominal mass due to either an adrenal/retroperitoneal primary or to hepatomegaly

Table 6.1 Malformation and/or condition associated with neuroblastoma

Family history of neuroblastoma and Hirschsprung disease
Congenital central hypoventilation syndrome (Ondine's curse)
Nesidioblastosis, hypoglycemia
Fetal hydantoin syndrome, microcephaly
Beckwith-Wiedemann syndrome (hypoglycemia, pancreatic islet hyperplasia)
Cystic fibrosis
Hypertension, cardiomegaly
Goldenhar syndrome
Potter sequence with absent L lung and L kidney, polycystic R kidney
Monozygotic twins with neuroblastoma
Multiple congenital anomalies, NOS
<i>Congenital heart defects</i> ^{a,b}
DiGeorge anomaly with multiple cardiac defects
Endocardial cushion defect, omphalocele
Dupl (3q), t(3;10), LOH11q, ventricular septal defect
Turner syndrome, 45×0, cystic hygroma, horseshoe kidney
Weaver syndrome, ventricular septal defect, patent ductus arteriosus
Transposition of great vessels
Truncus arteriosus
Tetralogy of Fallot, pulmonary atresia
Cardiomyopathy, asymmetric septal hypertrophy

Reprinted from Isaacs [26]. With kind permission of © Springer, 2007

^aOccur in 10–20 % of patients with neuroblastoma

^bPatrone et al. [18]. With kind permission of © Allen Press, 1990

secondary to extensive metastases [5, 9, 21, 31–33] (Figs. 6.2, 6.3, 6.4 and 6.5). Over half of neuroblastomas are noted within the abdominal cavity [5, 33]. Less frequently, the tumor occurs as a mass in the mediastinum or neck, the former more frequently than the latter (Figs. 6.6 and 6.7) (see Table 6.2 for additional clinical manifestations).

Stage 4S is a special pattern of metastatic neuroblastoma unique to the first year of life that one would not anticipate as having a more favorable outcome [34–38] (Table 6.3). Patients designated as stage 4S have small or undetectable primary

Table 6.2 Clinical manifestations of neuroblastoma in the fetus and infant

Abdominal mass
Neck mass
Fetal hydrops
Cutaneous metastases (“blueberry muffin baby”)
Progressive distress and pneumonia with bronchial obstruction from mediastinal tumor
Paralysis or weakness with spinal cord compression
Airway problems, stridor and swallowing difficulties due to a large neck tumor
Metastases to the umbilical cord leading to intrauterine death
Hemoperitoneum from spontaneous rupture of tumor during delivery
Neurogenic bladder
Hemiplegia secondary to paraspinal “dumbbell” tumor
Congenital chylothorax
Cervical sympathetic ganglia involvement with Horner syndrome
Myoclonic encephalopathy
Visible dorsal paravertebral mass
Intestinal tumor associated with omphalocele and ileal atresia
Orbital and intraocular metastases
Scrotal mass

Reprinted from Isaacs [9]. © Springer-Verlag, 2002; Reprinted from Isaacs [21]. With kind permission of © Mosby-Elsevier, 2007

neuroblastomas with metastases in one or more of the following sites: liver, skin, or bone marrow (not bone). The adrenal is the most common primary site, and other locations are the retroperitoneal area, mediastinum, pelvis, multiple, or no discernible primary site [26, 33, 37, 38] (Figs. 6.2 and 6.4). Multiple bluish cutaneous nodules producing a “blueberry muffin” appearance are noted in about a third with stage 4S neuroblastoma metastatic to the skin [33, 39, 40]. Skin lesions are almost always associated with liver metastases and usually a favorable prognosis [9, 33, 39]. Spontaneous regression and histological maturation are documented [8, 9, 35] (Figs. 6.4 and 6.10). However, the liver may be so extensively involved by tumor that fatal respiratory and cardiac failure may occur (Fig. 6.4).

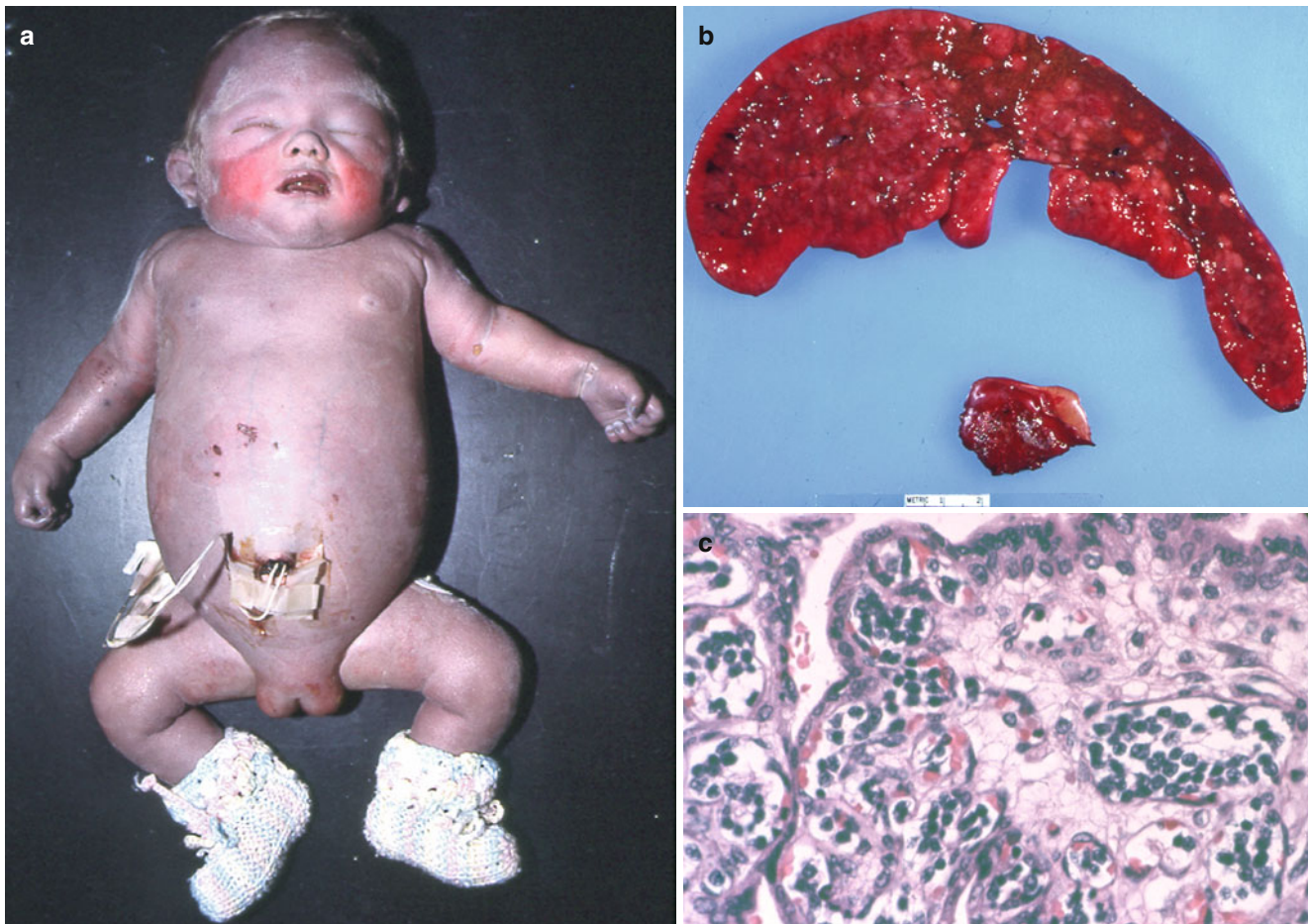


Fig. 6.1 Disseminated neuroblastoma with hydrops fetalis. **(a)** 1-week-old female with hydrops (generalized edema), ascites, and hepatomegaly. **(b)** Cut surfaces of the liver and adrenal with multiple *gray* nodular metastases. **(c)** Neuroblasts within placental villous capillaries. **(d)** Liver showing extensive replacement by a poorly differentiated neuroblastoma.

(e) Cerebral blood vessels are plugged with tumor emboli (*arrows*) with infarction of the adjacent cortical white matter. A cystic infarct is present in the upper right hand corner ((**a–c**) Reprinted from Isaacs [60]. With kind permission of © Chapman Hall, 1989. (**d, e**) Reprinted from Isaacs [9]. © Springer-Verlag, 2002)

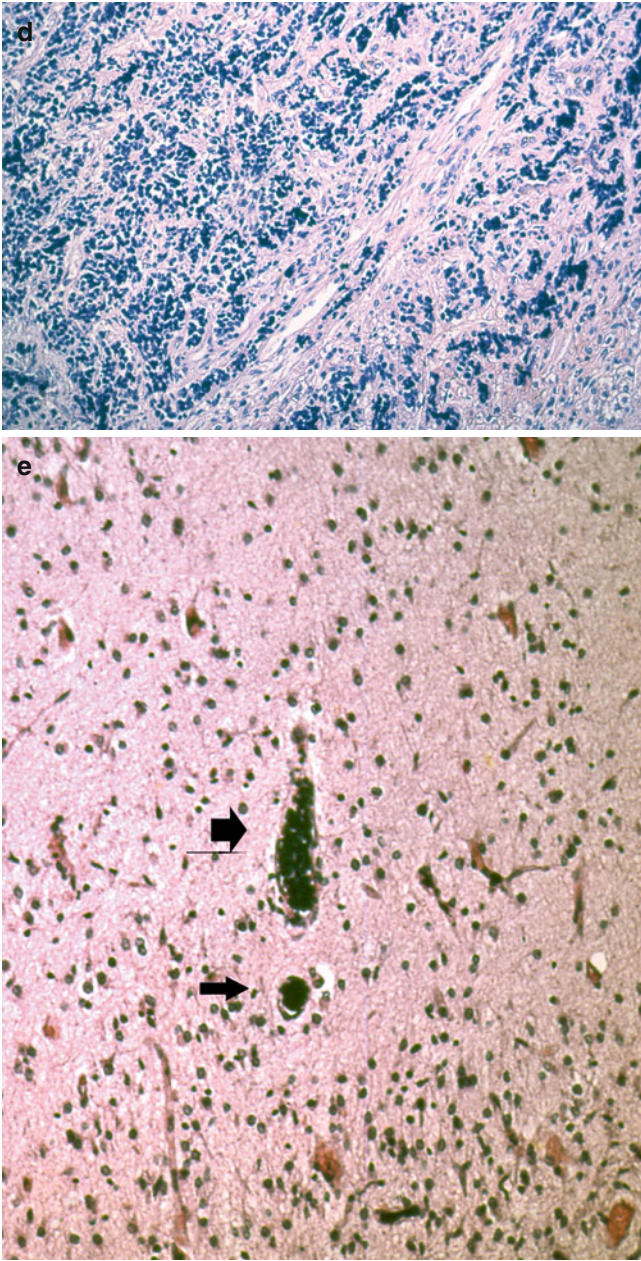


Fig. 6.1 (continued)

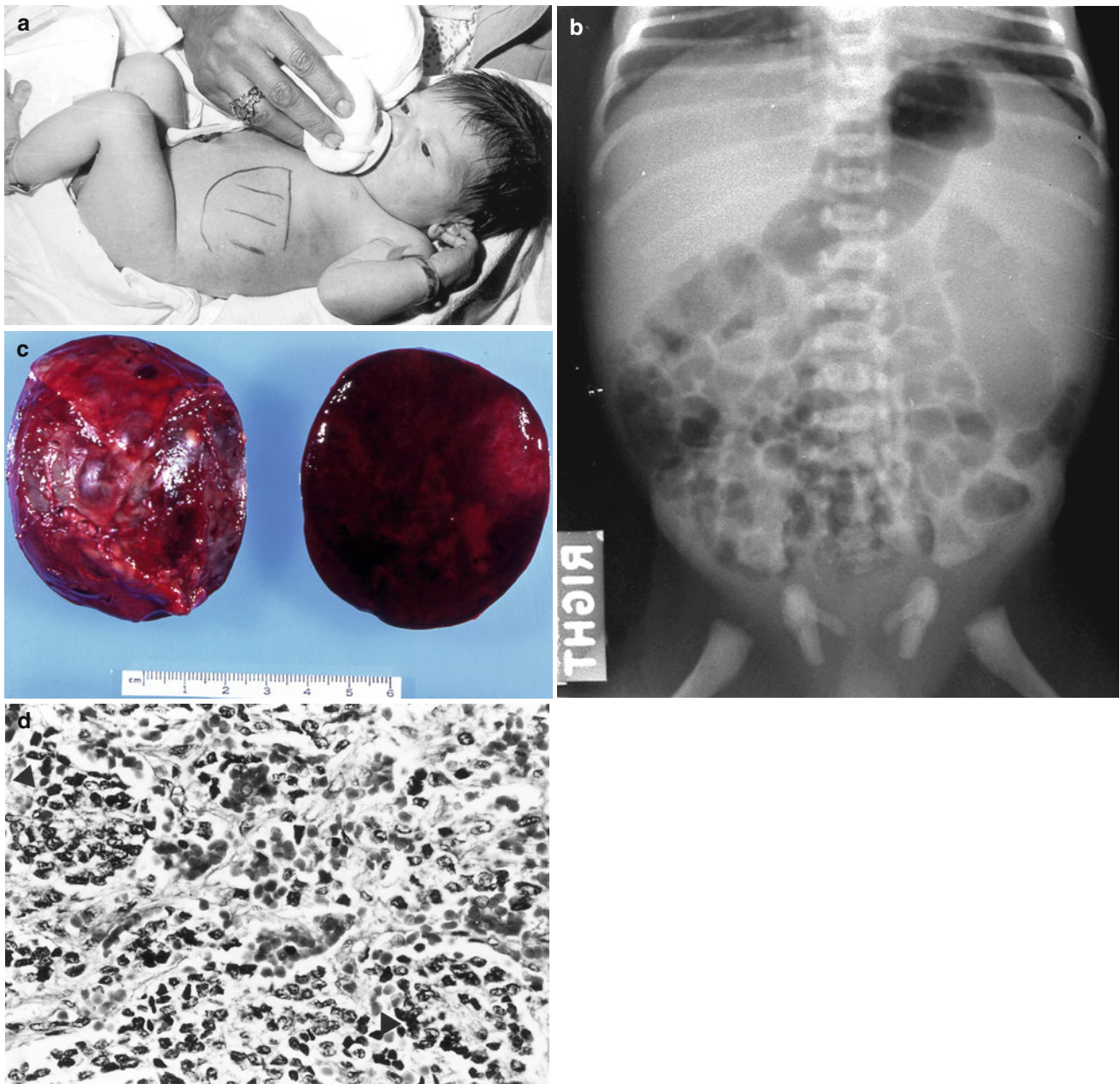


Fig. 6.2 Poorly differentiated, hemorrhagic neuroblastoma. (a) 3-day-old male with stage IV-S neuroblastoma. The left upper quadrant abdominal mass is outlined. (b) Abdominal X-ray film reveals hepatomegaly due to multiple metastases. The adrenal tumor is not well outlined. (c) 8×6 cm, 143-g tumor replacing the left adrenal. The specimen has a diffuse, hem-

orrhagic cut surface, which is on the right. (d) The tumor consists of small, round, darkly staining cells forming Homer-Wright rosettes with fibrillary material (*upper left corner*) (neuropil) in addition to extensive hemorrhage (stroma poor, low MKI, favorable histology) (Reprinted from Isaacs [8]. © WB Saunders 1997)



Fig. 6.3 Adrenal neuroblastoma. Solid tumor of 4 cm in diameter with areas of necrosis. Death from pulmonary hemorrhage at age 4 days (Reprinted from Isaacs [21]. With kind permission of © Mosby)

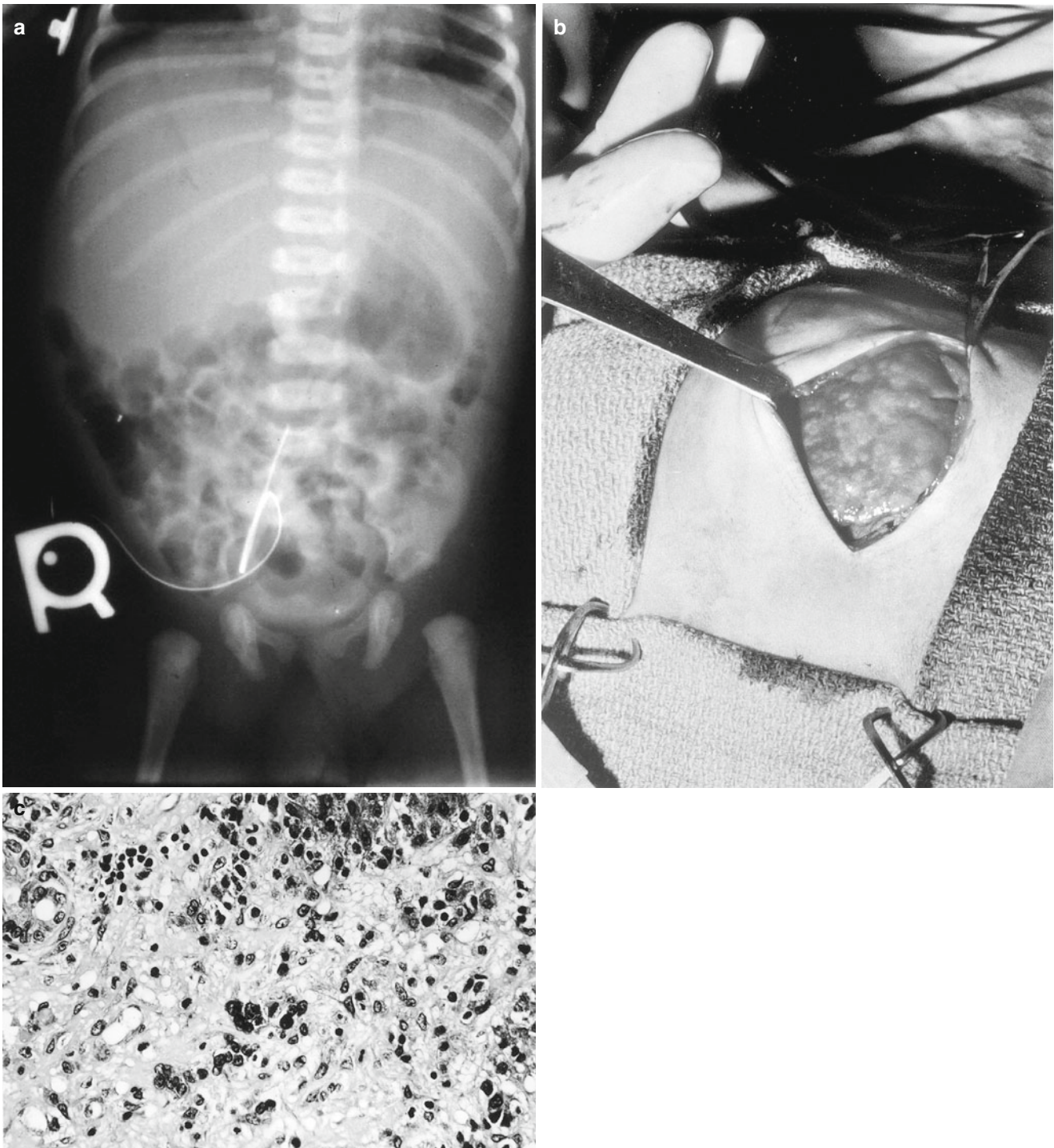


Fig. 6.4 Congenital neuroblastoma. 6-day-old female, Stage 4-S, with an enlarged liver presenting as an abdominal mass due to neoplastic hepatomegaly. (a) Massive liver enlargement depicted on an abdominal X-ray film. (b) Exploratory laparotomy showing multiple tumor nodules replacing most of the liver. (c) Liver biopsy reveals extensive fibrosis, parenchymal loss, and tiny nests of residual neuroblasts, many of

which are necrotic. Although the microscopic findings suggest spontaneous regression, infants with extensive metastatic liver disease may die from either pulmonary or hepatic failure resulting from upward displacement of the diaphragm and massive liver cell necrosis, respectively (Reprinted from Isaacs [8]. © WB Saunders 1997)

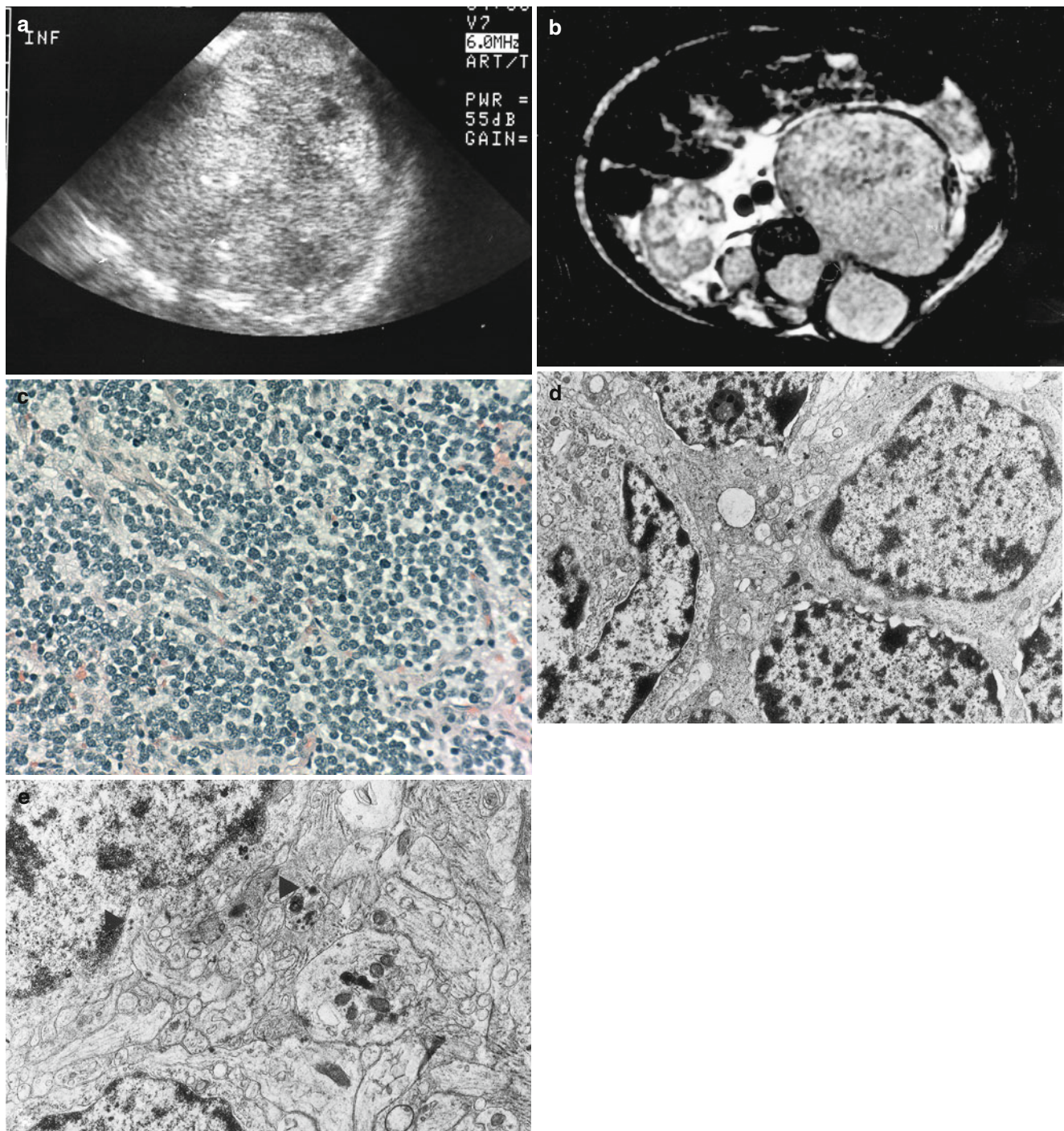


Fig. 6.5 Retroperitoneal, “dumbbell,” undifferentiated neuroblastoma. Newborn male with a retroperitoneal mass who was paraplegic at birth. (a) Ultrasound scan reveals a large abdominal mass. (b) The tumor extends through the intervertebral foramina in a “dumbbell-like fashion.” Other imaging studies showed a paraspinal mass going from T1 to L3 and liver metastases. (c) Low power reveals a small cell malignant tumor with scant fibrillary material. The tumor consists of small round to oval darkly staining cells with barely visible cytoplasm. The cells are surrounded by delicate fibrillary material (neuropil). Mitoses are present. Immunoperoxidase results: neurofilament +, synaptophysin –,

S-100 –, HBA71 –, LCA –, muscle markers –; No N-myc amplification, aneuploidy +, tumor cytogenetics 46XY, (DX: Shimada classification: stroma poor, high MKI, unfavorable histology). (d) EM photomicrograph displays finely dispersed chromatin and a high nuclear to cytoplasmic ratio. Few organelles are present. (e) Higher magnification reveals interdigitating cell processes with dense core neurosecretory granules and neurotubules (EM photomicrographs courtesy of Ann Peters, Department of Pathology, Children’s Hospital San Diego; Reprinted from Isaacs [9]. © Springer-Verlag, 2002)

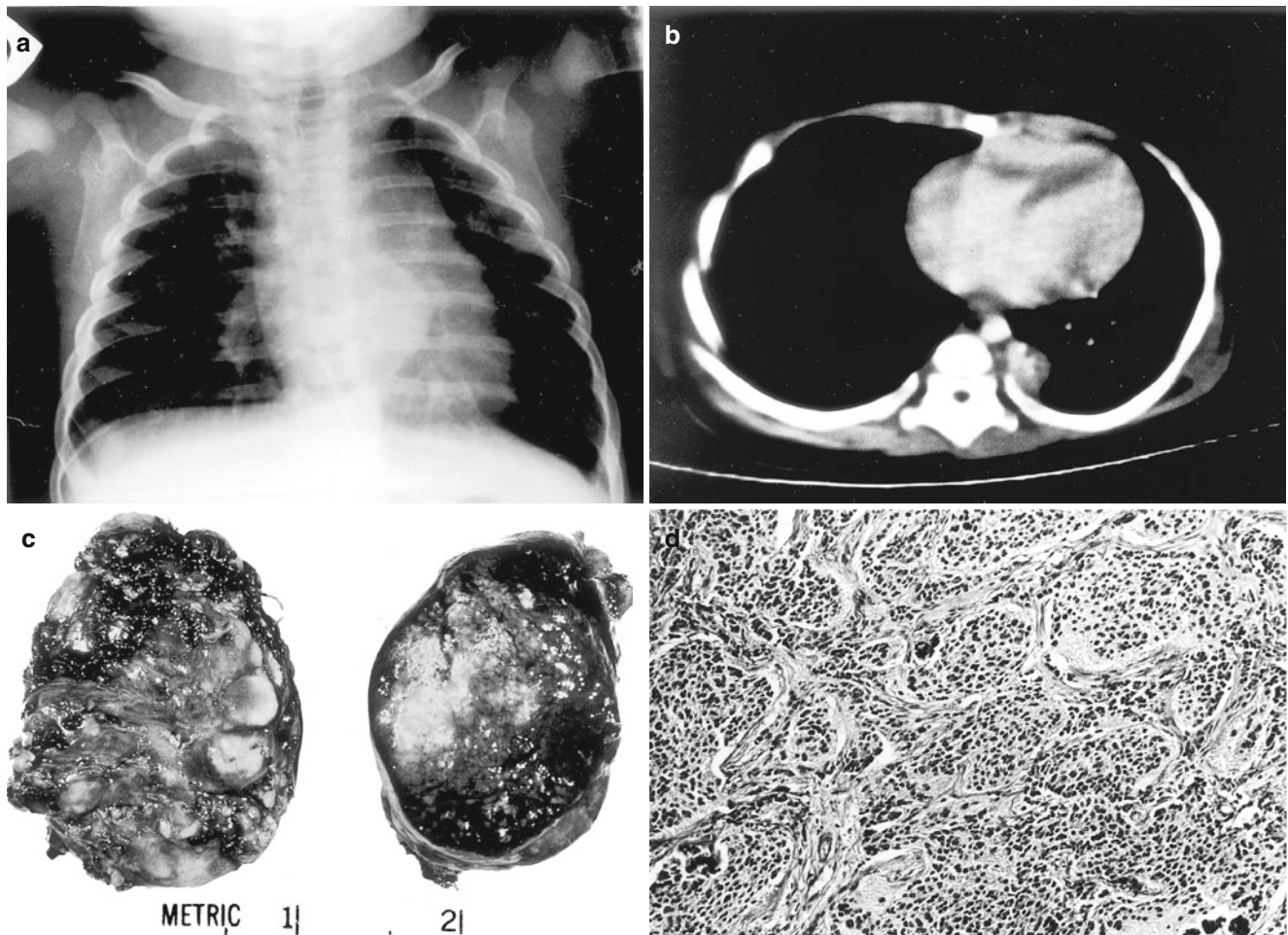


Fig. 6.6 Posterior mediastinal neuroblastoma in a 6-month-old female presenting with a mediastinal mass noted as an incidental finding on a chest film. **(a)** Chest radiograph reveals a posterior mediastinal mass with calcifications and suggestive hilar lymph node metastases. **(b)** CT scan shows a 4–5 cm, partially calcified posterior mediastinal mass situated in the thoracic paravertebral region. **(c)** The tumor, 5.1 g, 2.2×1.7 cm, has a dark-red, nodular capsular surface (*left side*) and a

soft white-pink cut surface (*right*) with focal hemorrhage and extensive calcification. **(d)** The tumor has a lobular pattern with nests of neuroblasts and abundant neuropil surrounded by delicate fibrovascular septae. Foci of calcification, an additional favorable sign, are present (differentiating, stroma poor, low MKI, favorable histology) (Reprinted from Isaacs [9]. © Springer-Verlag, 2002)

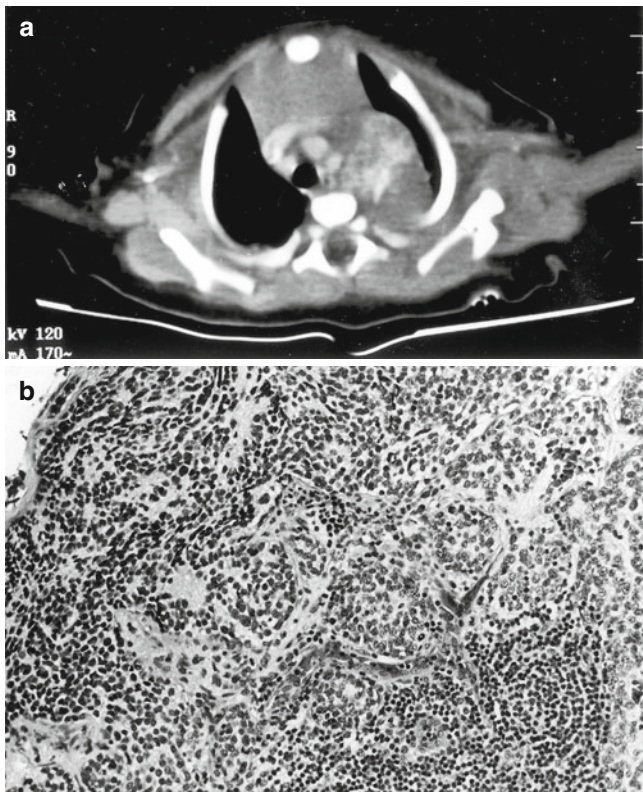


Fig. 6.7 Posterior mediastinal neuroblastoma. **(a)** Six-day-old female with respiratory distress and a mediastinal mass. CT scan shows a 3-cm partially calcified posterior mediastinal mass situated in the thoracic paravertebral region and hilar lymph node metastases. **(b)** Posterior mediastinal lymph node containing tumor metastases. Capsule of the node is situated in the *left upper corner*. Neuroblasts are slightly larger than lymphocytes in the lymphoid nodules. Tumor cells are surrounded by fine, delicate neuropil and form Homer-Wright rosettes, which aid in their identification. Low MKI and no *N-myc* amplification (differentiating, stroma poor, favorable histology, infant less than 1 year of age) (Reprinted from Isaacs [9]. © Springer-Verlag, 2002)

Table 6.3 International staging system for neuroblastoma

Stage	Description
1	Localized tumor with complete gross excision, with or without microscopic residual disease; representative ipsilateral lymph nodes negative for tumor microscopically (nodes attached to and removed with the primary tumor may be positive)
2A	Localized tumor with incomplete gross excision; representative ipsilateral non-adherent lymph nodes negative for tumor microscopically
2B	Localized tumor with or without complete gross excision, with ipsilateral non-adherent lymph nodes positive for tumor; enlarged contralateral lymph nodes must be negative microscopically
3	Unresectable unilateral tumor infiltrating across the midline, with or without regional lymph node involvement; or localized unilateral tumor with contralateral regional lymph node involvement; or midline tumor with bilateral extension with infiltration by infiltration (unresectable) or by lymph node involvement
4	Any tumor with dissemination to distant lymph nodes, bone marrow, liver, skin, or other organs (as except as defined by stage 4S)
4S	Localized primary tumor as defined for stage 1 or 2A or 2B with dissemination limited to liver, skin, bone marrow (limited to infants aged less than 1 year)

Reprinted from Brodeur and Maris[7]. With kind permission of © Williams and Wilkins, 2002

6.4 Diagnostic Tests

Most neuroblastomas, over 90 %, are biochemically active secreting varying quantities of *catecholamines* such as *vanillmandelic acid (VMA)* and *homovanillic acid (HVA)* [2, 8, 41]. Urinary catecholamine analysis is important not only for establishing the diagnosis but also for detecting recurrence or metastases.

Additional tests are of prognostic significance [2, 42]. Elevated levels of serum *ferritin* and *inhibition of E rosette formation by the patient's T lymphocytes* are unfavorable prognostic indicators that often correlate with advanced disease (stages 3 and 4) [2, 42]. Neuroblastoma cells produce ferritin that interferes with lymphocyte immune function. Ferritin-labeled immunoperoxidase is positive in neuroblastoma cells showing a *high mitotic-karyorrhexis (MKI) index* and *N-myc amplification*. Normal serum *neuron-specific enolase (NSE)* values are associated with a more favorable outcome than elevated ones [2, 42]. Serial serum *lactic dehydrogenase (LDH)* measurements are helpful for following tumor activity [43]. Patients whose LDH levels return to normal generally have a favorable prognosis; those whose levels tend to rise have recurrences and often a fatal outcome. *Nerve growth factor (neurotrophin) receptor*, which is expressed by the *TRK proto-oncogene*, is a transmembrane glycoprotein (a tyrosine kinase) that is produced in the developing nervous system and is responsible for neuronal differentiation. High levels of expression of the TRK nerve growth factor receptor are associated with a good prognosis in neuroblastoma [44].

Most of the serum markers described above used to predict outcome or follow disease activity do not appear to have the overall prognostic value as compared to the new genetic markers, for example, *N-myc* amplification and chromosomal analysis, and currently none is being used by major groups for risk determination [2] (Table 6.4).

DNA cytometric analysis (DNA index) of neuroblastoma specimens provides useful data that can be predictive of response to therapy and outcome [45]. The DNA index shows that a good prognosis is associated with aneuploidy and a low percentage of tumor cells in the S, G2, and M phases of the cell cycle [45]. Infants with tumor cells that have a hyperdiploid DNA content are more likely to have a lower stage of disease and respond to initial therapy compared to those with a diploid DNA content which are more likely to have advanced disease and do not respond. Aneuploidy in neuroblastoma cells correlates with a better prognosis than diploidy, which is contrary to what is observed in most other pediatric malignant tumors.

Table 6.4 Favorable prognostic indicators in infants with neuroblastoma

Feature	
Metastases at initial evaluation	Absent
Cystic pathological variant	Present
<i>N-myc</i>	1 copy (normal)
MKI	Low <2 %
DNA ploidy	Hyperdiploid
1p LOH	Absent
14q LOH	Absent
Translocation of 17q	Absent
TRK-A expression	High
ISSN stage	1, 2 or 4S
3-year survival	95 %

Reprinted from Lack [51]. With kind permission of © Armed Forces Institute of Pathology, 1997; Reprinted from Brodeur and Maris [7]. With kind permission of © Williams and Wilkins, 2002; Reprinted from Isaacs [26]. With kind permission of © Springer, 2007; Reprinted from Isaacs [2]. With kind permission of © Mosby, 2007
Abbreviations: LOH loss of heterozygosity, *N-myc* N-myc oncogene, *TRK-A* tyrosine kinase (receptor) growth factor

6.5 Genetic Factors

Tumor cells in patients with neuroblastoma show *deletions of the short arm of chromosome 1 (band 1p36)*, and of the *long arm of chromosome 11q*, extrachromosomal double minute chromatin bodies (observed with *N-myc* amplification), and homogeneously staining regions [2, 46–48]. *Unbalanced gain (translocation) of 17q* is a common genetic abnormality associated with a poor prognosis and is present in most neuroblastomas with *N-myc* amplification [2, 47]. Both the *N-myc (MYCN)* and *ras oncogenes* are found in neuroblastomas, and both are highly amplified in some tumor specimens, particularly from some patients with advanced disease. A relationship exists between *N-myc* amplification and loss of heterozygosity for chromosome 1p [48]. *N-myc* amplification correlates with prognosis and the extent of disease at the time of diagnosis [49]. Tumors from patients with stages 1 and 4S disease have single copies of *N-myc* gene, whereas stages 3 and 4 tumors show multiple ones (genomic amplification) [49]. Moreover, *N-myc* amplification is associated with an unfavorable histological pattern, namely, a high mitotic-karyorrhexis activity (index). Elevated levels of multidrug resistance-associated protein (MDRAP) gene expression in patients with neuroblastoma correlate strongly with poor outcome and suggest that expression of MDRAP accounts for the association between *N-myc* amplification and reduced survival [50]. Neuroblastoma cell lines show defects in the nerve growth factor receptor pathway which

may be responsible for initiation or maintenance of the undifferentiated state of the tumor [47].

6.6 Pathology

Neuroblastoma gross and microscopic findings in the newborn and infant are similar to those seen in the older child [1, 6, 8, 9, 21, 51]. Adrenal gland tumors vary in size from a few millimeters to several centimeters in diameter. They may be solid or cystic (Figs. 6.2, 6.3, 6.8 and 6.15). The cortical tissue of the adrenal gland usually persists and may surround the tumor or be visible only on one surface as a thin, orange-tan rind, while the rest is so attenuated that it cannot be distinguished on gross examination. The solid portions of the tumor are light gray to red brown—depending on the amount of hemorrhage—soft, and somewhat granular in appearance. Flecks of cream colored calcification are present in some tumors.

Microscopically, the tumor consists of small neuroblasts with poorly demarcated boundaries whose round or oval hyperchromatic nuclei are proportionately large in relation to total cell volume (Figs. 6.2, 6.5, 6.6, 6.7, 6.8, 6.9, 6.10, 6.11, 6.12, 6.13, 6.14 and 6.15). Fine fibrils (neuropil) either form a delicate interlacing network between the cells or are found in areas almost devoid of cells. Rosettes consisting of a small, pale, and finely granular central area surrounded by a petal-like arrangement of cells (Homer-Wright rosettes) are noted in least a third of specimens (Figs. 6.5, 6.6 and 6.10). Hemorrhagic necrosis and calcification are present particularly in larger tumors. Neuroblastoma is a classic example of one of the small, blue cell tumors of infancy and childhood raising diagnostic problems associated with this group of tumors [2, 9] (Fig. 6.11). The light microscopic, immunohistochemical, and EM features of small blue cell tumors are listed in Table 6.5.

Shimada et al. proposed a histopathologic classification for neuroblastoma which correlates certain histological patterns and prognosis [52, 53]. The histological criteria are based primarily on the evaluation of maturation of both neuroblastic and stromal elements and of nuclear morphology. Neuroblastomas are divided into two main categories, stroma rich and stroma poor; the terminology currently used also in

this system is “Schwannian stroma rich or poor” [53] (Table 6.6). The mitosis-karyorrhexis index (MKI) of the neuroblasts is evaluated, and the MKI appears to be the most important indicator for prognosis particularly in children less than 1 1/2 years of age [53]. The data of Shimada et al. suggest that a low MKI is more significant in this age group for survival than maturation [54]. Neuroblastomas of infants with stages 1 and 4S disease, the most favorable prognostic groups, typically have, in addition to a stroma-poor pattern, a low MKI and absent *N-myc* amplification. Generally, the stroma-rich pattern is not observed in neuroblastomas removed from fetuses and neonates [2, 53].

EM features of neuroblastoma are reported by several investigators [8, 9, 51, 54, 55]. The findings depend upon the degree of cytological differentiation (Figs. 6.5, 6.11 and 6.13) (Table 6.4). The neuroblastoma with the densely cellular, primitive, and “small blue cell tumor” appearance of undifferentiated neuroblastoma on H&E and thick sections may be difficult to distinguish by EM from other small cell malignant tumors such as the undifferentiated sarcoma, rhabdomyosarcoma, and leukemia-lymphoma (Fig. 6.11). The presence of *dense core* or *neurosecretory granules*, which are found also in small numbers in the primitive neuroectodermal tumor (PNET), establishes the diagnosis by EM [9, 54]. More differentiated neuroblastomas show in addition a network or neuropil composed of cells with neural processes, microtubules, neurofilaments, and cell attachments with some resembling synapses [8, 9, 54] (Fig. 6.13).

Immunoperoxidase techniques aid in establishing the diagnosis. Neuroblastoma cells are reactive with NB84 (neuroblastoma antigen), *neuron-specific enolase (NSE)*, *synaptophysin*, and *neurofilament* and are focally positive for S-100 protein but stain negatively for desmin, actin, leukocyte common antigen, cytokeratin, and the Ewing antigen [2] (Fig. 6.11c and Table 6.6).

The first clinical manifestations in greater than half of newborns and infants with neuroblastoma are the result of metastases [2, 26, 32]. In spite of the occurrence in disseminated disease (stage 4S), the prognosis is surprisingly good. Metastases occur most often to the liver, skin, and bone marrow [26, 32]. Adrenal is the leading primary site followed by the neck and mediastinum [26, 32]. The International Staging System for neuroblastoma is described in Table 6.2.

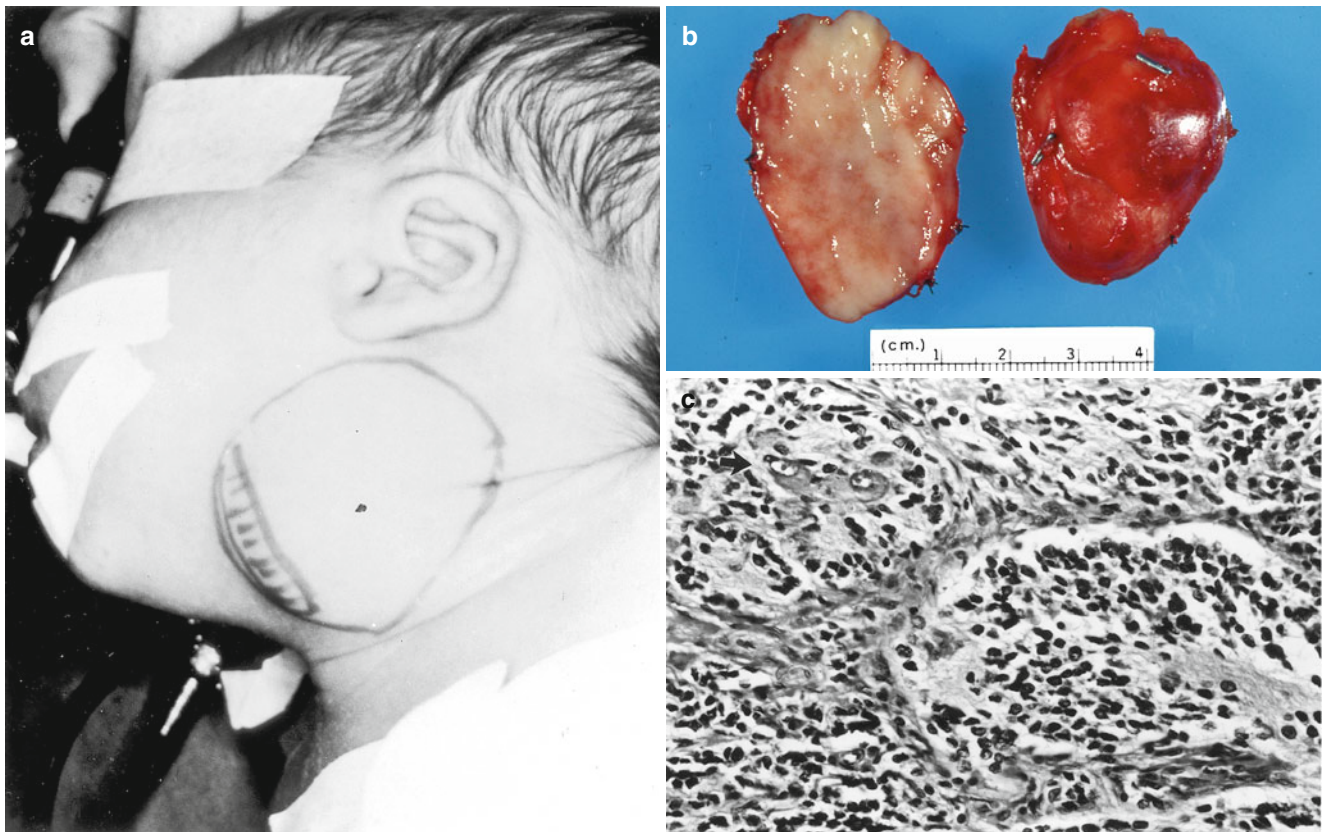


Fig. 6.8 Cervical neuroblastoma. Differentiating neuroblastoma, stage I. (a) 2-month-old male with a cervical mass and noisy respirations noted 1 month prior to hospitalization. The tumor, presumably arising from cervical sympathetic ganglia, is outlined on the patient. (b) The specimen, measuring 4.5×3.5 cm and weighing 20 g, has a rather uniform light-tan cut surface, on the left. (c) The tumor has histological

features of a differentiating neuroblastoma displaying a lobular pattern, abundant neuropil, and focal ganglioneuroblasts consisting of large vesicular nuclei, prominent nucleoli, and abundant cytoplasm (arrow). (Stroma poor, low MKI, favorable histology) (Reprinted from Isaacs [8]. © WB Saunders 1997)

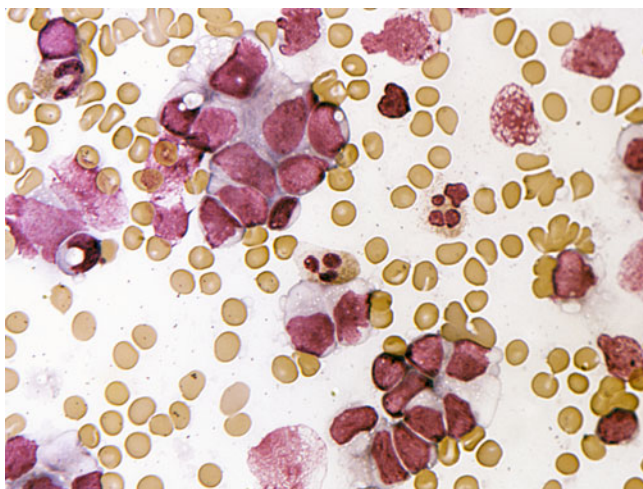


Fig. 6.9 Bone marrow smear with neuroblastoma metastases. Wright-Giemsa stained smear reveals small, round, darkly staining tumor cells forming *syncytia* (adherent clumps of tumor cells). The bone marrow aspirate was from a neonate with stage IV-S neuroblastoma who had high urinary VMA and HVA levels. The bone marrow cytology and the urinary catecholamine findings were sufficient to establish the diagnosis without resorting to a biopsy (Reprinted from Isaacs [8]. © WB Saunders 1997)

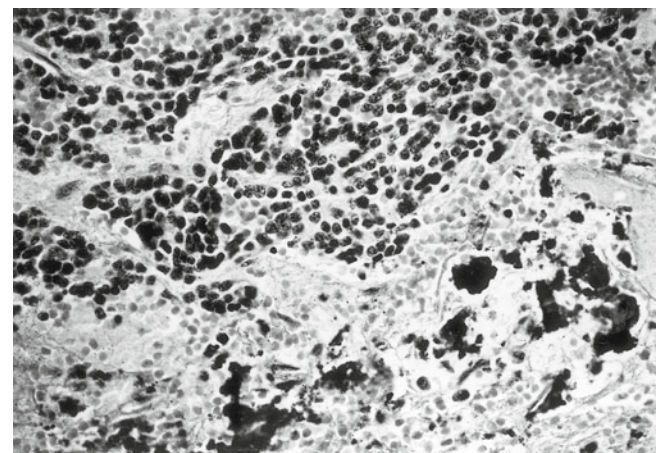


Fig. 6.10 Spontaneous regression of congenital neuroblastoma, stage IV-S. Extensive necrosis, hemorrhage, and calcification are evidence of tumor regression (Reprinted from Isaacs [8]. © WB Saunders 1997)

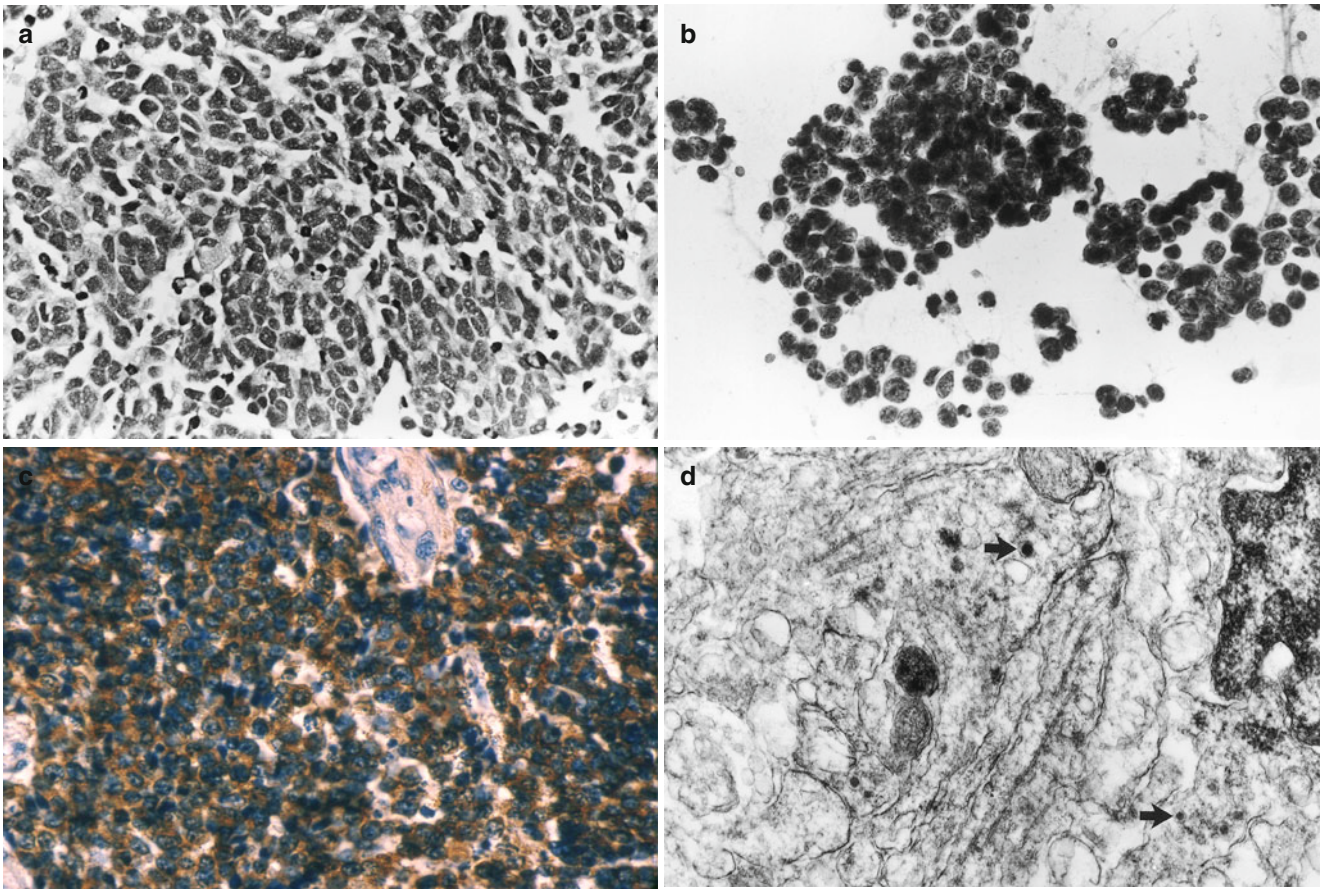


Fig. 6.11 Undifferentiated neuroblastoma. (a) A small, *blue* cell malignant tumor without rosettes or neuropil (stroma poor, high MKI, unfavorable histology). (b) Imprint (“touch preparation”) of the tumor. The cells are round to oval with a high nuclear to cytoplasmic ratio. Fine “peppery” chromatin pattern and One or more tiny nucleoli are present. (c) The cells stain positively with neuron-specific enolase, are reactive with synaptophysin, focally reactive with S-100 protein but

stain negatively with desmin, actin, leukocyte common antigen, anti- β 2-microglobulin, and HBA71 antibodies. The tumor exhibited *N-myc* amplification. (d) EM reveals microtubules and dense core (neurosecretory) granules (*arrows*). (Electron photomicrograph courtesy of Ann Peters, Rady Children’s Hospital San Diego; Reprinted from Isaacs [8]. © WB Saunders 1997)

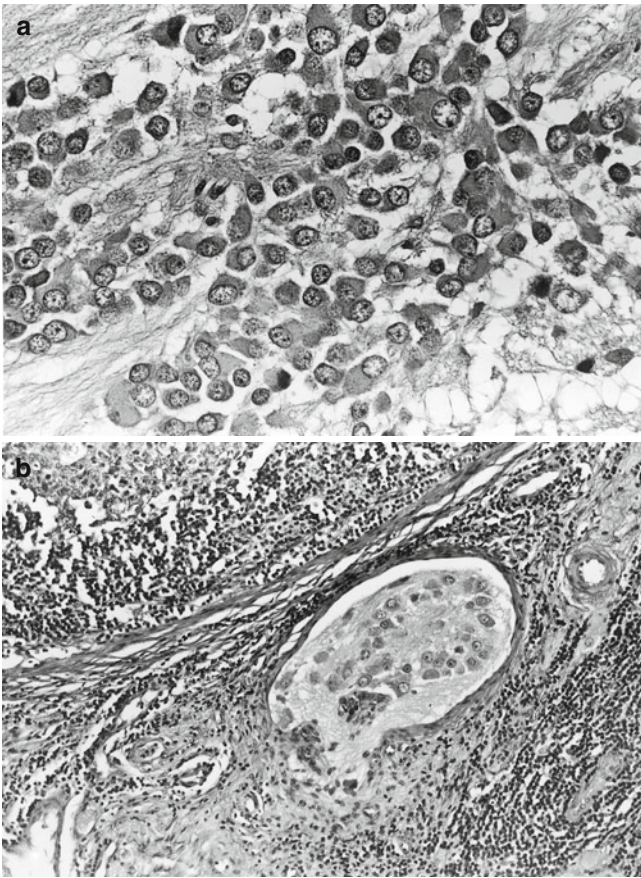


Fig. 6.12 Differentiating cervical neuroblastoma. Neck mass in an 8-month-old male with metastases to lymph nodes and bone marrow. **(a)** Biopsy reveals maturing neuroblasts with round to slightly oval nuclei, a fine, peppery chromatin pattern, and prominent cytoplasm. No mitoses are noted. Delicate fibrillar neuropil is present. NSE +, S-100+, tumor 46XY, *N-myc* normal (stroma poor, low MKI, favorable histology). **(b)** Section of a cervical lymph node reveals similar appearing tumor deposits in lymphatics (Reprinted from Isaacs [9]. © Springer-Verlag, 2002)

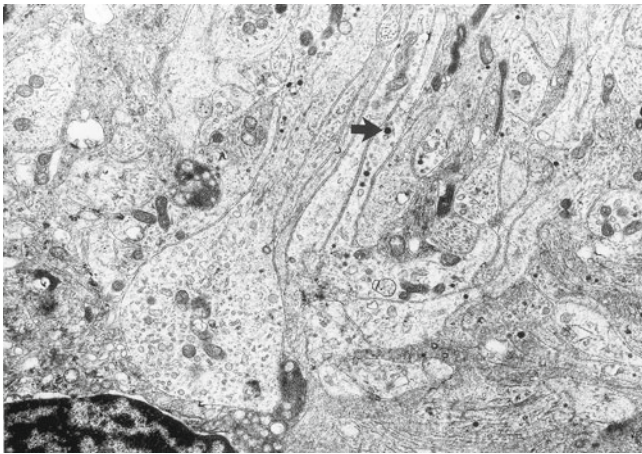


Fig. 6.13 Ultrastructure of a differentiating neuroblastoma. Neuropil composed of a network of neurites containing neurotubules and neurosecretory granules (*arrow*) is present. One neurite directly adjacent to the nucleus has a bulbous swelling suggestive of synaptic bouton. $\times 20,000$ (Courtesy of Darkin Chan, Childrens Hospital Los Angeles; Reprinted from Isaacs [8]. © WB Saunders 1997)

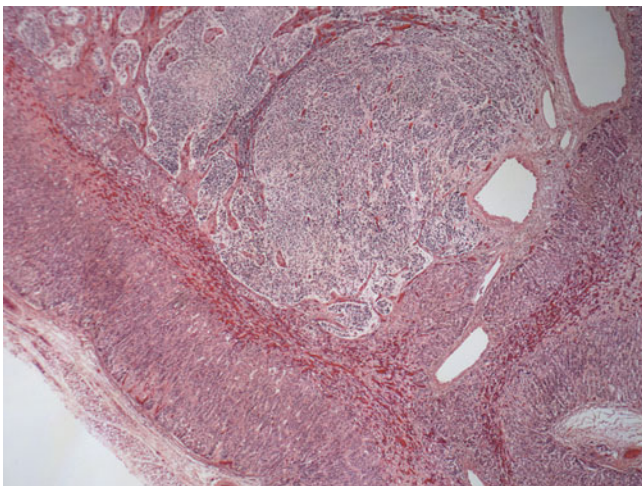


Fig. 6.14 Neuroblastoma in situ. The adrenal contains a small, central area of neuroblasts not invading the capsule. This was an incidental postmortem microscopic finding in a 2-day-old, 3-kg male who died from complications of the hypoplastic left heart syndrome (Reprinted from Isaacs [9]. © WB Saunders 1997)

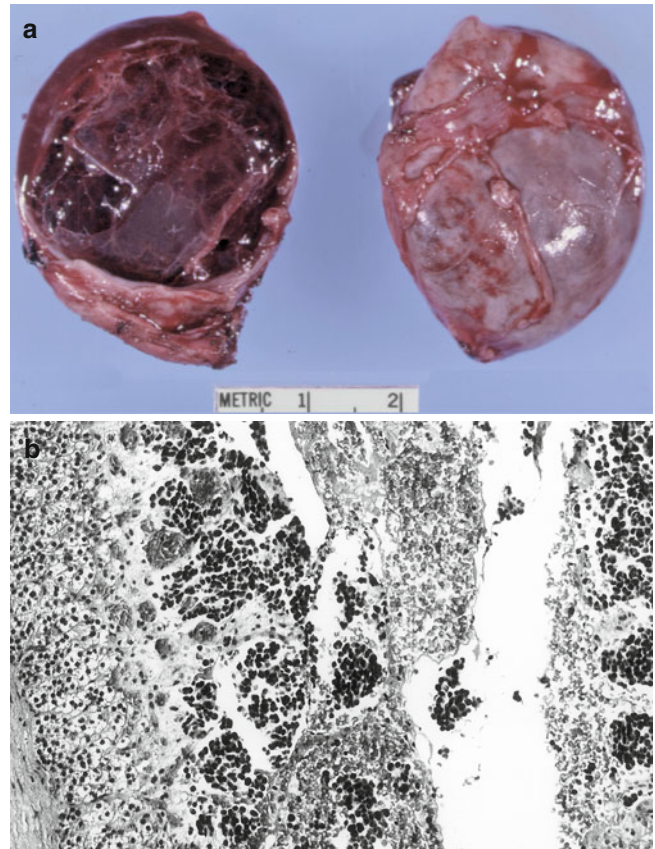


Fig. 6.15 Cystic adrenal hemorrhage with neuroblastoma. A cystic lesion thought due to adrenal hemorrhage was detected on antenatal sonography. (a) The gross specimen excised at 1 month of age reveals an opened cyst with a hemorrhagic cut surface which is on the left. (b) Microscopically, the adrenal capsule and cortex are on the left adjacent to nests of neuroblasts surrounded by hemorrhage (Reprinted from Isaacs [9]. © Springer-Verlag, 2002)

Table 6.5 Histopathologic differential diagnosis of the small blue cell malignant tumors

Tumor	Light microscopy	Immunohistochemistry	Electron microscopy
Neuroblastoma	Small round cells, rosettes, neurofilaments, nuclei with a peppery chromatin pattern	NSE+, NFP+, NF +, NB84+, synaptophysin +, chromogranin +, Des−, MSA−, LCA−, CK−, CD99−	Neurosecretory granules, microtubules, neurofilaments
Rhabdomyosarcoma	Spindle cells, tadpole cells, giant cells, eosinophilic cytoplasm, cross striations; embryonal, botryoid, and alveolar patterns	DES +, MSA +, Vim +, myogenin +, NFP −, CD 99−, CK −, LCA −, HBA71−, NB84−	Spindle cells, primitive attachments, Z bands, thick and thin filaments, basement membranes
Leukemia ^a	Diffuse infiltrates of small round cells with a high N/C ratio, granules±	LCA+, VIM ±, MSA −, NFP −, CK −, CD 99−	Round cells, no attachments, no matrix, granules ±
Primitive neuroectodermal tumor (PNET) ^b	Small round cells, rosettes ±; lobular pattern	NSE+, VIM+, HBA7 +, B2MG+, NFP ±, LCA −, DES −, MSA −, CK −	Primitive cells, few organelles, rare neurosecretory granules, few intermediate filaments; primitive attachments ±
Rhabdoid tumor	Polygonal cells with eosinophilic cytoplasm, red intermediate filament inclusions, round, vesicular nucleus with one large nucleolus (“rhabdoid cell”); PNET-like areas	Vim +; CK +; Des −; MSA −; NFP−; CD 99−; LCA −, NB84−	Bundles of cytoplasmic intermediate filaments
Wilms’ tumor, blastemal pattern	Lobules of small round to oval, darkly staining cells with a high N/C ratio	Blastema: Vim +; Des ±; Epithelium: CK +	–

Reprinted from Isaacs [2]. With kind permission of © Mosby, 2007; Reprinted from Isaacs [9]. © Springer-Verlag, 2002; Reprinted from Isaacs [21]. With kind permission of © Mosby

Abbreviations: B2MG anti-B2 microglobulin, CK cytokeratin, DES desmin, HBA71 Ewing antigen, LCA leukocyte common antigen, MSA muscle specific actin, NB84 neuroblastoma antigen, NSE neuron-specific enolase, NFP neurofibrillary protein, VIM vimentin

^aMyeloid leukemias may be present in extramedullary sites in the absence of diagnosable bone marrow involvement, for example, granulocytic sarcoma or chloroma, megakaryoblastic leukemia, M7

^bPrimitive neuroectodermal tumor (PNET) includes the entities Askin thoracopulmonary tumor and Ewing’s sarcoma

Table 6.6 Pathological features in the grading of neuroblastic tumors

Differentiation of neuroblasts
Undifferentiated
Poorly differentiated
Differentiating
Mitosis-karyorrhexis index (MKI)
Low (2 % or less of cells)
Intermediate (2–4 % of cells)
High (4 % or greater of cells)
Stroma (neuroma-like or Schwannian)
Poor
Rich
Calcifications
Present
Absent

Reprinted from Lack [51]. With kind permission of © Armed Forces Institute of Pathology, 1997

6.7 Spontaneous Regression

Spontaneous regression of neuroblastomas is not an uncommon event [6, 9, 31, 35]. In some instances, there is maturation of the tumor to ganglioneuroma or neurofibroma, while in others, there are foci of degeneration, necrosis, and disappearance particularly in newborns [9, 31] (Fig. 6.10). Neuroblastoma spontaneous regression occurs

more often in children than for any other neoplasm [21, 47]; however, the exact incidence of this outcome is unknown [35]. Serial biopsies taken from stage 4S neuroblastoma patients often show evidence of spontaneous regression [9, 35] (Figs. 6.10 and 6.16). Similar trends have been observed among congenital sacrococcygeal teratomas and retinoblastomas.

6.8 Neuroblastoma In Situ

The frequency in which small collections of neuroblasts are found in the adrenal glands in random sections of newborns (neuroblastoma in situ) suggests that maturation and cessation of growth of potentially lethal tumors is a relatively frequent occurrence [2, 56, 57]. Many such collections of cells have been observed (Fig. 6.14). The reported incidence of *neuroblastoma in situ* differs considerably in the literature varying from 1 in 10 to 1 in 500 necropsies [56, 57]. Most authors believe that the lesion most likely represents a precursor of neuroblastoma. *Congenital malformations* especially congenital heart disease, tracheoesophageal fistula, and genitourinary tract anomalies are found at necropsy in as many as 73 % of fetuses and newborns with neuroblastoma in situ [26, 56, 57]. Such collections of cells have been found in newborns with trisomy 18 [2].

The normal neural crest aggregates in the developing fetal adrenal gland can be distinguished by EM from in situ neuroblastoma cells. The former are composed of two cell types, neuroblasts and pheochromoblasts (chromaffin cells); the latter consist of only one cell type, neuroblasts [55].

There is a unique pathological variant occurring mostly in the perinatal period called “cystic neuroblastoma” that is considered to be a form of neuroblastoma in situ [25, 26]. This variant is associated with the highest survival rate of all forms of neuroblastoma [26]. The lesion consists of small, focal nests of neuroblasts situated within an intact cyst wall rather than diffuse infiltrates of tumor cells (Fig. 6.15). Generally, the cystic tumors are characterized by Shimada favorable histology and biological markers such as aneuploid DNA content, lack of chromosome 1p deletion, and absence of MYCN amplification [26] (Table 6.3). Fetuses and neonates with cystic neuroblastomas experience a much better outcome than those with non-cystic tumors, 92 and 70 %, respectively in one study [26] (Table 6.7).

6.9 Ganglioneuroma

Ganglioneuroma of the adrenal area seldom occurs in the fetus and infant [9] (Fig. 6.16). Typically, they are tumors of older children and adults. Ganglioneuromas are more highly differentiated than neuroblastoma and are considered as the benign end of the neuroblastoma spectrum [9, 37, 51, 58]. Histologically, ganglioneuroma consists of mature or slightly immature ganglion cells having an abundant pink cytoplasm, round nucleus with prominent nucleolus, surrounded by interlacing bundles of Schwann cells (the stroma resembling a neurofibroma) [51, 59] (Fig. 6.16). Mitotic figures should not be observed in ganglioneuromas nor do the tumor cells show *N-myc* gene amplification [2]. In the young, they may occur spontaneously or after therapy for neuroblastoma. Spontaneous and therapy-induced maturation of neuroblastoma to ganglioneuroma is well documented [8, 9, 35, 37, 42, 58] (Fig. 6.16). This maturation process occurs also in metastatic sites. Nevertheless, growth of ganglioneuroma may cause functional problems requiring surgical intervention [58]. Although some are not resectable, patients with ganglioneuromas generally experience a long-term disease-free survival [2, 58].

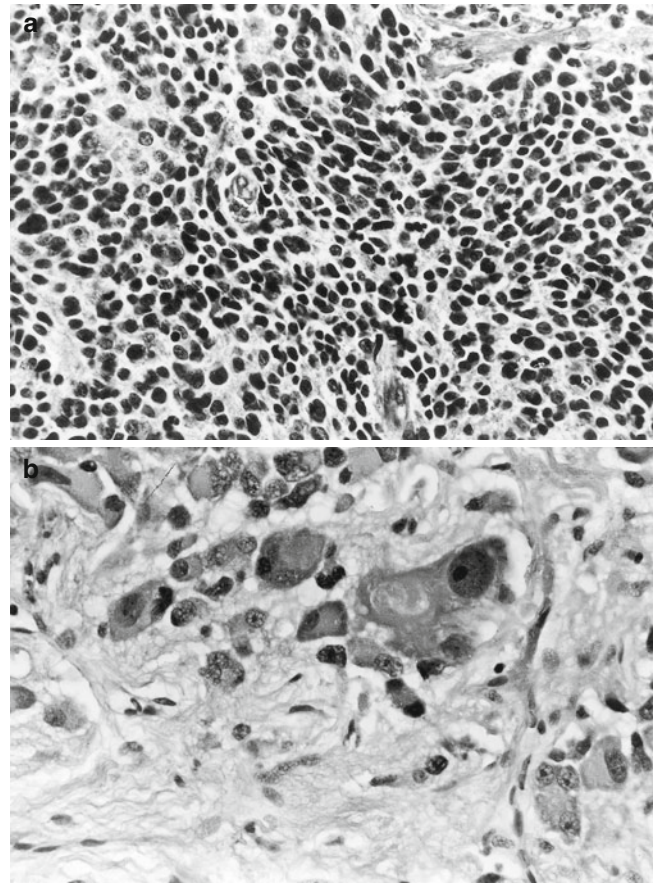


Fig. 6.16 Maturation of neuroblastoma to ganglioneuroma. 5-month-old male with a mediastinal mass and liver metastases, stage IVs. (a) Initial biopsy of the mediastinal mass reveals an undifferentiated neuroblastoma composed of small dark round to oval cells with inconspicuous cytoplasm and minimal intercellular fibrillar material. NSE +; synaptophysin focally, weakly +; LCA-; desmin -; (age less than 1 year, stroma poor, low MKI, favorable histology). Patient was treated with chemotherapy. (b) The patient’s mediastinal mass was biopsied again 7 months later. The biopsy shows maturation to ganglioneuroma (Reprinted from Isaacs [9]. © Springer-Verlag, 2002)

6.10 Prognosis

Favorable prognostic indicators in infants with neuroblastoma are listed in Table 6.3. The prognosis for newborns and infants is far better than that for older children, mainly because the former present more often with a treatable localized lesion or 4S disease. Biologically, neuroblastoma appears to be two

Table 6.7 Survival of fetuses and neonates with neuroblastoma ($n=271$)

	Number	Survival
Fetuses	112 (41) ^b	99/112 (88)
Neonates	159 (59)	101/159 (64)
Cystic neuroblastoma ^a	63 (24)	58/63 (92)
Non-cystic neuroblastoma	199 (76)	139/199 (70)
Cases before 1983	50	22/50 (44)
Cases after 1983	221	178/221 (80)
Patients alive, NED	191	191/271 (70)
Patients alive, with tumor	9	9/200 (4.5)
Overall survival	9	200/271 = 74 %

Reprinted from Isaacs [26]. With kind permission of © Springer, 2007
 Abbreviations: NED No evidence of disease

^aTen neuroblastomas were unclassifiable as to whether they contained cysts leaving 261 cases where the tumor could be evaluated

^b()=percent

different conditions, one affecting fetuses and infants and the older children. More fetuses and infants present with stages 1, 2, and 4S disease, which tend to regress spontaneously with little or no therapy, as compared with older children [34, 35]. Survival in one study was 100 % for stages 1 and 2, approximately 80 % for stage 4S, and 50 % for stage 4 [2]. Other than age and disease stage at the time of diagnosis, improved survival is attributed to one or more of the following factors: spontaneous regression; favorable histology; normal chromosomes 1, 11, and 17; aneuploidy; and low *N-myc* oncogene expression [2, 33] (Table 6.3). Newborns with cystic neuroblastoma have an overall survival rate of more than 20 % greater than the noncystic neuroblastoma group (Table 6.7).

References

- Bolande RP (1997) Neurocristopathy: its growth and development in 20 years. *Pediatr Pathol Lab Med* 17:1–25
- Isaacs H Jr (2007) Tumors. In: Gilbert-Barness E (ed) *Potter's pathology of the fetus, infant and child*, vol 2, 2nd edn. Mosby Elsevier, Philadelphia, pp 1677–1742
- Bader JL, Miller RW (1979) U.S. cancer incidence and mortality in the first year of life. *Am J Dis Child* 133:157–159
- Barson AJ (1978) Congenital neoplasia: the society's experience, abstracted. *Arch Dis Child* 53:436
- Campbell AN, Chan HSL, O'Brien A et al (1987) Malignant tumours in the neonate. *Arch Dis Child* 62:19–23
- Dehner LP (1981) Neoplasms of the fetus and neonate. In: Naeye RL, Kissane JM, Kaufman N (eds) *Perinatal diseases*, International Academy of Pathology Monograph number 22. Williams and Wilkins, Baltimore, p 286
- Brodeur GM, Maris JM (2002) Neuroblastoma. In: Pizzo PA, Poplack DG (eds) *Principles and practice of pediatric oncology*, 3rd edn. J.B. Lippincott, Williams and Wilkins, Philadelphia, pp 895–937
- Isaacs H Jr (1997) Neuroblastoma. *Tumors of the fetus and newborn*, vol 35, Major problems in pathology. W.B. Saunders, Philadelphia, pp 130–149
- Isaacs H Jr (2002) Neuroblastoma. *Tumors of the fetus and infant: an atlas*. Springer, New York, pp 137–160
- Mancini AF, Rosito P, Faldella G et al (1982) Neuroblastoma in a pair of identical twins. *Med Pediatr Oncol* 10:45–51
- Chatten J, Voorhess ML (1967) Familial neuroblastoma. Report of a kindred with multiple disorders including neuroblastoma in four siblings. *N Engl J Med* 277:1230–1236
- Bolande RP, Towler WF (1970) A possible relationship of neuroblastoma to Von Recklinghausen's disease. *Cancer* 26:162–175
- Isaacs H Jr (2010) Perinatal neurofibromatosis: two case reports and review of the literature. *Am J Perinatol* 27:285–292
- Grotting JC, Kassel S, Dehner LP (1979) Nesidioblastosis and congenital neuroblastoma. *Arch Pathol Lab Med* 103:642–646
- Bower RJ, Adkins JC (1980) Ondine's curse and neurocristopathy. *Clin Pediatr* 19:665–668
- Michna BA, McWilliams NB, Krummel TM et al (1988) Multifocal ganglio-neuroblastoma coexistent with total colonic aganglionosis. *J Pediatr Surg* 23:57–59
- Chitayat D, Friedman JM, Dimmick JE (1990) Neuroblastoma in a child with Beckwith-Wiedemann syndrome. *Am J Med Genet* 35:433–436
- Patrone PM, Chatten J, Weinberg P (1990) Neuroblastoma and DiGeorge anomaly. *Pediatr Pathol* 10:425–430
- Seeler RA, Israel JN, Royal JE et al (1979) Ganglioneuroblastoma and fetal hydantoin-alcohol syndromes. *Pediatrics* 63:524–527
- Nakissa N, Constine LS, Rubin P et al (1985) Birth defects in three common pediatric malignancies: Wilms' tumor, neuroblastoma and Ewing's sarcoma. *Oncology* 42:358–563
- Isaacs H Jr (1997) Tumors. In: Gilbert-Barness E (ed) *Potter's pathology of the fetus and infant*, 2nd edn. Mosby, St. Louis, pp 1248–1339
- Atkinson GO, Zaatari GS, Gay BB et al (1986) Cystic neuroblastoma in infants: radiographic and pathologic features. *AJR Am J Roentgenol* 146:113–117
- Jaffa AJ, Many A, Hartoov J et al (1993) Prenatal sonographic diagnosis of metastatic neuroblastoma: report of a case and review of the literature. *Prenat Diagn* 13:73–77
- Cassidy C, Winters WD (1997) Bilateral cystic neuroblastoma: imaging features and differential diagnoses. *Pediatr Radiol* 27:758–759
- Kozakewich HPW, Perez-Atayde AR, Donovan MJ et al (1998) Cystic neuroblastoma: emphasis on gene expression, morphology, and pathogenesis. *Pediatr Dev Pathol* 1:17–28
- Isaacs H Jr (2007) Fetal and neonatal neuroblastoma: retrospective review of 271 cases. *Fetal Pediatr Pathol* 26:177–184
- Smith CR, Chan HSL, DeSa DJ (1981) Placental involvement in congenital neuroblastoma. *J Clin Pathol* 34:785–789
- Moss TJ, Kaplan L (1987) Association of hydrops fetalis with congenital neuroblastoma. *Am J Obstet Gynecol* 132:905–906
- Anders D, Kindermann G, Pfeifer U (1973) Metastasizing fetal neuroblastoma with involvement of the placenta simulating fetal erythroblastosis. Report of two cases. *J Pediatr* 82:50–53
- Ohyama M, Kobayashi S, Aida N et al (1999) Congenital neuroblastoma diagnosed placental examination. *Med Pediatr Oncol* 33:430–431
- Bolande RP (1979) Developmental pathology. *Am J Pathol* 94:623–683
- Schneider KM, Becker JM, Krasna IH (1965) Neonatal neuroblastoma. *Pediatrics* 36:359–366
- Grosfeld JL, Rescoria FJ, West KW et al (1993) Neuroblastoma in the first year of life: clinical and biologic factors influencing outcome. *Semin Pediatr Surg* 2:37–46
- Evans AE, D'Angio GJ, Randolph J (1971) A proposed staging for children with neuroblastoma. *Children's cancer study group A. Cancer* 27:374–378
- Haas D, Ablin AR, Miller C et al (1988) Complete pathologic maturation and regression of stage IVS neuroblastoma without treatment. *Cancer* 62:818–825
- Stephenson SR, Cook BA, Mease AD et al (1986) The prognostic significance of age and pattern of metastases in stage IV-S neuroblastoma. *Cancer* 58:372–375

37. Hachitanda Y, Hata J-I (1996) Stage IVS neuroblastoma: a clinical, histological and biological analysis of 45 cases. *Hum Pathol* 27:1135–1138
38. Evans AE, Chatten J, D'Angio JG et al (1980) A review of 17 IV-S neuroblastoma patients at the Children's Hospital of Philadelphia. *Cancer* 45:833–839
39. Shown TE, Durfee MF (1970) Blueberry muffin baby: neonatal neuroblastoma with subcutaneous metastases. *J Urol* 104:193–195
40. Isaacs H (2011) Cutaneous metastases in neonates: a review. *Pediatr Dermatol* 28:85–93
41. Laug WE, Siegel SE, Shaw KNF et al (1978) Initial urinary catecholamine concentrations and prognosis in neuroblastoma. *Pediatrics* 62:77–83
42. Evans AE, D'Angio GJ, Probert K et al (1987) Prognostic factors in neuroblastoma. *Cancer* 59:1853–1857
43. Quinn JJ, Altman AJ, Frantz CN (1980) Serum lactic dehydrogenase, an indicator of tumor activity in neuroblastoma. *J Pediatr* 97:89–91
44. Nakagawara A, Arima-Nakagawara M, Scavarda NJ (1993) Association between high levels of expression of the TRK gene and favorable outcome in human neuroblastoma. *N Engl J Med* 328:847–854
45. Gansler T, Chatten J, Varello M (1986) Flow cytometric DNA analysis of neuroblastoma. Correlation with histology and clinical outcome. *Cancer* 58:2453–2458
46. Brodeur GM, Azar C, Brother M et al (1992) Neuroblastoma: effect of genetic factors on prognosis and treatment. *Cancer* 70:1685–1694
47. Brodeur GM (1994) Molecular pathology of human neuroblastomas. *Semin Diagn Pathol* 11:118–125
48. Komuro H, Valentine MB, Rowe ST et al (1998) Fluorescence in situ hybridization analysis of chromosome 1p36 deletions in human MYCN amplified neuroblastoma. *J Pediatr Surg* 33:1695
49. Seeger RC, Brodeur GM, Sather H et al (1985) Association of multiple copies of the N-myc oncogene with rapid progression of neuroblastomas. *N Engl J Med* 313:1111
50. Norris MD, Bordow SB, Marshall GM et al (1996) Expression of the gene for multidrug resistance-associated protein and outcome in patients with neuroblastoma. *N Engl J Med* 334:231
51. Lack EE (1997) Tumors of the adrenal gland and extra-adrenal paraganglia. In: *Atlas of tumor pathology, third series, fascicle 19*. Armed Forces Institute of Pathology, Washington, D.C.
52. Shimada H, Chatten J, Newton WA Jr (1984) Histopathologic prognostic factors in neuroblastic tumors: definition of subtypes of ganglioneuroblastoma and an age-linked classification of neuroblastomas. *J Natl Cancer Inst* 73:405–416
53. Shimada H, Ambros IM, Dehner LP et al (1999) The International Neuroblastoma Pathology Classification (the Shimada system). *Cancer* 86:364–372
54. Romansky SG, Crocker DW, Shaw KNF (1978) Ultrastructural studies on neuroblastoma. Evaluation of cytodifferentiation and correlation of morphology and biochemical survival data. *Cancer* 42:2392
55. Romansky SG (1979) Neural crest aggregates in the human fetal adrenal gland (abstract). *Lab Invest* 40:309
56. Beckwith JB, Perrin EV (1963) In situ neuroblastomas: a contribution to the natural history of neural crest tumors. *Am J Pathol* 43:1089–1104
57. Guin HG, Gilbert FE, Jones B (1969) Incidental neuroblastoma in infants. *Am J Clin Pathol* 51:126–136
58. Hayes FA, Green AA, Bhaskar NR (1989) Clinical manifestations of ganglioneuroma. *Cancer* 63:1211–1214
59. Joshi VJ, Silverman JF (1994) Pathology of neuroblastic tumors. *Semin Diagn Pathol* 11:107–117
60. Isaacs H Jr (1989) Congenital malignant tumors. In: Reed GB, Claireaux AE, Bain AD (eds) *Diseases of the fetus and newborn: pathology, radiology and genetics*. Chapman Hall, London

7.1 Introduction

The *leukemias* are a heterogeneous group of hematologic neoplasms characterized by the infiltration of abnormal hematopoietic cells in the bone marrow, peripheral blood, and various organs and tissues. Following this clonal overgrowth of leukemic cells, the patient eventually develops hematologic sequelae of bone marrow failure manifested by anemia, neutropenia, and thrombocytopenia [1, 2].

Acute leukemia is defined as *congenital* when diagnosed at birth, *neonatal* in the first month, and *infantile* when the disease occurs during the first year of life.

The clinical findings and biological features of leukemia in the fetus and infant are not exactly the same as those of older children and adults [1–4]. For example, the disease in the young has an unexplained natural tendency to undergo *spontaneous remission* [5–9]. Despite therapeutic advances in the treatment of acute leukemia in childhood, the prognosis for fetuses and infants regardless of therapy is still discouraging [2, 5, 10, 11]. With few exceptions, fetal and infant leukemias are classified as acute since they have a predominance of immature hematopoietic precursors. Traditionally, acute leukemia is divided into two main categories, *acute lymphocytic leukemia (ALL)* and *acute myeloid leukemia (AML)*. Most fetal and infant leukemias are designated as acute nonlymphocytic (ANLL), as high as 90 % in some series, as compared to acute lymphocytic leukemia (ALL) [2, 4, 5]. Congenital chronic myeloid leukemia is the subject of a rare case report during the first year of life [13, 14].

Infant ALL may express both B- and T-antigens simultaneously, a so-called *mixed lineage* or *biphenotypic leukemia* [1, 3, 5]. The expression of both ALL and AML can occur at the same time or present later in two separate blast populations. Lineage conversion of ALL to AML can occur also after relapse.

7.2 Incidence

Data from the Third National Cancer Survey reveal that the incidence of malignant tumors in newborns is 36.5 per million live births per year and that neuroblastoma ranks first with 19.7 per million live births (54 % of cases) and leukemia second with 4.7 per million live births (13 %) [6]. However, the mortality from leukemia (2.6 per million live births) exceeds 1.5 times that of neuroblastoma (1.8 per million). In several perinatal studies, leukemia is the second most common malignant tumor following neuroblastoma [1–5] (Table 1.1).

Leukemia does not occur as often in the infant as it does later in childhood. The incidence of leukemia in the infant and neonate is approximately 3 and 1 %, respectively, of the total pediatric population with this disease [5].

7.3 Hematopoiesis

Development of blood and blood vessels begins within the blood islands of the yolk sac and to a lesser extent in the chorion, body stalk, and allantois at approximately 19 days [15]. Cells within the center of the blood islands become the blood-forming cells, the hematopoietic stem cells, while those at the periphery form the endothelial cells which line vessels. Hematopoietic stem cells are carried in the blood from the yolk sac and populate the liver, bone marrow, spleen, lymph nodes, and other sites (e.g., thymus and kidney). Blood formation begins in the liver during the fifth week, and this organ becomes the main source of erythrocytes until near the end of fetal life (Fig. 7.1). By the end of the third month, hematopoiesis is found in the bone marrow, which becomes the major site of erythropoiesis during the latter part of the third trimester [15].

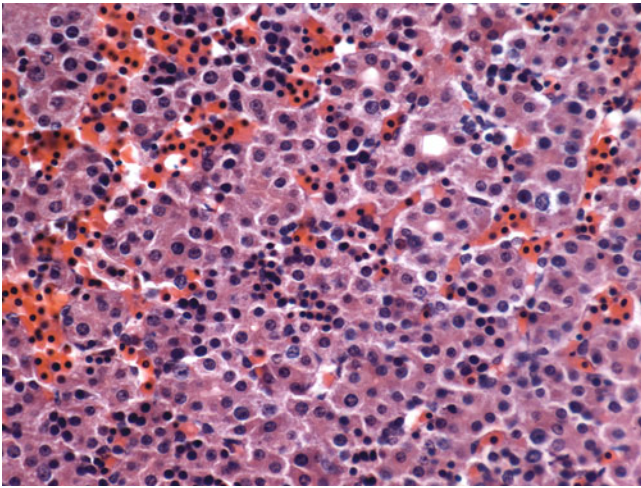


Fig. 7.1 Fetal liver with hematopoiesis. Liver from 16-mm fetus (approximately 6 weeks gestation) showing extensive hematopoiesis. Sinusoids are filled with enlarged nucleated erythrocytes and nests of smaller nucleated erythroblasts (Reprinted from Isaacs [1]. © Springer-Verlag, 2002)

Blood cells formed within the yolk sac and in the liver during the second trimester are predominately erythropoietic elements, many of which are large and nucleated having a megaloblastic appearance (Fig. 7.1). Leukocytes, namely, neutrophils, histiocytes, lymphocytes, and megakaryocytes, appear in the liver and yolk sac at approximately 5 weeks, and a few weeks later in the spleen, lymph nodes, and bone marrow [15].

7.4 Clinical Features

Hepatosplenomegaly, *hydrops*, and *polyhydramnios* (*hydramnios*) are the main presenting signs of leukemia detected by antenatal sonography [1, 16–23]. Leukemia is diagnosed in fetuses with Down syndrome as early as 33 weeks' gestation [17, 18, 20, 23]. Diagnosis can be established by fetoscopy and umbilical blood sampling [16–23]. Leukemic cells are readily identified on Wright-Giemsa stained umbilical blood smears.

Leukemia is an important cause of *stillbirth* [5, 12, 19, 24–27]. In one study, stillbirth was responsible for 5 of 69 (7 %) of the deaths in the Down syndrome group as compared to 5 of 145 (3 %) in the non-Down syndrome patients [5]. At postmortem examination, fetuses with leukemia are often hydropic and macerated, and their placentas are significantly enlarged and edematous, resembling those of

erythroblastosis fetalis (hemolytic disease of the newborn) [1, 12, 22, 24, 27].

The *clinical findings* of neonatal and infant leukemia are variable. The disease is characterized usually by a rapid downhill course, but it may be unpredictable. Some neonates show signs of leukemia at birth and die shortly thereafter, while others appear normal following delivery but develop clinical and hematological problems later on. In a third group, leukemia is not discovered until the third to sixth week of life with a history suggestive of hematologic abnormalities dating back a few weeks earlier [1, 5, 9].

Nodular cutaneous infiltrates (*leukemia cutis*, “blueberry muffin baby”) and *hepatosplenomegaly* are characteristic features of neonatal leukemia, especially AML (M4, M5) [5, 28–33]. Cutaneous nodules, ranging in color from blue to purple to brown to red, are observed in stillborns with the disease and are the initial presenting sign in about half of neonates, particularly those with AML (M5) [5, 30, 34, 35] (Fig. 7.2). Frequently, leukemia cutis is the initial clinical manifestation of the disease and precedes other signs of leukemia by as much as 4 months [5, 31, 35]. Other cutaneous manifestations are multiple *petechiae* and *ecchymoses related to thrombocytopenia* (Table 7.1).

When *respiratory distress* occurs at birth, it is attributed to pulmonary hemorrhage secondary to thrombocytopenia and/or extensive leukemic infiltration complicated by atelectasis [1]. *Neurological findings* are observed in neonates with central nervous system (CNS) involvement. A bulging fontanelle is the sign of meningeal leukemic infiltration or an intracranial bleed secondary to thrombocytopenia [1, 12]. Over a third of these neonates have leukemic cells either in their cerebrospinal fluid (CSF) or in their meninges and brain at necropsy.

Sepsis, *pneumonia*, and *other infections* are often the result of *neutropenia* [2]. Cardiac failure with nonimmune hydrops has been attributed to severe anemia [21]. Hyperviscosity and leukostasis with compromise of CNS, cardiac, and pulmonary function secondary to profound leukocytosis are other complications [2].

In the group of patients whose leukemia is discovered toward the end of the neonatal period and later in infancy, signs and symptoms tend to be more vague; for example, the baby may have a low-grade fever, pallor, lethargy, hepatosplenomegaly, a bleeding tendency, diarrhea, or generally “failure to thrive” [5, 12]. *Sepsis and hemorrhage* are the most common causes of death, which is the same as that observed in older children [5, 12].



Fig. 7.2 Congenital leukemia. (a) Multiple flat and elevated areas of involvement of the skin. The largest area is in the left antecubital fossa. Death occurred at 2 days (Reprinted from Gilbert-Barness [36]. With kind permission of © Mosby). (b) Bone marrow smear from a neonate

with monocytic leukemia (AML-M5) showing large leukemic blast cells with monocytoid features consisting of more than one light staining nucleoli, in-folded nuclei, and finely granular, bluish-purple cytoplasm [directly below]

Table 7.1 Conditions causing petechiae and purpura in the newborn

Congenital rubella
Toxoplasmosis
Cytomegalovirus
Platelet antibodies
Amegakaryocytic thrombocytopenia
Congenital leukemia
Hemolytic anemia (e.g., hereditary spherocytosis)
Twin-to-twin transfusion
Fetal-maternal transfusion
Isoimmunization

Reprinted from Isaacs [12]. © WB Saunders 1997

7.5 Leukemia Occurring in Infants with Chromosomal Anomalies, Syndromes, and Malformations

Chromosomal anomalies, syndromes, and malformations are found in association with leukemia [5, 22, 37–42]. The major chromosomal defect, *trisomy 21*, is found in patients with Down syndrome. *Chromosome 11q23* translocations are noted in about half of neonates with either AML or ALL [2, 5, 11, 37] (Table 7.2) (Fig. 7.3). The major translocations involving the 11q23 locus are t(4;11) and t(11;19) [5]. Chromosomal alterations more commonly associated with

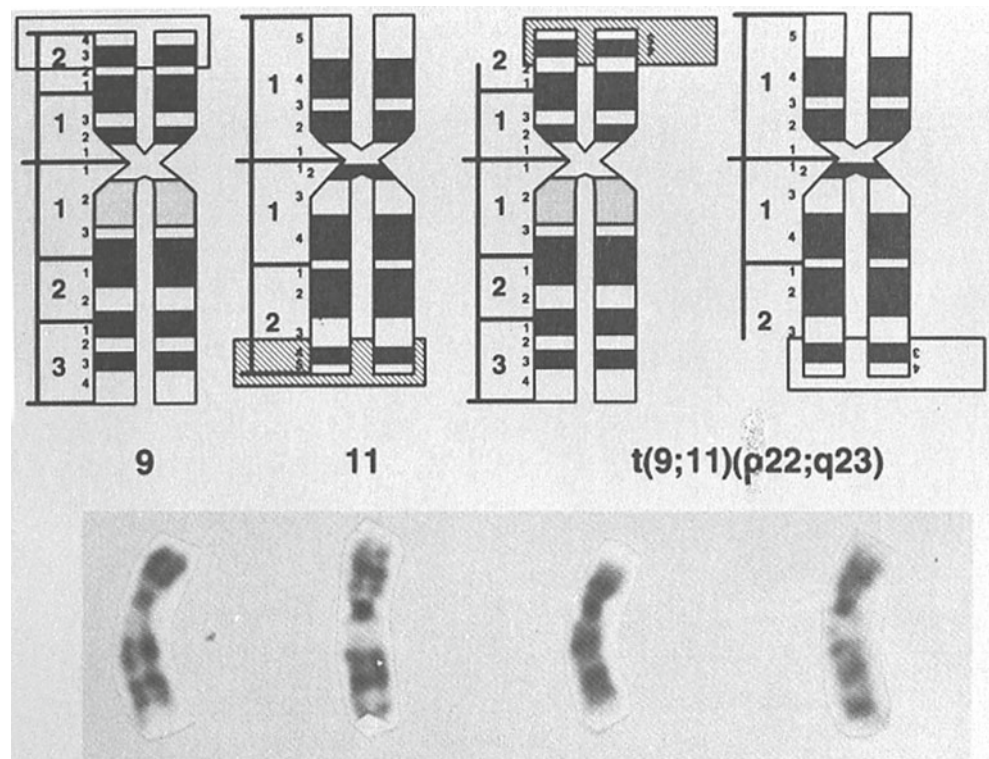
Table 7.2 Common immunophenotypes and karyotypes in congenital leukemias

	ALL	AML (M4 and M5)	AML (M7)
Immunophenotype			
Common	CD10 (CALLA) Surface immunoglobulin Sig+ CD79a (early B-cell) + HLA-DR, TdT+	CD33 CD13 CD14+	Iib/IIIa + GPIIIa + Platelet GpIb + Factor VIII antigen +
Variably present	CD33 (myeloid) + CD9, CD24, CD45+ (Mixed lineage leukemias)	HLA-DR	CD33+ CD13+, HLA-DR + CD34, CD41, CD61 +
Karyotype			
Common	t(4;11)(q21;q23)	t(11;19)(q23;p13) t(9;11)(p21;q23)	47,XX+21, 47, XY +21 & mosaics 46,XX/47,XX +21 or 46,XY/47,XY +21 t(1;22)(p13;q13) CATA-1 gene -
Less common	t(9;11)(p2;q23)	Many others involving 11q23 and various partners	

Reprinted from Isaacs [1]. © Springer-Verlag, 2002; Perkins [3]. With kind permission of © Mosby- Elsevier; Sande et al. [2]. With kind permission of © Elsevier, 1999

Abbreviations: ALL acute lymphoid leukemia, AML acute myeloid leukemia, TCR T-cell receptors, HLA-DR human leukocyte antigen-DR, TdT terminal DNA polymerases

Fig. 7.3 11q23 translocation. t(9;11)(p22;q23) is a frequent type of 11q translocation observed in ANNL monocytic leukemia (FAB M5) (Reprinted from Heim and Mittelman [43]. With kind permission of © Alan R. Liss, 1987)



acute megakaryocytic leukemia (AMKL) (M7) are t(1;22)(p13;q13) rearrangements [10, 38, 39] (Fig. 7.4). Trisomies 1, 8, 19, and 13; X;6 translocation; Turner syndrome (X0); Klinefelter syndrome (47 XXY); monosomy 7; and trisomy 9 are associations described less often [5, 40].

Examples of *congenital defects* and syndromes found in association with leukemia are Bloom syndrome, Diamond-Blackfan anemia, Klippel-Feil syndrome, Fanconi anemia, Ellis-van Creveld syndrome, neurofibromatosis 1, Shwachman syndrome, TAR syndrome (thrombocytopenia and absent



Fig. 7.4 The t(2;22)(p13;q13) rearrangement associated with acute megakaryoblastic leukemia. (a) Diagram showing the G-banded pattern of the derivative (*der*) chromosomes and normal homologues. The arrows indicate the approximate positions of the breakpoints. (b) Representative partial karyotypes from four patients (Reprinted from Carroll [10]) (With kind permission of © American Society of Hematology, 1991)

radii), Marfan syndrome, Klinefelter syndrome, and certain cardiac malformations [3, 5, 41, 42, 44, 45].

Cytogenetic abnormalities found in the leukemic cells of fetuses and infants are clearly different from those in older children and adults, and perhaps this may explain in part the unique biological characteristics of the disease in the younger age group [46]. 11q23-MLL gene rearrangements occur most often with AML, particularly monocytic subtypes, and less often with pre-B ALL. Neonates with 11q23-associated leukemia present often with marked leukocytosis and

hepatosplenomegaly [4, 37, 47, 48]. Leukemia cutis occurs more frequently in patients with acute monocytic leukemia, and CNS involvement is slightly more prevalent in ALL. Incidence of subtype M7 in AML is 20 % or more in infants [39].

The main translocation of acute megakaryocytic leukemia (AMKL) is a t(1;22) translocation in the leukemic cells of children with AMKL (M7) [10, 39]. There is a strong association between AMKL and Down syndrome. Occasionally, AMKL may present clinically as a solid tumor mass, similar to granulocytic sarcoma, which is rare also in infancy [1, 10, 39]. Bone marrow and other organs including soft tissues contain compact infiltrates of leukemic cells with megakaryocytic antigens accompanied by fibrosis [1, 10, 39].

Neonates and infants with either AML or ALL show a high frequency of *co-expression of lymphoid- and myeloid-associated antigens* in their leukemic cells [3, 5]. The cells are usually HLA/DR positive and CALLA (CD10) negative phenotype [11, 37, 47, 48]. Hyperleukocytosis, organomegaly, and CNS involvement often are common initial clinical findings.

The large leukemic cell burden and the unfavorable immunophenotype and chromosomal translocations are factors believed to contribute to the poor outcome for the neonate with leukemia [47].

7.6 Differential Diagnosis

Neonatal leukemia must be differentiated from *leukemoid reactions* (blood and clinical findings resembling true leukemia) observed in *response to infection, hemolytic disease, or hypoxia* [1, 5, 12, 30] (Table 7.3). It may be difficult to distinguish leukemia from the more common conditions causing leukemoid reactions [1, 2, 5, 12, 30, 35, 49]. Infections, hypoxia, and hemolytic disease of the newborn stimulate both erythroid and myeloid hematopoiesis in the sites where they normally occur in fetal life, and therefore exclusion of leukemoid reactions and blood group incompatibility is important but sometimes difficult. Occasionally, the distinction is not made easily on histological grounds alone [1].

Leukemoid reactions may mimic leukemia because neonates present with high peripheral leukocyte counts and increased numbers of circulating immature forms. The immature cells may be distinguished from leukemia on the basis of bone marrow examination and immunohistochemical findings, which are usually normal [1]. Moreover, peripheral blood smears do not show the monotonous cell population characteristic of leukemia. Cytogenetic studies are helpful in distinguishing the two. Leukocytosis, thrombocytopenia, and hepatosplenomegaly frequently accompany *congenital infections* such as toxoplasmosis, rubella, cytomegalovirus, herpes, syphilis, and bacterial sepsis. However, these

Table 7.3 Differential diagnosis of congenital leukemia

Infectious disease
Congenital cytomegalovirus
Congenital rubella
Toxoplasmosis
Congenital herpes virus
Viral hepatitis
Human immunodeficiency virus
Intrauterine parvovirus
Listeria monocytogenes
Congenital syphilis
Hematological
Immune processes
Rh factor in blood incompatibility
Other major or minor blood group incompatibilities
Nonimmune processes
α -Thalassemia
Congenital dyserythropoietic anemia
Diamond-Blackfan anemia
Intrauterine or birth-related hypoxia
Twin-to-twin transfusion
Malignant tumors
Neuroblastoma
Alveolar rhabdomyosarcoma
Rhabdoid tumor
Ewing sarcoma
Histiocytoses
Langerhans cell histiocytosis
Hemophagic lymphohistiocytosis

Gottesfeld et al. [30]. With kind permission of © American Academy of Dermatology, 1989; Sande et al. [2]. With kind permission of © Elsevier, 1999; Isaacs [1]. © Springer-Verlag, 2002

infections are usually accompanied by other clinical manifestations of intrauterine growth retardation, microcephaly, and hepatitis, all of which can be ruled out clinically, and by maternal and infant serologic tests [2].

Severe *hemolytic disease of the newborn* (immune erythroblastosis fetalis) may masquerade as leukemia (Fig. 7.5). Neonates with this disorder, if severe enough, have hepatosplenomegaly, skin nodules due to extramedullary hematopoiesis, numerous erythroblasts in the peripheral blood smear, and thrombocytopenia [1, 30, 35]. Hepatosplenomegaly and cutaneous nodules are present also in newborns with *disseminated neuroblastoma, stage 4S*. Peripheral blood counts are usually normal, but bone marrow aspirates reveal characteristic small syncytia of neuroblastoma cells [1, 12] (Figs. 6.9 and 7.7). Documentation of elevated urinary catecholamines is important for establishing the diagnosis of neuroblastoma. Dermal erythropoiesis causing a “blueberry muffin” appearance of the skin is found more often with *congenital infections* (e.g., rubella and cytomegalovirus) and hemolytic disease of the newborn than with either leukemia or neuroblastoma [30, 35].

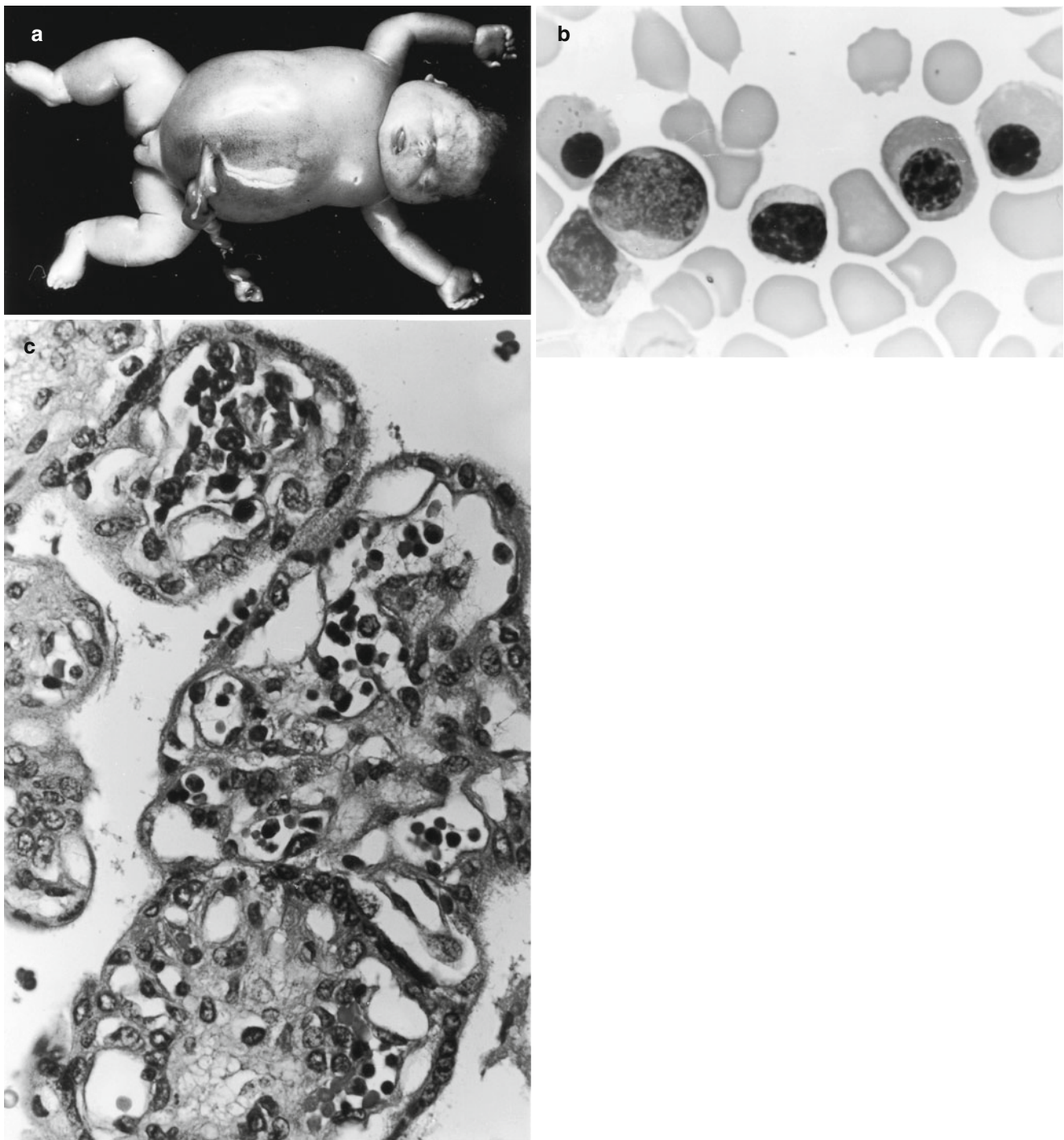


Fig. 7.5 Erythroblastosis due to Rh incompatibility. (a) Stillborn with hydrops fetalis. (b) Peripheral Wright-Giemsa stained smear from a newborn with erythroblastosis fetalis showing immature erythrocytes consisting of erythroblasts and normoblasts. Anisocytosis, poikilocytosis, and polychromasia are present. Hematologic values: hemoglobin 10 g/dL,

leukocyte count $39 \times 10^9/L$, platelet count $158 \times 10^9/L$. (c) Placenta from a hydropic newborn with erythroblastosis fetalis due to Rh incompatibility. Placenta was enlarged (780 g), pale, and edematous. H&E microscopic section reveals edematous villi with many nucleated erythrocytes within villous capillaries (Reprinted from Isaacs [12]. © WB Saunders 1997)

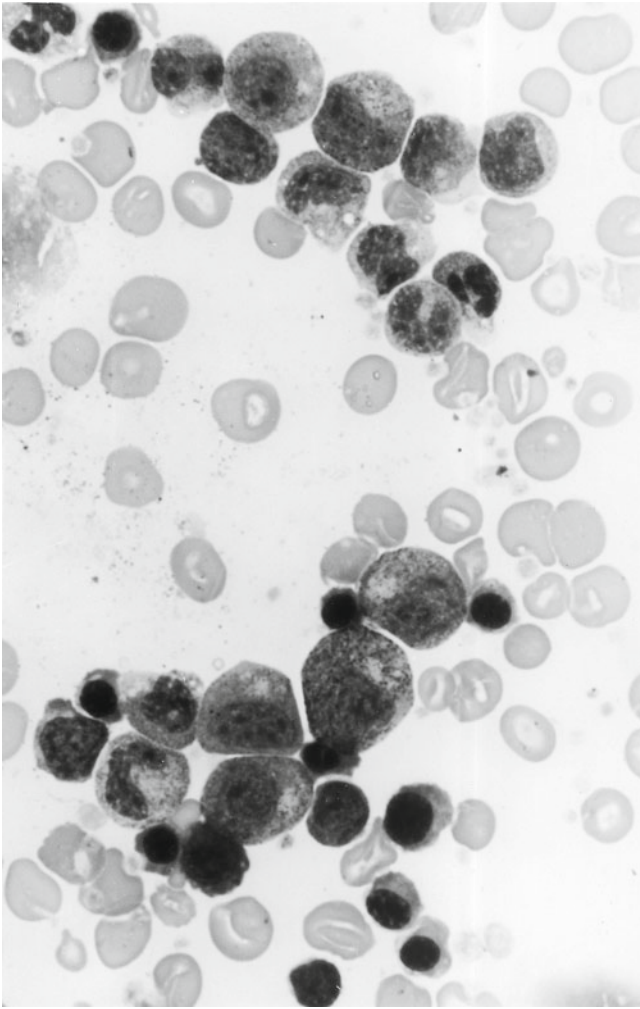


Fig. 7.6 Transient myeloproliferative disorder with Down syndrome. The patient was a 2-day-old male with Down syndrome. Evaluation for imperforate anus revealed a leukocyte count of $31 \times 10^9/L$ and RBC of 12.1 g/dL. The peripheral smear revealed 30 % immature granulocytes, 17 % bands, 31 % lymphocytes, 8 % monocytes, 1 % eosinophils, and 10 % blasts; 20 nucleated RBCs per 100 WBCs; reduced platelets. Bone marrow histochemical studies: nonspecific esterase and acid phosphatase reactive; peroxidase, Sudan black B, PAS and chloroacetate esterase negative. After a few weeks, his blood picture returned to normal without therapy. He is alive and well at age 15 years without recurrence of his leukemia. Wright-Giemsa stained bone marrow aspirate showing predominately myeloid elements and early erythroid forms (Reprinted from Isaacs [1]. © Springer-Verlag, 2002)

Congenital human immunodeficiency virus (HIV) infection may be mistaken for leukemia [3, 50]. Clonal B-cell proliferations in these patients are the cause of lymphadenopathy and worrisome marrow findings. Newborns with HIV infection may present with petechiae and thrombocytopenia [3, 50]. The bone marrow contains collections of large lymphocytes with scant cytoplasm and dense, homogeneously staining nuclei with clefts; they are of B-cell lineage and CD10 (CALLA) expression positive. Bone marrow DNA analysis and flow cytometry show gene rearrangements in both the immunoglobulin light- and heavy-chain loci, thus establishing the presence of a clonal B-cell lymphoid proliferation. Eventually, the B-cell lymphoid proliferation resolves [3, 50].

Three main criteria are required for the diagnosis of perinatal leukemia: the presence of immature hematopoietic cells in the peripheral blood and bone marrow; infiltration of non-hematopoietic tissues by these cells; and exclusion of conditions that should be considered in the differential diagnosis, such as hemolytic disease of the newborn, congenital infections, and neuroblastoma [1, 2, 12].

Approximately 10 % of newborns with Down syndrome develop an enigmatic myeloproliferative disorder that is clinically and morphologically indistinguishable from leukemia, often megakaryocytic in type; this condition is called transient congenital leukemia, or ineffective regulation of myelopoiesis, among other terms [1, 5, 16–19, 22] (Figs. 7.6 and 7.7). The disorder has been detected also prenatally [5, 17].

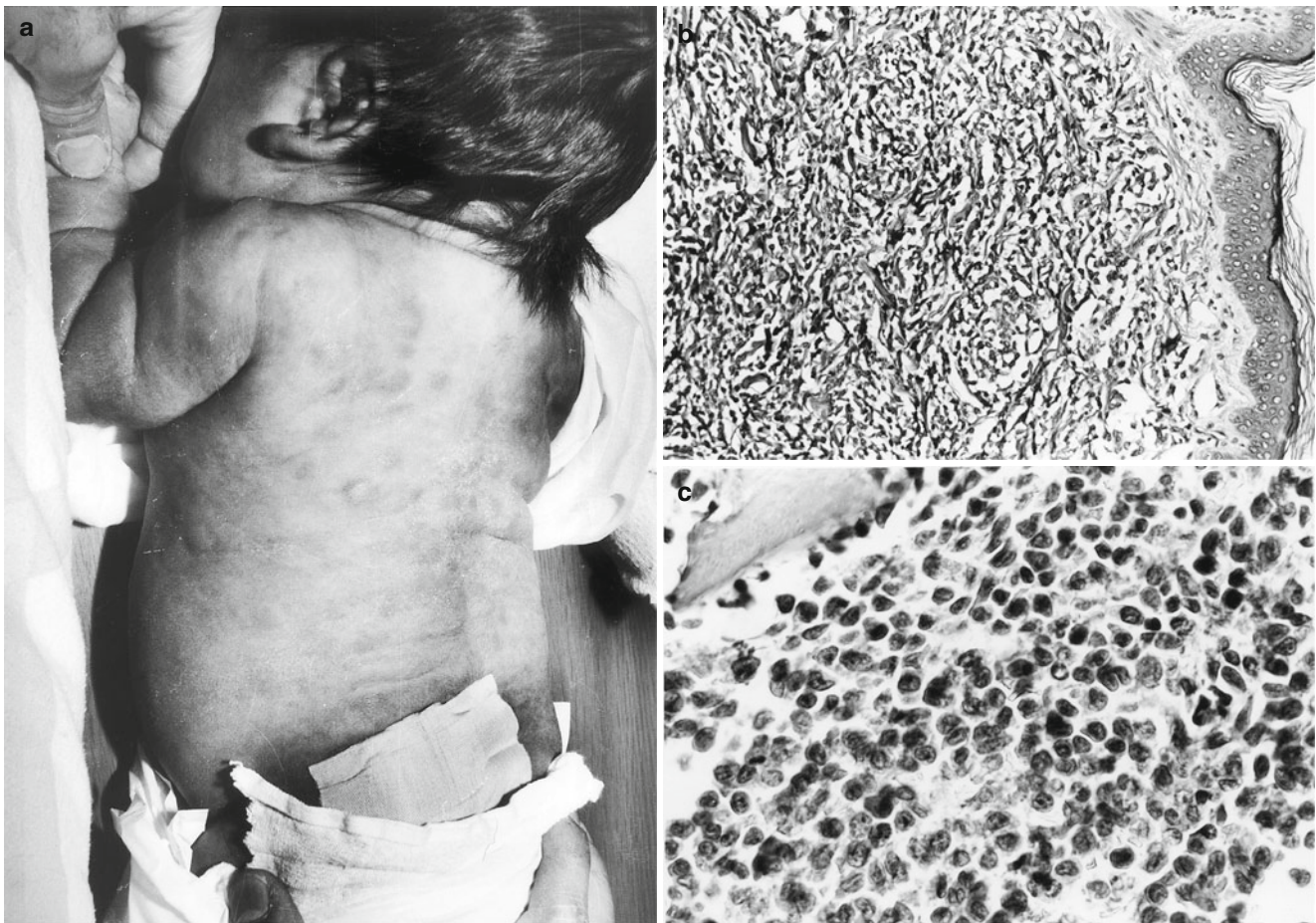


Fig. 7.7 Transient congenital leukemia. (a) Newborn male with multiple raised cutaneous nodules distributed over most of his body, fitting the description of a “blue berry muffin baby”. His karyotype, 46XY, was normal. The initial leukocyte count was $117 \times 10^9/L$ and hemoglo-

bin 12.7 g/dL. (b) Skin biopsy taken of one of the nodules showing diffuse dermal and subcutaneous leukemic cell infiltration. (c) The bone marrow is replaced by myeloblasts (Reprinted from Isaacs [12]. © WB Saunders 1997)

7.7 Diagnosis of Leukemia

Complete *morphologic, immunologic, and genetic examination of the leukemic cells is required to establish the diagnosis of leukemia*. Hematologic evaluation begins with performing a *complete blood cell count (CBC) and examination of the peripheral smear* [1, 5, 51, 52]. Although these tests can be performed on umbilical cord blood, they alone are often insufficient for either diagnosis or classification. Moreover, the presence of leukocytosis and blasts in the peripheral smear does not establish the diagnosis necessarily of leukemia since erythroblastosis fetalis, sepsis, and certain metastatic malignancies can cause increased leukocyte counts with release immature hematopoietic elements (Figs. 7.5 and 7.8). In addition to the CBC and peripheral smear, *bone marrow aspiration and biopsy* are indicated to study cellular morphology and to rule out infections and the other entities mentioned above. Normally there are less than 5 % blasts in the bone marrow; greater than 25 % blasts is

required for the diagnosis of leukemia [1, 5, 51, 52]. Blood and bone marrow cultures are an important part of the work-up.

When the diagnosis of acute leukemia is established, it is important particularly for therapeutic and prognostic reasons to determine whether the leukemia is lymphocytic or nonlymphocytic [1, 51, 52]. The next step is to decide the subclassification of ALL or ANLL to which the leukemia belongs. ALL and ANLL are diagnosed and classified on the basis of morphologic findings as the presence of granules or Auer rods and nuclear, nucleolar, and cytoplasmic appearance, and by cytochemical stains, flow cytometry, and cytogenetic studies (Table 7.4). Traditionally, the international *French-American-British classification (FAB)* based on these findings is used to classify the leukemias [53]. The FAB classification subdivides ALL into three groups: L1, L2, and L3 and ANLL into 7 groups: M1 to M7 (Table 7.4) [53]. Most infant ALL cases fall into the L1 or L2 FAB morphology [2, 5].

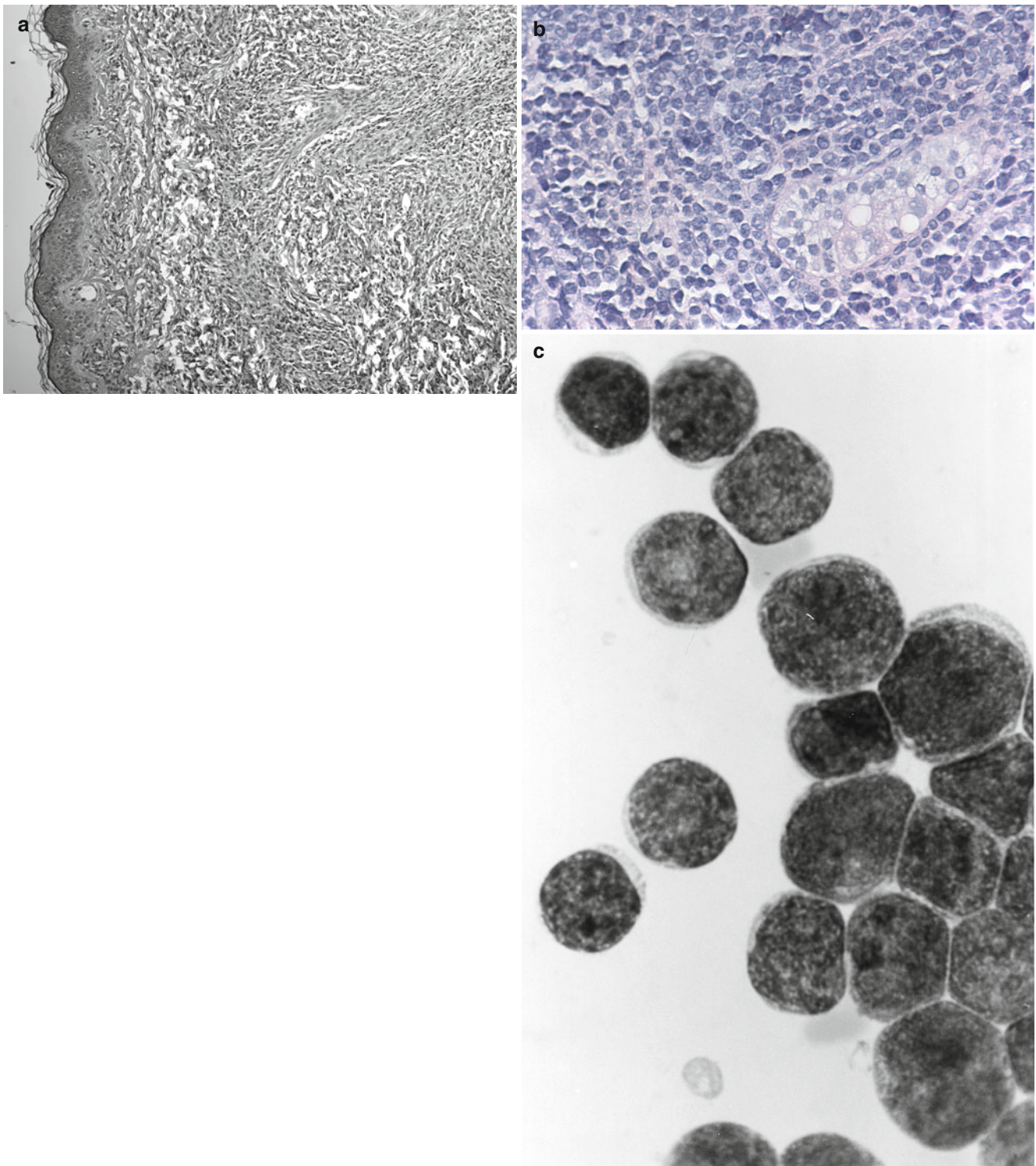


Fig. 7.8 Acute lymphoid leukemia (ALL). 3-month-old male with anemia (hemoglobin of 5.8 g/dL) and a leukocytosis of $25 \times 10^9/L$ with a differential of 96 % lymphoblasts and 4 % neutrophils. Platelet count was $104 \times 10^9/L$. Scattered bluish-purple nodules less than 1 cm in diameter were distributed over the chest, back, groin, and scalp, and bilateral testicular enlargement was noted on physical examination. His karyotype was normal. (a) Skin biopsy showing leukemic cells infiltrating the dermis and subcutaneous tissue. (b) Testis biopsy with extensive interstitial leukemic cell infiltrates. (c) An imprint (“touch

preparation”) of the testis biopsy showing small lymphoblasts having a high nuclear/cytoplasmic ratio, clumped chromatin pattern, and 1 or 2 small nucleoli consistent with FAB L1 morphology. Similar cells found in the bone marrow contained PAS-positive granules were CALLA, peroxidase, Sudan black, and α naphthyl esterase negative. The anti-DR antibody was positive, but no T-cell antibodies were detected. Interpretation of the findings was that the lymphoblasts were of pre-B-cell lineage falling into the so-called pre-B-cell ALL category (Reprinted from Isaacs [12]. © WB Saunders 1997)

Table 7.4 Morphological and cytochemical features of ALL and AML

Leukemia	FAB	Wright-Giemsa stain morphology	Cytochemistry									
			PAS	Sudan	MP	CAE	ANB	ANA	Gly	VIII	PPO	Iib
Acute lymphoid	L1	Predominately small cells High N:C ratio Indistinct 1–2 nucleoli Coarse nuclear chromatin Blue cytoplasm	+	–	–	–	–	–	–	–	–	–
	L2	Large cells, vary in size lower N:C ratio than L1 prominent nucleoli stippled chromatin Blue cytoplasm	+	–	–	–	–	–	–	–	–	–
Acute myeloid	M1-M3	Low N:C ratio	–	+	+	+	–	+	–	–	–	–
		Auer rods ± 2–5 nucleoli										
		Granules present										
		Fine nuclear chromatin Blue-gray cytoplasm										
Acute myelomonocytic	M4	Myeloblasts and monoblasts	–	+	+	+	±	+	–	–	–	
Acute monocytic	M5	Low N:C ratio; Nuclei lobular or reniform; cells resemble monocytes; fine nuclear chromatin +	–	±	±	–	+	+	–	–	–	
Acute erythroleukemia	M6	Bizarre erythroblasts	±	±	+	–	–	–	+	–	–	–
		Multiple lobed nuclei; multiple nuclei										
		Blast cells with ragged cytoplasmic borders										
		Vacuolated blue cytoplasm										
Acute megakaryoblastic	M7	Blasts with high N:C ratio; cytoplasmic blebs	+	–	–	–	–	±	–	+	+	+

Reprinted from Perkins [3]. With kind permission of © Mosby- Elsevier; Sande et al. [2]. With kind permission of © Elsevier, 1999; Isaacs [1]. © Springer- Verlag, 2002

Abbreviations: FAB French-American-British morphologic classification, N:C nuclear to cytoplasmic, PAS periodic acid Schiff, Sudan Sudan black B, MP myeloperoxidase, CAE chloroacetate esterase, ANB α -naphthyl butyrate esterase, ANA α -naphthyl acetate esterase, glyc glycophorin A, VIII factor VIII, PPO platelet peroxidase (by electron microscopy), Iib glycoprotein IIb/IIIa

Occasionally, leukemic blast cells are poorly differentiated making it impossible to determine whether the leukemia fits into any of the ALL or ANLL categories based only on morphology and cytochemistry. Therefore, the final interpretation of the type of leukemia depends on the use of a combination of supplemental methods as flow cytometry, cytogenetics, and molecular analysis which assist in the identification of the cellular lineage [3, 29, 52, 54]. Monoclonal antibodies for myeloid and lymphoid surface antigens are used to distinguish ANLL from ALL and to further subtype the leukemic cells [3, 29, 52, 54] (Table 7.4). Most newborn and infant ALL cells have an early pre-B-cell phenotype manifested by HLA/DR positivity and negativity for CALLA, T-cell, and B-cell antigens [3, 55, 56]. L1 and/or L2 FAB morphology is noted most often in this age group (Fig. 7.8c). *Acute monocytic leukemia (M5)* (42 %) is the most common form of ANLL in neonates and infants followed by *acute myelomonocytic leukemia (M4)* (4 %) and *acute myeloblastic leukemia (M1)* (17 %) [3, 5].

Immature cells of the megakaryocytic series in smears and in tissues frequently lack distinctive morphologic features that aid in their recognition. As a result, some AMKL cases have been classified as *acute undifferentiated leukemia* [1, 57]. The diagnosis of AMKL is made on the basis of morphology on Wright-Giemsa stained smears, the platelet peroxidase reaction by EM (which is positive also in erythroleukemic blasts), and reactivity with monoclonal platelet-specific antibodies by flow cytometry [3, 10, 57].

Megakaryoblasts in Wright-Giemsa stained smears display a variable morphology conforming to the *M7* category of the FAB classification [1, 10] (Fig. 7.9). *Small and large blast cells with cytoplasmic projections or blebs* are considered consistent with the diagnosis of AMKL. The small blasts have round nuclei, prominent nucleoli, stippled chromatin, and a moderate basophilic cytoplasm without granules and the latter a scant cytoplasm, a round nucleus with stippled chromatin, and an inconspicuous nucleolus.

The presence of *glycophorin A* in leukemic cells is considered diagnostic of erythroleukemia [58, 59].

Megakaryoblasts in blood and marrow smears react with *platelet glycoprotein GPIIb/IIIa antibody* [9, 57, 60]. However, the blasts are nonreactive for CALLA (CD10), TdT, OKM1, myeloperoxidase, and α -naphthyl butyrate esterase [57]. The AMKL cells are reactive with CD34, HLA-DR, and the platelet factors CD61 and CD 41 (glycoprotein IIa/IIIb) [60]. The syncytial appearance of AMKL cells in the marrow and the infiltrative nature in other organs accompanied by fibrosis suggest a non-hematopoietic metastatic malignancy. Markers such as neuron-specific enolase, NB-antigen, synaptophysin, desmin, and cytokeratin are required to exclude neuroblastoma, rhabdomyosarcoma, PNET, and other small cell malignant metastatic tumors [1, 10, 57].

7.8 Pathology

The gross and microscopic appearance of *leukemic placentas* resembles those of erythroblastosis fetalis (hemolytic disease of the newborn). They are enlarged, pale, and edematous, some weighing more than 700 g [1, 24, 27, 33]. Villi are swollen, uniformly enlarged, and composed of fetal blood vessels filled with leukemic blast cells, which do not invade the intervillous space of the maternal circulation (Fig. 7.9). Since leukemia, neuroblastoma, alveolar rhabdomyosarcoma, and other malignancies are known to involve the placenta, it may be difficult to distinguish between these conditions by H&E stained sections alone particularly if the affected fetus is macerated or stillborn. If tissues are well preserved, then immunocytochemical, flow cytometry, and chromosomal analysis can be performed to make a definite diagnosis [12].

Pallor and manifestations of bleeding such as petechiae, ecchymoses, and oozing from needle puncture sites, various orifices, and the umbilicus are typical *findings at post-mortem examination* of fetuses and infants dying of leukemia [1, 12] (Fig. 7.2). When the skin is involved, the nodular “blueberry muffin baby” appearance of leukemia cutis may be present. Stigmata of Down syndrome should be searched for such as epicanthal folds, transverse palmar creases, and clinodactyly of the fifth finger. If they are present, flow cytometry and chromosomal analysis should be done [61].

Organomegaly is typically present. The liver may weigh more than twice its normal expected weight and the spleen greater than four times normal. When the liver and spleen are

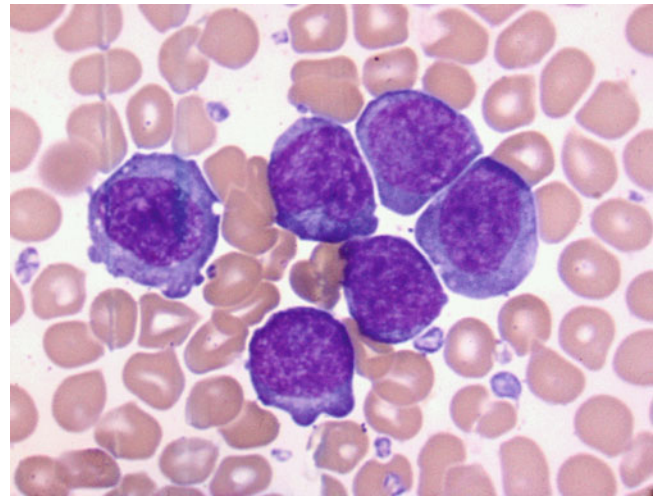


Fig. 7.9 (a) Acute megakaryoblastic leukemia. 1-month-old female presented with fever and leucocytosis of $50 \times 10^9/L$. Bone marrow aspirate revealed 87 % blasts consisting of small and large cells with cytoplasmic projections (blebs). The former have round nuclei, prominent nucleoli, stippled chromatin, and a moderate (basophilic) cytoplasm without granules and the latter a scant cytoplasm, a round or double nucleus with stippled chromatin and inconspicuous nucleoli. Cytochemistry: PAS, acid phosphatase, CD33 CD34, platelet antibodies CD 41, CD42a, and CD61 were positive; CAE, Sudan black B, and peroxidase negative; CD13 (Reprinted from Isaacs [1]. © Springer-Verlag, 2002)

greatly enlarged, they appear to occupy much of the abdominal cavity [1, 12] (Fig. 7.10b). *Renomegaly* secondary to leukemic infiltration is a common feature of the disease. Often the kidneys weigh almost twice their normal expected weight. They have tense, tan-gray, and smooth swollen capsules. Peripelvic hemorrhage and bulging cut surfaces with partial or total obliteration of the normal cortical-medullary architecture by gray to tan infiltrates are characteristic findings (Fig. 7.10d). The *spleen* has a swollen, purple-gray smooth capsule and a tan to red-brown bulging cut surface. Well-defined trabecular markings and white-pulp lymphoid nodules are generally absent (Fig. 7.10d). Splenic infarcts appear as irregular dark-red areas situated in the red pulp. The *liver* has a pale, tan smooth swollen capsule and a cut surface with gray to red markings representing foci of leukemic infiltrates and hemorrhage, respectively (Fig. 7.10c). *Lymphadenomegaly* is uncommon in the untreated or partially treated infant. When infiltrated, the lymph nodes are light tan to gray, swollen with small foci of hemorrhage. Lymphoid nodules generally are not seen.

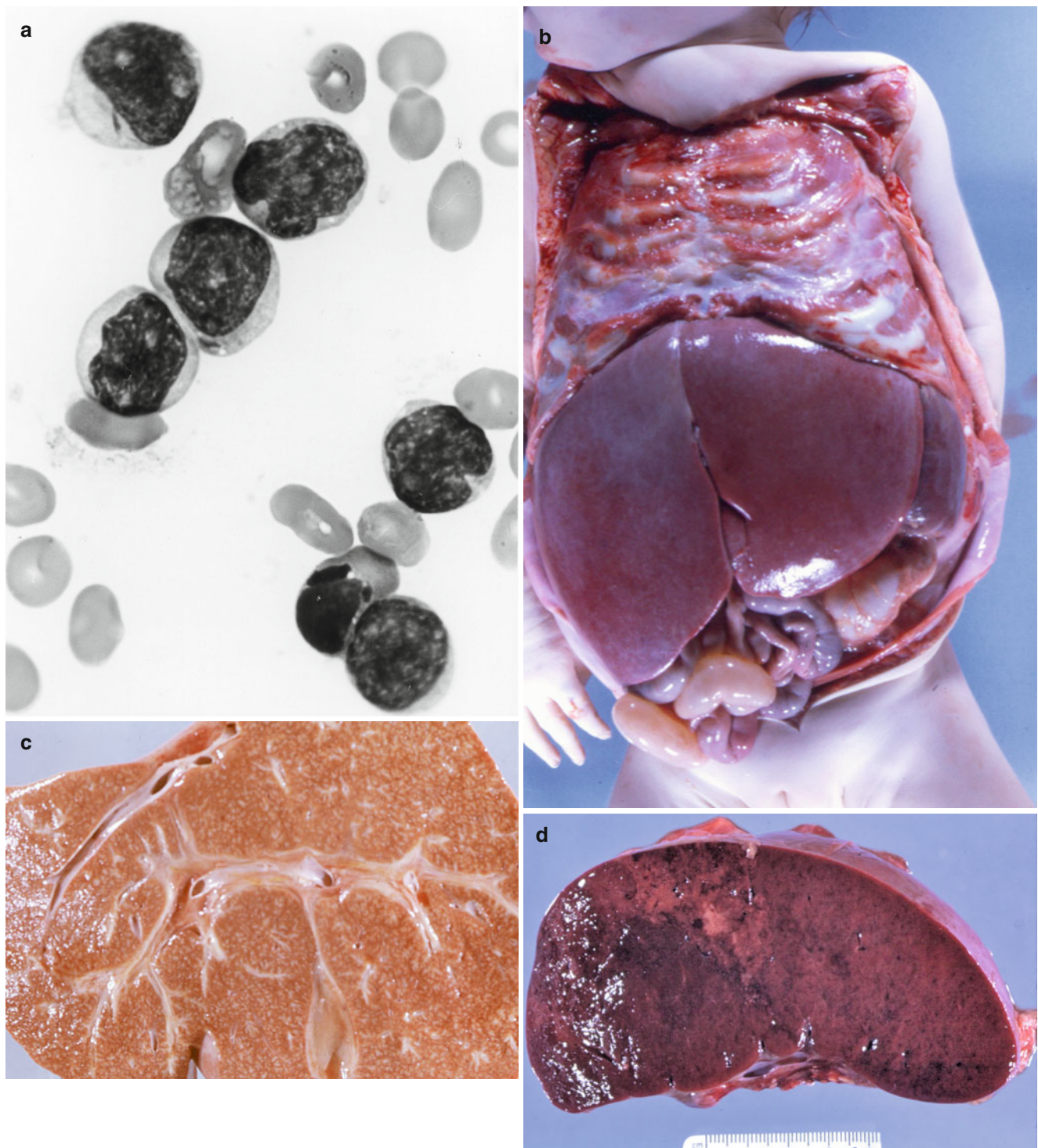


Fig. 7.10 Acute myeloid leukemia. 6-month-old-male with a 1-week history of fever and lethargy. Laboratory findings revealed an anemia (Hb 5.6 g/dL), leukopenia (WBC $28 \times 10^9/L$; 94 % blasts and 6 % neutrophils), and thrombocytopenia (platelets $32 \times 10^9/L$). (a) Wright-Giemsa stained bone marrow aspirate revealed myeloblasts showing features consistent with an M-2 FAB morphology; the leukemic cells have a relatively low nuclear-to-cytoplasmic ratio, nuclei with a fine chromatin pattern, and 2–3 prominent nucleoli. Auer rods are present in two blast cells, one in the upper left hand corner. Cytochemical findings: Sudan black, myeloperoxidase, and nonspecific esterase positive; PAS negative. (b) Postmortem examination revealed multiple petechiae and ecchymoses distributed over the skin and viscera, hepatosplenomegaly, renomegaly, and lymphadenomegaly. The photograph depicts impressive in situ hepatosplenomegaly. (c)

Cross section of the liver showing extensive whitish leukemic infiltrates. (d) The splenic cut surface with diffuse leukemic infiltration and an infarct on the left (dark area). (e) Capsular and cut surfaces of the kidney with central peripelvic hemorrhage and blurring of the cortical-medullary architecture by leukemic infiltrates. (f) Microscopic section of the liver reveals expansion of the portal tract by leukemic cells, which are noted also within the adjacent sinusoids. (g) The renal interstitium is heavily infiltrated by leukemic cells. (h) Collections of leukemic cells are noted within the edematous interstitial spaces. (i) Bone marrow elements are replaced by leukemic cell blasts. (j) There are areas of recent hemorrhage within cerebellar gray and white matter. Intracranial hemorrhage is an important cause of death in leukemia patients. (k) Foci of leukemic cell infiltrates are present within the cerebral cortex (Reprinted from; Isaacs [12]. © WB Saunders 1997)

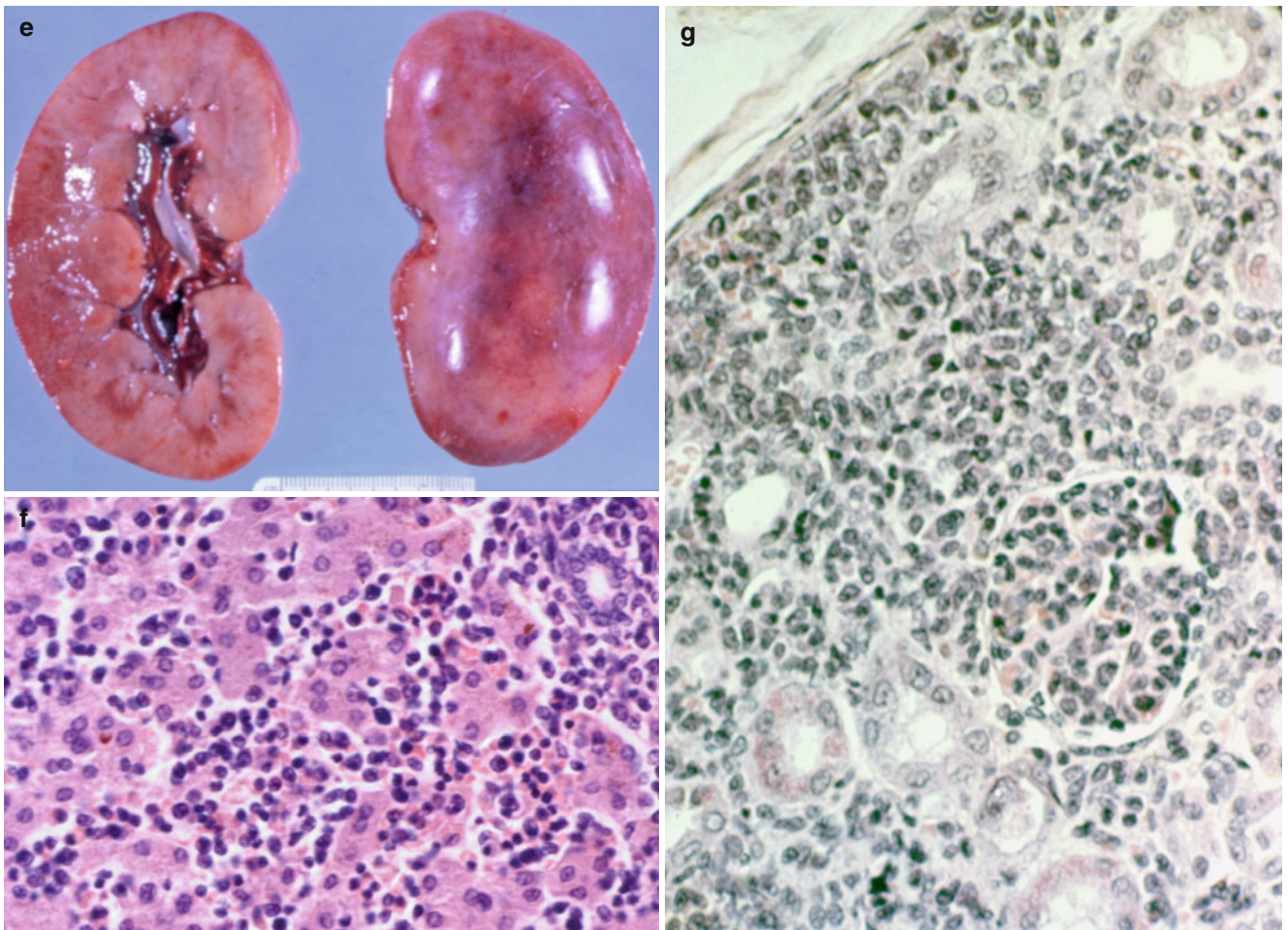


Fig. 7.10 (continued)

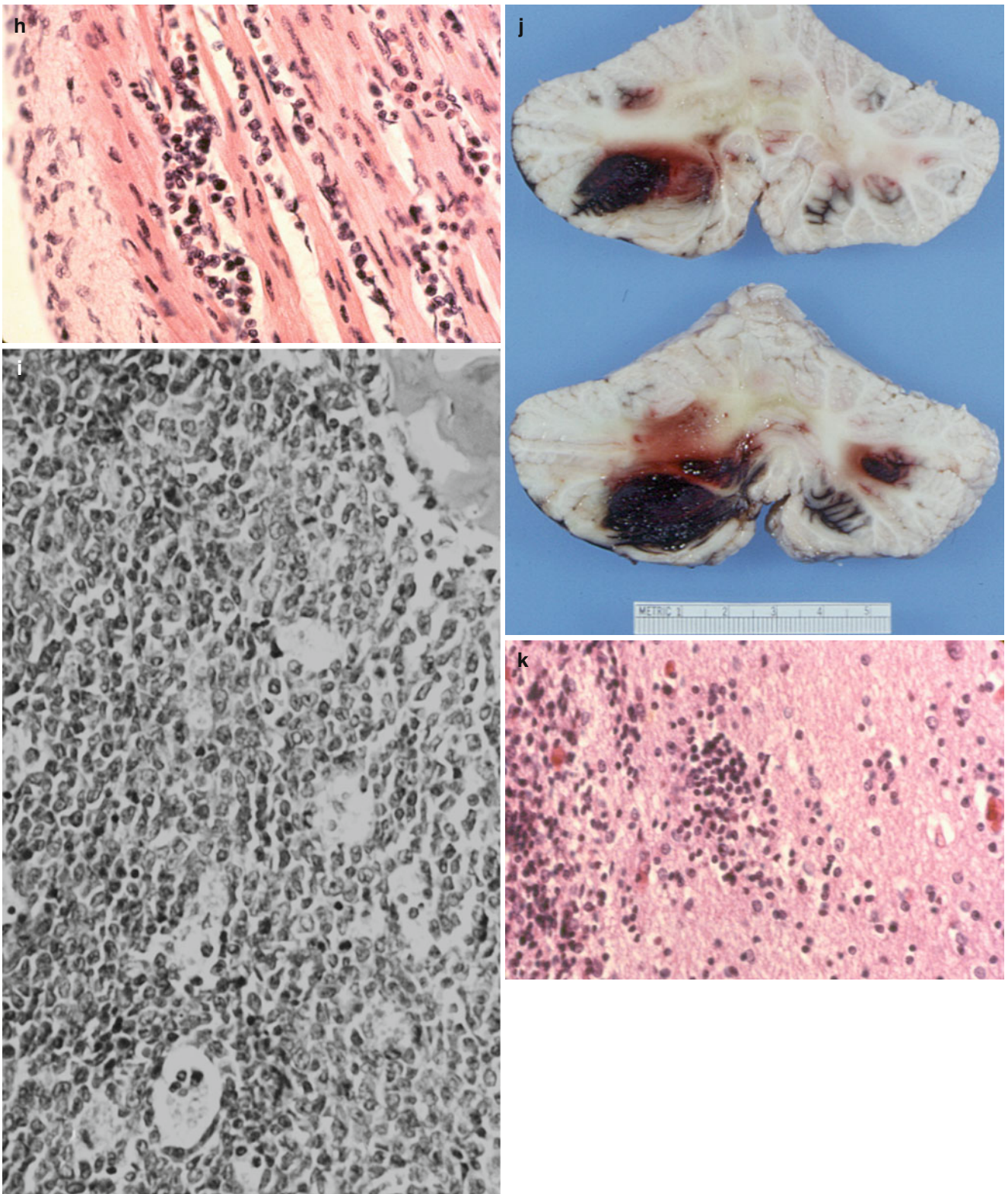


Fig. 7.10 (continued)

Grossly the *brain* displays varying degrees of meningeal involvement, sometimes minimal, manifested by a swollen, white, milky appearance of the leptomeninges. Perivascular hemorrhage and gross evidence of leukemic infiltration involving Virchow-Robin spaces and adjacent parenchyma are noted. *Intracerebral hemorrhage*, sometimes massive, is a common cause of death [1].

Microscopic examination reveals varying degrees of infiltration of the involved organs and tissues by immature lymphoid or myeloid elements, depending on the type of leukemia. Lymph nodes, spleen, and bone marrow in particular show diffuse infiltration by leukemic cells accompanied by variable numbers of young erythroid elements such as normoblasts and erythroblasts. Extramedullary organs including the lungs, kidneys, skin, and gastrointestinal tract are similarly involved. Lymphoid tissue atrophy is present in those patients who had received chemotherapy [12].

One must be cautious in making a histological diagnosis of leukemia in the fetus and newborn based only on the finding of hematopoietic infiltrates in the liver, spleen, and lymph nodes because these organs are normally the sites of extramedullary hematopoiesis occurring during the development of the fetus and neonate [1] (Fig. 7.1). Moreover, infiltration by immature hematopoietic cells occurs also in leukemoid reactions and in hemolytic disease of the newborn. *Demonstration of blast cells in tissues not ordinarily the site of fetal extramedullary hematopoiesis* is requisite for the diagnosis [1, 5].

Stillborns and newborns with *Down syndrome* and leukemia or those with a transient myeloproliferative disorder show foci of *visceral fibrosis*, which may be extensive, in the liver and pancreas and occasionally in the bone marrow [22, 62, 63]. Diffuse intralobular fibrosis surrounding proliferating bile ducts and residual hepatocytes constricting or obliterating central veins characterizes the histological findings in the liver [62]. The *pancreas* shows inter- and intralobular fibrosis with disorganization of the glands and ducts [62]. Hepatic fibrosis may be severe enough to cause *liver failure* in infants with AMKL and/or erythroleukemia [22, 59, 61]. Megakaryoblasts stimulate fibroblastic proliferation and fibrosis in patients with AMKL and megakaryocytosis [61, 62]. Moreover, in the differential diagnosis, extensive visceral fibrosis occurs also in infants with congenital syphilis.

Multiple petechiae, ecchymoses focal ulcerations, and nodular leukemic infiltrates are the main *cutaneous manifestations* of congenital leukemia [29, 33, 35, 64] (Figs. 7.2 and 7.7). *Leukemia cutis* is noted in over a third of newborns [5, 29, 35]. Skin involvement is particularly common with acute monocytic leukemia, which is the major type of ANML in the newborn [5, 35]. Firm red-brown to gray-blue nodular infiltrates may involve over half the body and range in size from a few millimeters to several centimeters in diameter giving the baby a “*blue berry muffin*” appearance [35] (Table 5.2 and Fig. 7.7). Histological findings consist of

infiltrates of myeloid or lymphoid cells, depending on the type of leukemia, within the epidermis, dermis, and subcutaneous tissue (Figs. 7.7b and 7.8a). In both Langerhans cell histiocytosis and leukemia cutis, the infiltrates involve the epidermis, the dermis, and subcutis [1, 33]. Other skin manifestations include *multiple petechiae and ecchymoses related to thrombocytopenia*.

Neuropathological findings consist of collections of leukemic cells in the leptomeninges, and depending on the amount of leukocytosis, distension of meninges, gray and white matter capillaries by blast cells. Perivascular parenchymal involvement is variable but extensive in patients with high peripheral leukocyte counts [12]. *Intracerebral and/or intraventricular hemorrhage* are an important cause of death.

Eye involvement is found in less than 10 % of infants and children diagnosed with acute leukemia. The disease has been diagnosed in the newborn by anterior chamber tap followed by centrifuge cytospin preparation, Wright-Giemsa staining, and identification of blast cells [65]. The major eye manifestations of leukemia are retinal hemorrhage and infiltration of the optic nerve, retina, uveal tract (iris, ciliary body, and choroid), and orbit [65–68]. Leukemia can involve almost any ocular structure by direct infiltration, hemorrhage, or infarction. The choroid is the most common site of leukemic infiltration. Usually the leukemic cells are more numerous in well-vascularized locations within the eye [67]. There is an important relationship between ocular involvement and the state of systemic disease in children with leukemia [68]. Nodular retinal infiltrates are noted with elevated leukocyte counts having a high proportion of blast cells. Choroidal involvement in acute leukemia is associated with widespread systemic disease. Optic nerve infiltration by leukemic cells is almost always correlated with meningeal leukemia [68].

7.9 Prognosis

The biological and clinical characteristics of leukemia in young infants differ significantly from those with leukemia in older children, and the *prognosis* generally is dismal. Newborns with AML fare much better than those with ALL once complete remission is achieved. Females with pre-B ALL have a much worse prognosis than older children with this disease. Although remissions occur, transient leukemia in the Down syndrome newborn is associated with significant morbidity. Close follow-up is recommended for the first few years of life because of the potential of developing acute leukemia, particularly AMKL (M7) [5].

References

1. Isaacs H Jr (2002) Leukemia. In: Isaacs H Jr (ed) Tumors of the fetus and infant: an atlas. Springer, New York, pp 161–180

2. Sande JE, Arceci RJ, Lampkin BC (1999) Congenital and neonatal leukemia. *Semin Perinatol* 23:274–285
3. Perkins JL (2007) Hematopoietic system. In: Gilbert-Barness E (ed) *Potter's pathology of the fetus, infant and child*, vol 2, 2nd edn. Mosby Elsevier, Philadelphia, pp 1453–1536
4. Bresters D, Reus AC, Veerman AJ et al (2002) Congenital leukaemia: the Dutch experience and review of the literature. *Br J Haematol* 117:513–524
5. Isaacs H Jr (2003) Fetal and neonatal leukemia. *J Pediatr Hematol Oncol* 25:348–361
6. Bader JL, Miller RW (1979) U.S. cancer incidence and mortality in the first year of life. *Am J Dis Child* 133:157–159
7. Dinulos JG, Hawkins DS, Clark BS et al (1997) Spontaneous remission of congenital leukemia. *J Pediatr* 131:300–303
8. Lampkin BC, Peipon JJ, Price JK et al (1985) Spontaneous remission of presumed congenital acute nonlymphoblastic leukemia (ANLL) in a karyotypically normal neonate. *Am J Pediatr Hematol Oncol* 7:346–351
9. Grundy RG, Martinez A, Kempinski H et al (2000) Spontaneous remission of congenital leukemia: a case for conservative treatment. *J Pediatr Hematol Oncol* 22:252–255
10. Carroll A, Civin C, Schneider N et al (1991) The t(1;22) (p13;q13) is nonrandom and restricted to infants with acute megakaryoblastic leukemia: a Pediatric Oncology Group study. *Blood* 78:748–752
11. Kaneko Y, Shikano T, Maseki N et al (1988) Clinical characteristics of infant acute leukemia with or without 11q23 translocations. *Leukemia* 2:672–676
12. Isaacs H Jr (1997) Leukemia. In: Isaacs H Jr (ed) *Tumors of the fetus and newborn*, vol 35, Major problems in pathology. W.B. Saunders, Philadelphia, pp 150–168
13. Clark RH, Taylor LL, Wells RJ (1984) Congenital juvenile chronic myelogenous leukemia: case report and review. *Pediatrics* 73:324–326
14. Hazani A, Barak Y, Berant M et al (1993) Congenital juvenile myelogenous leukemia: therapeutic trial with interferon alpha-2. *Med Pediatr Oncol* 21:73–76
15. Oyer CE, Singer DB (1998) The hematopoietic system. In: Wigglesworth JS, Singer DB (eds) *Textbook of fetal and perinatal pathology*, 2nd edn. Blackwell Science, Boston, p 1143
16. Gaedcke G, Kleihauer E, Terinde R (1990) Acute non-lymphocytic syndrome. *Lancet* 335:857
17. Foucar K, Friedman K, Llewellyn A (1992) Prenatal diagnosis of transient myeloproliferative disorder via percutaneous umbilical blood sampling. Report of two cases in fetuses affected by Down's syndrome. *Am J Clin Pathol* 97:584–590
18. Donnemfeld AE, Scott SC, Henselder-Kimmel M et al (1994) Prenatally diagnosed non-immune hydrops caused by congenital transient leukaemia. *Prenat Diagn* 14:721–724
19. Baschat AA, Wagner T, Malisius R et al (1998) Prenatal diagnosis of a transient myeloproliferative disorder in trisomy 21. *Prenat Diagn* 18:731–736
20. Nicolaidis KH, Rodeck CH, Lange I et al (1985) Fetoscopy in the assessment of unexplained fetal hydrops. *Br J Obstet Gynaecol* 92:671–679
21. Isaacs H Jr (2008) Fetal hydrops associated with tumors. *Am J Perinatol* 25:43–68
22. Zipursky A, Brown E, Christensen H et al (1997) Leukemia and/or myeloproliferative syndrome in neonates with Down syndrome. *Semin Perinatol* 21:97–101
23. Zerres K, Schwanitz G, Niesen M et al (1990) Prenatal diagnosis of acute nonlymphoblastic leukemia in Down syndrome. *Lancet* 335:117
24. Gray ES, Balch NJ, Kohler H et al (1986) Congenital leukemia: an unusual cause of stillbirth. *Arch Dis Child* 61:1001–1006
25. Greenbaum BH, Steinfeld J, Obermeyer-Imaizumi S et al (1996) Congenital monoblastic leukemia as a cause of third-trimester fetal loss: the role of monoclonal antibody testing. *J Perinatol* 16:202–204
26. Hunger SP, McGavran L, Meltesen L et al (1998) Oncogenesis in utero: fetal death due to acute myelogenous leukaemia with an MLL translocation. *Br J Haematol* 103:539–542
27. Las Heras J, Leal G, Haust MD (1986) Congenital leukemia: report of a case with ultrastructural study. *Cancer* 58:2278–2281
28. Scully RE, Galdabini JJ, McNeely BU (1976) Case records of the Massachusetts General Hospital. Weekly clinicopathologic exercises. Case 37–1976. *N Engl J Med* 295:608–614
29. Francis JS, Sybert VP, Benjamin DR (1989) Congenital monocytic leukemia: report of a case with cutaneous involvement, and review of the literature. *Pediatr Dermatol* 6:306–311
30. Gottesfeld E, Silverman RA, Coccia PF et al (1989) Transient blueberry muffin appearance of a newborn with congenital monoblastic leukemia. *J Am Acad Dermatol* 21:347–351
31. Resnik KS, Brod BB (1993) Leukemia cutis in congenital leukemia. *Arch Dermatol* 129:1301–1306
32. Garewal G, Marwaha RK, Ray R et al (1993) Congenital acute lymphoblastic leukemia: report of a case with unusual immunophenotype. *Am J Hematol* 44:147
33. Attal H, Kowal-Vern A, Husain AN et al (1996) Newborn infant with multiple purple skin nodules. *Arch Dermatol* 132:341–346
34. Hanada T, Ono I, Minosaki Y et al (1991) Translocation t(8;16) (p11;p13) in neonatal acute monocytic leukemia. *Eur J Pediatr* 150:323–324
35. Isaacs H Jr (2011) Cutaneous metastases in neonates: a review. *Pediatr Dermatol* 28:85–93
36. Gilbert-Barness E, Craig GM (1975) *Blood Potter's pathology of the fetus and infant*, 3rd edn. Mosby-Year Book, St Louis: pp 671–673
37. Abe R, Ryan D, Cecalupo A et al (1983) Cytogenetic findings in congenital leukemia: case report and review of the literature. *Cancer Genet Cytogenet* 9:139–144
38. Sait SN, Brecher ML, Green DM et al (1988) Translocation t(1;22) in congenital acute megakaryocytic leukemia. *Cancer Genet Cytogenet* 34:277–280
39. Lion T, Haas OA, Harbott J et al (1992) The translocation t(1;22) (p13;q13) is a nonrandom marker specifically associated with acute megakaryocytic leukemia in young children. *Blood* 79:3325–3330
40. Mahmoud HH, Ridge SA, Behm FG et al (1995) Intrauterine monoclonal origin of neonatal concordant acute lymphoblastic leukemia in monozygotic twins. *Med Pediatr Oncol* 24:77–81
41. Dehner LP (1981) Neoplasms of the fetus and neonate. In: Naeye RL, Kissane JM, Kaufman N (eds) *Perinatal diseases*. International Academy of Pathology, Monograph #22. Williams & Wilkins, Baltimore, p 286
42. Gale GB, Toledano SR (1984) Congenital acute lymphocytic leukemia in a newborn with Klinefelter syndrome. *Am J Pediatr Hematol Oncol* 6:338–339
43. Heim S, Mittelman F (1987) Acute nonlymphocytic leukemia. In: Heim S, Mittelman F (Eds) *Cancer cytogenetics*. AR Liss, New York: pp 11–20
44. Sharief N, Kingston JE, Wright VM et al (1991) Acute leukemia in an infant with Marfan's syndrome: a case report. *Pediatr Hematol Oncol* 8:323–327
45. Bader JL, Miller RM (1978) Neurofibromatosis and childhood leukemia. *J Pediatr* 92:925–929
46. Heerema NA, Arthur DC, Sather H (1994) Cytogenetic features of infants less than 12 months of age at diagnosis of acute lymphoblastic leukemia: impact of the 11q23 breakpoint on outcome: a report of the Childrens Cancer Group. *Blood* 83:2274–2284
47. Pui C-H, Raimondi SC, Murphy SB et al (1987) An analysis of leukemic cell chromosomal features in infants. *Blood* 69:1289–1293
48. Pui C-H, Kane JR, Crist WM (1995) Biology and treatment of infant leukemias. *Leukemia* 9:762–769

49. Pierce MI (1959) Leukemia in the newborn infant. *J Pediatr* 54:691–706
50. Voelkerding KV, Sandhaus LM, Belov L et al (1988) Clonal B-cell proliferation in an infant with congenital HIV infection and immune thrombocytopenia. *Am J Clin Pathol* 90:470–474
51. Altman AJ (1985) Cytologic diagnosis of the acute nonlymphoid leukemias. I. Morphologic, cytochemical, and ultrastructural features. *Am J Pediatr Hematol Oncol* 7:21–44
52. Altman AJ (1985) Cytologic diagnosis of the acute nonlymphoid leukemias. II. Flow cytometry, surface markers, cytogenetics, and use of cell culture techniques. *Am J Pediatr Hematol Oncol* 7:156–164
53. Bennett JM, Catovsky D, Daniel M-T (1976) Proposals for the classification of acute leukemias. French-American-British (FAB) co-operative group. *Br J Haematol* 33:451–458
54. Dinndorf PA, Reaman G (1986) Acute lymphoblastic leukemia in infants: evidence for B cell origin of disease by use of monoclonal antibody phenotyping. *Blood* 68:975–978
55. Ludwig W-D, Bartram CR, Harbott J (1989) Phenotypic and genotypic heterogeneity in infant acute leukemia. I. Acute lymphoblastic leukemia. *Leukemia* 3:431–439
56. Crist W, Pullen J, Boyett J (1986) Clinical and biologic features predict a poor prognosis in acute lymphoid leukemia in infants. Pediatric Oncology Group Study. *Blood* 67:135–140
57. Windebank KP, Tefferi A, Smithson WA et al (1989) Acute megakaryocytic leukemia (M7) in children. *Mayo Clin Proc* 64:1339–1351
58. Greaves MF, Sieff C, Edwards PAW (1983) Monoclonal antiglycophorin as a probe for erythroleukemia. *Blood* 61:645–651
59. Allan RR, Wadsworth LD, Kalousek DK et al (1989) Congenital erythroleukemia: a case report with morphological, immunophenotypic, and cytogenetic findings. *Am J Hematol* 31:114–121
60. Ng K-C, Tan A-M, Chong Y-Y et al (1999) Congenital acute megakaryoblastic leukemia (M7) with chromosomal t(1;22)(p13;q13) translocation in a set of identical twins. *J Pediatr Hematol Oncol* 21:428
61. Gilson TP, Bendon RW (1993) Megakaryocytosis of the liver in a trisomy 21 stillbirth. *Arch Pathol Lab Med* 117:738–739
62. Becroft DMO, Zwi LJ (1990) Perinatal visceral fibrosis accompanying the megakaryoblastic leukemoid reaction of Down syndrome. *Pediatr Pathol* 10:397–406
63. Yagihashi N, Watanabe K, Yagihashi S (1995) Transient abnormal myelopoiesis accompanied by hepatic fibrosis in two infants with Down syndrome. *J Clin Pathol* 48:973–975
64. Ruchelli ED, Uri A, Dimmick JE et al (1991) Severe perinatal liver disease and Down syndrome: an apparent relationship. *Hum Pathol* 22:1274–1280
65. Tabbara K, Beckstead JH (1980) Acute promonocytic leukemia with ocular involvement. *Arch Ophthalmol* 98:1055–1058
66. Ridgway EW, Jaffe N, Walton DS (1976) Leukemic ophthalmopathy in children. *Cancer* 38:1744–1749
67. Rodgers R, Weiner M, Friedman AH (1986) Ocular involvement in congenital leukemia. *Am J Ophthalmol* 101:730–732
68. Robb RM, Ervin L, Sallan SE (1979) An autopsy study of eye involvement in acute leukemia of childhood. *Med Pediatr Oncol* 6:171–177

8.1 Introduction

The histiocytoses are a diverse group of diseases characterized by the infiltration and accumulation of histiocytes primarily within the blood and tissues [1–12]. *The term histiocytosis denotes an increase in the number of histiocytes, which consist of two main types of cells: macrophages and dendritic cells* [1–3, 6, 8–11]. The histiocytoses range from cytologically benign proliferations of mature cells to clearly malignant ones (Table 8.1).

Abnormal or altered regulation of histiocyte activation plays an important role in the pathogenesis, and many of the signs, symptoms, and pathologic findings are attributed to the increased functional activity of these cells and their cytokine products. Lymphocytes are an integral part of the proliferative process. The differential diagnosis of the disseminated histiocytoses is sometimes difficult because they present with overlapping clinical and pathological findings [2, 5, 6, 11]. Nevertheless, the histiocytoses must be clearly differentiated from one another because they require different forms of treatment approaches and have different outcomes [3, 6, 11].

Not all diseases in which histiocytic infiltrates occur are classified as histiocytoses. The infiltrates may represent a secondary process or a reaction to a condition with a known etiology. Mycobacterial infections, histoplasmosis, graft-versus-host disease, chronic granulomatous disease of childhood, the X-linked lymphoproliferative syndrome, and the lysosomal storage diseases are but a few examples [3, 6, 9, 13] (Fig. 8.1).

Table 8.1 Classification of fetal and infant histiocyte disorders

Dendritic cell-related disorders
Langerhans cell histiocytosis (LCH)
Cutaneous LCH (Hashimoto-Pritzker syndrome)
Disseminated LCH
Juvenile xanthogranuloma
Cutaneous
Extracutaneous
Macrophage-related disorders
Hemophagocytic lymphohistiocytoses (HLH) ^a
Familial HLH (FLH, primary HLH)
Infection-associated HLH (IAH, secondary HLH, reactive HLH)
Sinus histiocytosis with massive lymphadenopathy (Rosai-Dorfman disease)
Malignant-related disorders
Acute monocytic leukemia
Malignant lymphoma, dendritic sarcoma ^b

Reprinted from Favara et al. [2]. With kind permission of © Wiley, 1997; Reprinted from Dehner [5]; Isaacs [9]. © Springer-Verlag, 2002; Huang and Arceci [6]. With kind permission of © Elsevier, 1999; Isaacs [11]. With kind permission of © Wiley, 2006

^aThe term hemophagocytic syndrome includes both familial HLH and infection-associated HLH

^bMalignant lymphoma and dendritic sarcoma usually do not occur during the first year of life



Fig. 8.1 Histiocytosis due to lysosomal storage disease. **(a)** Fifteen-day-old hydroptic female with the lethal infantile form of Gaucher's disease (type 2). The liver and spleen are massively enlarged. **(b)** The liver shows a histiocytosis consisting of large cells with eccentric small,

oval nuclei, and abundant cytoplasm, having a wrinkled appearance consistent with Gaucher's cells (*arrow*). The spleen, lymph nodes, and bone marrow were similarly involved (Reprinted from Sharma et al. [13]. With kind permission of © Thieme, 2000)

8.2 Ontogeny of the Monophagocytic System

The monocyte is the precursor of the macrophage and of related phagocytic cells that comprise the mononuclear phagocyte system. Cells of the monocytic and granulocytic series originate from a common bone marrow progenitor cell. Within the marrow, the monocyte matures through several stages from the monoblast, the promonocyte, and then the monocyte. The normal bone marrow contains from 1 to 3 % monocytes and their precursors [5, 6, 8, 9, 14].

When a monocyte leaves the blood stream and enters the tissues, it becomes a wandering macrophage (also called histiocyte) and subsequently undergoes further differentiation to form a variety of mononuclear phagocytic cells known by various names depending on their tissue location. For example, they become Kupffer cells in the liver, alveolar macrophages in the lung, sinus macrophages in the spleen, and Langerhans cells in the skin. Macrophages that have

accumulated at a site of chronic inflammation, for example, in a tuberculous lymph node, can differentiate further into epithelioid histiocytes (so named because they resemble epithelial cells), or they may fuse to form multinucleated giant cells. Moreover, macrophages can divide in tissues [5, 6, 8, 9, 14].

The properties and function of macrophages vary according to their location. Primarily, they are responsible for ingestion and killing of microorganisms. Macrophages have cytoplasmic granules composed of lysosomes which contain hydrolytic enzymes: the antibacterial enzyme lysozyme and Fc receptors for antigen-antibody complexes. Following exposure to antigens, for example, of an invading microorganism, T lymphocytes liberate lymphokines (soluble factors), such as interferon, that activate or assist the macrophage in disposal of the invader. Macrophages process antigen for presentation to lymphocytes in immune responses, thus initiating antibody formation. Moreover, activated macrophages secrete cytokines having important biological functions, for example, interleukin 1, which plays a role in cell activation

and in the body's febrile reaction, and the tumor necrosis factor (TNF), which participates in host defense against tumor growth. Macrophages clear from the blood effete erythrocytes, noxious substances, and cellular debris as they pass through organs of the monophagocytic system, for example, in the liver and spleen [5, 6, 9, 14].

8.3 Classification of Histiocytoses

Based on function, *cells of the mononuclear phagocytic system are divided into two main groups, phagocytic cells (antigen-processing cells) and dendritic cells (antigen-presenting cells)* [1, 2, 5, 8, 9, 14] (Tables 8.1 and 8.2). The current *classification of the histiocytic disorders includes three main categories: dendritic cell related, macrophage related, and malignant disorders* [2, 5, 8, 9]. Using this scheme, *the types of histiocytoses encountered in the fetus and infant would be (1) the dendritic cell disorders including Langerhans cell histiocytosis (LCH) and juvenile xanthogranuloma (JXG); (2) the macrophage disorders, the hemophagocytic lymphohistiocytoses (familial- and infection-associated lymphohistiocytosis) (HLH); and Rosai-Dorfman disease. Acute monocytic leukemia (AMoL) falls into the second main category, malignant disorders* [2, 5, 8, 9].

Histiocytoses occurring most often in the fetus and infant are LCH, HLH JXG, and AMoL in the malignant disorder category [5, 8–12]. X-linked lymphoproliferative disease,

sinus histiocytosis with massive lymphadenopathy (Rosai-Dorfman disease), and malignant histiocytoses of dendritic and macrophage types are unusual in infancy [3, 6, 9, 11, 15].

8.4 Dendritic Cell Disorders

8.4.1 Langerhans Cell Histiocytosis

The Langerhans cell is a member of the monophagocytic system originating from the bone marrow and migrating primarily to the skin and to other organs. It is one of the three types of dendritic cells occurring in the epidermis in addition to the melanocyte and the indeterminate dendritic cell [9]. The Langerhans cell is found also in extracutaneous sites such as lymph nodes, thymus, oral mucosa, and vagina. Normally it functions in the processing of antigens, for example, those of viruses, bacteria, and tumor cells, coming into contact with the skin, and in the presentation of antigens to T lymphocytes [8, 9].

Langerhans cell histiocytosis (LCH) is the term applied to the older generic one, histiocytosis X, which included the clinical triad of Letterer-Siwe disease, Hand-Schuller-Christian syndrome, and eosinophilic granuloma [1, 2, 4–6, 8, 11, 17]. Histologically, all three conditions are characterized by *granuloma-like lesions composed of Langerhans histiocytes* [3, 5, 8, 9]. *LCH is divided into two main groups: disseminated LCH and LCH limited to the skin (cutaneous LCH)* [12]. Involvement of two or more organ systems is the criterion required for the diagnosis of disseminated LCH [11, 16, 17].

8.4.1.1 Clinical Findings

Skin lesions consisting of a seborrheic, eczematoid, and occasionally a hemorrhagic rash distributed over the scalp, face, abdomen, and diaper areas are the first manifestation from birth in both disseminated and cutaneous LCH [9, 11, 12, 16–19] (Fig. 8.2a). The time interval before systemic symptoms appear varies from days to months [12]. Subsequently, hepatosplenomegaly, lymphadenopathy, and generally “failure to thrive” become evident. Hematologic studies reveal an anemia, a variable leukocytosis, abnormal clotting factors, and thrombocytopenia, all of which portend disseminated disease and a poor prognosis [9, 17]. Although the bone marrow is variably positive for LCH cells, the diagnosis is definitely established by skin or lymph node biopsy [9, 11].

Imaging studies reveal pulmonary infiltrates becoming more progressive as the disease evolves (Fig. 8.2b). LCH histiocytes, CD1a (thymocyte antigen), and S-100 positive are identified in bronchoalveolar lavage fluid [1, 3, 9]. Skeletal surveys show “punched out,” lytic lesions in the skull and long bones [20] (Fig. 18.1).

Table 8.2 Identifying features of histiocytes

Macrophage	Lysosome, CD45, CD14, and CD68 positive S-100, CD1a, and factor XIIIa negative Birbeck granules absent
Indeterminate cell	CD45, S-100, and CD1a positive Factor XIIIa negative Birbeck granules absent
Langerhans cell	CD45, S-100, and CD1a positive CD14 and factor XIIIa negative Birbeck granules present
Interdigitating dendritic cell	CD45 and S-100 positive CD14, CD1a, and factor XIIIa negative Birbeck granules absent
Dermal dendrocyte	Factor XIIIa, CD45, and CD68 positive S-100 and CD1a negative Birbeck granules absent
Follicular dendritic cell	KiM4, CD21, CD35 positive S-100 variable CD45 negative Birbeck granules absent

Reprinted from Favara et al. [2]. With kind permission of © Wiley, 1997

Symptomatic involvement of the gastrointestinal tract occurs in disseminated LCH and is manifested by vomiting, diarrhea, bloody stools, and a protein losing enteropathy which may manifest in the first month of life and is associated with widespread multisystem disease [21]. The patient with LCH first appearing in the thymus presents with stridor and respiratory distress and an anterior superior mediastinal mass on chest imaging studies [9].

8.4.1.2 Pathology

The gross appearance varies with the site and the age of the lesion. Specimens curetted from bones are soft, red, hemorrhagic, and necrotic. When visible, *soft grayish yellow to red granuloma-like nodules*, usually multiple, are found in the liver, spleen, and lymph nodes. Older lesions are firmer because of fibrosis and are tan yellow instead of grayish red due to the presence of foamy histiocytes [8, 9].

8.4.1.3 Histology

The Langerhans cell has a characteristic *infolded or coffee bean-shaped nucleus, small nucleolus, and eosinophilic cytoplasm* (Fig. 8.3a–c). Some lesions show nuclear atypia and mitotic figures, but these findings are not correlated with prognosis [9]. Extensive infiltration of histiocytes, accompanied by variable numbers of eosinophils, is the main histological finding. Histiocytic erythrophagocytosis (engulfment of erythrocytes by macrophages) is noted rarely. The LCH histiocyte has distinctly different immunohistochemical and EM properties compared to the normal monocyte and macrophage [1, 8, 9]. *LCH histiocytes are reactive with S-100 and CD1a surface antigens* (Table 8.2). By EM examination, the cytoplasm of the Langerhans histiocyte contains characteristic racket-shaped *Birbeck granules*, which support the diagnosis [1, 8, 9, 22, 23] (Fig. 8.3f). The significance and function of these structures are unknown. Often the granules are difficult to find, and multiple sections may be required to identify them. The granules are observed also in normal Langerhans cells within the epidermis but not in the intermediate dendritic cells or melanocytes.

Skin is the site most often involved at the time of presentation [3, 8, 9, 12]. Histiocytic infiltrates are situated primarily in the dermis directly beneath the epidermal-dermal junction. They invade the epidermis and extend into the stratum corneum (Fig. 5.16). The differential diagnosis of cutaneous nodular infiltrates in the newborn producing the so-called blueberry muffin baby appearance includes leukemia cutis, extramedullary hematopoiesis, urticaria pigmentosa (mast cell disease), and metastatic malignancies such as rhabdomyosarcoma, rhabdoid tumor, and neuroblastoma [8–10, 12] (Tables 7.1 and 5.2).

Infiltration of the pulmonary interlobular septae and alveolar spaces produces airway obstruction and eventually

the formation of cystically dilated, emphysematous areas. *LCH histiocytic infiltration of the lungs is an important cause of death particularly in young infants* [8, 9, 11, 12] (Fig. 8.2c). The infiltrates replace and obscure the normal lymph node architecture (Fig. 8.3). Bone marrow is similarly involved. The splenic red pulp is heavily infiltrated, while the white pulp and trabeculae generally are spared. Granuloma-like infiltrates are found also in the pancreas, gonads, liver, and salivary glands and less often in the pituitary, brain, and meninges [8, 9, 11, 12]. The liver shows variable degrees of periportal and sinusoidal histiocytic infiltration and fibrosis progressing to biliary cirrhosis [8, 9]. Skeletal surveys reveal lytic lesions involving the skull, ribs, pelvis, and occasionally the long bones and vertebra [9, 20]. The curettings show granuloma-like collections of LCH histiocytes and multinucleated giant cells, extensive necrosis with destruction of bone, eosinophilic “abscesses,” and variable numbers of lymphocytes and plasma cells. Subsequently, “end stage” or healing lesions consist primarily of histiocyte foam cells, which do not react with CD1a or S-100, and fibrosis. Fibrous lesions may resemble xanthofibroma or benign fibrous histiocytoma [8, 9].

Solitary osseous lesions rarely herald the onset of soft tissue and visceral involvement and a fatal outcome. Moreover, older infants with several bone lesions do survive [9, 20]. *Hand-Schuller-Christian syndrome* is the clinical manifestation of multifocal LCH involving primarily the cranial bones, the middle ear, and pituitary. The syndrome is very uncommon for only a few patients, usually older infants and children, actually fulfill the diagnostic criteria consisting of exophthalmos, diabetes insipidus, and histiocytic infiltrates in membrane bone [6].

Exophthalmos, or protrusion of the eye, results from a space-occupying histiocytic lesion in the orbit. Otitis media occurs with drainage following destructive infiltrates in the mastoid and petrous portion of the temporal bone. The lesions tend to be not as aggressive with less cellularity and monotony of cell type than in disseminated LCH but tend to exhibit more fibrosis [8, 9]. The clinical course is usually protracted, and the mortality rate is much lower, approximately half of the 50 % observed for disseminated disease. The least aggressive of the three forms, *eosinophilic granuloma*, typically occurs in older children and adolescents presenting as a single lytic bone lesion associated with a good prognosis.

A pure cutaneous form of LCH, known also as self-healing histiocytosis or the Hashimoto-Pritzker syndrome, is often congenital and correlated with a favorable outcome [11, 12, 22, 23]. The typical presentation of self-healing LCH is skin lesions in an otherwise well infant with no or mild systemic symptoms [11]. Skin lesions, which may be multiple and extensive, undergo rapid spontaneous regression.

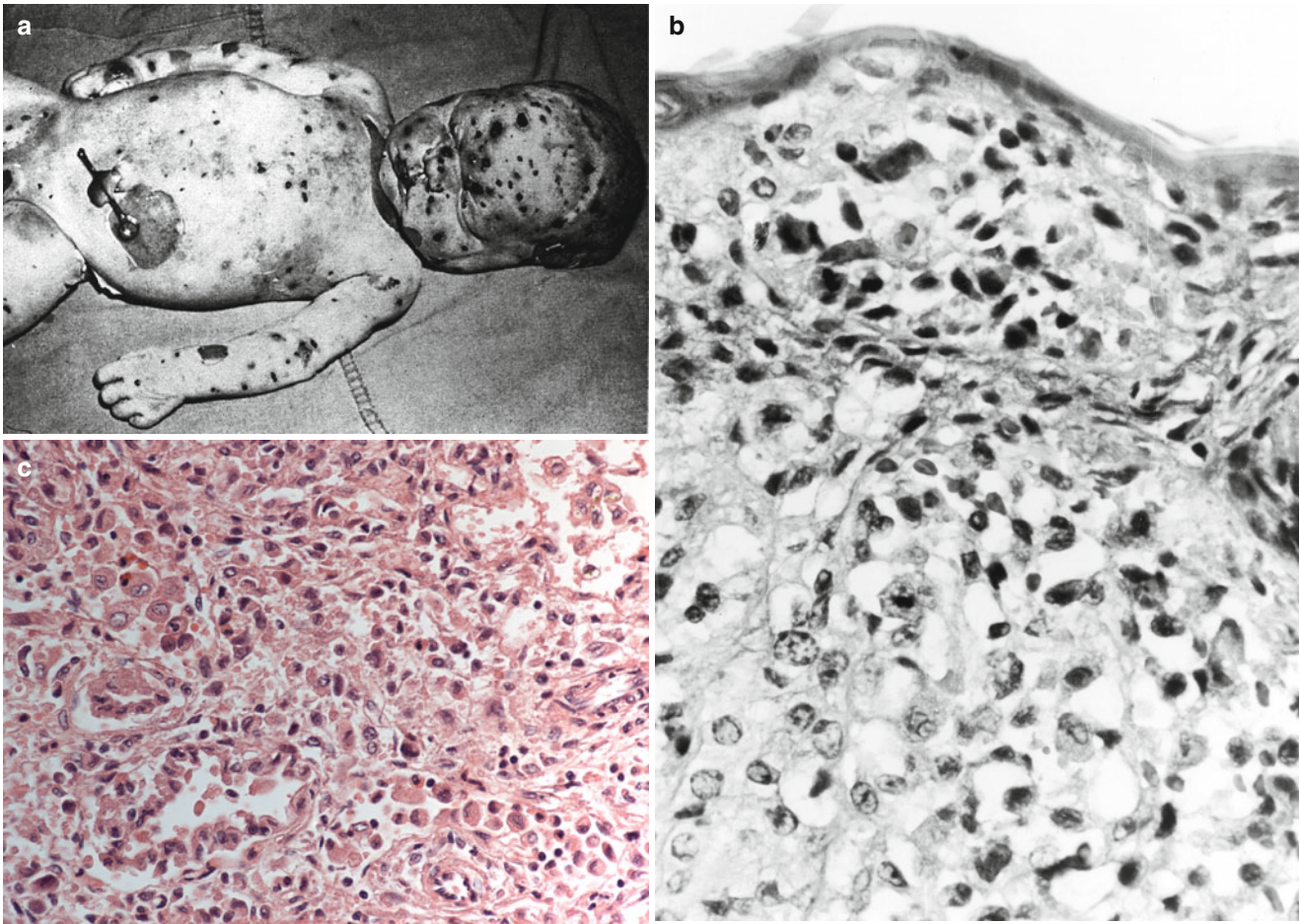


Fig. 8.2 Congenital disseminated Langerhans cell histiocytosis (Letterer-Siwe disease). **(a)** Term stillborn with widely distributed hemorrhagic, crusted, and scaling nodules accompanied by a focal, purpuric macular rash. Diagnosis was established by skin and lymph node biopsies. **(b)** Disseminated Langerhans cell histiocytosis (Letterer-Siwe disease) in similar 5-day-old female with a maculopapular rash and severe respiratory distress. There was a maternal history of polyhydramnios. The skin shows erosion of the stratum corneum and invasion of the

edematous epidermis and dermis by Langerhans cell histiocytes. **(c)** The pulmonary interstitium, alveolar ducts, and alveoli are diffusely infiltrated by Langerhans cell histiocytes with characteristic infolded, coffee bean-like nuclei. Pulmonary involvement is an important cause of death in newborns and infants with this disease (**(a)** Reprinted from Ahnquist and Holyoke [19]. With kind permission of © Elsevier, 1960; **(b, c)** Reprinted from Isaacs [9]. © Springer-Verlag, 2002)

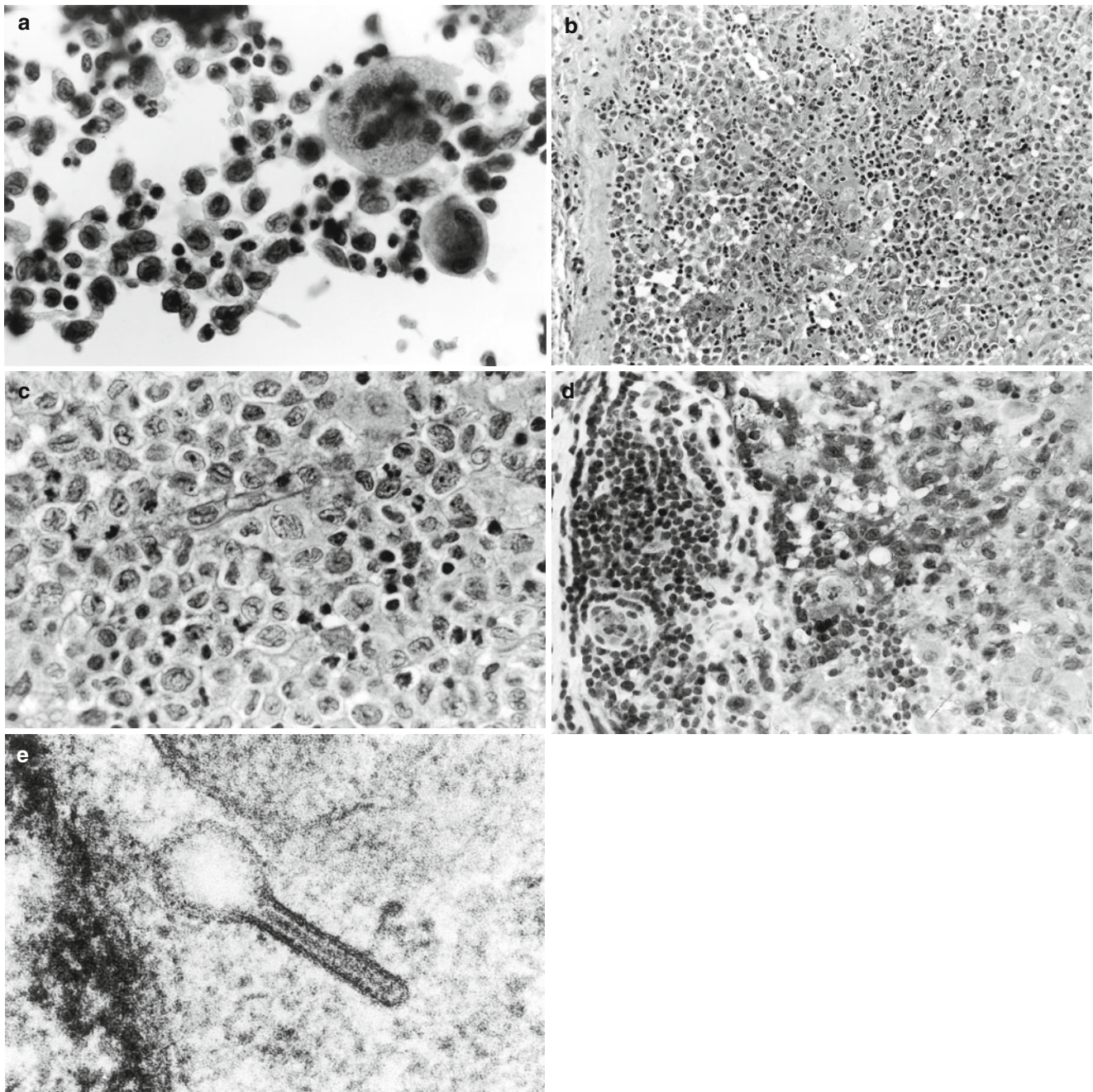


Fig. 8.3 Langerhans cell histiocytosis, lymph node biopsy. (a) Imprint (“touch preparation”) revealing histiocytes composed of scant eosinophilic cytoplasm and characteristic, folded, “coffee bean”-like nuclei containing one or more tiny nucleoli. Multinucleated giant cells consist of similar appearing nuclei. (b) Histiocytes flooding the subcapsular and cortical sinusoids. (c) Higher power view showing the histiocytes in

more detail. (d) The cytoplasm stains uniformly positive with S-100 protein. (e) Tennis racket-shaped Birbeck granule demonstrated by EM ((a–d) Reprinted from Isaacs [9]. © WB Saunders 1997; (e) Electron photomicrograph courtesy of Ann Peters, Department of Pathology, Rady Children’s Hospital of San Diego)

EM and immunohistochemical properties of the histiocytes from patients with congenital self-healing histiocytosis are essentially the same as those of both normal epidermal Langerhans cells and LCH cells [11, 12, 22, 23]. Nevertheless, patients with self-healing histiocytosis should be followed carefully for progression of disease because of the possibility of relapse [12].

8.4.1.4 Prognosis

Clinical outcome cannot be predicted from the histology alone [6, 8, 9, 11]. The *clinical findings, particularly the age of the patient and extent of organ involvement at the time of diagnosis, are the most reliable indicators for predicting prognosis* [9, 11, 16, 17]. Organ dysfunction may be more important

than the number of organs involved [6, 17]. Bone marrow involvement at the time of diagnosis is associated with a poor outcome [6, 9]. Disseminated LCH with multiple sites of involvement and organ dysfunction has an unfavorable prognosis with less than 50 % survival [6, 9]. Those who fall into this category are usually under 1 year of age and comprise less than 15 % of the total. The overall mortality rate of children under 2 years of age at diagnosis is 50–60 %, while that of children over 2 years decreases to 15 % [6, 9, 11, 12].

8.4.2 Juvenile Xanthogranuloma

Juvenile xanthogranuloma (JXG) may occur at birth presenting as one or more yellow nodules ranging in size from 1 cm to several cm particularly when the subcutaneous tissue is involved [6, 8, 9, 11, 12, 24–28]. The head and neck and extremities are common sites. There are two forms of JXG, cutaneous and extracutaneous [12, 24–28]. Significant morbidity and mortality result from extensive extracutaneous systemic involvement [11, 12, 24–28]. Cutaneous lesions are present in less than half of infants with disseminated disease. The most common extracutaneous sites in decreasing order are the subcutaneous soft tissues, liver, spleen, lung, eye, orbit, and oropharynx [11, 12, 25].

The dermal dendrocyte, found normally in the upper dermis, is considered to be the cell of origin of JXG and is phenotypically different from the indeterminate and Langerhans cells [5, 9] (Table 8.2).

8.4.2.1 Pathology

Microscopically, the tumor consists of histiocytes with eosinophilic or foamy cytoplasm, Touton multinucleated giant cells, which are large cells with a peripheral rim multiple nuclei forming a wreath-like arrangement beneath the basement membrane, and variable numbers of lymphocytes and eosinophils. The histiocytes appear reactive lacking S-100 and CD1a reactivity and Birbeck granules, characteristic of Langerhans cells [8, 9, 24, 25, 28]. Sudan black B and oil red O stains are variably positive for lipid. Early lesions in the young infant may not contain Touton multinucleated giant cells which could create a diagnostic problem. Solitary giant xanthogranuloma and benign cephalic histiocytosis are regarded as variants of JXG [29]. See Chaps. 4 and 5 for further discussion of JXG.

8.5 Macrophage-Related Disorders

8.5.1 Hemophagocytic Syndromes

The *hemophagocytic syndromes* are one of the most common macrophage-related disorders of varied biological behavior and are responsible for significant morbidity and

mortality [11, 33, 34, 42]. *Hemophagocytic lymphohistiocytosis (HLH)* is the major member of this group which includes most patients with macrophage-related disorders. *HLH consists of two main types: primary (familial) and secondary (infection or reactive associated)*. The term *hemophagocytic syndrome* is used to include both entities [2, 9]. There is a great deal of similarity between primary and secondary HLH for the clinical, biochemical, and pathological findings are practically the same [9, 30, 31, 40, 42] (Table 8.1).

8.5.1.1 Primary Hemophagocytic Lymphohistiocytosis

Primary hemophagocytic lymphohistiocytosis (familial hemophagocytic lymphohistiocytosis) is a rapidly fatal disease characterized by fever, hepatosplenomegaly, and pancytopenia frequently occurring in siblings [3, 6, 30]. The disease is found primarily in infants and young children. Most patients are less than 6 months of age at the time of diagnosis, and 10–15 % are neonates [30, 36]. The German/Austrian Registry for Histiocytic Disorders reports an incidence of one per million children under 15 years of age per year [30].

Familial hemophagocytic lymphohistiocytosis (familial HLH) is a disorder of unknown etiology of the monophagocytic system [3, 6, 8, 9, 30–35]. It has an autosomal recessive pattern of inheritance, but at least 25 % of the cases are non-familial [3, 6, 30]. The primary defect is believed to be related to mutations of the perforin gene on chromosome 10q [36].

Clinical Findings

The classical presenting signs are fever, hepatosplenomegaly, and pancytopenia [11, 33, 34, 37]. Other manifestations of this rare, usually fatal disease are irritability, anorexia, wasting, and “failure to thrive.” Hepatic dysfunction and bleeding diathesis are present [9, 33, 34, 36]. Usually there is a short period of normal growth and development and absence of symptoms after birth, but fever or hepatomegaly may be evident already [9, 11, 30]. Stupor, or coma, seizures with hemiplegia, and cranial nerve palsies are ominous neurological signs [37–39]. The onset of nervous system involvement heralds progression of the disease which is reflected by an elevated cerebrospinal fluid protein and pleocytosis [37–39]. In addition, laboratory studies reveal hypofibrinogenemia, hyperferremia, and hypertriglyceridemia [3, 6, 9, 30]. Thrombocytopenia is accompanied by severe bleeding, and the granulocytic series show a maturation arrest. *The tetrad of elevated triglycerides, increased liver enzymes, hyperferremia, and low fibrinogen levels suggests the diagnosis* [30].

The diagnosis of familial HLH is sometimes difficult to establish during life; it may be apparent only from postmortem findings and then going back and discovering a family history of a sibling with a similar disease [9, 30].

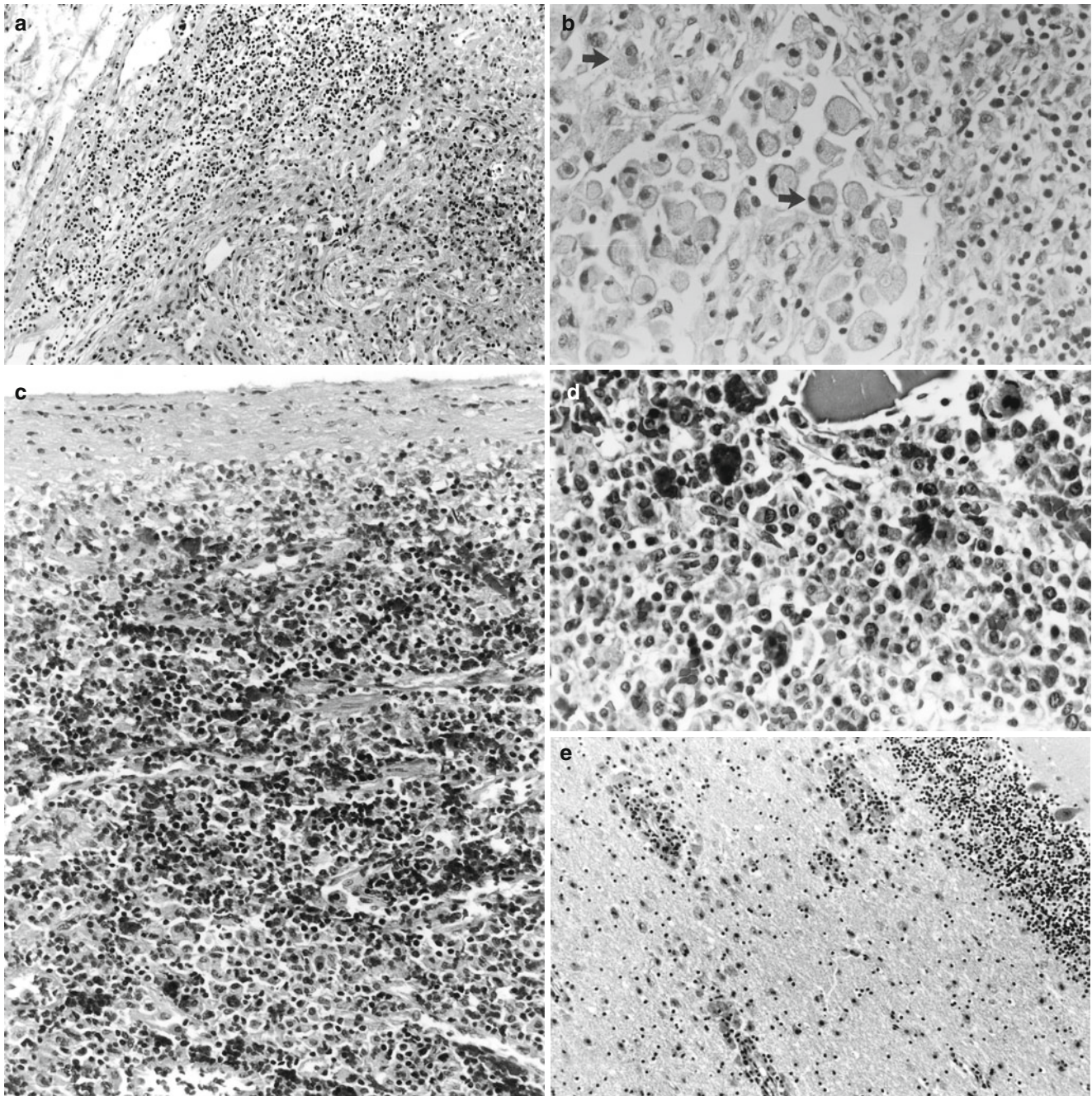


Fig. 8.4 Familial erythrophagocytic lymphohistiocytosis. Lymph node from a 1-year-old male with fever, hepatosplenomegaly, hemolytic anemia, hypofibrinogenemia, and elevated liver enzymes. Female sibling died from a similar condition. (a) The lymph node shows lymphoid depletion and infiltrates of macrophages and lymphocytes. (b) The lymphocytes and macrophages appear reactive without atypical features. Histiocytic hemophagocytosis is present (*arrows*). (c) The spleen is

heavily infiltrated by lymphocytes and histiocytes. Lymphoid follicles are not recognizable. (d) Normal marrow elements are replaced by lymphocytes and histiocytes, the latter displaying hemophagocytosis. (e) The cerebellum exhibits perivascular cuffing by lymphocytes and histiocytes accompanied by focal parenchymal necrosis (Reprinted from Isaacs [8]. © WB Saunders 1997)

Pathology

The histopathological hallmark of this disease is extensive lymphohistiocytic infiltration and erythrophagocytosis within the liver, spleen, lymph nodes, bone marrow, and leptomeninges [9, 11, 31, 32, 36–40] (Fig. 8.4). The spleen and liver are

markedly enlarged, up to 10 times and 2 times normal, respectively. Thymic involution and depletion of lymphoid tissue in lymph nodes and spleen are characteristic findings. Pulmonary infiltration is predominately centrilobular, peribronchial, and perivascular in location [9]. The submucosa of the tracheal

and major bronchi shows extensive involvement. Many different organs are affected [9, 11, 31, 32, 40].

The main neuropathological finding is focal or diffuse leptomeningeal lymphohistiocytic infiltration by erythrophagocytic histiocytes [37–40]. The arachnoid, choroid plexus, and Virchow-Robin perivascular spaces are affected in about a third to half of the cases [34, 37, 38]. Perivascular cuffing with extension of lymphocytes and histiocytes into adjacent cerebral or cerebellar cortex and brain stem occurs (Fig. 8.4e). Diffuse cerebral infiltration by histiocytes and multifocal necrosis are found in the most severely involved brains [37, 38]. The severity of the central nervous system lesions is related to the duration of the illness [38, 39]. The brain is affected much more than the rest of the body in some patients [34].

Postmortem orbital examination reveals infiltration of the anterior uveal tract, inner retina, and optic nerves by lymphocytes and histiocytes with hemophagocytosis [9, 38]. In addition, profound edema of the optic disks and small foci of necrosis and hemorrhage are noted in the optic nerves.

Histiocytes and lymphocytes within the infiltrates appear reactive but show no cellular atypia, abnormal mitotic activity, or other evidence of malignancy. Histiocytic phagocytosis of erythrocytes, and sometimes lymphocytes and platelets, is a characteristic finding. The proliferative histiocytes in familial HLH have immunohistochemical and ultrastructural properties of normal reactive histiocytes, that is, they are reactive for CD14, CD45, CD68, and HLA-DR but lack the S-100 protein, CD1a surface antigen, and Birbeck granules characteristic of LCH histiocytes [9] (Table 8.2). EM studies confirm the reactive nature of the histiocytes and lymphocytes and the absence of Birbeck granules.

An enlarged lymph node, if present, is recommended for diagnostic biopsy. The findings of lymphohistiocytic infiltrates, hemophagocytosis, and lymphoid depletion suggest the histological diagnosis [9, 31, 32, 40]. However, it should be kept in mind that these findings are rather nonspecific and that hemophagocytosis is present also in a variety of other conditions including a variety of infections, hemolytic anemia, and graft-versus-host disease. Lymphohistiocytic infiltrates with lymphoid depletion are found also in infection-associated hemophagocytosis, the X-linked lymphoproliferative syndrome, and the accelerated phase of Chediak-Higashi syndrome [9]. LCH, leukemia, nonspecific inflammation, and extramedullary hematopoiesis should be considered in the histological differential diagnosis. Splenic fine-needle aspiration biopsy can be used for demonstrating histiocytes with hemophagocytosis [9].

Prognosis

Familial HLH is nearly always a rapidly fatal disorder with death occurring in 3–6 months of onset. The cause of death is attributed to sepsis, bleeding, or central nervous system involvement [3, 6, 9, 30, 34, 37, 40].

8.5.1.2 Secondary Hemophagocytic Lymphohistiocytosis (Infection-Associated Hemophagocytic Syndrome)

Infection-associated hemophagocytic syndrome (IAH) was first reported by Risdall et al. in 1979 who described a disease characterized by a generalized histiocytic proliferation and hemophagocytosis associated with a systemic viral infection [41]. Cytomegalovirus, herpes simplex virus, adenovirus, enterovirus, and Epstein-Barr virus are examples of the viral agents implicated [41, 43–45]. The syndrome occurs also with other infections such as bacterial, fungal, and parasitic [46–49]. IAH occurs in immunocompromised and in normal individuals but more commonly in the former [41]. Infection-associated hemophagocytic syndrome is probably the most common histiocytic disorder in the infant which also occurs throughout all age groups including adults [9, 41]. Other terms applied to this lymphohistiocytosis are “reactive” or malignancy-associated hemophagocytic syndrome [2, 6, 42, 50].

Clinical Findings

The clinical manifestations of the infection-associated hemophagocytic syndrome (IAH) are practically identical to those of the familial HLH and include fever, failure to thrive, anemia, hepatosplenomegaly, and variable lymphadenomegaly [2, 9, 33, 34]. Leukopenia, abnormal liver function tests, hyperferremia, and coagulopathy are the main laboratory findings [41]. Bilateral pulmonary infiltrates may be present on chest radiographs.

Familial HLH is the entity causing the most problem in the differential diagnosis [30, 42]. There is considerable overlap between the two diseases making distinction between them often difficult. In contrast to the familial form, there is an underlying immune deficiency (iatrogenic or otherwise), a proven infection, recovery in most instances, and usually no family history in the infection-associated hemophagocytic syndrome. Patients are reported who were thought initially to have familial HLH initially but in whom eventually a viral or some other agent was recovered by tissue or other culture, EM, or by molecular studies [9, 30, 44].

Pathology

The diagnosis of IAH is made by bone marrow examination. Bone marrow smears reveal prominent histiocytic hemophagocytosis [9, 43] (Fig. 8.5d). *The reactive-appearing histiocytes contain phagocytized erythrocytes and platelets.* They show the cytologic, EM, and histochemical features of normal histiocytes in contrast to the Langerhans cell and malignant histiocytic disorders. *Atypical lymphocytes (“virocytes”) and immunoblasts* may be present also. The atypical lymphocytes have large reniform nuclei, prominent nucleoli, and a characteristic blue cytoplasm with white fluffy inclusions giving the cytoplasm a “snow storm”-like

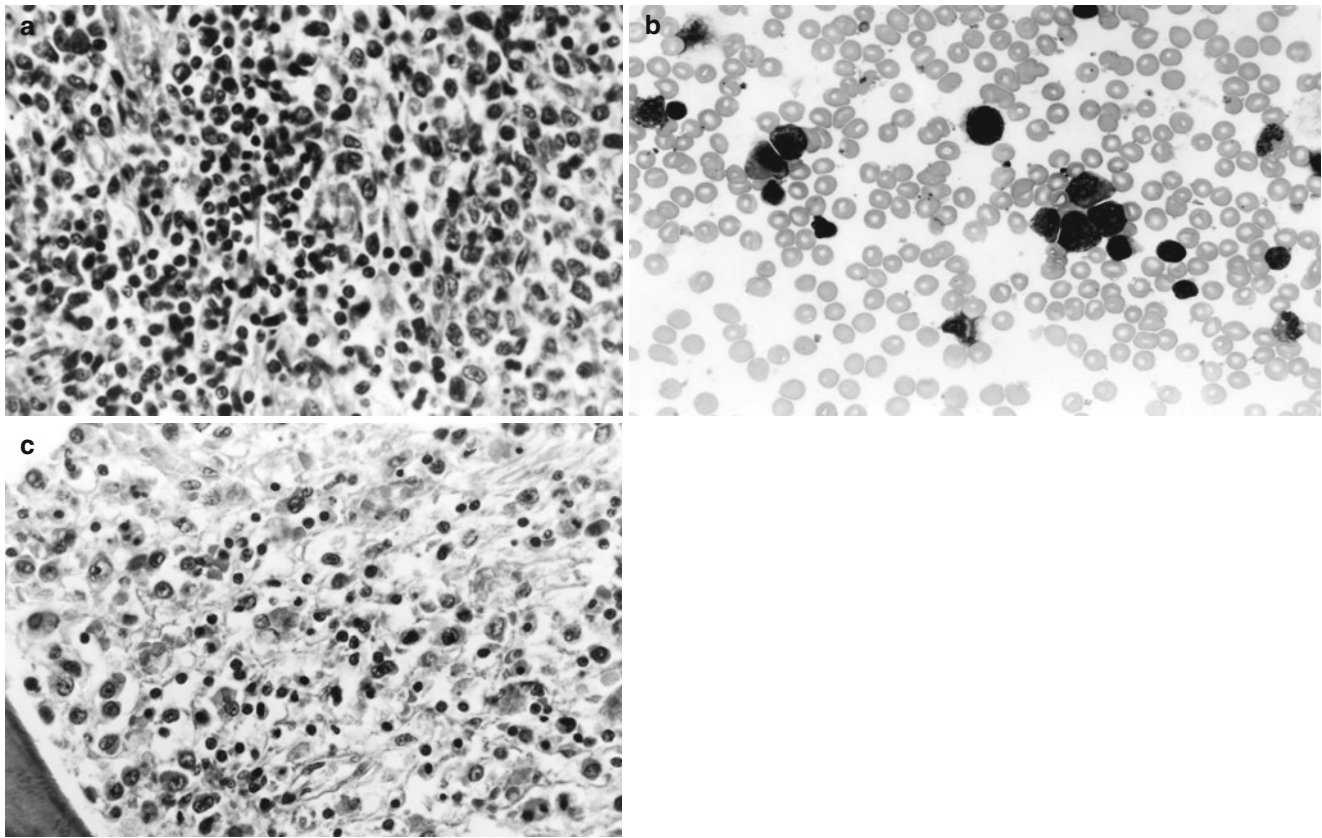


Fig. 8.5 Infection-associated hemophagocytic syndrome. Six-week-old female with fever, lethargy, vomiting, and diarrhea. Other findings were hepatosplenomegaly, anemia, thrombocytopenia, abnormal coagulation studies, and elevated liver enzymes. (a) The infiltrate is composed of reactive lymphocytes and histiocytes. (b) Postmortem bone

marrow aspirate shows only lymphocytes and histiocytes with very few normal marrow elements. (c) Section of rib lacks normal marrow elements. Lymphocytes and histiocytes, the latter with phagocytosed erythrocytes, comprise the cell population (Reprinted from Isaacs [8]. © WB Saunders 1997)

appearance. The peripheral blood smears exhibit varying degrees of cytopenia with or without atypical lymphocytes. Lymph nodes and spleen are depleted of lymphoid elements, have pale “burned-out” germinal centers, and are infiltrated by hemophagocytic histiocytes [9, 50] (Fig. 8.5a). Early in the disease, lymph nodes may show a florid immunoblastic proliferative response similar to that observed initially in human immunodeficiency virus (HIV) infections. Liver biopsy reveals prominent portal infiltrates composed of lymphocytes, erythrophagocytic histiocytes, and sometimes immunoblasts. If a viral or other infectious agent is found, then the diagnosis of IAH is confirmed [50, 51].

Postmortem findings in children with infection-associated hemophagocytic syndrome are described [9, 39, 40]. The histological features are practically identical to those of familial HLH. Reactive benign-appearing histiocytes with erythrophagocytosis are found in the portal tracts and sinusoids of the liver, in the red pulp of the spleen, and within the leptomeninges. Focal hepatocellular necrosis is variably present. Interstitial pneumonia with or without viral inclusions are the pulmonary findings. Viral inclusions may appear in many organs of patients infected by a viral inclu-

sion forming virus. Viral agents, for example, Epstein-Barr virus, cytomegalovirus, human herpes virus 6, and parvovirus 19, have been isolated from patients with this disease [51]. Polymerase chain reaction amplification using archival bone marrow material provides a useful technique to aid in confirming the presence of a viral infection [51]. Other infectious agents, for example, acid fast bacilli, have been identified in patients with this syndrome [46–49].

8.5.2 Sinus Histiocytosis with Massive Lymphadenopathy

The syndrome was established as a clinicopathologic entity by *Rosai and Dorfman in 1972 who described a benign, chronic massive enlargement of cervical lymph nodes accompanied by fever, leukocytosis, and hyperglobulinemia* [15, 52]. One of the largest and most comprehensive reviews is by Fourcar, Rosai, and Dorfman who analyzed 423 cases [53]. Less than 20 examples are reported in the newborn and infant.

This *macrophage disorder* occurs both in children and adults, in identical twins and siblings, and is equally prevalent

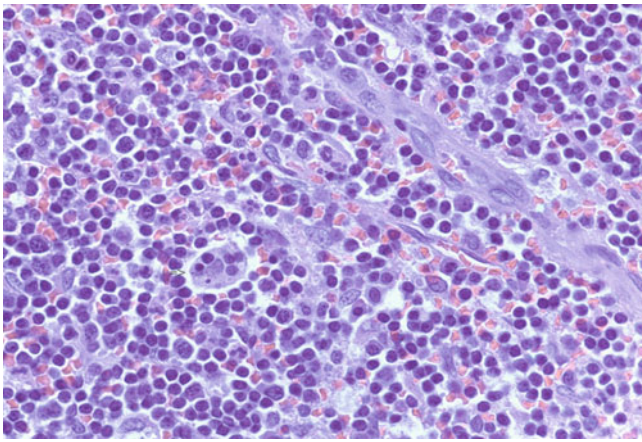


Fig. 8.6 Lymph node biopsy from a young child with Rosai-Dorfman disease

in Blacks and Caucasians [53]. *The most common presentation is cervical adenopathy which is often bilateral. Laboratory findings are normochromic anemia, leukocytosis, lymphopenia, polyclonal hyperglobulinemia, and an elevated erythrocyte sedimentation rate.* Approximately 10 % of the patients with sinus histiocytosis with massive lymphadenopathy have an underlying immune defect, and almost half with this association die from their immune problem [54].

8.5.2.1 Pathology

Marked expansion of lymph node sinusoids by collections of histiocytes and lymphocytes with focal effacement of the nodal architecture is the histological findings. The histiocytes are benign appearing having abundant cytoplasm and regular nuclei. *Leukocytophagocytosis (emperipolesis), where lymphocytes and plasma cells are phagocytized by histiocytes, is a distinguishing histological feature essential for establishing the diagnosis [15, 52–54]* (Fig. 8.6). Reactive, vacuolated histiocytes, many plasma cells, and extensive fibrosis are present. The lesions are focally destructive and can affect also extranodal sites as nasal mucosa, salivary gland, orbit, skin, and bones [15, 52–54].

The histiocytes show cytological and immunohistochemical findings similar to those of normal histiocytes and macrophages. In addition, placental alkaline phosphatase and S-100 are variably expressed by histiocytes. Molecular clonality studies suggest that Rosai-Dorfman disease is a polyclonal disorder [1].

8.5.2.2 Prognosis

Generally patients with sinus histiocytosis with massive lymphadenopathy have a good prognosis, but the course of the disease can be protracted lasting 3–9 months. However, significant morbidity and mortality do occur. Fourcar et al. analyzed the findings in 14 fatal cases [54]. The etiology of this syndrome is unknown, but an underlying immune defect has been proposed [2].

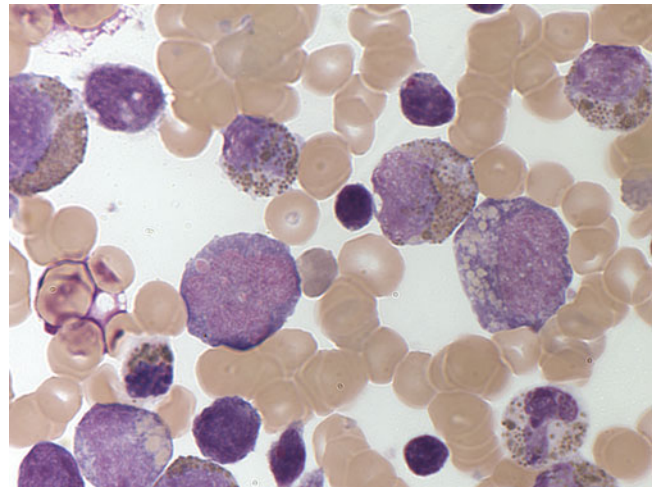


Fig. 8.7 Chediak-Higashi syndrome. Five-year-old female with oculocutaneous albinism, gray hair, developmental delay, susceptibility to infection, and neutropenia. Leukocytes contain diagnostic large, round lysosomal inclusions surrounded by a clear zone. Extensive intracellular hemosiderosis suggests that the patient had entered the accelerated phase of the syndrome with hepatosplenomegaly, lymphadenopathy, anemia, pancytopenia, abnormal liver function tests, and hemophagocytosis. Wright-Giemsa (Courtesy of Glenn Billman, M.D, Rady Childrens Hospital San Diego; Reprinted from Isaacs [8]. © WB Saunders 1997)

Death occurs in the Chediak-Higashi syndrome from infection or from a so-called accelerated phase of infection associated hemophagocytic syndrome [9] (Fig. 8.7).

8.6 Malignant-Related Disorders

8.6.1 Malignant Histiocytoses

The malignant histiocytoses are regarded as true neoplastic disorders of histiocytes. Malignant histiocytosis, acute monocytic leukemia, and histiocytic lymphoma are members of this group [2] of the three, acute monocytic leukemia (AMoL) is the major one occurring in the fetus and infant. Malignant histiocytosis, histiocytic lymphoma, and dendritic sarcoma are rare diseases occurring mostly in adults and the subject of a few infant cases.

8.6.2 Acute Monocytic Leukemia

According to the French-American-British (FAB) classification of leukemia, the criteria required for the diagnosis of acute monocytic leukemia (AMoL), in addition to other findings of leukemia, are the presence of over 30 % leukemic monoblasts or more mature leukemic monocytes (FAB M5) and fewer than 20 % leukemic granulocytic precursors in the bone marrow [10, 55] (Fig. 8.8). Leukemic monocytes are characteristically α -naphthyl esterase, myeloid surface markers CD13, CD33, CD14 immunoreactive. 11q23 translocations are common (see Chap. 7).

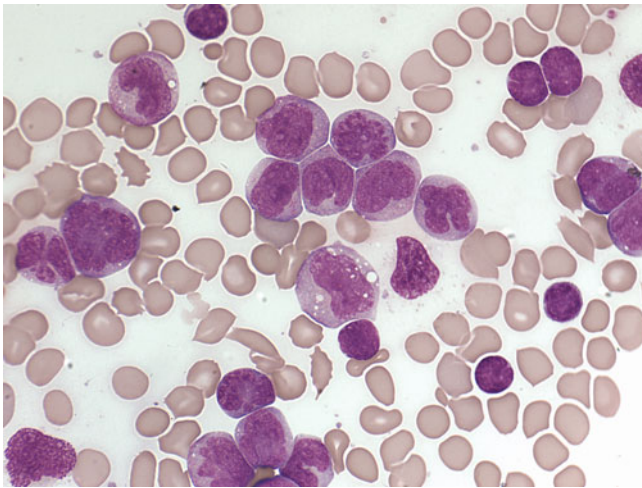


Fig. 8.8 Acute Monocytic leukemia. Many leukemic blast cells have a monocytoid appearance

Typically infants with AMoL present with a significant leukocytosis and a high frequency of involvement of non-hematopoietic tissues particularly the skin [10, 12, 55]. Hepatosplenomegaly and lymphadenomegaly are found initially in about half the cases [10, 12, 55].

8.7 Prognosis

HLH accounts for the highest mortality followed by AMoL and disseminated LCH. Newborns with LCH and JXG limited to the skin and/or subcutaneous tissue often survive without treatment which is attributed to spontaneous regression of these tumors [11].

References

- Favara BE (1989) Histiocytosis syndromes and related disorders of early infancy: a pathologists perspective. *Pediatr Hematol Oncol* 6:213
- Favara BE, Feller AC, Pauli M (1997) Contemporary classification of histiocytic disorders. The WHO committee on histiocytic/reticulum cell proliferations. Reclassification Working Group of the Histiocyte Society. *Med Pediatr Oncol* 29:157–166
- Stephan JL (1995) Histiocytoses. *Eur J Pediatr* 154:600–609
- Dehner LP (1981) Neoplasms of the fetus and neonate. In: Naeye RL, Kissane JM, Kaufman N (eds) *Perinatal diseases*, International Academy of Pathology, Monograph number 22. Williams and Wilkins, Baltimore, p 286
- Dehner LP (2003) Histiocytic disorders in children, something relatively old. Course title: AP104. College of American pathologists annual meeting, 11 Sept 2003, San Diego
- Huang F, Arceci R (1999) The histiocytoses of infancy. *Semin Perinatol* 23:319–331
- Arceci RJ (1999) The histiocytoses: the fall of the Tower of Babel. *Eur J Cancer* 35:747–767
- Isaacs H Jr (1997) Histiocytoses. In: *Tumors of the fetus and newborn. Major problems in pathology*, vol 35. W.B. Saunders, Philadelphia, pp 169–186
- Isaacs H Jr (2002) Histiocytoses. In: *Tumors of the fetus and infant: an atlas*. Springer, New York, pp 181–198
- Isaacs H Jr (2003) Fetal and neonatal leukemia. *J Pediatr Hematol Oncol* 25:348–360
- Isaacs H Jr (2006) Fetal and neonatal histiocytoses. *Pediatr Blood Cancer* 47:123–129
- Isaacs H Jr (2011) Cutaneous metastases in neonates: a review. *Pediatr Dermatol* 28:85–93
- Sharma R, Hudak ML, Perszyk AA et al (2000) Perinatal lethal form of Gaucher's disease presenting with hemosiderosis. *Am J Perinatol* 17:201–206
- Lasser A (1983) The mononuclear phagocytic system: a review. *Hum Pathol* 14:108–126
- Foucar E, Rosai J, Dorfman RF et al (1984) Immunologic abnormalities and their significance in sinus histiocytosis with massive lymphadenopathy. *Am J Clin Pathol* 82:515–525
- Stein SL, Paller AS, Haut PR et al (2001) Langerhans cell histiocytosis presenting in the neonatal period: a retrospective case series. *Arch Pediatr Adolesc Med* 155:778–783
- Lahey ME (1981) Prognostic factors in histiocytosis X. *Am J Pediatr Hematol Oncol* 3:57–60
- Minkov M, Prosch H, Steiner M et al (2005) Langerhans cell histiocytosis in neonates. *Pediatr Blood Cancer* 45:802–807
- Ahnquist G, Holyoke JB (1960) Congenital Letterer-Siwe disease (reticuloendotheliosis) in a term stillborn infant. *J Pediatr* 57:897–904
- Senac MO Jr, Isaacs H, Gwinn JL (1986) Primary lesions of bone in the 1st decade of life: retrospective survey of biopsy results. *Radiology* 160:491–495
- Boccon-Gibod LA, Krichen HA, Carlier-Mercier LMB et al (1992) Digestive tract involvement with exudative enteropathy in Langerhans cell histiocytosis. *Pediatr Pathol* 12:515–524
- Dehner LP, Bamford JT, McDonald EC (1983) Spontaneous regression of congenital cutaneous histiocytosis X: report of a case with discussion of nosology and pathogenesis. *Pediatr Pathol* 1:99–106
- Hashimoto K, Griffin D, Kohsbaki M (1982) Self-healing reticulo-histiocytosis: a clinical histologic and ultrastructural study of the fourth case in the literature. *Cancer* 49:331–337
- Dehner LP (2003) Juvenile xanthogranulomas in the first two decades of life: a clinicopathologic study of 174 cases with cutaneous and extracutaneous manifestations. *Am J Surg Pathol* 27:579–593
- Freyer DR, Kennedy R, Bostrom BC et al (1996) Juvenile xanthogranuloma: forms of systemic disease and their clinical implications. *J Pediatr* 129:227–237
- Sonoda T, Hashimoto H, Enjoji M (1985) Juvenile xanthogranuloma: clinicopathologic analysis and immunohistochemical study of 57 patients. *Cancer* 56:2280–2286
- Janssen D, Harms D (2005) Juvenile xanthogranuloma in childhood and adolescence: a clinicopathologic study of 129 patients from the Kiel pediatric tumor registry. *Am J Surg Pathol* 29:21–28
- Seo S, Min KW, Mirkin LD (1986) Juvenile xanthogranuloma: ultrastructural and immunocytochemical studies. *Arch Pathol Lab Med* 110:911–915
- Zelger BG, Zelger B, Steiner H et al (1995) Solitary giant xanthogranuloma and benign cephalic histiocytosis—variants of juvenile xanthogranuloma. *Br J Dermatol* 133:598–604
- Janka GE (1989) Familial hemophagocytic lymphohistiocytosis: diagnostic problems and differential diagnosis. *Pediatr Hematol Oncol* 6:219–225
- Gilbert EF, ZuRhein GM, Wester SM et al (1985) Familial hemophagocytic lymphohistiocytosis: report of four cases in two families and review of the literature. *Pediatr Pathol* 3:59–92
- Goldberg JC, Nezelof C (1989) Familial lymphohistiocytosis: the pathologist's view. *Pediatr Hematol Oncol* 6:199–205
- Hirst WJ, Layton DM, Singh S (1994) Hemophagocytic lymphohistiocytosis: experience at two U.K. centres. *Br J Haematol* 88:731–739

34. Arico M, Janka G, Fischer A (1996) Hemophagocytic lymphohistiocytosis. Report of 122 children from the International Registry: FHL study group of the histiocyte society. *Leukemia* 10:197–203
35. Arico M, Danesino C, Pende D et al (2001) Pathogenesis of haemophagocytic lymphohistiocytosis. *Br J Haematol* 114:761–769
36. Lipton JM, Westra S, Haverty CE (2004) Case records of the Massachusetts General Hospital. Weekly clinicopathological exercises. Case 28-2004. Newborn twins with thrombocytopenia, coagulation defects, and hepatosplenomegaly. *N Engl J Med* 351:1120–1130
37. Rettwitz W, Sauer O, Burow HM et al (1983) Neurological and neuropathological findings in familial erythrophagocytic lymphohistiocytosis. *Brain Dev* 5:322–327
38. Akima M, Sumi SM (1984) Neuropathology of familial erythrophagocytic lymphohistiocytosis. *Hum Pathol* 15:161–168
39. Henter J-I, Nennesmo I (1997) Neuropathologic findings and neurologic symptoms in twenty-three children with hemophagocytic lymphohistiocytosis. *J Pediatr* 130:358–365
40. Ost A, Nilsson-Ardnor S, Henter J-I (1998) Autopsy findings in 27 children with haemophagocytic lymphohistiocytosis. *Histopathology* 32:310–316
41. Risdall RJ, McKenna RW, Nesbit ME et al (1979) Virus-associated hemophagocytic syndrome; a benign histiocytic proliferation distinct from malignant histiocytosis. *Cancer* 44:993–1002
42. Janka G, Imashuku S, Elinder G et al (1998) Infection- and malignancy-associated hemophagocytic syndromes. Secondary hemophagocytic lymphohistiocytosis. *Hematol Oncol Clin North Am* 12:435
43. Chen RL, Su JJ, Lin KH (1991) Fulminant childhood hemophagocytic syndrome mimicking histiocytic medullary reticulosis. An atypical form of Epstein-Barr virus infection. *Am J Clin Pathol* 96:171–176
44. Danish EH, Dahms BB, Kumar ML (1985) Cytomegalovirus-associated hemophagocytic syndrome. *Pediatrics* 75:280–283
45. Barre V, Marret S, Mendel I et al (1998) Enterovirus-associated haemophagocytic syndrome in a neonate. *Acta Paediatr* 87:469–471
46. Aygun C, Tekinalp G, Gurgey A (2003) Infection-associated hemophagocytic syndrome due to *Pseudomonas aeruginosa* in preterm infants. *J Pediatr Hematol Oncol* 25:665–667
47. Pohl M, Niemeyer CM, Hentschel R et al (1999) Haemophagocytosis in early congenital syphilis. *Eur J Pediatr* 158:553–555
48. Shaw PH, Brown D, Shulman ST (2000) Tuberculosis-associated hemophagocytic syndrome in an infant. *Pediatr Infect Dis J* 19:475–477
49. Campo E, Condom E, Miro MJ et al (1986) Tuberculosis-associated hemophagocytic syndrome. A systemic process. *Cancer* 58:2640–2645
50. Arya S, Hong R, Gilbert EF (1985) Reactive hemophagocytic syndrome. *Pediatr Pathol* 3:129–141
51. Hoang MP, Dawson DB, Rogers ZR et al (1998) Polymerase chain reaction amplification of archival material for Epstein-Barr virus, cytomegalovirus, human herpesvirus 6, and parvovirus B19 in children with bone marrow hemophagocytosis. *Hum Pathol* 29:1074
52. Rosai J, Dorfman RF (1972) Sinus histiocytosis with massive lymphadenopathy: a pseudolymphomatous benign disorder: analysis of 34 cases. *Cancer* 30:1174–1188
53. Fourcar E, Rosai J, Dorfman R (1990) Sinus histiocytosis with massive lymphadenopathy (Rosai-Dorfman disease): review of the entity. *Semin Diagn Pathol* 7:19–73
54. Fourcar E, Rosai J, Dorfman RF et al (1984) Immunologic abnormalities and their significance in sinus histiocytosis with massive lymphadenopathy. *Am J Clin Pathol* 82:515–525
55. Sande JE, Arceci RJ, Lampkin BC (1999) Congenital and neonatal leukemia. *Semin Perinatol* 23:274–285

9.1 Introduction

Brain tumors occur less often in the first year of life than in the older child and adult [1–9]. The peak age incidence in children is between 5 and 8 years [10]. Central nervous system neoplasms are the leading solid tumor in children and adolescents and are surpassed only by leukemia and lymphoma in frequency [10]. Although fetal and newborn brain tumors are diagnosed less often than extracranial teratoma, neuroblastoma, and leukemia (Table 1.1), they cause 5–20 % of deaths due to neoplasms in this period of life [7, 9, 11–18].

9.1.1 Incidence

The annual incidence of brain tumors varies from one decade to the next, from one institution to another, and in different parts of the world [4, 6, 8, 11, 16, 18–21]. The rate of occurrence of brain tumors reported for the first year of life differs considerably ranging from 1 to 18 % [3, 4, 6, 11, 13, 18–22]. Congenital intracranial tumors comprise approximately 1 % of those occurring during childhood [6, 23].

The number of fetuses and infants diagnosed with intracranial lesions has increased dramatically since the inception of ultrasonography, computerized tomography, and magnetic resonance imaging which have significantly contributed to earlier treatment and survival [6, 9, 24]. Imaging studies are most helpful in identifying and distinguishing potentially curable tumors such as choroid plexus papillomas from rapidly fatal ones such as giant teratomas and PNETs where much of the brain may be destroyed by tumor [8, 9].

Fetal and infant brain tumors differ from those occurring in the older child and adult in several ways. First of all, the location is not entirely the same. Primary intracranial tumors in the older child and adolescent are mostly infratentorial, that is, they are located within the posterior fossa involving the brain stem and cerebellum in contrast to the fetus and neonate where many are found above the tentorium [3, 4, 7–9, 16, 22–29]. The clinical presentation and frequency

of the various histological types are not the same. The main presenting findings are *macrocephaly* (a large head) and an *intracranial mass* or *hydrocephalus* (dilatation of the cerebral ventricles resulting from obstruction of the CSF pathways) and followed by *stillbirth* (born dead) (Table 9.1). Intracranial teratoma is the leading tumor in several fetal and newborn studies. Next is astrocytoma followed by primitive neuroectodermal tumor (PNET), choroid plexus papilloma, and craniopharyngioma [7–9, 16] (Table 9.2). In utero most brain tumors are detected during the third trimester of pregnancy. Many are inoperable because they occupy much of the intracranial cavity involving large areas of the brain. Overall survival rate is dismal, less than 30 % [9].

Table 9.1 Fetal and neonatal brain tumors presenting signs and symptoms ($n=250$)

Initial signs and symptoms	No.	Percent
Macrocephaly	146	28.7
Hydrocephalus	83	17.3
Intracranial mass ^a	72	12.2
Stillborn	53	10.4
Eye signs ^b	28	5.5
Vomiting	20	3.9
Hydramnios	19	3.7
Hemorrhage	13	2.6
Seizures	13	2.6
Bulging cranial mass	13	2.6
Breech presentation	12	2.4
Dystocia	12	2.4
Bulging fontanel	8	1.5
Hypotonia	6	1.2
Cranial nerve palsy	6	1.2
Enlarged uterus for dates	5	1
Hydrops	5	1
	508 ^c	100

Reprinted from Isaacs [9]. With kind permission of © Elsevier, 2002

^aRepresents the number of patients

^bDetected by antenatal or postnatal imaging studies

^cEye signs: ptosis, exophthalmos, strabismus, nystagmus, doll's eyes, or setting sun sign

^dTotal number of all signs and symptoms of the 250 patients with tumors

Table 9.2 Fetal and neonatal tumors histological type and survival rate ($n=250$)

Tumor	No. (%) ^a	Living/dead	Stillborn	Percent stillborn ^b	Percent survival
Teratoma	74 (29.6)	9/65	25	34	12
Astrocytoma	47 (18.8)	16/31	6	13	34
Primitive neuroectodermal tumors ^c	33 (13.2)	4/29	11	33	12
Choroid plexus tumors ^d	33(13.2)	24/9	1	1	73
Craniopharyngioma	17 (6.8)	4/13	3	18	23.5
Meningeal tumors ^e	14 (5.6)	5/9	3	21	36
Ependymal tumors ^f	11 (4.4)	1/10	1	9	9
Ganglioglioma ^g	5 (2.0)	5/0	0	0	100
Spongiblastoma	3 (1.2)	0/3	2	67	0
Medulloepithelioma	3 (1.2)	0/3	0	0	0
Rhabdoid tumor	2 (0.8)	0/2	0	0	0
Astroblastoma	2 (0.8)	1/1	0	0	50
Hemangioblastoma	2 (0.8)	1/1	0	0	50
Oligodendroglioma	2 (0.8)	0/2	1	50	0
Atypical teratoid/Rhabdoid tumor	1 (0.4)	0/1	0	0	0
Hypothalamic hamartoma	1 (0.4)	0/1	0	0	0
Total	250(100 %)	70/180	53	21	28 ^h

Reprinted from Isaacs [9]. With kind permission of © Elsevier, 2002

^aPercent of total cases

^bOverall stillborn rate: $53/250 \times 100 = 21$

^cIncludes 19 medulloblastomas with only 1 of 19 survivors

^dIncludes 20 choroid plexus papillomas and 4 carcinomas (2 of 4 survivors)

^eIncludes 7 meningeal sarcomas (1 survivor) and 7 meningiomas (4 survivors)

^fIncludes 11 ependymomas and 3 ependymoblastomas (no survivors)

^gIncludes 1 gangliocytoma

^hOverall survival rate: $70/250 = 28\%$

9.1.2 Association of Brain Tumors with Heritable Disorders and Other Conditions

Definite associations are documented between brain tumors and heritable diseases, syndromes, and other conditions. *Neurofibromatosis and tuberous sclerosis* are prime examples [7, 30–35] (Tables 9.3 and 9.4, respectively). The types of tumors occurring in infants with neurofibromatosis are neurofibroma, meningioma, pilocytic astrocytoma, ependymoma, and optic nerve glioma [7, 32]. Cerebellar hemangioblastomas and retinal tumors occur with the *Von Hippel-Lindau disease*; medulloblastomas are found in individuals with the *nevoid basal cell carcinoma syndrome*, the *Turcot intestinal polyposis syndrome*, and *ataxia telangiectasia*. There is an important association between neonatal brain tumors and congenital anomalies [22, 36]. There is a significant increased incidence of brain tumors occurring in infants with renal tumors, for example, primitive neuroectodermal tumor (PNET) and rhabdoid tumor [18, 37, 38].

Table 9.3 Neurofibromatosis type 1 CNS findings

Plexiform neurofibroma
Malignant peripheral nerve sheath tumors
Schwannoma
Gliomas
Astrocytoma of optic pathway
Astrocytomas of hypothalamus, thalamus, cerebrum, cerebellum, and spinal cord ^a
Ependymoma
Medulloblastoma
Meningioma
Aqueductal stenosis
Hydrocephalus
Cerebrovascular malformations
Mental retardation
Seizures

Riccardi [32]. With kind permission of © Elsevier, 1992; Reprinted from Isaacs [9]. With kind permission of © Elsevier, 2002; Reprinted from Burger and Scheithauer [30]. With kind permission of © Armed Forces Institute of Pathology, 2007

^aAstrocytomas are usually pilocytic, while others are diffuse, fibrillary, or of varying grades

Table 9.4 Ages when lesions of tuberous sclerosis may first appear

Age	Lesion/sign
Between 20th week of gestation and birth	Cardiac rhabdomyoma, subependymal nodule(s)/tumor ^a
Perinatal period	Multiple renal cysts ^a Fetal hydrops Seizures in utero Wolff-Parkinson-White (WPW) syndrome
Newborn period	Forehead fibrous plaques Partial seizures with or without generalization Abdominal distension/uremia
Infancy (<1 year of age)	Infantile spasms/West syndrome Cutaneous hypomelanotic nodules Retinal hamartomas Regression of social-adaptive behavior Delayed motor development

Reprinted from Gomez [35]. With kind permission of © Oxford University Press, 1999

^aDetected by imaging studies

9.1.3 Clinical Findings

An abnormally large head circumference (macrocephaly) is the most common finding observed in the fetus or newborn with a brain tumor regardless of histological type. *Macrocephaly* is the result of either hydrocephalus or to the size of the tumor mass or both [3, 7–9, 25] (Table 9.1). *Hydrocephalus* (marked dilatation of the cerebral ventricles due to obstruction of the CSF pathways accompanied by accumulation of CSF), the second most common finding, results by either compression of the ventricular system or by hemorrhage from the tumor. Choroid plexus tumors produce hydrocephalus by hypersecretion of CSF (cerebrospinal fluid) [8, 9].

Although hydrocephalus is an important manifestation of brain tumors in the fetus and infant, most causes of this finding result from aqueductal stenosis or from other congenital malformations such as meningomyelocele. Intrauterine infections, intracranial vascular malformations, cysts, prenatal and intracranial hemorrhage are other etiologic factors [7–9].

Brain tumors can grow enormously in utero causing *dystocia (difficult delivery) or stillbirth* [8, 9, 16, 18, 26, 36]. The incidence of stillbirth, as high as 17 %, has been described especially with intracranial teratomas, glioblastomas, and PNETs [7, 9, 36]. Large tumors may require aspiration or decompression of the skull to permit vaginal delivery. Infants with rapidly growing neoplasms *show signs of increased intracranial pressure* manifested by vomiting, lethargy, macrocephaly, separation of cranial sutures, and bulging fontanelles.

Symptomatic *intracranial hemorrhage* in term infants is uncommon, but when it occurs, it is usually secondary to

trauma, coagulation disorders, and/or hypoxia [1, 9]. The possibility of a structural cause such as arteriovenous malformation or brain tumor is, unfortunately, not always seriously considered until very late, as late as the postmortem examination. The incidence of hemorrhage from perinatal brain tumors is significant, as high as 18 % in some studies [8, 9].

One constellation of findings unique to the infant with a brain tumor is the *diencephalic syndrome*. Typically, infants with this condition have an elfin-like facies, long, thin extremities, marked wasting in the presence of a voracious appetite, hyperalertness, and happy disposition [39, 40]. Most patients have a low-grade astrocytoma, usually pilocytic, situated in the region of the third ventricle and hypothalamus [39, 40]. Increased growth hormone production presumably by the hypothalamic-pituitary axis is believed to play a role in this rare and unusual syndrome characterized by a prolonged course and a high mortality [39, 40].

9.1.4 Pathology

The location and the histological types of brain tumors occurring in the fetus and newborn differ somewhat from those in the older child and adolescent. In several series, over 60 % of brain tumors are found above the tentorium cerebelli as compared to the older age group where most arise from below it [8, 9, 11, 17, 18].

Intracranial teratomas comprise almost one third of the total reported cases in fetuses and neonates [7–9, 17] (Table 9.2). Astrocytoma, medulloblastoma, ependymoma, and choroid plexus papilloma are the major neuroepithelial tumors [3, 8, 9, 11, 14, 18, 41].

In addition to routine histological examination by hematoxylin and eosin (H & E) stained paraffin sections, immunohistochemistry, cytogenetics, and EM are used for the diagnosis and classification of brain tumors [8, 30, 31, 42–48] (Table 9.5). Immunohistochemical markers are the glial fibrillary acidic protein (GFAP) and the neurofilament protein (NFP) antibodies [30, 31, 42] (Table 9.5). GFAP is used to distinguish glial from non-glial neoplasms and for the identification of astrocytic and ependymal elements [30, 42]. The neurofilament proteins are intermediate filament proteins found in neurons and their processes and are usually restricted to these cells [30, 31, 42]. Monoclonal antibodies employed to detect neuroectodermal-associated antigens are neuron-specific enolase (NSE) and the S-100 protein which cross-react also with several other types of tissues, both neural and nonneural. In spite of this, neuroblastoma, medulloblastoma, and other PNETs generally are immunoreactive with NSE and variably reactive with S-100. Nestin, an intermediate filament protein, and vimentin are expressed by primitive neuroepithelium, for example, medulloblastoma and ependymoma. Neurons and medulloblastomas are

Table 9.5 Immunohistochemical methods used in the diagnosis of central nervous system tumors

Antibody	Diagnostic use
Glial fibrillary acidic protein (GFAP)	Astrocytoma, ependymoma
S-100 protein	Tumors of neural crest origin: gliomas, nerve sheath and choroid plexus tumors, melanoma, granular cell tumor
Synaptophysin	Tumors with neurosecretory differentiation: neuroblastoma, medulloblastoma
Chromogranin	Neuroendocrine tumors
Neuron-specific enolase (NSE)	Meningiomas, ependymomas, choroid plexus papilloma, medulloblastoma, schwannoma
Neurofilament antibodies	Tumors of neural origin: ganglioneuroma, neuroblastoma, medulloblastoma, ganglioglioma
Epithelial membrane antigen	Epithelial tumors, chordoma, meningioma, choroid plexus tumors
Cytokeratins	Epithelial tumors, craniopharyngioma, choroid plexus tumors, chordoma, some germ cell tumors
Placental alkaline phosphatase, human chorionic gonadotropin and α -fetoprotein	Germ cell tumors
Vimentin	Meningioma, nerve sheath tumors, medulloblastoma, astrocytoma
S-antigen	Retinoblastoma
Nestin	Medulloblastoma, ependymoma

Reprinted from Bigner et al. [31]. With kind permission of © Arnold, 1998; Reprinted from Timperly [44]. With kind permission of © BMJ Publishing Group, 2000

reactive with synaptophysin [31]. Alpha-fetoprotein (AFP) and human chorionic gonadotropin (hCG) immunoperoxidase antibodies are intracranial germ cell tumor markers, for example, yolk sac tumor and choriocarcinoma, respectively [30, 31, 42] (Table 9.5).

9.1.5 Cytogenetics

Chromosomal abnormalities in pediatric brain tumors tend to be rather nonspecific but nevertheless are different from many of those found in adult brain tumors [45, 46, 48]. One of the most common anomalies occurs in medulloblastoma where there is a total or partial loss of chromosome 17, a monosomy, or i(17q), which is noted in approximately 60–70 % of tumors [42, 48]. Deletions involving 17p and absence of *C-Myc* or *N-Myc* amplifications are described in cerebral PNETs [46]. Chromosomal 1 deletions (del 1q) are found in childhood astrocytomas [49]. Chromosomal analysis performed on intracranial teratomas usually show a normal 46XY or 46XX karyotype for both the host and tumor [8, 45, 48]. Teratoid/rhabdoid tumor molecular analysis shows a mutation deletion involving chromosome 22q11 resulting in absence of the *hSNF5/INI1* gene and its product [9, 37].

9.2 Teratoma

Teratoma is the leading germ cell tumor occurring in the fetus and infant [3, 4, 7–9] (Tables 1.1 and 9.2). Historically, most intracranial teratomas were diagnosed at postmortem examination, but currently, they are detected in utero or in the neonatal period during routine sonography [8, 9, 29, 49–57].

Several forms of intracranial teratoma are described: massive tumors replacing the intracranial contents, smaller ones causing hydrocephalus, large intracranial teratomas with extension into the orbit or neck, and teratomas presenting as an incidental postmortem finding in a stillborn fetus [53, 55].

Teratomas arise from several locations within the CNS such as the pineal, hypothalamic areas, suprasellar region, and cerebral hemispheres [8, 9, 25, 49–57]. Due to the size of some tumors, recognizable anatomical landmarks are lost, and therefore, in these cases, it is practically impossible to determine the exact site of origin which occurs in about of a third of the cases [9, 29]. Large tumors may erode through the skull and extend into the orbit, oral cavity, or into the neck [50, 52, 53]. Spontaneous rupture of the fetal head during delivery is a common occurrence [52–54].

Intracranial teratomas present clinically in several ways. They are detected incidentally on “routine” prenatal sonography (Fig. 9.1a). Sonograms reveal an intracranial mass containing solid and cystic areas with or without foci of calcification accompanied by distortion or destruction of the normal brain architecture [52, 53]. The patient’s large head filled with tumor may prevent passage through the maternal birth canal causing dystocia (Fig. 9.1b). Mothers of fetuses with intracranial teratomas may present with a sudden increase in uterine size in an otherwise normal pregnancy [51, 52]. The rapid increase in maternal girth is attributed to tumor growth and the accompanying polyhydramnios (increased amniotic fluid). There is a high incidence of breech (feet first) presentation. The main initial findings in both the fetus and newborn are macrocephaly followed by hydrocephalus and an intracranial mass detected on imaging (Fig. 9.1). Eye signs, for example, setting sun sign and proptosis, are others [9].

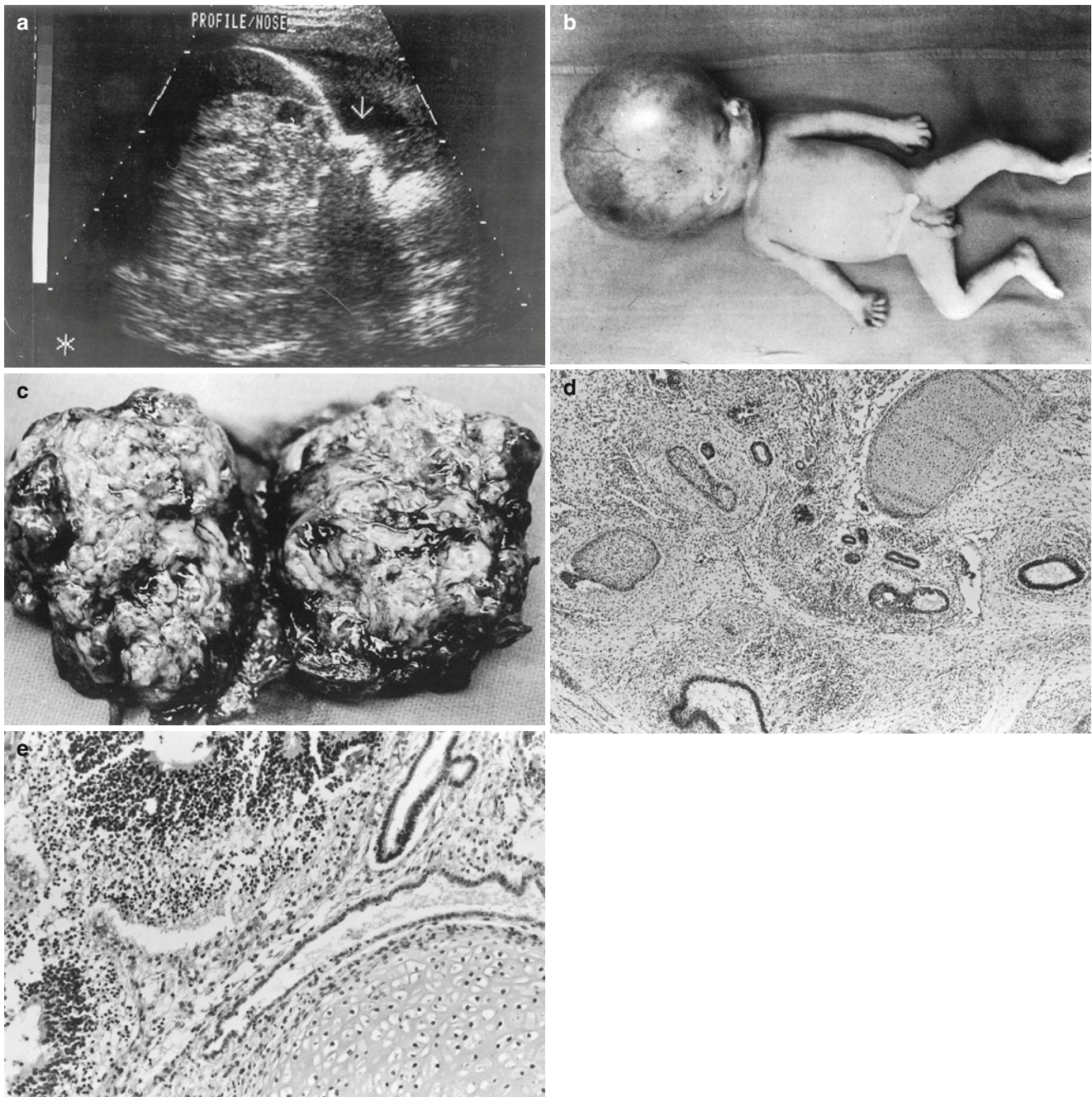


Fig. 9.1 Intracranial teratoma. (a) Ultrasound at 31 weeks gestation. Coronal view displays a large cystic and solid mass filling the cranial vault. The *arrow* is pointed at the nose. The forehead is the curved structure above the *arrow*, and the mouth and chin are below it. (b) The macrocephalic infant at birth. (c) The intracranial contents consist of a variety of cystic and solid tissues; there is no recognizable brain. (d) Photomicrograph reveals cartilage, squamous and respiratory

epithelium, and immature neuroglial elements. (e) Immature neuroglial elements, epithelium, and cartilage viewed at higher magnification. Courtesy of Val Catanzarite, M.D., Department of Neonatology Mary Birch-Sharp Hospitals, San Diego, CA; and Arturo Mendoza, M.D., Department of Pathology, Sharp Hospital, San Diego, CA; Reprinted from Weyerts et al. [56]. With kind permission of © British Medical Journal Group)

Gross and Microscopic Findings. Teratomas typically are large with cystic and solid areas replacing much of the brain [8, 9, 51, 52, 56]. Most tumors are composed of mature components derived from all three germ layers and in addition immature elements consisting mainly of embryonic neuroglial tissue [7–9, 50–54, 56, 57] (Fig. 9.1d, e). Immature

neuroglial components found in infant teratomas may be mistaken for a malignancy because of their hypercellularity, high mitotic rate, and nuclear atypia, thus mimicking the small blue cell tumor (Fig. 9.1e). However, malignant germ cell tumor components are rarely found in infant intracranial teratomas [8, 9].

Most patients with antenatally diagnosed intracranial teratomas expire before or shortly after birth. The prognosis worsens with increasing tumor size and decreasing gestational age at diagnosis [7–9, 52, 54]. Teratomas are associated with one of the lowest survival rates of all perinatal brain tumors, for example, only 12 % in one study [9].

9.3 Astrocytoma

Astrocytoma is the leading neuroglial tumor occurring throughout infancy and childhood and is derived from and composed of astrocytes showing various degrees of differentiation. As a group, astrocytomas differ in their gross and histological features as well as in their site of origin and clinical manifestations [8, 9, 28, 30, 31, 39–41, 58–73]. Astrocytomas occurring in the fetus and neonate are found often outside the posterior cranial fossa and above the tentorium. The cerebral hemisphere, optic nerve, thalamus-hypothalamus, mesencephalon, and pons are the main primary sites. Typically, those arising from the cerebral hemisphere are large, tend to involve more than one lobe, and displace the lateral ventricle(s) [1, 2, 11, 14, 18, 58–60] (Fig. 9.2a). Presenting findings are macrocephaly, the most

common one, hydrocephalus, hemorrhage, polyhydramnios, dystocia, and stillbirth [9, 59, 60] (Table 3). An intracranial mass detected on routine prenatal sonography may be the initial one.

Histologically, they range from benign (low grade) to malignant (high grade) tumors (Table 9.6) (Figs. 9.2, 9.3, 9.4, 9.5, and 9.6). The low-grade-1 *pilocytic astrocytoma* is on the benign end of the spectrum consisting of small bipolar and stellate-shaped cells with scanty processes forming loose and compact areas and microcysts (Figs. 9.2 and 9.3). Rosenthal fibers and eosinophilic granular (cytoid) bodies are characteristically but variably present. Anaplastic changes, that is, cellular and nuclear pleomorphism, nuclear hyperchromatism, neoplastic giant cells, and bizarre mitoses, are absent. Mitoses are uncommon. Pilocytic astrocytomas arise throughout the neuraxis, but the optic nerve and hypothalamic/chiasmatic regions are the most common sites in infants [8, 9]. Tumor cells show strong GFAP staining [9, 30, 31]. Some are associated with an indolent clinical behavior and a more favorable course [9, 30].

Pilocytic astrocytomas of the optic pathways (“optic gliomas”) occur about equally in the orbit and optic chiasm, in both locations and less often in segments of the optic pathways outside the main tumors [61]. In the orbital group, the

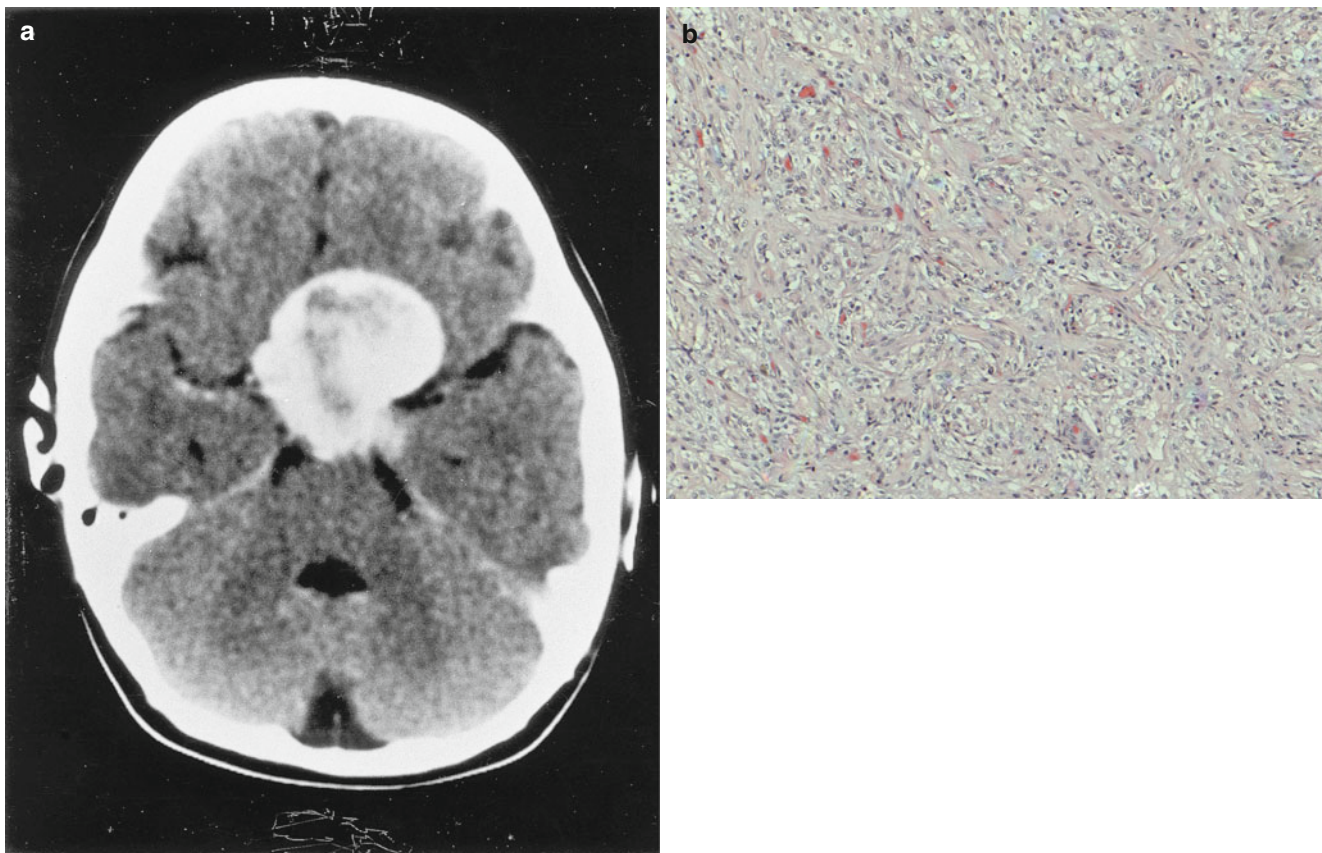


Fig. 9.2 Astrocytoma. Five-month-old female with intermittent vertical nystagmus. (a) CT scan of the head reveals a lobulated, midline mass occupying the suprasellar cistern and involving the optic chiasm

and left hypothalamus. (b) Photomicrograph displays a low-grade pilocytic astrocytoma with compact and microcystic areas (Reprinted from Isaacs [7]. © WB Saunders 1997)

main tumor mass is situated within the orbit, and the most common presenting sign is *proptosis* (exophthalmos, protrusion of the eye). In the optic chiasmatic group, the tumor is intracranial, and the presenting finding is *visual loss*. There is a high association between optic pathway pilocytic astrocytomas and *neurofibromatosis type 1* approaching 50 % in some patients [32, 33, 61]. This association carries an unfavorable prognosis.

Table 9.6 The World Health Organization (WHO) classification of astrocytoma

Astrocytoma (Grade 1) tumor composed primarily of pilocytic astrocytes
Astrocytoma (Grade 2) applies to low-grade diffuse astrocytomas
Astrocytoma (Grade 3) refers to anaplastic (malignant) astrocytoma
Astrocytoma (Grade 4) includes glioblastoma multiforme and variants

Reprinted from Burger and Scheithauer [30]. With kind permission of © Armed Forces Institute of Pathology, 2007

Optic pilocytic astrocytomas arise as fusiform or globular masses from the substance of the optic nerves [61]. They produce a dumbbell-shaped mass accompanied by cyst formations in both intraorbital and intracranial segments of the nerve. The leptomeninges of the optic nerve are frequently and irregularly infiltrated. Extension beyond the dura and invasion of orbital soft tissues is uncommon and usually found after surgical intervention. Neither extension into bone nor metastases occur [61].

Initially, tumor cells are confined to the substance of the optic nerve. With more extensive involvement, there is greater variation in the pattern of tumor growth resulting in looser and denser areas; fascicles of elongated pilocytic astrocytes with elongated nuclei alternate with areas of microcyst formation and round, stellate astrocytes [61] (Fig. 9.3a, b). The tumor cells possess a single nucleus with abundant chromatin. The cytoplasm contains variable amounts of fibrillar material that stains blue with the

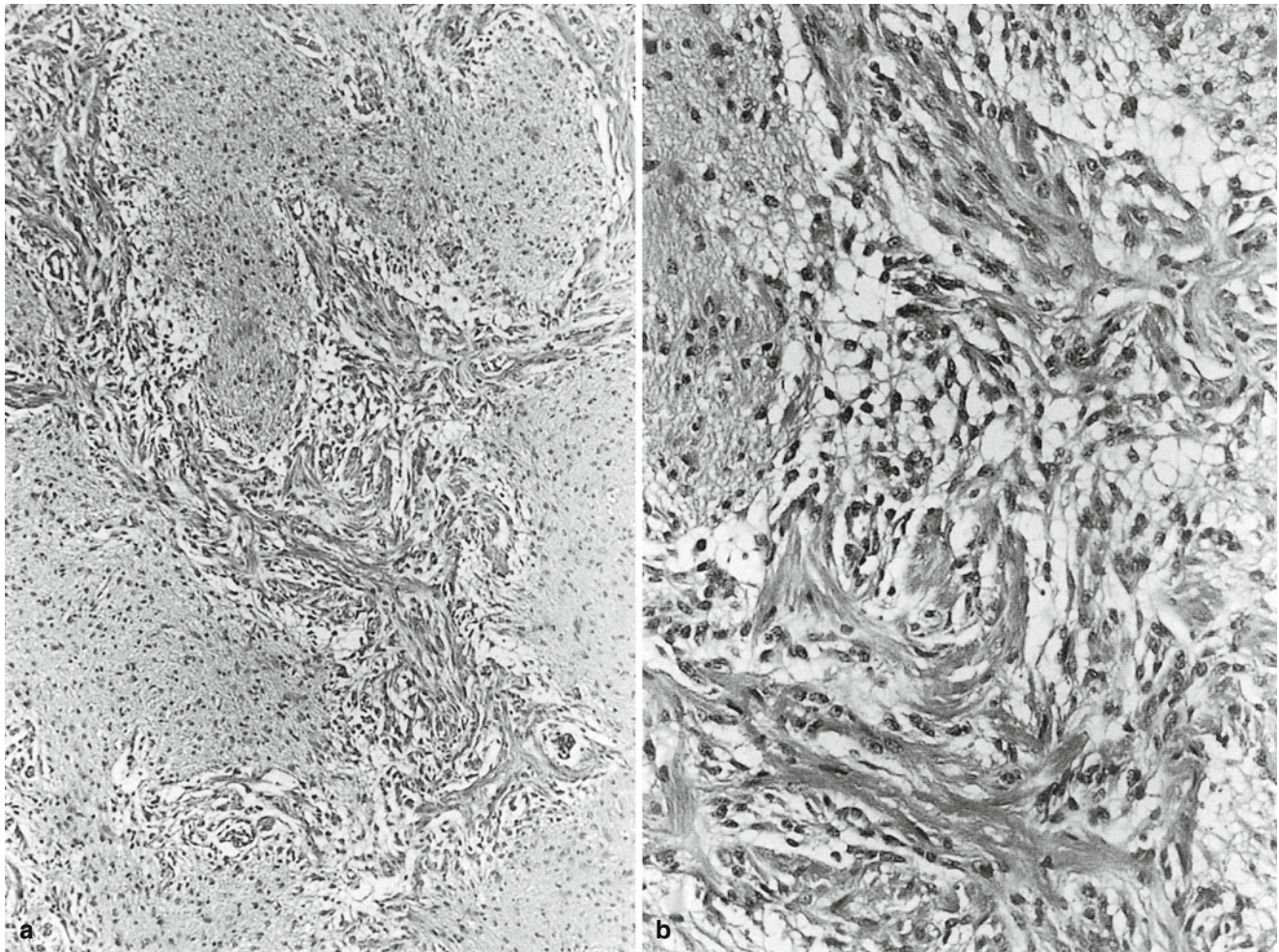


Fig. 9.3 Optic glioma. Seven-month-old male with seizures, facial twitching, and right-eye deviation. CT scan revealed obstructive hydrocephalus and a 3×4-cm suprasellar, solid, and cystic mass arising from the optic chiasm, compressing the third ventricle and producing enlargement of right optic foramen. (a) The cerebral cortex is infiltrated by a

pilocytic astrocytoma having histological features similar to those described in Fig. 9.1b. (b) Higher magnification showing the biphasic pattern consisting of compact fascicles of fibrillated, elongated bipolar cells alternating with more loosely arranged microcystic areas (Reprinted from Isaacs [7]. © WB Saunders 1997)

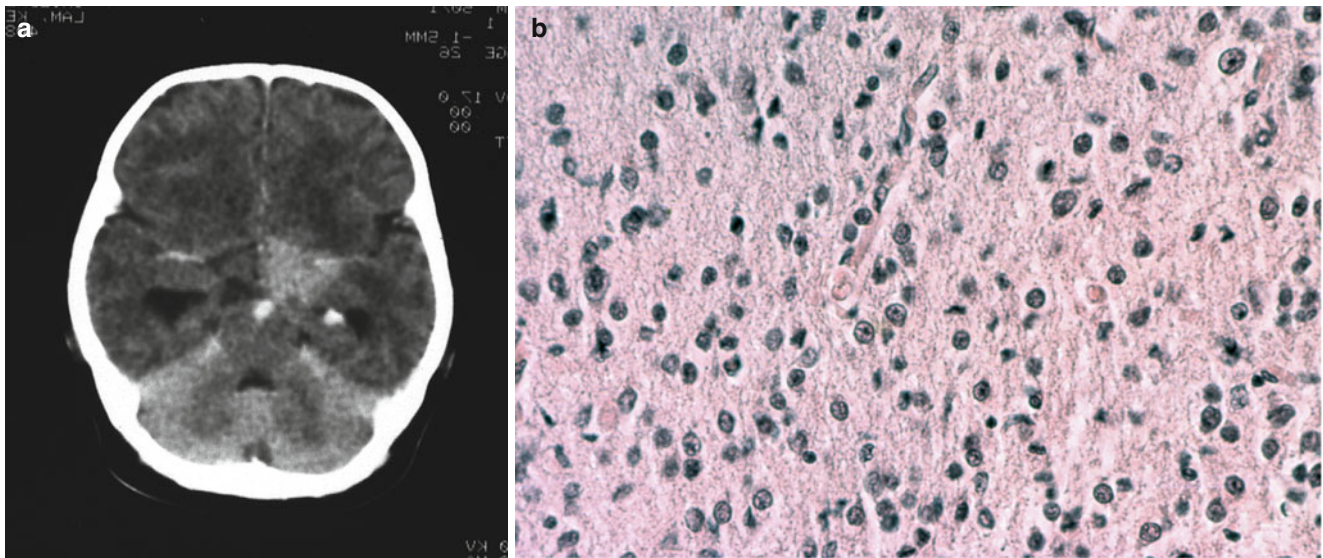


Fig. 9.4 Anaplastic astrocytoma. Two-month-old male with hydrocephalus and a mass in the left and right thalamus. (a) CT scan shows the infiltrative thalamic mass. (b) The tumor is hypercellular with moderate nuclear and cytoplasmic pleomorphism. The nuclei are darkly

staining; some have an angulated appearance (Reprinted from Isaacs [8]. © Springer-Verlag, 2002; (b) Courtesy of Ignacio Gonzalez, M.D., Department of Pathology, Children’s Hospital, Los Angeles)

PTAH or Holzer methods. Some glial fibers have a cork screwlike appearance. Eosinophilic *Rosenthal fibers* are a prominent feature. Mitotic figures are characteristically absent [9, 61].

Anaplastic astrocytoma occurs also in the fetus and infant [41, 60, 62]. The term “anaplastic astrocytoma” refers to astrocytomas of intermediate grade malignancy roughly corresponding to the WHO classification Grades 2 and 3. Microscopically, they show cytoplasmic and nuclear pleomorphism, hypercellularity, mitotic activity, and to a degree the anaplasia of glioblastoma but lack palisading necrosis, hemorrhage, and vascular proliferation found in the latter [8, 9, 30, 62] (Fig. 9.4). GFAP and vimentin antibodies are reactive, but NSE, synaptophysin, neurofilament, desmin, cytokeratin, and epithelial membrane antigen are not [30, 31]. Children with anaplastic astrocytomas have a better outcome than those with glioblastoma. Some long-term survivors are reported [60, 62].

Glioblastoma (malignant astrocytoma) arises from the cerebral hemispheres and basal nuclei of fetuses, stillborns, and infants [8, 9, 28, 30, 31, 58–60, 63–65] (Fig. 9.5a). It comprises approximately a third of astrocytomas reported in the young (Table 9.2). Prenatal ultrasound findings consist of a unilateral echogenic mass occupying most of one hemisphere, sometimes with a shift of midline structures and obstructive hydrocephalus [28, 59–65]. Hemorrhage within the tumor may be an initial imaging finding [55]. Serial sonographic studies show that malignant astrocytomas develop rapidly over a short period of time in utero [65]. Rapid growth may be the result of hemorrhage into the tumor. Perforation of the head and removal of tumor may be required for vaginal

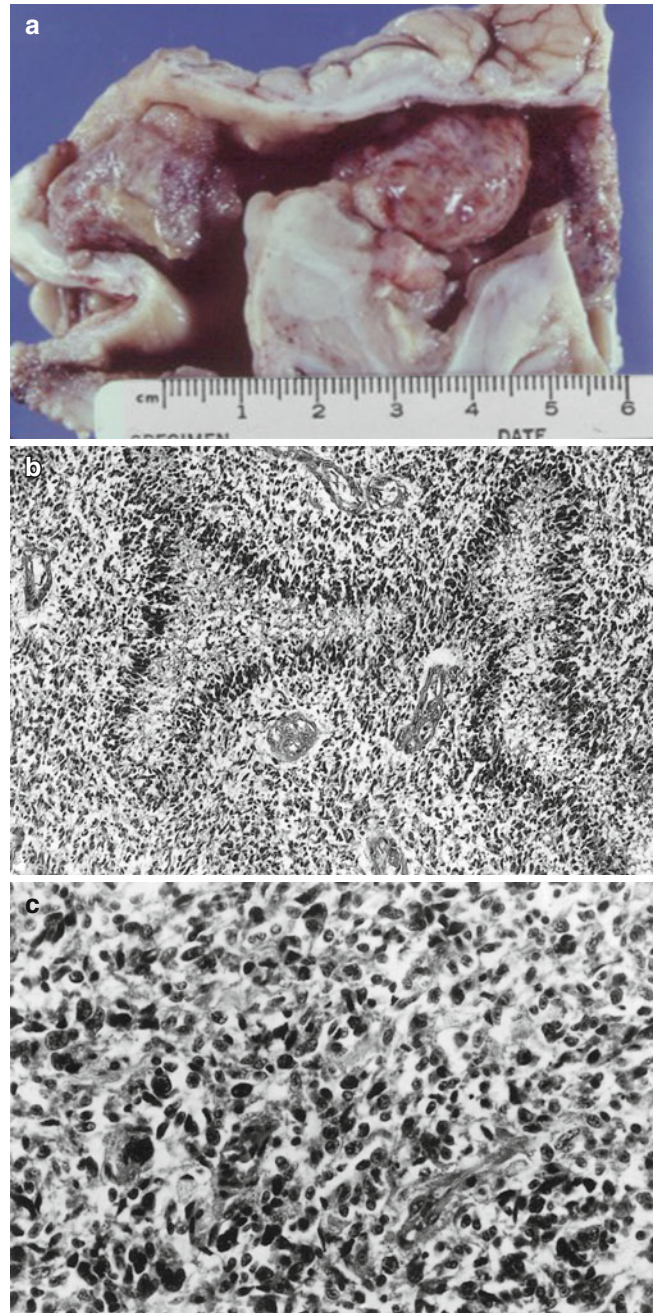
delivery in instances of cephalopelvic disproportion due to a large intracranial mass [8, 9]. Similar to the adult glioblastoma, the prognosis in the reported congenital cases is dismal [9]. Most patients whose tumors are detected antenatally are born usually moribund and die soon after birth [9].

Grossly, the tumors are large, bulky, soft pale-gray, and necrotic with variable hemorrhage [8, 9, 30, 31] (Fig. 9.5a). Microscopically, they appear as densely cellular tumors, showing marked hypercellularity, pleomorphism, microvascular proliferation, and neoplastic spindle-shaped cells forming palisades around central necrotic foci (“palisading necrosis”) [8, 9, 28, 30, 31, 59–65] (Fig. 9.4b, c). GFAP and vimentin immunoreactivity are characteristic features.

Subependymal giant-cell astrocytoma is a unique tumor found mainly in the brains of patients with *tuberous sclerosis*. Most occur during the first and second decades of life, but some examples are found in the fetus and infant [34, 67–70] (Table 9.4). Fetuses and neonates with tuberous sclerosis present more often with their cardiac problems such as uncontrollable arrhythmias and intracavitary outflow obstruction due to rhabdomyoma rather than manifestations of their CNS tumor [7, 8, 34]. Most patients with subependymal giant-cell astrocytoma are diagnosed subsequently with tuberous sclerosis and cardiac rhabdomyomas [9, 34].

Subependymal giant cell astrocytomas appear on sonograms as subependymal echogenic nodules situated in the walls of lateral ventricles often near the foramen of Monro. The tumor is nodular and of mixed signal or isodense to the brain, enhancing densely with contrast on CT scan. Calcification is present often [67–70].

Fig. 9.5 Glioblastoma. Eight-month-old female with congenital hydrocephalus. **(a)** The tumor originated from the right parietal lobe, crossed the midline, and invaded the left cerebral hemisphere and lateral ventricles. Large necrotic, hemorrhagic tumor masses are noted in the cerebral cortex, basal ganglia, and ventricular wall. Severe hydrocephalus is present. **(b)** The densely cellular tumor is composed of small, pleomorphic cells forming palisades around necrotic central areas. Microvascular proliferation is present. **(c)** Higher magnification reveals small cells displaying hyperchromatism, pleomorphism, and nuclear angulation. There are one or two tumor giant cells **(a)** Reprinted from Isaacs [8]. © Springer-Verlag, 2002; **(b** and **c)** Courtesy of Ignacio Gonzalez, M.D., Department of Pathology, Children's Hospital Los Angeles)



Grossly subependymal giant-cell astrocytomas appear as outgrowths in the walls of lateral ventricles; they may obstruct the foramen of Monro and block the third ventricle producing hydrocephalus [9, 34, 67–70] (Fig. 9.6a). Histologically, the tumors are characterized by large fusiform or pyramidal cells with prominent eosinophilic cytoplasm [9, 30, 31, 34, 67–70] (Fig. 9.6b). The tumor is immunoreactive with NSE and variably staining with GFAP and synaptophysin. Although the subependymal giant-cell astrocytoma resembles *gemistocytic astrocytoma*, the latter is more infiltrative and intra-

parenchymal rather than well-demarcated, exophytic intraventricular growths. Neoplastic gemistocytes are usually smaller than subependymal giant-cell astrocytoma cells; the former usually lack calcifications [30, 31].

Desmoplastic cerebral astrocytoma occurring during the first year of life is a variant associated with a fair prognosis [9, 71–73]. The tumor is detected prenatally by ultrasound [72]. Desmoplastic astrocytoma tends to be a large, cystic hemispheric tumor involving the cerebral cortex and adjacent leptomeninges.

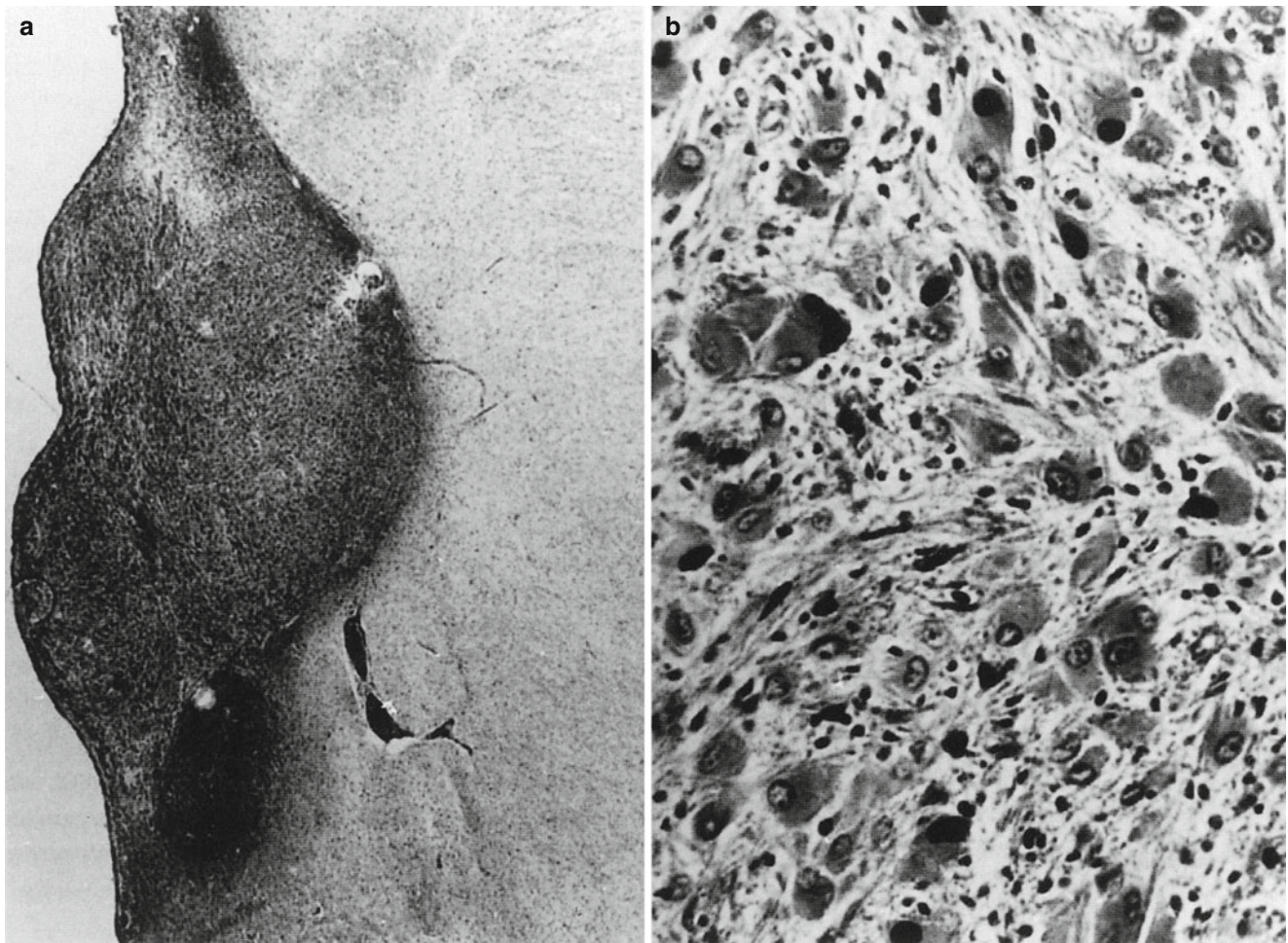


Fig. 9.6 Subependymal giant-cell astrocytoma. Tuberosus sclerosis in an infant aged 22 days. (a) Cellular subependymal nodule protruding into the lateral ventricle. (b) The tumor consists of large astrocytic cells

with abundant cytoplasm, eccentric slightly vesicular nuclei, and large nucleoli surrounded by numerous fibrillary processes (Reprinted from Isaacs [74]. With kind permission of © Mosby)

Microscopic examination reveals a cellular spindle cell tumor with a prominent collagenous stroma. Bipolar and spindle-shaped cells with eosinophilic cytoplasm and cells with long processes are present within the stroma. The astrocytic cells form bundles and nests separated by thick bands of collagen [8, 71–73]. Reticulin stain shows thick fibers surrounding nests of individual cells. Tumor cells and their processes are strongly reactive with GFAP and the collagen fibers with Masson's trichrome stain [73]. *Infantile desmoplastic ganglioglioma* is the main consideration in the differential diagnosis since both tumors are histologically similar. Whether they represent the same tumor is open to debate. Complete resection of the two astrocytomas is associated with a favorable outcome.

The overall survival rate for fetuses and neonates with astrocytoma remains discouraging. Only a third of patients in one perinatal study survived, and over 10 % were stillborn [9].

9.4 Primitive Neuroectodermal Tumors

The term *primitive neuroectodermal tumor (PNET)* is applied to a group of small cell malignant tumors of the central and peripheral nervous systems and soft tissues [43, 46, 75–88]. The neural crest is proposed as the site of origin of these highly aggressive neoplasms. PNETs occur primarily in the pediatric age group and are characterized by the capacity for differentiation along neuronal,

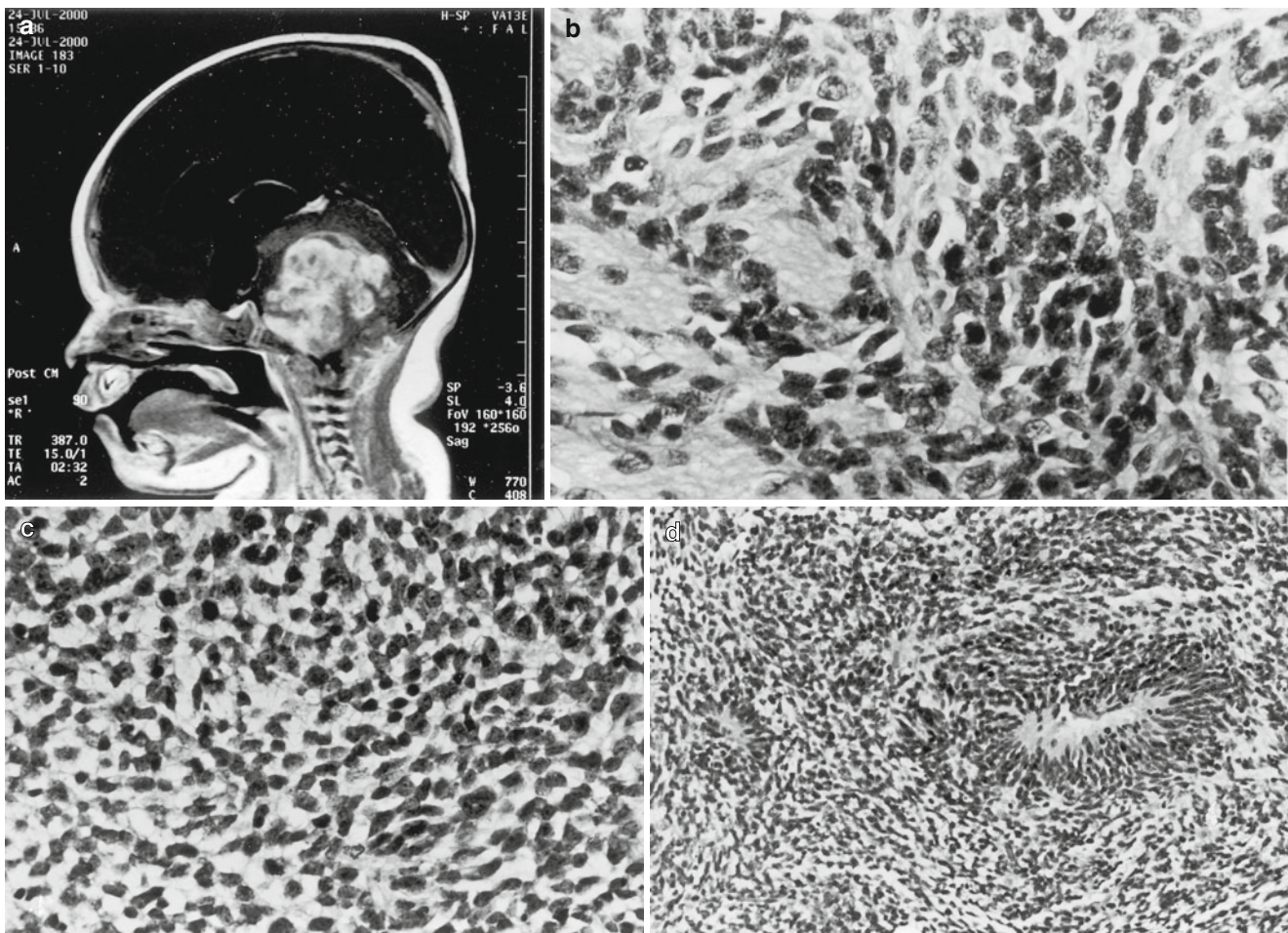


Fig. 9.7 Primitive neuroectodermal tumor (PNET) with divergent differentiation in a 1-day-old with hydrocephalus and a large posterior fossa mass. (a) Magnetic resonance imaging depicting the posterior fossa tumor displacing the cerebellum and adjacent structures. The ventricles are markedly dilated. (b) The hypercellular tumor consists primarily of small darkly staining cells with round to oval nuclei and scant

cytoplasm. No rhabdoid tumor cells are identified. (c) There are areas of neuroblastic differentiation consisting of neuropil. (d) The tumor shows also foci of ependoblastic differentiation characterized by small cells with rosette formation (Case courtesy of Hal Meltzer, M.D. Department of Neurosurgery, Childrens Hospital, San Diego, with permission; Reprinted from Isaacs [8]. © Springer-Verlag, 2002)

astrocytic, ependymal, muscular, and melanotic cell lines [30, 42, 79] (Figs. 9.7, 9.8, 9.9, and 9.10). Moreover, they share a similar biological behavior in the CNS regardless of their primary site. Although they comprise approximately 25 % of primary CNS tumors in children, perinatal PNETs are not as common [9]. Generally, PNETs have a poor prognosis because they are highly aggressive, metastasizing widely throughout the CSF pathways invading the meninges of the brain and spinal cord. A working group of the World Health Organization (WHO) recommended that the diagnosis of PNET be used as an operative term for cerebellar medulloblastomas in addition to

tumors that are indistinguishable morphologically from the medulloblastoma but arise also from other sites in the CNS [79].

PNETs are found in several locations including most commonly the cerebellum (where they are called *medulloblastoma*), the cerebral hemispheres (*cerebral neuroblastoma*, *ganglioneuroblastoma*), pineal (*pineoblastoma*), brain stem, spinal cord, olfactory nerve, and retina (*retinoblastoma*) [8, 9, 77]. PNETs metastasize not only locally to extracranial tissues but also to distant sites such as the lungs, liver, lymph nodes, and bone marrow [83, 84].

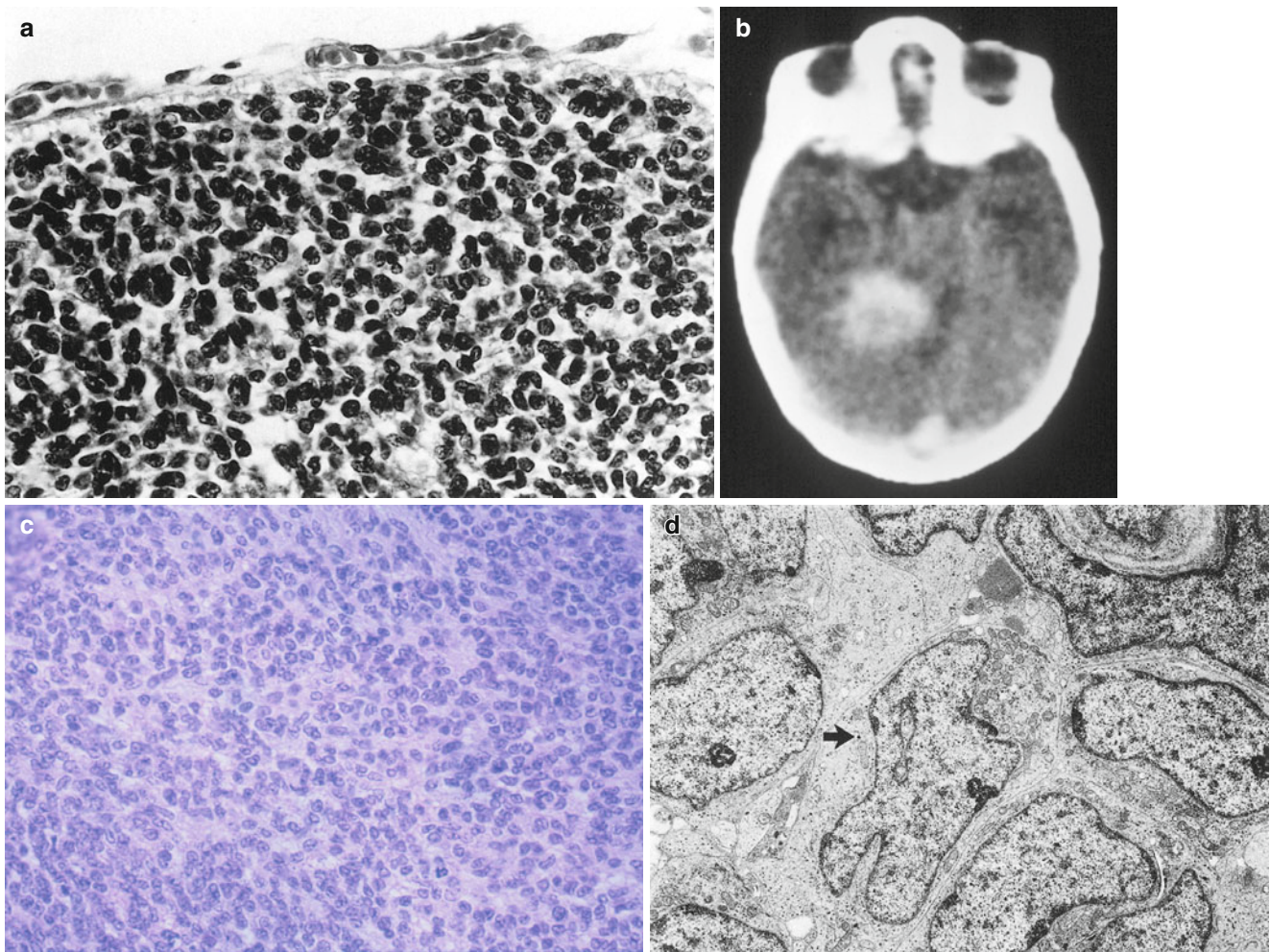


Fig. 9.8 Medulloblastoma. (a) Cerebellar biopsy from a 650 g, 10 hour-old-male infant of 26 weeks gestation showing the developing external granular layer in an immature but normally otherwise brain. Superficial biopsies of the external granular layer may be misinterpreted as a tumor such as medulloblastoma on frozen section. (b) Intracranial CT scan of a newborn with a several week history of poor feeding and vomiting and terminally bulbar paresis. There is a large enhancing mass within the medial aspect of the left cerebellar

hemisphere. (c) Photomicrograph reveals a small cell tumor with a fibrillary background and some suggestive pseudorosette formations. Several mitotic figures are present. (d) EM findings show primitive-appearing cells with irregular nuclei. The cytoplasm contains a few organelles mostly mitochondria and scattered ribosomes. Rare dense core granules are present. Microtubules are noted in some cytoplasmic processes (Reprinted from Isaacs [7]. © WB Saunders 1997)

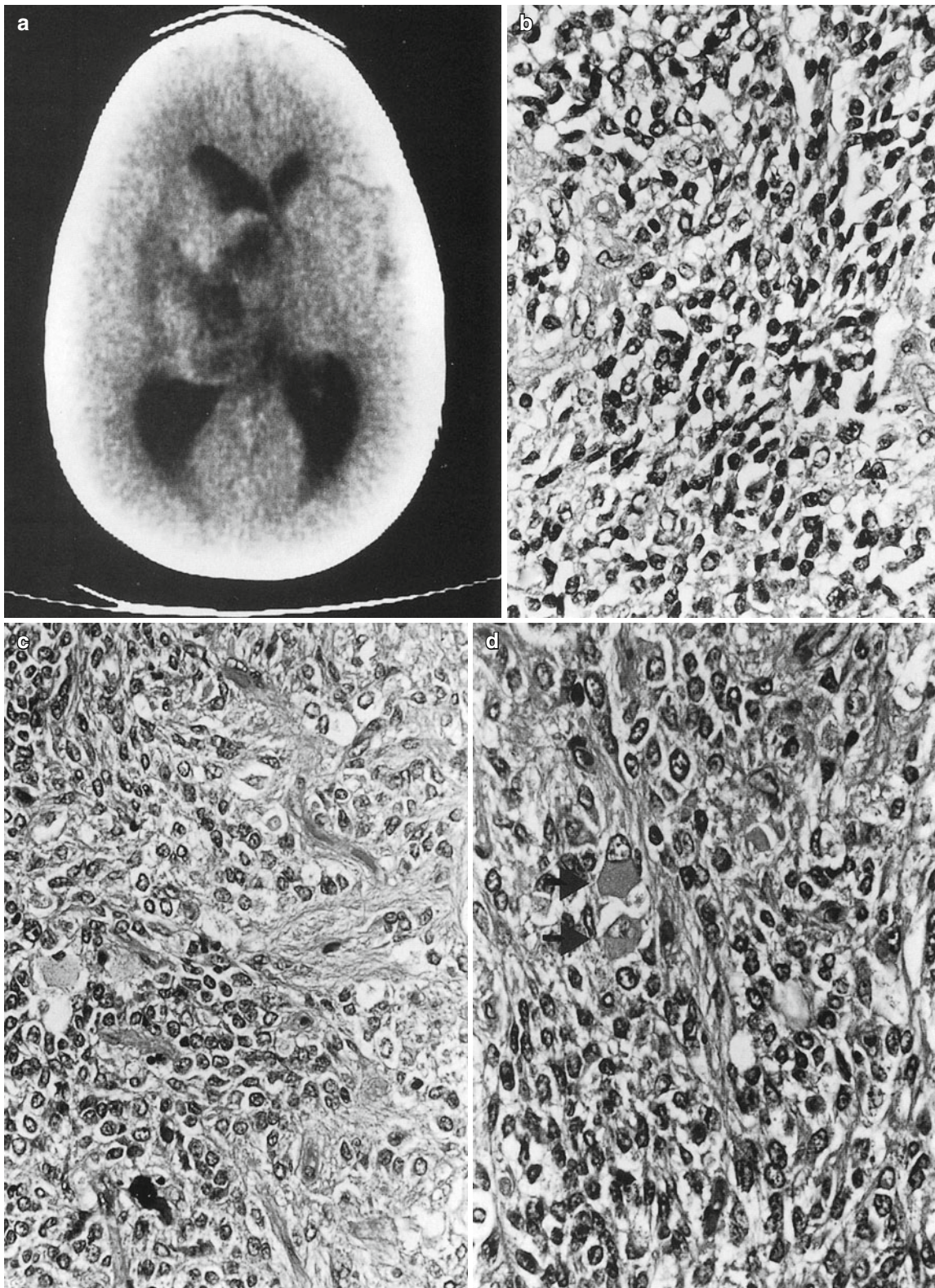


Fig. 9.9 Cerebral PNET (cerebral neuroblastoma). (a) CT scan of an 11-month-old male with vomiting and paresis of the left arm. A large heterogeneous enhancing mass is present in the right frontal-parietal area with irregular low-density areas in the right basal ganglia. The lateral ventricles are dilated. (b) The tumor consists of sheets of small,

poorly differentiated, darkly staining cells. (c) Areas of fibrosis (desmoplasia) and calcification (*black* staining material) are present. (d) Foci of astrocytic differentiation (*arrows*) (Reprinted from Isaacs [7]. © WB Saunders 1997)

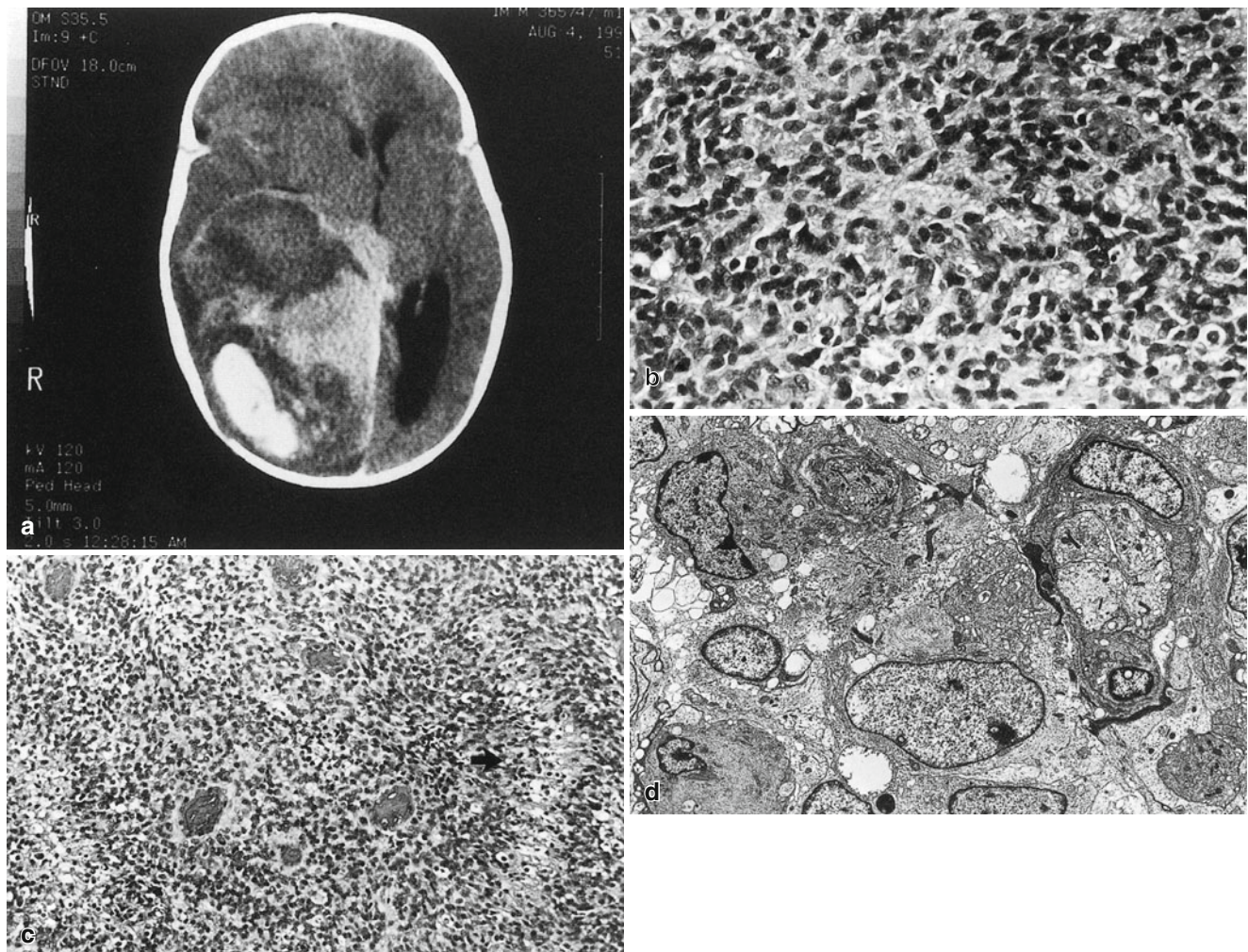


Fig. 9.10 Cerebral primitive neuroectodermal tumor. Six-week-old male with a 2-day history of vomiting and increasing lethargy. (a) CT scan reveals a large heterogeneous, enhancing mass with areas of hemorrhage and necrosis occupying much of the parieto-occipital lobes. Herniation across the midline and dilatation of the left lateral ventricle are present. (b) Section reveals a hypercellular, small cell malignant tumor with variable nuclei and indistinct cell borders surrounded by fibrillar material. Positive immunostaining for neuron-specific enolase, S-100, and GFAP suggests a neuroectodermal origin with glial differentiation. Cells cultured from this tumor yielded a normal male karyotype

46XY. (c) An area of palisading necrosis (*arrow*). PNET is one of the tumors other than glioblastoma to show necrosis with palisading. (d) EM depicting primitive-appearing cells with microfilaments. Some suggestive neurosecretory granules are found in other fields ((a–c) Reprinted from Isaacs [7]. © WB Saunders 1997; EM photomicrograph (d) Courtesy of Ann Peters, Department of Pathology, Rady Children’s Hospital San Diego)

9.5 Medulloblastoma

Medulloblastoma (cerebellar PNET) follows in frequency teratoma, astrocytoma, and choroid plexus tumors [7, 9] (Table 9.2) (Fig. 9.8). The tumor has been detected by imaging studies in both the fetus and infant [78, 82]. Macrocephaly and hydrocephalus are the main presenting findings [7–9]. Metastatic lesions may be the initial manifestation which is unusual for a brain tumor in this age group [81, 83].

Congenital anomalies are found in patients with medulloblastoma, for example, imperforate anus, omphalocele, cleft palate, myelomeningocele, cerebellar agenesis, dural arteriovenous malformations, and acrania [9, 22, 36, 85–89]. Of all brain tumors in the young, familial occurrence has been documented most often with medulloblastoma [9, 22]. It is reported in male siblings and in sisters with congenital tumors. There is a significant *association between medulloblastoma and rhabdoid tumor of the kidney* [9].

Medulloblastomas arise from the vermis of the cerebellum and grow into the fourth ventricle and adjacent cerebellar hemispheres. Subsequently, obstructive hydrocephalus and leptomeningeal seeding occur along the cerebrospinal axis [7–9, 75, 81–84]. At this time, the CSF cytological examination may reveal the presence of tumor cells.

With vascular invasion, the tumor enters the bloodstream and metastasizes, in 5–18 % of the time, to organs outside the CNS, primarily to the liver, lungs and bone marrow, and sometimes to the lymph nodes [83, 84]. Therefore, bone marrow examination and CSF cytology are an integral part of the initial metastatic work-up before starting therapy [7, 8].

Medulloblastoma falls into the category of the small blue cell tumor consisting of small darkly staining cells with varying amounts of intercellular pink-staining fibrillar material [8, 30, 46, 76–85] (Fig. 9.5b). Well-defined Homer-Wright rosettes are present in less than half the specimens and are similar to those found in neuroblastoma and retinoblastoma. Extensive necrosis and moderate mitotic activity are present [8, 30, 46, 76–85]. *Desmoplasia*, characterized by a nodular growth pattern with fibrosis, is observed in some tumors particularly in those removed from older infants but apparently has no prognostic significance [9]. Cerebellar PNETs with “divergent differentiation” show several different neuroepithelial components in addition to the small round, undifferentiated cells, for example, astrocytoma, oligodendroglioma, and ependymal elements [75, 77] (Fig. 9.7). Atypical teratoid/rhabdoid tumor, which has a much worse prognosis, can be confused with medulloblastoma [77]. The presence of the characteristic rhabdoid cell and INI1 gene mutational loss confirm the former diagnosis.

EM studies show that medulloblastoma shares some ultrastructural features in common with neuroblastoma [7, 43, 75]. The tumor is composed of small, primitive cells surrounded by cytoplasmic processes containing neurofilaments and neurotubules. In some specimens, dense core granules measuring 100 nm in diameter are present, but they are found in much smaller numbers compared to peripheral neuroblastoma (Figs. 9.6 and 9.7).

Prognosis for young patients with cerebellar PNETs in general remains bleak. Infants have clearly a worse outcome than older children [9].

9.6 Cerebral PNET

Cerebral PNET (Cerebral neuroblastoma) is an uncommon, highly malignant small blue cell tumor occurring primarily in young children and infants characterized by early recurrence, metastasis, and high mortality [9, 30, 75, 77, 78, 87, 88]. A fourth of all cerebral PNET’s occur before age 2 years (Table 8.3). The tumor has been detected by ultrasound in the perinatal period [46, 78, 82]. Some grow rapidly and enormously in utero replacing much of the brain causing macrocephaly and dystocia [46, 78, 87, 88].

Cerebral PNETs tend to be large with extensive cystic necrosis and hemorrhage occupying much of a cerebral hemisphere. The tumor is grayish tan, soft, and friable with focal firmer gliotic areas [8, 87, 88].

Microscopic examination reveals a highly cellular, small cell tumor with a high mitotic rate as the major component. Areas may be present with a histological appearance similar to the peripheral neuroblastoma such as Homer-Wright rosettes and pink fibrillar neuropil. Focal ganglion cell differentiation, a peripheral astrocytic component, and a prominent connective tissue stroma are additional but variable findings [8, 78, 87, 88] (Figs. 9.9 and 9.10). Focal ganglion cell differentiation, a peripheral astrocytic component and a prominent connective tissue stroma are additional but variable findings [78, 87, 88]. Other components such as ependymal, neuronal, retinal, or melanocytic cells are described [46, 75, 77]. Mesenchymal tissues, such as skeletal muscle, fibrous tissue, cartilage, and epithelium, are noted in some [43, 75–78]. Tumor cells are reactive with synaptophysin and neurofilament antibodies. Focal collections of hypertrophic astrocytes are immunoreactive with GFAP [88]. Neuronal processes containing microtubules and neurosecretory (dense core) granules are EM findings [88].

PNETs with glial differentiation tend to have a worse prognosis [46, 77]. The outcome of patients with this tumor is dismal [9] (Table 9.2).

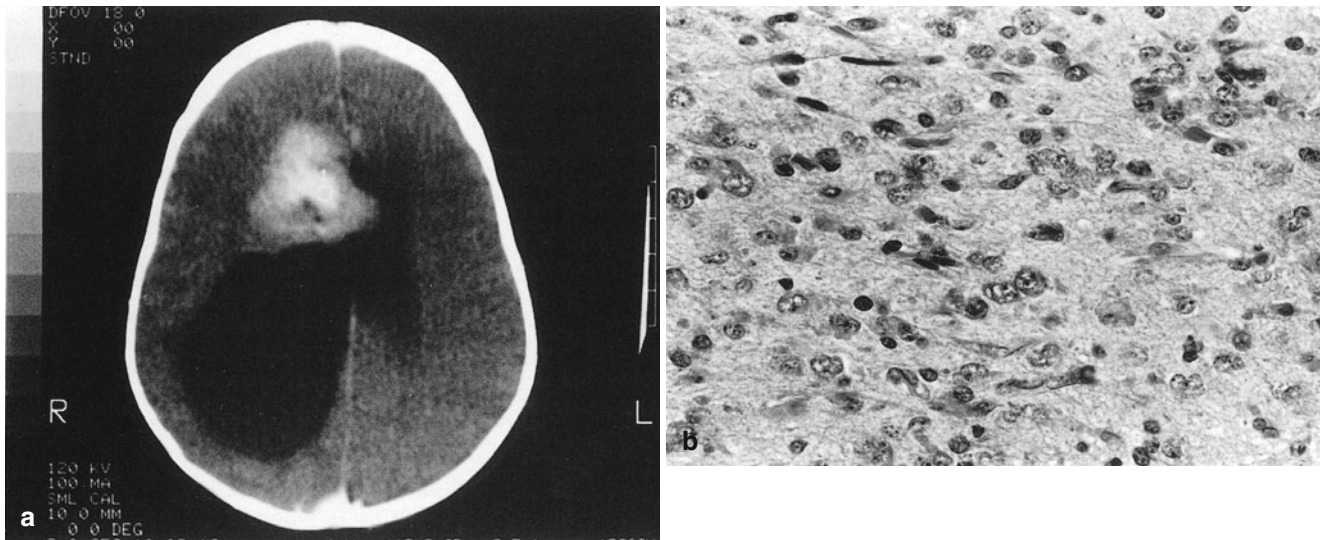


Fig. 9.11 Cerebral ganglioglioma. Seven-week-old male with macrocephaly, bulging tense fontanelles, conjugate eye deviation to the right, and left homonymous hemianopsia. (a) CT scan depicts a large enhancing mass occupying the right frontal lobe and extending into the adjacent ventricle. Obstruction of the foramen of Monro and dilatation of

the right lateral ventricle are present. (b) The tumor consists of atypical-appearing ganglion cells with slightly vesicular nuclei, one or two large nucleoli, and prominent eosinophilic cytoplasm accompanied by hypertrophic astrocytes (Reprinted from Isaacs [7]. © WB Saunders 1997)

9.7 Gangliocytoma

Gangliocytoma, by definition, is a tumor composed of mature, neoplastic ganglion cells with a minor non-neoplastic glial cell component [79, 90]. Grossly they are well delineated and often contain foci of calcification that may be seen on imaging studies. The tumors occur in any area of the CNS, but the frontal lobe is a common site. When located in the hypothalamic region, endocrine hyperfunction may occur [7]. Gangliocytomas are frequently of low cellularity and may be difficult to distinguish from neuronal heterotopias and hamartomas. The finding of bizarre binucleate or multinucleated neurons is considered diagnostic features [90]. Gangliocytomas are slow growing and usually do not undergo malignant change [31].

9.8 Ganglioglioma

Ganglioglioma is an uncommon CNS neoplasm found in patients of all ages including infants [7, 9, 90–93]. It comprises less than 5% of all brain tumors diagnosed in the pediatric age group. Macrocephaly and seizures are the main presenting signs [9, 91].

The tumors vary in size and are well circumscribed and finely granular on cross section. Histologically, they consist of collections of mature, sometimes atypical-appearing ganglion cells and astrocytes surrounded by a network of glial fibers and fibrosis [30, 91–93] (Fig. 9.11). Microcysts and foci of calcification are present occasionally.

9.9 Infantile Desmoplastic Ganglioglioma

This is a distinctive supratentorial neoplasm arising as a mass with solid and cystic cortical components. Typically, they are situated peripherally next to the meninges [8, 90, 93–95] (Fig. 9.12a). It may be discovered at birth [8, 94]. Sometimes spontaneous hemorrhage into the tumor is the initial finding [9].

Histologically, desmoplastic infantile ganglioglioma consists of a dominant fibrous tissue component composed of fascicles of spindle-shaped fibroblastic cells often displaying a storiform (“cart wheel”) growth pattern (Fig. 9.12b–d). Variable numbers of glial, neuronal, and sometimes primitive neuroectodermal components are present [8, 93–95]. Calcification and Schwann cell elements occur in a few tumors. Astrocytic cells are immunoreactive with GFAP, whereas the neural component stains positively with NSE and S-100 protein but not with GFAP. The fibroblastic areas are not reactive with either these antibodies but stain strongly with Masson’s trichrome (Fig. 9.12d). Moreover, focally positive macrophage antigens (Ki-M1P) are present in the fibrous areas [94].

EM features consist of astrocytic cells containing intermediate filaments and pericellular basal lamina and cells with neuronal differentiation composed of dense core granules. The fibroblastic cells have margined chromatin, ribosomes, intermediate filaments, and Golgi apparatus and are surrounded by collagen, features similar to those described for the fibroblasts of fibromatosis and fibrous histiocytoma [93, 94].

Infants with gangliocytoma, ganglioglioma, and desmoplastic ganglioglioma generally experience a favorable clinical outcome providing complete surgical resection is achieved

[92, 93] (Table 9.2). Nevertheless, seizures may persist in some patients following surgery.

Desmoplastic astrocytoma of infancy, previously mentioned above, and desmoplastic infantile ganglioglioma share

similar imaging, clinical, and pathological findings suggesting that perhaps they might be variations of the same neoplasm [93–95].

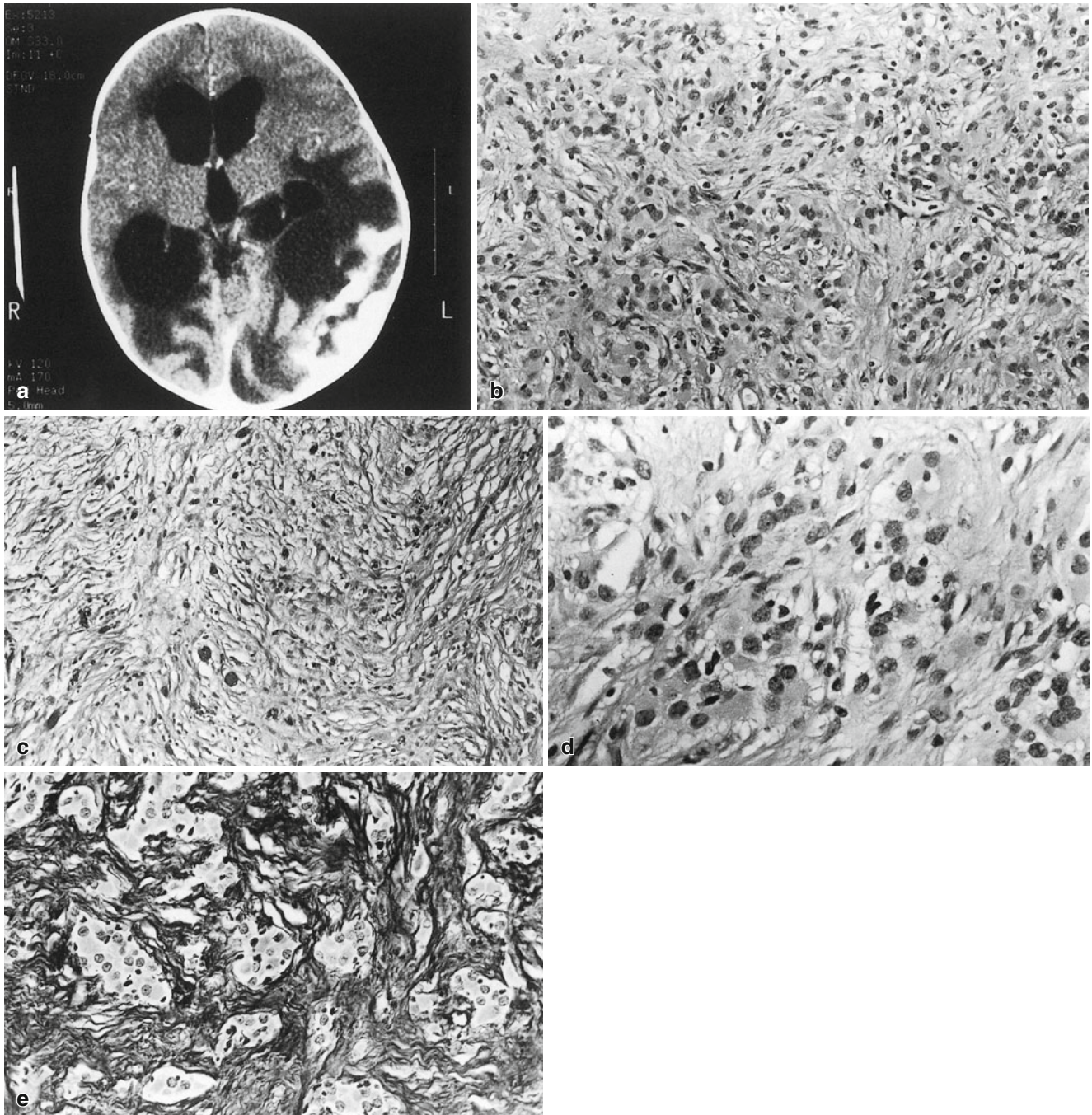


Fig. 9.12 Infantile cerebral desmoplastic ganglioglioma. Five-month-old female with macrocephaly and vomiting. (a) CT scan reveals a large, superficial contrast-enhancing, cystic mass within the left parieto-occipital lobes and marked ventriculomegaly. (b) Clusters of ganglion cells are surrounded by a fibrous tissue spindle cell component. (c) Dense desmoplastic areas consisting of spindle-shaped cells com-

prised most of this tumor. (d) Ganglion cells are round with slightly vesicular nuclei and prominent nucleoli. (e) Reticulin stain demonstrating collagen tissue surrounding ganglion cells. Immunohistochemical findings: vimentin, S-100, and GFAP positive; ganglion cells focally reactive with synaptophysin and NSE (Reprinted from Isaacs [7]. © WB Saunders 1997)

9.10 Ependymoma

Ependymoma comprises 10 % of all central nervous system tumors in children [96, 97]. In some series, it is the third most frequently diagnosed brain tumor in infants (16 % of the total) and fourth in rank in the newborn (10 %) [7, 9]. Most ependymomas of the fetus and infant arise from the region of the fourth ventricle [96–101] (Table 9.2 and Fig. 9.13a). Occasionally, they occur near the lateral ventricle, the main site in adults.

Neonates with ependymomas present with macrocephaly, hydrocephalus, and signs of increased intracranial pressure; some tumors cause dystocia, spontaneous intracerebral hemorrhage, and stillbirth [96–101] (Fig. 9.13b). CNS metastases may be present at the time of diagnosis [97].

Ependymomas are tumors derived from and consist of ependymal cells originating from within or near the ependymal lining of the ventricles or central canal of the spinal cord [31, 98, 102]. In the newborn and infant, most are classified as the cellular type and are composed of rather uniform darkly staining cells forming characteristic ependymal perivascular rosettes [8, 102] (Figs. 9.13c, d and 9.14b). Halos or clear zones distributed about blood vessels surrounded by tumor cells are helpful in making the diagnosis especially on frozen section [8]. Mitoses are not uncommon.

Touch smear preparations show fine processes extending out from tumor cells (Fig. 8.14b). GFAP reactivity is variable and is usually most prominent within the fibrillary processes radiating toward central vessels in the perivascular rosette.

The presence of perivascular rosettes by light microscopy and cilia, microvilli, cytoplasmic intermediate filaments, and long junctional complexes demonstrated by EM helps to distinguish ependymomas from other neuroepithelial tumors [102].

Anaplastic ependymomas are highly aggressive ependymal tumors with a poor prognosis classified as WHO Grade III. Distinguishing histological features include poorly differentiated tumor cells, increased cellularity, and mitotic activity accompanied by palisading necrosis and microvascular proliferation (Fig. 9.13e).

The primitive-appearing *embryonic ependymoblastoma* is a rare variant considered by some as a PNET with ependymal differentiation [96, 98, 103, 104]. This highly cellular, small blue cell tumor infiltrates the leptomeninges and spreads along the CSF pathways in a manner similar to medulloblastoma and other central nervous system PNETs. The tumor consists of small uniform cells lining canals, showing a high mitotic rate and forming rosettes and tubular structures [98, 103, 104]. Extensive necrosis is present.

Ependymoblastomas are immunoreactive with vimentin and S-100 but are not reactive with cytokeratin or neurofilament antibodies. Cells are focally positive for GFAP [104]. By EM, the tumor cells are characterized by a high nuclear to cytoplasmic ratio, scanty rosettes and cytoplasmic organelles, junctional complexes, rudimentary cilia, few basal bodies, and glial-like filaments [104].

Ependymal tumors generally have a poor prognosis regardless of cell type or age of the patient [9, 96, 98, 101].

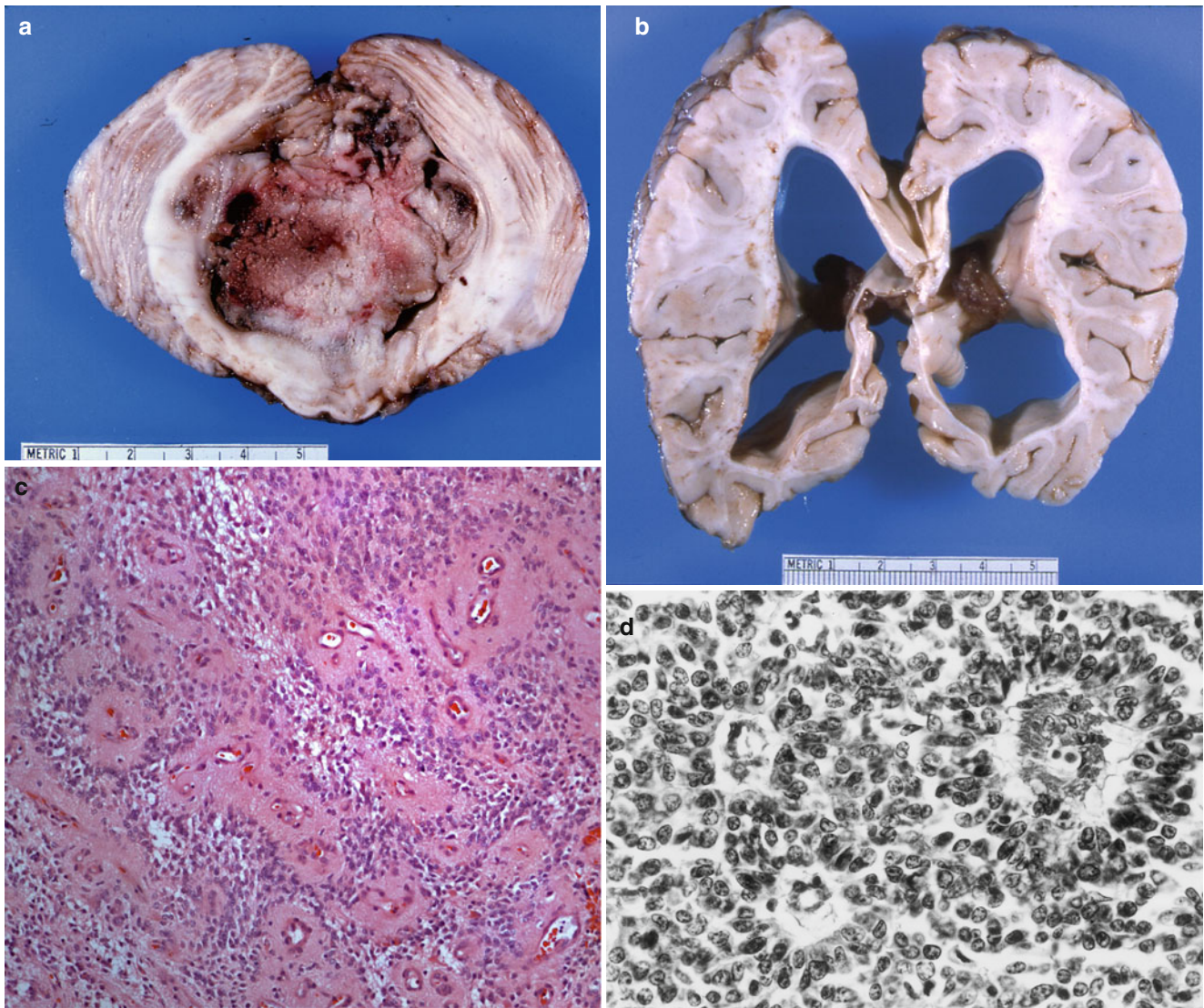


Fig. 9.13 Ependymoma. 9-month-old male with macrocephaly, vomiting, and marasmus progressing over a 5-month period. Imaging studies reveal severe hydrocephalus (the mantle measured only 1.5 cm in thickness), aqueduct stenosis, and a large midline cerebellar mass. **(a)** Gross photograph shows a 7×5×-cm, midline cerebellar tumor occupying the fourth ventricle, invading both hemispheres, the mesencephalon, pons,

and medulla. The immediate cause of death was a 3×3 cm recent hemorrhage within the fourth ventricle filling the aqueduct of sylvius. **(b)** Severe hydrocephalus is seen in a more proximal coronal section. **(c)** Low magnification reveals a cellular, rather uniform small cell neoplasm forming perivascular rosettes. **(d)** Higher magnification of the ependymal rosettes (Reprinted from Isaacs [7]. © WB Saunders 1997)

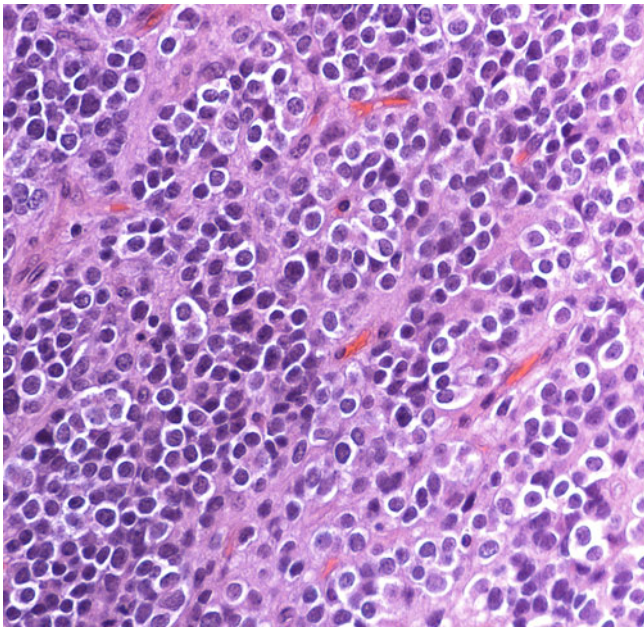


Fig. 9.14 Anaplastic Ependymoma of the fourth ventricle showing poorly differentiated tumor cells, increased cellularity, and mitotic activity accompanied by microvascular proliferation

9.11 Choroid Plexus Papilloma

Choroid plexus papillomas are tumors composed of epithelial cells that line the ventricular choroid plexuses [7, 8, 30, 31] (Fig. 9.15a–d). About half in the pediatric age group are diagnosed during the first year of life [3, 7, 8, 25, 105–112].

Choroid plexus papillomas comprise 10 % of all brain tumors in infants and 5 % of all perinatal brain tumors [4]. They are the cause of rapid onset of hydrocephalus in the fetus and infant and occasionally stillbirth [7–9, 26, 105–112] (Table 9.2).

Typically, the papilloma expands into the lateral ventricle producing a large space-occupying nodular lesion readily demonstrated by imaging studies [8, 105–112] (Fig. 9.15a). Less often, they arise from the third or fourth ventricle [108–110]. Large quantities of CSF are formed by the tumor resulting in marked dilatation of the ventricular system which may be noted at birth. Choroid plexus papillomas occur in association with the Aicardi syndrome and giant pigmented nevi [106, 112].

The papilloma has a finely nodular, pink, cauliflower-like gross appearance, and microscopically, the tumor consists of numerous fingerlike papillary formations covered by uniform, regular cuboidal to columnar epithelial cells resembling choroid plexus [8, 105–112] (Fig. 9.15b). Immunohistochemical findings are an expression of both epithelial (cytokeratin) and glial (GFAP) markers; like normal choroid plexus, microvilli, cilia, and zonula adherens junctions are observed by EM [105, 107, 113].

Choroid plexus papillomas may show atypical features such as hypercellular epithelium, mitoses, shortening, and broadening papillary formations (Fig. 9.16a–c).

Generally, complete surgical resection of choroid plexus papillomas results in cure. However, the procedure may be difficult and complicated by fatal hemorrhage because the tumors are so highly vascular [7–9].

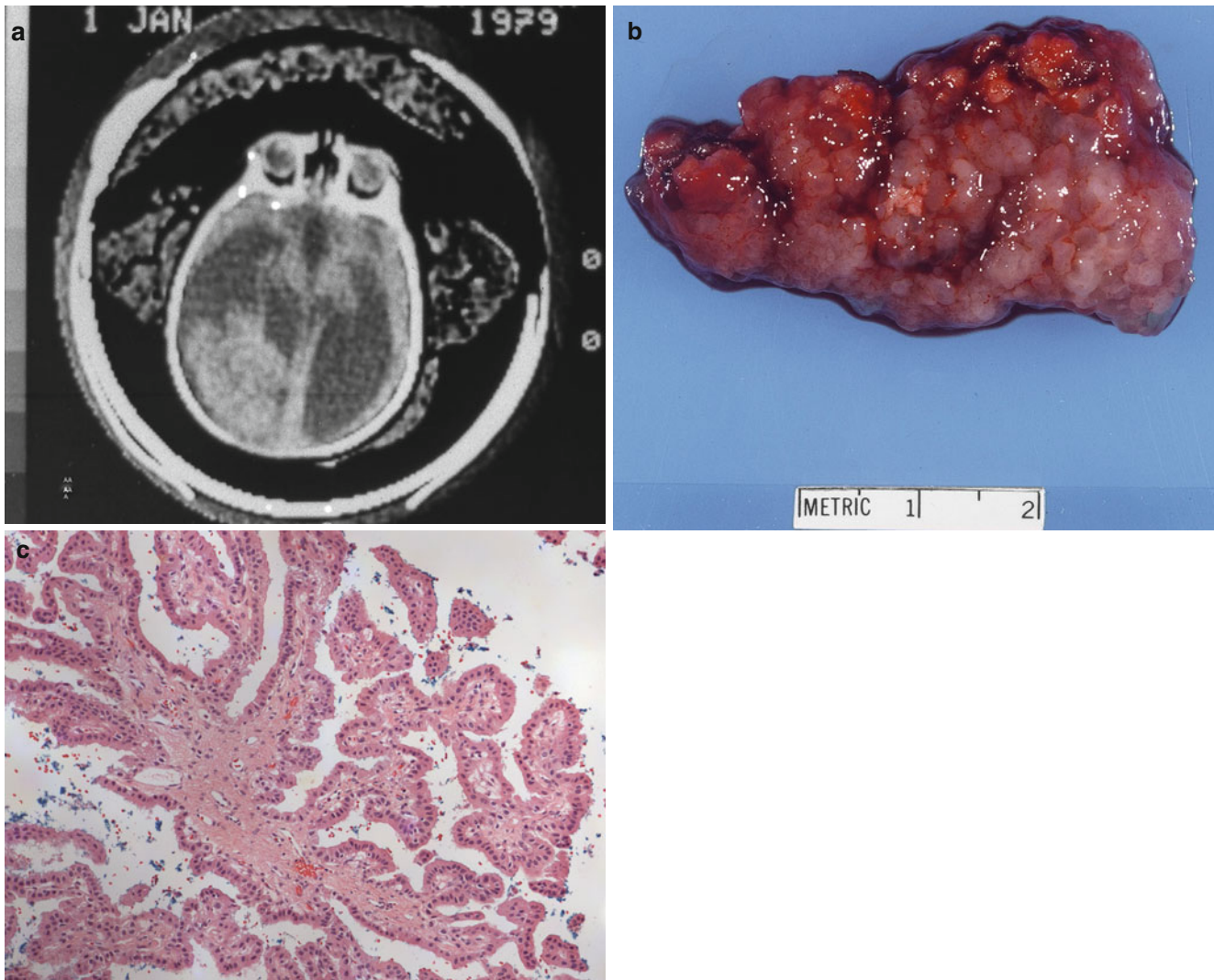


Fig. 9.15 Congenital choroid plexus papilloma. Rapidly progressive hydrocephalus, a bulging fontanelle, and vomiting were the presenting signs in this 1-month-old female. **(a)** CT scan reveals a large, enhancing mass partially filling the left lateral ventricle and severe hydrocephalus. **(b)** Two cauliflower-like masses, 5.5×2.7 cm and 4.7×3.5 cm, were

excised from the left lateral ventricle. The larger one is depicted in the gross photograph. **(c)** Low-power view showing the overall architecture and resemblance to normal choroid plexus. Edematous papillary structures are lined by small cells with regular, round to oval darkly staining nuclei (Reprinted from Isaacs [7]. © WB Saunders 1997)

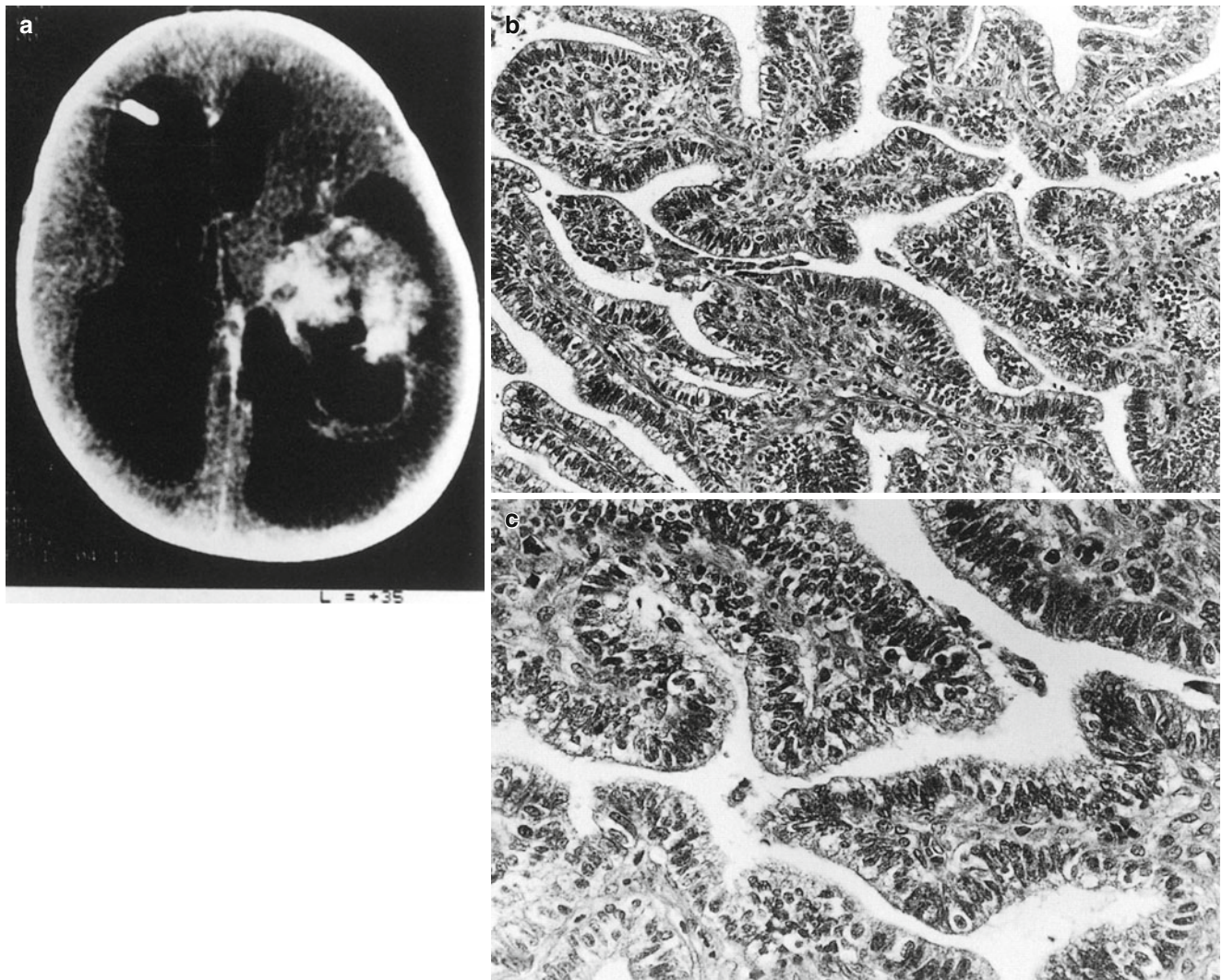


Fig. 9.16 Choroid plexus papilloma with atypical changes. Two-month-old male with hydrocephalus. **(a)** CT scan depicts a large nodular mass partially filling the left lateral ventricle. Severe hydrocephalus is present. **(b)** Low-power view reveals only slight resemblance to normal choroid plexus. The papillary formations have a more blunted appear-

ance than normal. **(c)** Moderate cytological atypia, increased nuclear/cytoplasmic ratio, and cellularity are noted (compare with Fig. 9.14c). There is no invasion into the underlying stroma. (Courtesy of Ignacio Gonzalez, M.D., Department of Pathology, Childrens Hospital Los Angeles; Reprinted from Isaacs [8]. © Springer-Verlag, 2002)

9.12 Choroid Plexus Carcinoma

Fewer than one third of *choroid plexus carcinomas* are diagnosed in the first year of life [8, 107, 113–115]. Most occur in the lateral ventricles. Widespread dissemination throughout the cerebrospinal subarachnoid space, a fatal complication, may be found at the time of diagnosis [115]. Sometimes the histological distinction between papilloma and carcinoma may prove difficult [113]. The diagnosis of malignancy depends on several histological criteria, namely, poorly formed

papillary structures, infiltration into adjacent tissues, hypercellularity, pleomorphic nuclei, increased mitotic activity, vascular proliferation, and necrosis [31, 107, 113] (Fig. 9.17a, b). In some areas, the tumor cells resemble undifferentiated carcinoma. Immunohistochemical studies may be useful in establishing the diagnosis of malignancy [107, 113].

Prognosis. Choroid plexus papillomas have one of the best survival rates of all infant CNS tumors [9], whereas the prognosis for choroid plexus carcinomas is much less encouraging [115, 116].

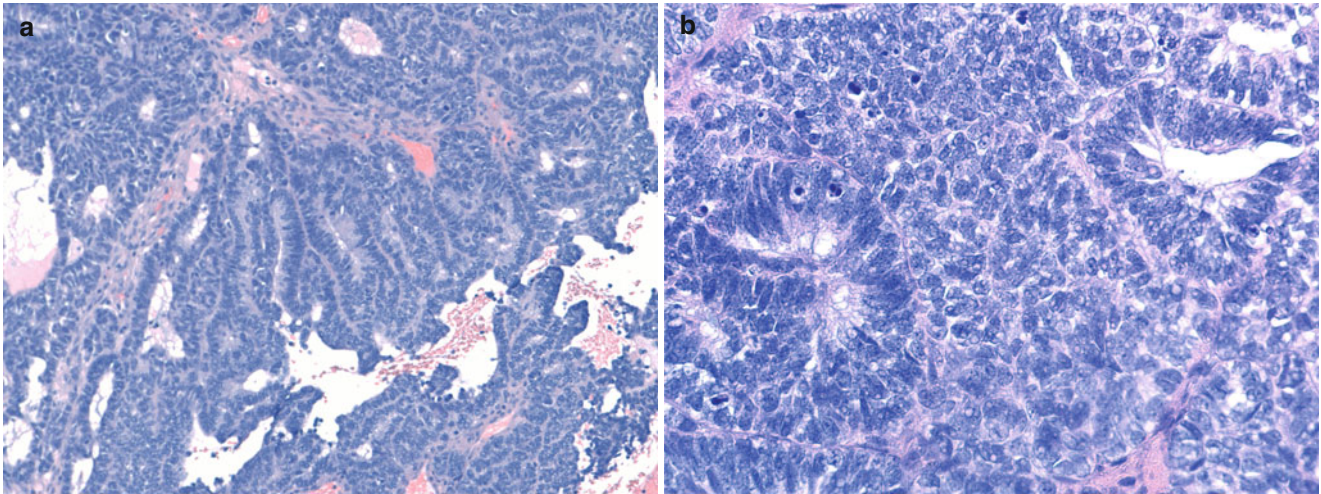


Fig. 9.17 Choroid plexus carcinoma, lateral ventricle. (a) The papillary architecture is only partially preserved with only a few fingerlike projections lined by atypical epithelium. (b) Higher magnification

reveals features of a poorly differentiated carcinoma (Reprinted from Isaacs [8]. © Springer-Verlag, 2002)

9.13 Oligodendroglioma

Oligodendrogliomas are exceptionally rare in fetuses and infants comprising less than 1 % of cases, for example, 2 of 250 patients, in one series [9]. The cerebrum is the main site of origin, and most are histologically benign. Seizures are common at presentation and, if large enough, signs and symptoms of increased intracranial pressure [30].

Microscopic findings are described by Burger and Scheithauer: histological and cytological monotony, round nuclei with small prominent nucleoli, clear perinuclear halos (fried egg effect), small curved capillaries (chicken wire pattern), and calcifications [30] (Fig. 9.18).

The tumors are often unresectable. The two newborns described above did not survive [9].

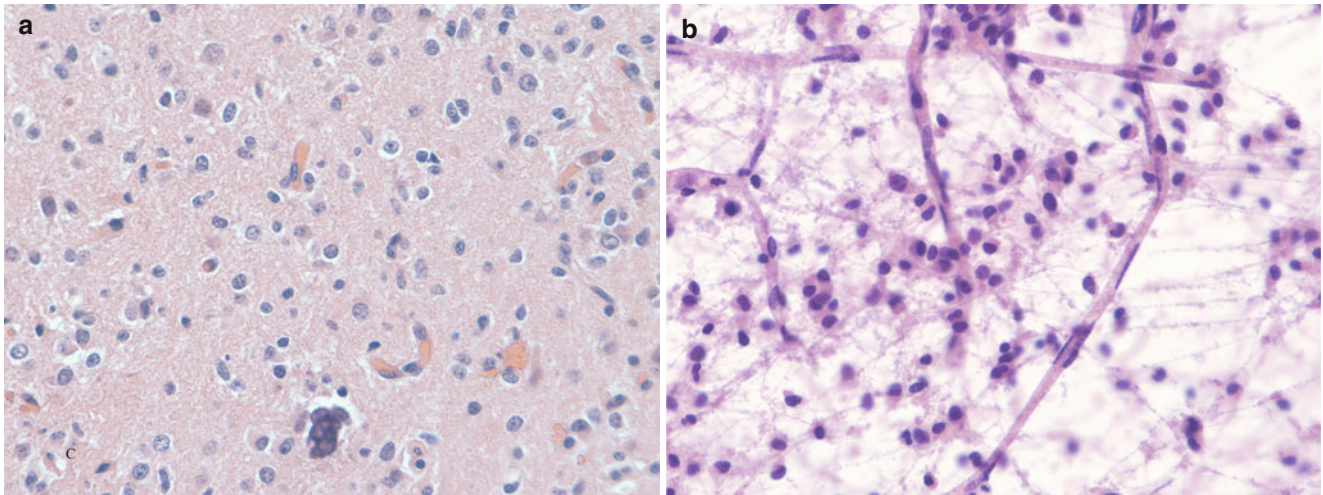


Fig. 9.18 Oligodendroglioma, cerebral cortex. **(a)** Round to oval tumor cells with tiny nucleoli, some cells with perinuclear halos, curved delicate capillaries, and foci of calcification. **(b)** The touch smear

reveals small round to oval tumor cells with tiny nucleoli accompanied by delicate branching capillaries

9.14 Craniopharyngioma

Although *craniopharyngioma* is a relatively common tumor of childhood comprising 10 % of intracranial neoplasms, it seldom occurs in the fetus and infant [7–9, 117–121]. Because of its epithelial morphology and location intimately related to the pituitary gland, it is thought to arise from Rathke’s pouch, an ectodermal diverticulum developing from the roof of the mouth. *Macrocephaly* and a *suprasellar mass* are the most frequent findings [7, 9, 117–121]. Polyhydramnios is variably present. The *CSF protein level is characteristically and significantly elevated* [7, 117]. Imaging studies

reveal a heterogeneous, calcified, cystic mass in the suprasellar region. Large tumors may completely replace all normal brain tissue in a manner similar to that of a teratoma [119, 120]. Microscopically, craniopharyngiomas display both *squamous* and *adamantinomatoid patterns* with keratin pearls and foci of calcification [8, 30, 120] (Fig. 9.19a, b). Clusters of necrobiotic squames are an important feature of the adamantinomatous pattern [30].

Fetuses and infants with large craniopharyngiomas generally have a poor prognosis with only a few survivors [9, 121] (Table 9.1).

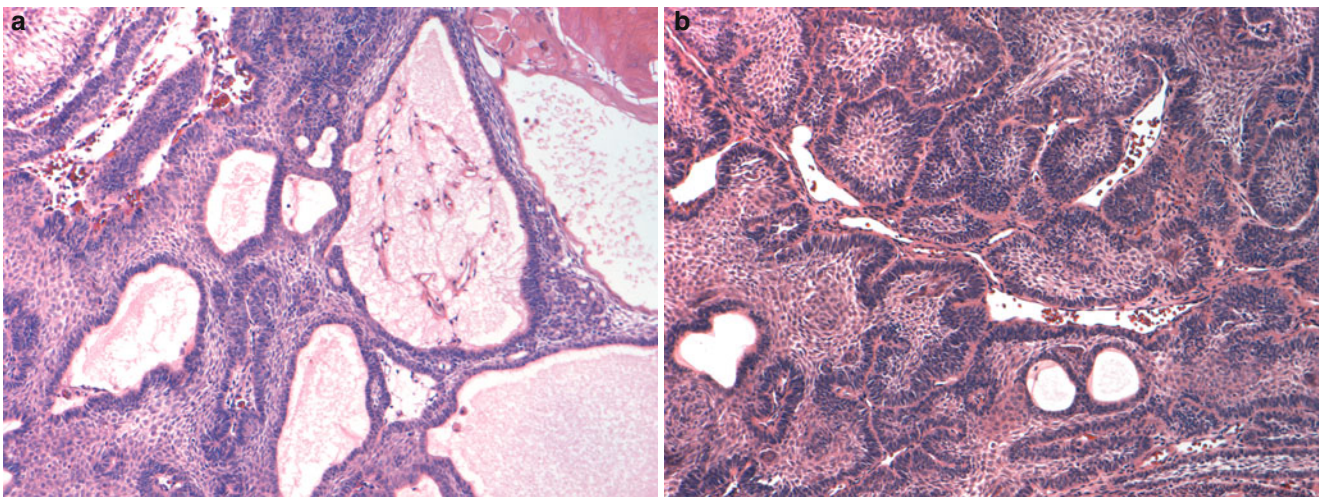


Fig. 9.19 Craniopharyngioma. Three-month-old female with upward gaze nystagmus and a suprasellar mass (with enhancement) detected on CT scan. **(a)** The tumor consists of epithelial cells forming compact masses or lining cysts. **(b)** Nests of epithelial cells are surrounded by a

layer of columnar “basal” cells separated by a myxoid stroma consisting of stellate cells forming the “adamantinomatous” pattern. Clusters of keratin pearls are noted in the *right side* of the photomicrograph (Reprinted from Isaacs [8]. © Springer-Verlag, 2002)

9.15 Atypical Teratoid/Rhabdoid Tumor

The highly malignant *atypical teratoid/rhabdoid tumor* (AT/RT) of the central nervous system is similar biologically and histologically to the rhabdoid tumor found in the kidney, soft tissues, and other sites [9, 37, 122–127]. This group of tumors is found primarily in infancy and early childhood and most prove fatal [9, 37, 122–127]. Since expression of multiple lineages in these CNS tumors suggests a teratomatous process, the term atypical teratoid/rhabdoid tumor was coined by Rorke et al. [122]. The posterior fossa particularly the cerebellum is the major site of origin. In this location, atypical teratoid/rhabdoid tumors show similar clinical and imaging findings as medulloblastoma but are characterized by a more fulminant course than the latter (Fig. 9.20a). Cerebral hemispheres and brain stem are other primary sites [37, 122, 125–127]. Congenital examples presenting with hydrocephalus or hydranencephaly (complete or almost absence of cerebral hemispheres) are described [9, 125, 126]. The tumor has been detected antenatally by sonography [122].

Grossly atypical teratoid/rhabdoid tumors consist of tan-gray friable tissue with areas of necrosis [9, 126, 127]. They are distinguished histologically from medulloblastoma and other PNETs by the presence of the characteristic rhabdoid cells, which have an eosinophilic cytoplasm, a round vesicular nucleus with a large nucleus, and a cytoplasmic eosinophilic paranuclear inclusion composed of intermediate filaments (Fig. 9.20b, c). Most atypical teratoid/rhabdoid tumors are composed of two main components, both rhabdoid and PNET, the latter having the

appearance of other “small blue cell tumors” of childhood [9, 122, 125]. Occasionally, epithelial glands and Homer-Wright rosettes are present. The tumors display a complex polyphenotypic immunophenotype. Vimentin, epithelial membrane antigen, cytokeratin, glial fibrillary acidic protein, and cytokeratin are variably immunoreactive [125]. Smooth muscle actin, chromogranin, and synaptophysin are variably expressed.

By EM, the presence of cells with circumscribed bundles of intermediate filaments forming tight whorls, corresponding to the eosinophilic cytoplasmic paranuclear inclusions observed by light microscopy, is a diagnostic feature of the rhabdoid cell [37, 122, 125, 127]. Moreover, demonstration of the mutation deletion of the INI1 gene located at chromosome 22q11 is required for definitely establishing the diagnosis [37]. Diagnosis of rhabdoid tumor is very important because this finding is predictive of a much worse prognosis than that for medulloblastoma, which also has a small blue cell malignant component [9, 122, 125, 126]. Brain invasion, recurrence, and early CSF spread contribute to a dismal overall short survival of less than a year [9, 30, 37] (Table 9.1).

9.16 Medulloepithelioma

The *medulloepithelioma* of the central nervous system is a rare malignant neoplasm of early childhood; average age of diagnosis is at 2 years of age. Only a few congenital cases are reported [6, 9, 128–130]. Overall, the paraventricular region of the cerebrum is the most common site, but tumors

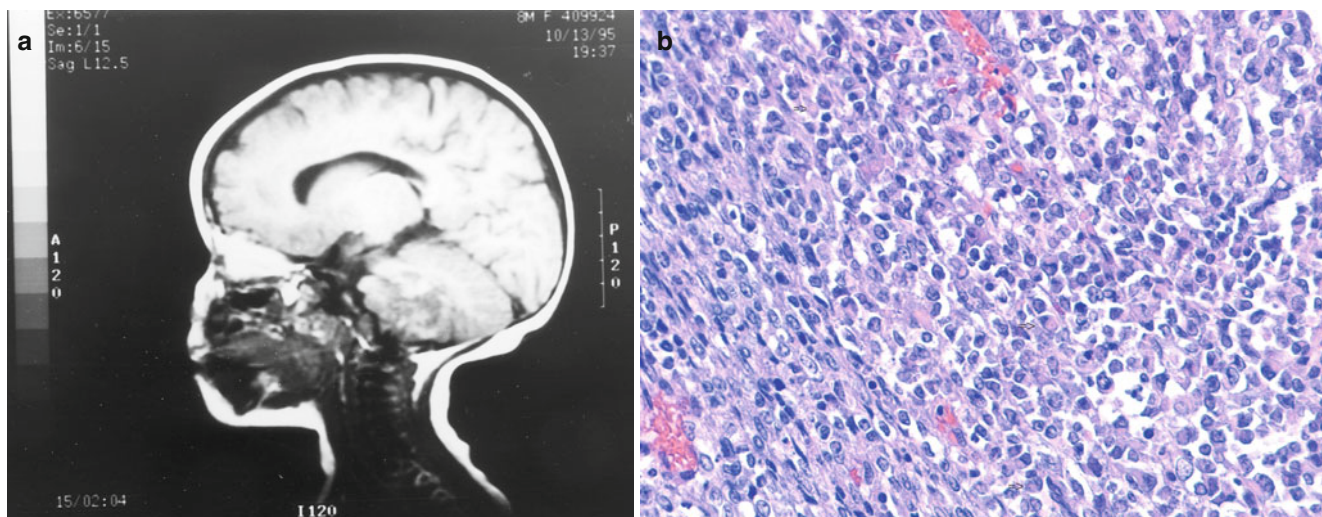


Fig. 9.20 Atypical teratoid/rhabdoid tumor. Eight-month-old girl with a posterior fossa mass. (a) MRI displays a 3-cm tumor in the left cerebellar peduncle which enhances slightly. (b) The tumor shows a varied histological appearance. Small vacuolated cells contain round to oval nuclei with a fine chromatin pattern and a prominent nucleolus. Larger oval to rectangular cells with eccentric nuclei and prominent nucleoli. Some

contain cytoplasmic paranuclear eosinophilic inclusions representing packets of intermediate filaments (arrows). Immunoperoxidase studies: NSE and EMA stain strongly positive, keratin and actin focally weakly reactive, and GFAP and synaptophysin negative. Cultured tumor cells yielded a 46XX karyotype and a chromosome 22 deletion with absence of INI1 activity (Reprinted from Isaacs [8]. © Springer-Verlag, 2002)

may occur in almost any location in the brain and spinal cord. The *midbrain and cerebellum are primary sites* described in the infant [128–130] (Table 10). *Increasing head size, seizures, strabismus, hemiparesis, lethargy, and coma are the presenting signs* [128–130]. These highly malignant neoplasms extensively invade structures locally and spread along the CSF pathways similar to other the PNETs described above.

Medulloepithelioma is a unique “embryonal tumor” which histologically resembles the primitive medullary epithelium of the medullary plate and neural tube. The tumor forms papillary and tubular structures composed of crowded pseudostratified columnar cells delineated by well-defined basement membranes. In addition, there is divergent differentiation ranging from embryonal to mature neuroepithelial and neuronal cell types [128–130]. The tumors consist of primitive medullary epithelium as described above with foci of astrocytes, oligodendroglia, ependymal cells, neuroblasts, and mature ganglion cells in varying amounts. The medulloepitheliomatous component is not immunoreactive with glial fibrillary acidic protein, neuron-specific enolase, or S-100 protein [129]. However, this component shows vimentin and microtubule-associated protein type-5 reactivity similar to what is found in primitive neural tube cells. The prognosis for patients with this tumor is bleak [9, 128–130] (Table 9.1).

9.17 Meningioma

Meninges are the primary site of a variety of benign and malignant mesenchymal tumors of childhood ranging from *meningiomas* to *sarcomas* and *melanomas* [8, 9, 131–136]. In one significant survey, 1.8 % of all intracranial tumors of childhood were meningeal in origin compared to 14 % for adults [131].

To date, less than 100 cases of *meningioma* have been reported in infants [1, 7–9, 131–136]. Meningiomas of the young are distinctly different from those occurring in older age groups [131, 134]. They are found more often in males and more frequently convex rather than infratentorial in location. The major signs and symptoms in infants are *macrocephaly, tense fontanelle, cranial asymmetry, vomiting, seizures, and diffuse spasticity* [9, 131–136]. Twenty percent of infants were *stillborn* in one study [9].

Some tumors attain a large size, for example, a meningioma removed from a 5-month-old male weighed 600 g [136]. About half the tumors arise from the parietal and/or occipital meninges, and about half are malignant (meningeal sarcomas) [9]. The histological type is usually *fibroblastic*

consisting of uniform spindle cells with a prominent vascular component [8, 9, 131, 134]. Moreover, other histological types include *angioblastic, meningothelial*, and the *sclerosing meningioma* composed of whorling collagen bundles and cells with perinuclear halos [8, 9, 31].

Surgery is the treatment of choice. The prognosis is good provided that the tumor is completely excised [9, 131, 134] (Table 9.1).

9.18 Vascular Malformations of the Brain

Although benign histologically, a variety of intracranial vascular conditions cause significant morbidity and mortality during the first year of life. *Arteriovenous malformations, Sturge-Weber syndrome, cavernous hemangioma, and neonatal hemangiomatosis* are examples involving the CNS [7, 8, 23, 137–140].

Cyanosis and congestive heart failure are manifestations of large intracranial arteriovenous malformations, and because of these findings, they may be mistaken for congenital heart disease [7, 23]. In one perinatal study, there were five newborns with large intracerebral arteriovenous malformations who presented with cyanosis and congestive heart failure [7, 23]. Because of their clinical presentation, three of five were given the presumptive diagnosis of a large congenital heart defect. However, audible cranial bruits in the other two were more consistent with an intracranial arteriovenous malformation. Postmortem examination performed on all five neonates who died within 3 days after birth revealed anastomoses or fistulae between the cerebral or meningeal arteries and cerebral veins, sagittal sinus, or vein of Galen. The adjacent brain showed variable amounts of hemorrhage, necrosis, and calcification. The hearts of these neonates were considerably enlarged and dilated with right ventricular hypertrophy suggestive of high-output heart failure resulting from the large intracranial arteriovenous shunts. Another infant in this study had the Sturge-Weber syndrome (flat facial hemangioma, meningeal hemangioma with seizures) and presented with intractable seizures and a port-wine stain hemangioma distributed over the left side of his face, forehead, and parietal area. CT scans revealed left cerebral atrophy and focal calcifications in the left parietal area which was confirmed on gross and microscopic examination of the hemispherectomy specimen [8] (Fig. 9.21a–d). Diffuse hemangiomatosis of the leptomeninges with focal involvement of gray and white matter of the temporal and occipital lobes was also found [8].

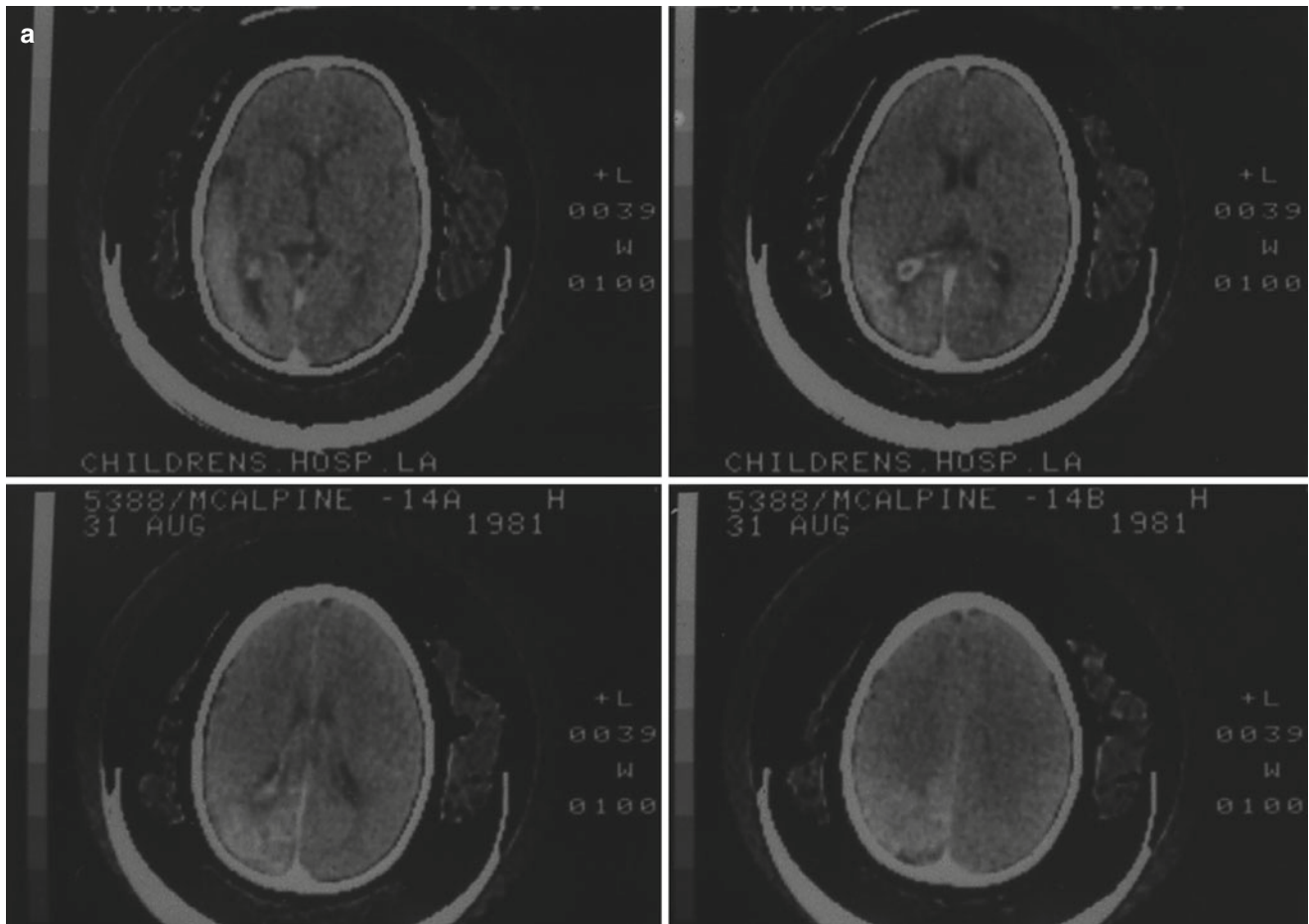


Fig. 9.21 Sturge-Weber syndrome. 1-year-old male with a “port-wine-stain” hemangioma distributed over the left side of the face, forehead, and parietal area and a history of intractable seizures. **(a)** CT scan reveals left cerebral atrophy and focal calcifications. **(b)** The cortical surface of the left cerebral hemispherectomy shows thickening and discoloration of the leptomeninges due to a diffuse hemangioma situated over the temporal, parietal, and occipital areas. **(c)** Cut surface of the cerebral hemisphere showing diffuse thickening of the leptomeninges

and a focal lesion in the cortical gray and white matter. **(d)** Photomicrograph of the temporal lobe depicting a leptomeningeal hemangioma composed of numerous thin-walled vessels lined by a single layer of flattened endothelium and separated by variable amounts of loose connective tissue. The adjacent gray and white matter show gliosis and focal neuronal necrosis (Reprinted from Isaacs [7]. © WB Saunders 1997)

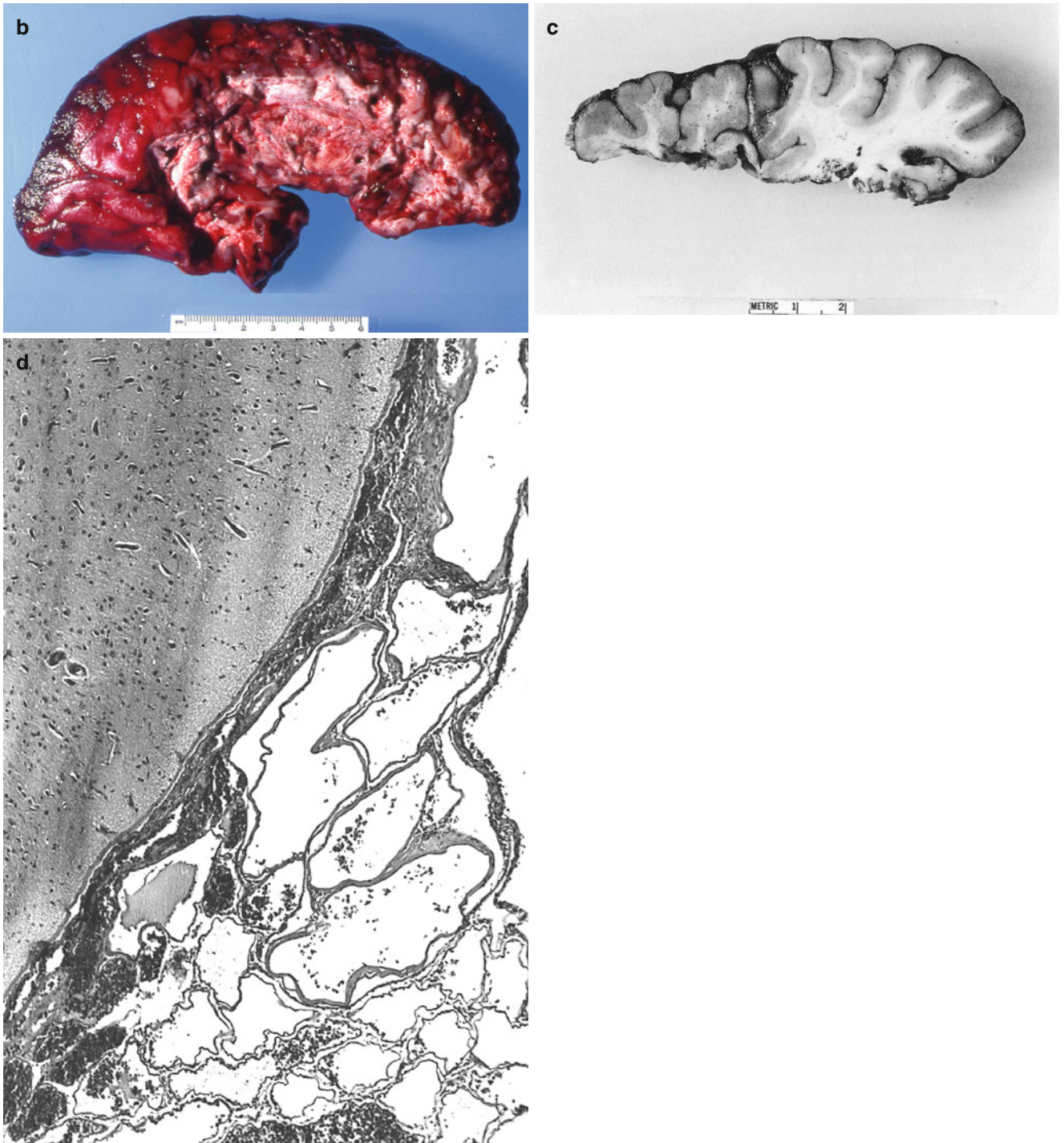


Fig. 9.21 (continued)

9.19 Prognosis for Infants with Brain Tumors

Outcome is related to the size and location of the tumor, the histological type, surgical resectability, and the condition of the infant at the time of diagnosis [9]. Fetuses and

infants with choroid plexus papillomas, gangliogliomas, and low-grade astrocytomas have the most favorable prognosis, whereas those with teratomas and primitive neuroectodermal tumors have the worst [9] (Fig. 9.22 and Table 9.1).

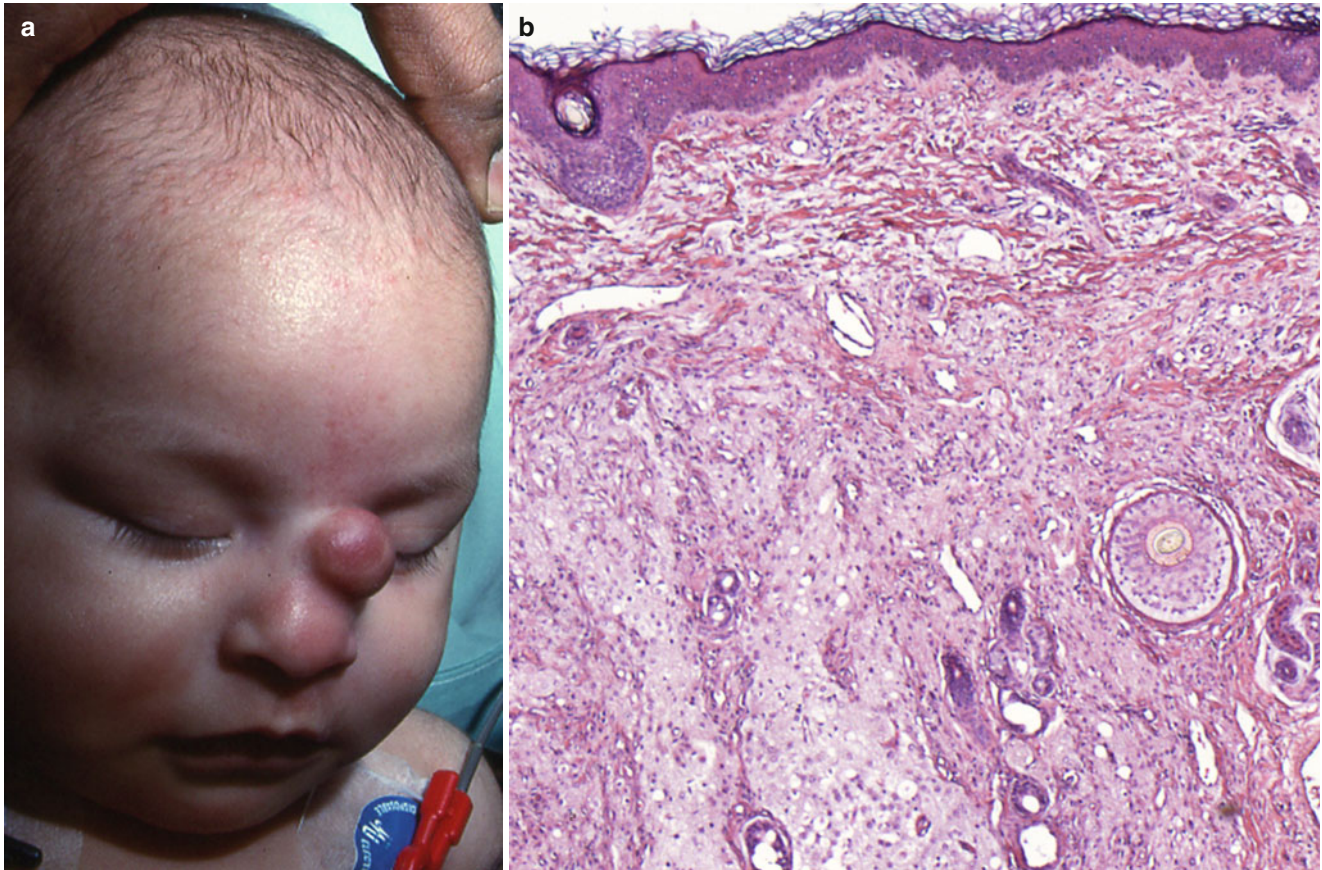


Fig. 9.22 Nasal encephalocele (“nasal glioma”). **(a)** Newborn with a firm, round nodule situated on the bridge of the nose. Intracranial CT scan does not reveal a communication with the brain. The nasal mass

has a firm, fibrous-appearing cut surface. **(b)** Collections of glial cells are present beneath the dermis (Reprinted from Isaacs [7]. © WB Saunders 1997)

9.20 Miscellaneous Craniofacial Anomalies

Encephaloceles are herniations of the brain or meninges through a defect in the skull [141]. Most occur in the occipital region. Others are found on the bridge of the nose where they have been called “nasal gliomas” (Fig. 9.22). Etiology is unknown.

References

- Jellinger K, Sunder-Plassman M (1973) Congenital intracranial tumors. *Neuropadiatrie* 4:46–63
- Farwell JR, Dohrman GJ, Flannery J (1978) Intracranial neoplasms in infants. *Arch Neurol* 35:533–537
- Jooma R, Kendall BE (1982) Intracranial tumors in the first year of life. *Neuroradiology* 23:267–274
- Oi S, Kokunai T, Matsumoto S (1990) Congenital brain tumors in Japan (ISPN Cooperative Study): specific clinical features in neonates. *Childs Nerv Syst* 6:86–91
- Takaku A, Kodama N, Ohara H, Hori S (1978) Brain tumors in newborn babies. *Childs Brain* 4:365–375
- Mazewski CM, Hudgins RJ, Reisner A, Geyer JR (1999) Neonatal brain tumors: a review. *Semin Perinatol* 23:286–298
- Isaacs H Jr (1997) Brain tumors. In: Tumors of the fetus and newborn. Major problems in pathology, vol 35. W.B. Saunders, Philadelphia, pp 187–228
- Isaacs H Jr (2002) Brain tumors. In: Tumors of the fetus and infant: an atlas. Springer, New York, pp 199–240
- Isaacs H (2002) I & II. Perinatal brain tumors: a review of 250 cases. *Pediatr Neurol* 27:249–342
- Young JL, Miller RW (1975) Incidence of malignant tumors in U.S. children. *J Pediatr* 86:254–258
- Parkes SE, Muir KR, Southern L, Cameron AH, Darbyshire PJ, Stevens MC (1994) Neonatal tumours: a thirty-year population based study. *Med Pediatr Oncol* 22:309–317
- Bader JL, Miller RW (1979) U.S. cancer incidence and mortality in the first year of life. *Am J Dis Child* 133:157–159
- Isaacs H Jr (1987) Congenital and neonatal malignant tumors: a 28-year experience at Children’s Hospital of Los Angeles. *Am J Pediatr Hematol Oncol* 9:121–129
- Gerlach VH, Janisch W, Schreiber D (1982) ZNS-Tumoren der perinatalperiode. *Zentralbl Allg Pathol* 126:23–28
- Buetow PC, Smirniotopoulos JG, Done S (1990) Congenital brain tumors: a review of 45 cases. *Am J Roentgenol* 155:587–593
- Di Rocco C, Iannelli A, Ceddia A (1991) Intracranial tumors of the first year of life: a cooperative survey of the 1986–1987 Education Committee of the ISPN. *Childs Nerv Syst* 7:150–153
- Raisanen JM, Davis RL (1993) Congenital brain tumors. *Pathology (Phila)* 2:103–116
- Janisch W (1985) Zur epidemiologie der primären Geschwulste des zentralnervensystems im ersten lebensjahr. *Arch Geschwulstforsch* 55:489–494
- Colangelo M, Buonaguro A, Ambrosio A (1980) Intracranial tumors in early infancy (under one year of age). *J Neurosurg Sci* 24:27–32
- Raimondi AJ, Tomita T (1983) Brain tumors during the first year of life. *Childs Brain* 10:193–207
- Sakamoto K, Kobayashi N, Ohtsubo H, Tanaka Y (1986) Intracranial tumors in the first year of life. *Childs Nerv Syst* 2:126–129
- Wakai S, Arai T, Nagai N (1984) Congenital brain tumors. *Surg Neurol* 21:597–609
- Isaacs H Jr (1985) Perinatal (congenital and neonatal) neoplasms: a report of 110 cases. *Pediatr Pathol* 3:165–216
- Kobayashi T, Kayama T, Yoshimoto T (1990–1991) Brain tumor in infancy: comparative study of before and after CT scan era. *Pediatr Neurosurg* 16:99, abstract
- Radkowski MA, Naidich TP, Tomita T et al (1988) Neonatal brain tumors: CT and MR findings. *J Comput Assist Tomogr* 12:10–20
- Tomita T, McLone DG, Flannery AM (1988) Choroid plexus papillomas of neonates, infants and children. *Pediatr Neurosci* 14:23–30
- Dehner LP (1981) Neoplasms of the fetus and neonate. In: Naeye RL, Kissane JM, Kaufman N (eds) Perinatal diseases, International Academy of Pathology, monograph number 22. Williams and Wilkins, Baltimore, pp 297–300
- Sabet LM (1982) Congenital glioblastoma multiforme associated with congestive heart failure. *Arch Pathol Lab Med* 106:31–34
- Rickert CH (1999) Neuropathology and prognosis of foetal brain tumours. *Acta Neuropathol* 98:567–576
- Burger PC, Scheithauer BW (2007) Tumors of the central nervous system. In: Atlas of tumor pathology, Fourth series, Fascicle 7. Armed Forces Institute of Pathology, Washington, D.C.
- Bigner DB, McLendon RE, Bruner JM (1998) Russell and Rubinstein’s pathology of tumors of the nervous system, vol I and II, 6th edn. Arnold, London
- Riccardi VM (1992) Type 1 neurofibromatosis and the pediatric patient. *Curr Probl Pediatr* 22:66–107
- Isaacs H (2010) Perinatal neurofibromatosis: two case reports and review of the literature. *Am J Perinatol* 27:285–292
- Isaacs H (2009) Perinatal (fetal and neonatal) tuberous sclerosis: a review. *Am J Perinatol* 26:755–760
- Gomez M (1999) Definition and criteria for diagnosis. In: Gomez MR, Sampson JR, Whittemore VH (eds) Tuberous sclerosis complex, 3rd edn. Oxford University Press, Oxford, p 18
- Werb P, Scurry J, Ostor A et al (1992) Survey of congenital tumors in perinatal necropsies. *Pathology* 24:247–253
- Isaacs H Jr (2010) Fetal and neonatal rhabdoid tumor. *J Pediatr Surg* 45:619–626
- Isaacs H (2008) Fetal and neonatal renal tumors. *J Pediatr Surg* 43:1587–1595
- DeSousa AL, Kalsbeck JE, Mealey J et al (1979) Diencephalic syndrome and its relation to opticochiasmatic glioma: review of twelve cases. *Neurosurgery* 4:207–209
- Perilongo G, Carollo C, Salvati L et al (1997) Diencephalic syndrome and disseminated juvenile pilocytic astrocytomas of the hypothalamic-optic chiasm region. *Cancer* 80:142–146
- Heckel S, Favre R, Gasser B et al (1995) Prenatal diagnosis of a congenital astrocytoma: a case report and literature review. *Ultrasound Obstet Gynecol* 5:63–66
- Kleihues P, Kiessling M, Janzer RC (1987) Morphological markers in neuro-oncology. *Curr Top Pathol* 77:307–338
- Boesel CP, Suhan JP, Bradel EJ (1978) Ultrastructure of primitive neuroectodermal neoplasms of the central nervous system. *Cancer* 42:194–201
- Timperly WR (2000) ACP best practice no 158. *Neuropathology. J Clin Pathol* 53:255
- Vagner-Capodano AM, Gentet GC, Gambarelli D et al (1992) Cytogenetic studies in 45 pediatric brain tumors. *Pediatr Hematol Oncol* 9:223–235
- Girschick HJ, Klein R, Scheurlen WG et al (2001) Cytogenetic and histo-pathologic studies of congenital supratentorial primitive neuroectodermal tumors: a case report. *Pathol Oncol Res* 7:67–71
- Cossu A, Massarelli G, Manetto V et al (1993) Rhabdoid tumors of the central nervous system: report of three cases with immunocytochemical and ultrastructural findings. *Virchows Arch A Pathol Anat Histopathol* 422:81–85

48. Fujii Y, Hongo T, Hayashi Y (1994) Chromosome analysis of brain tumors in childhood. *Genes Chromosomes Cancer* 11:205–215
49. Dolkart LA, Balcom RJ, Eisinger G (1990) Intracranial teratoma: prolonged neonatal survival after prenatal diagnosis. *Am J Obstet Gynecol* 162:768–769
50. Rostad S, Kleinschmidt-DeMasters BK, Manchester DK (1985) Two massive congenital intracranial immature teratomas with neck extension. *Teratology* 32:163–169
51. Sherer DM, Abramowicz JS, Eggers PC et al (1993) Prenatal ultrasonographic diagnosis of intracranial teratoma and massive craniomegaly with associated high-output cardiac failure. *Am J Obstet Gynecol* 168:97–99
52. Alagappan A, Shattuck KE, Rowe T et al (1998) Massive intracranial immature teratoma with extracranial extension into oral cavity, nose, and neck. *Fetal Diagn Ther* 13:321–324
53. Nanda A, Schut L, Sutton LN (1991) Congenital forms of intracranial teratoma. *Childs Nerv Syst* 7:112–114
54. Washburne JF, Magann EF, Chauhan SP et al (1995) Massive congenital intracranial teratoma with skull rupture at delivery. *Am J Obstet Gynecol* 173:226–228
55. Volpe JJ (2008) Brain tumors and vein of Galen malformations. In: Volpe JJ (ed) *Neurology of the newborn*, 5th edn. WB Saunders Co, Philadelphia, pp 989–1005
56. Weyerts LK, Catanzarite V, Jones MC, Mendoza A (1993) Prenatal diagnosis of a giant intracranial teratoma associated with pulmonary hypoplasia. *J Med Genet* 30:880–882
57. Felix I, Becker LE (1990–1991) Intracranial germ cell tumors in children: an immunohistochemical and electron microscopic study. *Pediatr Neurosurg* 16:156–162
58. Doren M, Tercanli S, Gullotta F et al (1997) Prenatal diagnosis of a highly undifferentiated brain tumour – a case report and review of the literature. *Prenat Diagn* 17:967–971
59. Geraghty AV, Knott PD, Hanna HM (1989) Prenatal diagnosis of fetal glioblastoma multiforme. *Prenat Diagn* 9:613–616
60. Roosen N, Deckert M, Nicola N et al (1988) Congenital anaplastic astrocytoma with favorable prognosis. Case report. *J Neurosurg* 69:604–609
61. Borit A, Richardson EP (1982) The biological and clinical behaviour of pilocytic astrocytomas of the optic pathways. *Brain* 105:161–187
62. Connolly B, Blaser SI, Humphreys RP et al (1997) Long-term survival of an infant with ‘anaplastic’ astrocytoma. *Pediatr Neurosurg* 26:97–102
63. Winters JL, Wilson D, Davis DG (2001) Congenital glioblastoma multiforme: a report of three cases and a review of the literature. *J Neurol Sci* 188:13–19
64. Mazzone D, Magro G, Lucentia A et al (1995) Report of a case of congenital glioblastoma multiforme: an immunohistochemical study. *Childs Nerv Syst* 11:311–313
65. Kamitomo M, Sameshima H, Uetsuhara K et al (1998) Fetal glioblastoma: rapid growth during the third trimester. *Fetal Diagn Ther* 13:339–342
66. Boop FA, Chaddock WM, Sawyer J et al (1991–1992) Congenital aneurysmal hemorrhage and astrocytoma in an infant. *Pediatr Neurosurg* 17:44–47
67. Mirkin LD, Ey EH, Chaparro M (1999) Congenital subependymal giant-cell astrocytoma: case report with prenatal ultrasonogram. *Pediatr Radiol* 29:776–780
68. Painter MJ, Pang D, Ahdab-Barmada M et al (1984) Congenital brain tumors in patients with tuberous sclerosis. *Neurosurgery* 14:570–573
69. Oikawa S, Sakamoto K, Kobayashi N (1994) A neonatal huge subependymal giant cell astrocytoma: case report. *Neurosurgery* 35:748–750
70. Ostör AG, Fortune DW (1978) Tuberous sclerosis initially seen as hydrops fetalis: report of a case and review of the literature. *Arch Pathol Lab Med* 102:34–39
71. Louis DN, von Deimling A, Dickersin GR et al (1992) Desmoplastic cerebral astrocytomas of infancy: a histopathologic, immunohistochemical, ultrastructural, and molecular genetic study. *Hum Pathol* 23:1402–1409
72. Aydin F, Ghatak NR, Salvant J et al (1993) Desmoplastic cerebral astrocytoma of infancy. A case report with immunohistochemical, ultrastructural and proliferation studies. *Acta Neuropathol* 86:666–670
73. de Chadarevian JP, Pattisapu JV, Faerber EN (1990) Desmoplastic cerebral astrocytoma of infancy. Light microscopy, immunocytochemistry, and ultrastructure. *Cancer* 66:173–179
74. Isaacs H Jr (1997) Tumors. In: Gilbert-Barness E (ed) *Potter’s pathology of the fetus and infant*, vol 2. Mosby, St. Louis, pp 1242–1339
75. Becker LE, Hinton D (1983) Primitive neuroectodermal tumors of the central nervous system. *Hum Pathol* 14:538–550
76. Dehner LP (1986) Peripheral and central primitive neuroectodermal tumors. A nosologic concept seeking a consensus. *Arch Pathol Lab Med* 110:997–1005
77. Rorke LB, Trojanowski JQ, Lee VM et al (1997) Primitive neuroectodermal tumors of the central nervous system. *Brain Pathol* 7:765–784
78. Friese M, Kern M (1998) Schroder: a prenatally diagnosed PNET with an extensive tumor mass in the brain. *Clin Neuropathol* 17:271 (Abstract p 9)
79. Kleihues P, Burger PC, Scheithauer BW (2000) Histological typing of tumours of the central nervous system, 2nd edn, World Health Organization histological classification of tumours. Springer, Berlin
80. Inwald D, Kempley S, Hird M (1998) Congenital primitive neuroectodermal tumour presenting as obstructed labour. *Arch Dis Child Fetal Neonatal Ed* 78:F222–F224
81. Yu IT, Ho DM, Wong T-T, Liu HC (1990) Congenital cerebral primitive neuroectodermal tumor with astrocytic differentiation and extracranial metastases. *Childs Nerv Syst* 6:179–182
82. Mitchell D, Rojiani AM, Richards D, Yachnis AT, Powell SZ (1995) Congenital CNS primitive neuroectodermal tumor: case report and review of the literature. *Pediatr Pathol Lab Med* 15:949–956
83. Mitchell CS, Wood BP, Shimada H (1994) Neonatal disseminated primitive neuroectodermal tumor. *Am J Roentgenol* 162:1160
84. McComb JG, Davis RL, Isaacs H Jr (1981) Extraneural metastatic medulloblastoma in childhood. *Neurosurgery* 9:548–551
85. Asai M, Kitamura H, Yanagibashi T, Asukai K, Katagiri N (1998) Case of acrania associated with congenital medulloblastoma. *Eur J Obstet Gynecol Reprod Biol* 81:115–117
86. Miller PD, Albright AL (1993) Posterior dural arteriovenous malformation and medulloblastoma in an infant: case report. *Neurosurgery* 32:126–130
87. Horten BC, Rubinstein LJ (1976) Primary cerebral neuroblastoma: a clinicopathological study of 35 cases. *Brain* 99:735–756
88. Eberhart CG, Brat DJ, Cohen KJ, Burger PC (2000) Pediatric neuroblastic brain tumors containing abundant neuropil and true rosettes. *Pediatr Dev Pathol* 3:346–352
89. Evans DGR, Farndon PA, Burnell H et al (1991) The incidence of Gorlin syndrome in 173 consecutive cases of medulloblastoma. *Br J Cancer* 64:959–961
90. Becker LE (1995) Central neuronal tumors in childhood: relationship to dysplasia. *J Neurooncol* 24:13–19
91. Smith NM, Carli MM, Hanieh A, Clark B, Bourne AJ, Byard RW (1992) Gangliogliomas in childhood. *Childs Nerv Syst* 8:258–262
92. Price DB, Miller LJ, Drexler S et al (1997) Congenital ganglioglioma: report of a case with unusual imaging appearance. *Pediatr Radiol* 27:748–749
93. VandenBerg SR (1993) Desmoplastic infantile ganglioglioma and desmoplastic cerebral astrocytoma of infancy. *Brain Pathol* 3:275–281
94. Paulus W, Schlote W, Perentes E et al (1992) Desmoplastic supratentorial neuroepithelial tumours of infancy. *Histopathology* 21:43–49

95. Rushing EJ, Rorke LB, Sutton L (1993) Problems in the nosology of desmoplastic tumors of childhood. *Pediatr Neurosurg* 19:57–62
96. Kudo H, Oi S, Tamaki N et al (1990) Ependymoma diagnosed in the first year of life in Japan in collaboration with the International Society for Pediatric Neurosurgery. *Childs Nerv Syst* 6:375–378
97. Comi AM, Backstrom JW, Burger PC et al (1998) Clinical and neuroradiologic findings in infants with intracranial ependymomas. *Pediatric Oncology Group. Pediatr Neurol* 18:23–29
98. Mork SJ, Loken AC (1977) Ependymoma. A follow up study of 101 cases. *Cancer* 40:907–915
99. Ernestus R-I, Schroder R, Klug N (1992) Spontaneous intracerebral hemorrhage from an unsuspected ependymoma in early infancy. *Childs Nerv Syst* 8:357–360
100. Nagib MG, O'Fallon MT (1996) Posterior fossa lateral ependymoma in childhood. *Pediatr Neurosurg* 24:299–305
101. Vinchon M, Soto-Ares G, Riffaud L et al (2001) Supratentorial ependymoma in children. *Pediatr Neurosurg* 34:77–87
102. Sara A, Bruner JM, Mackay B (1994) Ultrastructure of ependymoma. *Ultrastruct Pathol* 18:33–42
103. Rubinstein LJ (1970) The definition of the ependymoblastoma. *Arch Pathol* 90:35–45
104. Cruz-Sanchez FF, Haustein J, Rossi ML et al (1988) Ependymoblastoma: a histological, immunohistological and ultrastructural study of five cases. *Histopathology* 12:17–27
105. Gertz HJ, Unger M, Lobeck H et al (1990) Histological and immunocytochemical findings in a case of fetal choroid plexus papilloma. *Zentralbl Allg Pathol Anat* 136:719–722
106. McCune AB, Cohen BA, Gartner JC (1990) Congenital choroid plexus papilloma and giant nevocellular nevus: report of a case. *J Am Acad Dermatol* 22:849–851
107. Paulus W, Janisch W (1990) Clinicopathologic correlations in epithelial choroid plexus neoplasms: a study of 52 cases. *Acta Neuropathol* 80:635–641
108. Adra AM, Mejides AA, Salman FA et al (1994) Prenatal sonographic diagnosis of a third ventricle choroid plexus papilloma. *Prenat Diagn* 14:865–867
109. Lippa C, Abroms IF, Davidson R et al (1989) Congenital choroid plexus papilloma of the fourth ventricle. *J Child Neurol* 4:127–130
110. Costa JM, Ley L, Claramunt E et al (1997) Choroid plexus papillomas of the III ventricle in infants. Report of three cases. *Childs Nerv Syst* 13:244–249
111. Di Rocco C, Iannelli A (1997) Poor outcome of bilateral congenital choroid plexus papillomas with extreme hydrocephalus. *Eur Neurol* 37:33–37
112. Taggard DA, Menezes AH (2000) Three choroid plexus papillomas in a patient with Aicardi syndrome. A case report. *Pediatr Neurosurg* 33:219–223
113. Coffin CM, Wick MR, Braun JT, Dehner LP (1986) Choroid plexus neoplasms: clinicopathologic and immunohistochemical studies. *Am J Surg Pathol* 10:394–404
114. St Clair SK, Humphreys RP, Pillay PK et al (1991–1992) Current management of choroid plexus carcinoma in children. *Pediatr Neurosurg* 17:225–233
115. Packer RJ, Perilongo G, Johnson D et al (1992) Choroid plexus carcinoma of childhood. *Cancer* 69:580–585
116. Duffner PK, Kun LE, Burger PC et al (1995) Postoperative chemotherapy and delayed radiation in infants and very young children with choroid plexus carcinomas. *The Pediatric Oncology Group. Pediatr Neurosurg* 22:189–196
117. Tabaddor K, Shulman K, Dal Canto MC (1974) Neonatal craniopharyngioma. *Am J Dis Child* 128:381–383
118. Ueyama Y, Kuratsuji T, Lee JY et al (1985) Congenital giant craniopharyngioma. *Acta Pathol Jpn* 35:1273–1277
119. Bailey W, Freidenberg GR, James HE et al (1990) Prenatal diagnosis of a craniopharyngioma using ultrasonography and magnetic resonance imaging. *Prenat Diagn* 10:623–629
120. Yamada H, Haratake J, Narasaki T, Oda T (1995) Embryonal craniopharyngioma. *Cancer* 75:2971–2977
121. Muller-Scholden J, Lehrnbecher T, Muller HL, Bensch J, Hengen RH, Sorensen N, Stockhausen HB (2000) Radical surgery in a neonate with craniopharyngioma. *Pediatr Neurosurg* 33:265–269
122. Rorke LB, Packer RJ, Biegel JA (1996) Central nervous system atypical teratoid/rhabdoid tumors of infancy and childhood: definition of an entity. *J Neurosurg* 85:56–65
123. Biggs PJ, Garen PD, Powers JM et al (1987) Malignant rhabdoid tumor of the central nervous system. *Hum Pathol* 18:332–337
124. Weeks DA, Beckwith JB, Mierau GW et al (1989) Rhabdoid tumor of the kidney: a report of 11 cases from the National Wilms' Tumor Study Pathology Center. *Am J Surg Pathol* 13:439–458
125. Burger PC, Yu I-T, Tihan T et al (1998) Atypical teratoid/rhabdoid tumor of the central nervous system: a highly malignant tumor of infancy and childhood frequently mistaken for medulloblastoma: a Pediatric Oncology Group study. *Am J Surg Pathol* 22:1083–1092
126. Fernandez C, Bouvier C, Sevenet N et al (2002) Congenital disseminated malignant rhabdoid tumor and cerebellar tumor mimicking medulloblastoma in monozygotic twins: pathologic and molecular diagnosis. *Am J Surg Pathol* 26:266–270
127. Behring B, Bruck W, Goebel HH et al (1996) Immunohistochemistry of primary central nervous system malignant rhabdoid tumors: report of five cases and review of the literature. *Acta Neuropathol* 91:578–586
128. Sato T, Shimoda A, Takahashi T et al (1980) Congenital cerebellar neuroepithelial tumor with multiple divergent differentiations. *Acta Neuropathol* 50:143–146
129. Khoddami M, Becker LE (1997) Immunohistochemistry of medullo-epithelioma and neural tube. *Pediatr Pathol Lab Med* 17:913–925
130. Molloy PT, Yachnis AT, Rorke LB et al (1996) Central nervous system medulloepithelioma: a series of eight cases including two arising in the pons. *J Neurosurg* 84:430–436
131. Nakamura Y, Becker LE (1985) Meningeal tumors of infancy and children. *Pediatr Pathol* 3:341–358
132. Hockley AD, Hoffman HJ, Hendrick EB (1977) Occipital mesenchymal tumors of infancy: report of three cases. *J Neurosurg* 46:239–244
133. van Vliet MAT, Bravenboer B, Kock HCLV, Teepen JL (1983) Congenital meningeal sarcoma – a case report. *J Perinat Med* 11:249–254
134. Benli K, Cataltepe O, Oge HK et al (1990) Giant congenital meningioma in a newborn. *Childs Nerv Syst* 6:462–464
135. Niida H, Tanaka R, Takeda N et al (1992) Meningioma in a neonate: case report. *Surg Neurol* 38:273–276
136. Lopez MJ, Olivares JL, Ramos F et al (1988) Giant meningioma in a 5-month old infant. *Childs Nerv Syst* 4:112–115
137. Oakes WJ (1992) The natural history of patients with the Sturge-Weber syndrome. *Pediatr Neurosurg* 18:287–290
138. Tallman B, Tan OT, Morelli JG et al (1991) Location of port-wine stains and the likelihood of ophthalmic and/or central nervous system complications. *Pediatrics* 87:323–327
139. Sakai N, Yamada H, Nishimura Y et al (1992) Intracranial cavernous angioma in the 1st year of life and a review of the literature. *Childs Nerv Syst* 8:49–52
140. Capin DM, Gottlieb SM, Rosman NP (1997) Central nervous system hemangiomatosis in early childhood. *Pediatr Neurol* 17:365–370
141. Cohen MM Jr (2007) Craniofacial abnormalities. In: Gilbert-Barness E, ed. *Potter's Pathology of the Fetus, Infant and Child*, 3rd edition, vol 1. St. Louis, Mosby, pp 885–918

10.1 Retinoblastoma

Retinoblastoma is the principal intraocular neoplasm of infancy and childhood originating from the retina of one or both eyes as a single mass or multifocal tumors. Although it is relatively infrequent in the pediatric age group overall as compared to other neoplasms, it is responsible for morbidity and mortality during the first year of life [1–7]. Retinoblastoma occurs in fetuses and infants, and far advanced disease may be present already at birth [1, 2, 8–12]. The tumor is detected in utero by ultrasound as early as 21 weeks gestation [8].

10.1.1 Cytogenetics

The retinoblastoma gene, a suppressor gene, is situated at the 13q14 chromosome locus; deletions or mutations of both gene copies at this site are believed responsible for the formation of tumors [13–15]. The two alleles normally found at the 13q14 locus provide double protection against carcinogenesis [14]. This observation seems to apply not only to retinoblastoma but also to certain other childhood tumors such as neuroblastoma, Wilms' tumor, and osteosarcoma [14].

Genetic factors must be considered in the diagnosis and treatment of individuals with retinoblastoma and their families [2, 14]. Patients with retinoblastoma are divided into two main categories: *hereditary and nonhereditary* (or “*sporadic*”). The nonhereditary form, resulting from two somatic mutations, comprises 60 % of the cases; the hereditary form, resulting from one germinal mutation and one somatic mutation, accounts for the remainder [14, 15]. Only 5–6 % of hereditary cases have a family history of either unilateral or bilateral tumors. Unilateral, nonhereditary disease is present in 60 %; 15 % are hereditary and unilateral; 25 % are hereditary and bilateral. The bilateral cases are always hereditary. Bilateral disease is by far more prevalent in neonates and infants, almost 70 % occur in this age group, than in older children [1, 2]. Bilateral retinoblastoma is a dominant condition, and therefore, patients are heterozygous for chromosome 13

deletions, and the genotype (Rb+/Rb–) is transmitted to approximately half of their offspring [14]. Because so many retinal cells are at risk, one of three cells in each eye will undergo a second sporadic tumorigenic inactivation mutation resulting in loss of all tumor suppression and the appearance of tumor [14].

10.1.2 Clinical Findings

Infants diagnosed with retinoblastoma present with differences in laterality, stage, signs, symptoms, and respond differently to treatment when compared to older children [2, 3, 16]. The clinical findings depend upon when the tumor is discovered. The diagnosis of bilateral retinoblastoma is made more often during the first year of life than unilateral disease [2, 3, 16]. The inherited predisposition to retinoblastoma in bilateral cases shortens the time to the appearance of tumor. The highest percentage of patients (58 %) to develop new tumors is diagnosed before the age of 3 months and 95 % diagnosed before age 2 years [2].

Leukocoria or white pupillary reflex is the dominant early finding, noted in almost 60 % of infants [1] (Table 10.1 and Fig. 10.1). Funduscopic examination at this time reveals one or more yellow-white, creamy, rather smooth-shaped lesions on the retina. *Strabismus* is the presenting sign in 20 % of cases in infants older than 6 months of age [2]. Less common findings are *anisocoria, heterochromia, cataract, swelling, nystagmus, orbital cellulitis, and retinal detachment* [1–3, 14, 16]. Although children with retinoblastoma often present with leukocoria and strabismus, those diagnosed in the first 3 months generally are seen because of a *family history of the tumor* rather than leukocoria [2, 3, 14, 16]. When the optic nerve is involved by tumor, *rubeosis iridis* (the formation of blood vessels and fibrosis on the surface of the iris) is observed [14]. Later findings with advanced disease are *proptosis, perforation of the globe, and blindness*. When metastases occur outside the globe, the patient in time develops a large, disfiguring orbital mass with or without adjacent

Table 10.1 Clinical presentation of 71 infants less than 6 months of age with retinoblastoma

Finding	Number of patients
Family history	21
Leukocoria	41
Strabismus	3
Miscellaneous ^a	6

^aMiscellaneous findings were anisocoria, heterochromia, tearing, swelling, proptosis, cataract, nystagmus and perforation of the globe. Reprinted from Abramson and Notterman et al. [1]. With kind permission of © JAMA Network, 1983



Fig. 10.1 Leukocoria. White pupillary reflex (leukocoria) is the most common finding in the infant with retinoblastoma. The photograph depicts a 9-month-old female with leukocoria of the right eye which was noted by her mother 2 weeks prior to diagnosis (Courtesy of Linn Murphree, M.D. and Mr. Ben Szirth, Department of Ophthalmology, Children's Hospital Los Angeles; Reprinted from Isaacs [6]. © WB Saunders 1997)

bone and paranasal sinus invasion [7]. Irritability, vomiting, seizures, and coma are ominous signs of *CNS metastases*.

Less than 5 % of children with retinoblastoma have the *13q (del) syndrome* which is defined by, in addition to the chromosomal defect, a variety of abnormalities, including microcephaly, mental retardation, hypotonia, imperforate anus, malformed digits, and growth failure [14, 17].

Intraocular retinoblastoma is classified according to the *Reese-Ellsworth staging system* [18] (Table 10.2). The New York Hospital-Cornell Medical Center infant retinoblastoma study of 401 patients showed that the most common stage at diagnosis was group V [2]. Of infants diagnosed with bilateral tumors, 77 % of eyes were group V; 84 % of eyes with unilateral tumors were group V also. In the first 3 months of life, 71 % of bilateral affected eyes, and 83 % of unilateral affected eyes had group V tumors. Their study emphasizes that *earlier age of detection does not necessarily insure an earlier stage of ocular involvement*, contrary to what one would expect. Unfortunately, despite this earlier detection, the presenting eye is usually full of tumor and thus cannot be salvaged [2].

Table 10.2 Ellsworth criteria for staging of retinoblastoma

Group I very favorable
A. Solitary tumor, less than 4 disc diameters in size, at or behind the equator
B. Multiple tumors, none over 4 disc diameters in size, all at or behind the equator
Group II favorable
A. Solitary lesion, 4–10 disc diameters in size, at or behind the equator
B. Multiple tumors, 4–10 disc diameters in size, behind the equator
Group III doubtful
A. Any lesion anterior to the equator
B. Solitary tumors larger than 10 disc diameters behind the equator
Group IV unfavorable
A. Multiple tumors some larger than 10 disc diameters
B. Any lesion extending anterior to the ora serrata
Group V very unfavorable
A. Massive tumors involving over half the retina
B. Vitreous seeding

Reprinted from Ellsworth [18]. With kind permission of © The American Ophthalmological Society, 1969

Refers to chances of salvaging the affected eye and not systemic prognosis

10.1.3 Differential Diagnosis

Retinoblastoma can mimic other conditions involving the eye particularly hemorrhage and inflammation [1, 2, 13, 14]. *Hypopyon* (pus in the anterior chamber), *orbital cellulitis* (painful red eye), and *hyphema* (hemorrhage into the anterior chamber) are examples. *Coat's disease* (vascular malformation or hemangioma of the retina with retinal detachment), *retinopathy of prematurity* (Fig. 10.2), and *persistent hyperplastic primary vitreous* (fibrovascular membrane or plaque partially covering the retina) are conditions most easily mistaken for retinoblastoma [1, 13, 14]. Toxoplasmosis, toxocara canis, and other forms of *severe uveitis* have been confused with this tumor [13]. *Retinal astrocytoma* can mimic this malignancy, and the former would be more likely in a baby with tuberous sclerosis [19]. *Medulloepithelioma* can present with similar findings [13].

10.1.4 Spontaneous Regression

Occasionally, *spontaneous regression* occurs in infants and children with retinoblastoma, as with neuroblastoma. The process is heralded clinically by inflammation of the involved eye and microscopically by hemorrhage, necrosis, lymphocytic infiltrates, and vascular changes resulting in retinal gliosis of varying degree, *phthisis bulbi* (shrinkage, fibrosis, and disorganization of the eye), or even a normal

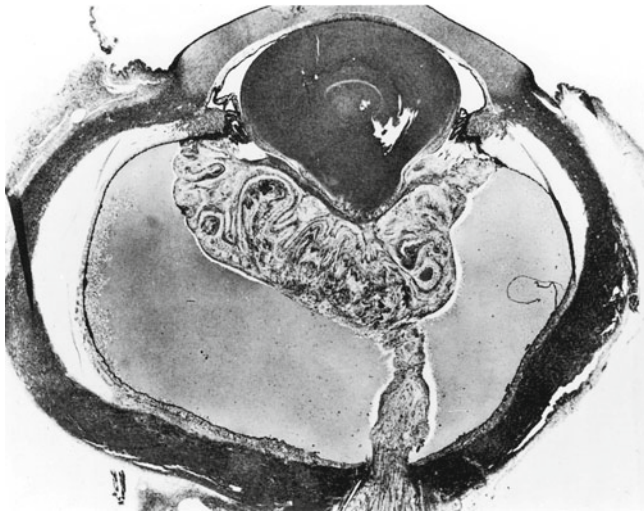


Fig. 10.2 Retinopathy of prematurity. The retina is detached and bound into a firm fibrous mass adherent to the posterior surface of the lens together with a mass of abnormally proliferated blood vessels. Infant weighed 1,100 g at birth. Eye removed because of erroneous diagnosis of retinoblastoma at age 6 months (Reprinted from Potter and Craig [48]. With kind permission of © Mosby-Year Book, 1976)

eye [14, 20, 21]. The exact incidence and the cause of spontaneous regression are unknown, but it is found more often in patients with bilateral retinoblastoma [21–23].

10.1.5 Pathology

Light and electron microscopic (EM) findings suggest that retinoblastoma develops from the retinal neural precursor cells of photoreceptor cells [13, 14, 23–26] (Fig. 10.3). Retinoblastoma arises from the retina of one or both eyes, most often as a single mass, but occasionally as multifocal lesions. The involved eye on cross section shows a well-defined soft gray-white mass in the retina containing tiny white flecks of calcification [13, 14, 22, 25] (Fig. 10.4c). When there are multifocal primary lesions or foci of vitreous seeding, they appear as white nodules or plaques on the retina or choroid. Large and mostly necrotic tumors tend to be less well demarcated and sometimes have the appearance of thick white paste within the vitreous cavity. Retinal detachment is found in both the *endophytic* and *exophytic growth patterns*, particularly in advanced disease, but it may be seen earlier in the former where the tumor grows toward the choroid from the retina. Most retinoblastomas are *exophytic*, that is, they grow anteriorly into the vitreous from the retina (Figs. 10.4c and 10.5a). The less common *diffuse infiltrating form* is characterized by diffuse infiltration of both the retina and choroid by tumor without a well-defined mass [13]. Choroidal invasion *per se* is not always an unfavorable prognostic sign, but it is frequently seen when the optic nerve is involved [14, 22, 26].

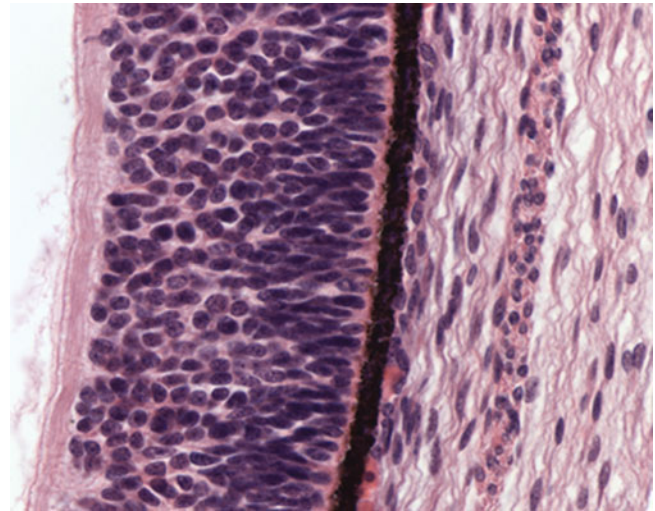


Fig. 10.3 Developing retina. The external layer of the optic cup contains retinal pigment and the inner layer the sensory (neural) retina. At this stage of development, the neural retina consists of four zones: proliferative (next to the pigment layer), external neuroblastic, transient fiber, and internal neuroblastic zone. From a fetus of 8–10 weeks estimated gestation (Reprinted from Isaacs [6]. © WB Saunders 1997)

Careful examination and taking proper microscopic sections of the optic nerve are required in the evaluation of a retinoblastoma specimen since the presence or absence of tumor at the line of resection determines the outcome [7, 14]. When tumor invades the nerve for a distance of 10 mm or more, it will eventually enter the subarachnoid space and lead to fatal dissemination of tumor cells into the cerebrospinal fluid with seeding of the leptomeninges at the base of the brain and spinal cord [29] (Fig. 10.5c and e). In approximately 40% of cases choroidal vessels are invaded by tumor cells, which then enter the circulation and metastasize primarily to the bone marrow, lymph nodes, and liver [29, 30]. In advanced disease with extensive involvement of the eye, the tumor perforates the globe and invades the periorbital soft tissues and bone forming a large disfiguring mass [7] (Fig. 10.5d).

Retinoblastoma is one of the “small blue cell tumors” of infancy and childhood and thus would fall into the category of “primitive neuroectodermal tumor” because it shares certain histological and clinical findings, for example, microfilaments, neurotubules, and neurosecretory granules, with other PNETs such as neuroblastoma and medulloblastoma [16, 21]. The main difference from the other PNETs is that more differentiated retinoblastomas show *photoreceptor cell differentiation*.

Typically, the tumor is very cellular consisting of sheets of small, round to oval, darkly staining cells with hyperchromatic basophilic nuclei and scant cytoplasm. Extensive necrosis and calcification and numerous mitoses are present usually. Although little or no recognizable stroma is noted, there is a prominent vascular network coursing through the

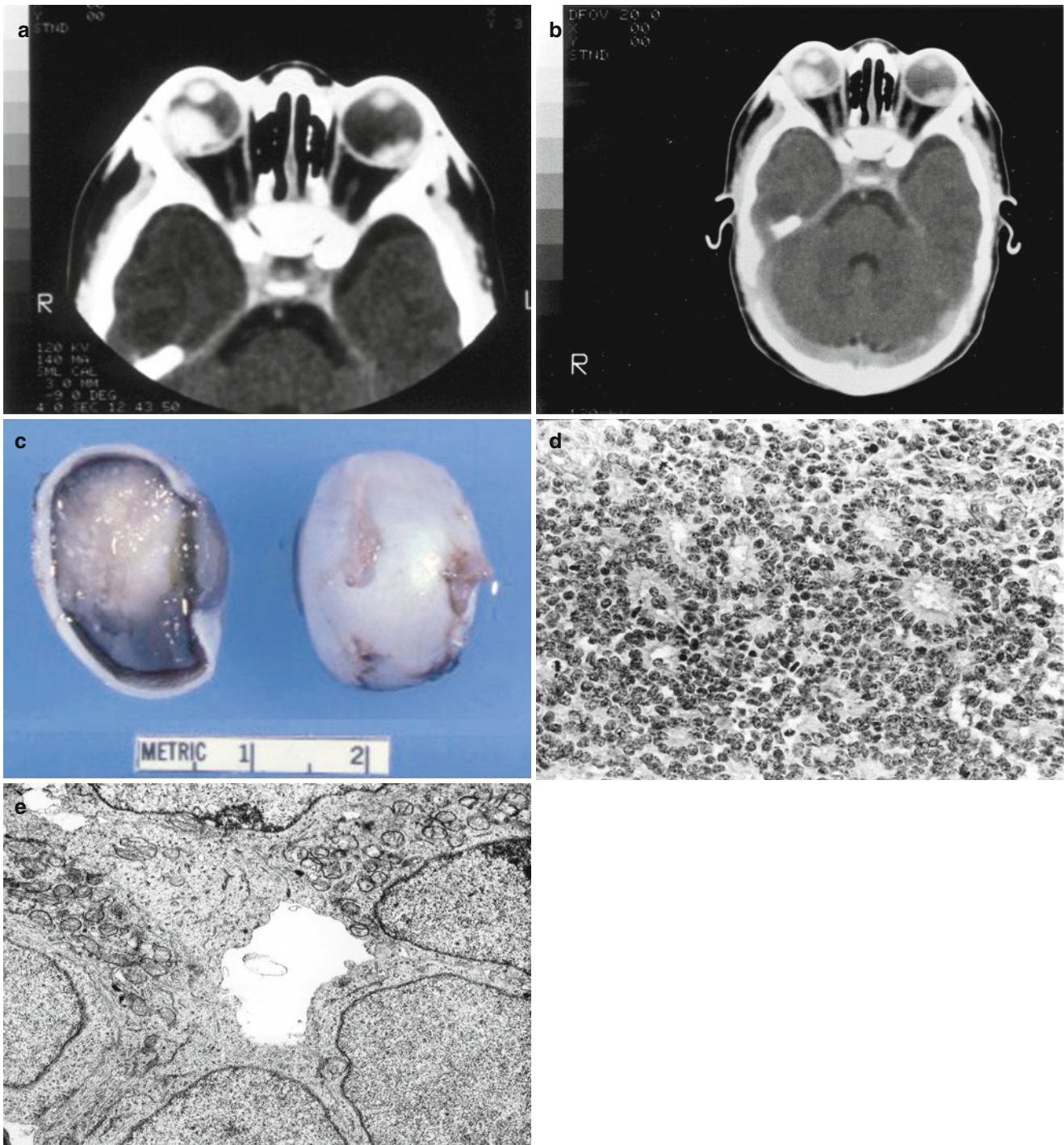


Fig. 10.4 Congenital bilateral retinoblastoma. One-month-old female presented with leukocoria of the right eye. (a) CT and (b) MRI scans demonstrate tumors in both eyes. (c) The globe of the right eye is hemisected revealing a gray-white tumor mass, 11 × 13 mm, filling most of the vitreous cavity, and containing white flecks of calcification. The stub of the optic nerve is situated on the posterior external surface of the globe on the right. Microscopically, it was not involved. At the time of the enucleation, the left eye was noted to have a 12 × 12-disc-diameter lesion in the posterior pole and four additional smaller ones. (d) The tumor is a differentiated retinoblastoma composed of small round cells

with scant cytoplasm and round to oval nuclei with a fine peppery chromatin pattern containing one or two small nucleoli. Several Flexner-Wintersteiner rosettes are present. (e) EM of a Flexner-Wintersteiner rosette having a clear space in the center surrounded by four immature-appearing tumor cells. Clusters of mitochondria and scattered microtubules are present in the cytoplasm. In the *left lower corner* of the photograph, there is a primitive cell junction ((e) EM ×18,900. Courtesy of Darkin Chan, Department of Pathology, Children's Hospital Los Angeles; Reprinted from Isaacs [6]. © WB Saunders 1997)

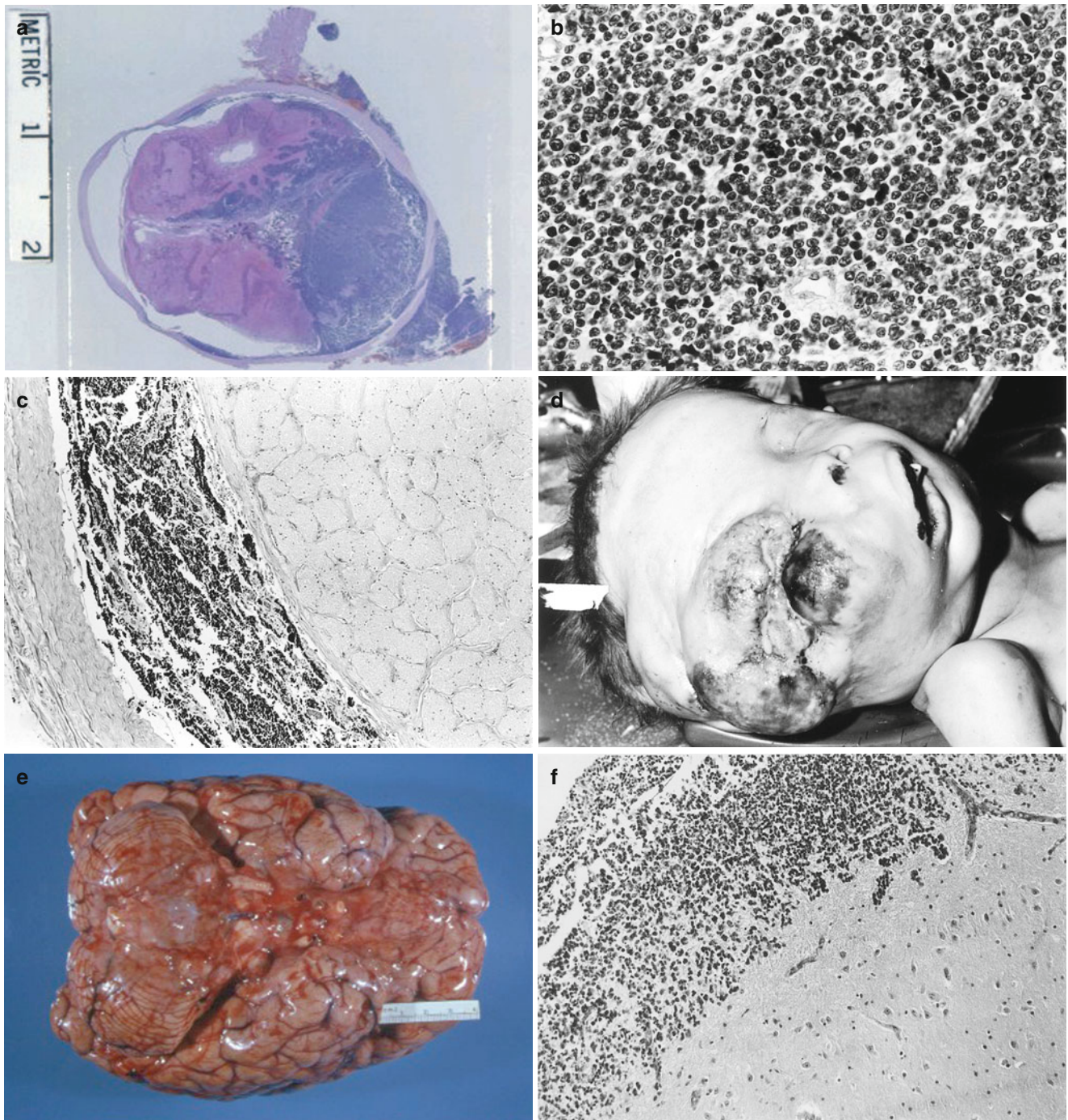


Fig. 10.5 Bilateral retinoblastoma with metastases, 1-year-old male. (a) Enucleated left eye with tumor filling the entire vitreous cavity. The tumor perforates the globe and invades the surrounding periorbital tissue (Ellsworth group 5). (b) The retinoblastoma has the appearance of a poorly differentiated small cell malignant tumor. Essentially, no photoreceptor cell differentiation is apparent. (c) Section of the optic nerve showing subarachnoid tumor spread. (d) The patient at postmortem examination had a fungating mass protruding from the right orbit and involving the right maxilla and frontal bone. The tumor spread inferi-

orly into the right maxilla and medially and posteriorly into the nasal cavity and pharynx obstructing these structures. It invaded the right orbital plate, extended into the floor of the anterior and middle cranial fossae, and involved the base of the brain. (e) The leptomeninges of the inferior and medial frontal and temporal lobes and cerebellar hemispheres are infiltrated by tumor. The cranial nerves, mesencephalon, pons, and medulla are encased by metastatic deposits. (f) The leptomeninges and adjacent insular cerebral cortex are invaded by tumor cells (Reprinted from Isaacs [6]. © WB Saunders 1997)

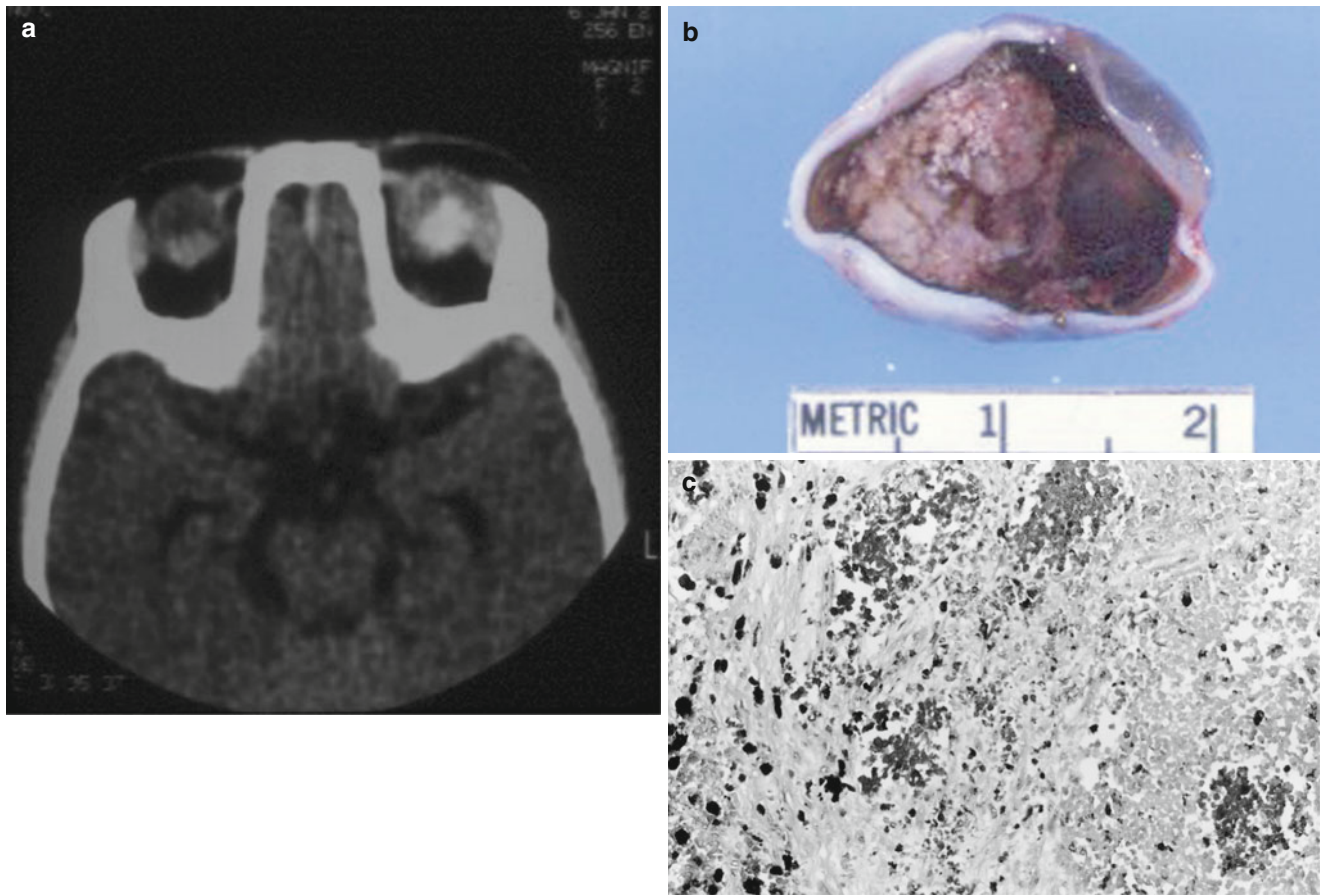


Fig. 10.6 Retinoblastoma with extensive necrosis and calcification. Two-month-old female presented with a swollen left eye several days prior to hospital admission. (a) CT scan reveals bilateral retinal tumors, the left larger than the right. (b) The hemisected left eye shows necrotic

and calcified tumor filling most of the vitreous cavity. (c) The tumor is totally necrotic and calcified. No recognizable “viable” tumor cells are evident (Reprinted from Isaacs [7]. © Springer-Verlag, 2002)

tumor with more viable cells forming sheaths about small vessels. Necrosis and calcification may be so extensive that a diagnosis cannot be established from histological findings alone (Fig. 10.6c). Cytodifferentiation, the amount varying with each specimen, is manifested by the formation of *Homer-Wright rosettes*, which consist of a ring of tumor cells situated about a central area containing pink fibrillary material (Figs. 10.7 and 10.8a) and *Flexner-Wintersteiner rosettes* composed of a single layer of cells aligned about a well-defined inner circular membrane having a clear zone in the center (Figs. 10.4d and 10.8a). Although several different kinds of tumor contain Homer-Wright rosettes, only the Flexner-Wintersteiner rosette is considered pathognomonic of retinoblastoma since it is related to photoreceptor cells and is seen in about half the specimens [13, 22, 23]. *Fleurette-like structures* consisting of clusters of cells having a “fleur-de-lis”-like arrangement representing still further cytodifferentiation are observed rarely [22–26]. Fleurettes are found in retinocytomas, the most differentiated form of retinoblastoma [26]. By EM, the cells forming the Flexner-Wintersteiner rosettes show at their luminal border clusters

of mitochondria, zonula adherens-like cell junctions, and characteristic cilia (Fig. 9.4e).

Immunohistochemical studies performed on both retinoblastoma and on human retina show certain features in common, further supporting the concept of the histogenesis of this tumor [27, 28]. For example, *neuron-specific enolase (NSE)* is immunoreactive in both tumor cells and in human retina neurons. NSE determination is especially helpful in the diagnosis in the bone marrow when there is a question of metastatic disease. However, it should be remembered that neuroblastoma (and other PNETs) is NSE immunoreactive also and that this staining procedure will not differentiate between these tumors. Moreover, the *retinal S antigen*, a component of photoreceptor cell outer segment, is present in the tumor and normal retina [14].

Three findings associated with an unfavorable outcome are *optic nerve invasion beyond the lamina cribrosa*, *choroidal involvement*, and *orbital extension* [1, 21, 31]. Retinoblastomas metastasize in four ways: direct extension, dispersion (into the vitreous and CSF), hematogenous dissemination, and lymphatic spread [13, 31, 32]. Generally,

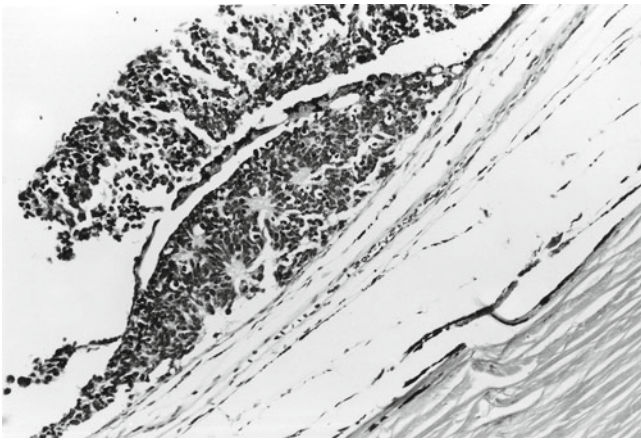


Fig. 10.7 Retinoblastoma, choroidal seeding. Nodules of tumor cells seeding onto the surface of the choroid. Several Homer-Wright rosettes are present (Reprinted from Isaacs [7]. © Springer-Verlag, 2002)

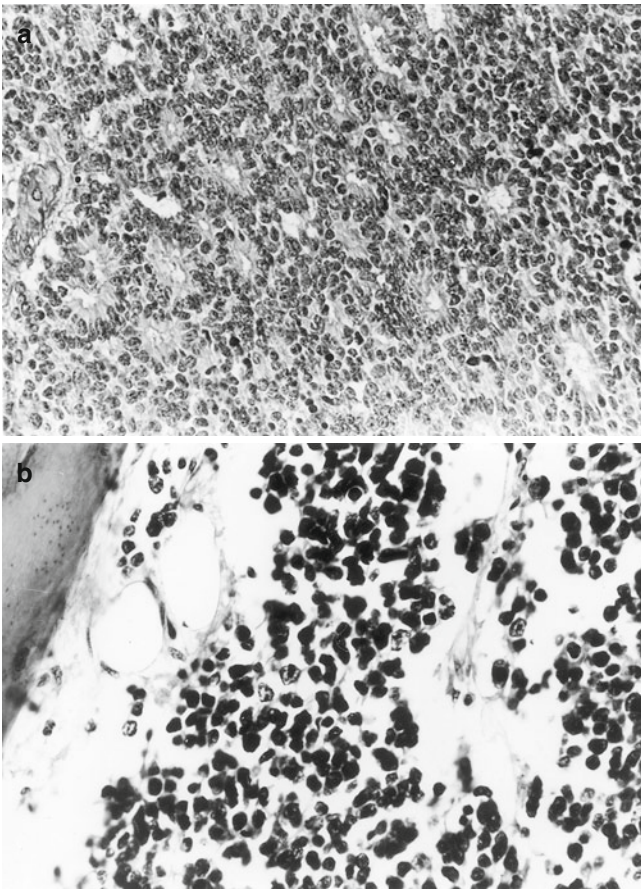


Fig. 10.8 Retinoblastoma, metastases are generally less differentiated than the primary tumor. (a) Photomicrograph of a well-differentiated retinoblastoma from an infant with bilateral tumors. Well-defined Flexner-Wintersteiner rosettes are present. (b) Postmortem bone marrow biopsy taken several months later after surgery and chemotherapy. The tumor consists of small, darkly staining cells without evidence of photoreceptor differentiation (Reprinted from Isaacs [7]. © Springer-Verlag, 2002)

retinoblastoma metastases appear much less differentiated than the intraocular primary tumor (Fig. 10.8a, b). Rosettes are hard to identify and poorly formed, and fleurettes are practically never found [13]. Postmortem studies reveal that the routes of metastases of retinoblastoma in addition to optic nerve and choroid invasion are, in decreasing order, the CSF, bone marrow, orbit-to-orbit extension through the meninges, and liver [7, 31, 32]. Once retinoblastoma spreads beyond the eye essentially, there are few or no survivors (Fig. 10.5).

10.1.6 Prognosis

The extent of the tumor, or *stage* of the disease at the time of diagnosis, is the most important factor with regard to the salvage of the eye(s) and prognosis [1, 14, 22, 31] (Tables 10.1 and 10.2). Usually, the prognosis is poor for patients with massive tumors involving over half the globe and in those with vitreous seeding (Ellsworth group 5) [18] (Table 10.2). A family history of retinoblastoma leads to earlier recognition of the disease but does not increase the probability of salvaging the eye(s); however, the prognosis and advanced stage is the same for infants with a family history and those without [2]. The two most important findings determining survival are *optic nerve involvement* and *extraorbital spread* [1, 14, 31, 32]. A definite relationship between cytodifferentiation of the tumor and prognosis has not been established [13, 14].

When distant metastases or local extension occurs outside the eye, the mortality rate approaches 100 % regardless of the form of therapy [1, 2, 14]. The length of survival after diagnosis of metastatic retinoblastoma ranges from 6 months to 1 year [14, 32]. *Second malignancies* particularly with treated bilateral retinoblastomas are not uncommon; patients are at risk for developing *osteosarcoma* and *other sarcomas* [13, 14, 32].

10.2 Trilateral Retinoblastoma

Bilateral retinoblastoma associated with retinoblastoma in the pineal has been termed “trilateral retinoblastoma” [33–39]. Pineoblastomas unassociated with retinoblastomas occasionally show photoreceptor differentiation [36, 38, 39]. Extraocular extension or local invasion into the central nervous system from the ocular retinoblastoma or from distant metastases occurs in the trilateral syndrome [35–38]. The histological appearance of bilateral and pineal retinoblastomas may be identical with or without photoreceptor differentiation [37]. Some trilateral lesions have the histological appearance of an undifferentiated, small blue cell tumor. This ultimately lethal condition is uncommon. The incidence

of trilateral retinoblastoma in patients with retinoblastoma is reported at approximately 3 % [34, 36]. Most patients with trilateral retinoblastoma had bilateral tumors and a positive family history or both [38]. In trilateral cases, a positive family history is obtained in over two thirds, and there is an earlier age of presentation of retinoblastoma, 7 months, as compared to classic bilateral retinoblastoma, 15 months [38]. Trilateral retinoblastoma is reported in infants as young as age 4 months who present with a calcified suprasellar mass and increased intracranial pressure due to obstructive hydrocephalus [38]. The most common presenting signs are lethargy, vomiting, and anorexia [35]. Mean survival from diagnosis of trilateral disease to death is approximately 7 months, and essentially, all patients die with cerebrospinal metastases [36, 38].

10.3 Medulloepithelioma

Medulloepithelioma is an extremely rare neoplasm thought to arise from the medullary epithelium lining the optic cup, which begins in early embryonic life as an out pouching of the neural tube. It is regarded as a tumor of neuroepithelium occurring most often in the ciliary body and/or iris and infrequently in the optic nerve or retina [13, 39–42]. The main initial clinical findings are a *cyst-like structure or mass in the iris, anterior chamber, or ciliary body and glaucoma*. Medulloepithelioma occurs in infants [41, 42].

Histologically, the tumor is composed of sheets and cords of small, blue, neuroblastic-like cells (“medullary epithelium”) forming tubular structures and cyst formations [39]. The netlike appearance formed by anastomosing cords of medullary epithelium is termed the *diktyomatous pattern* (from the Greek word *dikty* or “net”). When heterotopic tissues, for example, skeletal muscle, cartilage, or neuroglial tissue, are present, then the tumor is then classified as a *teratoid medulloepithelioma* [13, 39].

The neuroepithelium may differentiate toward retinal pigmented epithelium, non-pigmented, and pigmented ciliary epithelium, neurons, and neuroglia [13]. The tumor is defined as malignant when it is composed mostly of undifferentiated cells resembling retinoblastoma or if the heteroplastic tissue is anaplastic with a high mitotic rate [13]. About 20 % of eyes with medulloepithelioma also show histological evidence of hyperplastic primary vitreous [39].

Medulloepithelioma is the main primary ocular tumor that histologically resembles retinoblastoma, and thus, this may create a diagnostic problem. Undifferentiated foci in some malignant medulloepitheliomas contain cells that are indistinguishable from those of retinoblastoma [13].

Medulloepitheliomas are usually slow growing and associated with a favorable outcome provided they are localized to the eye and completely excised [40, 41]. However, the

tumors are potentially fatal when they perforate the globe and extend into the orbit. Death results from intracranial metastases. Therefore, the most important prognostic factor is *the presence or absence of orbital invasion* [13, 39].

10.4 Astrocytic Tumors of the Retina

Astrocytic tumors or hamartomas of the retina or optic nerve occur in association with *tuberous sclerosis* and are found in almost half the patients with this disease [19, 43]. Tuberous sclerosis is an autosomal dominant disorder that manifests with highly variable clinical manifestations including seizures, mental retardation, skin lesions, and hamartomas (overgrowths of cells normally found in the tissue of origin) affecting multiple organ systems such as the heart, brain, eye, and kidney [43–46].

Astrocytic tumors or hamartomas are observed also in children with *neurofibromatosis* and in those who do not have either one of these neurocutaneous syndromes (or “phakomatoses”). Neurofibromatosis-1 (NF-1) is one of the hereditary neurocutaneous syndromes that often affects the globe and ocular adnexa [44–46]. Almost half the infants with NF-1 have physical signs at birth consisting of multiple cafe-au-lait spots, plexiform neurofibromas, and lesions of the ocular structures. Survivors may develop serious ophthalmologic sequelae such as an enlarging, glaucomatous eye, an orbital mass, occurrence of malignant nerve sheath tumors, or other malignancies [46].

Early astrocytic tumors present as a small, flat transparent retinal thickenings and later on in childhood and adulthood as a raised nodular and calcified whitish masses within the retina or optic disc [13, 44]. The astrocytic lesions arise from the nerve fiber and ganglion cell layers, grow slowly in childhood, are confined to the eye, and generally do not invade adjacent structures.

Large retinal astrocytic hamartomas in patients with tuberous sclerosis may resemble retinoblastoma through the funduscope, especially if the mass is large, calcified, and accompanied by vitreous seeding. Although the ophthalmic presentation is suggestive of retinoblastoma, radiologic evidence of subependymal hamartomas and/or cardiac rhabdomyomas, characteristic of tuberous sclerosis, helps to establish the correct diagnosis [45, 46] (see Chap. 9 for further discussion). Skin lesions may be present also at birth.

Astrocytic retinal tumor histological findings consist of elongated, spindle-shaped (pilocytic) astrocytes with small, oval nuclei surrounded by a fine meshwork of glial fibers [13]. Foci of calcification may be present. Giant astrocytes are found in the tumors (hamartomas) of patients with tuberous sclerosis which occur also in the retina and in the brain [19].

10.5 Neurofibromatosis

Retinal tumors or hamartomas of astrocytic origin occur in association with *neurofibromatosis type 1* in 14 % of the patients afflicted with this disease [19]. Less than half the infants with neurofibromatosis have physical signs at birth consisting of multiple cafe-au-lait spots, plexiform neurofibromas, and hamartomas of the ocular structures [47]. Neurofibromatosis may involve the optic nerve and the entire uveal tract, which consists of the iris, ciliary body, and choroid

[13] (Fig. 10.9). When involved, the choroid shows diffuse thickening due to the presence of spindle-shaped Schwann cells, ganglion cells, nerve fibers, and ovoid bodies composed of Schwann cells and melanocytes [49] (Fig. 10.9d). Although *Lisch nodules*, which are focal collections of melanocytic cells situated on the anterior border of the iris, are the most common intraocular abnormality seen in adults, they are seldom found in children less than 5 years of age [47]. Plexiform neurofibroma of the eyelid correlates with a high incidence of congenital glaucoma [46] (Patient depicted in Fig. 10.9).

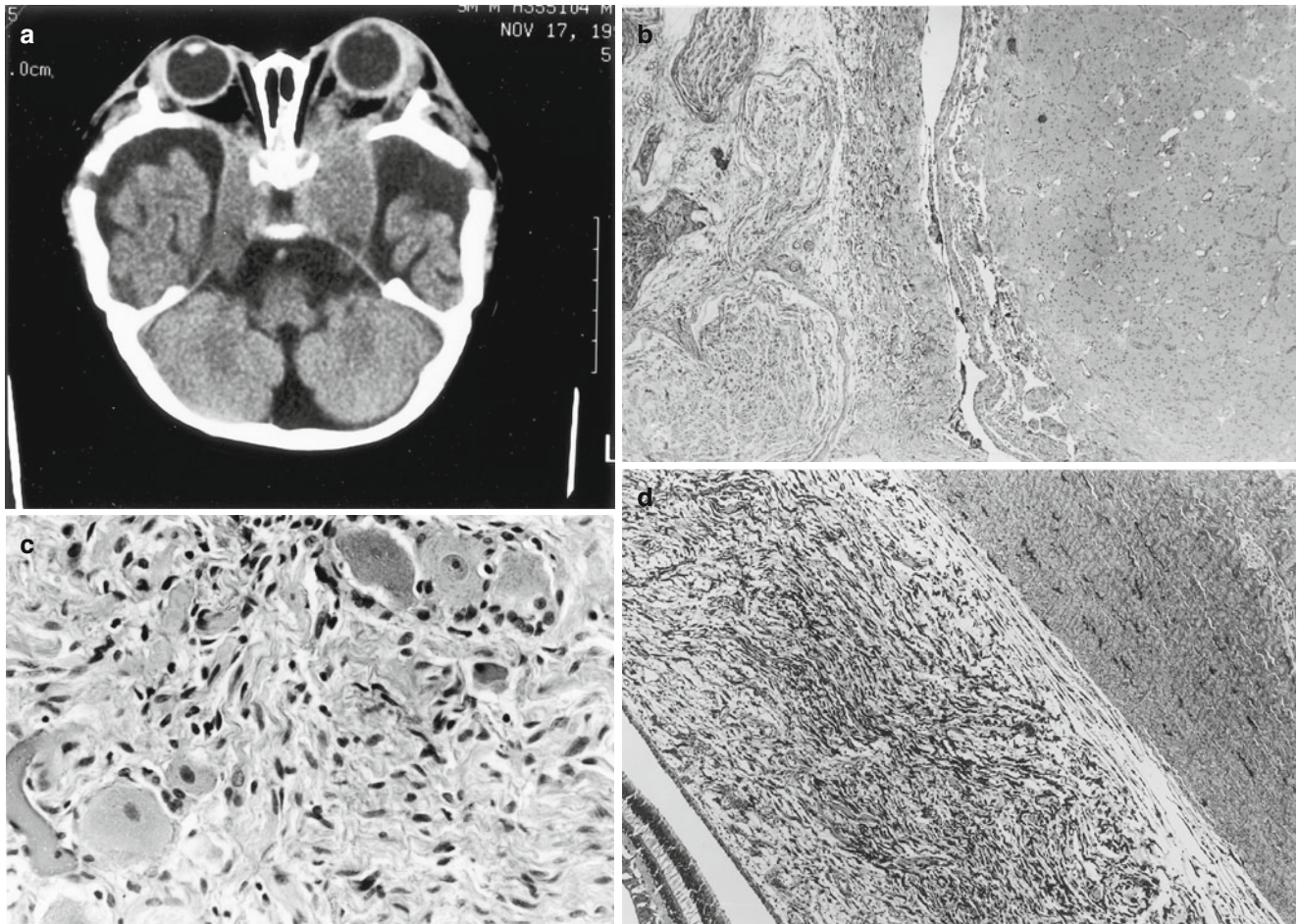


Fig. 10.9 Neurofibromatosis of the eye, optic nerve, and orbit. (a) MRI at age 5 months reveals tumor within the right orbit, cavernous, and paranasal sinuses. The right eye is exophthalmic. The eye was enucleated at age 21 months because of the severe, disfiguring proptosis and glaucoma. (b) The meninges are thickened. There is a plexiform neurofibroma adjacent to the optic nerve. (c) Microscopic section of the ciliary ganglion reveals diffuse infiltration by neurofibroma composed

of wavy elongated cells with regular oval or fusiform nuclei within a fibrillar matrix. (d) Section of sclera and retina. The sclera is diffusely thickened by collections of melanocytes, spindle-shaped Schwann cells, and fibrocytes. The sclera contains a small nerve with a plexiform neurofibroma (*upper right hand corner*) (Reprinted from Isaacs [6]. © WB Saunders 1997)

10.6 Optic Glioma

Astrocytoma is the main histological form of *optic glioma* and the foremost intracranial tumor associated with neurofibromatosis 1 (NF-1) [7, 13, 47]. Optic gliomas arise from the optic nerve and chiasm, consist of pilocytic astrocytes, and vary histologically from benign to malignant. Magnetic resonance imaging (MRI) scans through the orbits detect the presence of optic nerve gliomas which appear as thickenings of the entire nerve, usually a solid fusiform enlargement of the nerve. Tumors of the chiasm appear as a mass in the suprasellar region [47] (Fig. 9.2) (see Chap. 9 for further discussion of astrocytoma).

10.7 Orbital Tumors

Orbital tumors are uncommon and occasionally massive [48–58]. Typically, they present in the fetus and infant as abnormal protrusions (*ptosis*, *exophthalmos*) of the eyeball.

Other causes are *retrobulbar hemorrhage* and *congenital anomalies* of the eye, for example, cystic microphthalmia (Fig. 10.10) and congenital cystic eye. Encephalocele causes proptosis at birth in addition to trauma with retrobulbar hemorrhage [7]. Other features include rapid growth, extensive enlargement of the bony orbit, and often a normally developed eye. Since extension into the intracranial cavity (or an intracranial tumor with secondary orbital involvement) occurs making the tumor inoperable, orbital imaging studies prior to surgery are requisite to exclude this finding [7].

Although orbital tumors of the fetus and infant are uncommon, a variety of neoplasms arise from this site. The major ones are *teratoma* [7], *hemangioma* [7], *neurofibroma* [46–48], *rhabdomyosarcoma* [7, 58], and *metastatic neuroblastoma* [7]. Orbital teratoma is discussed also in Chap. 2. Much rarer examples of orbital tumors are *rhabdoid tumor* [49, 50], *polyphenotypic small cell tumor* [51], *myofibromatosis* [48, 52], *fibrosarcoma* [53], *malignant peripheral nerve sheath tumor* [54], *lipoblastoma* [55], and *melanotic neuroectodermal tumor* [56].



Fig. 10.10 Cystic microphthalmia. Two-week-old female with an orbital mass discovered on routine prenatal ultrasound. (a) Patient with a large left orbital mass, which clinically was thought to be a teratoma. (b) MRI reveals a cystic and solid mass occupying the left orbit. There were no recognizable ocular structures either by imaging studies or by gross inspection of the specimen. However, a 2 cm in diameter, empty cystic cavity was present. (c) The wall of the cyst consists of neuroglial

tissue and dysplastic retinal elements with pseudorosette formations. Portions of sclera, choroid, and ciliary body were identified microscopically within the mass. Along the right border of the photograph, there is a portion of immature retina bordering the cyst (Courtesy of Lynne Bird, M.D., Department of Dymorphology and Genetics, Rady Children's Hospital San Diego; Reprinted from Isaacs [7]. © Springer-Verlag, 2002)

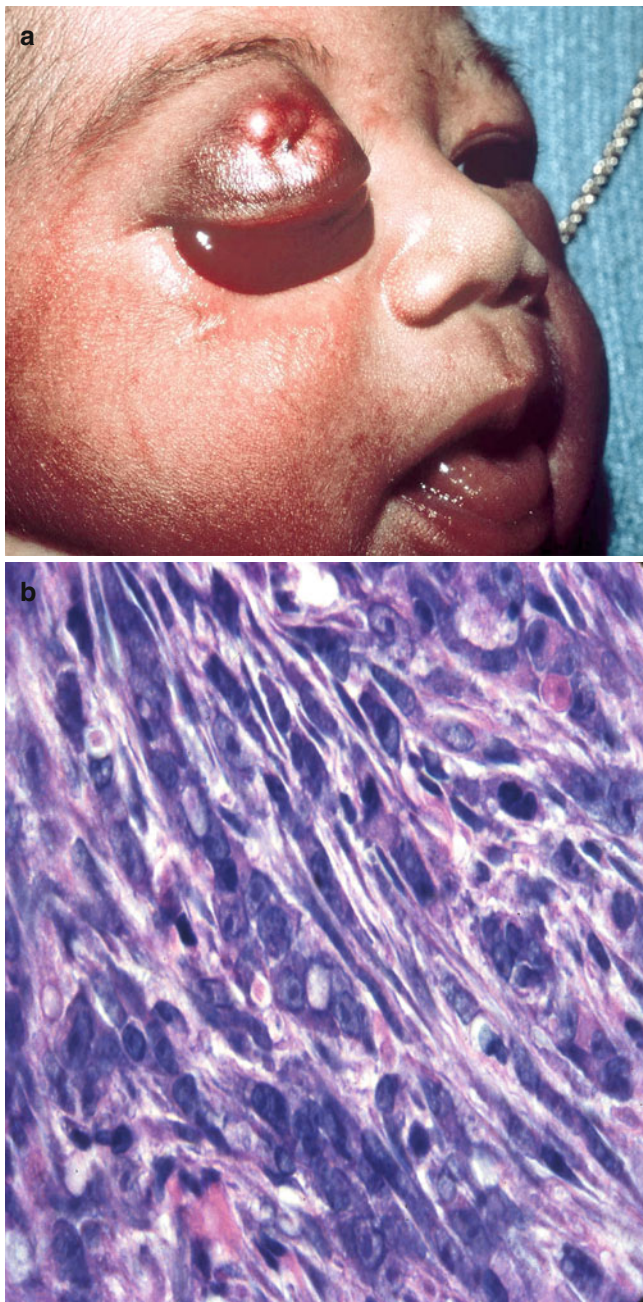


Fig. 10.11 Rhabdomyosarcoma of the eyelid. Six-day-old male with a nodular mass involving the right upper eyelid which was excised. (a) The patient shortly after birth with the eyelid tumor and underlying hemorrhagic, chemotic conjunctiva. (b) Photomicrograph of a right preauricular lymph node metastasis removed 9 days after the initial surgery. Large spindle-shaped cells consistent with rhabdomyoblasts are present (Reprinted from Isaacs [6]. © WB Saunders 1997)

Rhabdomyosarcoma of the eyelid and orbit is the subject of several case reports [6, 7, 13, 58] (Fig. 10.11). This highly malignant tumor accounts for most soft tissue sarcomas in infants, and it is second in frequency to fibrosarcoma in the newborn [7, 13]. Most rhabdomyosarcomas diagnosed during the first year of life are of the embryonal histological

type, which has a much better prognosis than the alveolar form [7, 58] (see Chap. 4 for further discussion).

References

1. Abramson DH, Notterman RB, Ellsworth RM et al (1983) Retinoblastoma treated in infants in the first 6 months of life. *Arch Ophthalmol* 101:1362–1366
2. Abramson DH, Servodidio CA (1992) Retinoblastoma in the first year of life. *Ophthalmic Paediatr Genet* 13:191–203
3. Abramson DH, Du TT, Beaverson KL (2002) (Neonatal) retinoblastoma in the first month of life. *Arch Ophthalmol* 120:738–742
4. Bader JL, Miller RW (1979) U.S. cancer incidence and mortality in the first year of life. *Am J Dis Child* 133:157–159
5. Isaacs H Jr (1987) Congenital and neonatal malignant tumors: a 28-year experience at Children's Hospital of Los Angeles. *Am J Pediatr Hematol Oncol* 9:121–129
6. Isaacs H Jr (1997) Tumors of the eye. In: *Tumors of the fetus and newborn. Major problems in pathology*, vol 35. W.B. Saunders, Philadelphia, pp 229–243
7. Isaacs H Jr (2002) Tumors of the eye. In: *Tumors of the fetus and infant: an atlas*. Springer, New York, pp 241–260
8. Plotsky D, Quinn G, Eagle R Jr (1987) Congenital retinoblastoma: a case report. *J Pediatr Ophthalmol Strabismus* 24:120–123
9. Campbell AN, Chan HSL, O'Brien A et al (1987) Malignant tumours in the neonate. *Arch Dis Child* 62:19–23
10. Parkes SE, Muir KR, Southern L et al (1994) Neonatal tumours: a thirty-year population based study. *Med Pediatr Oncol* 22:309–317
11. Maat-Kievit JA, Oepkes D, Hartwig NG et al (1993) A large retinoblastoma detected in a fetus at 21 weeks gestation. *Prenat Diagn* 13:377–384
12. Isaacs H Jr (1985) Perinatal (congenital and neonatal) neoplasms: a report of 110 cases. *Pediatr Pathol* 3:165–216
13. McLean IW, Burnier MN, Zimmerman LE, Jakobiec FA (1994) Tumors of the eye and ocular adnexa. In: *Atlas of tumor pathology*, Third series, fascicle 12. Armed Forces Institute of Pathology, Washington, D.C., p 97
14. Murphree AL, Munier FL (1994) Retinoblastoma. In: Ryan S (ed) *Retina*, vol I, 2nd edn. CV Mosby, St Louis, p 571
15. Friend SH, Dryja TP, Weinberg RA (1988) Oncogenes and tumor suppressing genes. *N Engl J Med* 318:618–622
16. Abramson DH, Frank CM, Susman M et al (1998) Presenting signs of retinoblastoma. *J Pediatr* 132:505–508
17. Gilbert F, Potluri VR, Short MP et al (1987) Retinoblastoma, chromosome abnormalities and oncogene expression. *Ophthalmic Paediatr Genet* 8:3–10
18. Ellsworth RM (1969) The practical management of retinoblastoma. *Trans Am Ophthalmol Soc* 67:462–534
19. Ulbright TM, Fulling KH, Helveston EM (1984) Astrocytic tumors of the retina: differentiation of sporadic tumors from phakomatosis-associated tumors. *Arch Pathol Lab Med* 108:160–163
20. Gangwar DN, Jain MSIS, Gupta A et al (1982) Bilateral spontaneous regression of retinoblastoma with dominant transmission. *Ann Ophthalmol* 14:479–480
21. Sang DN, Albert DM (1982) Retinoblastoma: clinical and histopathologic features. *Hum Pathol* 13:133–147
22. Shuangshoti S, Chaiwun B, Kasantikul V (1989) A study of 39 retinoblastomas with particular reference to morphology, cellular differentiation and tumor origin. *Histopathology* 15:113–124
23. Popoff NA, Ellsworth RM (1971) The fine structure of retinoblastoma. In vivo and in vitro observations. *Lab Invest* 25:389–402
24. Rootman J, Carruthers JDA, Miller RR (1987) Retinoblastoma. *Perspect Pediatr Pathol* 10:208–258

25. Ts'o M, Zimmerman LE, Fine BS (1970) The nature of retinoblastoma. I. Photoreceptor differentiation: a clinical and histopathologic study; II. Photoreceptor differentiation: an electron microscopic study. *Am J Ophthalmol* 69:339–359
26. Margo C, Hidayat A, Kopelman J et al (1983) Retinocytoma: a benign variant of retinoblastoma. *Arch Ophthalmol* 101:1519–1531
27. Donoso LA, Shields CL, Lee EY (1989) Immunohistochemistry of retinoblastoma. A review. *Ophthalmic Paediatr Genet* 10:3–32
28. Terenghi G, Polak JM, Ballesta J et al (1984) Immunocytochemistry of neuronal and glial markers in retinoblastoma. *Virchows Arch A Pathol Anat Histopathol* 404:61–73
29. Magrann I, Abramson DH, Ellsworth RM (1989) Optic nerve involvement in retinoblastoma. *Ophthalmology* 96:217–222
30. MacKay CJ, Abramson DH, Ellsworth RM (1984) Metastatic patterns of retinoblastoma. *Arch Ophthalmol* 102:391–396
31. Shields JA, Shields CL (1994) Current management of retinoblastoma. *Mayo Clin Proc* 69:50–56
32. Dickman PS, Barmada M, Gollin SM et al (1997) Malignancy after retinoblastoma: secondary cancer or recurrence. *Hum Pathol* 28:200–205
33. Bader JL, Meadows AT, Zimmerman LE et al (1982) Bilateral retinoblastoma with ectopic intracranial retinoblastoma: trilateral retinoblastoma. *Cancer Genet Cytogenet* 5:203–213
34. Amoaku WMK, Willshaw HE, Parkes SE et al (1996) Trilateral retinoblastoma: a report of five patients. *Cancer* 78:858–863
35. Blach LE, McCormick B, Abramson DH et al (1994) Trilateral retinoblastoma – incidence and outcome: a decade of experience. *Int J Radiat Oncol Biol Phys* 29:729–733
36. Pesin SR, Shields JA (1989) Seven cases of trilateral retinoblastoma. *Am J Ophthalmol* 107:122–123
37. Johnson DL, Chandra R, Fisher WS et al (1985) Trilateral retinoblastoma: ocular and pineal retinoblastoma. *J Neurosurg* 63:367–370
38. Lueder GT, Judisch F, Wen B-C (1991) Heritable retinoblastoma and pinealoma. *Arch Ophthalmol* 109:1707–1709
39. Broughton WL, Zimmerman LE (1978) A clinicopathologic study of 56 cases of intraocular medulloepitheliomas. *Am J Ophthalmol* 85:407–418
40. Canning CR, McCartney AC, Hungerford J (1988) Medulloepithelioma (diktyoma). *Br J Ophthalmol* 72:764–767
41. Shields JA, Eagle RC Jr, Shields CL (1996) Congenital neoplasms of the nonpigmented ciliary epithelium (medulloepithelioma). *Ophthalmology* 103:1998–2006
42. Steinkuller PG, Font RL (1997) Congenital malignant teratoid neoplasm of the eye and orbit: a case report and review of the literature. *Ophthalmology* 104:38–42
43. Shami MJ, Benedict WL, Myers M (1993) Early manifestations of retinal hamartomas in tuberous sclerosis. *Am J Ophthalmol* 115:539–540
44. Williams R, Taylor D (1985) Tuberous sclerosis. *Surv Ophthalmol* 30:143–154
45. Mullaney PB, Jacquemin C, Abboud E et al (1997) Tuberous sclerosis in infancy. *J Pediatr Ophthalmol Strabismus* 34:372–375
46. Isaacs H (2009) Perinatal (fetal and neonatal) tuberous sclerosis: a review. *Am J Perinatol* 26:755–760
47. Riccardi VM (1992) Type 1 neurofibromatosis and the pediatric patient. *Curr Probl Pediatr* 22:66–106
48. Waeltermann JM, Huntrakoon M, Beatty EC Jr, et al (1988) Congenital fibromatosis (myofibromatosis) of the orbit: a rare cause of proptosis at birth. *Ann Ophthalmol* 20:494–496
49. Rootman J, Damji KF, Dimmick JE (1989) Malignant rhabdoid tumor of the orbit. *Ophthalmol* 96:1650–1654
50. Stidham DB, Bugett RA, Davis MM, et al (1999) Congenital malignant rhabdoid tumor of the orbit. *J Am Assoc Pediatr Ophthalmol Strabismus* 3:318–320
51. Lyon DB, Dortzbach RK, Gilbert-Barnes E (1993) Polyphenotypic small cell orbitocranial tumor. *Arch Ophthalmol* 111:1402–1408
52. Shields CL, Husson M, Shields JA, et al (1998) Solitary intraosseous infantile myofibroma of the orbital roof. *Arch Ophthalmol* 116:1528–1530
53. Weiner JM, Hidayat AA (1983) Juvenile fibrosarcoma of the orbit and eyelid. A study of five cases. *Arch Ophthalmol* 101:253–259
54. Fezza JP, Wolfley DE, Flynn SD (1997) Malignant peripheral nerve sheath tumor of the orbit in newborn: a case report and review. *Pediatr Ophthalmol Strabismus* 34:128–131
55. Adams RJ, Drwiega PJ, Rivera CA (1997) Congenital orbital lipoblastoma: a pathologic and radiologic study. *Pediatr Ophthalmol Strabismus* 34:194–196
56. Lamping KA, Albert DM, Lack E, et al (1985) Melanotic neuroectodermal tumor of infancy (retinal anlage tumor) *Ophthalmol* 92:143–149
57. Gormley PD, Thompson J, Aylward GW, et al (1994) Congenital undifferentiated sarcoma of the orbit. *J Am Assoc Pediatr Ophthalmol Strabismus* 31:59–61
58. Kodet R, Newton WA, Hamoudi AB, et al (1997) Orbital rhabdomyosarcomas and related tumors in childhood: relationship of morphology to prognosis- an Intergroup Rhabdomyosarcoma Study *Med Pediatr Oncol* 29:51–60

11.1 Introduction

Pediatric renal tumors consist of separate distinct entities with different biologic behaviors and responses to treatment [1–15]. The National Wilms' Tumor Study (NWTs) demonstrated an important relationship between the histology of the various renal tumors and their prognosis [1, 2]. Classification of fetal and infant renal tumors and their distinguishing gross and microscopic findings are described in Tables 11.1 and 11.2, respectively. *Wilms' tumor (WT)*, *congenital mesoblastic nephroma (CMN)*, and *rhabdoid tumor (RTK)*, in that order, are the main neoplasms of the kidney occurring during the first year of life, and CMN is the leader followed by WT and RTK in the fetus and neonate [3–8, 10–15] (Table 11.2). An abdominal mass is the main clinical presentation of a renal tumor. Nonneoplastic diseases of the kidney, which appear also as abdominal masses, are by far more prevalent than neoplastic ones. *Hydronephrosis* and *renal cystic disease* account for roughly 40 % of all renal masses in infants [12, 15] (Figs. 11.1, 11.2, 11.3, and 11.4) (Table 1.2). The staging system for pediatric renal tumors is given in Table 11.3. This system depends on the identification of penetration of the renal capsule, involvement of renal sinus vessels, surgical margins, regional lymph nodes, and distant metastases [5].

Table 11.1 Classification of fetal and infant renal tumors

Congenital mesoblastic nephroma
Classic mesoblastic nephroma
Cellular mesoblastic nephroma
Mixed classic and cellular
Wilms' tumor
Classic triphasic
Epithelial (monomorphous)
Blastemal
Fetal rhabdomyomatous
Botryoid tumor of the renal pelvis
Wilms' tumor with anaplasia ^a
Nephroblastomatosis complex
Cystic renal tumors
Cystic nephroma (Multilocular cyst)
Cystic partially differentiated nephroblastoma
Cystic Wilms' tumor
Metanephric stromal tumor
Rhabdoid tumor of kidney
Clear cell sarcoma of kidney
Ossifying renal tumor of infancy
Renal cell carcinoma ^a

Reprinted from Isaacs [15]. © Springer-Verlag, 2002

^aUsually does not occur in infants

Table 11.2 Renal tumors and tumorlike conditions of the fetus and infant: distinguishing features

Tumor	Gross	Histopathology
Congenital mesoblastic nephroma		
Classic	Nonencapsulated, non-circumscribed, light tan, fingerlike projections, resembles leiomyoma	Monomorphous uniform spindle-shaped cells surrounding normal parenchymal elements, rare mitoses, Vim +, act +
Cellular	Encapsulated, pale gray, circumscribed, cystic, gelatinous	Monomorphous spindle-shaped cells, hypercellular, mitoses, nuclear atypia, Vim +, Act+, resembles infantile fibrosarcoma
Wilms' tumor	Encapsulated, well circumscribed, light tan-gray, soft, cystic necrosis, hemorrhage	<i>Epithelial</i> : primitive tubular and glomerular-like elements, scant stroma; <i>Blastemal</i> : small round to oval cells, many mitoses, may resemble a small blue cell malignancy; <i>Triphasic</i> : epithelial, blastemal, mesenchymal elements (e.g., skeletal muscle fibers, fibroblasts); <i>Fetal rhabdomyomatous</i> : triphasic histology with over 40 % skeletal muscle; <i>Botryoid</i> : tumors of the renal pelvis with a triphasic pattern ± skeletal muscle <i>Anaplasia</i> ^a : bizarre mulberry-like giant cells, large triphasic mitoses
Nephroblastomatosis complex		
Nephrogenic rests		
Perilobar (PLNR) ^b	Small tan-gray nodules present beneath the capsule, visible depending on their size	Nodules of small, dark embryonic-appearing tubules and glomeruli resembling the outer cortical nephrogenic zone of the developing kidney
Intralobar (ILNR)	Small tan-gray nodules situated within the cortex or medulla, visible depending on their size	Nodules of small, dark embryonic-appearing tubules and glomeruli resembling the outer cortical nephrogenic zone of the developing kidney
Combined (PLNR + ILNR)	Tan-gray confluent nodules present beneath the capsule, in the cortex and medulla, kidneys diffusely enlarged	Diffuse hyperplastic-appearing tubules, glomeruli, and blastemal occupying cortex and medulla, tubulointerstitial dysplasia, disorganized growth pattern
Metanephric stromal tumor	Tan-lobulated, cystic, and fibrous mass centered in the renal medulla	Variegated cellular stromal tumor with spindled or stellate cells forming a nodular pattern, onion skin collarette formation around entrapped tubules, angiodysplasia of intratumoral vessels, juxta-glomerular cell hyperplasia of entrapped glomeruli
Rhabdoid tumor	Encapsulated ±, tan-gray, ± well circumscribed, large areas of cystic necrosis, hemorrhage	Hypercellular population of polygonal cells with abundant eosinophilic cytoplasm, vesicular nucleus with single big nucleolus, globular cytoplasmic inclusion consists of intermediate filaments by EM, INI1 Chromosome 22 genetic deletion
Clear cell sarcoma of kidney	Encapsulated, well circumscribed, hemorrhagic and cystic	Hypercellular population of round to oval cells with water-clear cytoplasm, open (vesicular) nucleus, fine chromatin, and tiny nucleolus, few mitoses, rows of cells separated by delicate fibrous septae, vascular branching capillary pattern, palisading of tumor cells; Vim +, NSE-, cytoke-, des-. Actin-; EM: primitive small cells with sparse organelles and fluffy intra- and extracellular deposits
Ossifying renal tumor of infancy	Calcified mass projecting into dilated calyx arising from renal papilla	Osteoid islands surrounded by spindle-shaped fibroblastic cells resembling CMN
Cystic conditions of the kidney		
Multiloculated cyst	Multicystic mass situated in the upper or lower pole of the kidney well demarcated from the renal pelvis by a discrete light tan or white capsule, cysts vary in size, contain clear fluid, and consist of thin fibrous septae	Septae lack nephrogenic elements
Cystic partially differentiated nephroblastoma	Gross findings identical to multilocular cyst	Fibrous septae that separate cysts contain mature or immature nephrogenic elements
Cystic Wilms' tumor	Encapsulated, well circumscribed, light tan-gray, soft, focal or multifocal cysts	Well-differentiated Wilms' tumor with focal or multicystic change

Reprinted from Isaacs [11]. © WB Saunders 1997

Abbreviations: Vim vimentin, Act actin, CMN congenital mesoblastic nephroma, Cytok cytokeratin, Des desmin. NSE neuron-specific enolase, EM electron microscopy

^a“Unfavorable histology” associated with a poor prognosis, anaplasia is rare in infancy

^bFound in association with bilateral Wilms' tumor and congenital anomalies

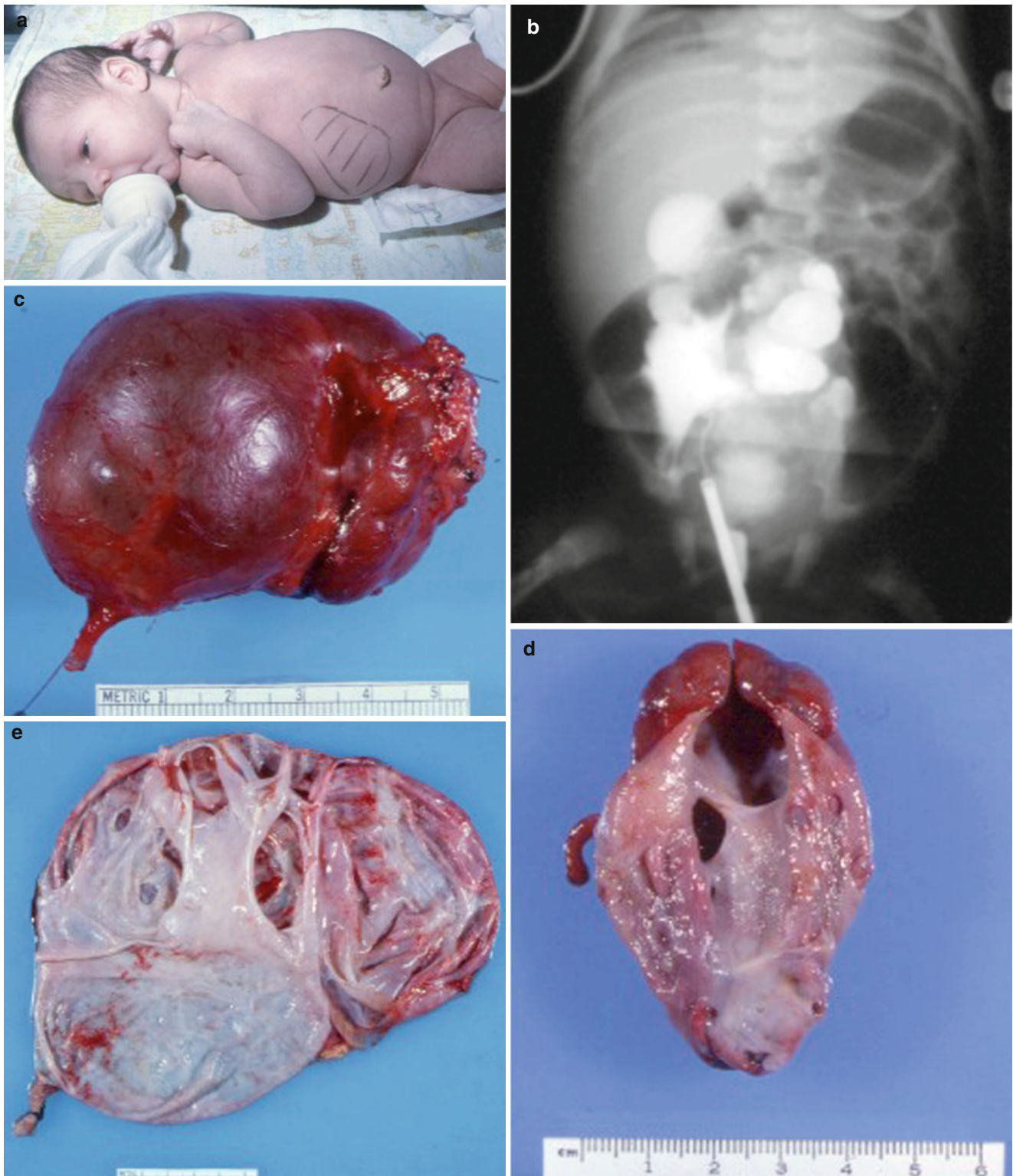


Fig. 11.1 Hydronephrosis presenting as an abdominal mass. This malformation is one of the most frequent ones detected on routine antenatal abdominal sonography. (a) 1-week-old female with an abdominal mass. (b) Retrograde pyelogram revealing the dilated renal pelvis outlined by injected contrast medium. (c) The dilated pelvis and portion of ureter are situated on the left side of the kidney. (d) The opened specimen

reveals the dilated pelvis and calyces. A ureteropelvic junction obstruction (stenosis) was found and considered to be the cause of the hydronephrosis. (e) Opened renal pelvis from an older child showing marked distension and thinning (Reprinted from Isaacs [11]. © WB Saunders 1997)

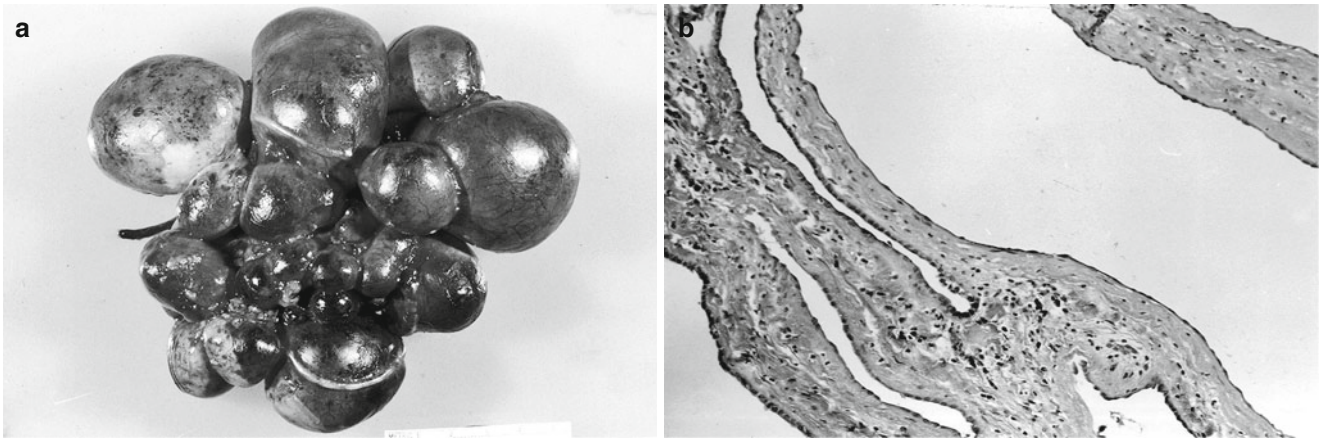


Fig. 11.2 Multicystic dysplastic kidney. 4-month-old female presented with an abdominal mass which was confirmed by imaging studies. **(a)** Almost the entire left kidney is replaced by multiple, grapelike cysts of various sizes filled with clear straw-colored fluid. The specimen weighed 368 g and measured 13×9×5 cm. An atretic ureter is attached to the cystic kidney on the left. **(b)** The thin-walled cysts are of various

sizes and lined by cuboidal and flattened epithelial cells. The cyst walls are composed mainly by dense fibrous tissue. Foci of residual renal tissue, cartilage, and medullary dysplasia (tubules lined by primitive urothelium and surrounded by collars of mesenchyme) not shown here but are present in other areas (Reprinted from Isaacs [11]. © WB Saunders 1997)

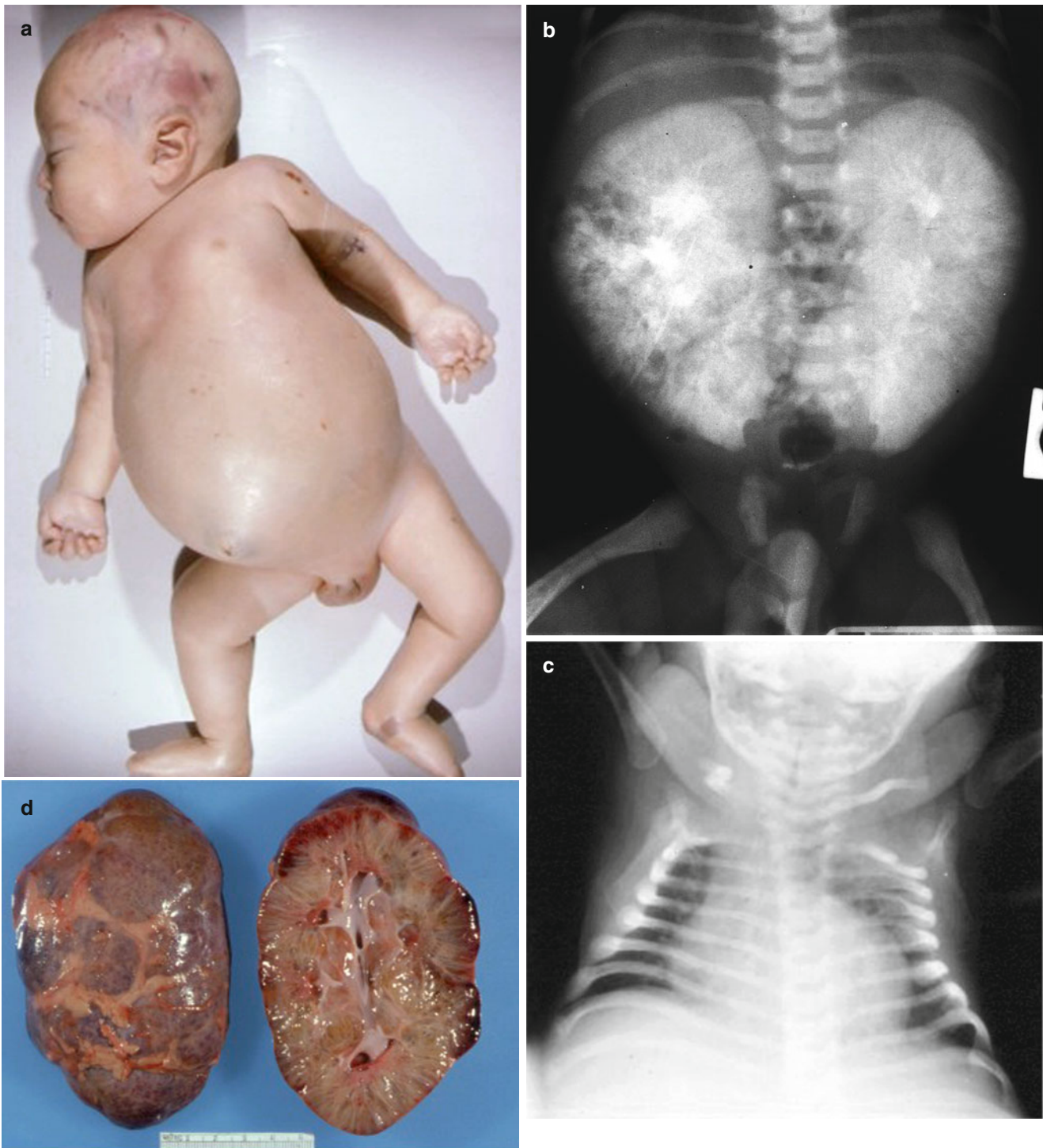


Fig. 11.3 Infantile polycystic disease of kidney and liver (autosomal recessive). (a) 3-month-old male infant with bilateral flank masses noted at birth died of renal and pulmonary failure complicated by *E. coli* sepsis. The abdomen is markedly distended by very large kidneys and liver. (b) Intravenous pyelogram displays bilateral renalomegaly and cystically tubules filled with dye. (c) Chest radiograph shows an abnor-

mally small thoracic cavity and hypoplastic lungs. (d) Radially arranged, fusiform cysts are situated in the cortex and medulla. The blackened cortical areas represent foci of acute pyelonephritis due to *E. coli*. (e) Cystically dilated collecting ducts are present (Reprinted from Isaacs [11]. © WB Saunders 1997)

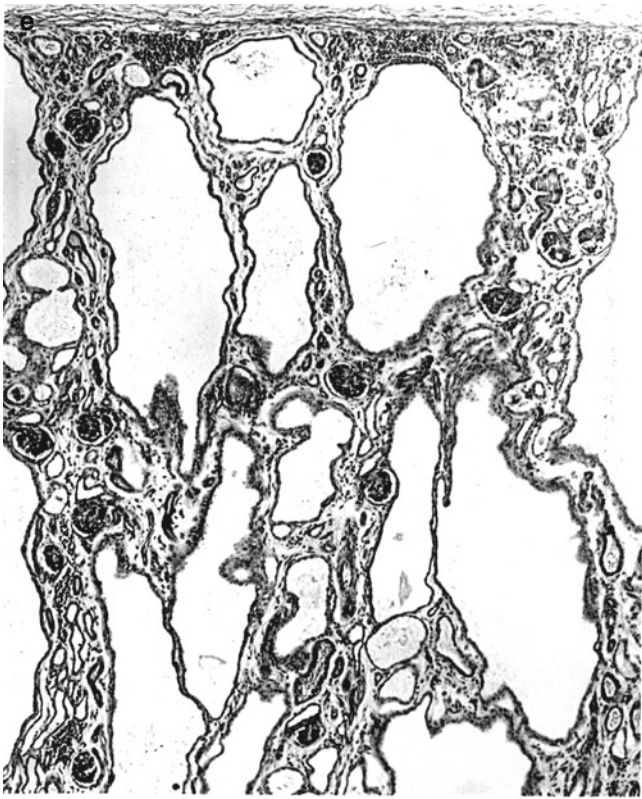


Fig. 11.3 (continued)

Fig. 11.4 Prune belly syndrome (megacystis, megaureter, and absence of abdominal musculature). (a) Infant with a distended, scaphoid, “doughy” abdomen, and bilateral undescended testes. (b) Intravenous pyelogram depicting a markedly dilated ureter and enlarged urinary bladder. (c) Skeletal muscle is absent from a full thickness biopsy of the abdominal wall. (d) Portion of megaureter shows intramural fibrosis

and decreased amount of smooth muscle. (e) Several small cysts lined by regular low cuboidal epithelium were present (Radiograph courtesy of Melvin O. Senac, Jr., M.D., Department of Radiology, Rady Children’s Hospital San Diego; Reprinted from Isaacs [11]. © WB Saunders 1997)

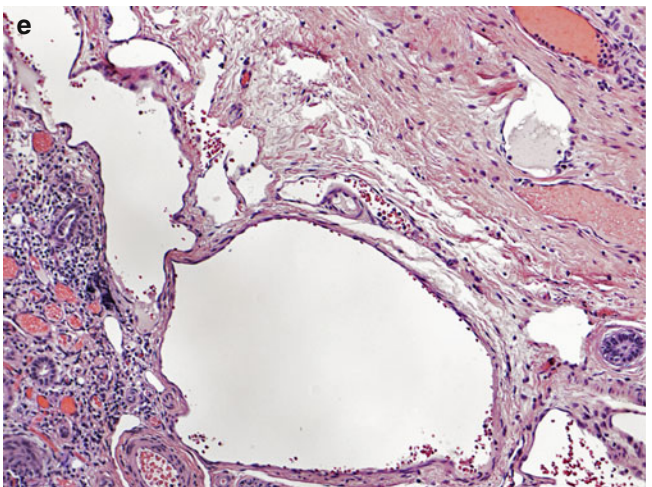
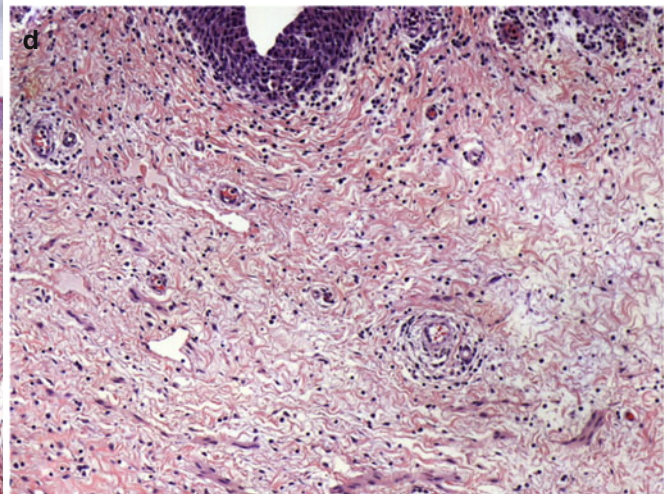
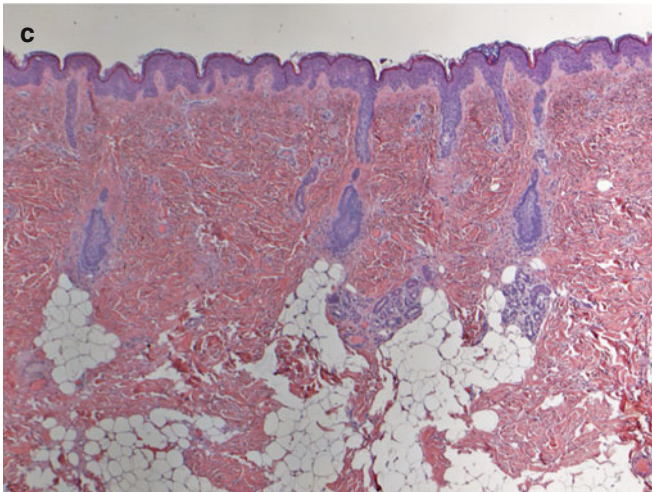
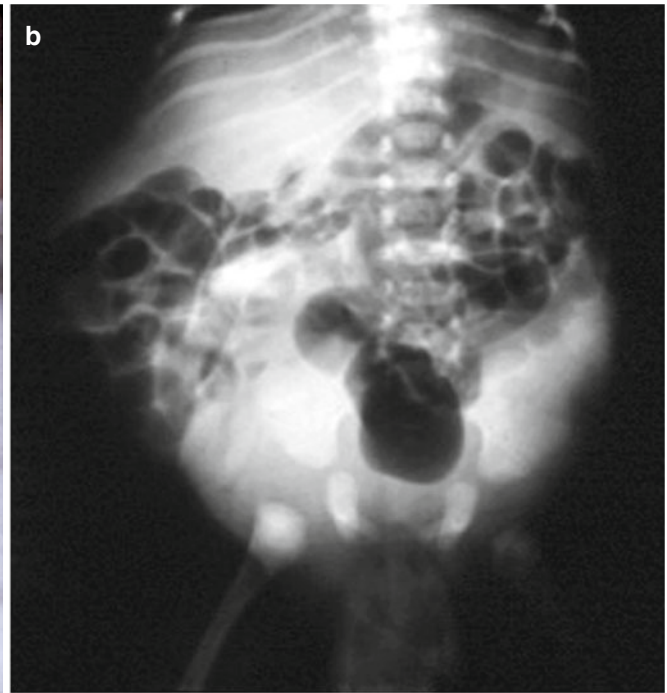


Table 11.3 Staging of pediatric renal tumors

Stage
I. Tumor confined to the kidney and totally resected
II. No evidence of tumor at or beyond the margins of resection, tumor totally resected, capsular invasion, tumor extends beyond the kidney involving renal sinus soft tissues and/or vessels
III. Residual tumor confined to the abdomen, involvement of abdominal lymph nodes, gross or microscopic lines of resection positive, tumor spillage and peritoneal implants, tumor not resectable
IV. Hematogenous metastases to distant organs, extra-abdominal lymph node metastases
V. Bilateral Wilms' tumors

Reprinted from Pearlman [5]. With kind permission of © Mosby-Elsevier, 2007

11.2 Wilms' Tumor

Embryonic nephrogenic tissue normally differentiates into the *metanephric blastema*, the precursor of nephrons, and mesenchymal stroma (Fig. 11.5). Abnormal proliferation of the metanephric blastema may produce epithelial and/or stromal renal tumors found almost exclusively in young individuals [12]. *Wilms' tumor* (WT) is the malignant embryonal tumor derived from the metanephric blastema [2].

Ten to twenty percent of all *Wilms' tumors* are diagnosed during the first year of life [7, 9, 15]. WT occurs less often in the fetus and neonate than in the older child [6, 7, 9, 15–19]. It presents as an abdominal mass either on prenatal sonography or during physical examination. The malignancy is associated with specific congenital defects and malformation syndromes in 10 % of affected individuals (Table 11.4).

Karyotypic analyses of WTs may show a deletion in the short arm of chromosome 11, del 11p13 [5, 20, 21]. Chromosome 11 deletions occur both in the leukocytes as well as in the tumor and can be used for identifying individuals and families at risk for developing the tumor and to the confirm histological diagnosis; for example, some poorly differentiated, blastemal, small blue cell WTs may present a diagnostic problem.

11.2.1 Pathology

Wilms' tumor on section has a pale tan to light gray cut surface with or without areas of necrosis or cyst formation. The tumor is encapsulated and well circumscribed (Figs. 11.6, 11.7, 11.8, 11.9, 11.10, 11.11, and 11.12). Rupture of the capsule with evidence of spillage and/or extension of tumor through the capsule is present in some specimens, particularly in the larger ones. Renal vein invasion is noted in about one fourth of the involved kidneys [12, 15]. Microscopically, most infant WTs show the *classic "triphasic" histological pattern* consisting of epithelial elements with varying degrees of differentiation, spindle-shaped blastema cells, and interstitial fibroblastic or myoblastic stromal cells [2] (Figs. 10.6 and 10.7). Some tumors are composed predominantly of either *epithelial tubular* or blastemal components (Figs. 11.8 and 11.9). The *blastemal pattern* is the least differentiated of the various histological patterns [2, 22] (Fig. 11.9). *Anaplastic features*, characterized by the presence of large, mulberry-like giant cells with hyperchromatic nuclei and multipolar mitotic figures, are associated with an adverse prognosis; anaplasia occurs more often in older children [1, 2, 23, 24] (Fig. 11.11). Both focal and diffuse anaplasia may occur in the same tumor [23]. The mortality associated with *diffuse anaplasia* rises rapidly with increasing stage and the type of cells involved by anaplasia [23, 24]. The presence of *focal anaplasia* in a WT has prognostic significance as well.

Some unique histological patterns of WT are noted particularly in the first year of life. The *fetal rhabdomyomatous nephroblastoma*, tumors with a prominent skeletal muscle component, and *botryoid tumors* of the renal pelvis showing a triphasic pattern, with or without skeletal muscle differentiation, are examples [15, 25, 26] (Fig. 11.12). The prognosis correlated with these microscopic variants is practically the same as the typical triphasic WT with favorable histology [15].

Most WTs occurring in infants are classified as *stage I* or *II* and have a "favorable histology," that is, triphasic, epithelial, or blastemal elements, which conceivably accounts for their better prognosis in this age group [7, 16] (Table 11.3).

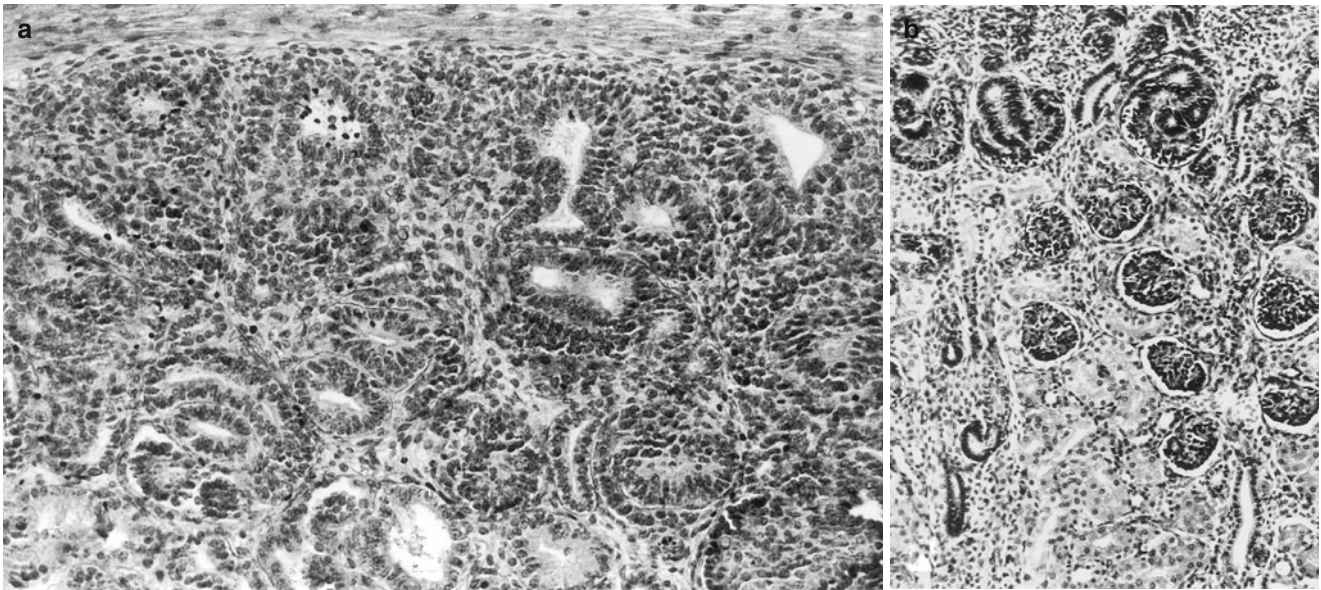


Fig. 11.5 Development of the kidney. **(a)** Glomeruli and tubules are beginning to form in the cellular metanephric blastema of the nephrogenic zone situated directly beneath the renal capsule. From an embryo of estimated 10–12 weeks gestation. **(b)** At the *top of the photograph*,

there is a row of immature glomeruli and tubules arising from the metanephric blastema. Three or four layers of definitive glomeruli are noted beneath (Reprinted from Isaacs [11]. © WB Saunders 1997)

Table 11.4 Conditions associated with Wilms' tumor

Aniridia
Hemihypertrophy
Genitourinary anomalies
Hypospadias
Undescended testes
Ambiguous genitalia
Nephroblastomatosis
Beckwith-Wiedemann syndrome ^a
WAGR syndrome ^b
Drash syndrome ^c
Perlman syndrome ^d
VATER association ^e
Bloom syndrome ^f
Prader-Willi syndrome ^g
Fraser syndrome

Reprinted from Isaacs [15] © Springer-Verlag, 2002

^aOmphalocele, macroglossia, visceromegaly and gigantism, abnormalities, and the 11p deletion syndrome

^bAmbiguous genitalia, nephritis, and Wilms' tumor

^cFetal gigantism, renal hamartomas, and nephroblastomatosis with Wilms' tumor

^dVertebral malformations, anal atresia, tracheoesophageal fistula, limb dysplasias, and renal anomalies

^eGrowth failure, sun sensitive facial telangiectasia, and defective immunity

^fObesity, short stature, hypogonadism, and mental retardation

^gCryptophthalmos, malformed ears, aberrant umbilicus, and incomplete development of external genitalia

The incidence of *bilateral WTs (stage V)* is reported as 5–10 % with figures ranging from 2 to 50 %, depending on the study [15–17, 27]. Patients with bilateral tumors tend to be younger at diagnosis, have an increased frequency of congenital malformations and nephrogenic rests, and have favorable histology (epithelial or a triphasic histological pattern). Although bilateral WTs generally have a favorable prognosis with adequate treatment, they present a therapeutic dilemma to balance curative surgical resection with preservation of functional renal tissue [27].

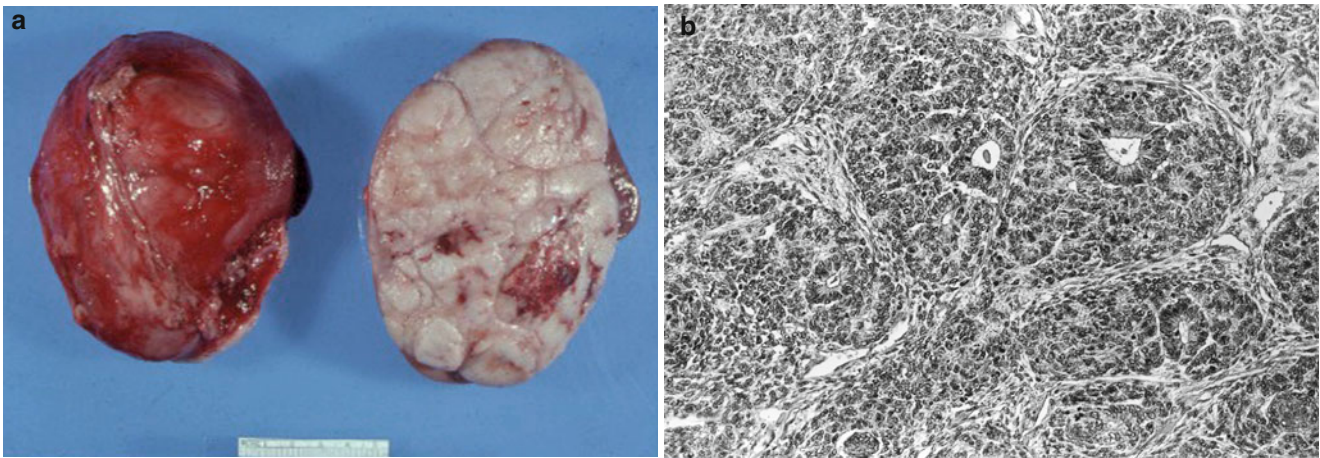


Fig. 11.6 Wilms' tumor. 1-year-old male was found to have an abdominal mass by his pediatrician while being evaluated for an upper respiratory infection. An abdominal mass is the most common physical finding in a child with a Wilms' tumor. (a) The kidney, 658 g and $13 \times 11 \times 9$ cm, is replaced by a soft, tan-gray lobular neoplasm that is encapsulated and well circumscribed. Areas of hemorrhagic necrosis are present. (b) The tumor consists the triad of blastemal, epithelial, and fibrous connective tissue components. The "triphasic" histological pattern (epithelial,

blastemal, and mesenchymal stromal components) is the most common one seen in Wilms' tumors in children overall. Epithelial Wilms' tumor is next in frequency in the newborn. Notice the manner in which spindle-shaped stromal cells blend imperceptively with the small, round more darkly staining blastemal cells. This finding is helpful when attempting to make the diagnosis especially on operative frozen section (Reprinted from Isaacs [15]. © Springer-Verlag, 2002)

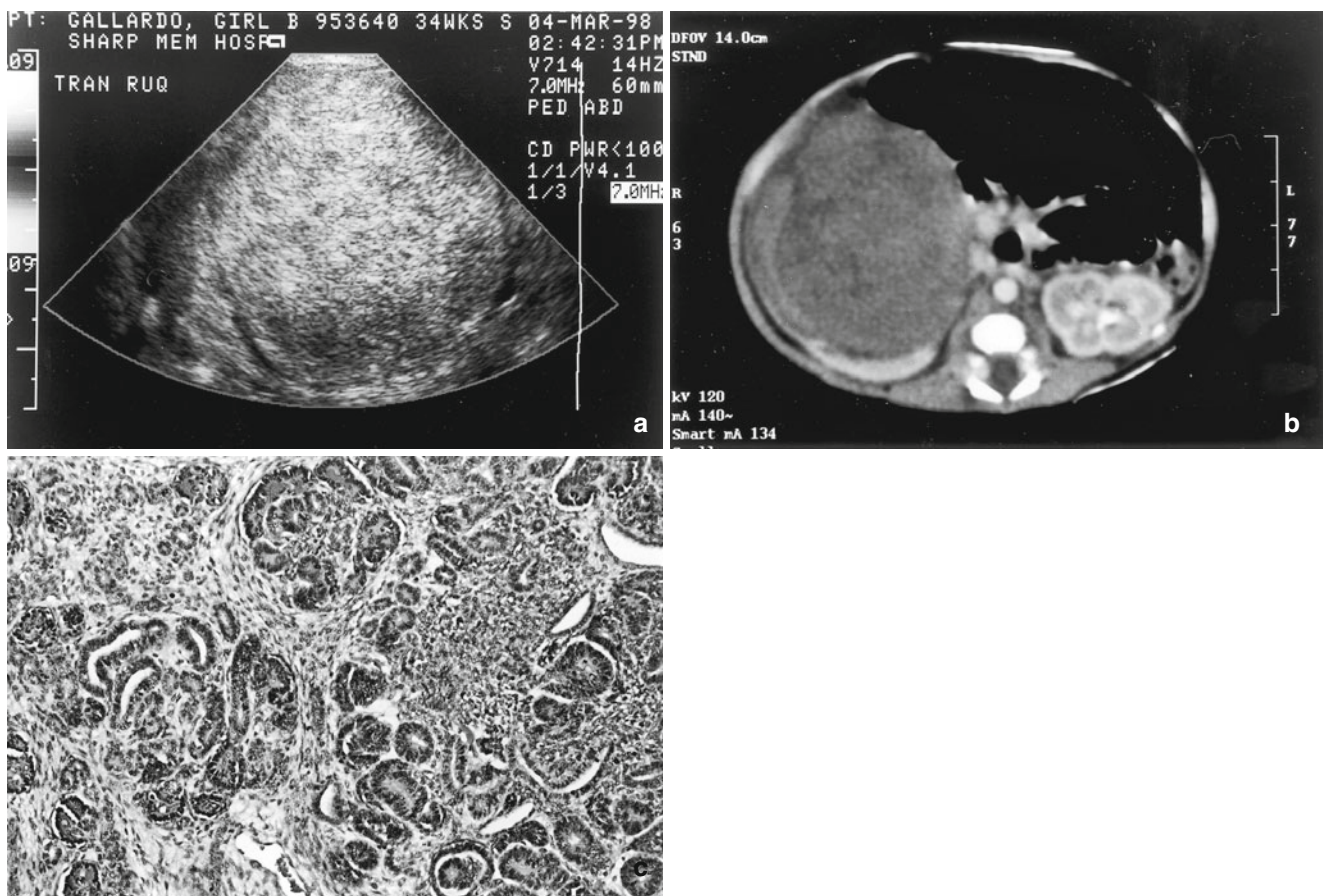


Fig. 11.7 Congenital Wilms' tumor ($6 \times 5 \times 4$ cm, 98 g, stage 1). Six-day-old female, one of twins, with an abdominal mass detected on prenatal ultrasonography at 34 weeks gestation. (a) Prenatal ultrasound showing the abdominal mass. (b) Abdominal CT scan reveals the tumor replacing most of the right kidney. The classic peripheral "claw sign"

characteristic of Wilms' tumor is present on the periphery of the mass. (c) The tumor is well differentiated with a triphasic histological pattern resembling developing kidney (c.f. Fig. 11.5). Nests of small, dark blue blastemal cells are present on the *right side* (Reprinted from Isaacs [15]. © Springer-Verlag, 2002)

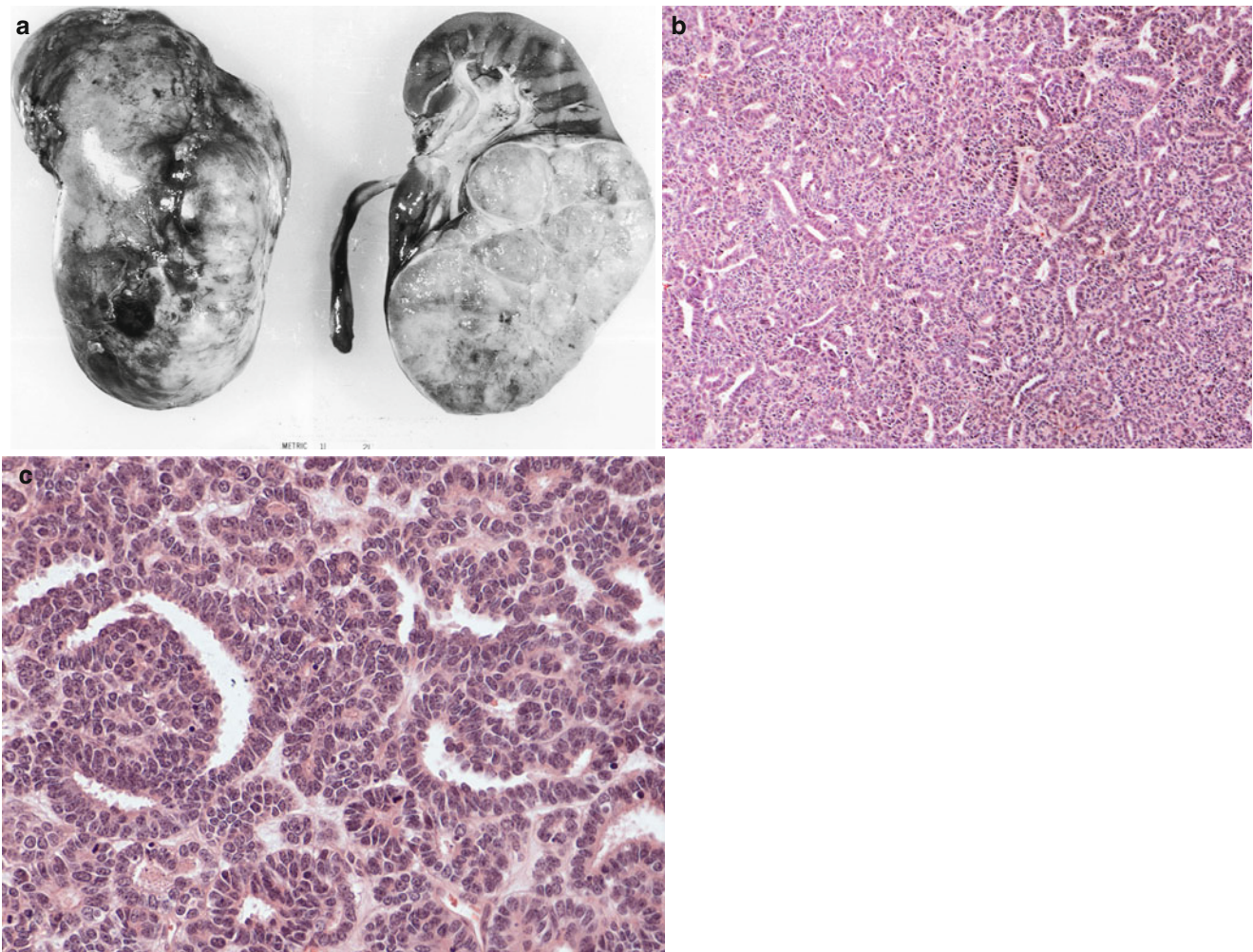


Fig. 11.8 Epithelial Wilms' tumor. (a) Renal tumor, 250 g and 9×5.5 cm, excised from an 11-month-old male with an abdominal mass. The cut surface of the kidney on the right shows a bulging, lobulated, encapsulated, and well-circumscribed neoplasm with a pale, slimy translucent appearance. (b) Low-power view revealing predomi-

nately epithelial tubular elements with very little stroma in between. (c) Higher magnification showing "back to back" tubular formations composed of vacuolated columnar cells with pleomorphic nuclei and moderate mitotic activity (Reprinted from Isaacs [11]. © WB Saunders 1997)

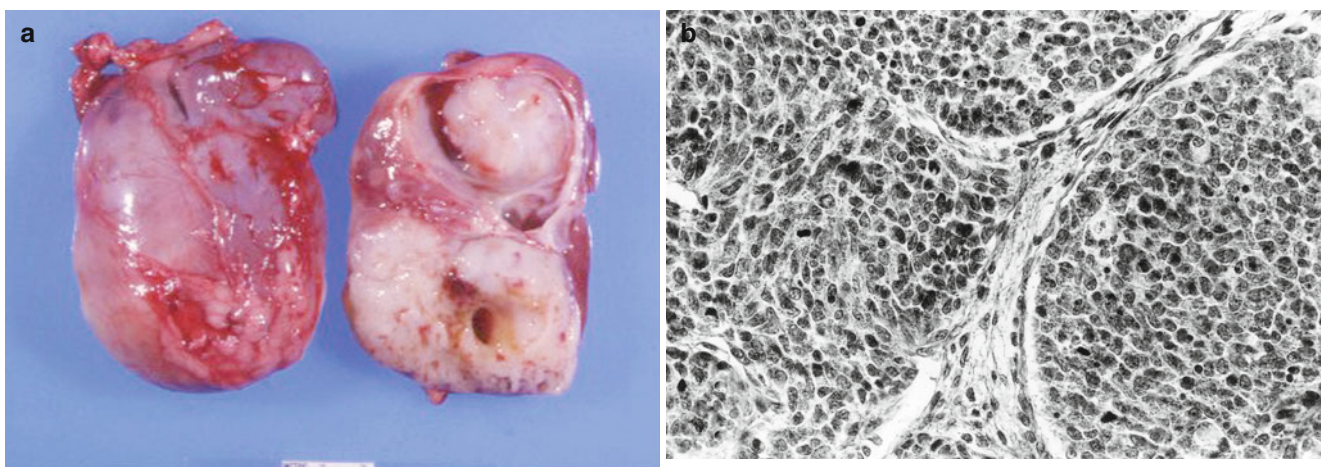


Fig. 11.9 Blastemal Wilms' tumor. (a) A 192 g, 9.5×7 cm, solid, and cystic neoplasm removed from a 4-month-old female, presenting with an abdominal mass. (b) Lobules of small round to oval blastemal cells with a high nuclear to cytoplasmic ratio are separated by delicate

fibrovascular septae. Sometimes, the blastemal pattern has the appearance of a "small, blue cell malignant tumor" (Reprinted from Isaacs [11]. © WB Saunders 1997)

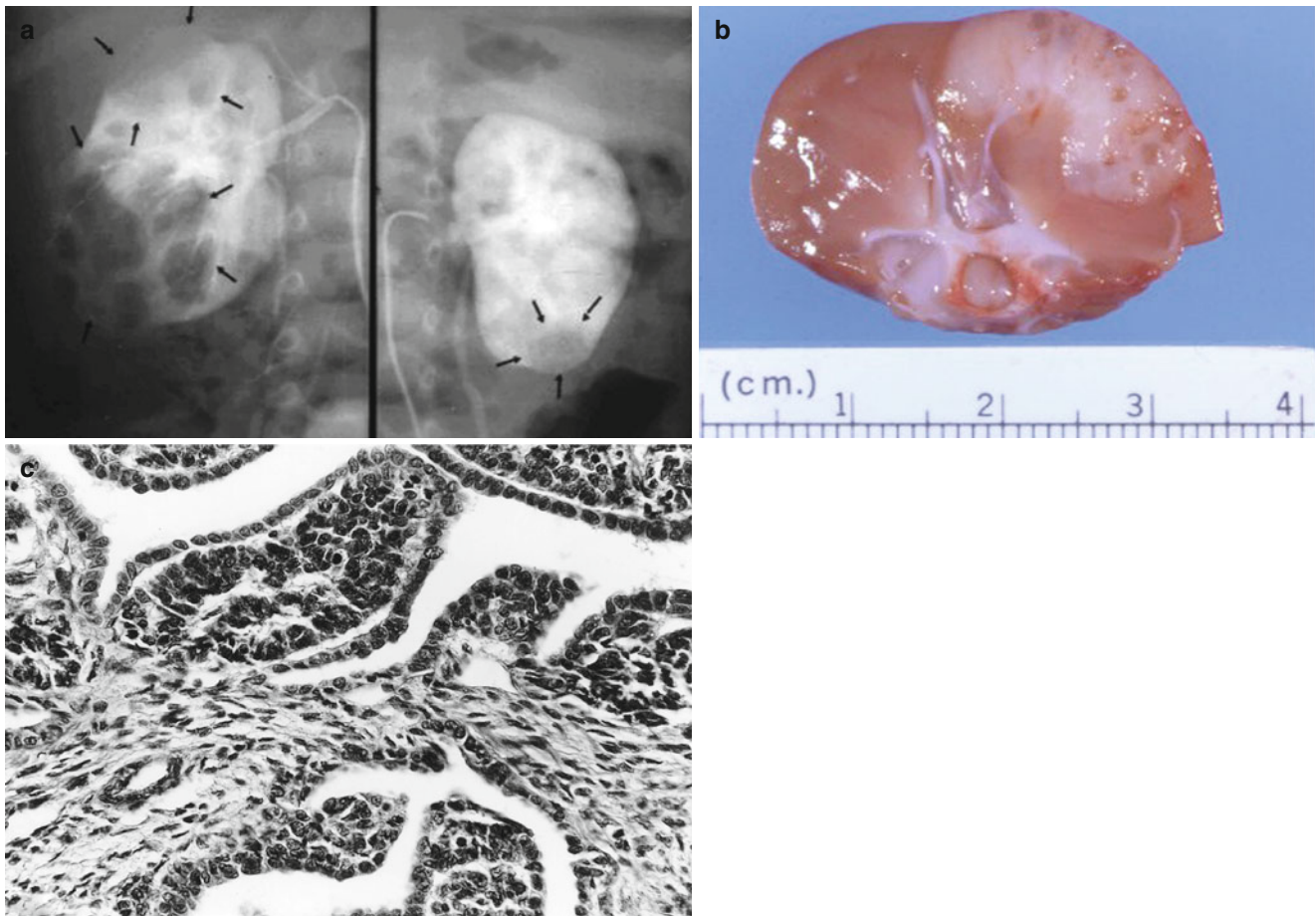


Fig. 11.10 Bilateral Wilms' tumor. 1-year-old male with congenital anomalies often associated with this malignancy. The clinical presentation of hypospadias, bilateral undescended testes, and aniridia prompted an investigation for the possibility of Wilms' tumor. (a) Arteriogram demonstrating two large masses in the right kidney and a smaller one in the left. The lesions are outlined by *arrows*. The baby had a total right nephrectomy, since this kidney was most involved, and a partial left nephrectomy. (b) A 2 × 1-cm tumor nodule situated beneath the capsule

of the lower pole of the left kidney has a light tannish-gray, cystic gelatinous appearance which was similar to the two larger ones in the right kidney. (c) All three tumors had the same histological appearance with triphasic and epithelial patterns. The "botryoid" polypoid epithelial component consists of papillary formations lined by single rows of cuboidal cells and nests of more atypical-appearing epithelial cells beneath (Reprinted from Isaacs [11]. © WB Saunders 1997)

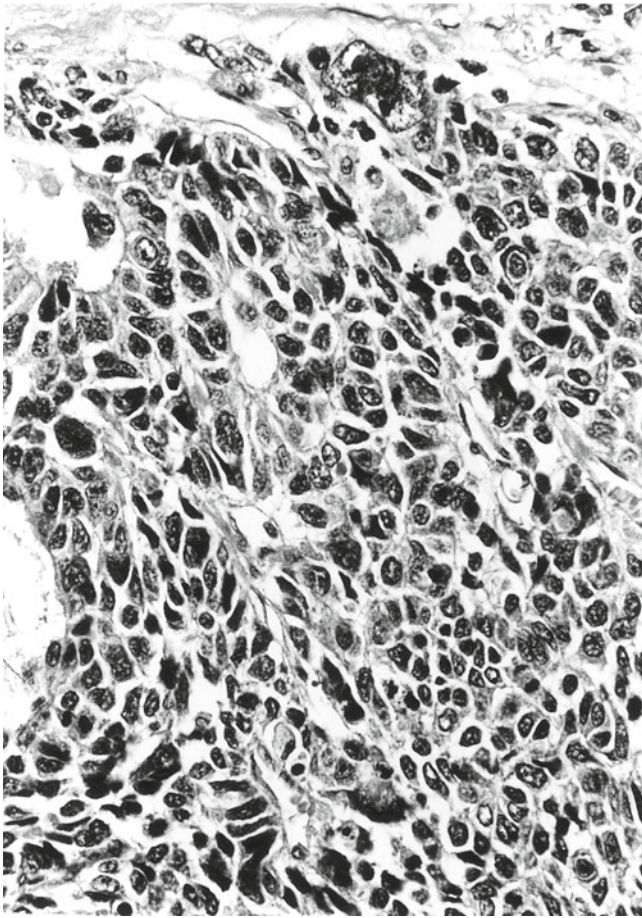


Fig. 11.11 Wilms' tumor with "anaplasia." Wilms' tumor with "unfavorable histology" from a 5-year-old girl. There are ill-defined tubule formations composed of anaplastic, darkly staining cells showing marked pleomorphism in cell size and shape. Bizarre-appearing giant cells and mitotic figures are present (Reprinted from Isaacs [15]. © Springer-Verlag, 2002)

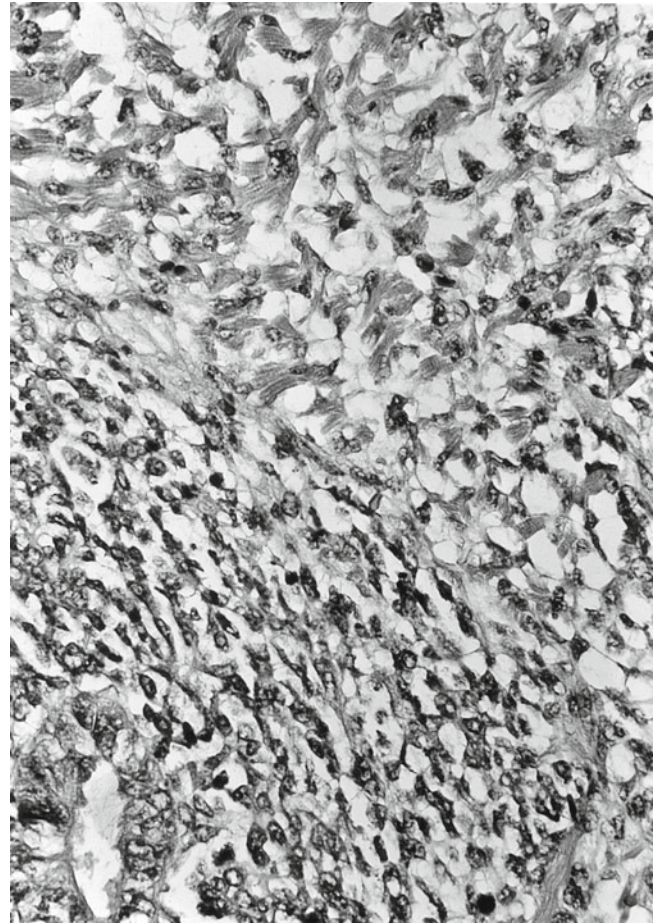


Fig. 11.12 Fetal rhabdomyomatous Wilms' tumor with a predominantly skeletal muscle component ("fetal rhabdomyomatous" Wilms' tumor). Rhabdomyoblasts with cytoplasmic cross striations (*upper right side of the field*) are bordered by blastemal cells and an embryonic tubule formation (*left lower corner*). The renal tumor, 845 g and 15×11 cm, was removed from a 10-month-old male. The renal pelvis was extensively involved by tumor (Reprinted from Isaacs [15]. © Springer-Verlag, 2002)

11.3 Nephrogenic Rests and Nephroblastomatosis

Nephrogenic rests and *nephroblastomatosis* are terms used to designate a group of renal lesions resembling the *metanephric blastema (nephrogenic zone)* of the developing kidney [15, 28–31] (Fig. 11.5). Nephrogenic rests are regarded as abnormally persistent nests of embryonal cells, representing microscopic malformations (dysplasias) of the developing kidney (Beckwith JB, personal communication, 1983) [28–33]. They are considered as WT precursor lesions. Nephrogenic rests are described in association with a variety of syndromes (Table 11.5). The lesions may be single, multiple, or bilateral in distribution and may be seen either grossly or microscopically depending on their size. *Nephrogenic rests* are divided into two main types: *perilobar (PLNR)* and *intralobar (ILNR)*; *nephroblastomatoses* are of four types: *perilobar*

(*PLNR, multifocal and diffuse*) and *intralobar (ILNR, deep cortical and panrenal)* (Fig. 11.13). PLNR, occurring at the lobar cortical surface (Fig. 11.14), is the most common form of nephrogenic rest, whereas ILNR is less frequent and found anywhere in the cortex or medulla. Combined nephroblastomatosis designates both PLNR and ILNR. *Panrenal (panlobar, diffuse) nephroblastomatosis* is the rarest form and often fatal; microscopically, there is no recognizable renal cortex or medulla [31]. Diffuse nephroblastomatosis is detected antenatally by sonography [32].

The fourth National Wilms' Tumor Study showed a high incidence of nephrogenic rests in kidneys with WTs, both unilateral and bilateral (29 % for the former and 99 % for the latter), and a high risk of developing a WT in the contralateral kidney when nephrogenic rests were found. Beckwith lists the risk figures as 26 % for PLNR alone, 59 % for ILNR alone, and 94 % for combined ILNR and PLNR [30]. Most nephrogenic

Table 11.5 Conditions associated with nephroblastomatosis

Wilms' tumor
Hemihypertrophy
Drash syndrome ^a
Thanatophoric dwarfism
Klippel-Trenaunay syndrome ^b
Trisomies 13 and 18
Perlman syndrome
Beckwith-Wiedemann syndrome
Congenital heart disease (high incidence)

Reprinted from Beckwith [29]. With kind permission of © Wiley, 1998; Reprinted from Bove [4]. With kind permission of © Elsevier, 1999; Reprinted from Isaacs [15]. © Springer-Verlag, 2002

^aSee previous table for description of other syndromes

^bCutaneous hemangiomas, varicose veins, and bony and soft tissue hypertrophy

rests regress and do not develop into a WT [29, 30], a situation perhaps analogous to neuroblastoma in situ [4, 30]. The importance of the rests, in addition to being potentially malignant (conceivably, they represent the first mutational event in carcinogenesis), is that they are associated with certain syndromes, trisomies, and congenital defects [5, 12, 28] (Table 11.5). Nephrogenic rests are detected before evolution to WT by serial imaging studies [4]. The type of rest is associated with certain histological types of WT; for example, the perilobar rests are seen in conjunction with the blastemal or epithelial WT with little stroma, and intralobar rests are noted with WTs having a prominent stroma, embryonic nephron-like elements, and heterologous cell types. Actual progression of nephrogenic rests to nephroblastomatosis to WT is documented by serial biopsies [30]. Occasionally, it is difficult or practically impossible to distinguish between a true WT and nephroblastomatosis. Neither the size of the lesion nor the microscopic appearance is always helpful in making this distinction (Beckwith JB, personal communication, 1983) [30]. Furthermore, this situation is particularly difficult in attempting to decide whether primitive nephrogenic structures, for example, in a biopsy of a bilateral WT treated with chemotherapy, represent nephrogenic rests, residual Wilms' tumor, recurrent Wilms' tumor, or *de novo* tumor growth. *Following the patient with serial imaging studies to see whether the lesion has grown or not should be of help in resolving this issue* (Beckwith JB, personal communication, 1983).

11.4 Congenital Mesoblastic Nephroma

Congenital mesoblastic nephroma (CMN), clearly distinct from Wilms' tumor (WT), is the leading renal tumor of the fetus and newborn, following WT in frequency over all during the first year of life [3, 6, 9–11, 15]. The tumor occurs in association with *hemihypertrophy and the Beckwith-Wiedemann syndrome* [12].

Typically, patients with CMN present with an abdominal mass that is discovered on physical examination or by

routine antenatal sonography [3, 15, 34, 35] (Figs. 11.15, 11.16, 11.17, and 11.18). The tumor's characteristic sonographic findings are different from those of WT. The abdominal mass in the fetus may be so large as to produce serious complications such as dystocia, hydramnios, hydrops, and stillbirth [3, 13, 36].

11.4.1 Pathology

Often the diagnosis of CMN can be made from its distinctive gross appearance, which is clearly different from that of WT, CCSK, RTK, and cystic conditions. *There are two main types of CMN, classical CMN and cellular CMN.* The *classical CMN* occupies half or more of the involved kidney, and the cut section reveals an unencapsulated mass having a whorled pattern similar to a uterine leiomyoma [3, 11, 15, 37] (Figs. 11.15 and 11.16). Fingerlike projections of tumor extend into the adjacent renal parenchyma. Although unusual, extension into the renal vein, vena cava, extrarenal soft tissues, and cystic variants occurs [37]. Only a few bilateral examples have ever been documented [3]. Microscopically, the classic CMN shows a proliferation of uniform spindle-shaped cells, demonstrated by EM to be myofibroblasts and fibroblasts. The tumor cells infiltrate the renal parenchyma and appear to push aside the glomeruli and tubules rather than invading them [15, 37] (Figs. 11.15 and 11.16). Mitotic figures and small islands of cartilage may be present. Both vimentin and actin are immunoreactive, and desmin is focally expressed [37].

The *cellular CMN* is characterized histologically by hypercellularity, nuclear atypia, and increased mitotic activity [37–40] (Figs. 11.17 and 11.18). Some years ago, often these tumors were called “renal sarcoma” (personal observation). EM, immunohistochemical, and cytogenetic findings suggest that cellular CMN shares certain biological and histological properties in common with infantile fibromatosis and other myofibroblastic tumors of childhood [37, 41, 42] (see Chap. 4). For example, ETV6-NTRK3 gene fusions and trisomy 11 are found in both cellular CMN and congenital fibrosarcoma suggesting a histogenetic link between the two [41, 42].

Grossly, cellular CMN has a softer, more cystic, and hemorrhagic cut surface than classic form and appears more well circumscribed without the interdigitating periphery (Figs. 11.17 and 11.18). Large cystic cellular CMNs weighing as much as 1,300 g are found in older infants [39]. The cellular variant is noted in almost a third of infants less than 3 months of age with CMN and apparently has no prognostic significance in this younger age group provided that *the lesion is completely removed*. However, in older infants and children, the risk of recurrence or metastases is significantly increased especially if there is vascular and renal capsular invasion [40]. Both classical and cellular CMN forms may coexist in the same tumor. Complete surgical resection is the recommended treatment of choice [43].

Fig. 11.13 Location of different types of nephroblastomatosis. (a) Perilobar multifocal; (b) Perilobar diffuse; (c) Intralobar (*deep cortical*); (d) Panrenal (Reprinted from Isaacs [15]. © Springer-Verlag, 2002)

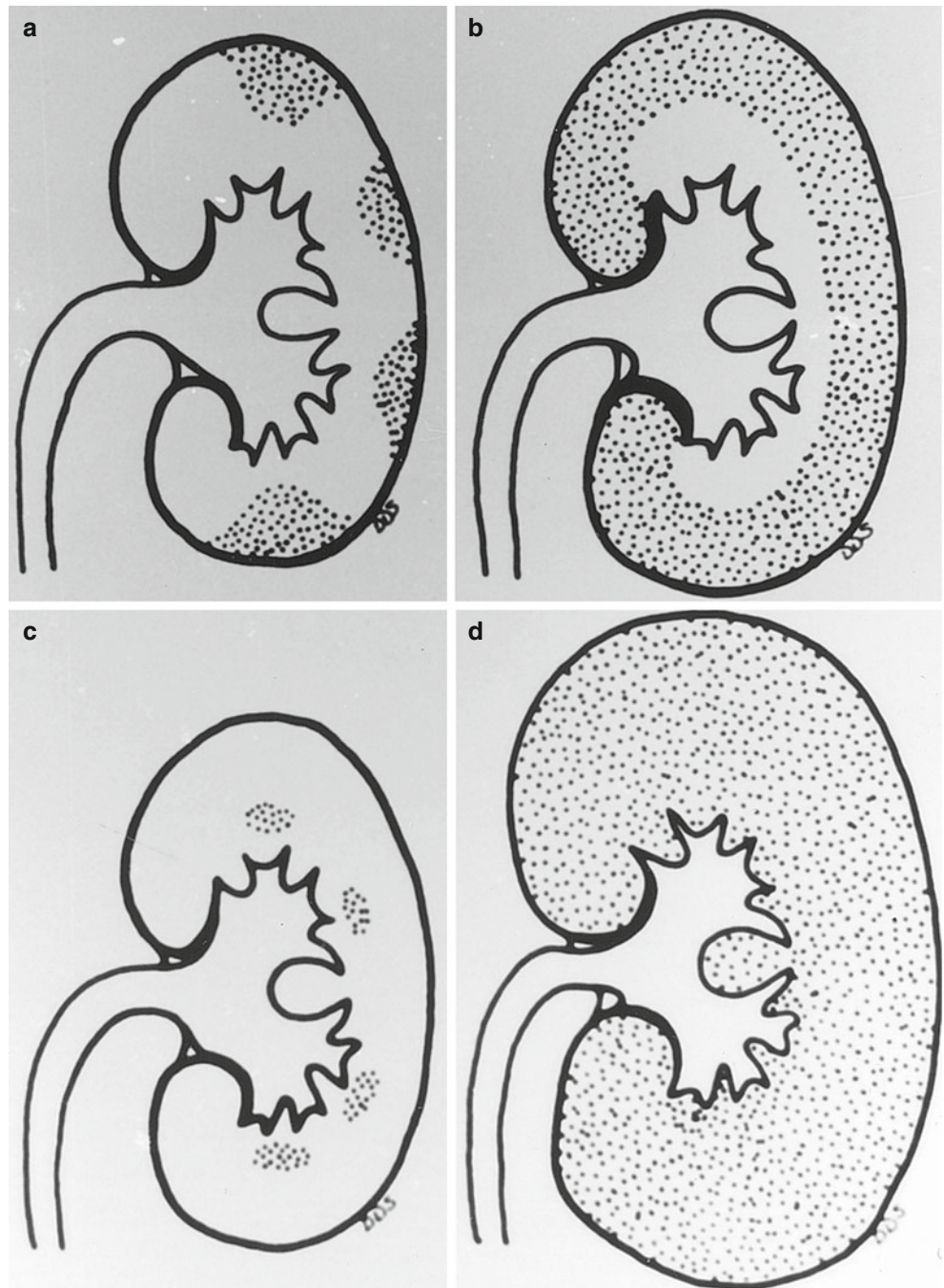


Fig. 11.14 Nephrogenic rests. Well-circumscribed nodules of darkly staining nephrogenic rests are situated directly beneath the renal capsule at the top of the photomicrograph (perilobar nephrogenic rests). Early tubule and glomerulus formations are evident. This was an incidental postmortem microscopic finding in both kidneys of a 3-week-old, 1,984 g, female of 35 weeks gestation with the Pierre-Robin syndrome and terminal bronchopneumonia. In addition, malformations of the genitourinary tract including a hypoplastic right kidney with a double collecting system and hydronephrosis were found (Reprinted from Isaacs [11]. © WB Saunders 1997)

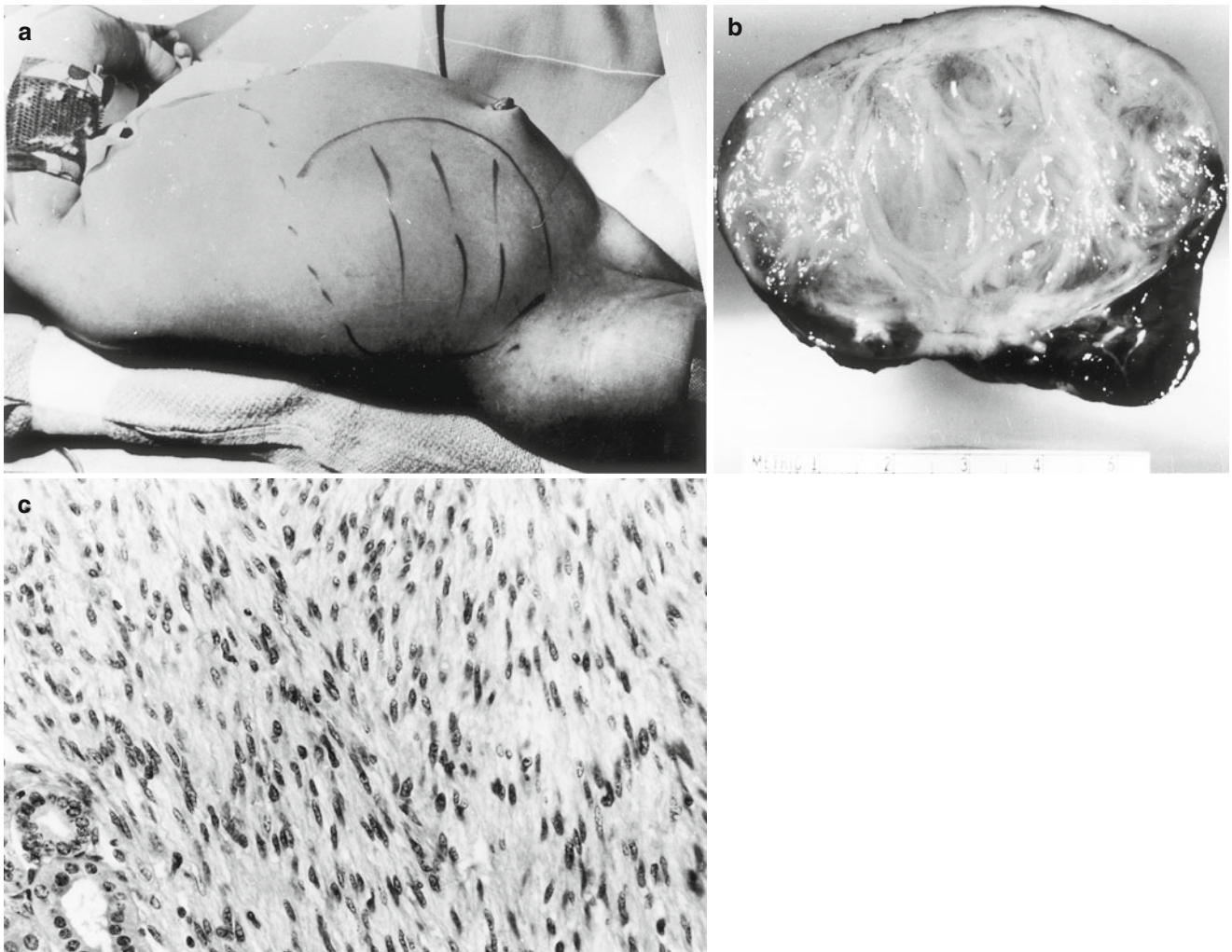
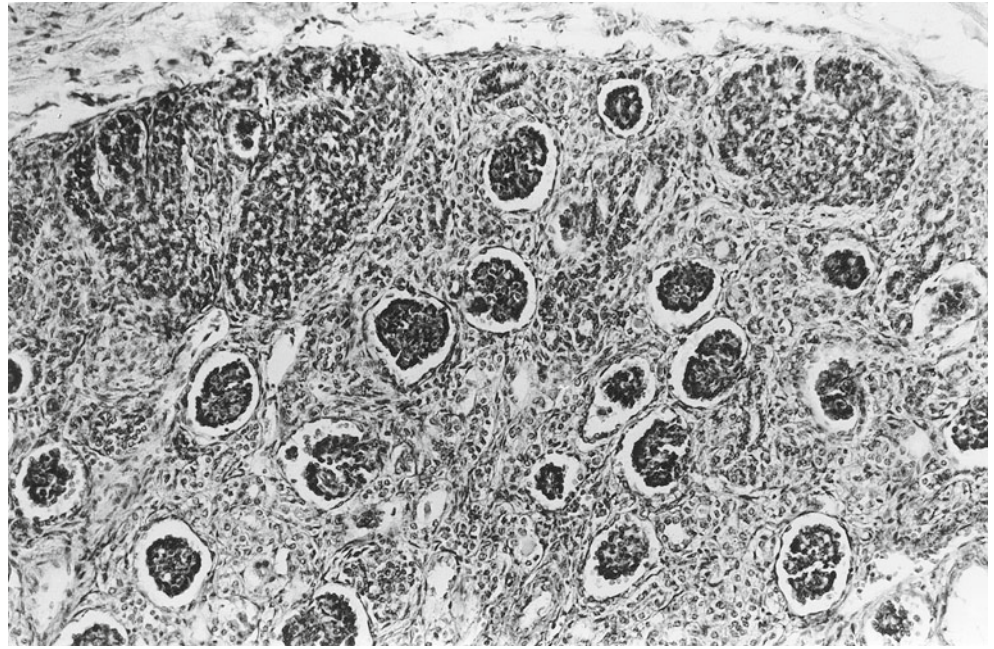


Fig. 11.15 Congenital mesoblastic nephroma, classic. (a) 1-week-old female with an abdominal mass, the most common physical finding in this condition, and a maternal history of polyhydramnios. (b) The tumor, 94 g and 8×5 cm, replaces the lower two thirds of the kidney and has a light

tan-yellow whorled appearance. It is nonencapsulated with small, fingerlike projections extending into adjacent hemorrhagic kidney. (c) The tumor is composed of uniform, small spindle-shaped cells surrounding "entrapped" tubules (Reprinted from Isaacs [11]. © WB Saunders 1997)

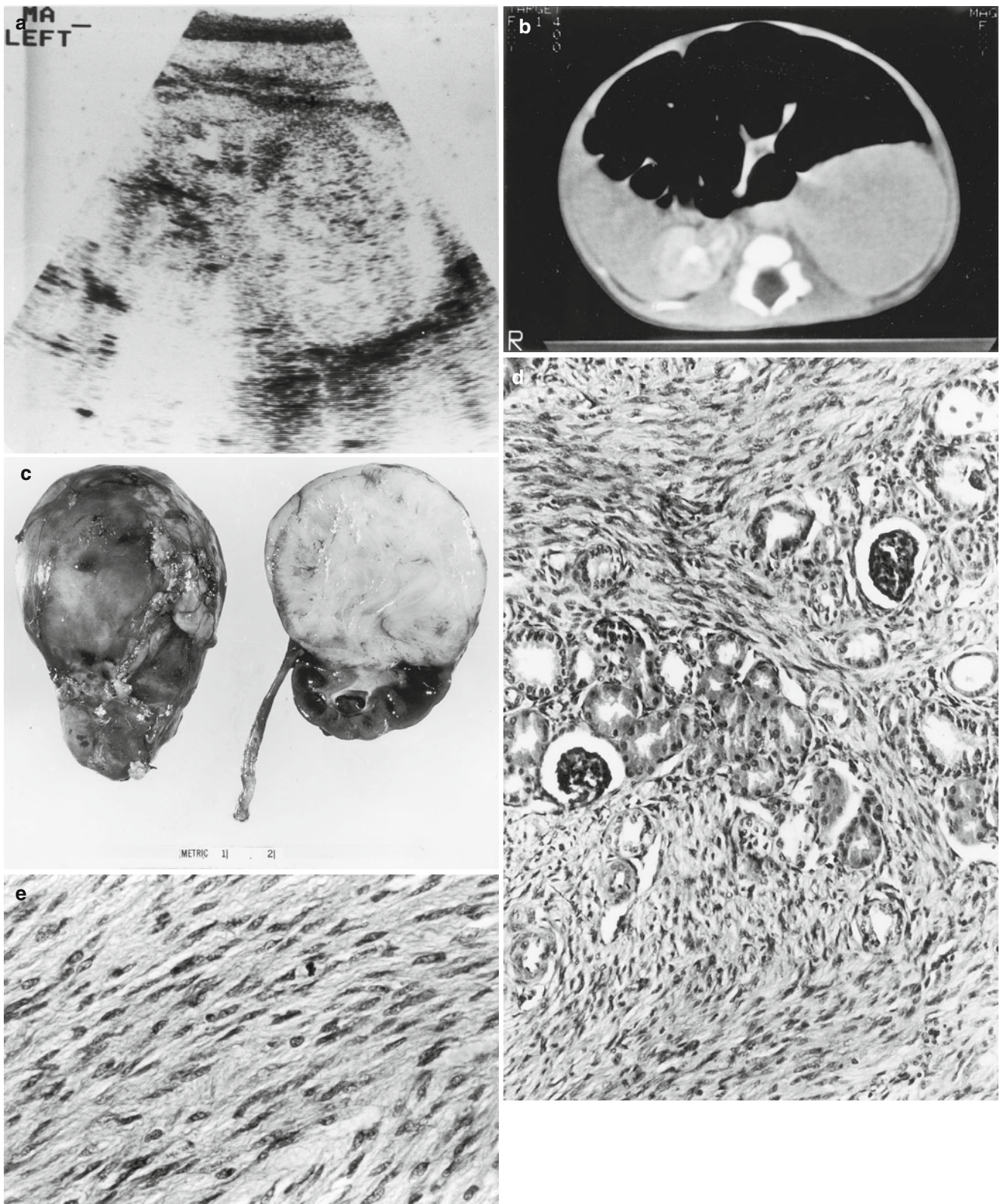


Fig. 11.16 Congenital mesoblastic nephroma, classic. (a) Sonogram of a 5-day-old male with a left flank mass noted at birth demonstrating the lesion. (b) CT scan confirms the sonographic findings. (c) The tumor, 50 g and 5×5 cm, has a whorled appearance similar to a uterine

leiomyoma and involves the pelvis and calyces. (d) Regular spindle-shaped cells encircle tubules and glomeruli. (e) Tumor cells are elongated, spindle shaped with regular oval to fusiform nuclei. Mitoses are seldom noted (Reprinted from Isaacs [11]. © WB Saunders 1997)

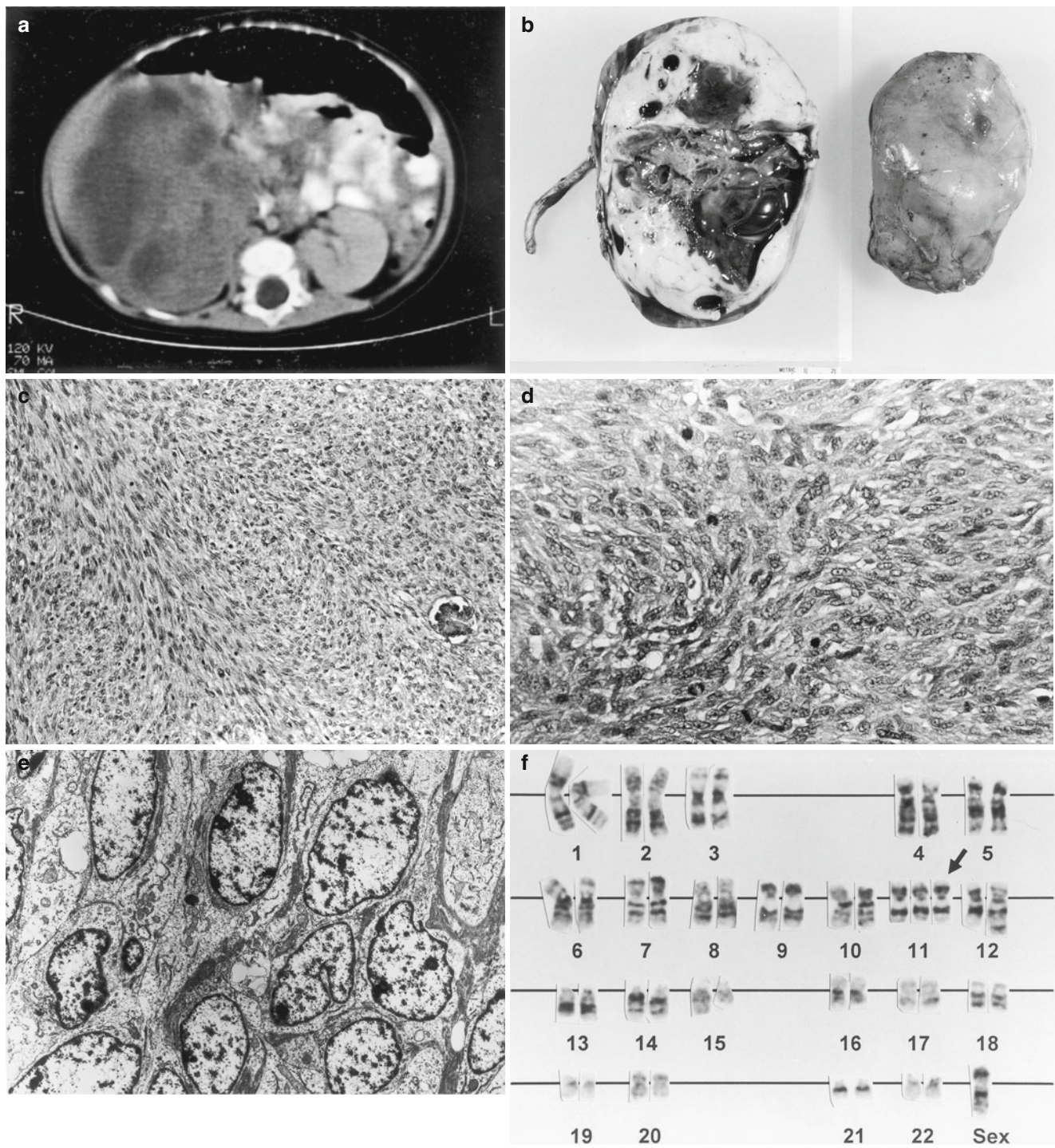


Fig. 11.17 Cellular congenital mesoblastic nephroma. (a) CT scan of a 4-month-old female with an abdominal mass revealing a large right renal lesion composed of both solid and cystic areas. (b) The right kidney, 254 g and 10×8 cm, is replaced by a soft, light tan-gray tumor with a prominent cystic component. In contrast to the “classic” congenital mesoblastic nephroma described above, this tumor is encapsulated, circumscribed, cystic, and hemorrhagic. (c) Spindle-shaped cells with plump oval or fusiform nuclei are separated by a slightly vacuolated fibrillary stroma. It displays an interdigitating (“herring bone”) growth pattern. (d) The tumor is more cellular than the “classical” mesoblastic

nephroma described in Figs. 11.15 and 11.16, and the nuclear atypia and mitotic activity are greater. (e) EM reveals spindle cells with features consistent with fibroblasts. Cytoplasmic fibrillar material is present. (f) Karyotype reveals a trisomy 11, which is described for this tumor [42, 43] (Electron photomicrograph courtesy of Ann Peters, Department of Pathology, Children’s Hospital San Diego; Karyotype courtesy of James Mascarello, Ph.D., Department of Genetics, Children’s Hospital San Diego; Reprinted from Isaacs [11]. © WB Saunders 1997)

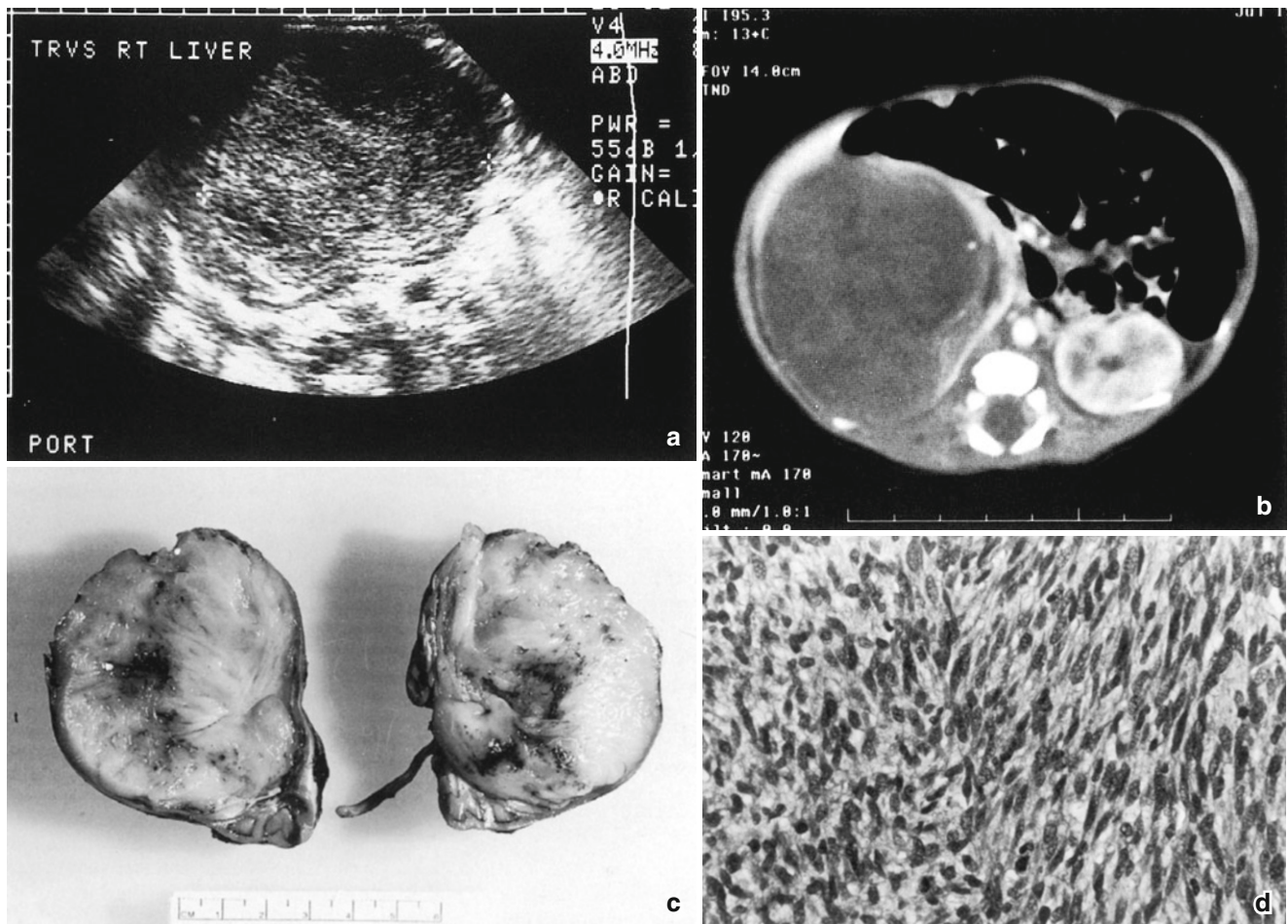


Fig. 11.18 Congenital cellular mesoblastic nephroma. (a) Sonogram shows a right abdominal mass. (b) CT scan reveals a large mass replacing most of the kidney. (c) The tumor, 122 g and 6.5×5.5 cm, has a white-yellow, gelatinous cut surface with foci of hemorrhagic necrosis. It occupies almost the entire kidney except for a small portion of renal

tissue in the lower pole and hilar region. (d) The hypercellular tumor shows an interdigitating growth pattern. The cells are small round to spindle-shaped cells with hyperchromatic, pleomorphic nuclei and accompanied by a few mitoses (Reprinted from Isaacs [15]. © Springer-Verlag, 2002)

11.5 Rhabdoid Tumor of the Kidney

Rhabdoid tumor of the kidney (RTK) was given its name because microscopically, it resembles rhabdomyosarcoma although it does not show skeletal muscle markers either by immunohistochemical studies or by EM [1–3] (Fig. 11.19). This highly aggressive, malignant neoplasm, characterized clinically by early metastases and a high mortality rate, occurs primarily in the infant and newborn (60–70 % of all rhabdoid tumors of the kidney) [5, 8, 13–16, 44–46]. RTK is the second most common malignant renal tumor, following WT and surpassing CCSK [15, 16].

In addition to the kidney, the malignancy occurs in the soft tissues, skin, CNS, and other extrarenal sites [11, 13, 15, 44]. Rhabdoid tumor may appear as one or more cutaneous nodules similar to the “blueberry muffin baby” of neonatal leukemia or neuroblastoma prior to the discovery of the primary tumor [13, 14, 44] (see Chaps. 4, 7 and 9). It may manifest in newborns as a widely disseminated metastatic disease

without a known primary and prove to be rapidly fatal [5, 14]. The tumor metastasizes to multiple sites such as the skin, placenta, bones, lungs, lymph nodes, brain, and liver. Molecular genetic analyses of kidney, brain, and soft tissue RTs show *deletions of chromosome 22q11 and mutations of the hSNF5/INI1 gene* [5, 14]. In older infants and children, rhabdoid tumors occur more often within the kidney or CNS rather than present in the soft tissues as compared to the fetus and neonate where the extrarenal non-CNS (soft tissue) sites predominate [8, 14]. There is a high incidence of concomitant occurrence of RTKs and CNS malignancies such as PNETs and atypical teratoid rhabdoid tumors [14, 15].

11.5.1 Pathology

The cut surface of the tumor is soft, friable, and gray pink to tan with focal cystic necrosis and hemorrhage [13, 45]

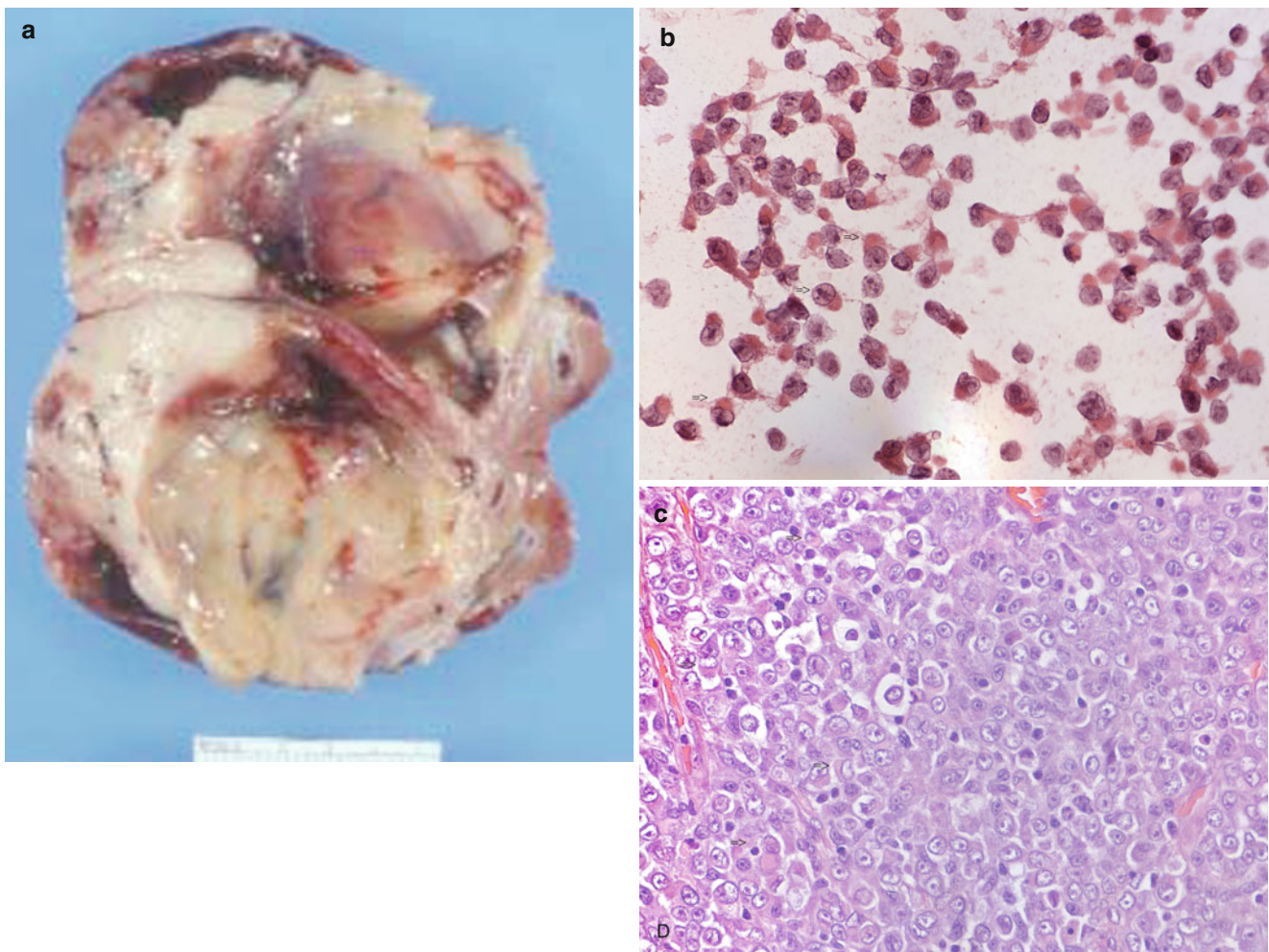


Fig. 11.19 Rhabdoid tumor of the kidney. A 2-year-old girl with gross hematuria and an abdominal mass. (a) The opened kidney reveals extensive tumor necrosis and hemorrhage. There is capsular invasion. (b) Smear preparation reveals round, oval, and teardrop-shaped cells

with vesicular nuclei and a single, large nucleolus. (c) Within the cytoplasm, there are ill-defined round to oval hyaline inclusions (arrows) composed of intermediate filaments, which are demonstrated by EM (Reprinted from Isaacs [15]. © Springer-Verlag, 2002)

(Fig. 11.17a). RTK tends to show more necrosis and hemorrhage than the typical WT. Even in a young child, the former may be as large as 15 cm across replacing most of the kidney and abdominal cavity [14, 15].

Microscopically, RTK consists of a monomorphous population of cells composed of large round to oval cells with a prominent eosinophilic cytoplasm, large vesicular nucleus, characteristically a big single nucleolus, and round hyaline cytoplasmic inclusions [5, 13, 14] (Fig. 11.19). By EM, the inclusions are composed of a meshwork of intermediate filaments. Immunoperoxidase studies reveal that tumor cells are vimentin and cytokeratin immunoreactive but nonreactive for the skeletal muscle markers myoglobin and desmin; NSE is variably reactive [5, 45].

Some rhabdoid tumors have a biphasic appearance of a small, blue cell malignancy consisting of only a few scattered, diagnostic rhabdoid cells, that is, a biphasic pattern. Cell cultures of RTK show mesenchymal features, and unlike neuroblastoma, the cells express the C-myc rather than the N-myc oncogene [46].

11.6 Clear Cell Sarcoma of the Kidney

Clear cell sarcoma of the kidney (CCSK) was found in 2.5 % of the patients enrolled on the National Wilms' Tumor Study [2]. The tumor has a tendency to metastasize to bones and carries a poor prognosis [2, 5, 7, 13, 47–49]. Several cases are described in newborns and infants [11, 13, 15, 47, 48]. CCSK occurs mostly in males but is not associated with any specific congenital anomaly, clinical condition, or malformation syndrome with rare exception [13, 47–49].

11.6.1 Pathology

The gross features of Clear cell sarcoma (CCSK) are similar to WT [11–13, 48] (Figs. 11.20 and 11.21). On cut surface, the tumor is well circumscribed. Prominent cyst formations are often present. Microscopically, the tumor displays a characteristic *monomorphous appearance consisting of rows of round to oval clear staining cells separated by delicate septae*

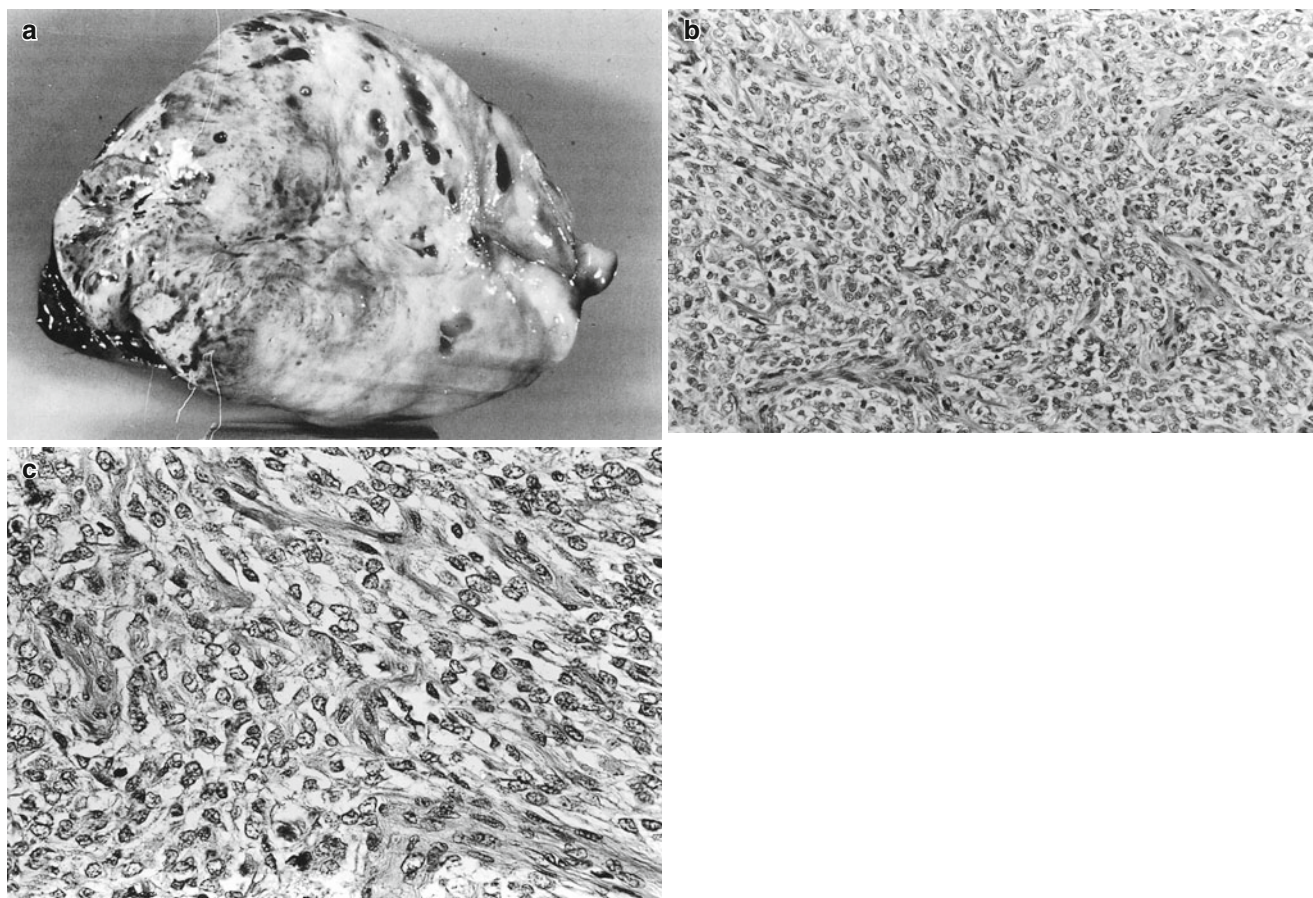


Fig. 11.20 Clear cell sarcoma of the kidney. 15-month-old male with an abdominal mass. (a) 735 g, 16.5×11.5 cm, right renal tumor has a soft gray-white to gray-pink cut surface. It invades the renal hilum and adjacent liver. (b) The tumor consists of fields of cells with “open” (empty) nuclei within a pale myxoid stroma. There is a prominent

branching vascular pattern which is a diagnostic feature of this neoplasm. (c) Higher magnification revealing polygonal-shaped cells consisting of water-clear cytoplasm, round to oval, “open” nuclei with finely dispersed chromatin and inconspicuous nucleoli (Reprinted from Isaacs [15]. © Springer-Verlag, 2002)

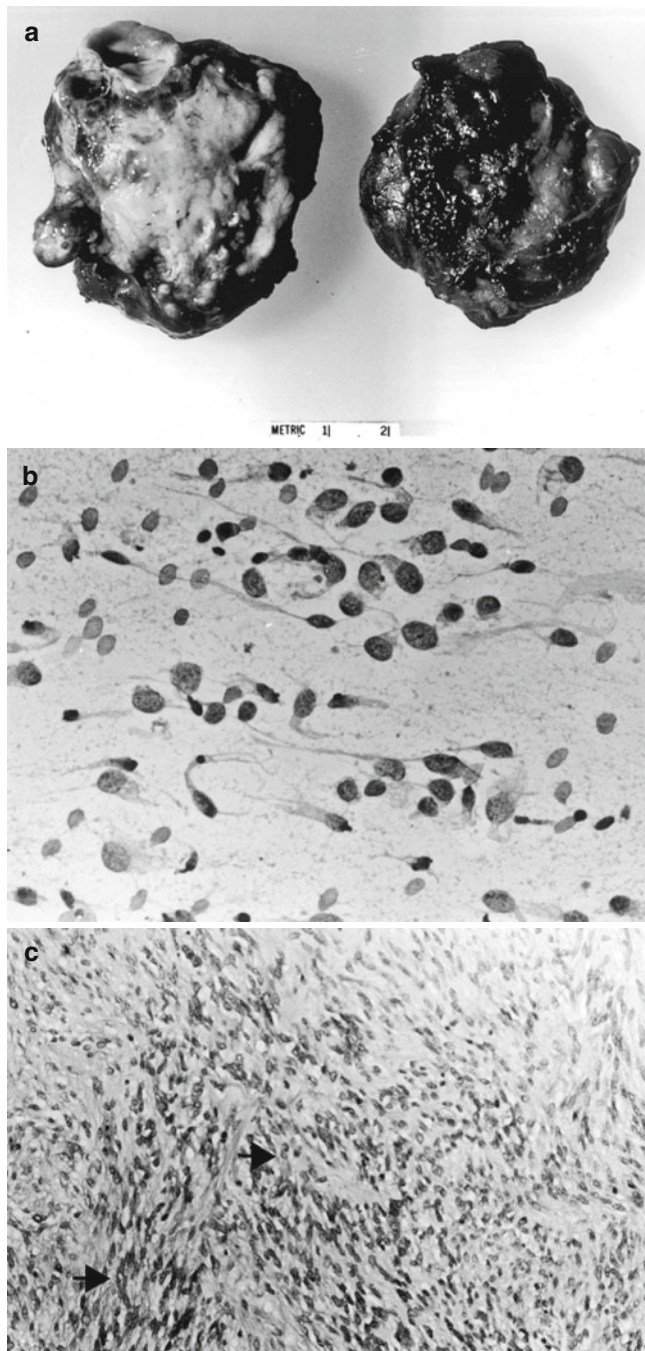


Fig. 11.21 Clear cell sarcoma of the kidney. 4-month-old female with a right abdominal mass discovered by her pediatrician on routine physical examination. Solid and cystic areas were noted not only on imaging studies but also on gross inspection of the tumor. (a) Most of the kidney is replaced by the tumor, 254 g and 10×8×7 cm, which has light tan-gray, gelatinous, and hemorrhagic cut surface. The renal sinus was invaded (stage II). (b) Cytological touch preparation displays tumor cells having a sperm-like configuration embedded in mucoid material. The nuclei show a fine chromatin pattern and one or more tiny nucleoli. (c) The interdigitating spindle cells form a storeform (*cartwheel*) growth pattern. The tumor shows nuclear palisading suggestive of Antoni A areas of a schwannoma (*arrows*) (Reprinted from Isaacs [15]. © Springer-Verlag, 2002)

(Figs. 11.20 and 11.21). The nuclei are small, round, and irregular with fine chromatin or a vesicular or clear appearance (“open nuclei”). Mitoses are rare. There is a *prominent vascular component* composed of branching capillaries within thin fibrous septae. Cysts are not uncommon. The tumor appears to surround or push aside preexisting glomeruli and tubules, which have an embryonic metaplastic appearance. Although the neoplasm is called a sarcoma, neither the EM nor the immunoperoxidase findings actually support this concept [47, 48]. At present, its histogenesis is unknown.

Several other histological patterns are described for CCSK. The *palisaded “verocay-body” pattern* consists of parallel rows of cells resembling a schwannoma (Fig. 11.21c); the *sclerosing pattern* has areas of fibrosis and stromal hyalinization mimicking osteoid; the *epithelioid trabecular pattern* shows an epithelial trabecular arrangement resembling tubules, and the spindle cell pattern with spindle cells produces storiform formations simulating fibrohistiocytic neoplasms [15, 47, 48] (Fig. 11.21c).

11.7 Cystic Conditions of the Kidney

Cystic renal lesions occur in fetuses and infants and include both true tumors and neoplastic-like conditions of probable developmental origin [5, 12, 15, 50–54]. *Hydronephrosis and multicystic kidney* are responsible for most abdominal masses during the first year of life. Cystic renal lesions may antedate the classical features of tuberous sclerosis in the infant and may be mistaken clinically and on imaging studies for tumor [50, 51].

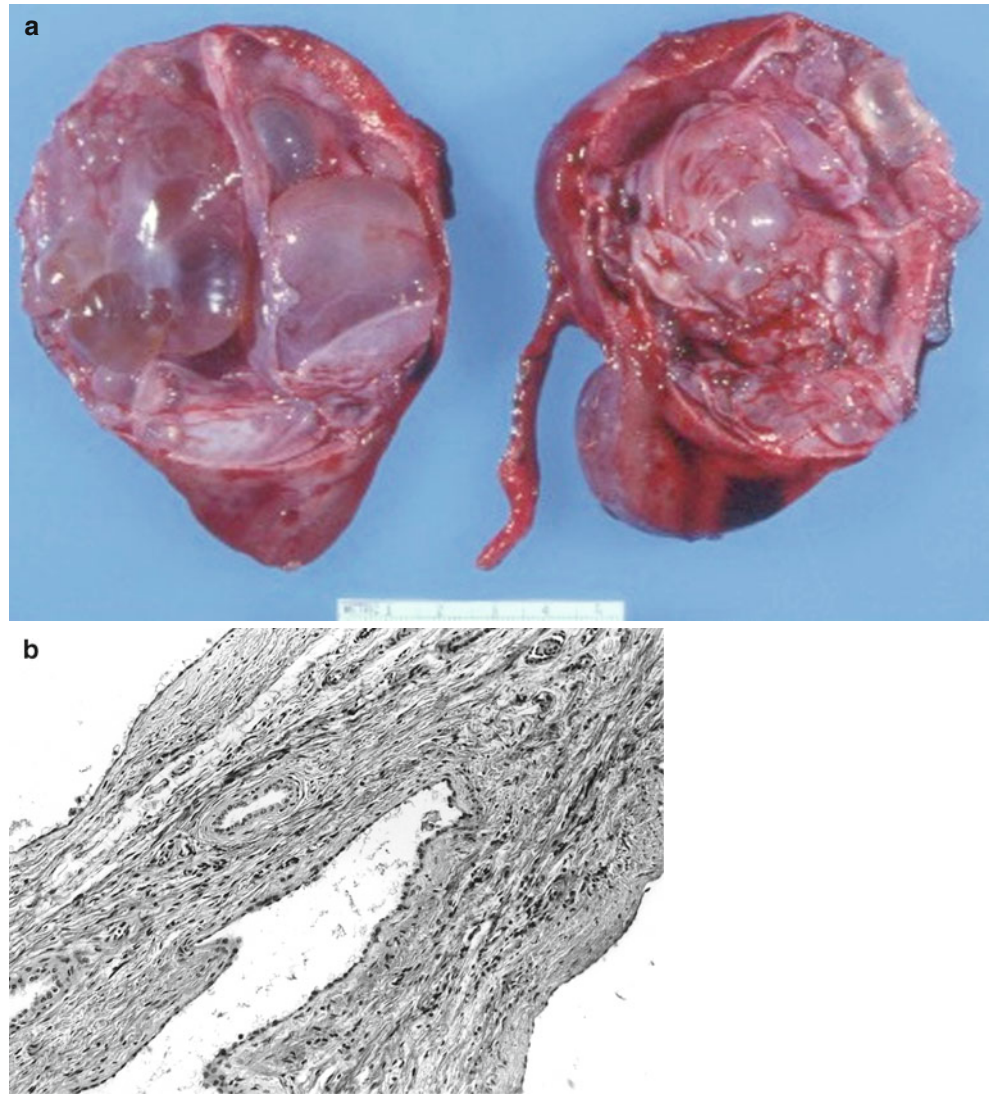
Multilocular cyst (cystic nephroma) presents clinically as an abdominal mass and is detected preoperatively by imaging studies. Most are unilateral, but bilateral examples are described [5]. The lesion consists of a multicystic mass situated in the upper or lower pole of the kidney well demarcated from the renal pelvis by a discrete light tan to white capsule (Figs. 11.22 and 11.23).

The cysts vary in size, contain clear fluid, and consist of thin fibrous septae, which lack nephrogenic elements on microscopic examination [11, 15, 52, 53]. Multilocular cyst has been described in association with both CMN and WT [15].

Cystic partially differentiated nephroblastoma (CPDN) is another multicystic condition grossly identical to CN but microscopically different because it contains immature or mature nephrogenic (metanephric) elements within the fibrous septa that separate the cysts [5, 52, 53]. CPDN occurs both in neonates and in older children.

Cystic Wilms’ tumor is the third member in the spectrum of cystic “neoplastic” conditions of the kidney. A well-differentiated WT with focal or multifocal cystic change sometimes creates a problem in the differential diagnosis of a multicystic renal mass. Although unusual, a multilocular cyst may occur in the same kidney with a WT [5, 15].

Fig. 11.22 Multilocular cyst of the kidney. A 2-year-old girl with a left abdominal mass. **(a)** The specimen, 405 g and 13 × 10 cm, consists of a multiloculated cyst occupying most of the kidney. The lesion does not communicate with the renal pelvis. The cysts range in size from 0.2 cm up to 4 cm in diameter and contain clear straw-colored fluid. The cyst is well encapsulated and surrounded by a capsule measuring 2–3 mm in thickness. **(b)** Cysts of various sizes are separated by fibrous connective tissue septae and are lined by cuboidal and flattened epithelium. No nephrogenic elements are present within the cyst walls (Reprinted from Fobi M, et al. [58]. With kind permission of © Elsevier, 1979)



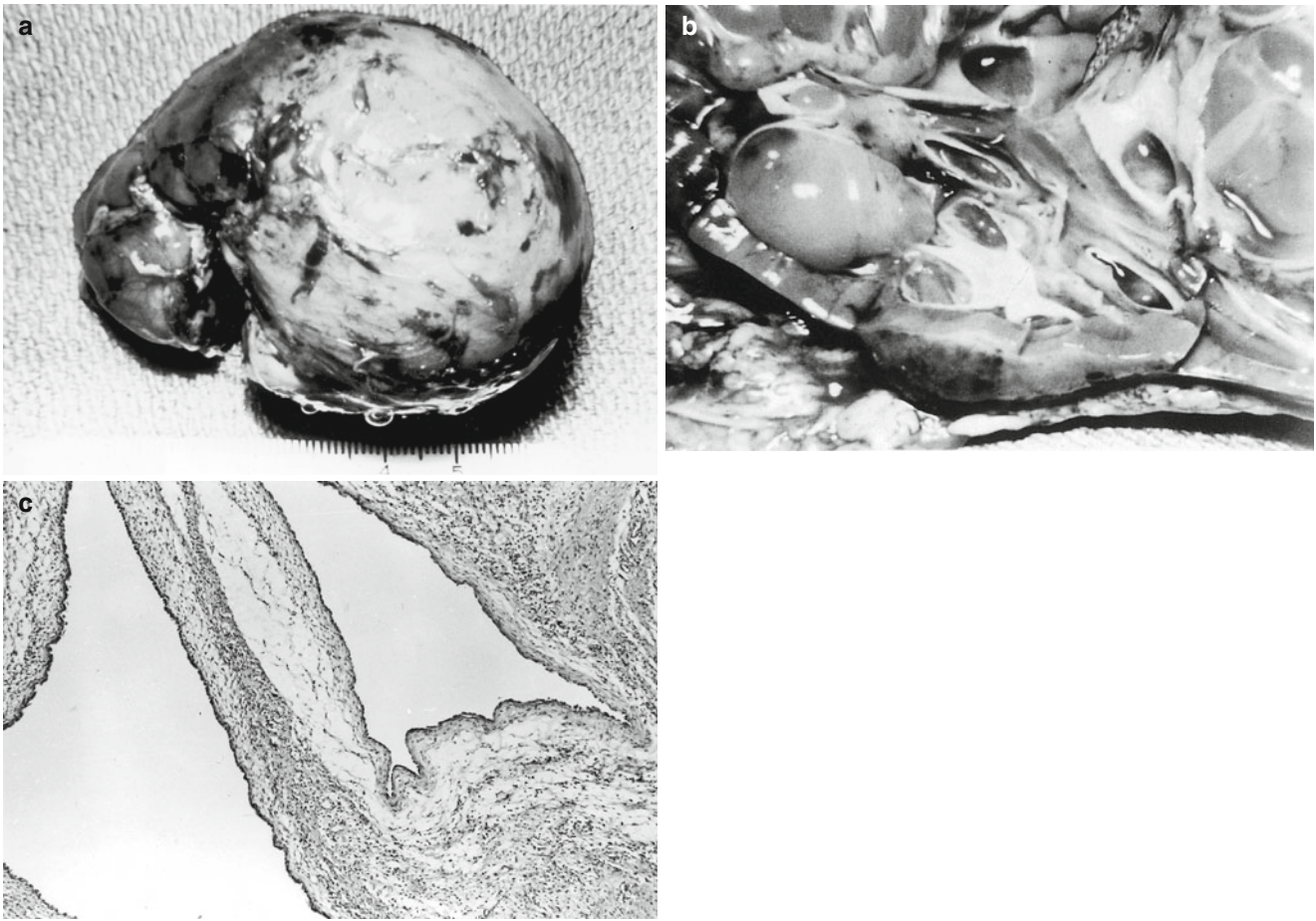


Fig. 11.23 Multilocular cyst of the kidney. Infant with an abdominal mass. (a) 6×5-cm cystic lesion situated within the upper and middle third of the right kidney. (b) The cut surface reveals multiple cysts of

various sizes containing clear fluid. (c) The cysts are separated by slightly vascular fibrous connective tissue and lined by flattened epithelial cells (Reprinted from Isaacs [15]. © Springer-Verlag, 2002)

11.8 Ossifying Renal Tumor of Infancy

Ossifying renal tumor of the kidney consists mostly of bone and soft tissue spindle cells and typically presents clinically with hematuria [15, 56, 57]. These benign lesions appear as a calcified, polypoid mass arising from the upper or middle pole collecting system. Less than 30 cases have been reported [5, 15, 56, 57]. Infants, usually male, present with gross

hematuria and a calcified renal lesion demonstrated by imaging studies [15, 56, 57]. Ossifying renal tumor is regarded as a benign neoplastic condition rather than a reactive process [56].

Grossly the specimens consist of a rock hard mass, 2–3 cm in diameter, attached to a renal papilla by a broad pedicle [55–57] (Fig. 11.24). Histologically, ossifying renal tumors are composed of *three main components: osteoid, osteoblasts,*

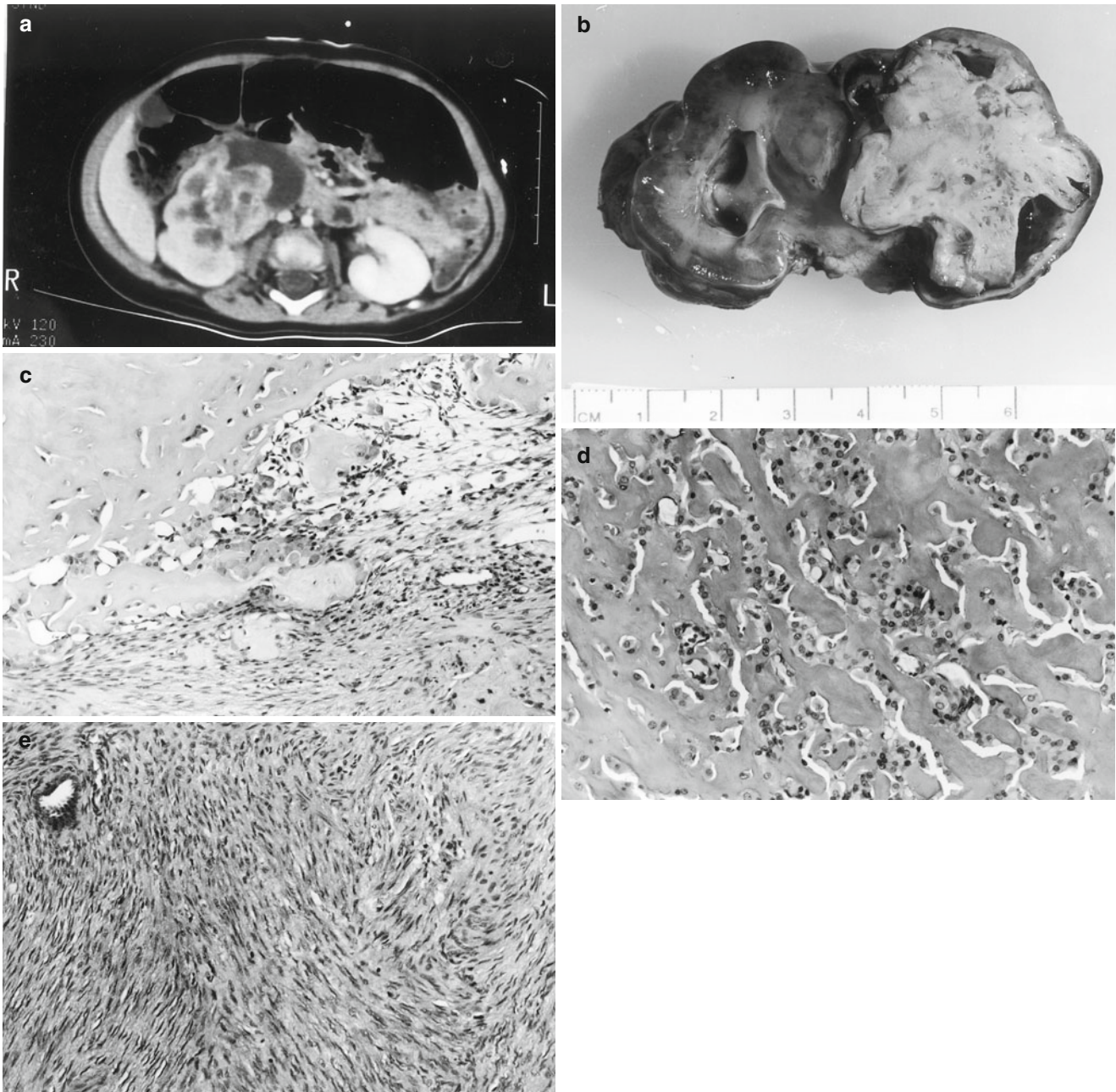


Fig. 11.24 Ossifying renal tumor of infancy. 4-month-old male with an abdominal mass and hematuria. (a) Magnetic resonance image showing a partially calcified mass arising from the right kidney. (b) The kidney, 45 g, contains an irregular, firm, gray-white, rock hard mass, 3.5×3.0×2.5 cm situated within the middle third and lower pole. The pelvis and calyces are dilated, and the renal papillae blunted. Chronic pyelonephritis is present also. (c) Junction between an area of bone and

nests of regular spindle-shaped cells. (d) Osteoid trabeculae are separated by clusters of osteoblasts and osteocytes with small, regular round nuclei. (e) An area adjacent to bone consisting of interdigitating small, regular spindle cells histologically resembling congenital mesoblastic nephroma. Note the lack of mitoses and nuclear atypia in all the microscopic sections illustrated (Reprinted from Isaacs [15]. © Springer-Verlag, 2002)

and spindle cells. The tumor contains a central nidus of mineralized osteoid admixed with polygonal cells having a plump nucleus, large nucleolus, and eosinophilic to amphophilic cytoplasm, features consistent with osteocytes and/or osteoblasts (Figs. 11.24c, d). Islands of osteoid are surrounded by mesenchyme composed of spindle-shaped cells which blend in imperceptively with the surrounding renal medulla. The mesenchymal cells have the appearance of CMN (Figs. 11.16e). The polygonal cells appear to originate from the spindle cells. Variable perivascular fibrosis is present. Mitotic figures and cytological atypia are absent [15, 56, 57]. Immunohistochemical studies reveal strong reactivity of the tumor cells with vimentin but no staining with either epithelial or vascular markers, which react only with adjacent renal tubules and blood vessels [57]. Surgical resection of the tumor results in cure. To my knowledge, no recurrences have been reported.

References

- Beckwith JB, Palmer N (1978) Histopathology and prognosis of Wilms' tumor. Results of the first National Wilms' Tumor Study. *Cancer* 41:1937–1948
- Beckwith JB (1983) Wilms' tumor and other renal tumors of childhood: a selective review from the National Wilms' Tumor Study Pathology Center. *Hum Pathol* 14:481–492
- Bolande RP, Brough AJ, Izant RJ (1967) Congenital mesoblastic nephroma of infancy. A report of eight cases and the relationship to Wilms' tumor. *Pediatrics* 40:272–278
- Bove KE (1999) Wilms' tumor and related abnormalities in the fetus and newborn. *Semin Perinatol* 23:310–318
- Pearlman E (2007) Renal tumors. In: Gilbert-Barnes E (ed) *Potter's pathology of the fetus, infant and child*, vol 2, 2nd edn. Mosby Elsevier, Philadelphia, pp 1345–1355
- Dehner LP (1981) Neoplasms of the fetus and neonate. In: Naeye RL, Kissane JM, Kaufman N (eds) *Perinatal diseases*, International Academy of Pathology, Monograph number 22. Williams and Wilkins, Baltimore, p 286
- Marsden HB, Lawler W (1983) Primary renal tumors in the first year of life. *Virchows Arch A Pathol Anat Histopathol* 399:1–9
- Weeks DA, Beckwith JB, Mierau GW et al (1989) Rhabdoid tumor of the kidney. A report of 111 cases from the National Wilms' Tumor Study Pathology Center. *Am J Surg Pathol* 13:439–458
- Isaacs H Jr (1985) Perinatal (congenital and neonatal) neoplasms: a report of 110 cases. *Pediatr Pathol* 3:165–216
- Isaacs H Jr (1987) Congenital and neonatal malignant tumors: a 28-year experience at Children's Hospital of Los Angeles. *Am J Pediatr Hematol Oncol* 9:121–129
- Isaacs H Jr (1997) Renal tumors. In: *Tumors of the fetus and newborn*. W.B. Saunders, Philadelphia, pp 244–277
- Isaacs H Jr (1997) Tumors. In: Gilbert-Barnes E (ed) *Potter's pathology of the fetus and infant*, vol 2. Mosby, St. Louis, pp 1242–1339
- Isaacs H Jr (2008) Fetal and neonatal renal tumors. *J Pediatr Surg* 43:1587–1595
- Isaacs H Jr (2010) Fetal and neonatal rhabdoid tumor. *J Pediatr Surg* 45:619–626
- Isaacs H Jr (2002) Renal tumors. In: *Tumors of the fetus and infant: an atlas*. Springer, New York, pp 261–302
- Hrabovsky EE, Othersen HB, de Lorimer A Jr et al (1986) Wilms' tumor in the neonate: a report from the National Wilms' Tumor Study. *J Pediatr Surg* 21(5):385–387
- Campbell AN, Chan HSL, O'Brien A et al (1987) Malignant tumours in the neonate. *Arch Dis Child* 62:19–23
- Applegate KE, Ghei M, Perez-Atayde AR (1999) Prenatal detection of a Wilms' tumor. *Pediatr Radiol* 29:65–67
- Beckwith JB (1999) Prenatal detection of a Wilms' tumor [editorial; comment]. *Pediatr Radiol* 29:64
- Koufos A, Hansen MF, Copeland NG et al (1985) Loss of heterozygosity in three embryonal tumors suggests a common pathogenetic mechanism. *Nature* 316:330–334
- Coppes MJ, Haber DA, Grundy PE (1994) Genetic events in the development of Wilms' tumor. *N Engl J Med* 331:586–590
- Chatten J (1976) Epithelial differentiation in Wilms' tumor: a clinicopathologic appraisal. *Perspect Pediatr Pathol* 3:225–254
- Faria P, Beckwith JB, Mishra K et al (1996) Focal versus diffuse anaplasia in Wilms tumor—New definitions with prognostic significance. A report from the National Wilms Tumor Study Group. *Am J Surg Pathol* 20:909–920
- Beckwith JB (1998) National Wilms Tumor Study: an update for pathologists. *Pediatr Dev Pathol* 1:79–84
- Gonzalez-Crussi F, Hsueh W, Ugarte N (1981) Rhabdomyogenesis in renal neoplasia of childhood. *Am J Surg Pathol* 5:525–532
- Weinberg AG, Currarino G, Hurt GE Jr (1984) Botryoid Wilms' tumor of the renal pelvis. *Arch Pathol Lab Med* 108:147–148
- Tomlinson GS, Cole CH, Smith NM (1999) Bilateral Wilms' tumor: a clinicopathologic review. *Pathology* 31:12–16
- Bove KE, McAdams JA (1976) The nephroblastomatosis complex and its relationship to Wilms' tumor: a clinicopathologic treatise. In: Rosenberg HS, Bolande RP (eds) *Perspectives in pediatric pathology*, vol 3. Year Book Medical Publishers, Chicago, pp 185–223
- Beckwith JB (1998) Nephrogenic rests and the pathogenesis of Wilms tumor: developmental and clinical considerations. *Am J Med Genet* 79:268–273
- Beckwith JB (1993) Precursor lesions of Wilms' tumor: clinical and biological implications. *Med Pediatr Oncol* 21:158–168
- de Chadarevian J, Fletcher BD, Chatten J et al (1977) Massive infantile nephroblastomatosis: a clinical, radiological, and pathological analysis of four cases. *Cancer* 39:2294–2305
- Ambrosino MM, Hernanz-Schulman M, Horii SC et al (1990) Prenatal diagnosis of nephroblastomatosis in two siblings. *J Ultrasound Med* 9:49–51
- Kulkarni R, Baile MD, Bernstein J (1980) Progression of nephroblastomatosis to Wilms' tumor. *J Pediatr* 96:178
- Haddad B, Haziza J, Touboul C et al (1996) The congenital mesoblastic nephroma: a case report of prenatal diagnosis. *Fetal Diagn Ther* 11:61–66
- Howey DD, Farrell EE, Sholl J et al (1985) Congenital mesoblastic nephroma: prenatal ultrasonic findings and surgical excision in a very-low-birth-weight infant. *J Clin Ultrasound* 13:506–508
- Isaacs H Jr (2008) Fetal hydrops associated with tumors. *Am J Perinatol* 25:43–68
- Pettinato G, Manivel JC, Wick MR et al (1989) Classical and cellular (atypical) congenital mesoblastic nephroma: a clinicopathologic, ultrastructural, immunohistochemical and flow cytometric study. *Hum Pathol* 20:682–690
- Beckwith JB, Weeks DA (1986) Congenital mesoblastic nephroma. When should we worry? *Arch Pathol Lab Med* 110:98–99
- Kelly DR (1985) Cystic cellular mesoblastic nephroma. *Pediatr Pathol* 4:157–162
- Gormley TS, Skoog SJ, Jones RV et al (1989) Cellular congenital mesoblastic nephroma: what are the options. *J Urol* 142:479–483
- Knezevich SR, Garnett MJ, Pysker TJ et al (1998) ETV6-NTRK3 gene fusions and trisomy 11 establish a histogenetic link between

- mesoblastic nephroma and congenital fibrosarcoma. *Cancer Res* 58:5046–5048
42. Mascarello JT, Cajulis TR, Krous HF et al (1994) Presence or absence of trisomy 11 is correlated with histologic subtype in congenital mesoblastic nephroma. *Cancer Genet Cytogenet* 77:50–54
 43. Howell CG, Otherson HB, Kiviat NE et al (1982) Therapy and outcome in 51 children with mesoblastic nephroma: a report of the National Wilms' Tumor Study. *J Pediatr Surg* 17:826–831
 44. Hsueh C, Kuo T (1998) Congenital malignant rhabdoid tumor presenting as a cutaneous nodule: report of 2 cases with review of the literature. *Arch Pathol Lab Med* 122:1099–1102
 45. Vujanic GM, Sandstedt B, Harms D et al (1996) Rhabdoid tumour of the kidney: a clinicopathological study of 22 patients from the International Society of Paediatric Oncology (SIOP) nephroblastoma file. *Histopathology* 28:333–340
 46. Gansler T, Gerald W, Anderson G et al (1991) Characterization of a cell line derived from rhabdoid tumor of the kidney. *Hum Pathol* 22:259–266
 47. Sotelo-Avila C, Gonzalez-Crussi F, Sadowinski S et al (1986) Clear cell sarcoma of the kidney: a clinicopathologic study of 21 patients with long term follow-up evaluation. *Hum Pathol* 16:1219–1230
 48. Argani P, Perlman EJ, Breslow NE et al (2000) Clear cell sarcoma of the kidney: a review of 351 cases from the National Wilms Tumor Study Group Pathology Center. *Am J Surg Pathol* 24:4–18
 49. Uzoaru I, Podbielski FJ, Chou P et al (1993) Familial adenomatous polyposis coli and clear cell sarcoma of the kidney. *Pediatr Pathol* 13:133–141
 50. Miller ID, Gray ES, Lloyd DL (1989) Unilateral cystic disease of the neonatal kidney: a rare presentation of tuberous sclerosis. *Histopathology* 14:529–532
 51. Isaacs H (2009) Perinatal (fetal and neonatal) tuberous sclerosis: a review. *Am J Perinatol* 26:755–760
 52. Andrews MJ Jr, Askin FB, Fried FA et al (1983) Cystic partially differentiated nephroblastoma and polycystic Wilms' tumor: a spectrum of related clinical and pathologic entities. *J Urol* 129:577–580
 53. Domizio P, Risdon RA (1991) Cystic renal neoplasms of infancy and childhood: a light microscopical, lectin histochemical and immunohistochemical study. *Histopathology* 19:199–209
 54. Beckwith JB, Kiviat NB (1981) Multilocular renal cysts and cystic renal tumors. *Am J Roentgenol* 136:435–436
 55. Chatten J, Bishop HC (1977) Bilateral multilocular cysts of the kidney. *J Pediatr Surg* 12:749–750
 56. Chatten J, Cromie WJ, Duckett JW (1980) Ossifying tumor of infantile kidney: report of two cases. *Cancer* 45:609–612
 57. Sotelo-Avila C, Beckwith JB, Johnson JE (1995) Ossifying renal tumor of infancy: a clinicopathologic study of nine cases. *Pediatr Pathol* 15:745–762
 58. Fobi M, Mahour GH, Isaacs H Jr (1979) Multilocular cyst of the kidney. *J Pediatr Surg* 14:282

12.1 Introduction

Tumors and tumorlike conditions of the liver are uncommon in newborns and infants, comprising only 3 and 8 %, respectively, of the total neoplasms of various types [1, 2]. The incidence of malignant liver tumors during the first year of life as determined from the Third National Cancer Survey is 7.5 per million live births per year [3]. Hepatic malignancies ranked seventh as the cause of infant deaths from cancer in that survey. Hepatic tumors seldom occur in the perinatal period comprising approximately 5 % of the total neoplasms of different kinds occurring in this age group [1–3].

Infantile hemangioma is the leading primary liver tumor followed in order by mesenchymal hamartoma and hepatoblastoma [1, 2, 4–10]. All three present clinically as an abdominal mass and are detected by antenatal or postnatal imaging [1, 2]. During the first year of life, hepatoblastoma rather than hepatocellular carcinoma is the principal primary malignant hepatic tumor [1, 2, 4, 11, 12]. Including the total surgical and necropsy specimens, most hepatic tumors are metastatic rather than primary [2, 4]. *Neuroblastoma* is the main neoplasm that metastasizes to the liver in the fetus and infant, and leukemia and renal tumors are next.

Classification of liver tumors and tumorlike conditions is given in Table 12.1.

Table 12.1 Classification of liver tumors and tumor-like conditions in the fetus and infant

Infantile hemangioma
Focal (solitary)
Multifocal ^a
Hemangioendothelioma type 1 ^b
Capillary hemangioma
Cavernous hemangioma
Hemangioendothelioma type 2 (angiosarcoma)
Mesenchymal hamartoma
Cyst (s)
Solitary unilocular cyst
Polycystic kidney and liver disease
Tuberous sclerosis
Adenoma
Focal nodular hyperplasia
Hepatoblastoma
Epithelial
Fetal
Embryonal
Mixed: epithelial and mesenchymal
Teratoid
Anaplastic
Hepatocellular carcinoma
Germ cell tumors
Teratoma
Fetus-in-fetu
Yolk sac tumor
Choriocarcinoma
Rhabdoid tumor
Hepatic sarcoma
Rhabdomyosarcoma
Undifferentiated (embryonal) sarcoma
Metastatic neoplasms
Neuroblastoma
Leukemia
Renal tumors (Wilms' tumor, rhabdoid tumor and clear cell sarcoma)
Yolk sac tumor
Choriocarcinoma

Reprinted from Isaacs [2]. © Springer-Verlag, 2002

^aMultifocal includes diffuse or disseminated hemangiomatosis

^bWith or without arteriovenous malformation

12.2 Hemangioma

Hemangioma is the leading primary hepatic tumor in infancy [2, 4, 6–8, 10, 13]. The majority of hemangiomas are diagnosed before 6 months of age, and almost half are found within the first week of life [4–6, 14, 15] (Figs. 12.1, 12.2, 12.3, and 12.4). More occur than are actually recorded since many are asymptomatic (“silent”) conditions that regress. They are discovered as an abdominal mass on physical examination, incidental imaging study, or postmortem finding [2, 4, 14, 15, 17]. Some hemangiomas cause hepatomegaly only while others are responsible for life-threatening conditions in the perinatal period, for example, hydrops, rupture with hemoperitoneum during delivery, and high-output cardiac failure [5–7, 14, 18–22] (Fig. 12.2). Consumptive coagulopathy resulting from disseminated intravascular coagulation and sequestration of platelets, bleeding diathesis (Kasabach-Merritt syndrome), and anemia are other complications [5, 10] (Fig. 12.3). Hydramnios and nonimmune fetal hydrops are prognostic signs heralding an unfavorable outcome [15, 17–20].

In 40–50 % of infants, hepatic hemangiomas are associated with those in the skin and other organs [2, 4, 5, 7]. Because of this, hepatic hemangioma should be considered in the differential diagnosis when a newborn presents with multiple cutaneous hemangiomas, an abdominal mass, and congestive heart failure [1, 2] (Fig. 12.2). Prognosis for infants with hepatic hemangioma is favorable providing there are no major clinical complications as those described above [2, 4, 7, 8].

Hepatic hemangiomas are divided into two main groups, *focal (solitary)* and *multifocal* (which also includes diffuse or disseminated hemangiomatosis). Focal hemangiomas are more prevalent than multifocal ones, almost two to one [2, 7]. The all-inclusive term “infantile hemangioma,” as defined by Dehner, includes hemangioendothelioma type 1, cavernous, capillary hemangioma, and most hepatic arteriovenous malformations [4].

Grossly the hepatic hemangioma appears as a single mass in the right or left lobe or less often as multicentric lesions distributed throughout both lobes. The cut surface of the liver reveals a dark reddish brown mass(s) composed of blood vessels filled with blood with or without areas of fibrosis, calcification, and hemorrhage [2, 4] (Figs. 12.3 and 12.4). Infantile hemangiomas are subdivided further into two types: capillary and cavernous, depending only on the size of the vascular spaces. Cavernous hemangiomas have larger vessels than capillary hemangiomas [2, 7, 10] (Fig. 12.2). The vascular channels are lined by layers of flat or plump, regular endothelial cells, which are GLUT1 positive. The

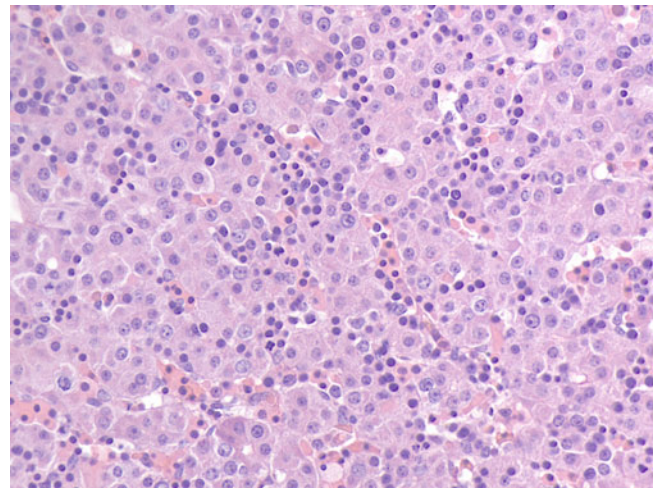


Fig. 12.1 Developing liver from a 12-mm human embryo. Hepatoblasts are composed of cells of variable size with regular, round nuclei and one or two prominent nucleoli. Irregularly arranged, early liver cell cord formations are bordered by sinusoids containing nucleated erythrocytes (erythroblasts) (Reprinted from Isaacs [16]. © WB Saunders 1997)

pale-staining connective tissue stroma between the vascular spaces is variable in amount and contains small bile ducts and foci of *extramedullary erythropoiesis*. Capillary hemangiomas can become cavernous as shunting increases. Thrombosis, necrosis, and fibrosis leave large residual vessels [1, 2] (Figs. 12.3 and 12.4). Approximately two thirds of hemangiomas undergo spontaneous regression, characterized histologically by thrombosis, fibrosis, and calcification or disappearance of the lesion [2] (Fig. 12.4c, d). Both types of hemangiomas can coexist in the same tumor (Figs. 12.2 and 12.3) that may be accompanied by an arteriovenous malformation. Associated extrahepatic hemangiomas are found most often in the skin, brain, placenta, lungs, and eyes [7]. Hemangioendothelioma type 2 (angiosarcoma) rarely occurs in the newborn and infant [21].

Since noninvasive imaging procedures are currently available, surgical exploration and biopsy, which may prove fatal, often are not required to establish the diagnosis [14, 15, 22]. When a relatively nondescript mass lesion is present in the liver and the imaging studies are equivocal, a biopsy is indicated particularly if a hepatoblastoma or sarcoma are suspected. Indicators of a poor prognosis in a patient with an hemangioma are the presence of congestive heart failure, jaundice, multiple nodules, and histological absence of cavernous differentiation [2, 7, 15]. Initially hepatic hemangiomas should be treated conservatively; surgery is reserved for patients with intractable cardiac failure and/or refractory consumptive coagulopathy [22].

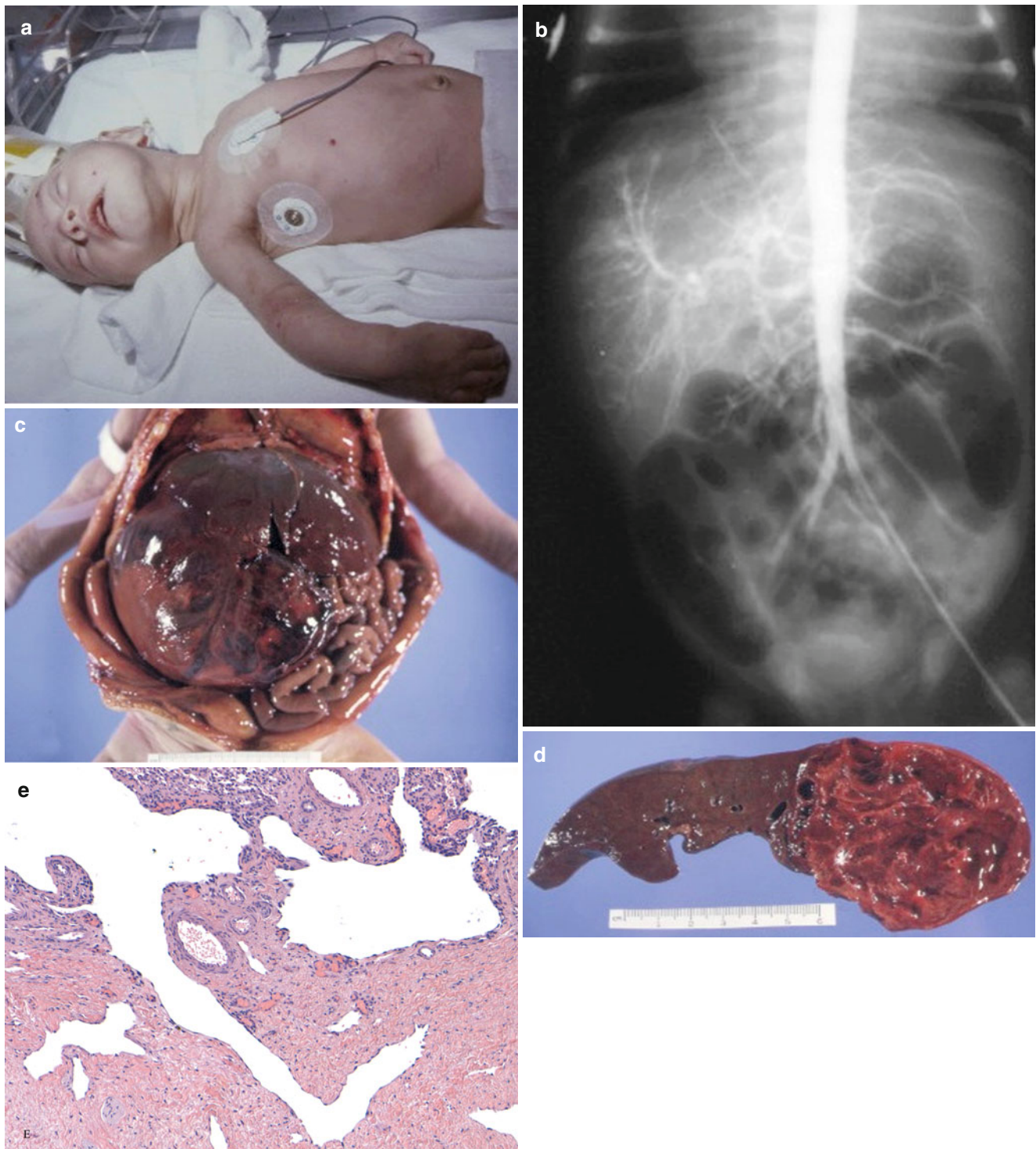


Fig. 12.2 Hemangioma of the liver. (a) Newborn with congestive heart failure and multiple cutaneous hemangiomas. (b) Arteriogram demonstrates a highly vascular lesion occupying most of the right lobe of the liver. (c) Postmortem photograph showing the hepatic hemangioma in situ arising from the right lobe. The tumor occupies much of

the abdominal cavity. (d) Cross section of the liver showing the sponge-like hemangioma filled with blood. (e) The cavernous hemangioma consists of large vascular channels. The adjacent parenchyma exhibits fibrosis and atrophy. (Reprinted from Isaacs [16]. © WB Saunders 1997)

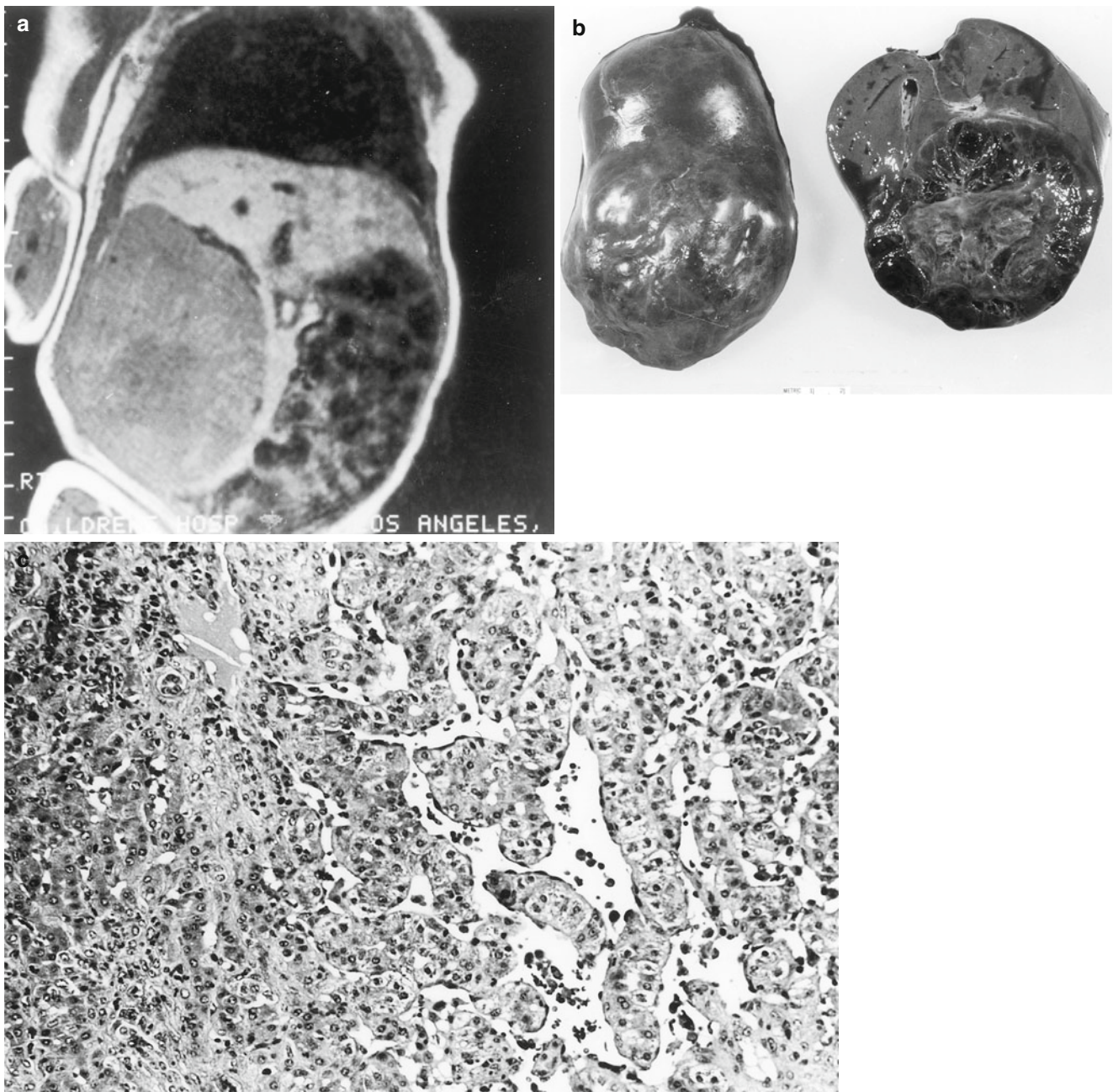


Fig. 12.3 Hemangioma of the liver. Six-day-old male with an abdominal mass and the Kasabach-Merritt syndrome. (a) MRI scan demonstrating a large mass of variable density situated in the right lobe of the liver with features consistent with a hemangioma.

(b) The right lobe of the liver, 225 g, 10×7 cm, contains a 6.5×6 cm hemorrhagic, spongy lesion. (c) The hemangioma is composed of both capillary and cavernous components (Reprinted from Isaacs [16]. © WB Saunders 1997)

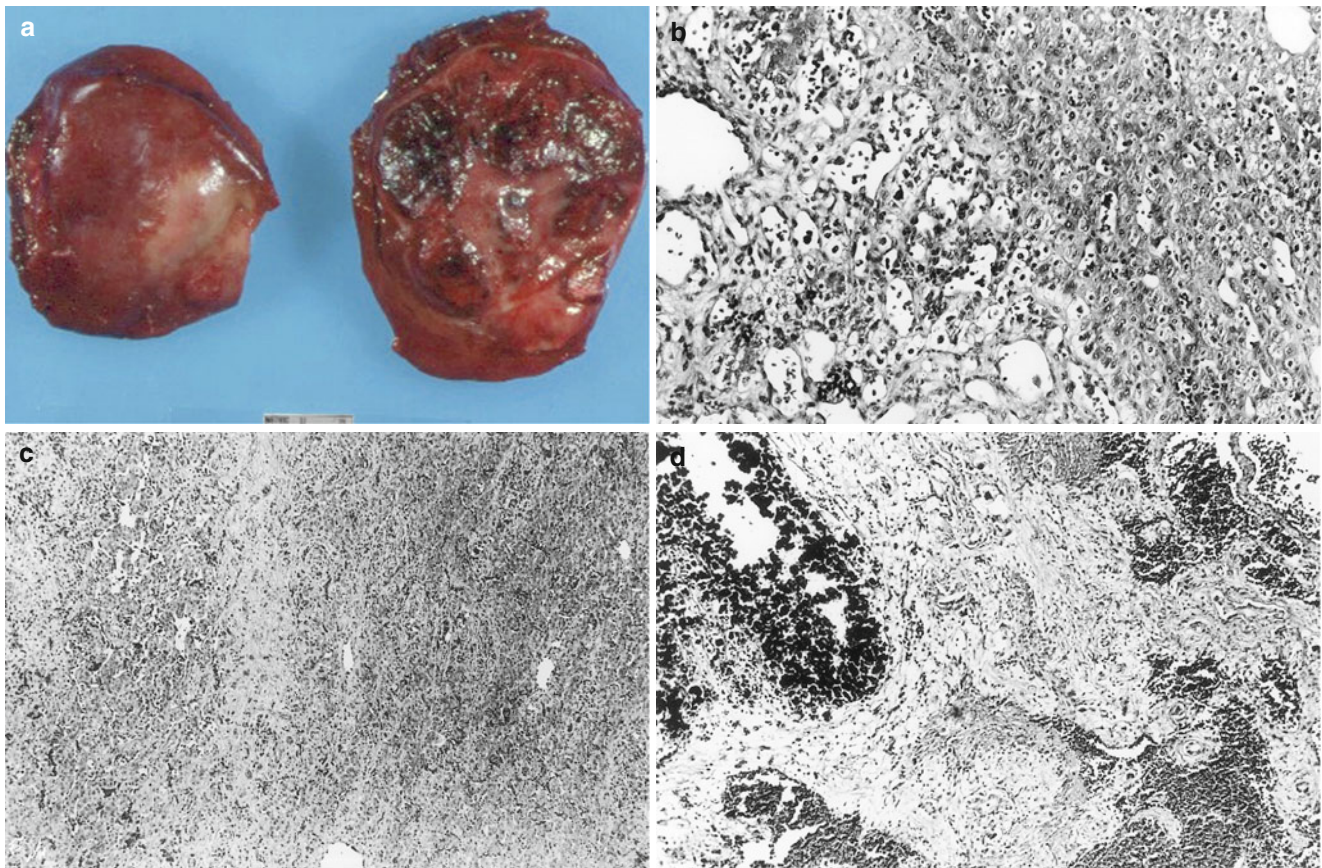


Fig. 12.4 Hemangioma of the liver. Twenty-day-old female with hepatomegaly and thrombocytopenia (platelet count 55,000) noted at birth. Imaging studies revealed a 6-cm-diameter mass in the right lobe of the liver. (a) Right lobe and portion of middle lobe of the liver, 136 g and $9 \times 8 \times 5$ cm, containing a well-encapsulated, circumscribed, dark, red-purple mass, 6×5.5 cm. (b) The tumor consists of

vascular channels of various caliber lined by regular endothelium surrounded by loose fibrous connective tissue. Both capillary and cavernous components are present. (c) Areas of necrosis and fibrosis are noted. (d) Extensive necrosis, fibrosis, and calcification are findings consistent with spontaneous regression (Reprinted from Isaacs [2]. © Springer-Verlag, 2002)

12.3 Mesenchymal Hamartoma

Mesenchymal hamartoma is the second most common benign hepatic lesion in the first year of life following hemangioma [1, 2, 5–8, 13, 23, 24]. Over half the pediatric cases are observed in infants and about a fourth in newborns [1, 5, 6]. The chief presenting finding is an expanding abdominal mass (Fig. 12.6). The diagnosis is often suggested preoperatively by imaging studies [1, 2] (Figs. 12.5, 12.6, and 12.7). Although benign histologically, mesenchymal hamartomas can cause life-threatening complications in the perinatal period similar to the ones as hemangioma, for example, hydrops, cardiac failure, anemia, coagulopathy, and stillbirth [7, 23–25]. Mesenchymal hamartoma is detected antenatally by sonography as early as 29 weeks

gestation [25–28]. Sonograms reveal a complex multicystic, well-circumscribed mass in the upper fetal abdomen predominately in the right lobe of the liver. The mass contains areas of echolucency surrounded by multiple echodense membranes (Fig. 12.5a). Over time the multicystic lesion expands rapidly, displacing adjacent abdominal organs, and if large enough causes hydramnios, placentomegaly, nonimmune hydrops, and stillbirth [25–28].

Generally mesenchymal hamartomas do not occur in association with specific congenital malformations or other conditions [6]. However, there are reports of mesenchymal hamartomas having a translocation involving chromosome 19q13.4 and of children who have had a mesenchymal hamartoma removed previously subsequently developing hepatic embryonal sarcoma [29–31]. Bove et al. propose that

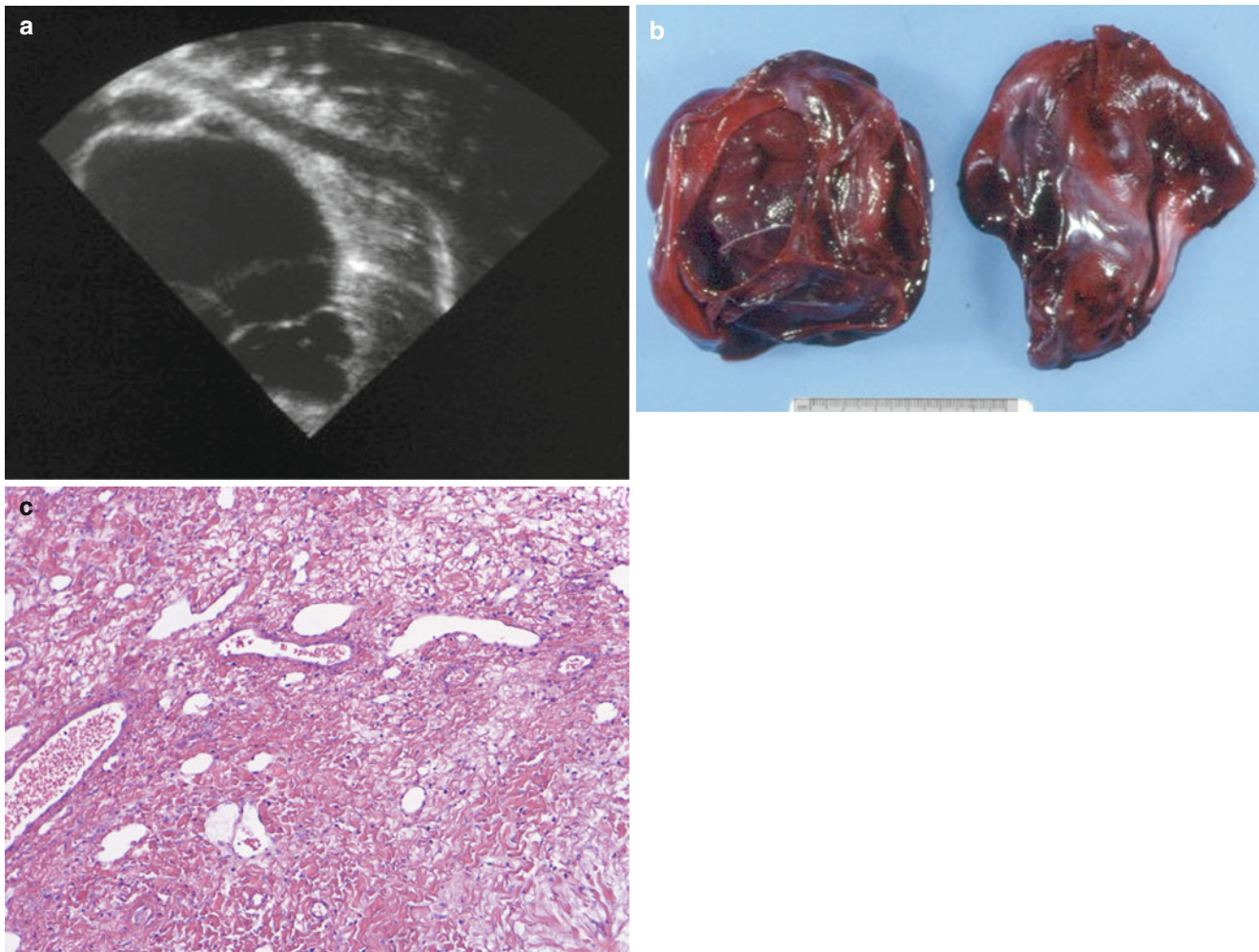


Fig. 12.5 Mesenchymal hamartoma of the liver. One-day-old female, 37 weeks gestation, with abdominal distension noted at birth. (a) Sonogram reveals a large cystic multilocular mass within the right lobe of the liver filled with sonolucent fluid. (b) The specimen consists of a multiloculated hepatic mass, 600 g and 15×12×7 cm, with thick

cyst walls. The cut surface is on the *left side*, and the external surface is on the *right*. (c) Irregular cystic spaces of varying size are surrounded by a loose vascular connective stroma and are lined by flattened endothelium or by low cuboidal epithelium (Reprinted from Isaacs [2]. © Springer-Verlag, 2002)

mesenchymal hamartomas with this translocation represent a subset with neoplastic potential. Moreover, the presence of the 19q13.4 anomaly in hepatic *embryonal sarcomas* as well also tends to support a histogenetic link between the two tumors [23, 30, 31].

Most mesenchymal hamartomas arise from the right lobe of the liver but some, 10 %, originate from both lobes [4–6]. The tumors are cured by surgical excision, providing they are resectable, completely excised, and that there are no associated serious clinical problems such as congestive heart failure, hydrops, pulmonary compromise, or fatal operative complications [2, 7, 10].

The diagnosis of mesenchymal hamartoma is suggested by its characteristic gross appearance, which consists of a well-circumscribed, demarcated multiloculated cystic

hepatic mass with a light gray or pale white bosselated external surface [2, 4, 6, 23] (Figs. 12.5, 12.6, and 12.7). Usually the adjacent liver is grossly normal. The specimens range considerably in size from 100 g to over a kilogram. Cut surfaces of the hamartoma reveal multiple cysts varying in size from a few millimeters to 10 cm or more in diameter. The cysts have gray-white, smooth and glistening lining and contain clear, pale yellow fluid. Some specimens are composed chiefly of multiple cysts (Figs. 12.5 and 12.6) while others are more solid containing dense fibrous connective tissue and only several small cysts (Fig. 12.7). Large necrotic centers are noted in some. Microscopically the cysts are lined by endothelium and cuboidal bile duct epithelium or lack a well-defined epithelium (Figs. 12.5, 12.6, and 12.7). Cysts are surrounded by pale, myxoid fibrous connective

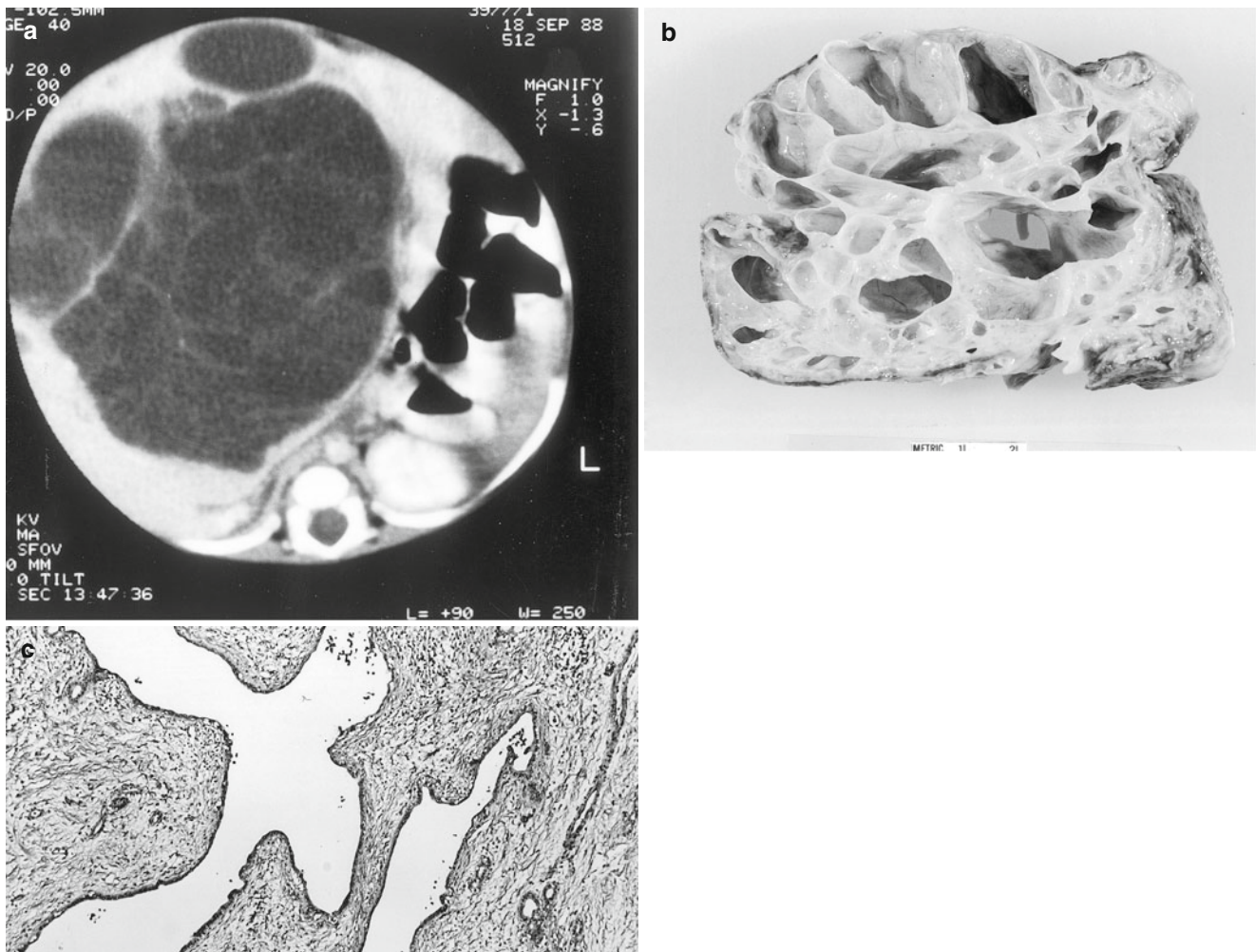


Fig. 12.6 Mesenchymal hamartoma of the liver. Six-month-old male with a rapidly growing abdominal mass first noticed at 4 months of age. (a) CT scan reveals a large, multiloculated, cystic lesion within the liver. (b) Only a small portion of the lesion, which weighed over a kilogram and occupied both the right and left lobes of the liver, is illustrated. It consists of multiple large cysts (filled with clear fluid) separated

by white fibrous connective tissue septae. (c) The cysts are lined cuboidal and endothelial cells separated by fibrovascular septae. The interstitial connective tissue contains a few small bile ducts. The cysts within a mesenchymal hamartoma progressively fill with fluid, presumably lymph and bile, and may expand at an alarming rate thus mimicking a malignant tumor (Reprinted from Isaacs [16]. © WB Saunders 1997)

tissue septae containing blood vessels, lymphatics, and small bile ducts [1, 2, 4, 23]. The periphery of the lesion is encircled either by a thick fibrous capsule or it blends imperceptibly with the adjacent liver parenchyma. EM shows mostly connective tissue, fibroblasts, bile ducts, and normal hepatocytes [4].

It may be difficult to distinguish between mesenchymal hamartomas and hepatic hemangiomas either grossly or microscopically, particularly if there is extensive hemorrhage into the lesion, since the two share similar histological features in common, namely, the presence of septae, blood vessels, and fibrous connective tissue stroma [1].

Pathogenesis of mesenchymal hamartoma remains unknown. Several etiologies have been proposed [4, 6, 29–32]. The cyto-

genetic relationship between mesenchymal hamartoma and *embryonal sarcoma* suggests a neoplastic etiology [31].

Recurrence once the lesion has been completely removed is unusual [2, 4, 7, 9, 23, 24]. The main cause of death is progressive abdominal distension due to a rapidly expanding, fluid-filled, multicystic hepatic mass that produces severe respiratory distress and compression of normal intra-abdominal blood vessels and other structures [7]. Congestive heart failure secondary to A-V shunting within the hamartoma, fetal hydrops, and stillbirth are other causes. Some of the large tumors are not resectable [2, 7]. Moreover, there appears to be a risk of developing hepatic embryonal sarcoma several years after the initial removal of the hamartoma [30, 31].

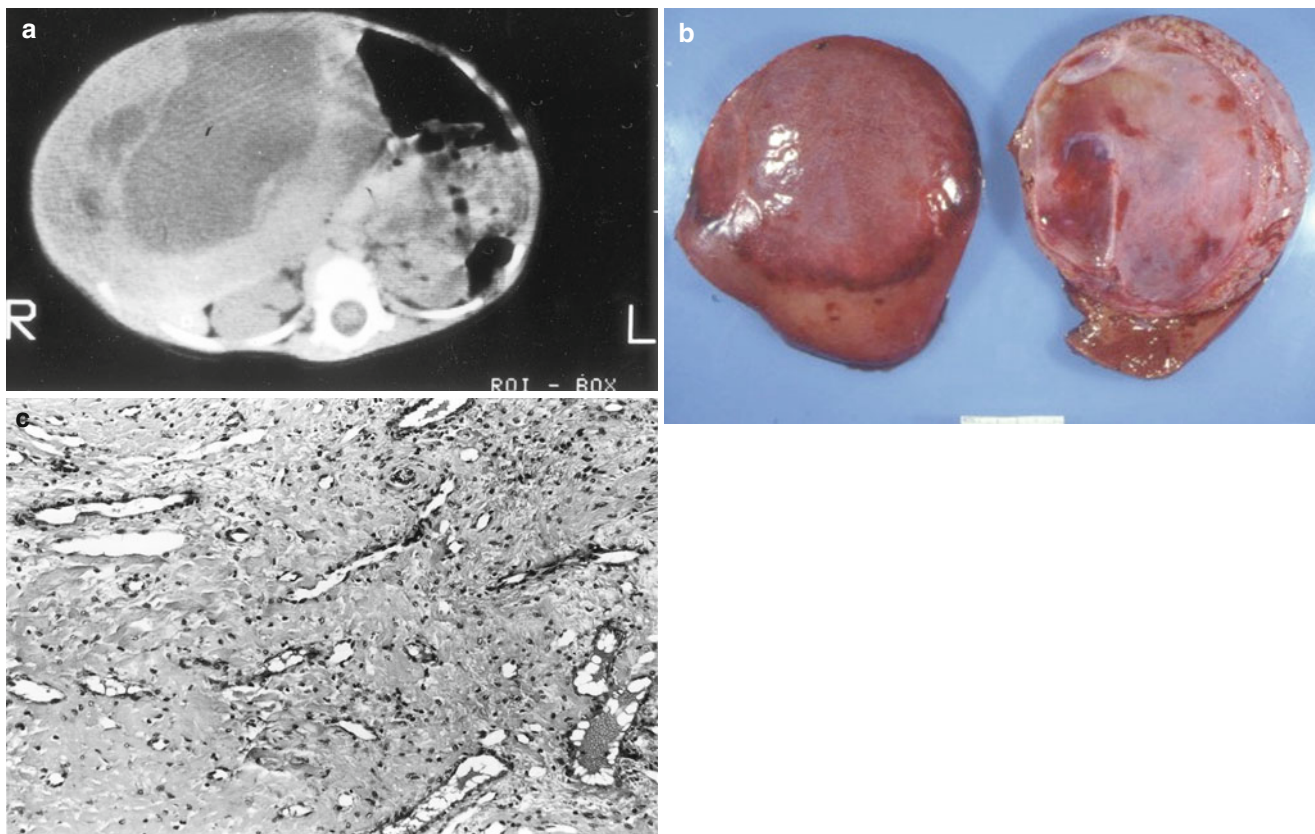


Fig. 12.7 Mesenchymal hamartoma of the liver. Eleven-month-old female with an abdominal mass. **(a)** CT scan reveals a solid and cystic mass within the right lobe of the liver. **(b)** The partial right hepatectomy specimen consists of solid and cystic myxoid-appearing structures. The

capsular surface of the liver is on the left side, and the cut surface is on the right. **(c)** Compact fibrovascular tissue containing slit-like spaces lined by flattened endothelium (mostly) and by low cuboidal epithelium (Reprinted from Isaacs [2]. © Springer-Verlag, 2002)

12.4 Hepatoblastoma

Hepatoblastoma is the leading liver malignancy during the first year of life [1, 2, 4–12, 33]. Over half the tumors are diagnosed in infants, and less than 10 % are seen in neonates [1, 6, 8, 33–40]. Although the number of hepatoblastomas reported in the older infant and child exceed all benign hepatic lesions combined, in the newborn hemangioma and mesenchymal hamartoma are more prevalent [2, 6, 12]. Hepatocellular carcinoma rarely occurs in patients younger than 6 years where usually there is an underlying condition such as cirrhosis, prolonged hyperalimentation, or a congenital metabolic storage disease [2, 5, 10–12]. Including the total surgical and necropsy specimens, most hepatic tumors are metastatic rather than primary [2, 4, 7]. *Neuroblastoma* metastasizes most often to the liver in the fetus and infant followed by *leukemia* and *renal tumors*. *Yolk sac tumor*, *rhabdomyosarcoma*, and *rhabdoid tumor* are examples of other malignancies metastasizing to the liver in this age group [2, 4, 7] (Table 12.1).

Hepatoblastoma commonly presents as an upper abdominal mass arising as a solitary tumor more often from the right lobe of the liver than the left [2, 11, 12]. (In the fetus, it is detected on prenatal ultrasound [1, 2, 8, 35, 36].) Additional clinical findings are respiratory distress and/or gastrointestinal symptoms related to a massively enlarged liver, spontaneous rupture with hemoperitoneum during delivery, anemia and jaundice, sexual precocity in males, hydramnios, and nonimmune fetal hydrops [1, 2, 4, 8, 35, 36, 38]. In addition to neuroblastoma and leukemia, hepatoblastoma is another pediatric malignancy responsible for placental metastases and fetal death [37, 38].

Various congenital anomalies and malformation syndromes are associated with hepatoblastoma [2, 10, 39–42] (Table 12.2). *Hemihypertrophy*, present in 2–3 %, the *Beckwith-Wiedemann syndrome*, and *intestinal adenomatous polyposis* are the ones cited most often [5, 6, 39, 41, 42]. Additional conditions associated with hepatoblastoma are listed in Table 12.2. Some of the same congenital malformations and syndromes occur also in patients with Wilms' tumor [41] (see Chap. 11). There is an increased incidence of

Table 12.2 Conditions associated with hepatoblastoma

Aicardi syndrome
Beckwith-Widemann syndrome
Hemihypertrophy
Wilms' tumor
Polyposis coli syndromes
Isosexual precocity
Fetal alcohol syndrome
Hydrops fetalis
Cystathioninuria
α -1-antitrypsin deficiency
Maternal contraceptive use
Trisomy 18
Umbilical hernia
Adenomatoid transformation of renal epithelium
Very low birth weight

Reprinted from Stocker [11]. With kind permission of © Elsevier, 1994; Reprinted from Lack et al. [12]. With kind permission of © Lippincott Williams & Wilkins, 1982; Reprinted from Isaacs [2]. © Springer-Verlag, 2002

hepatoblastoma occurring in *infants of very low birth weight* [43]. The Children's Oncology Group Hepatoblastoma Study revealed a 16–23-fold excess of extreme prematurity in children with this tumor. The low birth weight is correlated more often with unfavorable histology (embryonal vs. fetal hepatoblastoma) and aggressive biological behavior (advanced stage of disease at time of diagnosis) [43]. Because of this association, screening with serum α -fetoprotein is recommended by some for patients with very low birth rates [43].

Practically all patients with hepatoblastoma have significantly elevated serum α -fetoprotein, a valuable diagnostic tumor marker [2, 5, 6]. However, it should be mentioned that serum α -fetoprotein is normally elevated during the first few months of life (see Table 2.4 for normal serum levels in newborns and infants). Moreover, levels are increased also in patients with yolk sac tumor [1, 2].

Grossly hepatoblastomas consist of a single, round mass replacing a part or almost the entire lobe of the liver, some measuring 10–20 cm or more [1, 2, 4, 6, 10–12] (Figs. 12.8, 12.12, and 12.13). The tumor is often well-circumscribed and demarcated from the adjacent normal liver by a whitish-gray, fibrous pseudocapsule. The cut surface is light tan- or cream-colored, soft in consistency with or without gray myxoid areas and yellow necrotic zones. Tiny white foci of calcification are noted in the mixed hepatoblastomas cut surfaces. Hepatoblastoma is classified histologically into two main groups, *epithelial or mixed*, depending on whether mesenchymal elements are present [4, 6, 11, 12, 33, 44] (Table 12.3). The epithelial components occurring in both the epithelial and mixed hepatoblastomas are subdivided further into four main cell types designated as *fetal*, *embryonal*,

macrotrabecular, and *small cell undifferentiated* (or “*anaplastic*”). The fetal cell type, as the name implies, resembles fetal liver cells composed of small regular cells with minimal nuclear atypia and low mitotic rates (Fig. 12.8). The fetal-like cells form narrow cords one or two cells thick with bordering sinusoids and prominent foci of hematopoiesis. The *fetal type* consists of both light and dark cells, the former containing more glycogen and lipid than the latter as shown by histochemical and EM studies [1, 6].

Embryonal epithelial hepatoblastoma consists of more atypical, pleomorphic, larger cells than the fetal type; the atypical hepatocytes tend to grow in a more solid pattern (Figs. 12.9, 12.10, 12.11, 12.12, and 12.13). Frequent mitoses are noted. Portal triad structures are missing from within the tumor which is a helpful clue in deciding whether the liver tumor is benign or malignant. Both fetal and embryonal cell types coexist in the same tumor with transition zones between the two (Fig. 12.11). EM studies show that the embryonal hepatoblast is a more primitive cell containing fewer organelles than the fetal hepatoblast [45–47] (Fig. 12.11e). The type of epithelial component present in hepatoblastomas, that is, fetal versus embryonal, is more important in predicting prognosis than whether the tumor has mesenchymal elements or not.

Immunohistochemical studies show a wide variety of immunostaining with monoclonal antibodies particularly those specific for epithelial antigens [11]. Embryonal and fetal tumor cells are immunoreactive with cytokeratins numbers 8 and 18 and the bile duct cytokeratin 19. Cells associated with osteoid express vimentin and the cytokeratins 7, 18, and 19 [46, 47]. Like α -fetoprotein, hepatocyte paraffin 1 and the polyclonal anti-carcinoembryonic antigen are helpful in making the diagnosis of either hepatoblastoma or hepatocellular carcinoma [47] (Fig. 12.11). Hepatoblastomas express hepatocyte paraffin 1 with a characteristic granular intracytoplasmic pattern, less intense in embryonal than fetal type. Fetal-type hepatoblastomas react with anti-carcinoembryonic antigen, whereas the embryonal type does not.

Sometimes it is difficult to tell the difference between *embryonal epithelial hepatoblastoma with the “macrotrabecular” pattern* (Fig. 12.12) and hepatocellular carcinoma (Fig. 12.17). The latter tends to be *multifocal and associated with an underlying condition* such as cirrhosis, tyrosinemia, or other inborn metabolic disease. This is an important distinction because infants with hepatocellular carcinoma have a much worse prognosis and the tumors are treated differently [6, 33]. The macrotrabecular pattern is defined by the presence of trabeculae greater than ten embryonal hepatocyte cells thick [33] (Fig. 12.17b, c). Hepatocellular carcinoma has a larger cell size, striking cellular pleomorphism, tumor giant cells, multinucleated tumor cells, and sometimes foci of bile pigment [33] (Fig. 12.17c, d). EM is less helpful

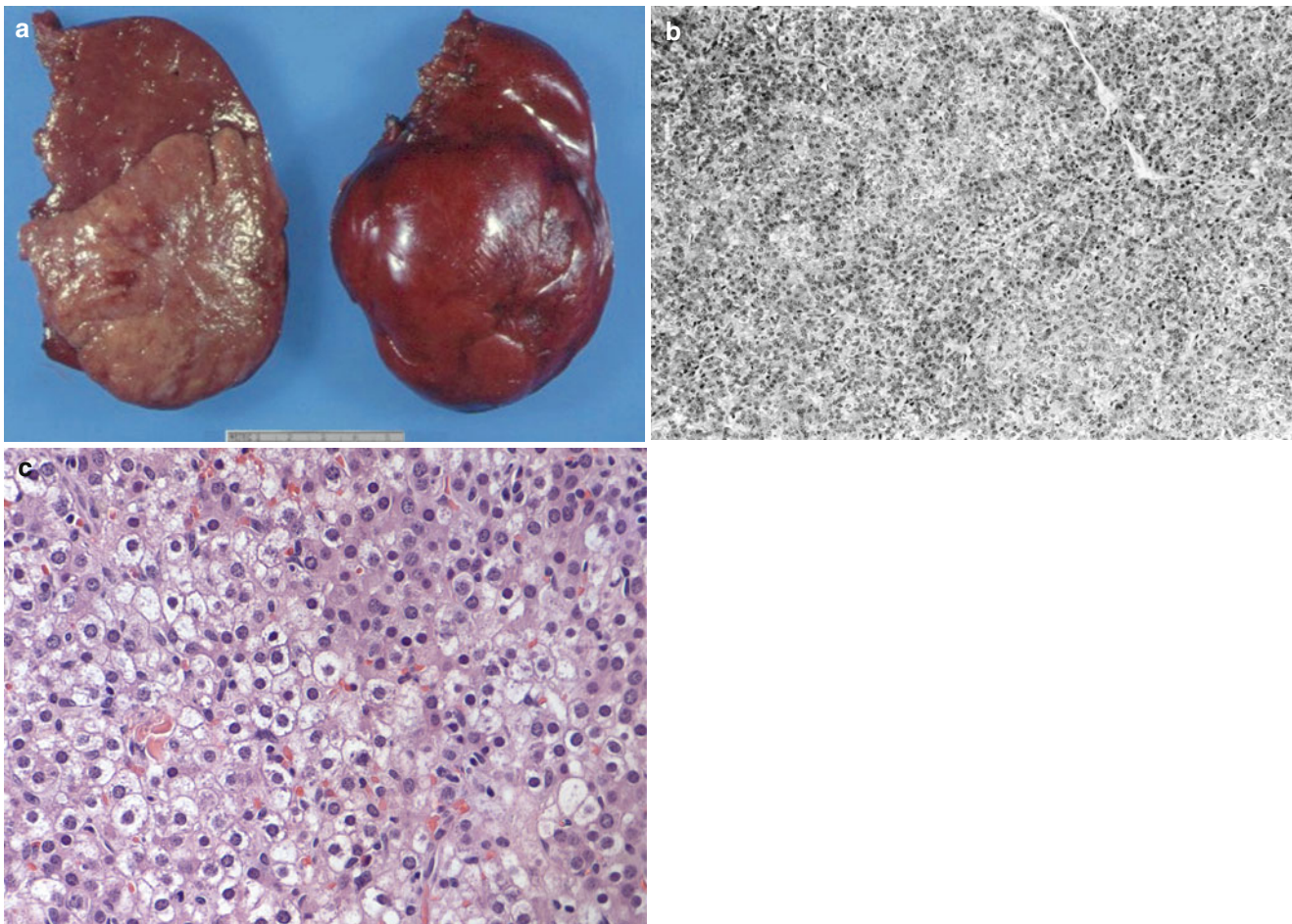


Fig. 12.8 Hepatoblastoma (epithelial, fetal). One-year-old male with an abdominal mass and an elevated serum α -fetoprotein (levels six times normal). (a) Right lobe of the liver, 347 g, 13×7 cm, containing a 9×7 cm, soft, tannish-yellow bulging mass. (b) The tumor is composed of small, uniform, immature liver cells (compare the photomicrograph

with developing liver, Fig. 12.1). Low magnification illustrates the small size of the tumor cells. (c) Higher magnification reveals light and dark cells and transition forms between the two types of fetal hepatoblasts (Reprinted from Isaacs [16]. © WB Saunders 1997)

Table 12.3 Histological classification of hepatoblastoma

Epithelial
Fetal pattern
Embryonal pattern
Macrotrabecular pattern
Small cell undifferentiated (“anaplastic”) pattern
Mixed epithelial and mesenchymal
Mixed with teratoid components ^a

Reprinted from Conran et al. [44]. With kind permission of © Allen Press, 1992

^aTissues from all three germ layers

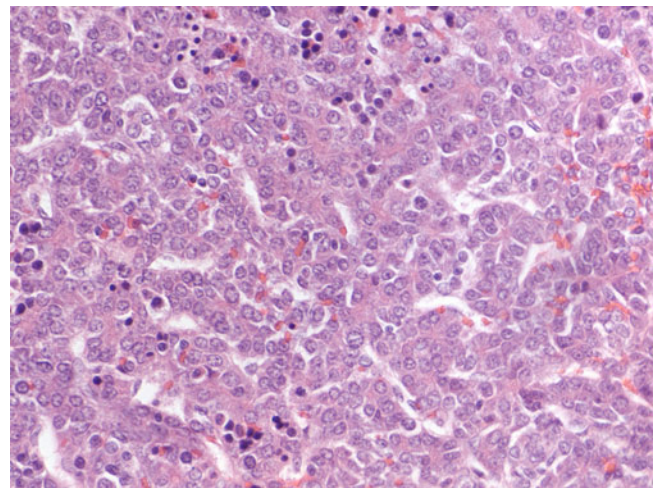


Fig. 12.9 Congenital hepatoblastoma (epithelial, embryonal). Newborn male with increasing respiratory distress and abdominal distension noted at birth. The tumor, 11×9.5 cm, consists of cord-like and pseudoacinar structures. Tumor cells show slight to moderate variation in nuclear size and shape. Several mitoses are noted. The cells with small, round darkly staining “naked” nuclei are nucleated erythrocytes (erythroblasts) (Reprinted from Isaacs [16]. © WB Saunders 1997)

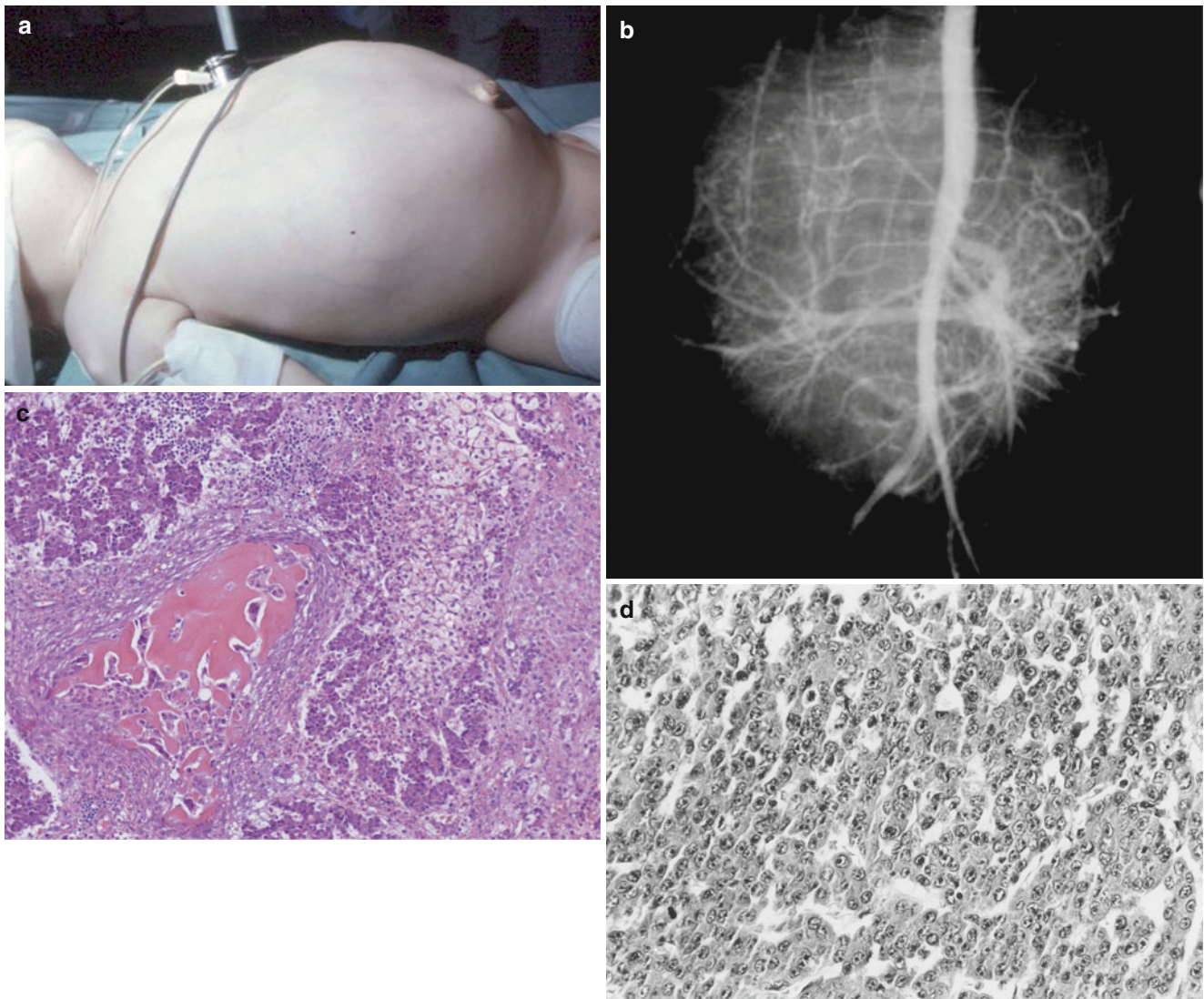


Fig. 12.10 Hepatoblastoma (mixed; fetal and embryonal epithelial components). Five-month-old male with a 3-month history of progressive abdominal distension. **(a)** The large abdominal mass arising from the liver is depicted. **(b)** Arteriogram reveals involvement of almost the entire liver by tumor. **(c)** Liver biopsy shows a mixed hepatoblastoma

with both osteoid and epithelial components, the latter consisting of fetal and embryonal cell types. **(d)** Higher magnification of the embryonal hepatoblasts showing more irregularity in nuclear configuration and cell size as compared to the fetal hepatoblastoma pictured in Fig. 12.8 (Reprinted from Isaacs [16]. © WB Saunders 1997)

in distinguishing hepatoblastoma from *hepatocellular carcinoma* [4, 45]. Cells of the former are less mature compared to the latter since they contain fewer cytoplasmic organelles and less well-developed microvilli.

The very rare, small cell undifferentiated (“anaplastic”) epithelial pattern is observed during the first 6 months of life [33, 48]. It consists of small, round, darkly staining cells resembling neuroblasts having little evidence of liver cell differentiation by H&E staining; in contrast to neuroblastoma, pools of mucoid material (acid mucopolysaccharide) are present between the cells [12, 33, 44, 48]. EM studies confirm the liver cell origin of the tumor by the presence of abundant glycogen, a prominent endoplasmic reticulum, tonofilaments, desmosomes, and canalicular microvilli [48].

Tumor cells are cytokeratin positive but do not react with vimentin, desmin, S-100, or neuron-specific enolase [48]. When fetal or embryonal epithelial components are found in addition to the small, dark round cells, the diagnosis of the small cell undifferentiated pattern can be made. Moreover, a t(10;22) chromosomal translocation has been described for the anaplastic variant [49].

In addition to the epithelial components described above, *mixed hepatoblastomas* contain *mesenchymal elements* consisting of spindle-shaped fibroblastic cells surrounded by a pale-staining myxoid stroma and foci of osteoid, bone, and less often cartilage or skeletal muscle located within nests of fetal or embryonic epithelium. *Osteoid* is the most common differentiated tissue, and it is found in 20–35 %

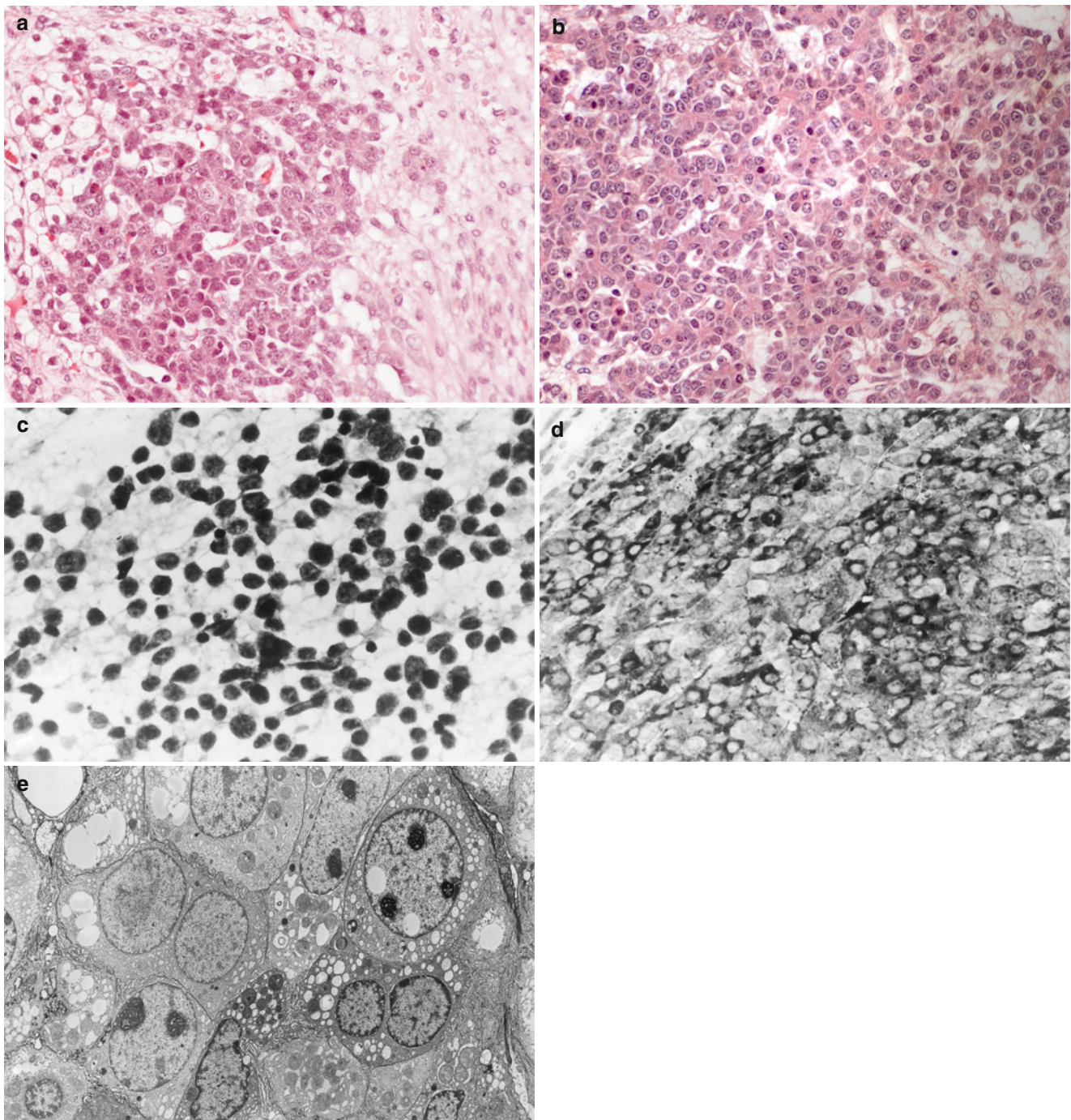


Fig. 12.11 Hepatoblastoma (epithelial with fetal and embryonal components). (a) The tumor is composed of two types of tumor cells, smaller fetal hepatoblasts along the left edge and larger embryonal. (b) Higher-power view of the embryonal tumor cells shows more nuclear and cytoplasmic pleomorphism and crowding with pseudoacinar formation. (c) Cytological preparation (smear) depicting the two cell populations of hepatoblasts. Note the scant cytoplasm of the mostly round tumor cells. (d) The tumor cells are strongly immunore-

active with α -fetoprotein antibody. In addition, they were focally, intensively reactive with α -1-antitrypsin. (e) EM depicts small and large tumor cells with single round nuclei, one to three nucleoli, and cytoplasm containing scattered mitochondria, profiles of rough endoplasmic reticulum, lipid droplets, and polyribosomes. (Electron photomicrographs courtesy of Ann Peters, Department of Pathology, Rady Children's Hospital San Diego) (Reprinted from Isaacs [2]. © Springer-Verlag, 2002)

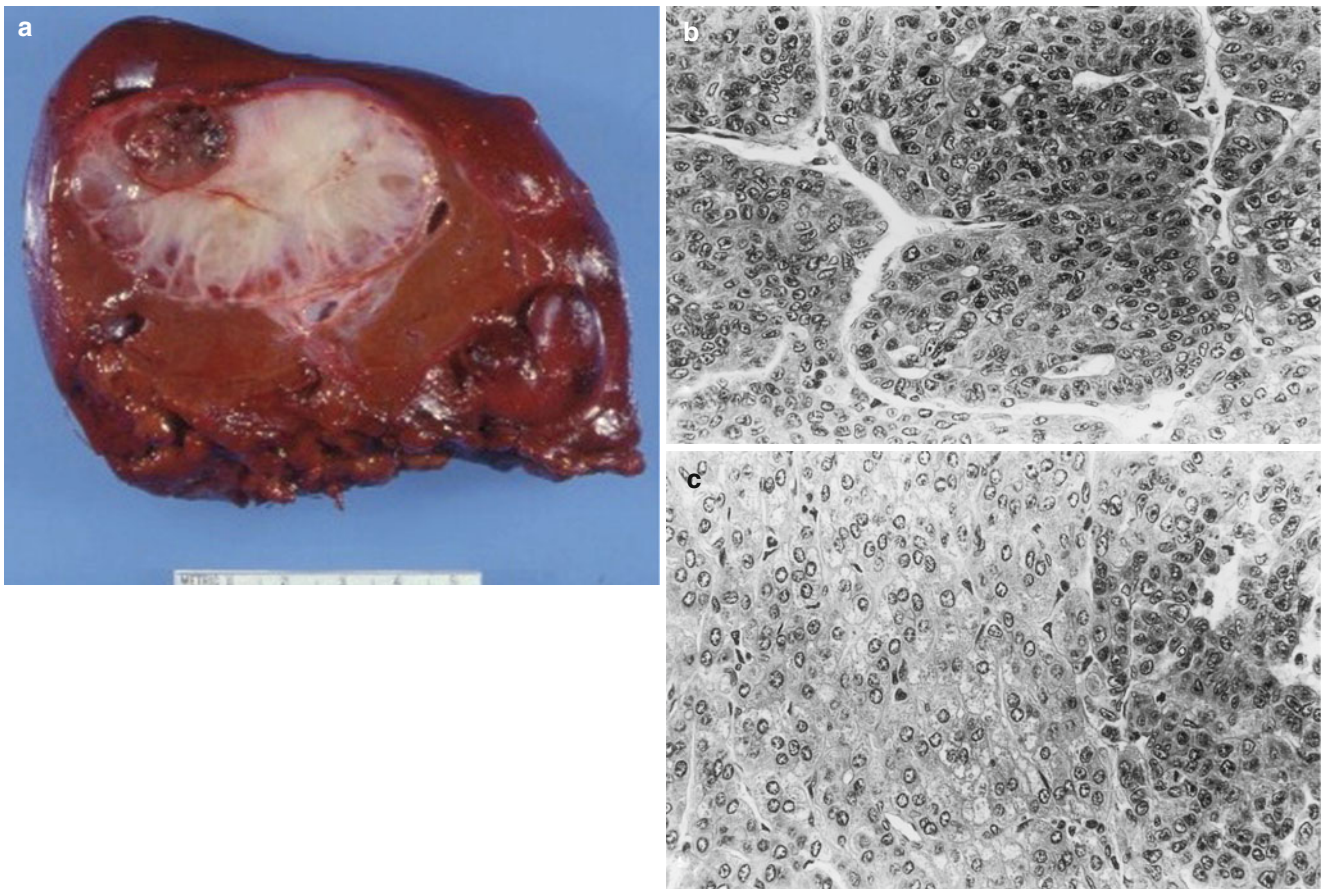


Fig. 12.12 Hepatoblastoma (epithelial, embryonal with macrotrabecular pattern). One-year-old male with an abdominal mass. (a) Partial hepatic lobectomy composed of a 7×5 cm tumor with both smooth, pale white-gray and nodular areas. (b) The macrotrabecular pattern shown is characterized by trabeculae (cords) greater than ten cells thick

composed of embryonal hepatoblasts. Occasionally this morphological pattern of hepatoblastoma is difficult to distinguish from hepatocellular carcinoma (compare with Fig. 12.16, hepatocellular carcinoma). (c) Higher magnification reveals trabecular and pseudoacinar formations in greater detail (Reprinted from Isaacs [2]. © WB Saunders 1997)

of hepatoblastomas [4] (Fig. 12.10). Osteoid is formed by tumor mesenchymal cells [4, 6].

The number of cases of “pure” epithelial versus mixed hepatoblastoma varies but in most series the epithelial type predominates rather than the mixed [2, 4, 12, 33]. The presence of a mesenchymal component has no bearing on prognosis [2, 6].

The term “teratoid” is reserved for mixed hepatoblastomas with tissues from all three germ layers, for example, cartilage, skeletal muscle, intestinal, and keratinizing stratified squamous epithelium [44, 50, 51]. Deposits of melanin pigment are present in some. Hepatoblastoma can occur along with a yolk sac tumor component [51]. Parenthetically teratomas may contain fetal liver cells.

Common sites of metastases of hepatoblastoma in decreasing order are the lungs, abdomen, brain, lymph nodes, and vena cava [7, 10].

Survival depends on four main factors: complete resection of the tumor, absence of metastases, lack of “unfavor-

able histology,” that is, presence of embryonal or undifferentiated cell types and the clinical condition of the affected infant [2, 6, 7, 12]. If the tumor is small in size and is completely resected before it has metastasized (i.e., stage I), then the patient has the best chance for survival (Table 12.4). One exception is the small cell undifferentiated (anaplastic) variant which has a particularly poor prognosis since it metastasizes early [4, 48].

When hepatoblastomas are sensitive to chemotherapy, which produces necrosis, fibrosis, and shrinkage, this allows resection of an originally inoperable tumor.

Patients die from the mass effect caused by the tumor which leads to abdominal distension, vascular compromise, anemia, hydrops, fetal hydrops, severe respiratory distress, and stillbirth [7]. Metastases to the abdominal cavity, lungs, and placenta are other important causes of death.

Hepatoblastoma current staging and treatment regimens are described by the Children’s Oncology Group publication [52].

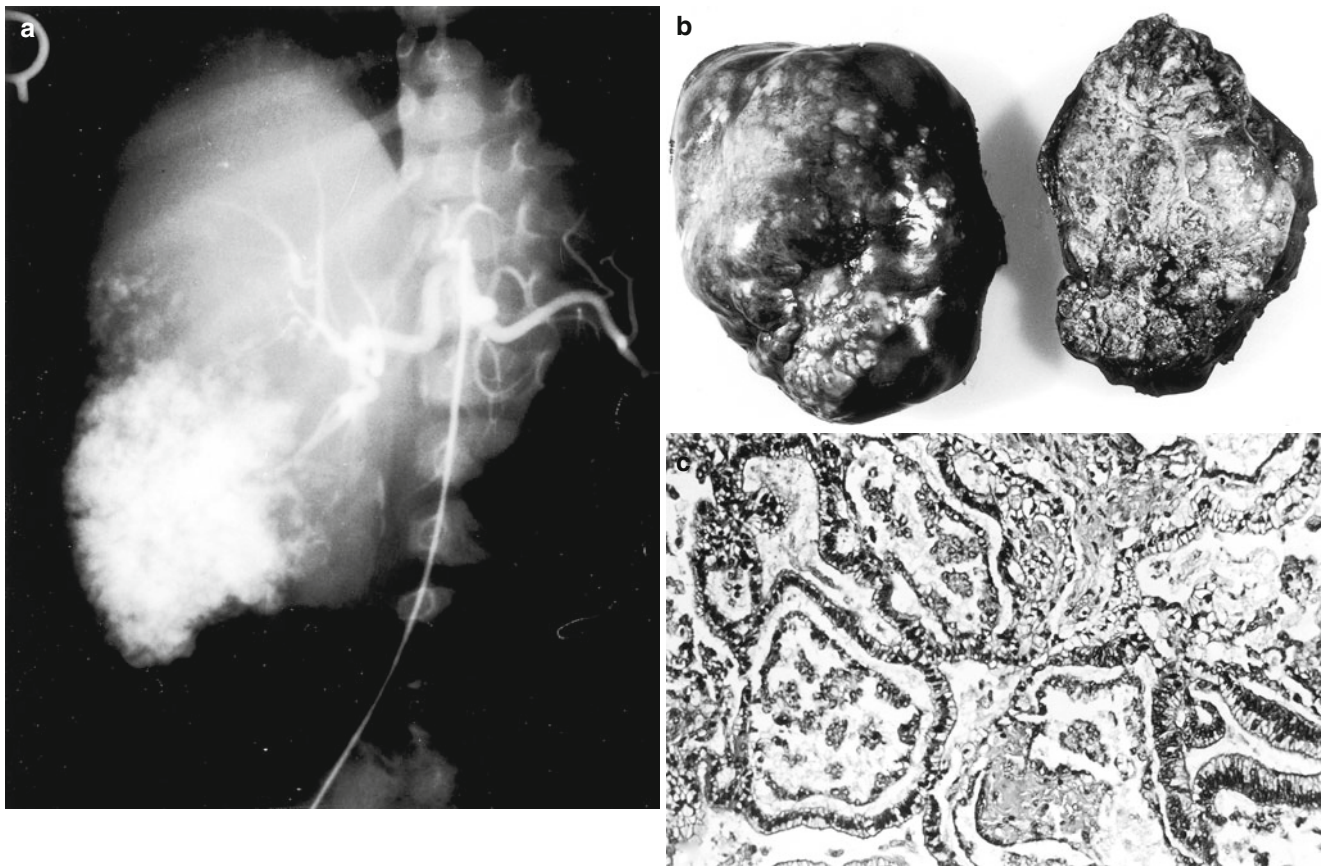


Fig. 12.13 Hepatoblastoma (epithelial, embryonal with intestinal-type epithelium). (a) The arteriogram reveals a large mass in the right lobe of the liver with flecks of calcification. (b) Most of the right lobe of the liver is replaced by a soft gray-white, finely nodular tumor mass.

(c) Portions of the tumor show irregular gland formations suggestive of intestinal-type epithelium composed of vacuolated columnar cells with hyperchromatic, pleomorphic nuclei (Reprinted from Isaacs [2]. © Springer-Verlag, 2002)

Table 12.4 Children's Oncology Group staging system for hepatoblastoma

Stage I	Complete gross resection at diagnosis with clear margins
Stage II	Complete gross resection at diagnosis with microscopic residual disease at the margins of resection
Stage III	Biopsy only at diagnosis; or gross total resection with nodal involvement; or preoperative tumor spill/rupture; or incomplete resection with gross residual
Stage IV	Distant metastatic disease at diagnosis

Reprinted from Meyers et al. [52]. With kind permission of © Wiley, 2009

12.5 Primary Sarcomas of the Liver

Embryonal rhabdomyosarcoma and *embryonal (undifferentiated) sarcoma* are the two main primary malignant mesenchymal tumors of the liver in childhood [4, 6, 53, 54]. Hepatic sarcomas are noted rarely in the newborn and infant [53].

Embryonal sarcoma affects mostly older children, 6–10 years of age, whereas rhabdomyosarcoma is found primarily in younger children between the ages of 2 and 4 years [4, 6]. There are instances of embryonal sarcoma arising from a mesenchymal hamartoma and the presence of a common 19q13.4 translocation in these entities suggesting a histogenetic link between the two [30, 31].

Embryonal sarcoma (undifferentiated sarcoma) is another entity that should be considered in the differential diagnosis of a primary liver tumor [4, 6, 30, 31, 53, 54]. An abdominal mass and pain are the main clinical findings. Imaging studies reveal a space-occupying lesion often situated in the right lobe of the liver with solid and cystic areas. Cysts and septations found on imaging may render distinction from mesenchymal hamartoma sometimes difficult [2]. Embryonal sarcomas tend to be large, measuring 30 cm or more in diameter. They are surrounded by a fibrous pseudocapsule. The cut surface has a tan to light gray, gelatinous appearance with extensive necrosis and cyst formation

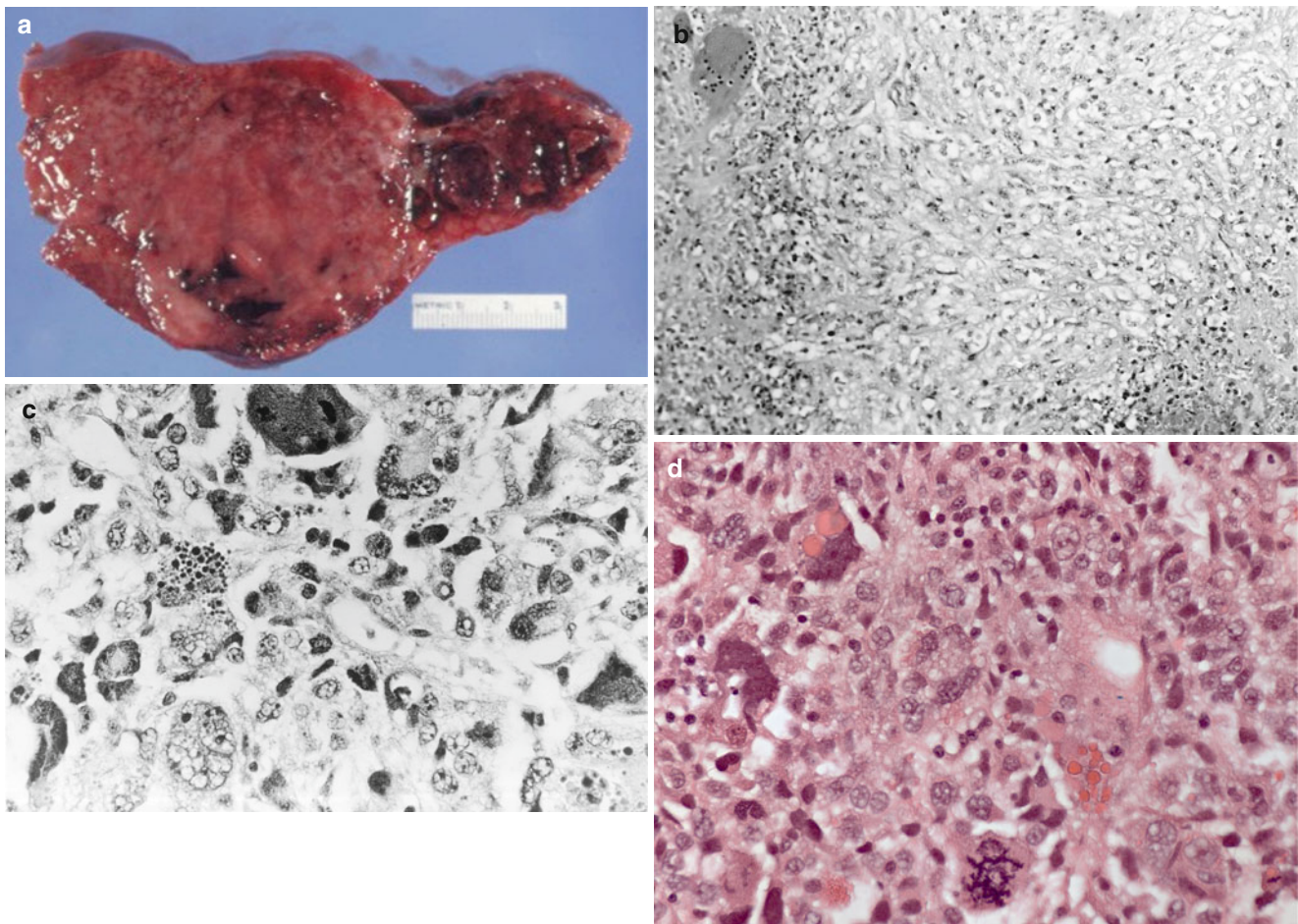


Fig. 12.14 Embryonal (undifferentiated) sarcoma of the liver. Two-year-old girl with an abdominal mass. Initial imaging studies revealed a large tumor with solid and cystic areas situated within the right lobe of the liver. Hepatic abscess was one of the diagnostic considerations. **(a)** Most of the liver is replaced by friable, gelatinous tissue with large areas of cystic necrosis and hemorrhage. **(b)** The tumor consists of an abundant, pale-staining, myxoid stroma with clusters of small round, oval, or spindle-shaped vacuolated cells. Extensive necrosis is present which is characteristic finding. Pieces of tumor with this histological

appearance are often submitted for frozen section diagnosis creating a diagnostic problem—neoplasm versus chronic hepatic abscess (e.g., due to *Entamoeba histolytica*). **(c)** Large tumor cells with bizarre nuclei and characteristic eosinophilic staining, PAS-positive, diastase-resistant, cytoplasmic spherules are present. Mitoses are not uncommon. Vascular invasion by tumor cells, not pictured here, is another important diagnostic finding. **(d)** Higher-power view showing the anaplastic giant cells, spherules, and vacuolated cells in more detail (Reprinted from Isaacs [2]. © Springer-Verlag, 2002)

(Fig. 12.14a). Microscopically there are abundant pale-staining myxoid stroma and extensive necrosis with clusters of small dark round, oval, or spindle-shaped cells (Fig. 12.14b). In addition, there are tumor giant cells with bizarre nuclei and diagnostic eosinophilic staining PAS-positive, diastase-resistant *cytoplasmic spherules* (Fig. 12.14c, d). Mitoses are not uncommon. Entrapped liver cells and bile ducts are noted about the periphery. Vascular invasion is an important feature. Vimentin and the histiocytic markers, lysozyme and α -1-antitrypsin, are variably reactive, but α -fetoprotein is not [54]. By EM, embryonal sarcomas are composed primarily of spindle-shaped fibroblastic cells with cytoplasm containing well-developed

rough endoplasmic reticulum. In addition, there are primitive mesenchymal cells with scanty cytoplasm and few organelles. Other cell types present include histiocytoid cells having lysosomal granules and microvillus-like cytoplasmic projections and myofibroblastic cells composed of serrated nuclei, abundant rough endoplasmic reticulum, filamentous condensations beneath the cytoplasmic membrane, and focal basal lamina formation [54].

Outcome of patients with embryonal sarcoma is generally dismal; few live longer than 18 months after diagnosis [2, 6, 53, 55]. However, recently the prognosis has improved somewhat with the advent of newer chemotherapeutic agents.

The liver is an uncommon primary site for *embryonal rhabdomyosarcoma* arising from either the intrahepatic bile ducts or from the extrahepatic biliary system [2, 4, 6, 55]. The child presents with an abdominal mass accompanied by jaundice if the biliary tract is obstructed. When the sarcoma is located in one of the major bile ducts, it forms tiny, pale, tan-gray grapelike, polypoid masses filling the ductal lumen similar to those arising from hollow viscera elsewhere, for example, urinary bladder, vagina, and ear. The histological appearance is that of a *botryoid embryonal rhabdomyosarcoma* consisting of polypoid projections composed of a pale myxoid stroma and a cellular rind of small dark round or spindle-shaped rhabdomyoblastic cells situated beneath the bile duct epithelium [2]. Cytoplasmic cross striations are variably present with H & E staining. Desmin and other skeletal markers are immunoreactive, and EM is diagnostic (see Chap. 4). When the tumor arises from the liver parenchyma, it forms a light tan-gray, gelatinous-appearing intrahepatic mass with foci of necrosis and hemorrhage.

Historically the prognosis of newborns with intrahepatic rhabdomyosarcoma was disappointing because the tumor metastasizes early to the lungs, brain, and lymph nodes, and due to its location, it is difficult to resect [4]. The prognosis has improved somewhat [55].

12.6 Germ Cell Tumors

Germ cell tumors metastatic to the liver, namely, *yolk sac tumor* spreading from the sacrococcygeal area or testis, for example, are observed more often than primary ones during the first year of life [1, 2, 6, 51, 56, 57] (Fig. 12.15). Although few in number, *teratoma* of the liver is reported more frequently than *primary yolk sac tumor* [2, 6, 56, 58]. Teratoma of the liver is more prevalent in the newborn and infant than in older children or adults. Hepatic *fetus-in-fetu* detected by antenatal sonography is described in association with separate nodules of mature teratoma in the same liver [58].

Hepatic teratomas are cystic, composed of mature tissues as found elsewhere and to a lesser extent immature neuroglial elements. They usually lack a malignant germ cell tumor component. Surgical excision results in cure providing no residual tumor is left behind [2].

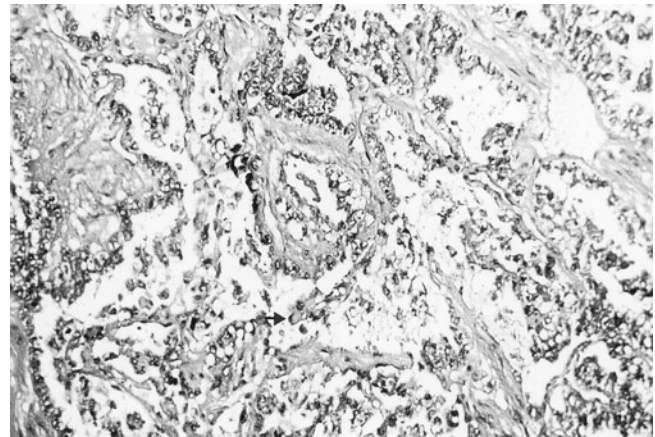


Fig. 12.15 Yolk sac tumor. One-year-old male with a large friable mass invading the abdominal wall along the falciform ligament and extending into the left lobe of the liver. Serum α -fetoprotein was 76,000. The tumor shows papillary and reticular growth patterns consisting of small vacuolated cells with irregular nuclei. Within the center of the field there is a vascular structure surrounded by tumor cells (endodermal sinus structure) (From Atkinson et al. [57]. With kind permission of © Elsevier, 1992)

12.7 Liver Cell Adenoma and Focal Nodular Hyperplasia

Adenoma and focal nodular hyperplasia are considered benign proliferations of liver cells which are noted more often in adults than in infants and children [4, 6, 13, 59, 60]. They seldom occur in the fetus and newborn [2, 60, 61].

Grossly *hepatic adenomas* are confined to one lobe, moderately soft with a yellow-brown cut surface. A thin connective tissue capsule is variably present. Microscopic examination reveals a well-encapsulated lesion with uniform cells resembling normal hepatocytes [60]. Tumor cells consist of a pale-staining cytoplasm and are arranged in sheets or anastomosing cords two to three cells wide with indistinct sinusoidal lining cells. Some binucleated or trinucleated cells are present. Normal *portal tracts and central veins are characteristically absent* [60]. Complete surgical removal is recommended when technically feasible because of the lingering suspicion of possible malignant change and diagnostic difficulties in differentiating hepatic adenoma from a well-differentiated hepatocellular carcinoma [60].

Focal nodular hyperplasia is a benign liver condition characterized by a round to oval, multinodular mass of hepatocytes separated by a stellate scar situated within the center

[4, 6, 60]. Similar to the adenoma, bile ducts, portal tracts, and recognizable central veins are absent within the lesion. The etiology is unknown. Most cases in children occur between ages 7 and 14 years [60, 62]. Focal nodular hyperplasia is cured by surgical excision [60].

Nodular regenerative hyperplasia is an uncommon liver condition in infants and children presenting as hepatomegaly and/or splenomegaly with or without portal hypertension [63]. It may be an incidental finding at necropsy. The lesion is reported together with other conditions such as Wilms' tumor, mental retardation, VATER syndrome, renal angiomyolipoma, and in patients treated with anticonvulsant therapy [63]. The entire liver may be replaced by multiple tan to yellow, nonencapsulated nodules varying in size from a few millimeters to several centimeters. Histologically the nodules are composed of hepatocytes slightly larger than normal ones causing compression atrophy of the adjacent parenchyma.

12.8 Miscellaneous Tumors and Tumorlike Conditions

Several other distinct hepatic tumors occur in the fetus and infant. *Rhabdoid tumor* primary in the liver, for example [2, 64–66]. The diagnosis can be established by examination of a metastatic site from the liver such as placenta or skin [64–66]. Rhabdoid tumor occurs in association with brain

tumors especially medulloblastoma [66] (see Chaps. 4, 5, 9, and 11).

Hepatocellular carcinoma is uncommon in children less than 6 years of age [4]. Often there is an underlying condition associated with this malignancy, for example, cirrhosis, biliary atresia, inborn error of metabolism (e.g., glycogen storage disease, tyrosinemia), or prolonged neonatal parental nutrition [67–69] (Table 12.2). Grossly the liver contains a large mass or is replaced by multiple grayish-white, necrotic, hemorrhagic tumor nodules (Fig. 12.16a). Microscopically the tumor consists of broad trabecular and acinar formations. Considerable nuclear pleomorphism, prominent nucleoli, giant cells, and presence of bile pigment are characteristic features of hepatocellular carcinoma (Fig. 12.16c, d). Tumor cells are strongly reactive with α -fetoprotein antibody which is present also with hepatoblastoma.

Angiomyolipoma of the liver is detected by sonography in infants with tuberous sclerosis [70]. The lesions are often asymptomatic and are found in the kidneys as well. Hepatic inflammatory pseudotumor (*proliferative fasciitis*) is reported in this age group [71].

Some *hepatic* (“nonparasitic”) *cysts* reach an enormous size in the fetus and infant, fill the peritoneal cavity, and produce an abdominal mass and respiratory distress [1, 2, 4, 72] (Fig. 12.17). Autosomal recessive *infantile polycystic disease of the kidneys and liver* may become apparent at birth manifested by *renohepatomegaly* abdominal masses [1, 2] (Fig. 12.18).

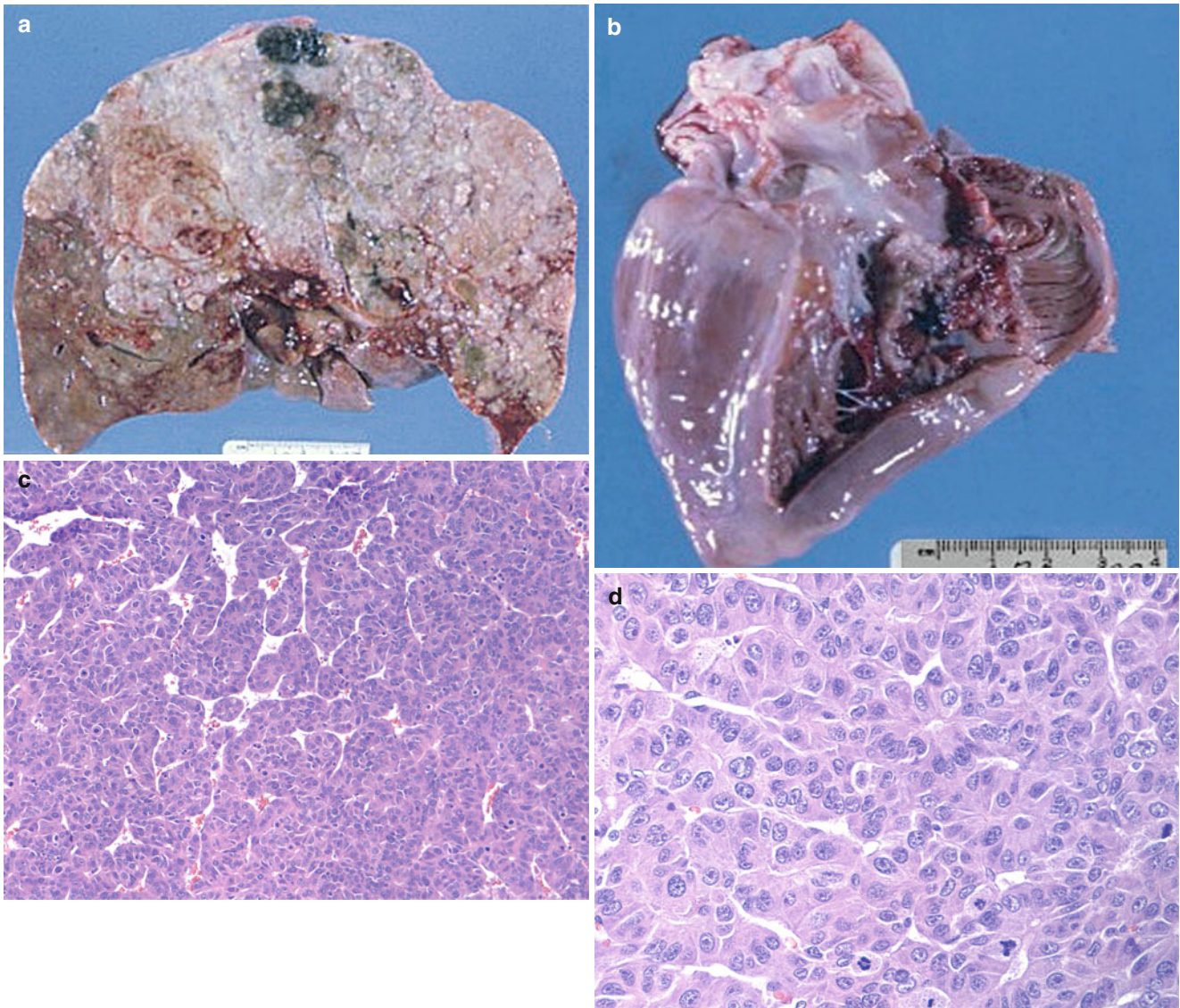


Fig. 12.16 Hepatocellular carcinoma. Six-year-old girl with cirrhosis and hepatocellular carcinoma. **(a)** Almost the entire fibrotic liver is replaced by multiple grayish-white tumor nodules accompanied by hemorrhage and necrosis. **(b)** An incision through the posterior wall of the right ventricle reveals grayish-white tumor nodules distributed

along the edge of the tricuspid valve and within the cardiac chamber. **(c)** The tumor displays a broad trabecular and acinar pattern. **(d)** Considerable nuclear pleomorphism, prominent nucleoli, and giant cells are characteristic of hepatocellular carcinoma (Reprinted from Isaacs [2]. © Springer-Verlag, 2002)

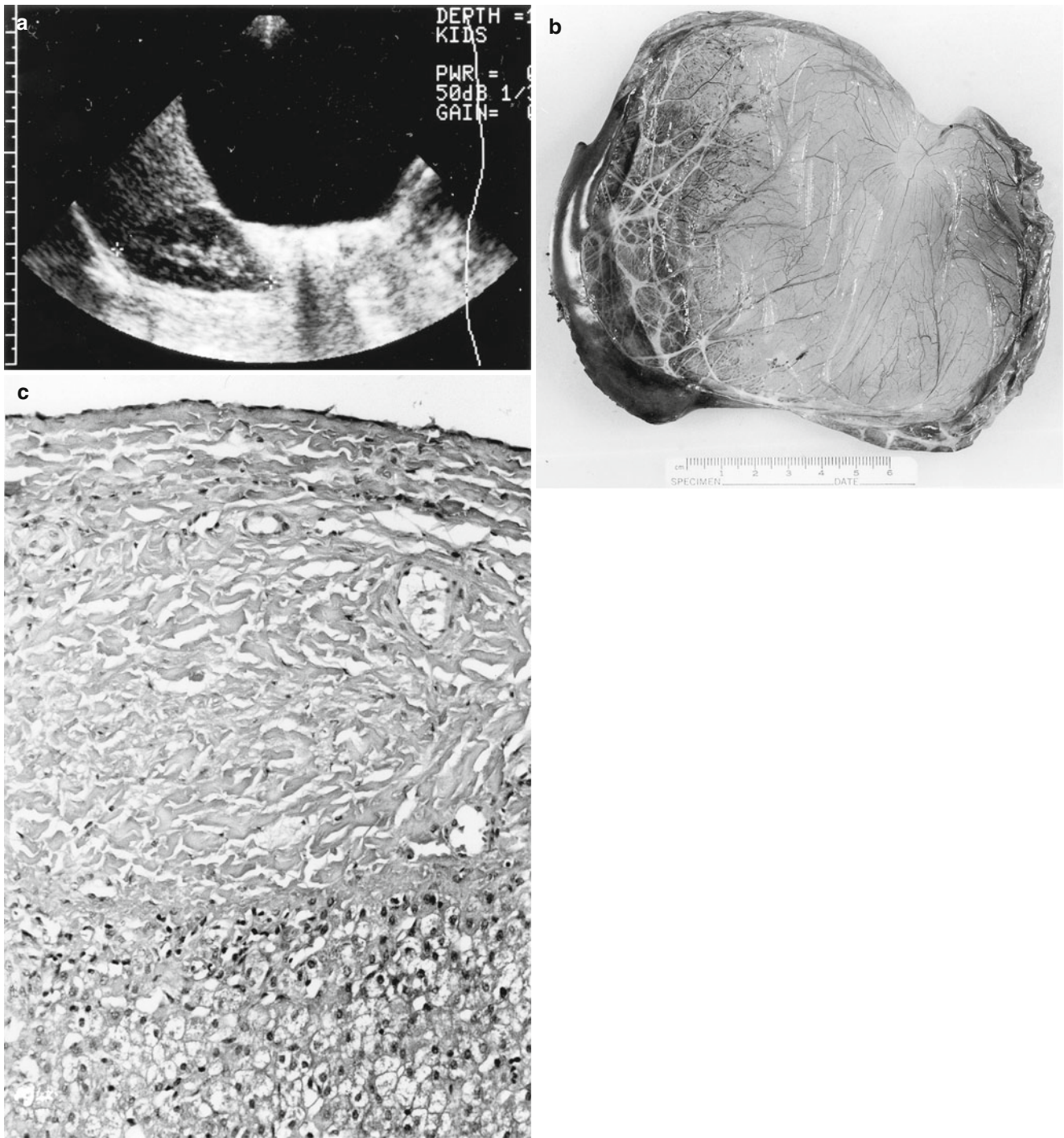


Fig. 12.17 Unilocular cyst of the liver. Eleven-month-old female with a history of progressive abdominal distension. (a) Sonogram reveals a cystic mass occupying the abdominal cavity without a definite site of origin. (b) The hepatic cyst, 1.1 kg, 18 cm in diameter, has a smooth,

glistening lining. (c) The cyst is lined by both cuboidal and flattened squamous epithelium situated on a thick layer of fibrous connective tissue. The underlying liver parenchyma is unremarkable (Reprinted from Isaacs [16]. © WB Saunders 1997)

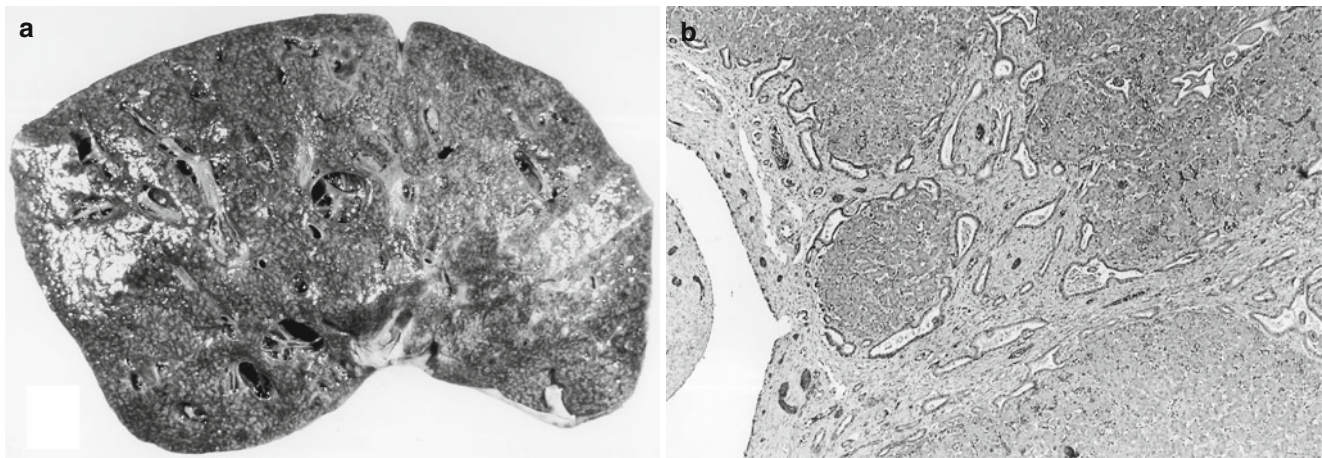


Fig. 12.18 Infantile polycystic disease of the kidneys and liver (autosomal recessive). The patient and his cystic kidneys are pictured in Fig. 10.3a. (a) The gross appearance of the liver with multiple cysts. (b)

Microscopic examination reveals angulated branching cystically dilated bile ducts and portal fibrosis (Reprinted from Isaacs [16]. © WB Saunders 1997)

References

- Isaacs H Jr (1997) Tumors. In: Gilbert-Barness E (ed) *Potter's pathology of the fetus and infant*, vol 2., pp 1242–1339
- Isaacs H Jr (2002) Liver tumors. In: *Tumors of the fetus and infant: an atlas*. Springer, New York, pp 303–336
- Bader JL, Miller RW (1979) Cancer incidence and mortality in the first year of life. *Am J Dis Child* 133:157–159
- Dehner LP (1978) Hepatic tumors in the pediatric age group: a distinctive clinical pathologic spectrum. *Perspect Pediatr Pathol* 4:217–268
- Dehner LP (1981) Neoplasms of the fetus and neonate. In: Naeye RL, Kissane JM, Kaufman N (eds) *Perinatal diseases*. International Academy of Pathology, Monograph number 22. Williams and Wilkins, Baltimore, p 286
- Weinberg AG, Finegold MJ (1986) Primary hepatic tumors in childhood. In: Finegold M (ed) *Pathology of neoplasia in children and adolescents*, vol 18, Major problems in pathology. WB Saunders Co, Philadelphia
- Isaacs H Jr (2007) Fetal and neonatal hepatic tumors. *J Pediatr Surg* 42:1797–1803
- von Schweinitz D (2003) Neonatal liver tumours. *Semin Neonatol* 8:403–410
- Isaacs H Jr (1985) Perinatal (congenital and neonatal) neoplasms: a report of 110 cases. *Pediatr Pathol* 3:165–216
- Isaacs H Jr (2007) Tumors. In: Gilbert-Barness E (ed) *Potter's pathology of the fetus, infant and child*, vol 2, 2nd edn. Mosby-Elsevier, Philadelphia, pp 1677–1708
- Stocker JT (1994) Hepatoblastoma. *Semin Diagn Pathol* 11:136–143
- Lack EE, Neave C, Vawter GF (1982) Hepatoblastoma: a clinical and pathological study of 54 cases. *Am J Surg Pathol* 6:693–705
- Ehren H, Mahour GH, Isaacs H Jr (1983) Benign liver tumors in infancy and childhood: report of 48 cases. *Am J Surg* 145:325
- Stanley P, Geer GD, Miller JH et al (1989) Infantile hepatic hemangiomas: clinical features, radiologic investigations, and treatment of 20 patients. *Cancer* 64:936–949
- Selby DM, Stocker JT, Waclawiw MA et al (1994) Infantile hemangioendothelioma of the liver. *Hepatology* 20:39–45
- Isaacs H Jr (1997) *Tumors of the fetus and newborn*. W.B. Saunders, Philadelphia
- Dreyfus M, Baldauf JJ, Dadoun K et al (1996) Prenatal diagnosis of hepatic hemangioma. *Fetal Diagn Ther* 11:57–60
- Albano G, Pugliese A, Stabile M et al (1998) Hydrops foetalis caused by hepatic haemangioma. *Acta Paediatr* 87:1307–1309
- Shturman-Ellstein R, Greco MA, Myrie C, Goldman EK (1978) Hydrops fetalis, hydramnios and hepatic vascular malformation associated with cutaneous hemangioma and chorangioma. *Acta Paediatr Scand* 67:239–243
- Petrovic O, Haller H, Rukavina B et al (1992) Prenatal diagnosis of a large liver cavernous hemangioma associated with polyhydramnios. *Prenat Diagn* 12:70 (letter)
- Noronha R, Gonzalez-Crussi F (1984) Hepatic angiosarcoma in a child. *Am J Surg Pathol* 8:863–871
- Samuel M, Spitz L (1995) Infantile hepatic hemangioendothelioma: the role of surgery. *J Pediatr Surg* 30:1425–1429
- Stocker JT, Ishak KG (1983) Mesenchymal hamartoma of the liver: report of 30 cases and review of the literature. *Pediatr Pathol* 1:245–267
- DeMaioribus CA, Lally KP, Sim K et al (1990) Mesenchymal hamartoma: a 35-year review. *Arch Surg* 125:598–600
- Dickinson JE, Knowles S, Phillips JM (1999) Prenatal diagnosis of hepatic mesenchymal hamartoma. *Prenat Diagn* 19:81–84
- Hirata GI, Matsunaga MI, Medearis AL et al (1990) Ultrasonographic diagnosis of a fetal abdominal mass: a case of a mesenchymal liver hamartoma and a review of the literature. *Prenat Diagn* 10:507–512
- Bessho T, Kubota K, Komori S et al (1996) Prenatally detected hepatic hamartoma: another cause of non-immune hydrops. *Prenat Diagn* 16:337–341
- Tovbin J, Segal M, Tavori I et al (1997) Hepatic mesenchymal hamartoma: a pediatric tumor that may be diagnosed prenatally. *Ultrasound Obstet Gynecol* 10:63–65
- Mascarello JT, Krous HF (1992) Second report of a translocation involving 19q13.4 in a mesenchymal hamartoma of the liver. *Cancer Genet Cytogenet* 58:141–142
- de Chadarevian JP, Pawel BR, Faerber EN et al (1994) Undifferentiated (embryonal) sarcoma arising in conjunction with mesenchymal hamartoma of the liver. *Mod Pathol* 7:490–493
- Bove KE, Blough RI, Soukup S (1998) Third report of t(19q)(13.4) in mesenchymal hamartoma of the liver with comments on link to embryonal sarcoma. *Pediatr Dev Pathol* 1:438–442
- Lenington WJ, Gray GF Jr, Page DL (1993) Mesenchymal hamartoma of liver: a regional ischemic lesion of a sequestered lobe. *Am J Dis Child* 147:193–196

33. Gonzalez-Crussi F, Upton MP, Mauer HS (1982) Hepatoblastoma: attempt at characterization of histologic subtypes. *Am J Surg Pathol* 6:599–612
34. Herzog CE, Andrassy RJ, Eftekhari F (2000) Childhood cancers: hepatoblastoma. *Oncologist* 5:445–453
35. Kazzi NJ, Chang C-H, Roberts EC et al (1989) Fetal hepatoblastoma presenting as non-immune hydrops. *Am J Perinatol* 6:278–280
36. Lee SC, Chung JW, Kim KH et al (1999) Successful transumbilical embolization of congenitally ruptured hepatoblastoma. *J Pediatr Surg* 34:1851–1852
37. Robinson HBJR, Bolande RP (1985) Fetal hepatoblastoma with placental metastases. *Pediatr Pathol* 4:163–167
38. Doss BJ, Vicari J, Jacques SM et al (1998) Placental involvement in congenital hepatoblastoma. *Pediatr Dev Pathol* 1:538–542
39. Hartley AL, Birch JM, Kelsey AM et al (1990) Epidemiological and familial aspects of hepatoblastoma. *Med Pediatr Oncol* 18:103–109
40. Orozco-Florian R, McBride JA, Favara BE et al (1991) Congenital hepatoblastoma and beckwith-wiedemann syndrome: a case study including DNA ploidy profiles tumor and adrenal cytomegaly. *Pediatr Pathol* 11:131–142
41. Sotelo-Avila C, Gooch WM (1976) Neoplasms associated with the Beckwith-Wiedemann syndrome. In: Rosenberg HS, Bolande RP (eds) *Perspectives in pediatric pathology, vol II*. Year Book Medical Publishers, Chicago, pp 255–272
42. Giardiello FM, Offerhaus GJA, Krush AJ et al (1991) Risk of hepatoblastoma in familial adenomatous polyposis. *J Pediatr* 119:766–768
43. Ikeda H, Hachitanda Y, Tanimura M et al (1998) Development of unfavorable hepatoblastoma in children of very low birth weight: results of a surgical and pathologic review. *Cancer* 82:1789–1796
44. Conran RM, Hitchcock CL, Waclawiw MA et al (1992) Hepatoblastoma: the prognostic significance of histologic type. *Pediatr Pathol* 12:167–183
45. Horie A, Kotoo Y, Hayashi I (1979) Ultrastructural comparison of hepatoblastoma and hepatocellular carcinoma. *Cancer* 44:2184–2193
46. Van Eyken P, Sciot R, Callea F et al (1990) A cytokeratin immunohisto-chemical study of hepatoblastoma. *Hum Pathol* 21:302–308
47. Fasano M, Theise ND, Nalesnik M et al (1998) Immunohistochemical evaluation of hepatoblastomas with use of hepatocyte-specific marker, hepatocyte paraffin 1, and the polyclonal anti-carcinoembryonic antigen. *Mod Pathol* 11:934–938
48. Gonzalez-Crussi F (1991) Case 1 undifferentiated small cell (“anaplastic”) hepatoblastoma. *Pediatr Pathol* 11:363
49. Hansen K, Bagtas J, Mark HF et al (1992) Undifferentiated small cell hepatoblastoma with a unique chromosomal translocation: a case report. *Pediatr Pathol* 12:457–462
50. Manivel C, Wick MR, Abenzo P et al (1986) Teratoid hepatoblastoma: the nosologic dilemma of solid embryonic neoplasms of childhood. *Cancer* 57:2168–2174
51. Cross SS, Variend S (1992) Combined hepatoblastoma and yolk sac tumor of the liver. *Cancer* 69:1323–1326
52. Meyers RL, Rowland JR, Krailo M et al (2009) Predictive power of pretreatment prognostic factors in children with hepatoblastoma: a report from the Children’s Oncology Group. *Pediatr Blood Cancer* 53:1016–1022
53. Stocker JT, Ishak KG (1978) Undifferentiated (embryonal) sarcoma of the liver. *Cancer* 42:336–348
54. Aoyama C, Hachitanda Y, Sato JK et al (1991) Undifferentiated (embryonal) sarcoma of the liver: a tumor of uncertain histogenesis showing divergent differentiation. *Am J Surg Pathol* 15:615–624
55. Horowitz ME, Etcubanas E, Webber BL et al (1987) Hepatic undifferentiated (embryonal) sarcoma and rhabdomyosarcoma in children: results of therapy. *Cancer* 59:396–402
56. Hart WR (1975) Primary endodermal sinus (yolk sac) tumor of the liver: first reported case. *Cancer* 35:1453–1458
57. Atkinson JB, Foster CE III, Lally KP, Isaacs H, Siegel SE (1992) Primary endodermal sinus (yolk sac) tumor of the falciform ligament. *J Pediatr Surg* 27:105–107
58. Magnus KG, Millar AJ, Sinclair-Smith CC et al (1999) Intrahepatic fetus-in-fetu: a case report and review of the literature. *J Pediatr Surg* 34:1861–1864
59. Dehner LP, Parker ME, Franciosi RA et al (1979) Focal nodular hyperplasia and adenoma of the liver. A pediatric experience. *Am J Pediatr Hematol Oncol* 1:85–93
60. Lack EE, Ornvold K (1986) Focal nodular hyperplasia and hepatic adenoma: a review of eight cases in the pediatric age group. *J Surg Oncol* 33:129–135
61. Applegate KE, Ghei M, Perez-Atayde AR (1999) Prenatal detection of a solid liver adenoma. *Pediatr Radiol* 29:92–94
62. Stocker JT, Ishak KG (1981) Focal nodular hyperplasia of the liver: a study of 21 pediatric cases. *Cancer* 48:336–345
63. Moran CA, Mullick FG, Ishak KG (1991) Nodular regenerative hyperplasia of the liver in children. *Am J Surg Pathol* 15:449454
64. Scheimberg I, Cullinane C, Kelsey A et al (1996) Primary hepatic malignant tumor with rhabdoid features: a histological, immunocytochemical, and electron microscopic study of four cases and review of the literature. *Am J Surg Pathol* 20:1394–1400
65. Ohyama M, Ijiri R, Tanaka Y et al (2000) Congenital primitive epithelial tumor of the liver showing focal rhabdoid features, placental involvement and clinical features mimicking multifocal hemangioma or stage 4S neuroblastoma. *Hum Pathol* 31:259–263
66. Isaacs H (2010) Fetal and neonatal rhabdoid tumor. *J Pediatr Surg* 45:619–626
67. Siciliano M, De Candia E, Ballarin S et al (2000) Hepatocellular carcinoma complicating liver cirrhosis in type IIIa glycogen storage disease. *J Clin Gastroenterol* 31:80–82
68. Patterson K, Kapur SP, Chandra RS (1985) Hepatocellular carcinoma in a noncirrhotic infant after prolonged parenteral nutrition. *J Pediatr* 106:797–800
69. McGoldrick JP, Boston VE, Glasgow JF (1986) Hepatocellular carcinoma associated with congenital macronodular cirrhosis in a neonate. *J Pediatr Surg* 21:177–179
70. Jozwiak S, Pedich M, Rajszyz P et al (1992) Incidence of hepatic hamartomas in tuberous sclerosis. *Arch Dis Child* 67:1363–1365
71. Shek TW, Ng IOL, Chan KW (1993) Inflammatory pseudotumor of the liver: report of four cases and review of the literature. *Am J Surg Pathol* 17:231–238
72. Takano H, Sato Y, Kao SCS et al (1997) Enlarging liver cyst in Beckwith-Wiedemann syndrome. *Pediatr Radiol* 27:619–620

13.1 Introduction

The adrenal cortex is the source of several tumors and tumorlike conditions with unusual clinical manifestations in the fetus and infant [1–19] (Table 13.1). *Adrenocortical tumors (ACTs)* are uncommon in this age group and throughout childhood. Relatively few examples of adrenal cysts, cortical adenomas, and carcinomas have been described, some in association with the Beckwith-Wiedemann syndrome, hemihypertrophy, cancer family (Li-Fraumeni) syndrome, or with other tumors [5, 6, 10]. Some ACTs exhibit structural abnormalities involving *chromosome 11p15* and include loss of heterozygosity, paternal isodisomy, and overexpression of the gene for insulin-like growth factor II (IGF2) [20].

Overall the adrenal medulla is by far a more common site of origin of tumors in the young than is the cortex with an incidence ratio of 10 to 1 of *neuroblastoma* to ACTs in children [8]. *Adrenal cortical hyperplasia* associated with the adrenogenital and Cushing's syndromes occurs more frequently than true adrenal cortical neoplasms in the first year of life [1].

Table 13.1 Tumors and tumorlike conditions of the adrenal cortex in fetuses and infants

Adrenal cortical hyperplasia
Congenital adrenal hyperplasia (adrenogenital syndrome)
Adrenal cortical hyperplasia associated with Cushing's syndrome
Adrenocortical tumors
Adrenocortical adenoma
Adrenocortical carcinoma
Adrenocortical cytomegaly
Adrenal cyst
Adrenal enlargement due to hemorrhage
Adrenal enlargement due to infection or abscess

Reprinted from Isaacs [17]. © WB Saunders 1997

13.2 Incidence

ACTs are uncommon in the pediatric age group occurring in less than 15 children per year in the USA [1, 3, 21] and in less than three per year in England [11]. *Adrenal cortical carcinoma (ACC)* may produce signs and symptoms in the

first year of life. In both infants and children, females are affected in a ratio of greater than two to one [3, 9]. Over half the adrenocortical tumors are found in children less than 3 years of age.

13.3 Clinical Findings

An *abdominal mass*, *virilization*, and/or *Cushing's syndrome* are the main presenting findings in newborns and infants [1, 3, 9, 15, 16]. They depend largely upon the type of the hormone(s) secreted by the tumor [1] (Fig. 13.1). Virilization is found considerably more often than either Cushing's syndrome or an abdominal mass per se, but these conditions may be seen alone or in combination [4]. *Hyperaldosteronism* and *feminizing signs* described infrequently in older children and adults are even rarer in the young. Carcinomas outnumber adenomas at least three to one from birth to 3 years of age; they have essentially the same histological appearance as those seen in tumors of older children and adults [3, 9].

Neoplasms of the adrenal cortex share with *Wilms' tumor* and *hepatoblastoma* an increased association with both *hemihypertrophy* and the *Beckwith-Wiedemann syndrome* suggesting a common etiology probably of genetic origin [3, 8, 23]. Cytogenetic studies show that a locus exists on chromosome 11p15 (a deletion or loss of heterozygosity) which is found in both adrenal cortical carcinoma and the Beckwith-Wiedemann syndrome [11]. Loss of tumor suppressor genes at loci on the short arm of chromosome 11p may be involved

with the formation of other childhood malignancies such as hepatoblastoma, Wilms' tumor, and possibly rhabdomyosarcoma [11, 23]. Certain families with children who have ACTs exhibit an increased susceptibility to malignancy as part of the *SBLA* (sarcoma, breast and brain tumor, leukemia, laryngeal and lung cancer, and ACC) cancer family syndrome, which is probably transmitted in an autosomal dominant fashion [4, 10].

Congenital anomalies of the genitourinary tract, hamartomas, and brain tumors, that is, astrocytoma and medulloblastoma, are reported in patients particularly with virilizing cortical tumors [1, 22]. Those infants and children with hemihypertrophy and/or Beckwith-Wiedemann syndrome should be followed closely by physical examinations and imaging studies for at least every 6 months to facilitate early diagnosis of tumor formation.

Investigation of a patient suspected of having an adrenocortical tumor should include imaging studies of the abdomen and measurement of urinary steroids. A suprarenal mass with or without calcification displacing the kidney downward and laterally is a characteristic finding on imaging scans. Abdominal sonography and computerized tomography are recommended for determining tumor localization. If a tumor is discovered in the adrenal, imaging studies of the lungs is required to rule out metastases. Analysis of 24-h urine specimens for *17-ketosteroids*, namely, dehydroepiandrosterone (DHEA), and *17-hydroxysteroids* and demonstration of steroid production independent of pituitary control after dexamethazone suppression are required for diagnosis [1]. Steroid secretion is suppressed in patients with *congenital*

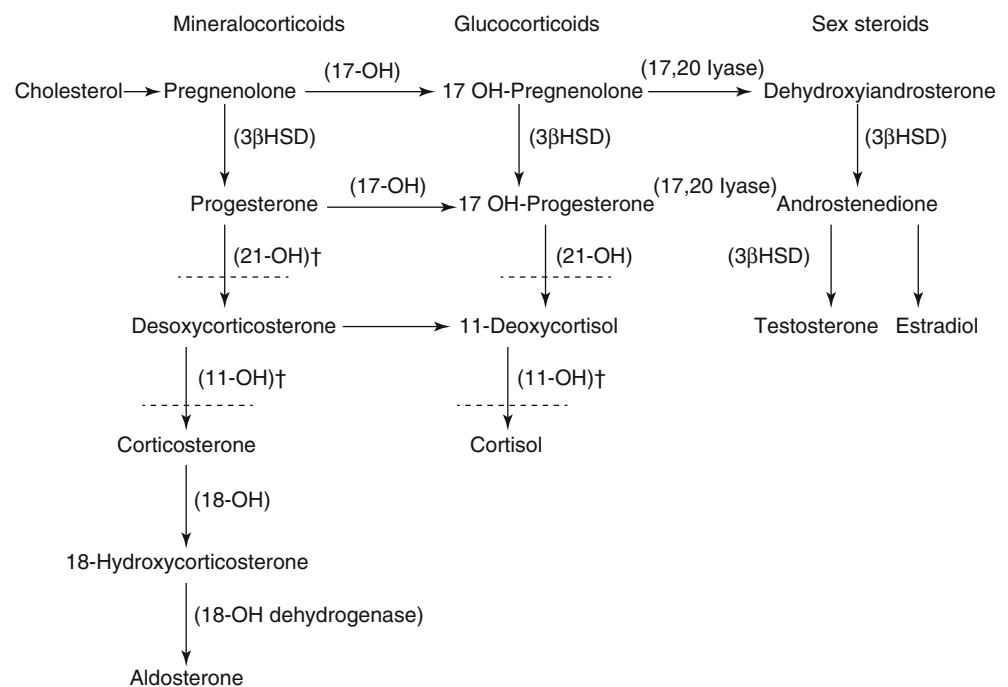


Fig. 13.1 Adrenocortical steroid biosynthetic pathways. *Dashed line* enzyme block, Enzymes: *3βHSD* 3β-hydroxysteroid dehydrogenase, *17βHSD* 17β-hydroxysteroid dehydrogenase, *17-OH* 17-hydroxylase, *11-OH* 11-hydroxylase, *18-OH* 18-hydroxylase, *21-OH* 21-hydroxylase, † Most common enzyme defects associated with the adrenogenital syndrome (Sources: Reprinted from New et al. [1]. With kind permission of © Elsevier-Saunders, 1990; Reprinted from Hughes [27]. With kind permission of © Endocrine Society, 1982; Reprinted from Isaacs [18]. © Springer Verlag, 2002)

adrenal hyperplasia (CAH) but not in those with a neoplasm. *Urinary 17-ketosteroids* are usually markedly elevated in patients with ACC and ACA. Ultimately the final diagnosis rests on microscopic examination of the tumor.

Most adrenal tumors are encapsulated even when malignant. Both adenomas and carcinomas have large cells with bizarre hyperchromatic nuclei. The histological distinction between a benign and malignant adrenal cortical tumor is not always clear, which makes predicting prognosis on the basis of histology alone difficult. Pathologists tend to disagree about distinctions between hyperplasia, adenomatous hyperplasia, and adenoma [16–18].

13.4 Adrenal Cortical Adenoma

An *adrenocortical adenoma (ACA)* may be responsible for *Cushing's syndrome with or without virilization* in infants and young children but nodular hyperplasia, ACC, and CAH are more common causes of this syndrome [1, 19] (Figs. 13.2, 13.3, and 13.4). There is a significant female predominance of about four to one in patients with ACA.

ACA is a single encapsulated mass usually surrounded by a thin fibrous capsule. The cut surface is smooth and bulging, varying in color from tannish-gray, tannish-yellow to orange brown. Cyst formations, hemorrhage, and necrosis are not seen except in some of the larger ones. Adjacent to the

adenoma, the atrophic adrenal cortex may be compressed into an almost paper-thin, orange-tan shell [15–18].

Microscopic examination reveals cords and clusters of round, oval to polygonal cells having the appearance of adrenal cortical cells surrounded by a prominent sinusoidal network (Figs. 13.2, 13.3, and 13.4). Two types of cells are present in ACAs from young patients with clinical signs and symptoms of Cushing's syndrome and virilization (Figs. 13.2d, 13.3d, and 13.4d). One is morphologically similar to the eosinophilic compact cells of the zona reticularis, observed commonly in patients with virilization. The other is a larger cell with a vacuolated spongy appearance due to increased lipid content comparable to cells of the zona fasciculata [9] (Fig. 13.2e). Not infrequently blending of the two types of cells is found. Moderate variation in cell size and focally giant cells with atypical nuclei may be present. Large areas of necrosis, anaplasia, and significant mitotic activity usually are not observed. *Capsular and vascular invasion*, two important criteria of malignancy, generally are absent, but the latter is sometimes difficult to evaluate particularly in adrenocortical and in other endocrine neoplasms because of the inherent intimate relationship between tumor cells and adjacent vascular channels [15–18].

The EM features of ACA, ACC, and hyperplasia associated with virilization are practically the same [17, 18, 24, 25]. Thus, EM is not a useful tool in distinguishing these conditions.

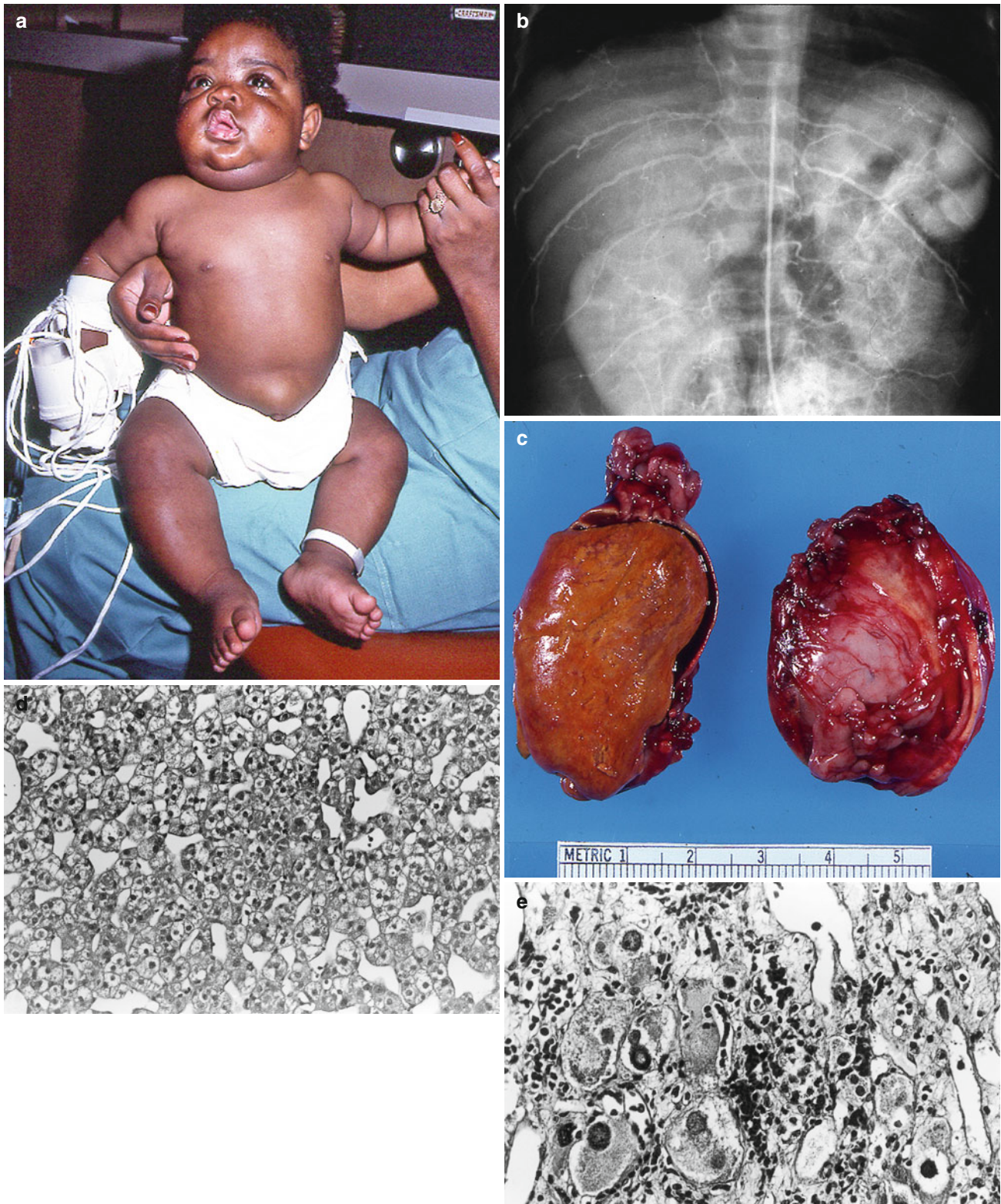


Fig. 13.2 Adrenocortical adenoma. Eight-month-old female with Cushing's syndrome (obesity, hypertension, acne) and a right adrenal mass. (a) Hemihypertrophy on the right side of the body and a protuberant umbilicus are present. (b) Arteriogram displays a right suprarenal mass and a large right kidney as compared to the left. (c) The adrenal is replaced by a 21-g, 5.5 × 3.5 cm, tumor with a bright orange-tan, smooth bulging cut surface. (d) Microscopic examination reveals nests and cords of clear vacuolated cells with regular nuclei and cells with

eosinophilic cytoplasm and more variable nuclei. Neither increased mitoses nor nuclear atypia is seen. (e) Focus of adrenal cytomegaly in the residual fetal cortex which normally involutes at age 3 months. The patient appears to have two conditions, hemihypertrophy and the Beckwith-Wiedemann syndrome, both of which are associated with a high incidence of adrenal and other tumors (Reprinted from Isaacs [17]. © WB Saunders 1997)

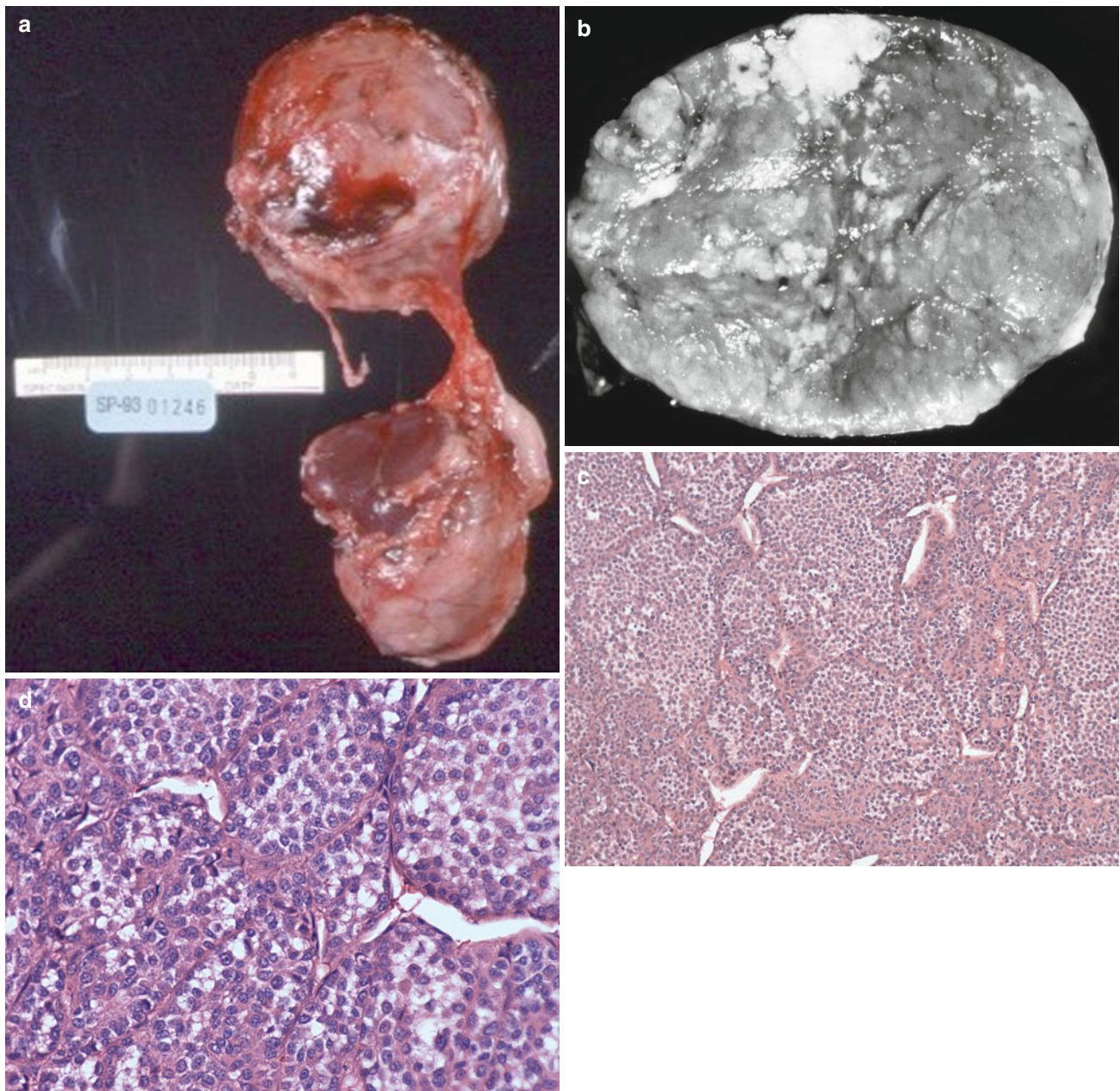
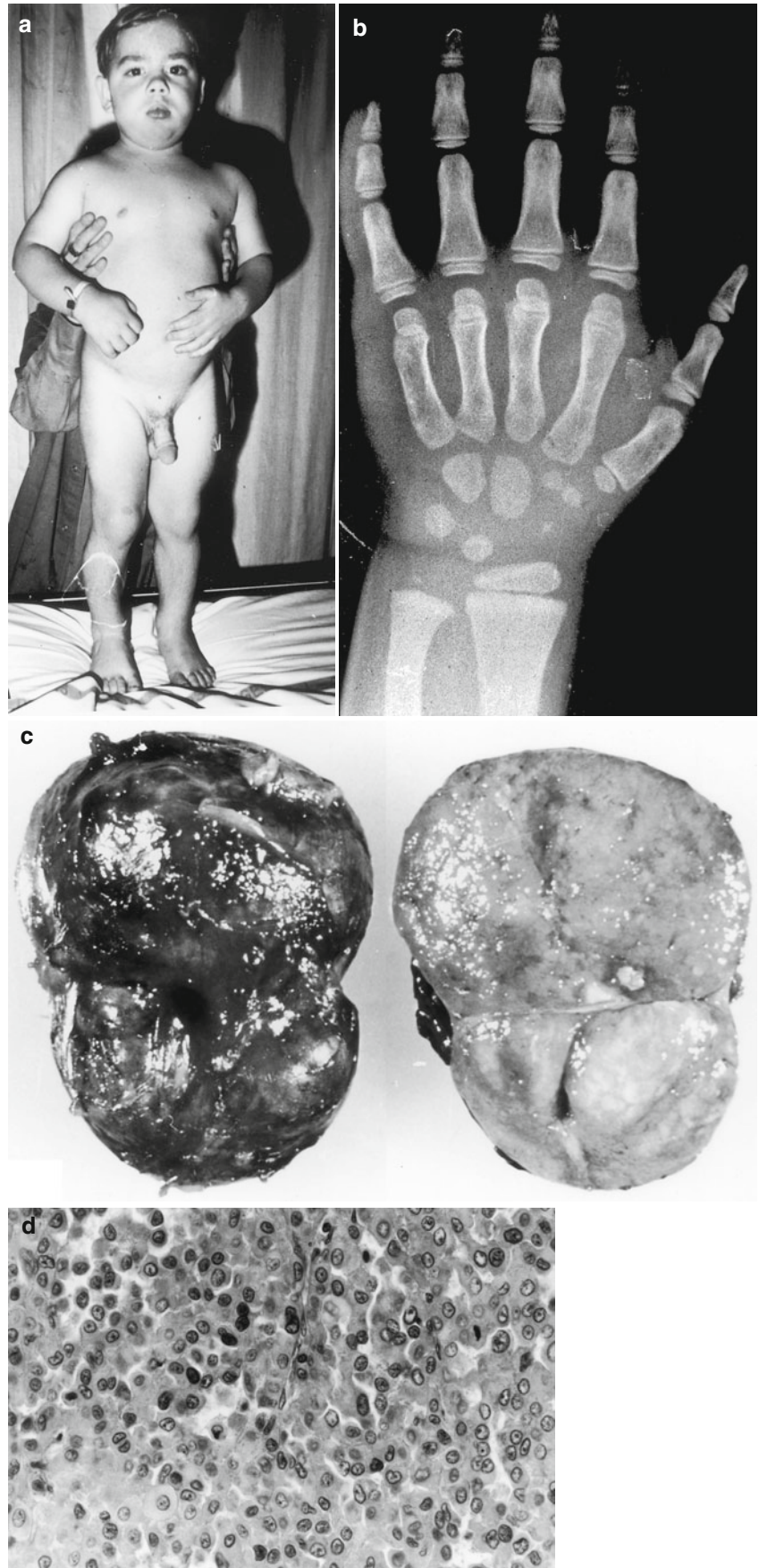


Fig. 13.3 Adrenocortical adenoma. Six-month-old female with Cushing's syndrome and an abdominal mass. **(a)** The left adrenal mass (*above*), 120 g and 6.5×6 cm, is attached to the left kidney (*below*) by fibrofatty adhesions. **(b)** The cut surface of the tumor is multilobulated, tan to tannish pink with small yellow-white areas of necrosis. **(c)** The tumor shows lobular and trabeculated growth patterns with a prominent vascular component. The cells are relatively uniform with round to oval

nuclei showing minimal pleomorphism. **(d)** Higher magnification with occasional enlarged or irregular nuclei. An average of one to two mitoses per ten high-power fields are present (Courtesy of Stephen G. Romansky, M.D., Department of Pathology, Long Beach Memorial Medical Center, Long Beach, CA; Reprinted from Isaacs [18]. © Springer-Verlag, 2002)

Fig. 13.4 Adrenocortical adenoma.

Two-year-old male with a masculinizing adrenal cortical tumor. **(a)** The patient with markedly enlarged genitalia, pubic and body hair, and facial acne. **(b)** X-ray of the left hand and wrist showing the advanced bone age of a 6-year-old child. **(c)** The tumor, 17.1 g and 4 × 3 cm, has a slightly roughened, brown capsular surface with yellow highlights (*left side of gross photograph*). The cut surface on the left is orange-yellow, bulging with small, flat yellow-white areas of necrosis. **(d)** The tumor forms cords and nests of cells resembling adrenocortical cells. There are two types of cells, one with regular, small, round occasionally vesicular nuclei and prominent pink cytoplasm and the other, larger round cells with abundant pale, slightly foamy cytoplasm and regular, round nuclei with prominent nucleoli. Minimal nuclear atypia and rare mitoses are noted (Reprinted from Isaacs [18]. © Springer-Verlag, 2002)



13.5 Adrenocortical Carcinoma

Adrenocortical carcinoma (ACC) is an uncommon neoplasm in children and is even rarer in infants [3] (Fig. 13.5). Its incidence is estimated at 0.2–0.4 % of all childhood malignancies [3, 4, 7]. Surprisingly enough ACC has been recorded more often than ACA in the newborn [7]. Two age peaks of carcinoma are found, one in infancy and the other in adolescence.

Female predominance is at least two to one. *An abdominal mass, signs and symptoms of Cushing's syndrome, and virilization are the presenting findings; most tumors are endocrinologically active, and virilization is found in over 60 % of infants and children* [3, 9]. Infrequently young patients are seen with *metastases* as the initial finding [7]. *Nonfunctioning ACCs* occur in the pediatric age group; some patients may show signs of metastatic disease at the time of diagnosis,

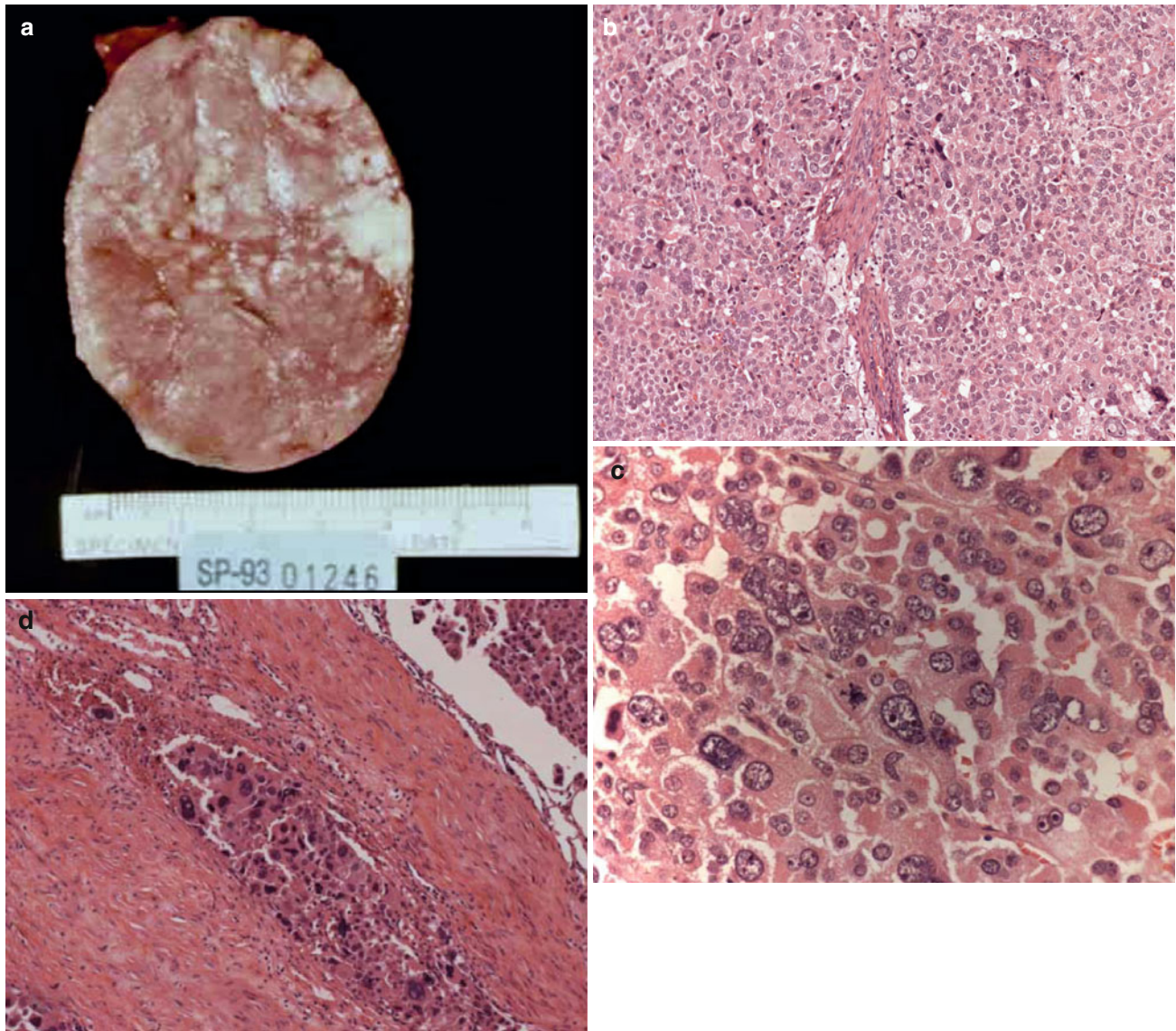


Fig. 13.5 Adrenocortical carcinoma. 8 month-old-male with a masculinizing adrenocortical tumor. The boy was large for his age. He was noted to have enlarged genitalia and pubic hair. Abdominal CT revealed a large left adrenal tumor. Testosterone levels were markedly elevated. (a) The tumor, 160 g and 9.1 × 6.5 cm, is composed of multiple nodules of various sizes and color. The largest nodule consists of firm tan tissue with focal areas of hemorrhage and calcification. There are nodules composed of bright yellow and brown hemorrhagic tissues. (b) Microscopically the tumor shows a diffuse arrangement of

pleomorphic cells. There are bizarre giant cells with abundant eosinophilic cytoplasm with one or more big, irregular nuclei. In addition cells having more uniform nuclei with dispersed chromatin and clear to vacuolated cytoplasm are present. (c) Higher magnification showing the various types of tumor cells in more detail. There 15 mitoses per 10 high power fields. (d) Capsular invasion is present at the top of the photomicrograph. In other areas not pictured the tumor extends to the line of resection without a capsule (Reprinted from Isaacs [18]. © Springer-Verlag, 2002)

for example, in the form of skin metastases resembling the “blueberry muffin baby,” and have a much worse prognosis [3, 7].

ACC may affect more than one child in a sibship and may occur in families with certain malignancies [10]. The various tumors described in family cancer syndromes are found excessively in patients as *second malignancies*, indicating a probable genetic influence. Hemihypertrophy, the Beckwith-Wiedemann syndrome, the cancer family (“SBLA”) syndrome, genitourinary malformations, and brain and liver tumors are found more often in patients with ACC than in the general population [4, 5]. Various *urinary tract malformations* occur also in patients with ACC [3]. Carcinomas range in size from 5 to 20 cm in diameter, and some weigh up to a kilogram [3, 9] (Fig. 13.5a). Most are encapsulated, but extension through the capsule into adjacent tissues or into the vena cava is seen especially in the larger ones. Cut surfaces are soft, lobular, and varying in color and consistency. Some tumors have a mushy light tan-gray appearance, while others are firmer, yellow-orange to tan. Prominent fibrous bands are observed in the latter and are one of the features of malignancy. Large areas of necrosis, hemorrhage, and cystic degeneration with or without calcification are typically seen [3, 8, 26]. The most frequent sites of metastases in decreasing order are the lung, liver, peritoneum, regional lymph nodes, kidney, and brain [1, 3, 19, 26].

ACC cells, like those of the adenoma, resemble those of the adrenal cortex. Typically they are arranged in nests and cords adjacent to dilated vascular structures. Some ACCs consist of cells with compact eosinophilic cytoplasm, while others have larger cells composed of clear or vacuolated cytoplasm due to abundant lipid droplets similar to those described above for the ACA (Fig. 13.5b–d). Mixtures of the two cell types are seen. Sometimes the tumor cells have the appearance of the peculiar giant cells of *adrenal cortical cytomegaly* found incidentally in stillborns and neonates with a variety of conditions. Adrenal cortical cytomegaly cells are one of the hallmarks of the Beckwith-Wiedemann syndrome. Bizarre-appearing tumor giant cells are observed also in both ACAs and ACCs. Generally poorly differentiated ACCs are unusual during the first year of life.

EM findings are similar to those of the ACA. Adrenocortical tumors, as a group, are immunoreactive with inhibin, vimentin, CK5, and focally with p53 and Ki-67 [26]. However, immunohistochemical studies do not reliably indicate malignancy [3, 14].

Histological criteria proposed for establishing the diagnosis of ACC include *capsular and vascular invasion, a diffuse growth pattern, broad fibrous bands, increased mitotic rate, single-cell necrosis, and extreme pleomorphism* [3, 9]. Non-histological factors such as *tumor weight over 200 g and weight loss in the patient* have been used also as other indicators of malignancy [13]. It is important to remember that small tumors have been known to metastasize, whereas some

Table 13.2 Staging criteria for pediatric adrenocortical tumors

Stage	Description
I	Complete surgical resection
	Tumor <100 g or <200 cm ⁴
	Normal hormone levels postoperatively
II	Microscopic residual tumor
	Tumor >100 g or >200 cm ⁴
	Tumor spillage during surgery
	Abnormal hormone levels postoperatively
III	Gross residual or inoperable primary tumor
IV	Metastatic tumor

Reprinted from Lack [35]. With kind permission of © Armed Forces of Pathology, 1997; Reprinted from Stewart et al. [36]. With kind permission of © Elsevier, 2004

larger ones have not. Obviously the ACT is considered malignant if it has metastasized [18]. The clinical staging of ACC is described in Table 13.2.

The prognosis in children is clearly more favorable when compared with adults [2, 18, 26]. Recent studies show that children younger than 5 years of age at diagnosis with a completely resectable ACT, which weighs less than 400 g, has less than 15 mitotic figures per 20 high-power microscopic fields, and minimal necrosis are findings associated with a favorable clinical outcome [2, 26].

Most pediatric ACTs behave in a benign fashion regardless of histology. The prognosis in children is clearly more favorable when compared with adults [2, 14, 26]. Pediatric ACTs generally behave in a benign fashion regardless of histology [2]. Infants with ACC have a much better prognosis than adolescents and adults, who have survival rates of about 53 and 17 %, respectively [14, 15, 26].

Local spread within the abdomen connotes a poor outcome. Recurrence of tumor or death due to metastases generally occurs within 2 years of diagnosis but some deaths have been reported as late as 5 years after the original diagnosis [19]. Staging criteria for pediatric adrenocortical tumors is described in Table 13.2.

13.6 Adrenal Cortical Hyperplasia

Hyperplasia of the adrenal cortex occurs in the fetus and infant. The excess hormone secretion associated with this condition results in recognizable clinical syndromes, the manifestations depending on the type(s) of steroid produced [1–3, 27–31] (Fig. 13.1). *The hormone excess produces one or more characteristic findings (or a combination): Cushing’s syndrome from hypersecretion of glucocorticoids, hypertension and hypokalemia from excess mineralocorticoids, or virilization or feminization from increased levels of androgens and estrogens, respectively* [1, 27–31, 35]. Inherited enzyme defects in steroid hormone biosynthesis are

responsible for most adrenocortical disorders in infants and children [1, 29]. *Congenital adrenal hyperplasia (adrenogenital syndrome)* and *Cushing's syndrome* are the two main endocrine diseases associated with adrenocortical hyperplasia, the former by far more common than the latter [1, 3, 27].

13.6.1 Congenital Adrenal Cortical Hyperplasia Associated with Adrenogenital Syndrome

Congenital adrenal hyperplasia (CAH) is an autosomal recessive disease caused by one of the five or more known enzymatic defects (blocks) in cortisol biosynthesis from cholesterol [1, 27–31] (Fig. 13.1). It is *the most frequent cause of ambiguous genitalia in the newborn* [29, 30] (Fig. 13.6). Neonatal screening studies indicate a frequency of 1 in 5,000 to 1 in 15,000 which is relatively common for an inborn error of metabolism [30]. Cortisol is synthesized principally in the zona fasciculata of the adrenal cortex. The secretion of cortisol is regulated by a negative feedback mechanism that involves this steroid and adrenocorticotropic hormone (ACTH). Low cortisol levels lead to increased ACTH production by the pituitary gland which in turn produces continued stimulation of the adrenal cortex. The end result of this adrenal-pituitary imbalance is bilateral adrenocortical hyperplasia and increased cortical steroid synthesis with excessive secretion of sex hormones and other steroids depending on the enzymatic block. If not treated promptly, some forms of CAH, particularly *the salt-losing forms, can be rapidly fatal in the neonate* [29–31].

Diagnosis of *21-hydroxylase deficiency* is established by detecting markedly elevated serum levels of 17-hydroxyprogesterone, the substrate for the 21-hydroxylase enzyme [29–31] (Fig. 3.1). In patients with *11-hydroxylase deficiency*, plasma deoxycortisol concentrations are markedly elevated, whereas 17-hydroxyprogesterone concentrations are not as high. *Deficiency of the 21-hydroxylase enzyme accounts for more than 90 % of cases of CAH* [1, 27]. Next in frequency is *11-hydroxylase deficiency*. The genetic defect of CAH is localized to the 6p chromosome for the 21-hydroxylase deficiency and the 8q chromosome for the 11-hydroxylase deficiency [1, 30, 31]. The 21-hydroxylase defect is closely linked to the HLA major histocompatibility complex situated on the short arm of chromosome 6 [27].

Cortisol is not synthesized effectively in patients with the 21-hydroxylase defect since 17-hydroxyprogesterone is not converted to 11-deoxycortisol, the immediate precursor of cortisol (Fig. 13.1). The lack of negative feedback then leads to high levels of ACTH and in turn the hypersecretion of steroid precursors proximal to the 21-hydroxylation step. These precursors are converted to androgens and, in two thirds of the patients with the 21-hydroxylase defect, the mineralocorticoid aldosterone. Androgens regulate the growth and

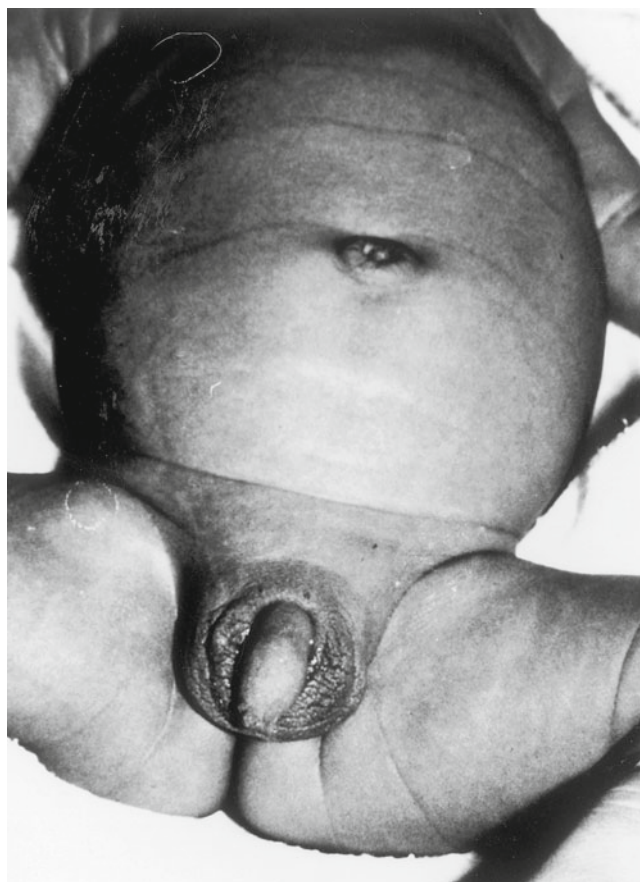


Fig. 13.6 Congenital adrenal hyperplasia (adrenogenital syndrome). Newborn female with this syndrome has striking clitoral enlargement, labial fusion (“scrotalization”), and hyperpigmentation. This endocrinopathy is one of the most common causes of ambiguous genitalia (Courtesy of Francine Kaufman, M.D., Division of Endocrinology and Metabolism, Children’s Hospital Los Angeles; From Isaacs [16, 18]. With permission)

development of both the male and female external genitalia of the fetus but not the internal female organs, that is, the uterus, fallopian tubes, and ovaries [1, 27, 30, 31].

13.6.2 Clinical Findings

Virilization is the end result of high levels of circulating androgens and is the most important physical finding in newborns with both the 11- and 21-hydroxylase enzyme defects. It is manifested in the female by clitoral hypertrophy (a phallus like clitoris), labial fusion, and sometimes scrotalization of the labia majora [1, 15, 17, 18, 27, 31] (Fig. 13.6). The internal female organs are essentially normal. The presence of “ambiguous genitalia” should alert the clinician of the possibility of the diagnosis of the adrenogenital syndrome, the discovery of which could be life-saving [1, 30]. Virilization in the newborn male is not as obvious as it is in the female and may not become apparent in the former until

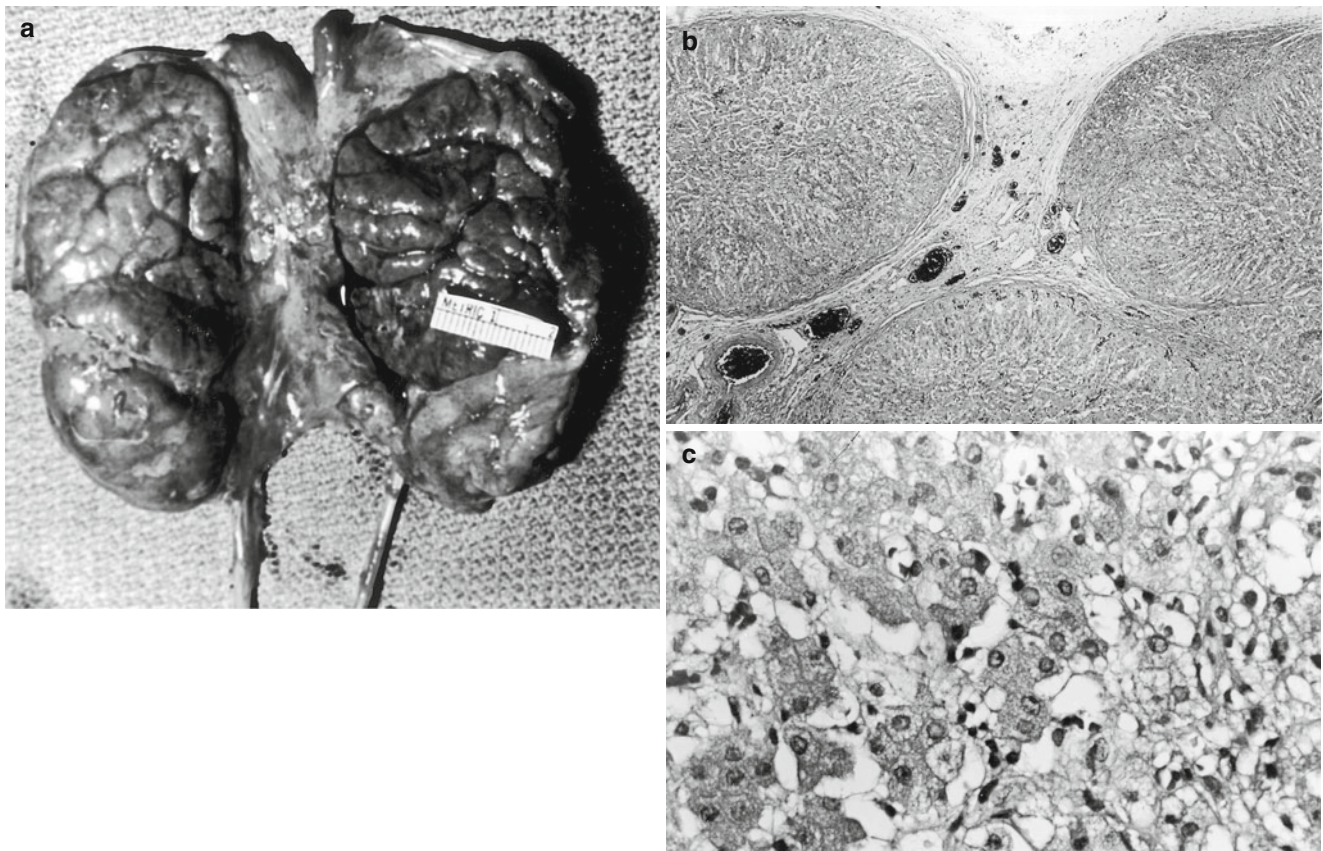


Fig. 13.7 Congenital adrenal hyperplasia. Three-year-old male with the salt-losing form of congenital adrenal hyperplasia due to 21-hydroxylase deficiency. (a) The kidneys are dwarfed by large convoluted adrenals (*top*), weighing 25 g together (normal combined weight for age is 5.2 g) and having a wrinkled, cerebriform appearance. (b) The cortex is thrown into numerous folds. The hyperplasia involves primar-

ily the zona fasciculata and zona reticularis. The zona glomerulosa is abnormally small in size. (c) The adrenal cortical cells are large, vacuolated, and filled with lipid. The darker staining cells in the left half of the field have eosinophilic staining cytoplasm (Reprinted from Isaacs [18]. © Springer-Verlag, 2002)

the baby is several months old. It should be kept in mind that virilization present at birth due to ACA or ACC can be mistaken for the adrenogenital syndrome [15, 16, 18].

In approximately one half to two thirds of patients with the classic 21-hydroxylase defect, aldosterone synthesis is impaired [30, 31]. This form of the metabolic defect is called the “salt wasting type” of CAH [29–31] (Fig. 13.7). “Simple virilizing disease” is the term used for infants and children without impaired aldosterone synthesis. Excessive salt loss from the renal tubules, secondary to low levels of aldosterone, leads to feeding difficulties, vomiting, hypovolemia, and shock. If left untreated, the salt-losing type results in death within the first weeks of life [1, 29, 30].

Sonography is helpful in making the diagnosis of CAH, particularly in newborns with ambiguous genitalia. The cerebriform pattern of the enlarged adrenals observed on sonography is characteristic of the disease [32–34]. The sonographic findings per se are not diagnostic of the particular enzyme deficiency in CAH, and the exact etiology should be pursued with laboratory investigation [18].

13.6.3 Pathology

The adrenal glands of patients with CAH have a striking, distinctive gross appearance [3, 17, 18, 35]. The adrenals are markedly enlarged weighing as much as 15 g or more than the normal expected weight, which is 3–10 g [3, 17, 18, 35]. Characteristically the cortex is thrown into numerous folds or convolutions giving the gland a wrinkled or cerebriform external surface that is even more evident on cross section (Fig. 13.7).

Microscopic examination reveals cortical hyperplasia, often nodular in configuration, with increased numbers of eosinophilic cortical cells extending out toward the cortical surface (Fig. 13.7). The cortical cells show a decreased amount of lipid as compared to normal cells [3, 16–18, 35]. By EM, the cells of the hyperplastic nodules closely resemble those of the zona reticularis [24, 25]. They show abundant smooth endoplasmic reticulum, spherical and elongated mitochondria with tubulovesicular cristae in addition to many lysosomes and lipofuscin granules. However, as

mentioned previously, EM is not helpful in distinguishing CAH from either ACA or ACC nor can it be used to determine whether a cortical lesion is functioning or not [24].

13.6.4 Adrenocortical Hyperplasia Associated with Cushing's Syndrome

Adrenal cortical hyperplasia (ACH) occurs also in infants who do not have a known enzymatic block in steroid metabolism. *Cushing's syndrome* develops when there is excessive cortisol production by either a neoplasm or hyperplasia of the adrenal cortex [1, 3, 27, 37, 38]. The syndrome should be distinguished from Cushing's disease, which results from excessive ACTH secretion by a basophilic adenoma of the anterior pituitary gland which leads to excessive production of cortisol by the adrenal cortex. Nevertheless, the clinical signs and symptoms of both the syndrome and disease are similar. For all practical purposes, Cushing's disease secondary to a pituitary tumor does not occur in the fetus and infant [38].

13.6.5 Clinical Findings

The presenting signs and symptoms of an infant with Cushing's syndrome due to either neoplasm or adrenal hyperplasia are variable. They may appear abruptly or gradually or they may be subtle or obvious [1, 37, 38]. In most studies, *obesity* is the most frequent presenting sign in the young [1]. Other clinical findings are "moon facies" with *plump cheeks*, *buffalo hump*, and *hypertension* as observed in older children and adults. Excessive *weight gain*, without normal growth, is characteristic of this condition in the infant [1]. *Virulism* is a common presenting sign. *Insulin-resistant diabetes* is found in all age groups although the pathogenesis is not well understood. The diabetes is cured usually following removal of the adrenal lesion. *Hypertension* accompanies the syndrome, and its pathogenesis also is unclear. The effects of high blood pressure may be serious and result in heart failure if not corrected.

13.6.6 Pathological Findings

The adrenal glands of infants with Cushing's syndrome associated with adrenal cortical nodular hyperplasia are usually but not always enlarged and show *numerous irregular, ill-defined nodularities*, which are seen both on the external and cut surfaces [17, 35, 37, 38]. Histologically the hyperplastic nodules range in size and involve mostly the zona fasciculata. They consist of active-appearing cortical cells varying in size and in degrees of lipid vacuolization. The intervening cortical tissue between the nodules tends to be atrophic. The nodules in the neonate may consist of fetal cortical cells.

Adrenals of infants with the *McCune-Albright syndrome* presenting with the Cushing's syndrome also appear enlarged and contain numerous hyperplastic nodules, 2–6 mm in diameter, composed of a uniform population of polygonal cells with a small central nucleus and abundant granular to eosinophilic cytoplasm. Neither mitoses nor cellular pleomorphism are present [37]. The McCune-Albright syndrome (fibrous dysplasia of bone, cafe-au-lait skin pigmentation, and sexual precocity) associated with Cushing's syndrome and adrenal nodular hyperplasia may become evident shortly after birth [17, 35, 37–39]. Large, asymmetric ovaries with luteinized follicular cysts, Leydig cell hyperplasia, vaginal bleeding, and breast enlargement are evidence of sexual precocity in these patients. Bone lesions of fibrous dysplasia, for example, osteoporosis, may appear as early as the neonatal period [17, 39]. *The McCune-Albright syndrome complicated by Cushing's syndrome may be responsible for a life-threatening neonatal illness or sudden, unexpected death* [17].

13.7 Adrenal Cortical Cytomegaly

Large, peculiar-appearing adrenal cortical cells were first described by Kampmeier in 1927 [40] and reported later in a detailed study by Craig and Landing, who also noted similar cells in the developing fetal cortex of stillborns and infants up to 2 months of age [41]. Adrenal cytomegaly, a term coined by Potter [15], is defined as the presence of large, bizarre-looking eosinophilic cells with huge nuclei distributed focally or diffusely within the fetal cortical zone [16–18, 40–44]. The cytomegalic cells are found only in the fetal cortex and are thought to arise from the large single cells noted early in the developing fetal cortex. They may occur singly or in large numbers as wedge-shaped clusters extending to the surface of the adrenal or as collections of cells distributed diffusely throughout the fetal cortex (Fig. 13.8).

An increased incidence of adrenal cytomegaly is noted in fetuses and newborns with a variety of conditions including erythroblastosis fetalis, maternal toxemia, multiple pregnancies, congenital heart malformations, hemihypertrophy, and particularly in those with the Beckwith-Weidemann syndrome [16–18, 41, 44]. The most characteristic and consistent histological finding in the adrenal glands in patients with the Beckwith-Weidemann syndrome is diffuse, bilateral cytomegaly of the fetal cortex [15, 17, 18]. Cytomegaly is described essentially in every patient with this syndrome where the adrenals are examined microscopically.

In addition, there is a significant association between adrenal cytomegaly and congenital malformations [17]. Cardiac anomalies as truncus arteriosus, atrial and ventricular septal defects, and various types of atresias are the most common ones mentioned [17, 18].

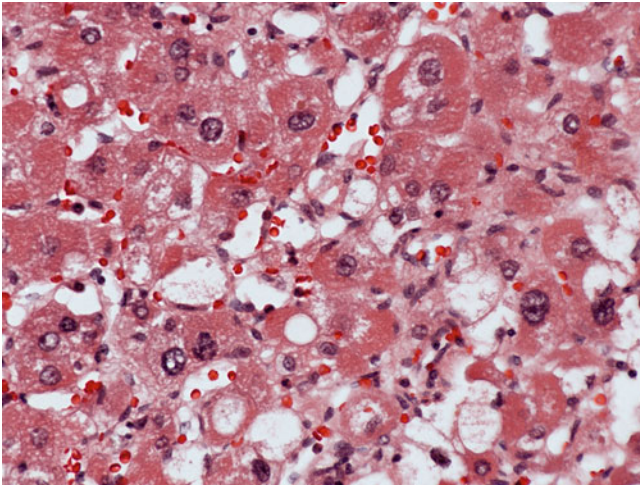


Fig. 13.8 Adrenal cortical cytomegaly. Incidental necropsy finding in a 4-day-old male with the Pena-Shokeir syndrome (dysmorphic facies, multiple joint contractures, and pulmonary hypoplasia). Large, peculiar-looking cells with huge nuclei are present within the developing fetal adrenal cortex. Focal infiltrates of lymphocytes are noted. Adrenal cortical cytomegaly is one of the important findings in the Beckwith-Wiedemann syndrome [16, 18] (Reprinted from Isaacs [17]. © WB Saunders 1997)

Typically the external appearance of the adrenals is usually normal, but sometimes they are enlarged. The presence of cytomegaly is an unexpected microscopic finding in post-mortem examinations performed on fetuses, stillborns, and newborns [16–18, 44]. Microscopically there is significant enlargement of the fetal zone, with many diffusely scattered cells with big nuclei (two to three times the normal size). The nuclei are darkly staining, and their shape may be irregular with pseudoinclusions and intranuclear vacuoles (Fig. 13.8). The cytoplasm stains uniformly eosinophilic similar to the rest of the fetal cortical cells and contains circumscribed masses of finely granular material. There is a peripheral rim of small vacuoles giving the cell a characteristic foamy appearance. Like the smaller cells of the fetal cortex, the cytomegalic cells have a polygonal outline. Mitoses are found rarely. The cytomegalic cells show degenerative and involutionary changes similar to those observed in the ordinary fetal cortical cells. The nuclear alterations consist of loss and fraying of the nuclear membrane with fragmentation, pyknosis, and karyorrhexis. Inflammatory infiltrates composed of neutrophils and large mononuclear cells are found in the rapidly involuting areas of the fetal cortex. The cause of adrenal cytomegaly is unknown [16–18].

13.8 Adrenal Cyst

Adrenal cysts are described in both infants and children but are more common in adults [15–17, 45–47]. Fewer than 20 cases are reported in the newborn [16, 18, 45].

They may present as an abdominal mass, thus mimicking a tumor, sometimes apparent at birth, or may be an incidental finding on imaging studies. Many are asymptomatic and spontaneously resolved but should be considered in the differential diagnosis of a cystic abdominal mass in a newborn or infant [18].

Most adrenal cysts in newborns result from *perinatal adrenal hemorrhage*, which is found in up to 1 % of post-mortem examinations performed on newborns [16]. Trauma associated with delivery is the most important cause. Sometimes they arise from a *hematoma within a tumor such as neuroblastoma in situ* [17, 18, 46, 47]. Organization of an *adrenal hemorrhage* may lead to a large cyst occasionally the size of an orange. On cross section, the cyst is uni- or multilocular and ranges from 2 to 11 cm in diameter.

Microscopically the cyst wall consists of fibrous connective tissue containing clusters of adrenal cortical cells. The wall lacks an epithelial lining, and sometimes focal calcification, if extensive enough, is present which can be seen on imaging studies. The cyst contents are variable and are composed of fibrin, necrotic debris, and erythrocytes. If the lesion is infected, inflammatory granulation tissue or exudate may be present. Adrenal cysts have been found in association with neuroblastoma and adrenal cortical cytomegaly in the newborn [16, 18, 45–47] (Fig. 6.16).

References

1. New MI, del Balzo P, Crawford C et al (1990) The adrenal cortex. In: Kaplan SA (ed) *Clinical pediatric endocrinology*. WB Saunders, Philadelphia, pp 181–234
2. Dehner LP (2003) Pediatric adrenocortical neoplasms: on the road to some clarity. *Am J Surg Pathol* 27:1005–1007
3. Lack EE, Mulvihill JJ, Travis WD et al (1992) Adrenal cortical neoplasms in the pediatric and adolescent age group: clinicopathological study of 30 cases with emphasis on epidemiological and prognostic factors. *Pathol Annu* 27(1):1–53
4. Hartley AL, Birch JM, Marsden HB et al (1987) Adrenal cortical tumors: epidemiological and familial aspects. *Arch Dis Child* 62:683–689
5. Sotelo-Avila C, Gonzalez-Crussi F, Fowler JW (1980) Complete and incomplete forms of Beckwith-Wiedemann syndrome. Their oncogenic potential. *J Pediatr* 96:47–50
6. Tank ES, Kay R (1980) Neoplasms associated with hemihypertrophy, Beckwith-Wiedemann syndrome and aniridia. *J Urol* 124:266–268
7. Saracco S, Abramowsky C et al (1988) Spontaneously regressing adrenal cortical carcinoma in a newborn: a case report with DNA ploidy analysis. *Cancer* 62:507–511
8. Dehner LP, Franciosi RA (1984) Adrenocortical neoplasia in the pediatric age group. A clinicopathologic study of seven cases. In: Humphrey FB, Grindley LP, Dehner LP et al (eds) *Adrenal and endocrine tumors in children*. Martinus Nijhoff Publishers, Boston, pp 291–302
9. Weatherby RP, Carney JA (1984) Pathologic features of childhood adrenocortical tumors. In: Humphrey FB, Grindley LP, Dehner LP et al (eds) *Adrenal and endocrine tumors in children*. Martinus Nijhoff Publishers, Boston, pp 217–248

10. Lynch HT, Katz DA, Bogard PJ et al (1985) The sarcoma, breast, cancer and adrenocortical carcinoma syndrome revisited. *Am J Dis Child* 139:134–136
11. Henry I, Grandjouan S, Coullin P et al (1989) Tumor specific loss of 11p15.5 alleles in del 11p13 Wilms' tumor and in familial adrenocortical carcinoma. *Proc Natl Acad Sci* 86:3247–3251
12. King DR, Lack EE (1979) Adrenal cortical carcinoma: a clinical and pathologic study of 49 cases. *Cancer* 44:239–244
13. Hawkins HP, Cagle PT (1992) Adrenal cortical neoplasms in children. *Am J Clin Pathol* 98:382–383
14. Medeiros LJ, Weiss LM (1992) New developments in the pathologic diagnosis of adrenal cortical neoplasms: a review. *Am J Clin Pathol* 97:73–83
15. Isaacs H Jr (1997) Tumors. In: Gilbert-Barness E (ed) *Potter's pathology of the fetus and infant*, vol 2. Mosby, St. Louis, pp 1242–1339
16. Isaacs H Jr (2007) Tumors. In: Gilbert-Barness E (ed) *Potter's pathology of the fetus, infant and child*, vol 2, 2nd edn. Mosby Elsevier, Philadelphia, pp 1677–1742
17. Isaacs H Jr (1997) Adrenocortical tumors. In: *Tumors of the fetus and newborn*, vol 35, Major problems in pathology. W.B. Saunders, Philadelphia, pp 298–316
18. Isaacs H Jr (2002) Adrenocortical tumors. In: *Tumors of the fetus and infant: an atlas*. Springer, New York, pp 337–352
19. Isaacs H Jr (2010) Fetal and newborn adrenocortical tumors. *Fetal Pediatr Pathol* 29:99–107
20. Wilkin F, Gagné N, Paquette J et al (2000) Pediatric adrenocortical tumors: molecular events leading to insulin-like growth factor II gene overexpression. *J Clin Endocrinol Metab* 85:2048–2056
21. Bader JL, Miller RW (1979) U.S. cancer incidence and mortality in the first year of life. *Am J Dis Child* 133:157
22. Bolande RP (1976) Neoplasia of early life and its relationships to teratogenesis. In: Rosenberg HS, Bolande RP (eds) *Perspectives in pediatric pathology*, vol 3. Year Book Medical Publishers, Chicago, pp 145–183
23. Koufos A, Hansen MF, Copeland NG et al (1985) Loss of heterozygosity in three embryonal tumors suggests a common pathogenetic mechanism. *Nature* 316:330–334
24. Ghadially FN (1985) *Diagnostic electron microscopy of tumours*, 2nd edn. Butterworths, London, pp 291–298
25. Hashida Y, Kenny FM, Yunis EJ (1970) Ultrastructure of the adrenal cortex in Cushing's disease in children. *Hum Pathol* 1:595–614
26. Wieneke JA, Thompson LD, Heffess CS (2003) Adrenal cortical neoplasms in the pediatric population: a clinicopathologic and immunophenotypic analysis of 83 patients. *Am J Surg Pathol* 27:867–881
27. Hughes IA (1982) Congenital and acquired disorders of the adrenal cortex. *Clin Endocrinol Metab* 11:89–125
28. Telander RL, Wolf SA, Simmons PS et al (1986) Endocrine disorders of the pancreas and adrenal cortex. *Mayo Clin Proc* 61:459–466
29. Mininberg DT, Levine LS, New MI (1982) Current concepts in congenital adrenal hyperplasia. *Pathol Annu* 17:179–195
30. White PC, New MI, Dupont B (1987) Congenital adrenal hyperplasia. *N Engl J Med* 316:1580–1586
31. Speiser PW, White PC (2003) Congenital adrenal hyperplasia. *N Engl J Med* 349:776–788
32. Avni EF, Rypens F, Smet MH et al (1993) Sonographic demonstration of congenital adrenal hyperplasia in the neonate: the cerebri-form pattern. *Pediatr Radiol* 23:88–90
33. Al-Alwan I, Navarro O, Daneman D et al (1999) Clinical utility of adrenal ultrasonography in the diagnosis of congenital adrenal hyperplasia. *J Pediatr* 135:71–75
34. Bentsen D, Schwartz DS, Carpenter TO (1997) Sonography of congenital adrenal hyperplasia due to partial deficiency of 3 β -hydroxysteroid dehydrogenase: a case report. *Pediatr Radiol* 27:594–595
35. Lack EE (1997) Tumors of the adrenal gland and extra-adrenal paraganglia. In: *Atlas of tumor pathology*, 3rd series, fascicle 19. Armed Forces of Pathology, Washington, D.C., pp 1–168
36. Stewart JN, Flageole H, Kavan P (2004) A surgical approach to adrenocortical tumors in children: the mainstay of treatment. *J Pediatr Surg* 39:759–763
37. Danon M, Robboy SJ, Kim S et al (1975) Cushing syndrome, sexual precocity, and polyostotic fibrous dysplasia (Albright syndrome) in infancy. *J Pediatr* 87:917–921
38. McArthur RG, Bahn RC, Hayles AB (1982) Primary adrenocortical nodular dysplasia as a cause of Cushing's syndrome in infants and children. *Mayo Clin Proc* 57:58–63
39. Kirk JMW, Brain CE, Carson DJ et al (1999) Cushing's Syndrome caused by nodular adrenal hyperplasia in children with McCune-Albright syndrome. *J Pediatr* 134:789–792
40. Kampmeier OF (1927) Giant epithelial cells of the human fetal adrenal. *Anat Rec* 37:95
41. Craig JM, Landing BH (1951) Anaplastic cells of fetal adrenal cortex. *Am J Clin Pathol* 21:940–949
42. Oppenheimer EH (1970) Adrenal cytomegaly: studies by light and electron microscopy. *Arch Pathol* 90:57–64
43. Aterman K, Kerényi N, Lee M (1972) Adrenal cytomegaly. *Virchows Arch* 355:105–122
44. Beckwith JB (1969) Macroglossia, omphalocele, adrenal cytomegaly, gigantism and hyperplastic visceromegaly. *Birth Defects Orig Artic Ser* 5:188
45. Zivković SM, Jancić-Zguricas M, Jokanović R et al (1983) Adrenal cysts in the newborn. *J Urol* 129:1031–1033
46. Tubergen DG, Heyn RM (1970) In situ neuroblastoma associated with an adrenal cyst. *J Pediatr* 76:451–453
47. Isaacs H Jr (2007) Fetal and neonatal neuroblastoma: retrospective review of 271 cases. *Fetal Pediatr Pathol* 26:177–184

14.1 Introduction

True neoplasms of the pancreas are unusual in the fetus and infant [1–6]. Lesions arising from islet cells, for example, *nesidioblastosis* and *adenomatous hyperplasia*, occur more often than exocrine tumors in this age group [1, 5–14]. The “embryonic” tumor of the pancreas, pancreatoblastoma,

a neoplasm unique to infants and children, is the subject of a few case reports [1, 5, 12–17]. Table 14.1 is a classification proposed for the various pancreatic tumors and tumorlike conditions found in the fetus and infant.

Table 14.1 Tumors and tumorlike conditions of the pancreas in fetuses and infants

Endocrine
Nesidioblastosis
Adenomatous hyperplasia
Islet cell adenoma
Exocrine
Cystadenoma
Ductal adenocarcinoma ^a
Acinar adenocarcinoma ^a
Pluripotential
Pancreatoblastoma
Mesenchymal
Hemangioma
Lymphangioma
Fibromatosis
Metastatic neoplasms
Neuroblastoma
Leukemia
Wilms tumor
Rhabdoid tumor
Yolk sac tumor
Miscellaneous
Extramedullary hematopoiesis
Lymphocytic infiltration

Reprinted from Isaacs [16]. © Springer-Verlag, 2002

^aUsually does not occur in the infant

14.2 Endocrine Tumors and Tumorlike Conditions of the Pancreas

14.2.1 Hypertrophy and Hyperplasia of the Islets of Langerhans

Pancreatic islets in the fetal and neonatal pancreas are normally more prominent than in the older child due to the relative underdevelopment of acinar tissue in early infancy [14]. Islet tissue is even more conspicuous in several newborn conditions where both islet hypertrophy and hyperplasia coexist.

14.2.2 Nesidioblastosis, Nesidioblastoma

In 1938 Laidlaw created the term “nesidioblastosis” to describe the neof ormation of islets of Langerhans from pancreatic duct epithelium [18] (Fig. 14.1). It is derived from the Greek words *nesidion* for “islet” and *blastos* for “germ.” He proposed also the term “nesidioblastoma” for an adenoma composed of islet cells. Yakovac in 1971 was one of the first to describe nesidioblastosis in a group of 12 infants with *intractable hypoglycemia* [19]. He demonstrated by histochemistry the presence of single or clusters of two to six islet cells separate from the islets of Langerhans located in acini and in small pancreatic ducts (Fig. 14.3).

Nesidioblastosis represents the normal endocrine cell development of the pancreas in the fetus and newborn infant and thus should not be considered a pathologic disorder per se in this age group (Figs. 14.1 and 14.2) [7, 8, 13, 16, 20, 22].

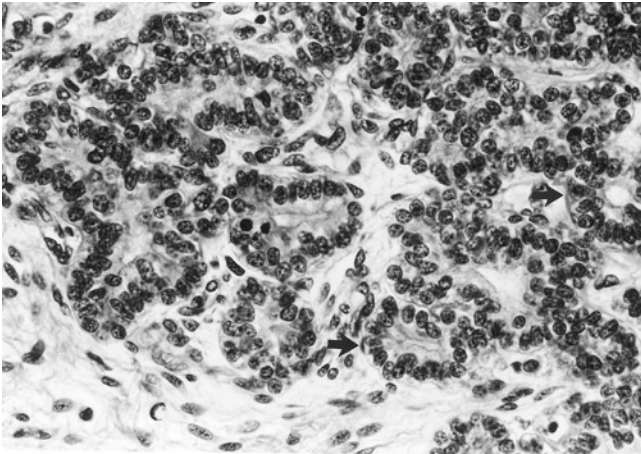


Fig. 14.1 Developing pancreas. Acini (*arrow*) are budding off from proliferating ducts. From an embryo of estimated 10–12 weeks gestation (Reprinted from Isaacs [15] © WB Saunders 1997)

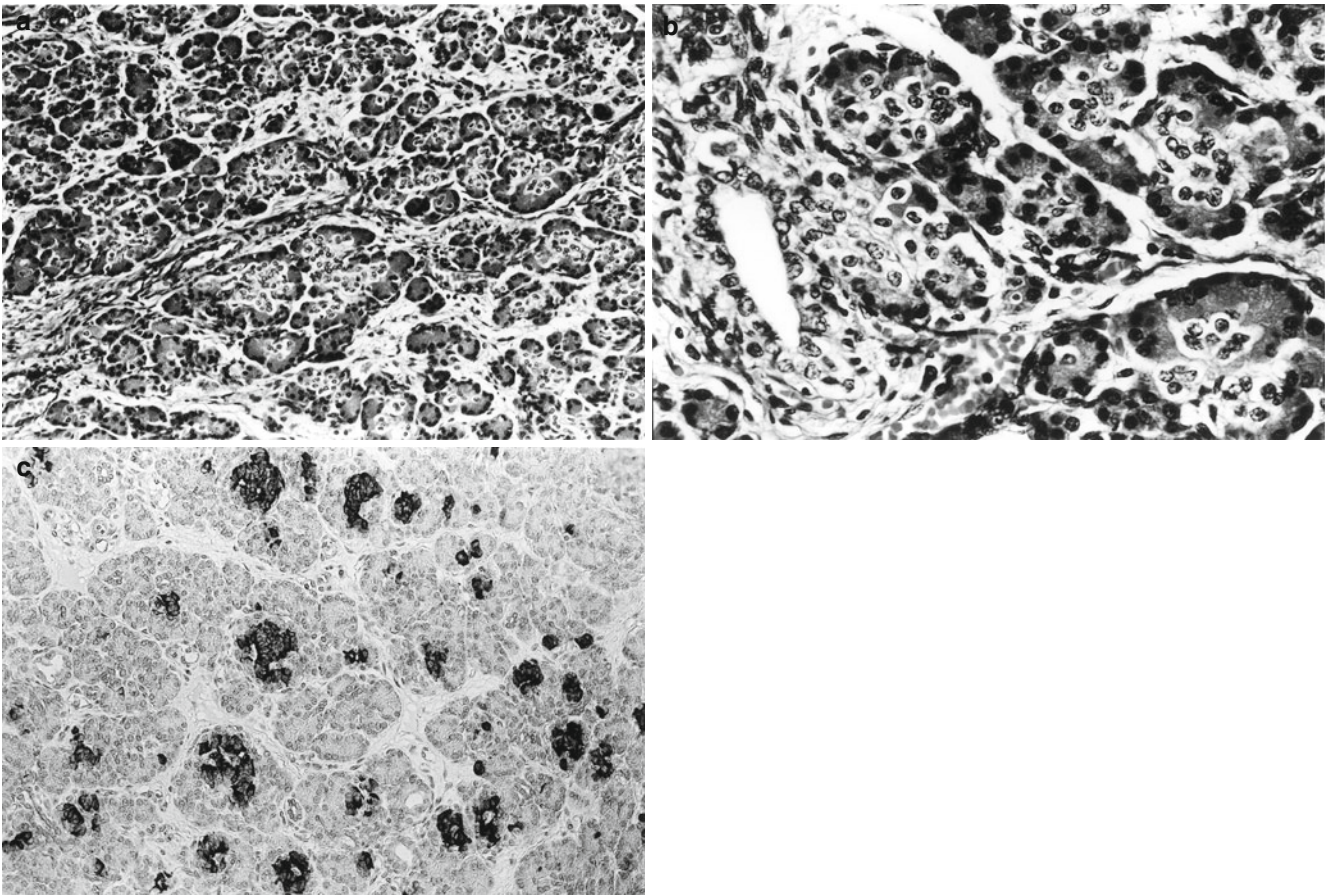


Fig. 14.2 Nesidioblastosis. Normal pancreas from a 650-g fetus. (a) Clusters of one or more islet cells separate from the islets of Langerhans are situated in acini and small pancreatic ducts. (b) Higher magnification.

(c) Insulin immunoperoxidase stain showing the presence of β cells outside of the islets (Reprinted from Isaacs [15]. © WB Saunders 1997)

14.2.3 Persistent Hyperinsulinemic Hypoglycemia of Infancy

Persistent hyperinsulinemic hypoglycemia of infancy is a term used to designate patients less than a year of age with hyperinsulinism and profound hypoglycemia, many of whom require pancreatic resection [7]. *Nesidioblastosis* is the name given to the histological findings associated with this condition where there are increased numbers of islet cells situated

throughout acinar tissue, separate from the islets of Langerhans. The islets of Langerhans are enlarged (islet cell hypertrophy) and irregular. Foci of islet cells are noted within ducts or ductile epithelium. Typically they show nuclear enlargement and pleomorphism [7] (Fig. 14.3).

Adenomatous hyperplasia of islet cells is the hallmark of the *Beckwith-Wiedemann syndrome* in the pancreas [5, 8, 20, 21] (Fig. 14.4) and pancreatoblastoma, the exocrine tumor associated with this syndrome [5, 24] (see below).

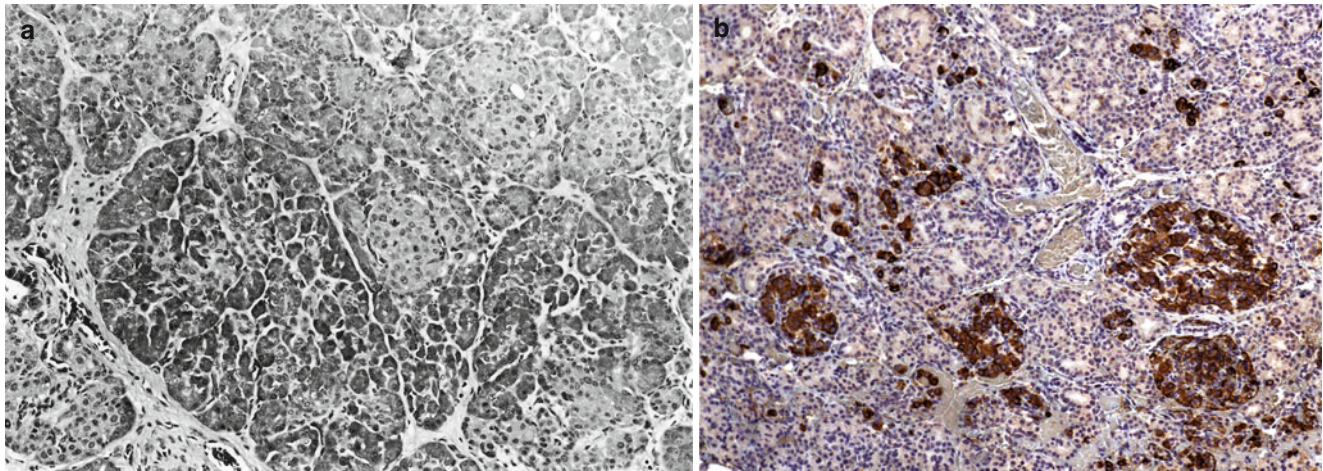


Fig. 14.3 Nesidioblastosis in a 1-month-old female with severe persistent hyperinsulinemic hypoglycemia. (a) Islets of Langerhans are irregularly distributed throughout the pancreas and vary considerably in size. Some within the interlobular septa are exceedingly large.

(b) Immunostaining for insulin reveals intense reactivity for islet cells not only within islets but also as individual cells and clusters within acini. Immunostains for glucagon somatostatin show intense immunoreactivity also (Reprinted from Isaacs [16]. © Springer-Verlag, 2002)

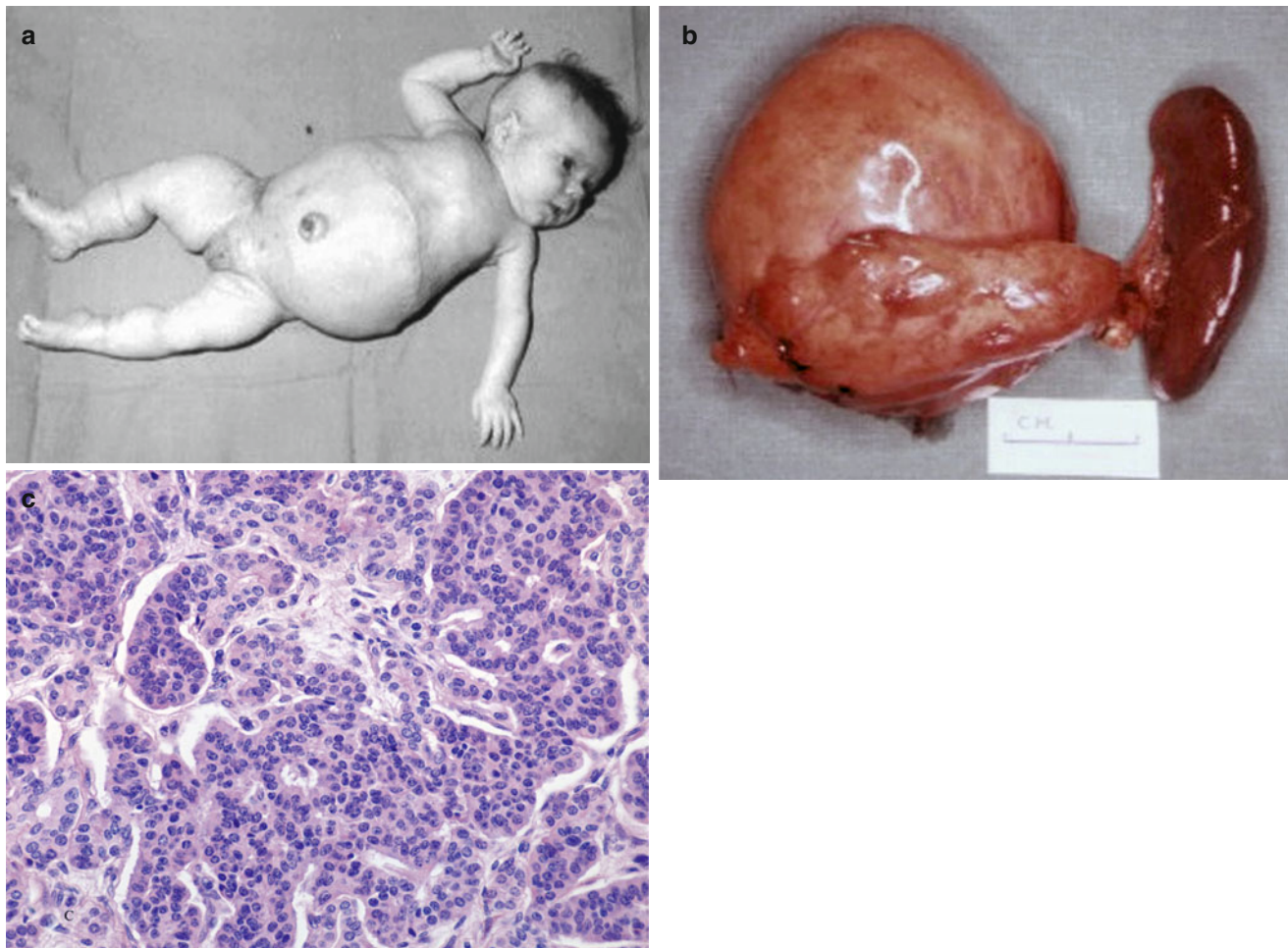


Fig. 14.4 Pancreas of the Beckwith-Wiedemann syndrome. This 3-week-old female had severe intractable hyperinsulinemic hypoglycemia, right hemihypertrophy, omphalocele, and abdominal visceromegaly. **(a)** Photograph of patient illustrating right sided hemihypertrophy. A protuberant abdomen due to abdominal organomegaly, and a prominent umbilicus. **(b)** The excised pancreas, 71 g (normal expected weight 4 g), and spleen are illustrated. **(c)** The pancreas reveals diffuse hyperplasia of the islet cells with marked reduction in acinar tissue. There is disorganized

proliferation of ductal and islet tissue, which is confluent and occupies a much larger area than the acinar pancreas. Additional findings in this patient associated with the Beckwith-Wiedemann syndrome were enlarged adrenal glands with cortical cytomegaly, renomegaly with nephroblastomatosis, and an umbilical myxoma (**(a, b)**) Courtesy of Jordan Weitzman, M.D., Department of Surgery, Children's Hospital Los Angeles; Reprinted from Roe et al. [21]. With kind permission of © American Academy of Pediatrics, 1973; Reprinted from Isaacs [16]. © Springer-Verlag, 2002)

14.2.4 Islet Cell Adenoma

Islet cell adenoma (nesidioblastoma, islet cell tumor, insulino- *ma)* is described in the newborn and infant [3, 16, 25, 26]. The lesion occurs more often in males than in females with a ratio of 2.7:1. The tumors cause persistent hypoglycemia and if not treated promptly may lead to seizures and permanent brain damage and even death. *Islet cell adenoma* consists of focal areas of excessive islet cell proliferation, usually greater than 40 % of a given low power field, pushing acinar elements aside or haphazardly incorporating them [3, 7, 22, 23, 25, 26] (Fig. 14.5).

Most islet cell adenomas are found in the head of the pancreas but some are located in the body and tail. Typically

they are small in size measuring between 0.1 and 1 cm in diameter. Occasionally the nodules are not identified or palpable on the external surface of the pancreas. In this situation, multiple cross sections of the pancreas are required to demonstrate the tumor(s). The tumor nodules have a cut surface varying from reddish-tan to white and gritty. Serially sectioning the paraffin blocks of the excised specimens may be required to find a tiny lesion [13, 16].

Microscopically the adenoma is composed of nests of islet cells separated from acinar tissue by a thin fibrous capsule with small ducts at the periphery of the nests (Fig. 14.5). Delicate fibrous connective tissue septae divide the tumor into small lobules. The term “nesidioblastoma” is given also to these lesions because of the intimate relationship of the

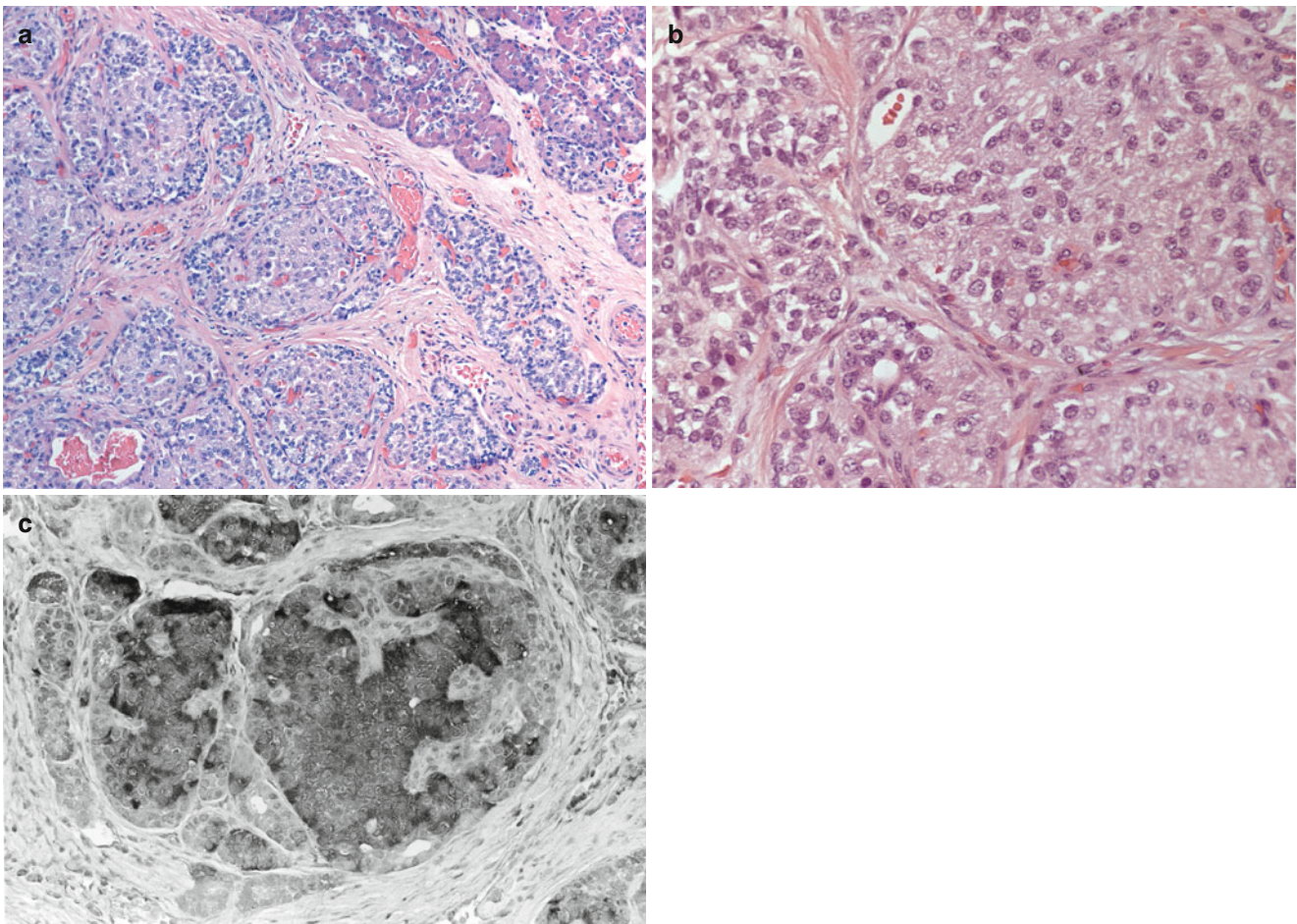


Fig. 14.5 Islet cell adenoma. Seventeen-day-old male with severe persistent hyperinsulinemic hypoglycemia. Within the head of the pancreas, there was a reddish-tan tumor nodule $2 \times 1 \times 1$ cm. **(a)** Nodules of endocrine cells are surrounded by ductules and bands of fibrosis shown in the left side of the photomicrograph. The tumor is separated from the rest of the pancreas by a fibrous capsule. **(b)** Higher magnification showing the nodular architecture in more detail. The endocrine cells are small, round, and regular, indistinguishable from islet tissue. **(c)**

Immunostain for insulin reveals intense staining of the tumor cells. However, immunostains for glucagon and somatostatin were nonreactive. Immunostain for insulin in the pancreas outside the tumor revealed intense staining of islet cells not only within islets but also in individual cells and nests within acini similar to that described in Fig. 14.2c. Nesidioblastosis and islet tumor may coexist in the same pancreas (Reprinted from Isaacs [16]. © Springer-Verlag, 2002)

islet cells to small pancreatic ducts [3]. Immunoperoxidase and EM studies indicate that the tumors are composed primarily of β -cells and ductal cells [3].

Nesidioblastosis may be present along with an islet cell adenoma [26]. Pancreatic function tests, that is, the oral glucose tolerance, diazoxide, somatostatin, and C-peptide suppression tests, do not distinguish hyperinsulinism caused by nesidioblastosis from that resulting from an adenoma [26].

Treatment of an islet cell adenoma requires prompt recognition and early excision of the tumor otherwise persistent hypoglycemia occurs resulting in brain damage. Treatment can be accomplished relatively easily if the lesion is readily palpable. However, if the tumor is small and deeply embedded in pancreatic tissue, this may give rise to surgical and other technical problems [23].

14.3 Exocrine Tumors and Tumorlike Conditions of the Pancreas

Neoplasms arising from the exocrine pancreas in patients less than 1 year of age are rare [1, 4, 6]. *Cystadenoma*, *pancreatoblastoma*, and *pancreatic ductal adenocarcinoma* are examples of some of the tumors reported [1, 4, 5, 9, 27].

14.3.1 Adenoma and Cystadenoma

Cystadenoma of the pancreas is a benign, well-circumscribed, multilocular cystic neoplasm often presenting as an abdominal mass [4, 9, 13, 15, 16, 27, 28]. To date a few histologically documented cystadenomas have been described in the first year of

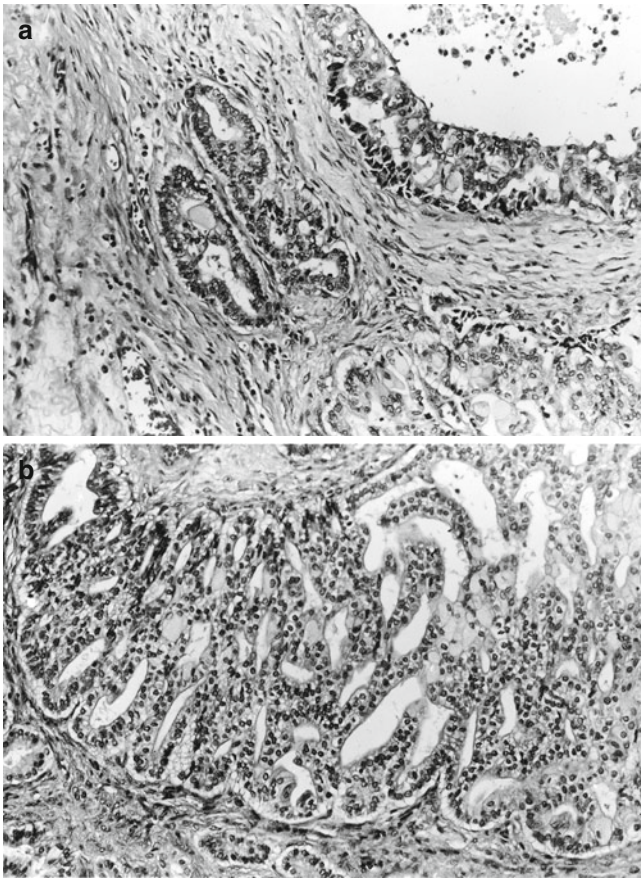


Fig. 14.6 Cystadenoma of the pancreas. 3-week-old female with a large cystic tumor, 440 g and 13 × 14 cm, arising from the body of the pancreas. (a) The wall of the cyst is lined by several rows of vacuolated epithelial cells. Acinar structures are present within the wall. (b) The tumor consists of cuboidal to columnar cells with regular round nuclei and vacuolated cytoplasm forming glandular and duct-like structures (Courtesy of Stephen G. Romansky, M.D., Department of Pathology, Long Beach Memorial Medical Center, Long Beach, CA; Reprinted from Isaacs [15]. © WB Saunders 1997)

life including a few neonates [15, 16, 27]. The tumor consists of a multiloculated mass with cysts containing serous fluid situated within the head and/or body of the pancreas. Histologically the cysts are lined by one or more layers of regular cuboidal to columnar epithelium separated by fibrous septae (Fig. 14.6).

14.3.2 Adenocarcinoma

Pancreatic adenocarcinoma seldom occurs in infants and children [1, 9, 29]. The patient presents with an abdominal mass with or without jaundice or abdominal pain [1]. The diagnosis is rarely if ever made preoperatively Rich [10]. Metastases may be present at the time of exploratory laparotomy and are found primarily within the liver and regional lymph nodes [6, 30].

Ductal adenocarcinoma is the leading tumor of the pancreas accounting for approximately 80 % of the malignancies [29]. It is primarily a tumor of adults. To my knowledge, the youngest patient with adenocarcinoma was a 7-month-old female who presented with a large tumor in the head of the pancreas that had metastasized to the liver, regional lymph nodes and pleura [30]. Some ductal adenocarcinomas are multifocal and located throughout the body of the pancreas. Larger tumors show foci of necrosis and cyst formation. Microscopically they display small, atypical duct-like structures surrounded by a dense fibrous stroma [1, 29].

14.3.3 Pancreatoblastoma

The term *pancreatoblastoma* (“*infantile carcinoma of the pancreas*”) was coined in 1977 by Horie et al. to describe a unique childhood tumor with distinct histological features having a better prognosis than adult pancreatic carcinomas [12]. In the first year of life, pancreatoblastoma occurs predominantly in males; over half are associated with the Beckwith-Wiedemann syndrome [2, 5, 17]. Usually the patients present with an abdominal mass [2].

Pancreatoblastomas are encapsulated, often cystic, and are situated mostly in the head but sometimes in the body of the pancreas [2, 13–16, 31–35] (Fig. 14.7). The specimens obtained from the neonates reported by Robey et al. and by Drut and Jones consisted of 6- and 12-cm diameter, respectively, cystic, necrotic tumors [5, 6] (Fig. 14.7). Histologically pancreatoblastomas display lobules of regular small cells with vacuolated cytoplasm and uniform round nuclei forming ductular canals and foci of squamous differentiation (Fig. 14.7). They show an organoid growth pattern consisting of nodules of squamous cells surrounded by an intermediate medullary zone of small round darkly staining cells and a peripheral rim of duct-like tubular structures [2, 5, 12, 31]. By immunohistochemistry, the tumors show *acinar, endocrine, and ductal differentiation*: all immunoreactive for pancreatic enzymes, endocrine markers, CEA, and keratin [2, 31]. α -1-antitrypsin is immunoreactive, suggesting an acinar cell component [2, 5, 31, 32]. Esterase and esterase are strongly positive in the squamous cell areas, which is helpful in establishing the diagnosis [32]. The tumor cells by EM contain zymogen-like granules, luminal microvilli, junctional complexes, and a lamellar arrangement of the granular endoplasmic reticulum similar to that observed in normal pancreatic acinar cells [2, 5, 12, 30, 32]. Endocrine differentiation has been observed only in a few specimens [2].

Pancreatic adenocarcinoma has an overall survival rate of only 1–4 % [6, 10, 12, 29, 33]. However, certain pediatric pancreatic malignancies such as pancreatoblastoma

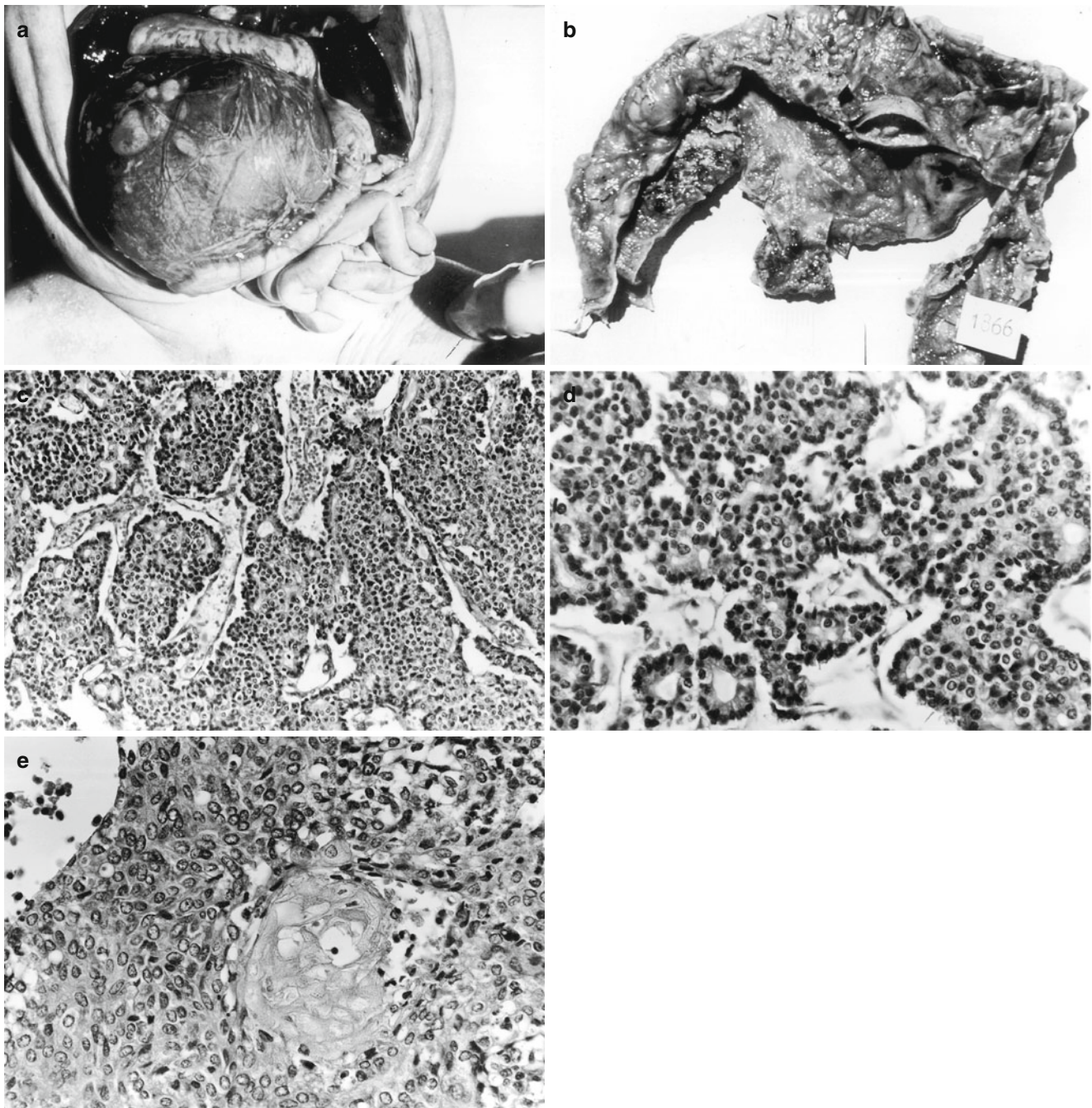


Fig. 14.7 Pancreatoblastoma. (a) In situ cystic pancreatoblastoma, 12 cm in diameter in a neonate with the Beckwith-Wiedemann syndrome. (b) The opened specimen reveals a large, cystic necrotic tumor. (c) Low magnification showing the lobular architecture separated by thin fibrovascular septa. The tumor is composed of uniform cells with

round, regular nuclei and vacuolated cytoplasm forming ductular canals. (d) Higher magnification showing ducts in more detail. (e) Foci of squamous differentiation are noted in some areas (Courtesy of Ricardo Drut, M.D.; Reprinted from Drut and Jones [5]. With kind permission of © Allen Press; Reprinted from Isaacs [16]. © Springer-Verlag, 2002)

appear to have a much better prognosis than the ductal adenocarcinoma occurring in adults [2, 9]. Primary resection of pancreatic tumors in infants and children is the treatment of choice if technically feasible [34]. The prognosis for patients with pancreatoblastoma is generally favorable, and usually complete surgical resection results

in cure [2, 17]. About half of pediatric patients are cured by resection [31, 35]. Of the six infants with this tumor found in the literature by the author, there were four survivors, one stillborn and one with the Beckwith-Wiedemann syndrome who died at 10 days of age [2, 5, 17, 24].

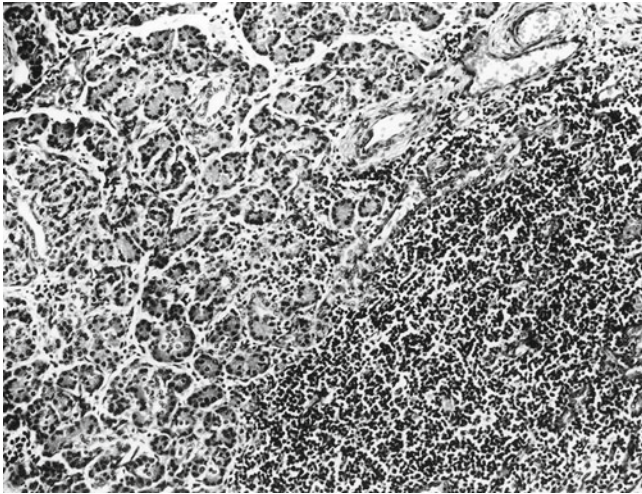


Fig. 14.8 Lymphocytic infiltration of the pancreas. Photomicrograph was taken from the same 650-g fetus depicted in Fig. 14.2. The head of the pancreas contains extensive infiltration by lymphocytes, which are small, round, and regular without atypical features. This benign, probably reactive lesion has been interpreted as leukemia or lymphoma on occasion (Reprinted from Isaacs [15]. © WB Saunders 1997)

14.4 Miscellaneous Tumors and Tumorlike Conditions

Non-epithelial, mesenchymal pancreatic tumors are uncommon in the fetus and infant. Hemangioma and fibromatosis involving the pancreas are some examples [36, 37]. Extensive leukemic infiltration is seen in patients with congenital leukemia [8, 16]. Retroperitoneal small cell malignant tumors such as rhabdomyosarcoma, rhabdoid tumor, and neuroblastoma metastasize to the pancreas [13, 16].

In the fetus and newborn, foci of extramedullary erythroid and myelopoiesis occur frequently in the pancreas which may be present even at term. This finding can be mistaken for *congenital myelocytic leukemia*. Excessive myelopoiesis is found in patients with a generalized leukemoid reaction associated with infection, trisomies 18 and 21 [8]. *Lymphocytic infiltrates* normally located in the head of the pancreas are common in premature and term infants. Occasionally the infiltrates may be so extensive that they are misinterpreted as lymphoma or leukemia rather than a reaction to some other condition such as degenerating islet tissue or infection [8, 13, 16] (Fig. 14.8).

References

- Lack EE, Cassady JR, Levey R et al (1983) Tumors of the exocrine pancreas in children and adolescents. *Am J Surg Pathol* 7:319–327
- Klimstra DS, Wenig BM, Adair CF et al (1995) Pancreatoblastoma: a clinicopathologic study and review of the literature. *Am J Surg Pathol* 19(2):1371–1389
- Carney CN (1976) Congenital insulinoma (nesidioblastoma): ultrastructural evidence for histogenesis from pancreatic ductal epithelium. *Arch Pathol Lab Med* 100:352–356
- Chang CH, Perrin EV, Hertzler J et al (1980) Cystadenoma of the pancreas with cytomegalovirus infection in a female infant. *Arch Pathol Lab Med* 104:7–8
- Drut R, Jones MC (1988) Congenital pancreatoblastoma in Beckwith-Wiedemann syndrome: an emerging association. *Pediatr Pathol* 8:331–339
- Robey G, Daneman A, Martin DJ (1983) Pancreatic carcinoma in a neonate. *Pediatr Radiol* 13:284–286
- Jack MM, Walker RM, Thomsett MJ et al (2000) Histologic findings in persistent hyperinsulinemic hypoglycemia of infancy: Australian experience. *Pediatr Dev Pathol* 3:532–547
- Jaffe R (1998) The pancreas. In: Wigglesworth JS, Singer DB (eds) *Textbook of fetal and perinatal pathology*, 2nd edn. Blackwell, Oxford, p 921
- Grosfeld JL, Vane DW, Rescoria FJ et al (1990) Pancreatic tumors in childhood: analysis of 13 cases. *J Pediatr Surg* 25:1057–1062
- Rich HR, Weber JL, Shandling B (1986) Adenocarcinoma of the pancreas in the neonate managed by pancreatoduodenectomy. *J Pediatr Surg* 21:806–808
- Burt TB, Condon VR, Matlak ME (1983) Fetal pancreatic hamartoma. *Pediatr Radiol* 13:287–289
- Horie A, Yano Y, Kotoo Y et al (1977) Morphogenesis of pancreatoblastoma, infantile carcinoma of the pancreas: report of two cases. *Cancer* 39:247–254
- Isaacs H Jr (1997) Tumors. In: Gilbert-Barness E (ed) *Potter's pathology of the fetus and infant*, vol 2. Mosby, St. Louis, pp 1242–1339
- Roberts DJ, Goldstein AM, Graeme-Cook F, Barrett Dahms B (2007) Gastrointestinal tract and pancreas. In: Gilbert-Barness E (ed) *Potter's pathology of the fetus, infant and child*, vol 2, 2nd edn. Mosby Elsevier, Philadelphia, pp 1157–1206
- Isaacs H Jr (1997) Pancreatic tumors. In: *Tumors of the fetus and newborn*, vol 35, Major problems in pathology. W.B. Saunders, Philadelphia, pp 317–327
- Isaacs H Jr (2002) Pancreatic tumors. In: *Tumors of the fetus and infant: an atlas*. Springer, New York, pp 353–366
- Potts SR, Brown S, O'Hara MD (1986) Pancreatoblastoma in a neonate associated with Beckwith-Wiedemann syndrome. *Z Kinderchir* 41:56–57
- Laidlaw GF (1938) Nesidioblastoma, the islet cell tumor of the pancreas. *Am J Pathol* 14:125–134
- Yakovac WC, Baker L, Hummeler K (1971) Beta cell nesidioblastosis in idiopathic hypoglycemia of infancy. *J Pediatr* 79:226–231
- Dahms BB, Landing BH, Blascovics M et al (1980) Nesidioblastosis and other islet cell abnormalities in hyperinsulinemic hypoglycemia of childhood. *Hum Pathol* 11:641–649
- Roe TF, Kershner AK, Weitzman JJ et al (1973) Beckwith's syndrome with extreme organ hyperplasia. *Pediatrics* 52:372–381
- Sempoux C, Guiot Y, Lefevre A et al (1998) Neonatal hyperinsulinemic hypoglycemia: heterogeneity of the syndrome and keys for differential diagnosis. *J Clin Endocrinol Metab* 83:444–449
- Craver RD, Hill CB (1997) Cure of hypoglycemic hyperinsulinism by enucleation of a focal islet cell adenomatous hyperplasia. *J Pediatr Surg* 32:1526–1527
- Koh THHG, Cooper JE, Newman CL et al (1986) Pancreatoblastoma in a neonate with Wiedemann-Beckwith syndrome. *Eur J Pediatr* 145:435–438
- Kirkland J, Ben-Menachem Y, Akhtar M et al (1978) Islet cell tumor in a neonate: diagnosis by selective angiography and histological findings. *Pediatrics* 61:790–791
- Amendt P, Kohnert KD, Kunz J (1988) The hyperinsulinaemic hypoglycaemia in infancy: a study of six cases. *Eur J Pediatr* 148:107–112

27. Jenkins JM, Othersen HB Jr (1992) Cystadenoma of the pancreas in a newborn. *J Pediatr Surg* 27:1569
28. Tyson RW, Ruyle SZ, Bass K et al (1998) Serous pancreatic cystadenoma in children under 1 year of age: a report of two cases. *Pediatr Dev Pathol* 1:250 (abstract)
29. Cubilla A, Fitzgerald PJ (1978) Pancreas cancer. I. Duct adenocarcinoma: a clinical-pathologic study of 380 patients. *Pathol Annu* 13(1):241–289
30. Corner BD (1943) Primary carcinoma of the pancreas in an infant aged seven months. *Arch Dis Child* 18:106–108
31. Kissane JM (1994) Pancreatoblastoma and solid and cystic papillary tumor: two tumors related to pancreatic ontogeny. *Semin Diagn Pathol* 11:152–164
32. Cooper JE, Lake BD (1989) Use of enzyme histochemistry in the diagnosis of pancreatoblastoma. *Histopathology* 15:407–414
33. Cooperman AM (1981) Cancer of the pancreas: a dilemma in treatment. *Surg Clin North Am* 61:1071–15
34. Jaksic T, Yaman M, Thorner P et al (1992) A 20-year review of pediatric pancreatic tumors. *J Pediatr Surg* 27:1315–1317
35. Klimstra DS, Wenig B, Heffess CS (1994) Pancreatoblastoma: a clinicopathologic study. *Lab Invest* 70:133A (abstract)
36. Ure BM, Holschneider AM, Gharib M et al (1988) Clinical aspects, classification and prognosis of 7 cases of pediatric fibromatosis. *Z Kinderchir* 43:27–30
37. Tunell WP (1976) Hemangioendothelioma of the pancreas obstructing the common bile duct and duodenum. *J Pediatr Surg* 11:827–830

15.1 Introduction

Cardiac tumors are rare in all age groups. The majority are histologically benign. *Rhabdomyoma*, the major cardiac tumor of the fetus and infant, is most likely a hamartoma rather than a true neoplasms [1–9]. *Hamartoma* is defined as an overgrowth of tissue normally present at the site of origin. Because of their location, benign tumors and hamartomas of the heart may severely compromise blood flow, interfere with myocardial function, or cause arrhythmias leading to their clinical discovery, stillbirth, or to sudden death [1–3, 7]. Disturbances in hemodynamic function are correlated with the size and location of the tumor. Murmurs, cyanosis, respiratory distress, cardiac insufficiency, and arrhythmias are the main presenting signs, which should raise suspicion of an underlying cardiac tumor [6, 7]. Primary cardiac tumors are found more often than metastasis to the heart in infants [4, 7–9].

Cardiac tumors are often unsuspected during life, and death may occur suddenly with no previous symptoms of cardiovascular disease [1]. In other instances, symptoms may be present, and the diagnosis is established before or after birth through imaging studies [1, 2, 9].

Cardiac tumors may imitate other neonatal conditions including sepsis and some forms of congenital heart disease (e.g., hypoplastic left heart syndrome, subaortic stenosis, mitral stenosis, and tricuspid insufficiency) [2, 7, 9, 10]. In the fetus, a cardiac tumor may cause congestive heart failure and hydrops, which may lead to stillbirth [9, 11, 12].

Certain tumors notably intrapericardial teratomas and fibromas may be removed successfully as may obstructive intracavitary rhabdomyomas [1, 13]. Primary tumors in a malformed heart are well documented, but their coexistence is unusual. When present, they adversely affect the surgical management and prognosis [7, 10]. Cardiac tumors should be considered in the differential diagnosis of a child with

unexplained heart murmurs, congestive heart failure, or arrhythmias [1, 7].

Cardiac neoplasms may be an early manifestation of certain genetic disorders such as *tuberous sclerosis*, *neurofibromatosis*, *the Gorlin syndrome (nevoid basal cell carcinoma syndrome)*, *familial myxomas*, and rarely *the Beckwith-Wiedemann syndrome* [5, 14–16].

Table 15.1 lists the various cardiac tumors and tumor-like conditions found in the fetus and infant.

Table 15.1 Cardiac tumors and tumor-like conditions of the fetus and infant

Primary
Rhabdomyoma
Teratoma
Fibroma
Myxoma
Oncocytic (histiocytoid) cardiomyopathy
Infantile hemangioma
Lymphangioma
Intravascular fasciitis
Rhabdomyosarcoma
Fibrosarcoma
Rhabdoid tumor
Juvenile xanthogranuloma
Metastatic tumors
Neuroblastoma
Leukemia
Rhabdomyosarcoma
Rhabdoid tumor
Miscellaneous tumor-like conditions
Epithelial cysts
Blood cyst of heart valves

Reprinted from McAllister and Fenoglio [11]. With kind permission of © Armed Forces Institute of Pathology; Reprinted from Isaacs [6]. © Springer-Verlag, 2002

The “true” incidence of fetal or infant cardiac tumors is often difficult to determine. Primary cardiac tumors are found in approximately 1 in 10,000 (0.01 %) routine necropsies on infants [3]. In a retrospective study of 14,000 fetal echocardiograms recorded over an 8-year period in seven centers, the incidence found was 0.14 %; in most instances, a fetal cardiac mass was detected on routine prenatal sonography [17]. Fetal cardiac tumors occur more frequently than necropsy studies suggesting perhaps that rhabdomyomas may regress and are not present in necropsy examinations performed in later life [17]. Most cardiac tumors are benign,

and of these, rhabdomyoma is the leader, followed by teratoma, fibroma, oncocytic cardiomyopathy, vascular tumors, and myxoma (Table 15.2) [7]. During the first year of life, rhabdomyoma and pericardial teratoma comprise over 75 % of the primary cardiac tumors [8, 18, 19]. Malignant and metastatic tumors are described but rare [7, 8].

Certain tumors, for example, *myxoma*, are found more often in adults and rarely observed in the young, whereas neoplasms such as *fibromas* and *intracardiac teratomas* are uncommon in adults but more prevalent in infants and children [1, 7, 8, 16].

Table 15.2 Fetal and neonatal cardiac tumors ($n=224$)

Cardiac tumor	No. (%)	Alive	% survival
Rhabdomyoma ^a	120 (53.8) ^b	72	60
Teratoma ^c	40 (17.8)	30	75
Cardiac fibroma	28 (12.4)	8	29
Oncocytic cardiomyopathy	15 (6.6)	1	7
Vascular tumors	13 (5.8)	11	85
Myxoma	6 (2.7)	1	17
Sarcoma ^d	3 (1.3)	0	0
<i>Overall survival</i>	224 (100)	123	55

Reprinted from Isaacs [7]. With kind permission of © Springer-Verlag, 2004

^aSeven of 120 (6 %) were stillborn

^bPercentage of total number of fetal and neonatal cardiac tumors

^cSix of 40 (15 %) were stillborn

^dIncludes one example each of rhabdomyosarcoma and infantile fibrosarcoma

15.2 Cardiac Rhabdomyoma

Cardiac rhabdomyoma occurs predominately in infants and children, approximately 75 % of those affected being 1 year of age or less [1–4, 6–9, 17–20]. It is the major cardiac tumor of the fetus and infant, followed in line by teratoma and fibroma [7]. Cardiac rhabdomyoma may be found unexpectedly on routine prenatal sonography, on postmortem examination of a stillborn, or a newborn with nonimmune fetal hydrops [1, 6, 7, 9, 12]. Rhabdomyomas that interfere with the conduction system or obstruct left or right ventricular blood flow result in recurrent arrhythmias or sudden death [1–3]. Cardiomegaly, congestive heart failure, and cardiac murmurs are other manifestations. *Fetal arrhythmia* is the most frequent initial sign and is a definite indication for sonography [9, 13]. Half of prenatally diagnosed rhabdomyomas are asymptomatic and are detected on routine sonography [9] (Fig. 15.1). They have been detected as early as 22 weeks gestation [6, 7]. Rhabdomyoma is not often found in association with congenital heart malformations [10].

Although they occur independently, rhabdomyomas are often only one manifestation of *tuberous sclerosis*, a neurocutaneous disorder (phakomatosis) transmitted as an autosomal dominant trait of variable expression [5, 21, 22]. The disease is classically manifested by the triad of mental retardation, epilepsy, and angiofibromas of the face. At least one third of infants and children with cardiac rhabdomyomas have tuberous sclerosis, and the reverse is also true [7, 18, 21].

Other manifestations of tuberous sclerosis may be present in the infant with rhabdomyomas. Skin lesions such as “mountain ash” macules are observed at birth and adenoma sebaceum (angiofibromatous hamartoma) later on in childhood. Cortical and subependymal tubers (gliomas) are seen on imaging studies or at necropsy [7, 11, 18, 21, 22] (see Chap. 9). Although grossly normal, the kidneys have multiple cysts on microscopic examination [21, 22]. Renal angiomyolipomas, consisting of vascular, smooth muscle, and adipose tissue elements, are found later in life.

On gross inspection, cardiac rhabdomyoma consists of one or more white to yellow-tan circumscribed nodules in the myocardium situated most often within the ventricular wall and in the ventricular septum (Fig. 15.2). Some are located in the subepicardial region and in the atria. In about half the patients, the rhabdomyomas are intracavitary causing outflow obstruction [1, 3, 5, 7, 8, 11, 13] (Fig. 15.2).

Rhabdomyomas are considered overgrowths of cardiac muscle (hamartomas) showing only mildly abnormal changes and not true neoplasia. Their most characteristic components are large round or oval cells with small central nuclei and a thin peripheral rim of cytoplasm. Connecting the nucleus with the cell wall are delicate radiating strands of myofibrils responsible for the designation “*spider cells*.” Cross striations are found in these strands and at the periphery of the cells. The intervening vacuoles are filled with *glycogen*, recognizable

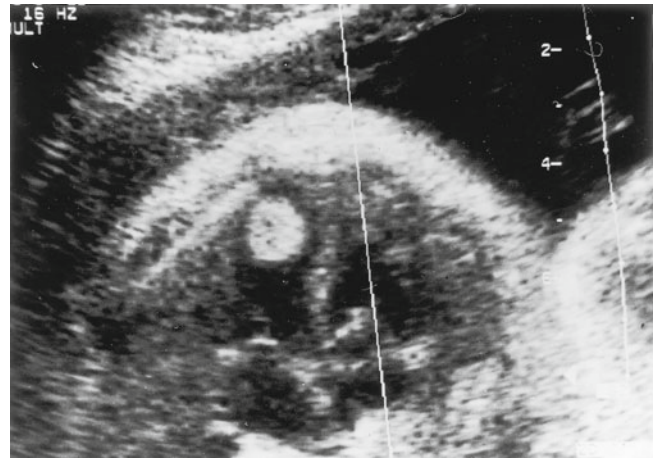


Fig. 15.1 Cardiac rhabdomyoma. Sonogram of a fetus at 32 weeks gestation demonstrating a round echogenic mass bulging into the cavity of the left ventricle. Several additional tumors were visible in other views. The baby proved to have tuberous sclerosis but survived (Courtesy of Val Catanzarite, M.D., Perinatology, Sharp Memorial Hospital, San Diego; Reprinted from Isaacs [4]. © WB Saunders 1997)

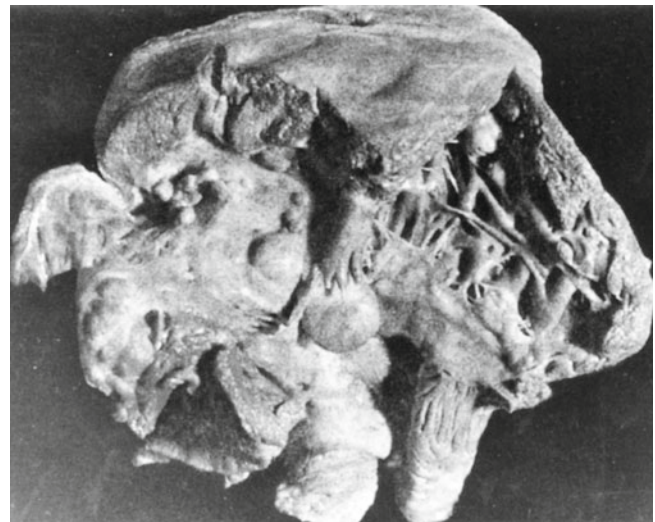


Fig. 15.2 Cardiac rhabdomyoma. Gross tumors are visible beneath the endocardium. The child with tuberous sclerosis died at age 6 months (Reprinted from Isaacs [5]. With kind permission of © Mosby, 1997)

with appropriate staining [5, 6] (Figs. 15.3 and 15.4). Such cells are scattered in small groups throughout the musculature and in masses. Immunohistochemical studies show diffuse immunoreactivity with myoglobin, actin, desmin, and vimentin; however, S-100 protein is nonreactive [19]. EM confirms the presence of cross striations as well as abundant β -glycogen within the cells [5, 6, 19]. Other ultrastructural features include leptofibrils, a poorly developed sarcoplasmic reticulum, and scattered desmosomes [19].

Because spontaneous regression of cardiac rhabdomyomas often occurs, surgical intervention is recommended only for patients with severe hemodynamic compromise or persistent arrhythmias [2, 17, 19]. Despite occasional spontaneous regression, prognosis is generally unfavorable overall [21].

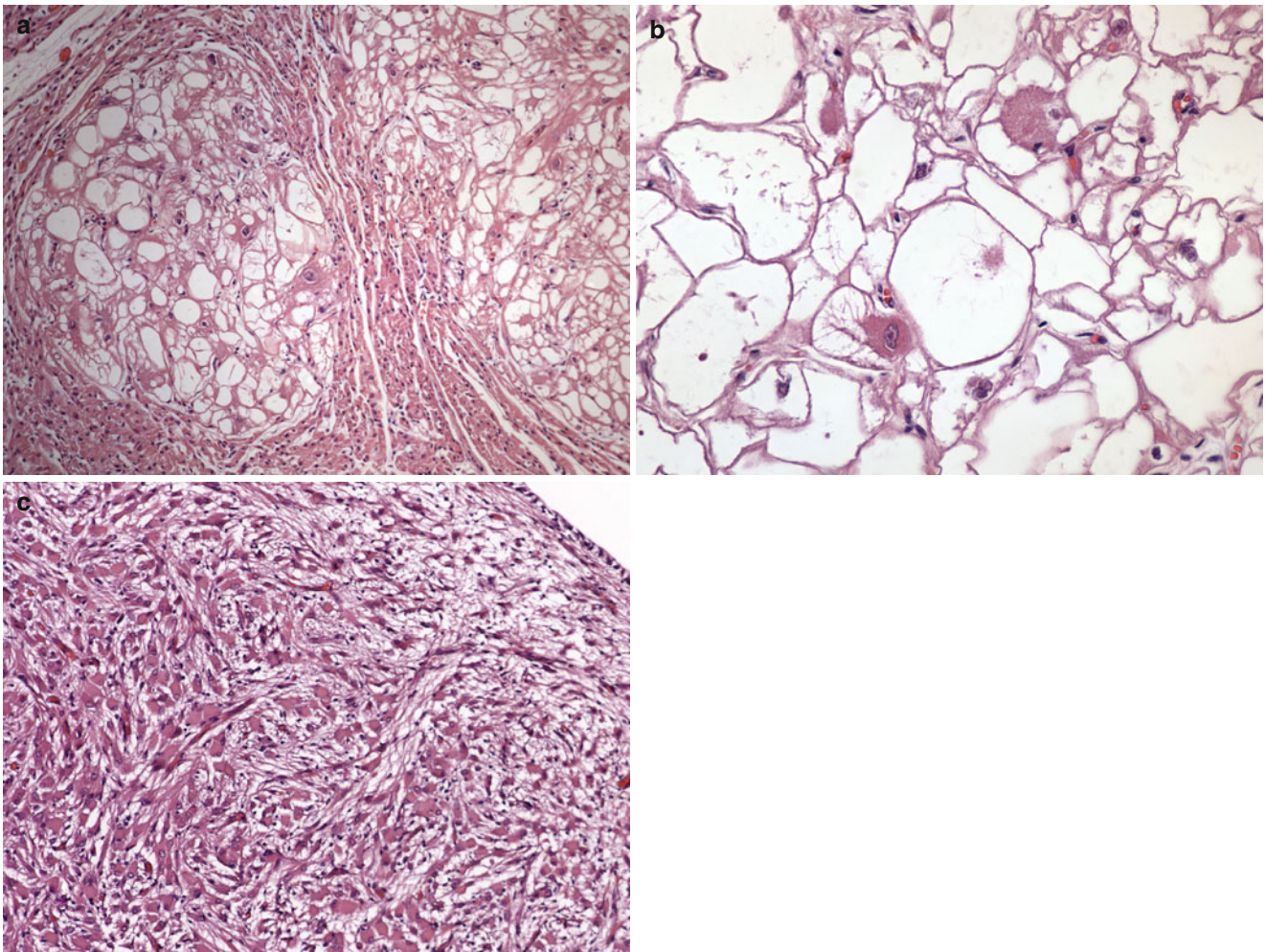


Fig. 15.3 Cardiac rhabdomyoma. Six-week-old male developed an arrhythmia at 1 week of age. Cardiac catheterization revealed a tumor in the posterior wall of the left ventricle. Four grams of yellow white and lobulated tissue was excised. **(a)** Large myocardial cells have cytoplasm distended by glycogen-filled vacuoles. Some contain central nuclei with delicate strands extending from the nucleus to the cell wall.

These are the so-called spider cells considered pathognomonic for cardiac rhabdomyoma. **(b)** Spider cells at higher magnification. At post-mortem examination, the patient had several additional cardiac rhabdomyomas. **(c)** Numerous subependymal glial nodules were found in the cerebrum and basal ganglia (Reprinted from Isaacs [5]. With kind permission of © Mosby, 1997)

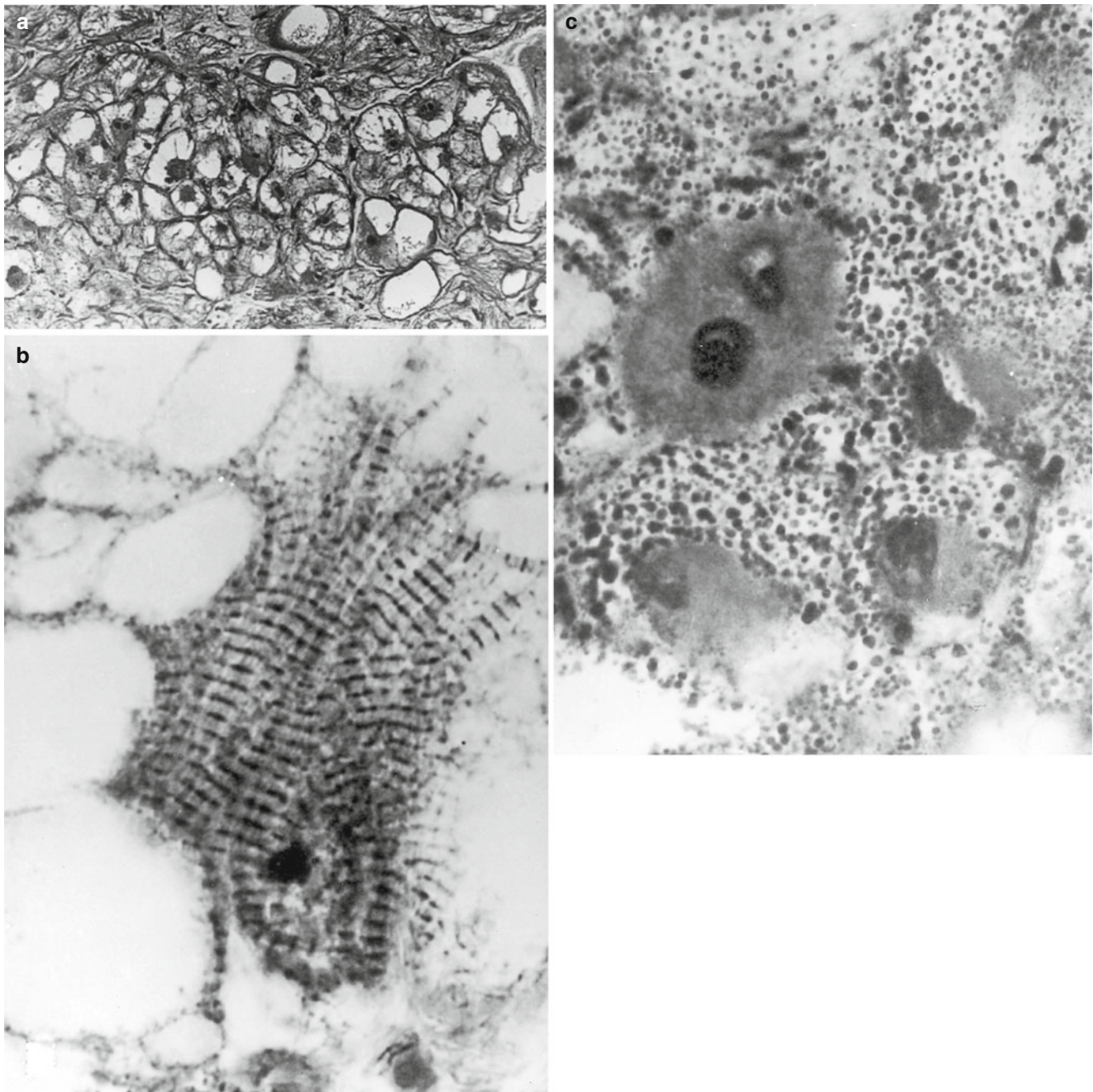


Fig. 15.4 Cardiac rhabdomyoma. (a) Rhabdomyoma showing typical “spider cells” in a child with tuberous sclerosis who died at 22 days of age. See Fig. 9.5 for other lesions found in the brain. (b) Cells showing

characteristic muscular striations. (c) Cells containing large amounts of glycogen (Reprinted from Isaacs [5]. With kind permission of © Mosby, 1997)

15.3 Pericardial and Cardiac Teratoma

Teratoma is an uncommon primary germ cell tumor of the heart or pericardium at any age [4–6, 9, 23–26]. Nearly two thirds are found in infants; it is second in frequency following rhabdomyoma in most series [5, 7, 11, 20, 25]. The majority of cardiac teratomas arise from the pericardium (intrapericardial teratoma) as compared to the atrium or ventricle (intracardiac), where only a few cases are described [5, 7]. The clinical

findings in newborns and infants with intrapericardial teratomas are dyspnea, cardiomegaly, and congestive heart failure which may be accompanied by cyanosis and a murmur. Pericardial effusion is characteristic, sometimes producing life-threatening tamponade. Pericardial teratoma is one of the most common causes of massive pericardial effusion in the fetus and neonate [1, 23, 25]. Fetal hydrops has been described in both [12]. The teratoma may cause sudden unexpected death [1, 11, 19].

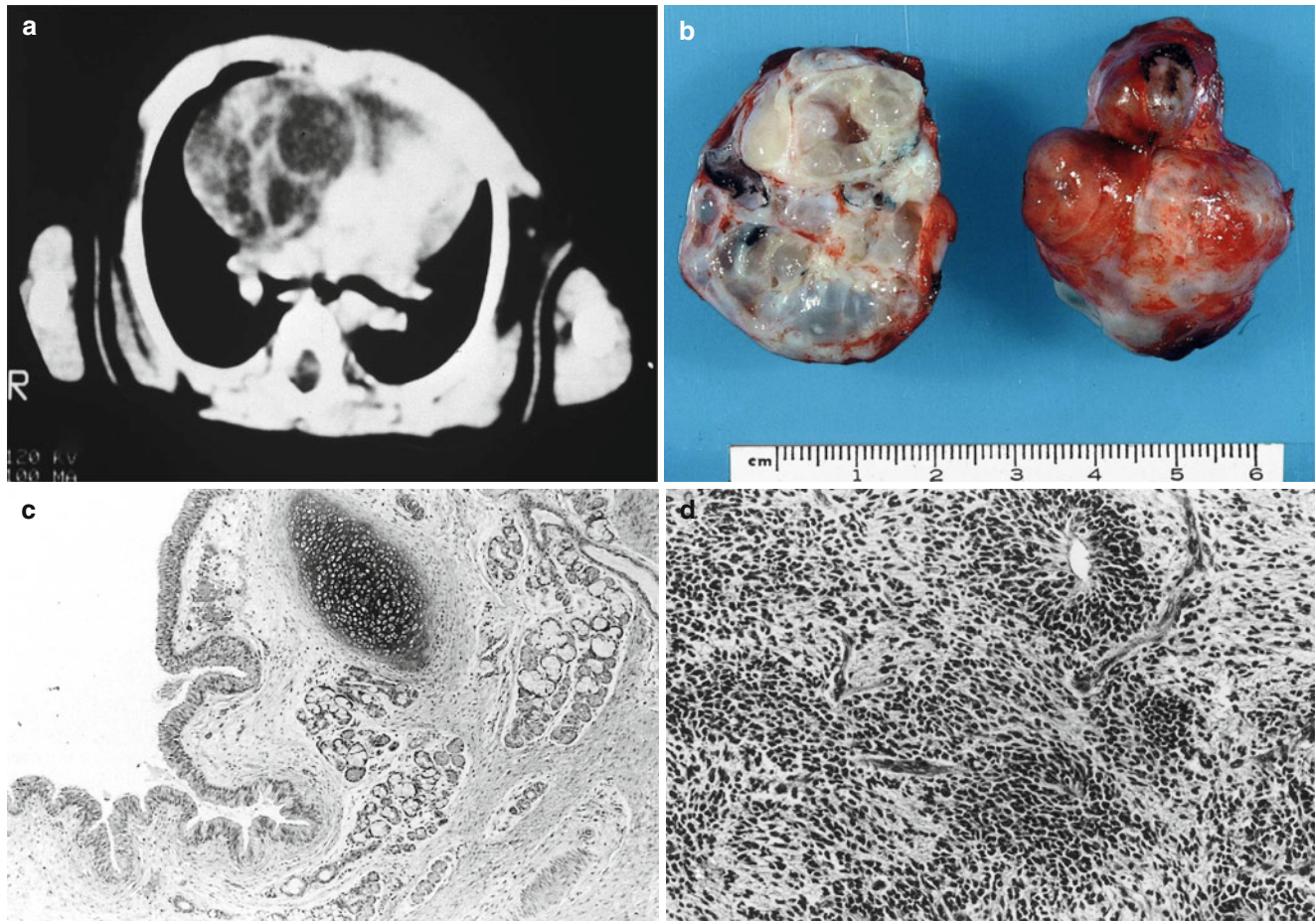


Fig. 15.5 Intrapericardial teratoma. Two-month-old male with a history of increasing respiratory distress. (a) CT scan of the thorax showing a nodular, cystic density arising from the pericardium and bulging into the right pleural cavity. (b) The tumor, 27.5 g and 5.5×3.6 cm, is situated within the pericardial cavity attached to the aorta. It has a lobu-

lated appearance and contains multiple cysts. (c) Mature respiratory epithelium, cartilage, and seromucinous glands comprise the teratoma. (d) In addition, there are immature neuroglial elements (Reprinted from Isaacs [4]. © WB Saunders 1997)



Fig. 15.6 Teratoma of the right atrium in a neonate. Gross appearance. Microscopically the tumor consisted of squamous epithelium, neuroglia, and glands similar to what is shown in (Fig 15.5c, d) (Reprinted from Isaacs [5]. With kind permission of © Mosby, 1997)

Infants and newborns with intracardiac tumors present with cyanosis, cardiomegaly, congestive heart failure, and a murmur [7, 24]. Teratoma is detected both antenatally and postnatally by imaging studies [6, 9, 25–27] (Fig. 15.5a).

Intrapericardial teratomas typically arise from the base of the heart and are attached to the root of the pulmonary artery and aorta. The tumor has a smooth, lobulated surface (Fig. 15.5b). On section, it consists of multiloculated cysts with intervening solid areas. The intracardiac tumors arise from the atrial and/or ventricular wall as nodular masses projecting into the cardiac chamber(s) [5–7, 11] (Fig. 15.6). Histologically, intrapericardial and intracardiac teratomas are identical to those found in other locations with all three germ layers represented in most specimens [6, 7, 23]. The cysts are lined by a variety of epithelium including stratified squamous, cuboidal, mucin-secreting, or respiratory epithelium. The more solid areas contain *mature* or *immature neuroglial tissue*, thyroid,

pancreas, smooth and skeletal muscle, and foci of bone and cartilage (Fig. 15.5c, d).

Early recognition of a cardiac teratoma is important because most can be cured by pericardiocentesis and surgical resection [11, 23–25, 27]. They have been successfully removed both in the neonate and infant and next to hemangioma have the highest cure rate in this age group [7, 24, 25].

15.4 Cardiac Fibroma

Cardiac fibromas are the third most common primary cardiac tumor of fetuses and infants, following rhabdomyoma and teratoma [1, 4, 5, 7, 8, 19, 28]. They are considered benign connective tissue tumors arising from *fibroblasts* and *myofibroblasts* having practically the same gross and microscopic appearance and biological behavior as their soft tissue counterpart (see Chap. 4). Other names applied to this tumor are fibromatosis, myofibromatosis, fibrous hamartoma, and congenital mesoblastic tumor [6, 11, 14, 29–31].

Cardiac fibromas are almost always solitary usually, arising from the myocardium of the ventricular septum or free wall of the right or left ventricle, more often the left [1, 7, 11]. The clinical findings depend on the location and extent of the tumor [1–3, 7]. Fibromas arising from the ventricular septum may involve the conduction system resulting in ventricular fibrillation. *Cardiomegaly* and *sudden unexpected death* occur with tumors situated both within the free wall of the ventricle and in the septum [2, 7]. At either location, the lesion may obstruct the inflow or outflow tract of the ventricle leading to progressive congestive heart failure [1, 2]. Since most fibromas occur in the left ventricle, the signs and symptoms of obstruction relate mostly to the left side of the heart [3] and are similar to signs and symptoms of the hypoplastic left heart syndrome and of subaortic stenosis [1–3, 29].

Extracardiac malformations or syndromes are seldom associated, but the tumor has been observed in association with cleft lip and palate [32], with the Beckwith-Wiedemann syndrome [30] and with the nevoid basal cell carcinoma syndrome (Gorlin-Goltz syndrome) [14, 33]. In congenital generalized (visceral) fibromatosis, fibromas may involve the heart [5–7, 31]. Cardiac fibromas have a firm, white, myxoid, or trabeculated gross appearance measuring 5 cm or more in diameter. The tumor is not encapsulated blending imperceptibly with the adjacent myocardium. Foci of calcification may be present within the center [1, 11, 14, 28]. Histologically, the tumor is composed of spindle-shaped fibroblastic cells surrounded by abundant collagen fibers [1, 7, 11, 14]. Mitoses are noted rarely. Central areas show foci of calcification, elastic fibers, and cystic change. Characteristically entrapped myocardial fibers are present

within the tumor [1, 14]. Immunohistochemical studies reveal diffuse vimentin and focal smooth muscle actin activity [14]. By EM, the fibroma consists of fibroblasts and spindle-shaped cells with abundant myofilaments and dense bodies consistent with myofibroblasts, findings similar to those of the soft tissue fibromatoses [7, 14]. Spontaneous regression has not been observed. Operative intervention is required for cure [2, 7, 14].

15.5 Cardiac Myxoma

Although *myxoma*, a benign neoplasm thought to be derived from cardiac multipotential mesenchymal cells, is the leading primary tumor of the heart in adults, it is the subject of only a few case reports in the fetus and infant [7, 8, 11, 16, 34, 35]. However, the tumor has been reported in stillborns [7, 11, 12]. The majority of myxomas occurring in the newborn and infant arise from the right atrium and most have proved fatal [8, 11, 34, 35]. Total surgical excision is the treatment of choice [1, 11, 36]. The reader is referred elsewhere for description of the pathological findings [1, 7, 11].

15.6 Vascular Tumors

Cardiac hemangiomas comprise about 2.8 % of all primary cardiac tumors, and most are diagnosed in the neonatal period [7, 36–40]. They can arise from anywhere in the vicinity of the heart. *Pericardial effusion* is often present. Other associated findings are cardiomegaly, congestive heart failure, fetal hydrops, hemopericardium, and thrombocytopenia [1, 13, 39, 40]. Echocardiography shows mixed echogenicity with echogenic and hyperechoic areas. The formation of hyperechoic and cystic spaces has been attributed to cavernous lakes; thrombosis and calcification are changes possibly related to spontaneous regression [7, 13].

The tumors appear as sessile, lobulated, and nonencapsulated masses ranging in size from 1.5 to 2.5 cm [1, 7, 11]. Thrombosis and calcification are variably present. Microscopically, the hemangioma consists of capillary and/or cavernous components [6, 7, 13] (see Chap. 4). Although neonates with hemangiomas have died from serious complications such as hydrops, bleeding, and congestive heart failure, most fetal and infant cardiac vascular tumors are associated with a favorable outcome [11, 36–40]. Intrapericardial *lymphangioma* may manifest in the neonate with respiratory distress, cardiomegaly, pericardial effusion, and a mass situated in the pericardial cavity between the atrium and ventricle [41].

Vascular tumors have the best prognosis of all cardiac tumors [7].

15.7 Oncocytic (“Histiocytoid”) Cardiomyopathy

Cardiac hamartoma-like conditions distinctly different morphologically from rhabdomyomas occur in infants and young children who typically present with refractory arrhythmias or sudden unexpected death [5, 7, 42–52]. Females are affected considerably more often than males. This condition of controversial etiology has been given a variety of exotic names, including infantile *histiocytoid cardiomyopathy*, *oncocytic cardiomyopathy*, *histiocytoid cardiomyopathy*, *Purkinje cell tumor*, *focal lipid cardiomyopathy*, and *idiopathic infantile cardiomyopathy* [7, 42–45, 47, 48]. Morphologically, the disease is characterized by the presence of focal yellowish nodules or yellow areas of discoloration composed of vacuolated histiocyte-like cells within the myocardium [46, 48, 51]. Although it is a distinct entity, the histogenesis and etiology of this condition are unknown. However, light and EM studies show that the vacuolated cells actually represent altered myocardial cells containing increased numbers of mitochondria. The term *oncocytic cardiomyopathy* was proposed when it was discovered that the characteristic cardiac lesions were associated also with oncocytes (cells containing increased numbers of mitochondria) in other organs [44, 50]. The cardiomyopathy is associated with both cardiac and extracardiac anomalies in approximately one third of patients, the former consisting of atrial and ventricular septal defects and hypoplastic left heart syndrome and the latter of cleft palate and anomalies of the central nervous system, eyes, and skin (microphthalmia with linear skin defects, “MLS”) [42–44, 46, 49].

Neonates with oncocytic cardiomyopathy present with arrhythmias (the most common clinical manifestation) or sometimes sudden unexpected death [42, 43, 45, 46, 49, 51]. Ventricular fibrillation, ventricular tachycardia, premature ventricular contractions, supraventricular tachycardia, and partial or complete heart block are the conduction defects described which may be present at birth [46, 49, 51].

Although the clinical diagnosis of oncocytic cardiomyopathy may prove difficult, the condition should be suspected particularly in female infants, who are initially seen with refractory arrhythmias, particularly supraventricular tachycardia, ventricular tachycardia, or junctional tachycardia [51]. The finding of nodular deposits on the ventricular endocardium or valves by sonography should prompt investigation by echocardiography or other imaging studies [51]. *Oncocytic cardiomyopathy is an important cause of sudden unexpected death in infancy*; therefore, the hearts of these patients must be carefully examined at postmortem examination for the presence of oncocytic myocytes [42].

At postmortem examination, practically all involved hearts are enlarged, 1.5–3 times normal, and dilated [7, 42, 44, 46, 48]. If large enough, tiny, raised, yellow-tan nodules

are visible grossly on the cut surfaces of the myocardium. They range in size from 1 to 2 mm in diameter or more. The conduction system and the left ventricle are the most common sites, followed by a diffuse distribution of oncocytes throughout most of the heart. The nodules are situated beneath the endocardium and less often beneath the epicardium [7, 46, 48, 49]. However, the only gross finding may be a poorly defined, pale yellow appearance of the endocardial surface of the ventricles or papillary muscles, or there may be no definite changes [7, 42, 44–46, 48].

Histologically, the lesion consists of collections of large, round to oval cardiac myocytes composed of a coarsely granular or foamy, pale cytoplasm. The cells are weakly PAS positive and desmin, myosin, and myoglobin immunoreactive, but they are negative for macrophage (histiocyte) markers, for example, lysozyme, α 1-antitrypsin, and CD68 [7, 42, 44]. Foci of fibrosis and lymphocytic infiltrates may be present around clusters of involved cells [46]. Transitional cells having mild vacuolation are present between the severely vacuolated cells and the adjacent normal myocytes. Serial histological sectioning of the cardiac conduction system may reveal involvement of the atrioventricular node, bundle of His, or bundle branches [48, 49, 51]. By EM, the granules correspond to numerous mitochondria that appear to replace the myofibrils, hence the derivation of the term oncocytic cardiomyopathy. The cytoplasm of these cells is almost completely filled with altered mitochondria. In addition, the cells contain few desmosomes, intercalated discs, scant Z-band material, and elongated, oval leptomeric fibers with bundles of thin filaments forming cross striations [42, 44, 46, 47, 49, 51].

Approximately one third of infants with oncocytic cardiomyopathy have oncocytic cells in other organs, such as the adrenals, thyroid, anterior pituitary, and tracheal and salivary glands [43, 45, 50, 51].

If left untreated, oncocytic cardiomyopathy is often fatal by the age of 2 years [42, 47]. Some patients with this disease have been cured with electrophysiologic mapping and surgical excision [49, 52]. Overall, the prognosis is bleak, especially for infants with multiple unresectable lesions [51]. To my knowledge, there are no reports of fetal diagnosed oncocytic cardiomyopathy. The survival rate for infants with this condition is low [7].

15.8 Miscellaneous Conditions

Primary *rhabdomyosarcoma*, the main malignancy of the heart, has been described infrequently in both newborns and older infants [4, 11, 53]. This ultimately fatal condition may present with congestive heart failure and arrhythmias. When the tumor extends into the cardiac chamber, it produces obstruction and murmurs that change in intensity [11].

Fibrosarcoma and *rhabdoid tumor* primary in the heart are recorded occasionally in infants [54, 55]. Systemic *juvenile xanthogranuloma* with cardiac involvement may present in the newborn as a murmur and small masses in the septum and ventricular outflow tracts [56] (see Chap. 8).

Blood cysts are a common finding in neonates dying of various causes and probably have no clinical significance [57]. They may persist and enlarge to form giant cysts of heart valves that occur most frequently on the tricuspid and mitral valves of fetuses and infants. Congenital blood cysts are believed to form from infoldings of the valvular endothelium that bulges into the atria because of the transvalvular pressure [57].

References

1. Arey JB (1984) Tumors of the heart and pericardium. In: Cardiovascular pathology in infants and children. Saunders, Philadelphia, pp 372–383
2. Freedom RM, Benson LN (1992) Cardiac neoplasms. In: Freedom RM, Benson LN, Smallhorn JF (eds) Neonatal heart disease. Springer, London, p 723
3. Nadas AS, Ellison RC (1968) Cardiac tumors in infancy. *Am J Cardiol* 21:363–366
4. Isaacs H Jr (1997) Cardiac tumors. In: Tumors of the fetus and newborn, vol 35. W.B. Saunders, Philadelphia, pp 330–343
5. Isaacs JR H (1997) Tumors. In: Gilbert-Barness E (ed) Potter's pathology of the fetus and infant, vol 2. Mosby, St. Louis, pp 1319–1323
6. Isaacs H Jr (2002) Tumors of the fetus and infant: an atlas. Springer, New York, pp 377–386
7. Isaacs HJR (2004) Fetal and neonatal cardiac tumors. *Pediatr Cardiol* 25:252–273
8. Chan HS, Sonley MJ, Moes CA et al (1985) Primary and secondary tumors of childhood involving the heart, pericardium and great vessels. A report of 75 cases and review of the literature. *Cancer* 56:825–836
9. Groves AMM, Fagg NLK, Cook AC et al (1992) Cardiac tumours in intrauterine life. *Arch Dis Child* 67:1189–1192
10. Russell GA, Dhasmana JP, Berry PJ et al (1989) Coexistent cardiac tumours and malformations of the heart. *Int J Cardiol* 22:89–98
11. McAllister HA JR, Fenoglio Jr JJ (1978) Tumors of the cardiovascular system, Fascicle 15, 2nd series. Armed Forces Institute of Pathology, Washington, D.C.
12. Isaacs H Jr (2008) Fetal hydrops associated with tumors. *Am J Perinatol* 25:43–68
13. Holley DG, Martin GR, Brenner JI (1995) Diagnosis and management of fetal cardiac tumors: a multicenter experience and review of published reports. *J Am Coll Cardiol* 26:516–520
14. Coffin CM (1992) Congenital cardiac fibroma associated with Gorlin syndrome. *Pediatr Pathol* 12:255–262
15. Vidaillet HJ (1988) Cardiac tumors associated with hereditary syndromes. *Am J Cardiol* 61:1355
16. Carney JA (1985) Differences between non-familial and familial cardiac myxoma. *Am J Surg Pathol* 9:53–55
17. Smythe JF, Dyck JD, Smallhorn JF et al (1990) Natural history of cardiac rhabdomyoma in infancy and childhood. *Am J Cardiol* 66:1247–1249
18. Webb DW, Thomas RD, Osborne JP (1993) Cardiac rhabdomyomas and their association with tuberous sclerosis. *Arch Dis Child* 68:367–370
19. Burke AP, Virmani R (1991) Cardiac rhabdomyoma: a clinicopathologic study. *Mod Pathol* 4:70–74
20. Fyler DC (1980) Report of the New England Regional Infant Cardiac Program. *Pediatrics* 65(suppl):376
21. Isaacs H (2009) Perinatal (fetal and neonatal) tuberous sclerosis: a review. *Am J Perinatol* 26:755–760
22. Ostor AG, Fortune DW (1978) Tuberous sclerosis initially seen as hydrops fetalis: report of a case and review of the literature. *Arch Pathol Lab Med* 102:34–39
23. Isaacs H Jr (2004) Perinatal (fetal and neonatal) germ cell tumors. *J Pediatr Surg* 39:1003–1013
24. Costas C, Williams RL, Fortune RL (1986) Intracardiac teratoma in an infant. *Pediatr Cardiol* 7:179–181
25. Bruch SW, Adzick NS, Reiss R et al (1997) Prenatal therapy for pericardial teratomas. *J Pediatr Surg* 32:1113–1115
26. Catanzarite V, Mehalek K, Maida C et al (1994) Early sonographic diagnosis of intrapericardial teratoma. *Ultrasound Obstet Gynecol* 4:505–507
27. Paw PT, Jamieson SW (1997) Surgical management of intrapericardial teratoma diagnosed in utero. *Ann Thorac Surg* 64:552–554
28. Beghetti M, Gow RM, Haney I et al (1997) Pediatric primary benign cardiac tumors: a 15-year review. *Am Heart J* 134:1107–1114
29. Gonzalez-Crussi F, Eberts TJ, Mirkin DL (1978) Congenital fibrous hamartoma of the heart. *Arch Pathol Lab Med* 102:491–493
30. Reddy JK, Shinke RN, Chang CHJ et al (1972) Beckwith–Wiedemann syndrome, Wilms' tumor, cardiac hamartoma, persistent visceromegaly, and glomeruloneogenesis in a 2 year old boy. *Arch Pathol* 94:523–532
31. Rosenberg HS, Stenback WA, Spjut HJ (1978) The fibromatoses of infancy and childhood. In: Rosenberg HS, Bolande RP (eds) Perspectives in pediatric pathology, vol 4. Year Book, Chicago, pp 269–348
32. Back LM, Brown AS, Barot LR (1988) Congenital cardiac tumors in association with orofacial clefts. *Ann Plast Surg* 20:558–561
33. Gorlin RJ (1987) Nevoid basal-cell carcinoma syndrome. *Medicine* 66:98–113
34. Hals J, Ek J, Sandnes K (1990) Cardiac myxoma as the cause of death in an infant. *Acta Paediatr Scand* 79:999–1000
35. Balsara RK, Pelias AJ (1983) Myxoma of right ventricle presenting as pulmonic stenosis in a neonate. *Chest* 83:145–146
36. Burke A, Johns JP, Virmani R (1990) Hemangiomas of the heart. A clinicopathologic study of ten cases. *Am J Cardiovasc Pathol* 3:283–290
37. Platt LD, Geierman CA, Turkel SB et al (1982) Atrial hemangioma and hydrops fetalis. *Am J Obstet Gynecol* 141:107–109
38. Cartagena AM, Levin TL, Issenberg H et al (1993) Pericardial effusion and cardiac hemangioma in the neonate. *Pediatr Radiol* 23:384–385
39. Thorp JA, Geidt A, Gelatt M et al (2000) Decompression of fetal cardiac tamponade caused by congenital capillary hemangioma of the pericardium. *Obstet Gynecol* 96:816–817
40. Tseng JJ, Chou MM, Lee YH et al (1999) In utero diagnosis of cardiac hemangioma. *Ultrasound Obstet Gynecol* 13:363–365
41. Daubeney PE, Ogilvie BC, Moore IE et al (1996) Intrapericardial lymphangioma presenting as neonatal cardiac tamponade. *Pediatr Cardiol* 17:129–131
42. Baillie T, Chan YF, Koelmeyer TD et al (2001) Test and teach. III-defined subendocardial nodules in an infant. *Histiocytoid cardiomyopathy*. *Pathology* 33:230–234
43. Bird LM, Krous HF, Eichenfield LF et al (1994) Female infant with oncocytic cardiomyopathy and microphthalmia with linear skin defects (MLS): a clue to the pathogenesis of oncocytic cardiomyopathy? *Am J Med Genet* 53:141–148
44. Franciosi RA, Singh A (1988) Oncocytic cardiomyopathy syndrome. *Hum Pathol* 19:1361–1362
45. Gelb AB, Van Meter SH, Billingham ME et al (1993) Infantile histiocytoid cardiomyopathy – myocardial or conduction system hamartoma: what is the cell type involved? *Hum Pathol* 24:1226–1231

46. Malhotra V, Ferrans VJ, Virmani R (1994) Infantile histiocytoid cardiomyopathy: three cases and literature review. *Am Heart J* 128:1009–1021
47. Shehata BM, Patterson K, Thomas JE et al (1998) Histiocytoid cardiomyopathy: three new cases and a review of the literature. *Pediatr Dev Pathol* 1:56–69
48. Bruton D, Herdson PB, Becroft DM (1977) Histiocytoid cardiomyopathy of infancy: an unexplained myofibre degeneration. *Pathology* 9:115–122
49. Kearney DL, Titus JL, Hawkins EP et al (1987) Pathologic features of myocardial hamartomas causing childhood tachyarrhythmias. *Circulation* 75:705–710
50. Silver MM, Burns JE, Sethi RK et al (1980) Oncocytic cardiomyopathy in an infant with oncocytosis in exocrine and endocrine glands. *Hum Pathol* 11:598–605
51. Keller BB, Mehta AV, Shamszadeh M et al (1987) Oncocytic cardiomyopathy of infancy with Wolff–Parkinson–White syndrome and ectopic foci causing tachydysrhythmias in children. *Am Heart J* 114:782–792
52. Murphy MC, Sweeney MS, Putnam JB Jr et al (1990) Surgical treatment of cardiac tumors: a 25-year experience. *Ann Thorac Surg* 49:612–617
53. Schmaltz AA, Apitz J (1982) Primary rhabdomyosarcoma of the heart. *Pediatr Cardiol* 2:73–75
54. Lazarus KH, D’Orsogna DE, Bloom KR et al (1989) Primary pericardial sarcoma in a neonate. *Am J Pediatr Hematol Oncol* 11:343–347
55. Small EJ, Gordon GJ, Dahms BB (1985) Malignant rhabdoid tumor of the heart in an infant. *Cancer* 55:2850–2853
56. Isaacs H Jr (2006) Fetal and neonatal histiocytoses. *Pediatr Blood Cancer* 47:123–129
57. Zimmerman KG, Paplanus SH, Dong S et al (1983) Congenital blood cysts of the heart valves. *Hum Pathol* 14:699–703

16.1 Introduction

Less than 5 % of primary neoplasms of the salivary glands are found in children [1–12], and 8 % or less of these occur in infants [4, 5, 8–10]. Inflammatory conditions and mucoceles are by far more prevalent than neoplasms [5, 12]. *Vascular lesions, hemangioma and lymphangioma*, are more common in the fetus and infant than epithelial salivary gland tumors [5, 8] (Fig. 16.1). *Capillary hemangioma* (“infantile hemangioma”) is the leading parotid tumor in infancy and can present as a facial mass in the neonate [1, 5, 12, 13] (Fig. 4.3). The parotid gland is the primary site of tumor involvement more often than the submandibular or sublingual glands [5, 12].

Mesenchymal tumors, excluding vascular lesions, are less common than tumors of epithelial origin. *Plexiform neurofibroma*, the hallmark of *neurofibromatosis 1*, involves the major salivary glands producing gland enlargement. The tumor occurs in newborns with neurofibromatosis 1 and occasionally causes considerable disfigurement [5, 14] (Fig. 16.2).

Sialoblastoma is the major epithelial salivary gland tumor of the fetus and infant [3, 5, 8, 10–12, 15–19, 22]. *Congenital pleomorphic adenoma, mucoepidermoid carcinoma, and undifferentiated carcinoma* are described much less often [5, 6, 8, 10–12, 20–22]. Table 16.1 lists the various salivary gland tumors and tumorlike conditions found in the fetus and infant.

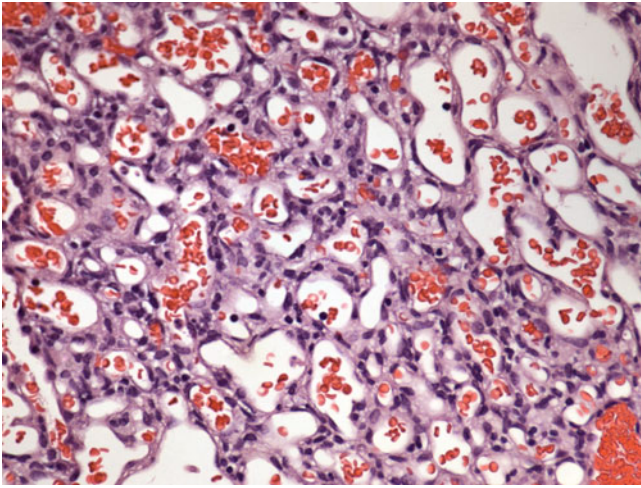


Fig. 16.1 Capillary hemangioma of the sublingual gland. Eight month-old male with a sublingual mass. Biopsy reveals lobules of proliferating capillaries. The capillary endothelium consists of regular, small round to oval cells (Reprinted from Isaacs [12]. © Springer-Verlag, 2002)

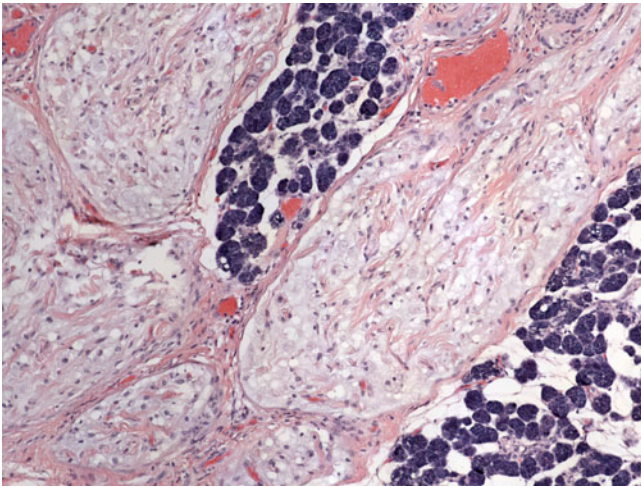


Fig. 16.2 Plexiform neurofibroma of the parotid gland. One-year-old male with neurofibromatosis one and a disfiguring mass involving the face and forehead present since birth. The tumor consists of enlarged, myxoid-appearing nerve trunks with proliferations of neurites and Schwann cells. There are portions darkly staining parotid gland present in the upper left and lower right-hand corner. The face and parotid gland are common sites for neurofibroma in infants [14] (Reprinted from Isaacs [12]. © Springer-Verlag, 2002)

Table 16.1 Fetal and infant salivary gland tumors and tumor-like conditions

Sialoblastoma
Salivary gland anlage tumor (congenital pleomorphic adenoma)
Undifferentiated carcinoma
Pleomorphic adenoma (mixed tumor) ^a
Mucoepidermoid carcinoma ^a
Acinic cell carcinoma ^a
Infantile hemangioma
Capillary hemangioma
Cavernous hemangioma
Hemangioendothelioma
Arteriovenous malformation
Lymphatic malformation (“lymphangioma”)
Teratoma
Nasopharyngeal dermoid (“hairy polyp”)
Neurofibroma
Fibromatosis
Myofibromatosis
Lipoma
Rhabdomyosarcoma ^a
Rhabdoid tumor ^a
Submandibular hamartoma

Reprinted from Isaacs [12]. © Springer-Verlag, 2002

^aRarely recorded in the fetus and infant

16.2 Sialoblastoma

The congenital salivary gland tumor originally described and termed “embryoma” by Vawter and Tefft [16], the monomorphic adenoma, congenital basal cell adenoma, basaloid adenocarcinoma, congenital hybrid basal cell adenoma, and adenoid cystic carcinoma share histological features in common, namely, epithelial and myoepithelial cell components [3, 5, 8, 15, 17–19, 22]. Currently, the accepted term for this group is “sialoblastoma” which is probably appropriate because the tumor’s histological findings resemble those of developing salivary gland [17, 18].

Sialoblastoma presents as a facial or submandibular mass sometimes found at birth (Fig. 16.3a). When the parotid gland is involved, a seventh nerve facial palsy may be present. Because of its size, the tumor may cause dystocia [19]. The parotid gland is involved more frequently than the submandibular salivary gland [10, 12].

Sialoblastoma varies considerably in size ranging from 1 to 15 cm in diameter and has a tan-gray to yellow, lobulated, sometimes cystic, and focally necrotic cut surface. They tend to be well circumscribed [3, 5, 16, 18].

The characteristic histological features include solid nests of epithelial cells containing small duct-like structures surrounded by narrow bands of fibrous connective tissue [3, 16, 17, 19, 22] (Fig. 16.3b). Tumor cells are composed of round to oval nuclei with a fine chromatin pattern, one or more large nucleoli, and a pale to amphophilic-staining cytoplasm.

There are small to moderate numbers of mitoses. Focal squamous cell nests are noted in some tumors.

Immunohistochemical studies show that only ductal cells stain positively for cytokeratin, whereas both ductal and epithelial cells express vimentin [3, 19, 22]. Spindle-shaped myoepithelial cells situated peripherally about the epithelial cell nests react with smooth muscle actin, myosin, and S-100.

EM confirms the immunohistochemical findings [3, 18]. Epithelial nest cells contain smooth oval nuclei, abundant endoplasmic reticulum, numerous ribosomes, and few primitive cell junctions. Ductal epithelial cells are larger with irregular nuclei and less prominent cytoplasm composed of many lysosomes and free ribosomes. Tight junctions and microvilli are present also. Ductal epithelium is partially surrounded by slender myoepithelial cells with elongated nuclei, intracytoplasmic thin filaments, and replicated basement membranes [3, 18].

Of 30 infant cases reviewed from the literature, there was local recurrence in seven, regional lymph node metastases in three; there were no instances of distant metastases. All but one survived (Table 16.2). These findings suggest that sialoblastoma is locally aggressive but will recur if not adequately excised. To my knowledge, distant metastases have not been recorded. Sialoblastoma is regarded as a tumor of low-grade malignancy and treated as such. Surgery is the treatment of choice with complete resection at the first surgical procedure if technically feasible [3, 15]. The long-term prognosis is generally favorable.

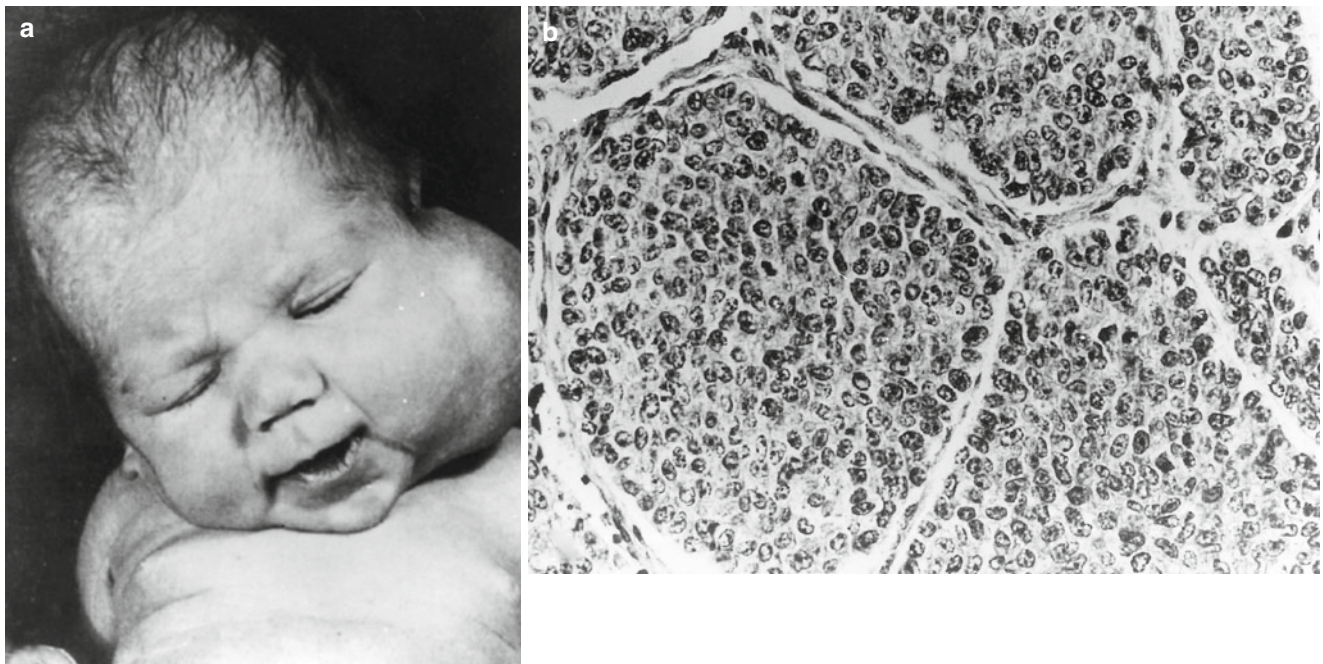


Fig. 16.3 Sialoblastoma. (a) Newborn with a large tumor of the left parotid salivary gland. It overlies the angle of the mandible and distorts the contour of the ear. (b) Irregular lobules and sheets of small, irregular

cells with vesicular nuclei are separated by delicate connective tissue septae (Reprinted from Lack [5]. With kind permission of © JAMA Network, 1988; Reprinted from Isaacs [12]. © Springer-Verlag, 2002)

Table 16.2 Sialoblastoma ($n=30$)

Sex	
Male	16 M/F=1.3
Female	12
Sex not stated	2
Antenatal diagnosis	3
Postnatal diagnosis	27
Initial presentation	
Mass over mandible	20 (57.1) ^a
Mass beneath mandible	8 (22.9)
Facial mass on antenatal sonography	3 (8.6)
Dystocia	3 (8.6)
Facial paralysis at birth	1 (2.8)
Location	
Parotid gland	22 (73.3), P/S=3.1
Submandibular gland	7 (23.3)
Salivary gland, not specified	1 (3.4)
Pathology	
Gross	
Tumor greatest dimension (cm)	6 cm, range 1–15
Tumor weight (g)	233 g, range 50–530
Facial nerve invasion by tumor	6 (20)
Recurrences ^b	7 (23)
Metastases ^c	3 (10)
Treatment and survival	
Patients treated	29 (97)
Patients not treated ^d	1 (3)
Survival with surgery alone	21/22 (95)
Outcome	
Fetal survival	3/3 (100)
Postnatal survival	25/27 (93)
Patients treated survived	29/30 (97)
Patients not treated survived	0/1
Overall survival	28/30=93 %

Source: 30 cases selected from the literature

^aValues in parentheses are percentages

^bTwo patients had two recurrences and five had one

^cMetastases to regional lymph nodes and/or adjacent soft tissues

^dPatient not treated died at age 10 days of unrelated causes, tumor diagnosed at necropsy

16.3 Congenital Pleomorphic Adenoma (Salivary Gland Anlage Tumor)

The *congenital pleomorphic adenoma of the nasopharynx* presents in the first 3 months of life with airway obstruction, progressive respiratory distress, and feeding problems [2, 12, 20, 23] (Fig. 16.4 and Table 16.3). Larger lesions may mimic choanal atresia because of the obstructive symptoms produced.

This midline, pedunculated polypoid tumor of the nasopharynx measures 1–3 cm in diameter. Histologically, it shows an outer surface epithelium composed of nonkeratinized stratified squamous epithelial cells, a hypocellular sub-

mucosa with duct-like structures and nests of squamous epithelium communicating with the surface mucosa, and central (mesenchymal) stromal-like nodules blending in with ductules [2, 10, 20] (Fig. 16.4c–e).

Immunohistochemical studies reveal diffuse immunoreactivity for salivary gland amylase, cytokeratin, and epithelial membrane antigen in epithelial structures and reactivity with vimentin, cytokeratin, and muscle-specific actin in the stroma-like nodules [2]. Myoepithelial cells characteristically express cytokeratin and actin. EM findings are consistent in the immunohistochemical studies. Myoepithelial cells with basal lamina, desmosomes, and bundles of microfilaments are noted in the nodules in addition to cells with epithelial features [2].

Congenital pleomorphic adenoma is distinguished from sialoblastoma, which occurs predominately within the parotid. The adenoma arises from the nasopharynx, has a different histological appearance, and conceivably represents a different stage of development of the salivary gland [2]. The main differential diagnosis of a midline nasopharyngeal mass in a newborn, other than the pleomorphic adenoma, is teratoma, dermoid hairy polyp, craniopharyngioma, encephalocele, glial heterotopia, rhabdomyosarcoma, and hemangioma [23].

Dehner et al. suggest that the salivary gland anlage tumor¹ represents a hamartoma² of minor salivary gland origin that histologically recapitulates the development of the gland because of the presence of the myxoid stroma with ductules and squamous nests [2].

There were no instances of recurrence or metastases in the 20 cases of salivary gland anlage tumor reviewed from the literature. Surgical excision results in cure [2, 12, 20] (Table 16.3).

16.4 Miscellaneous Salivary Gland Tumors and Tumorlike Conditions

The most common benign and malignant major salivary gland tumors in the pediatric age group are the pleomorphic adenoma (mixed tumor) and mucoepidermoid carcinoma, respectively [5]. They are extremely rare in the first year of life [12]. Krolls et al. reported a pleomorphic adenoma of the parotid in a 10-day-old male, which apparently was an incidental postmortem finding, and a parotid mucoepidermoid carcinoma in a 6-month-old male that had metastasized to the maxilla and regional lymph nodes [6]. Of 34 major salivary gland tumors in the study of Kaufman and Stout, only three (9 %) occurred in infants (two were congenital), and all three were diagnosed as undifferentiated carcinoma [1]. The

¹Anlage or *primordium* is the first indication of an organ or structure, its earliest stage of development.

²Hamartoma is an overgrowth of mature cells and tissues that normally occur in the affected part.

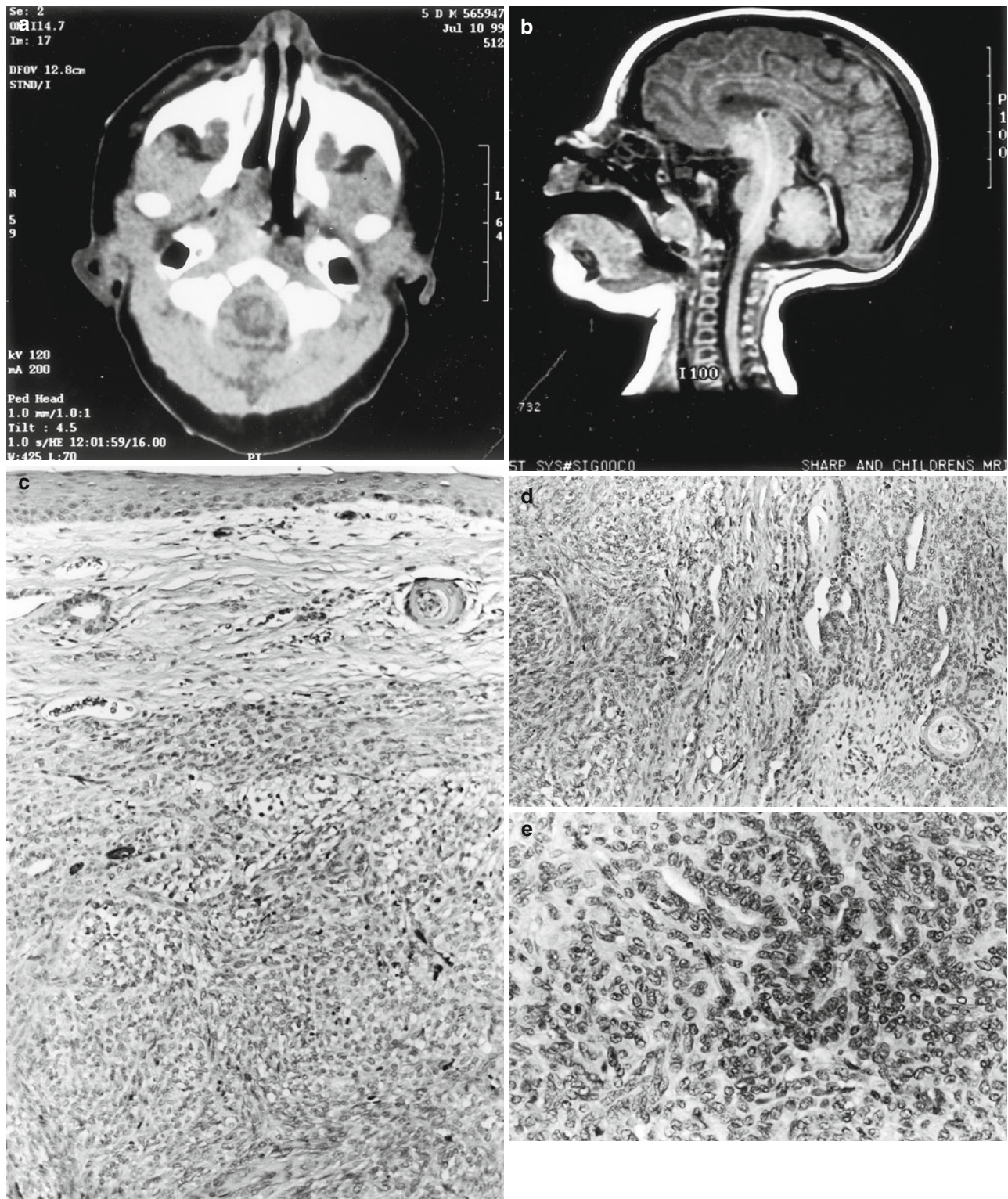


Fig. 16.4 Pleomorphic adenoma (salivary gland anlage tumor). Ten-day-old male with respiratory and feeding difficulties since birth. (a) CT axial scan through the skull base without contrast reveals a nasopharyngeal mass of soft tissue density extending from the nasal choanae to the retropharyngeal soft tissues. (b) MRI shows a 2×1.4×1.3-cm, pedunculated, enhancing, soft tissue mass within the nasopharynx (c) low magnification revealing an intact, nonkeratinized, stratified squamous epithelial mucosa on the top, hypocellular submucosa containing a duct-like structure and a round nest of squamous cells. (d)

Cystic squamous nest and duct-like structures adjacent to a stromal-like nodule (*on the left*). (e) Higher magnification of a stromal-like nodule displaying the relationship between ducts or glands and stroma. (f) Squamous nests and cells within stromal-like nodule showing cytokeratin immunoreactivity. In addition, vimentin and actin were expressed by cells comprising stromal-like nodules. (b, c) H&E; (d) PAS; (e) Cytokeratin immunoperoxidase (Louis Dehner, M.D., kindly reviewed the case and provided us with the diagnosis. Reprinted from Isaacs [12]. © Springer-Verlag, 2002)

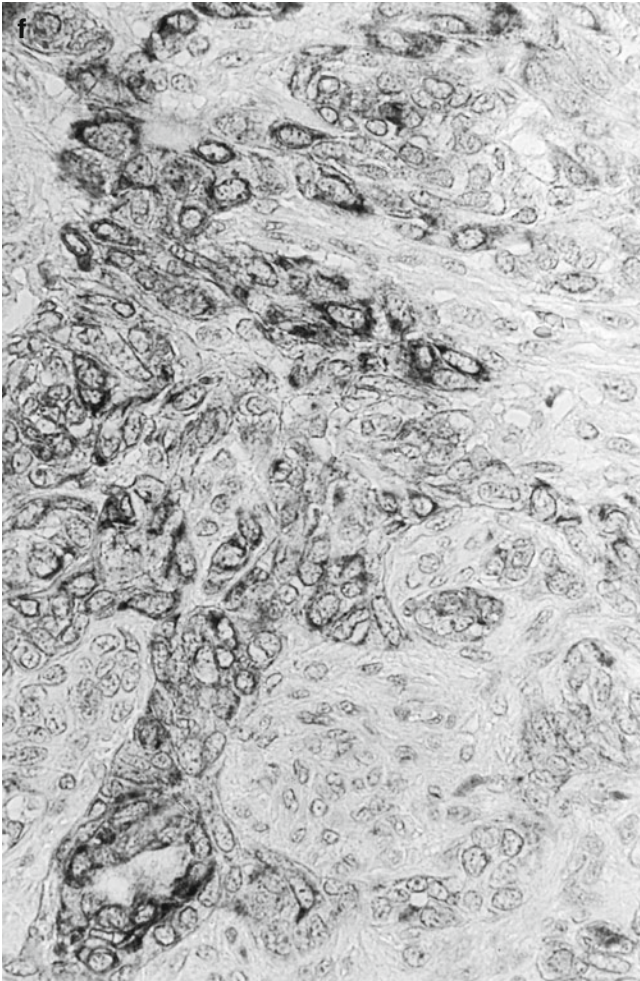


Fig. 16.4 (continued)

Table 16.3 Neonatal salivary gland anlage tumor ($n=20$)

Sex	
Male	15 M/F=3.75/1
Female	4
Sex not stated	1
Antenatal diagnosis	None
Postnatal diagnosis	20
Clinical presenting findings	
Nasopharyngeal mass ^a	17
Respiratory distress	15
Difficulty feeding	5
Nasal obstruction	4
Epistaxis	1
Stridor	1
Facial plethora	1
Location	
Nasopharynx	20
Wall	15
Posterior nasal septum	5
Tumor attached by pedicle	14
Size, greatest dimension (cm)	2.4 cm, range 1.3–4 cm
Treatment	
Patients treated	19/20 (95) ^b
Patients not treated ^a	1
Survival with excision	19/19 (95)
Recurrence after surgery	0
Outcome	
Patients treated survived ^c	18/19 (94)
Patients not treated survived	1/1
Patients lost to follow-up	1
Overall survival	19/20=95 %

Source: 20 cases selected from the literature

^aSpontaneous expulsion of the tumor occurred during resuscitation in one patient

^bValues in parentheses are percentages

^cOne patient died at age 6 months of sepsis; no residual tumor was found at necropsy

carcinomas were characterized as rapidly growing, inoperable tumors fixed to adjacent structures, local and distant metastases, and a short survival [1]. This malignancy occurred also in a 2,300-g male newborn who had a large submandibular gland primary that metastasized to the bones of the face and skull, larynx, palate, regional lymph nodes, and adrenal [12] (Fig. 16.5).

*Mucocele*s are the foremost minor salivary gland lesion in children. Surgical excision is a common procedure for correction of this curable condition. Congenital *cystic choristomas*³ of the submandibular gland composed of gut and respiratory epithelium are described [24, 25]. A *gastric heterotopia*⁴ occurred in a cyst of the submandibular gland in an 8-month-old male[1].

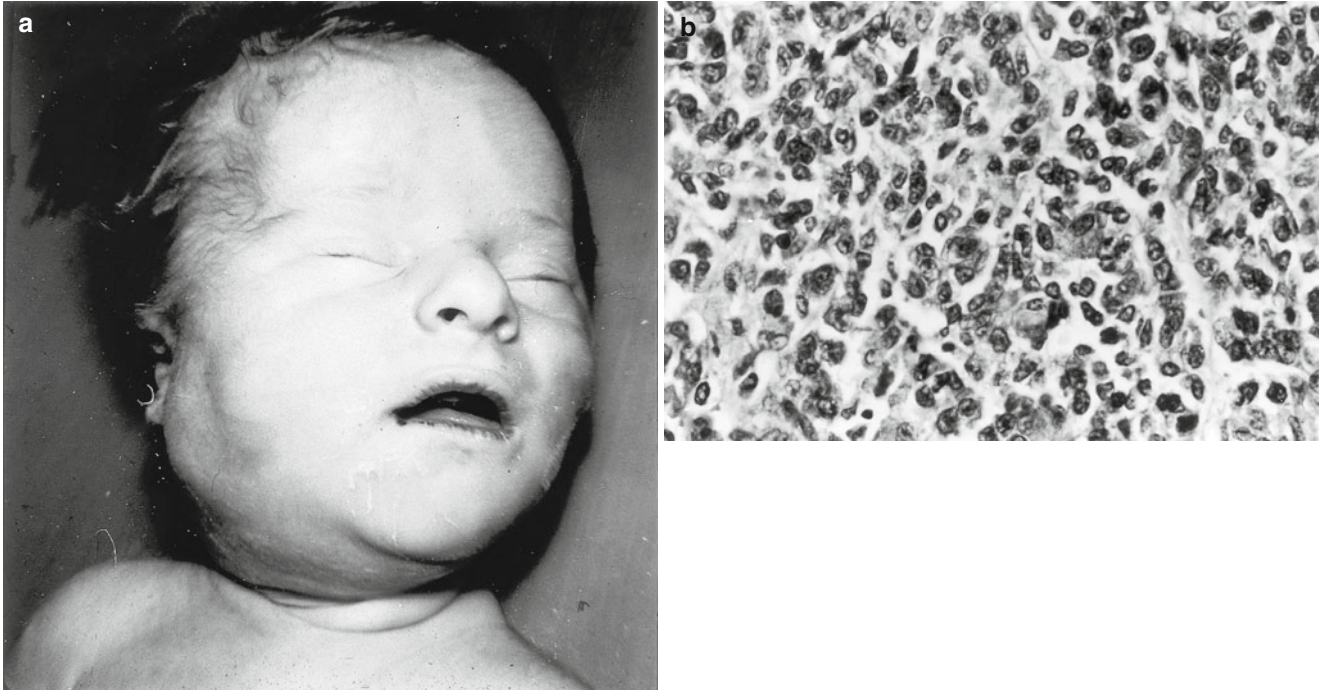


Fig. 16.5 Congenital undifferentiated carcinoma of submaxillary gland. (a) One-day-old, 2,300-g male with a large cervicofacial mass, respiratory distress, and a maternal history of polyhydramnios. (b) The tumor consists of cells with pleomorphic, atypical nuclei, and vacuo-

lated cytoplasm. Mitoses are present. In the lower right-hand corner, there is a duct-like structure (Reprinted from Isaacs [10]. © WB Saunders 1997)

³ *Choristoma* is tissue histologically normal for an organ or part other than the area at which it is situated.

⁴ *Heterotopia* is the presence of a tissue in an abnormal location.

References

1. Kauffman SL, Stout AP (1963) Tumors of the major salivary glands in children. *Cancer* 16:1317–1331
2. Dehner LP, Valbuena L, Perez-Atayde A et al (1994) Salivary gland anlage tumor (“congenital pleomorphic adenoma”). A clinicopathologic, immunohistochemical and ultrastructural study of nine cases. *Am J Surg Pathol* 18:25–36
3. Hsueh C, Gonzalez-Crussi F (1992) Sialoblastoma: a case report and review of the literature on congenital epithelial tumors of salivary gland origin. *Pediatr Pathol* 12:205–214
4. Fonseca I, Martins AG, Soares J (1991) Epithelial salivary gland tumors of children and adolescents in southern Portugal. *Oral Surg Oral Med Oral Pathol* 72:696–701
5. Lack EE, Upton MP (1988) Histopathologic review of salivary gland tumors in childhood. *Arch Otolaryngol Head Neck Surg* 114:898–906
6. Kroll SO, Trodahl JN, Boyers RC (1972) Salivary gland lesions in children: a survey of 430 cases. *Cancer* 30:459–469
7. Schuller DE, McCabe BF (1977) Salivary gland neoplasms in children. *Otolaryngol Clin North Am* 10:399–412
8. Seifert G, Donath K (1997) The congenital basal cell adenoma of salivary glands. Contribution to the differential diagnosis of congenital salivary gland tumours. *Virchows Arch* 430:311–319
9. Bianchi A, Cudmore RE (1978) Salivary gland tumors in children. *J Pediatr Surg* 13:519–521
10. Isaacs H Jr (1997) Salivary gland tumors. In: *Tumors of the fetus and newborn*, vol 35. W.B. Saunders, Philadelphia, pp 365–369
11. Isaacs H Jr (1997) Tumors. In: Gilbert-Barnes E (ed) *Potter’s pathology of the fetus and infant*, vol 2. Mosby, St. Louis, pp 1242–1339
12. Isaacs H Jr (2002) Salivary gland tumors. In: *Tumors of the fetus and infant: an atlas*. Springer, New York, pp 367–376
13. Dehner LP (1981) Neoplasms of the fetus and neonate. In: Naeye RL, Kissane JM, Kaufman N (eds) *Perinatal diseases*, International Academy of Pathology, Monograph number 22. Williams and Wilkins, Baltimore, pp 286–345
14. Isaacs H (2010) Perinatal neurofibromatosis: two case reports and review of the literature. *Am J Perinatol* 27:285–292
15. Roth A, Micheau C (1986) Embryoma (or embryonal tumor) of the parotid gland: report of two cases. *Pediatr Pathol* 5:9–15
16. Wawter GF, Tefft M (1966) Congenital tumors of the parotid gland. *Arch Pathol* 82:242–245
17. Ortiz-Hidalgo C, de Leon-Bojorge B, Fernandez-Sobrinho G et al (2001) Sialoblastoma: report of a congenital case with dysembryonic alterations of the adjacent parotid gland. *Histopathology* 38:79–80
18. Batsakis JG, Frankenthaler R (1992) Embryoma (sialoblastoma) of salivary glands. *Ann Otol Rhinol Laryngol* 101:958–960
19. Taylor GP (1988) Case 6 congenital epithelial tumor of the parotid-sialoblastoma. *Pediatr Pathol* 8:447–452
20. Har-EL G, Zirkin HY, Tovi F et al (1985) Congenital pleomorphic adenoma of the nasopharynx (report of a case). *J Laryngol Otol* 99:1281–1287
21. Ito M, Nakagawa A, Nakayama A et al (1990) Undifferentiated carcinoma of the parotid gland in a 10-month old child. *Acta Pathol Jpn* 40:149–152
22. Harris MD, McKeever P, Robertson JM (1990) Congenital tumours of the salivary gland: a case report and review. *Histopathology* 17:155–157
23. Boccon-Gibod LA, Grangeponde MC, Boucheron S et al (1996) Salivary gland anlage tumor of the nasopharynx: a clinicopathologic and immunohistochemical study of three cases. *Pediatr Pathol Lab Med* 16:973–983
24. Tang TT, Glicklich M, Siegesmund KA et al (1979) Neonatal cystic choristoma in submandibular salivary gland simulating cystic hygroma. *Arch Pathol Lab Med* 103:536–539
25. Smart PJ, Lendon M (1992) Choristoma of the submandibular gland: a rare cause of cervical swelling. *J Pediatr Surg* 27:1498–1499

17.1 Introduction

Both benign and malignant lung tumors are uncommon in the fetus and infant. Metastatic disease is more prevalent [1–7]. Rhabdomyosarcoma, Wilms' tumor, hepatoblastoma, rhabdoid tumor, and yolk sac tumor are the main malignant neoplasms that metastasize to the lungs during the first year of life. In patients with Leukemia, the pulmonary vessels may contain leukemic cells, and these cells may infiltrate the alveolar wall; perivascular infiltrates are found in severe cases [1, 5, 7].

Some nonneoplastic conditions may mimic tumors, for example, abscess and organizing bacterial pneumonia, or congenital anomalies such as bronchogenic cyst, extrapulmonary sequestration, cystic adenomatoid malformation, and pulmonary lymphangiectasis [2, 5, 8–14] (Figs. 17.1, 17.2, and 17.3). Lymphoproliferative disorders may present with pulmonary nodules simulating metastatic tumor [12] (Fig. 17.4).

Table 17.1 lists the various tumors and tumorlike conditions of the lung found in the fetus and infant.

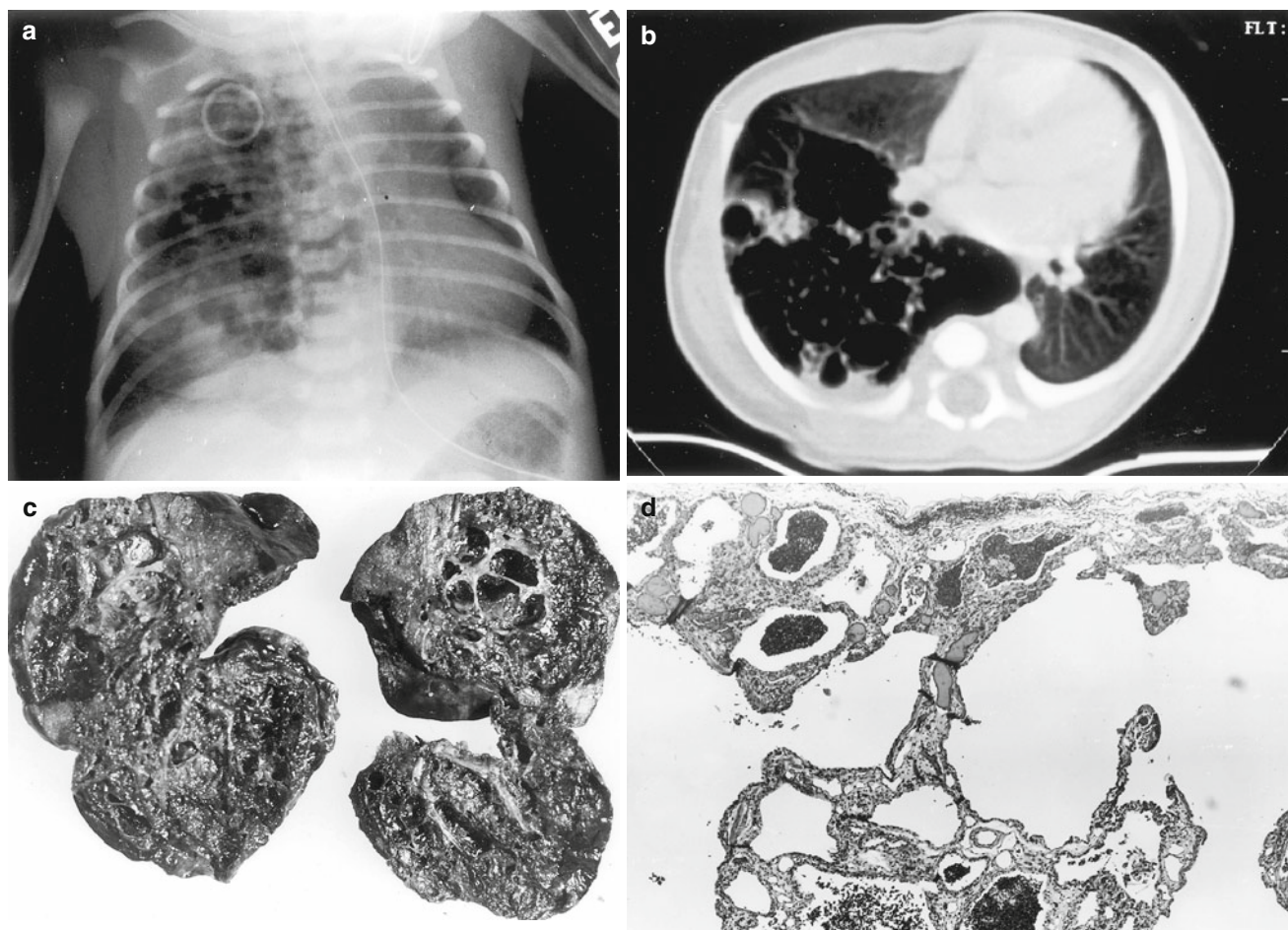


Fig. 17.1 Cystic adenomatoid malformation, type I. Eight-day-old male with progressive respiratory distress since birth. **(a)** Chest X-ray reveals multiple large cysts within the right upper lobe with a shift of mediastinal structures to the left chest. **(b)** CT scan shows the cysts and compression of the right lower and middle lobes in more detail. **(c)** The

specimen consists of the right upper lobe and a portion of the middle lobe measuring $6.0 \times 6.0 \times 1$ cm and weighing 23 g. The upper lobe contains several multilocular cysts, the largest measuring 2.5 cm. **(d)** Several irregular, small, and large cysts are lined by columnar epithelium (Reprinted from Isaacs [7]. © Springer-Verlag, 2002)

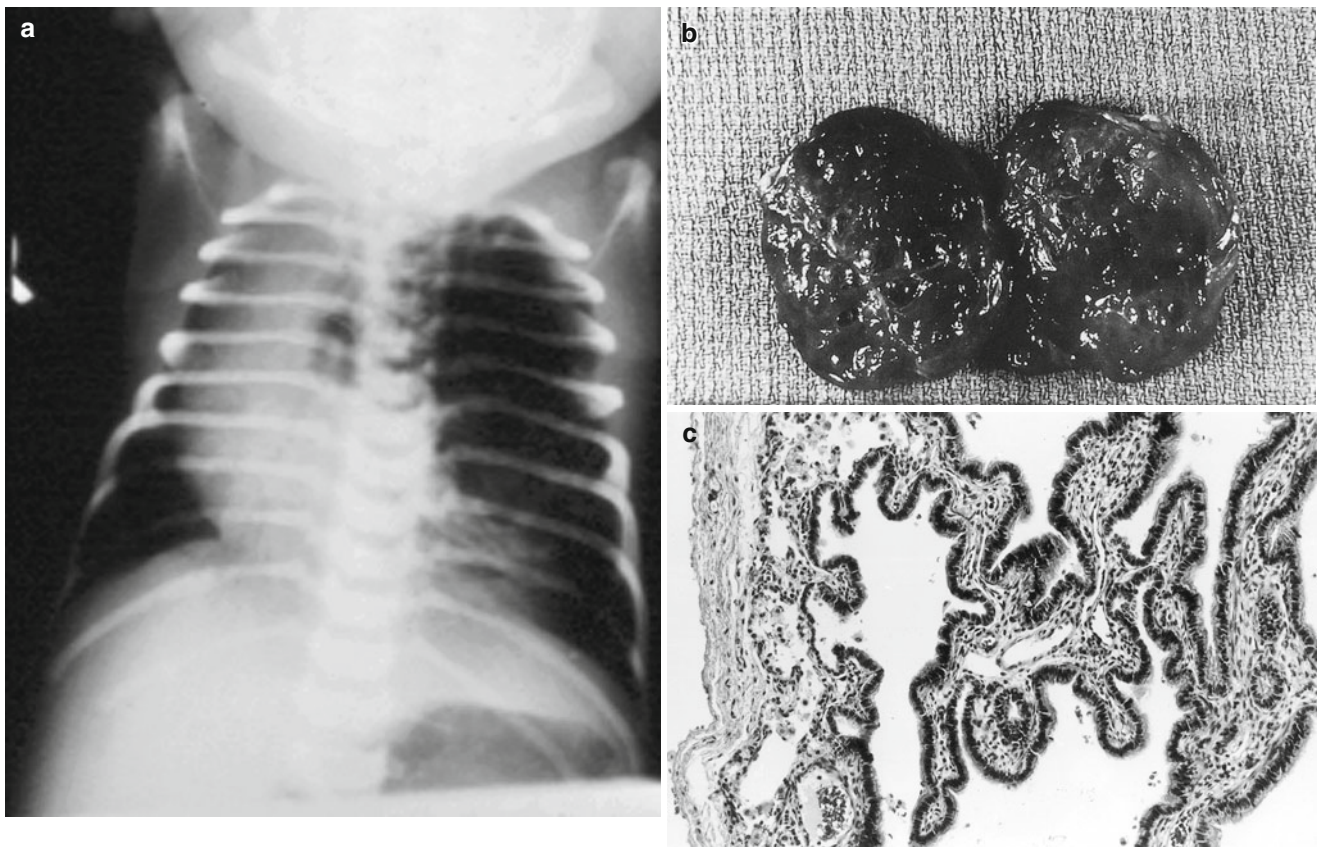


Fig. 17.2 Cystic adenomatoid malformation, type II. Newborn presented with severe respiratory distress. **(a)** Chest X-ray demonstrating a cystic lesion in the right lung, upper lobe, producing a mediastinal shift to the right. **(b)** The specimen consists of firm, congested lung with many

small cysts less than 1 cm in diameter. **(c)** The cysts are lined by cuboidal to columnar epithelium, resembling ectatic terminal bronchioles. The wall of the cysts contains only a few, scattered smooth muscle fibers and capillaries (Reprinted from Isaacs [7]. © WB Saunders 1997)

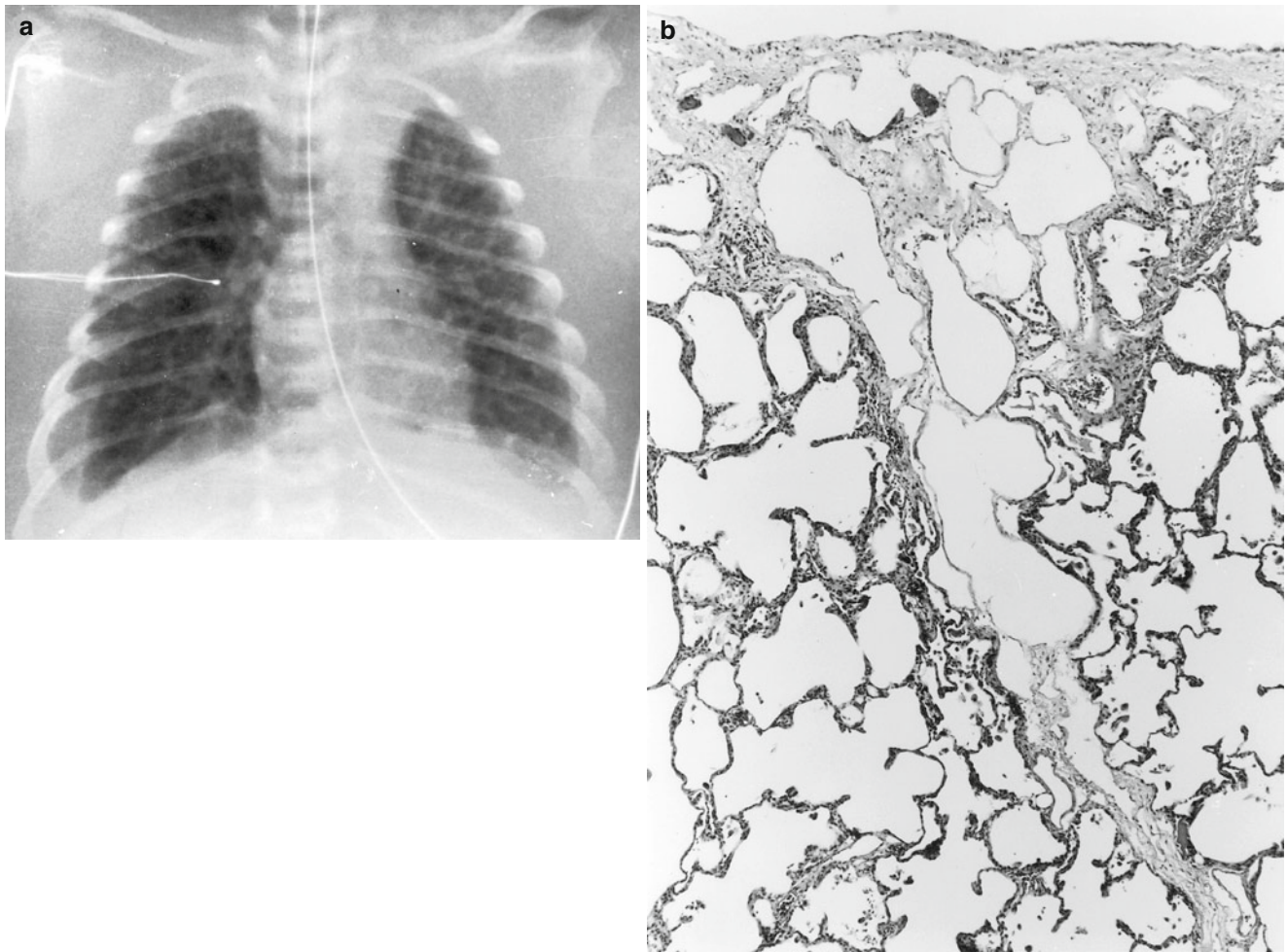


Fig. 17.3 Congenital pulmonary lymphangiectasis. Five-month-old female with increasing chronic pulmonary insufficiency. (a) Chest film reveals a coarse reticulonodular pattern within both lungs consistent

with pulmonary lymphangiectasis. (b) Severely dilated lymphatics are present within the interlobular septa and beneath the pleura (Reprinted from Isaacs [7]. © Springer-Verlag, 2002)

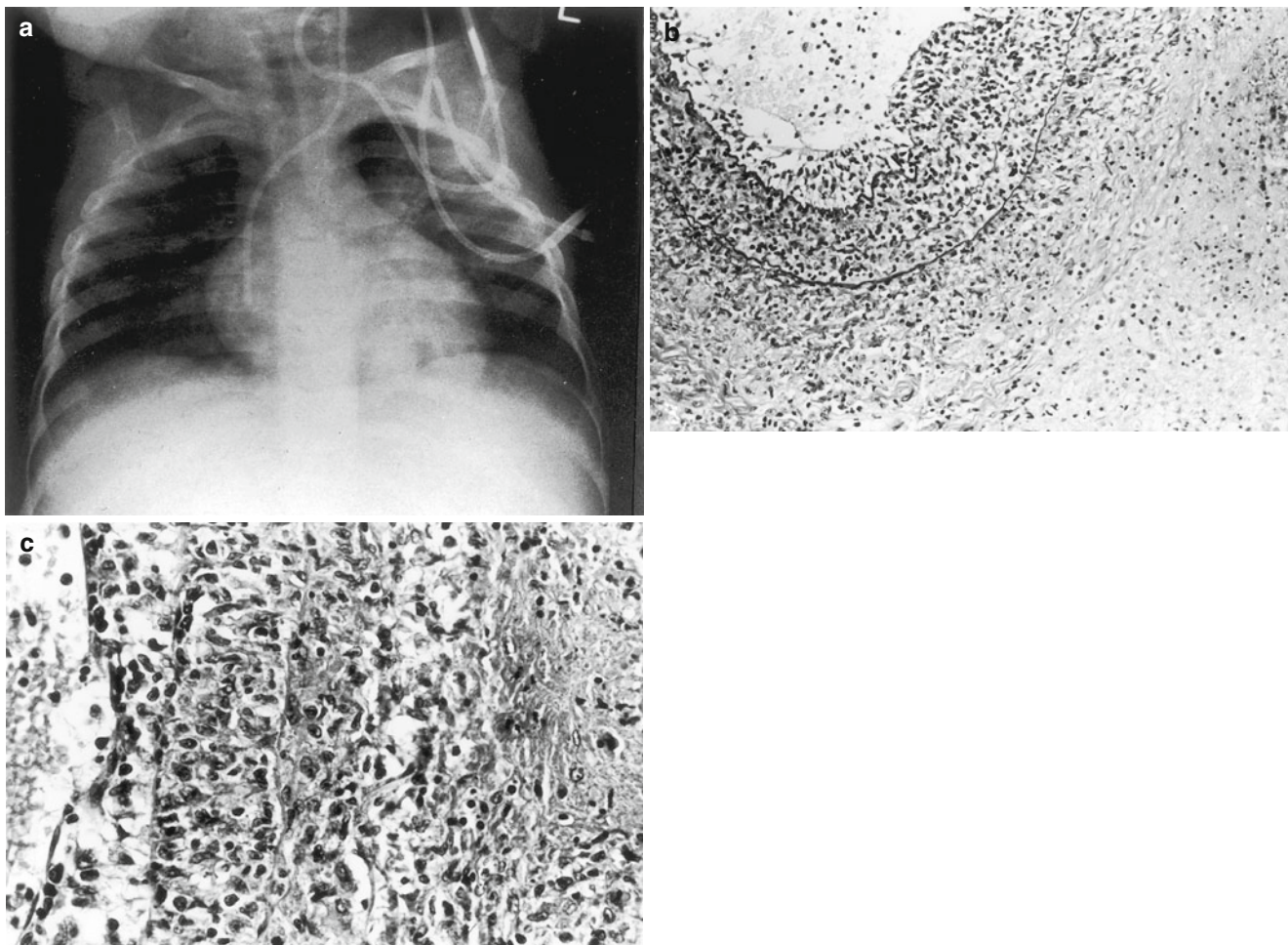


Fig. 17.4 Lymphomatoid granulomatosis. One-year-old male with chronic otitis media and failure to thrive. The baby had hypogammaglobulinemia and Epstein-Barr virus infection. (a) Chest radiogram reveals bilateral pulmonary nodules. (b) Lung biopsy shows a necrotizing vasculitis involving a pulmonary artery (the artery has both an internal and external elastic lamina) accompanied by adjacent infarcts. (c) Higher magnification displays vascular necrosis, edema, and infiltration by lymphocytes, plasma cells, and atypical lymphoid cells. The vascu-

lar lumen is on the left. At postmortem examination, similar yellow-tan, necrotic, vasculitic nodules were found in the kidneys, adrenals, liver, and lymph nodes. Giant cells and palisading epithelioid cells characteristic of Wegener's granulomatosis were not found. (b) Verhoff-Van Giesen (elastic) stain; (c) H&E (Reprinted from Lehman et al. [12]. With kind permission of © Journal of Rheumatology, 1989; Reprinted from Isaacs [7]. © Springer-Verlag, 2002)

Table 17.1 Fetal and infant tumors and tumorlike conditions of the lung

Inflammatory pseudotumor (plasma cell granuloma, inflammatory myofibroblastic tumor)
Rhabdomyomatous dysplasia (rhabdomyomatosis)
Cystic adenomatoid malformation
Extralobar pulmonary sequestration
Congenital pulmonary lymphangiectasis
Lymphangioma
Hemangioma
Myofibromatosis (fibromatosis)
Pulmonary myofibroblastic tumor
Pleuropulmonary blastoma
Primitive neuroectodermal tumor of the chest wall
Teratoma
Langerhans cell histiocytosis
Laryngotracheal papillomatosis
Juvenile xanthogranuloma
Lymphoproliferative disorders
Tumors metastatic to the lung
Leukemia
Hepatoblastoma
Rhabdomyosarcoma
Neuroblastoma
Wilms' tumor
Rhabdoid tumor
Yolk sac tumor

Reprinted from Isaacs [7]. © Springer-Verlag, 2002

17.2 Inflammatory Pseudotumor

Inflammatory pseudotumor is one of the major tumor or tumorlike conditions of the lung in children [2, 5, 7]. However, it seldom occurs during the first year of life. Inflammatory pseudotumor is a benign lesion, probably a reactive inflammatory process, that can mimic a neoplasm. Although the lung is the most common and well-known site, it occurs also in brain, orbit, small intestine, bladder, mesentery, spleen, retroperitoneum, heart, liver, and skin [2, 5, 13, 14]. Other names for this condition are plasma cell granuloma, inflammatory pseudotumor, and inflammatory myofibroblastic tumor [2, 5, 8, 12, 13]. Inflammatory pseudotumor is characterized by slow growth, instances of spontaneous resolution, and generally a favorable prognosis in infants.

Grossly, the inflammatory pseudotumor consists of a firm, circumscribed grayish-white to yellow nodule situated usually at the periphery of the lung. Three different histological patterns are described: organizing pneumonia, fibrous histiocytoma, and lymphoplasmacytic [2, 14] (Fig. 17.5). Immunohistochemical and EM studies show that the spindle cells are fibroblasts and myofibroblasts; hence, the term *inflammatory myofibroblastic tumor* has been applied by some [8]. Morphological evaluation for cellularity, mitosis, or inflammatory infiltrate does not appear to be useful for prediction of clinical outcome [13].

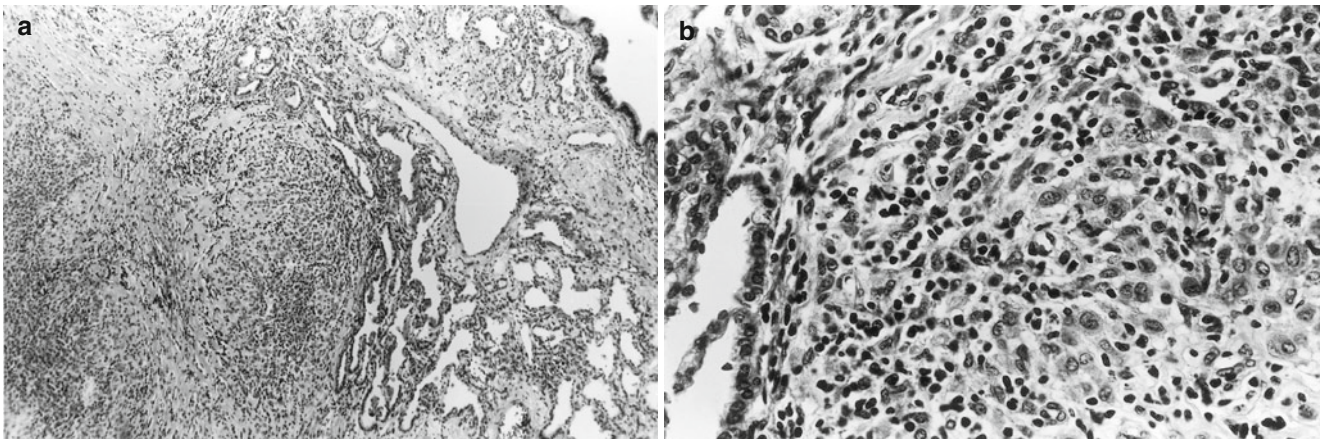


Fig. 17.5 Inflammatory pseudotumor. One-week-old female with a 3.5×2.5-cm, subpleural mass removed from the left lung, upper lobe. (a) Within the lung, there is a nodular inflammatory cell infiltrate with

fibrosis. (b) The infiltrate consists mostly of lymphocytes and histiocytes with a rare plasma cell (Reprinted from Isaacs [6]. © WB Saunders 1997)

17.3 Fibromatoses (Myofibromatoses)

Fibromatosis of the lungs usually occurs as part of a congenital disseminated disease termed generalized or *visceral fibromatosis (myofibromatosis)* [1, 5, 7, 15]. In this condition, multiple fibrous nodules are found in the skin, musculoskeletal system, and viscera. The tumors are composed of fibroblasts and myofibroblasts showing storiform, vascular, and hemangiopericytomatous growth patterns. Congenital generalized fibromatosis is classified into two main types: type I, patients with involvement of the skin, subcutaneous tissue, muscle, and bone, and type II, those with visceral involvement [15]. Pulmonary lesions in generalized fibromatosis portends a poor prognosis [7, 15] (see Chap. 4).

17.4 Vascular Conditions

Vascular conditions are unusual in the lungs of infants and children. *Hemangiomas* of the lung are uncommon [5, 8]. Many lesions reported as hemangiomas are *congenital malformations of the pulmonary vasculature*, variously called pulmonary arteriovenous fistula or aneurysms, congenital arteriovenous malformation, and pulmonary angiomatosis [5, 7]. Patients with these conditions may have associated vascular malformations in other organs such as in the mucus membranes, skin, and brain forming part of a more generalized syndrome of *hereditary telangiectasia*, for example, in the Rendu-Osler-Weber disease. Familial occurrence is reported [5, 7]. Multiple pulmonary hemangiomas may occur as part of a fatal syndrome, *diffuse hemangiomatosis of the newborn*, where cutaneous hemangiomas are associated with similar lesions in the brain, liver, lung, and other organs (see Chaps. 4 and 5).

Similar to the soft tissues and skin, *infantile hemangiomas* are composed of either capillary and/or cavernous components typically showing a lobular growth pattern. They are accompanied by prominent “feeding” arterial and venous blood vessels sometimes forming large arteriovenous-like malformations. Capillary and cavernous hemangiomas are lined by regular plump or flattened endothelial cells and differ only in their diameter [5–7] (see Chap. 4).

17.5 Congenital Pulmonary Cystic Diseases

Congenital cystic diseases of the lung, for example, *congenital cystic adenomatoid malformation (CCAM)*, may clinically mimic a neoplasm and later on become a source of malignancy within the cyst(s) [1, 2, 5–9, 16–20]. Rhabdomyosarcoma and pleuropulmonary blastoma are examples of malignancies arising from lung cysts [16, 17].

17.5.1 Congenital Cystic Adenomatoid Malformation

Congenital cystic adenomatoid malformation (CCAM) is a relatively common congenital pulmonary anomaly with a variable prognosis depending on the size of the lesion, the pathological subtype, and the presence or absence of clinical complications [5, 7, 18, 19]. In fetuses where large lesions are associated fetal hydrops, the prognosis for survival is bleak [18, 19]. The malformation is almost always unilateral without predilection for right or left side and usually limited to one lobe. An arrest in lung development has been suggested as one of the causes [20]. There are a wide variety of congenital anomalies associated with CCAM. Bilateral renal

agenesis, renal dysplasia, hydrocephalus, extralobar pulmonary sequestration, cardiac defects, and diaphragmatic hernia are a few examples [5, 7, 20]. The lesion is detected antenatally as early as 21 weeks gestation presenting as a mediastinal shift by sonography [19]. Many affected infants develop respiratory distress on the first day of life but the malformation may not become clinically evident until later on in childhood [19].

On the basis of its gross and histological findings, CCAM has been divided into three main types: I, II, and III [2, 8]. *Type I* consists of one or more *large cysts* with fibrous septae lined by columnar or cuboidal epithelial cells (Fig. 17.1). *Type II* contains many smaller cysts less than 1.2 cm lined by ciliated columnar epithelial cells resembling dilated terminal bronchioles (Fig. 17.2). Skeletal muscle may be found in the septa or adjacent to the cysts. The least common form, *solid type III*, is composed of a firm, bulky mass that occupies much of a lung lobe. Histologically, type III consists of *dilated irregularly branching bronchiole-like structures separated by alveolar-like spaces* lined by low cuboidal epithelium [2, 8]. The more prevalent macrocystic lesion, type I, is less often associated with fetal hydrops and has a more favorable prognosis than the other types, II and III. Particularly the solid (type III) can mimic a tumor on imaging studies, grossly and sometimes microscopically.

17.6 Laryngotracheal Papilloma

Laryngotracheal papilloma (*juvenile papilloma, squamous papilloma*) is a relatively frequent, benign tumor arising most often in the larynx [5, 7, 21–25]. The occurrence of many, recurrent papillomas in the larynx and tracheobronchial tree is called *papillomatosis*. In 5–10 % of individuals, papillomas

extend distally into the trachea and in less than 1 % into the adjacent lung [2]. The stated incidence is 1,500–2,000 infants and children in the USA per year [7]. *Human papillomavirus (HPV), types 6 and 11*, is considered to be the etiologic agent; condylomata situated around the birth canal have been proposed as the source of the virus [2, 21, 22]. Papillomas occur most often during the first 3 years of life.

Papillomas in the larynx cause hoarseness and inspiratory stridor eventually leading to severe respiratory distress if not treated [2, 21]. Typically, the clinical course is characterized by multiple recurrences requiring numerous resections and sometimes a lifesaving tracheostomy. Extensive laryngeal-tracheal papillomatosis can be the cause of sudden unexpected death from suffocation in a young child [6].

Spontaneous regression usually occurs by late adolescence, but occasionally, there is extension into the peripheral airway and lungs with cavity formations filled with numerous papillomas [2, 23–25]. Progression to squamous cell carcinoma has been documented [25].

Papillomas present as one or more tiny, papillary or sessile, wartlike growths projecting from the laryngeal and tracheal mucosa. Occasionally, the mucosa is covered by numerous lesions which obstruct the airway (Fig. 17.6). Microscopically, they consist of papillary formations composed of stratified squamous epithelium displaying maturation toward the surface and varying degrees of *koilocytosis*. Focal atypia and increased mitotic activity are not unusual. The epithelium rests on a slender fibrovascular core. *Koilocytosis, the presence of vacuolated epithelial cells with clear cytoplasm or perinuclear halos and angular nuclear pyknosis*, is a prominent feature indicative of *viral cytopathic effect*. Human papillomavirus, specifically type 11 and less often type 6, has been isolated from these lesions and from maternal condylomas [22, 23].

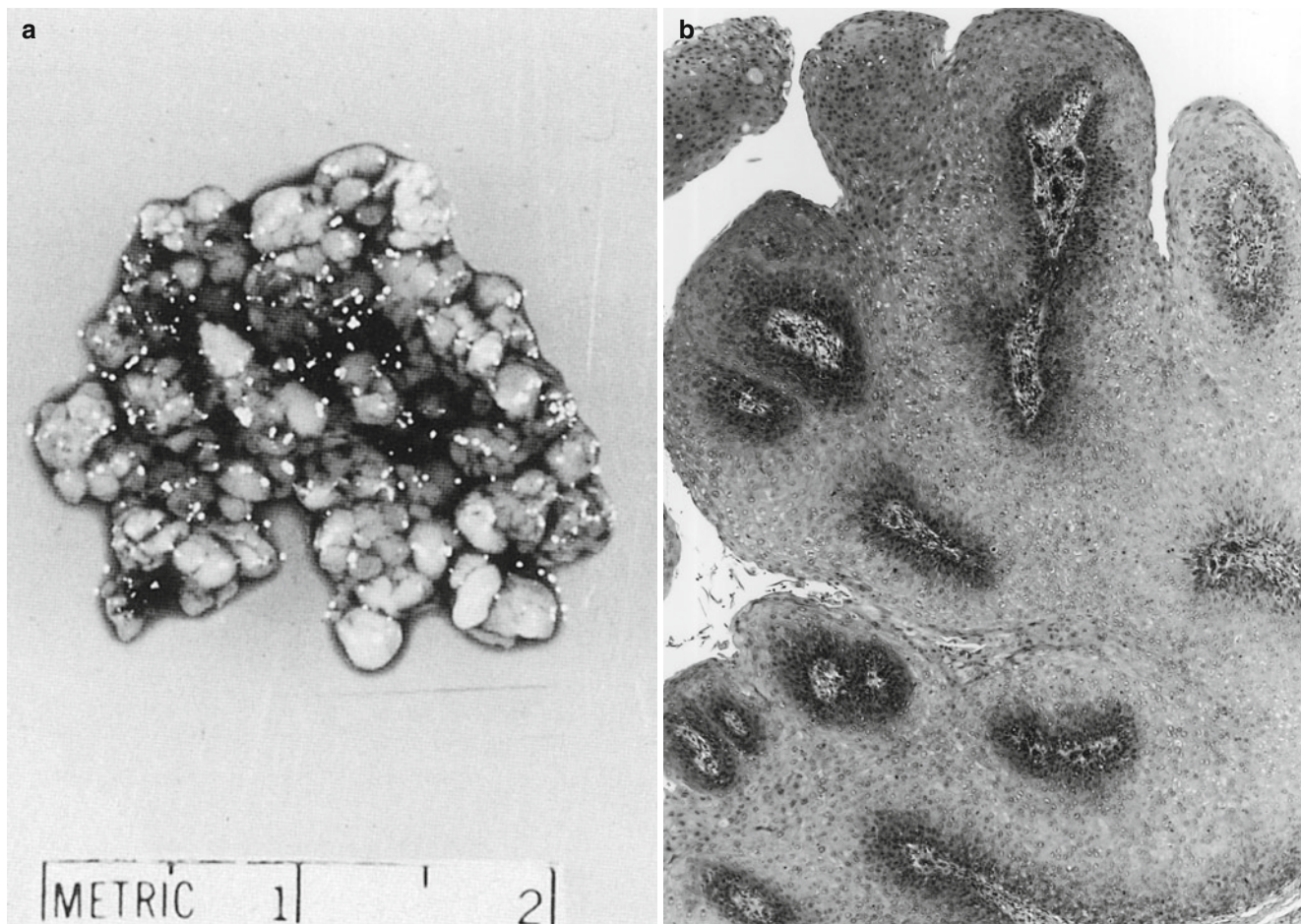


Fig. 17.6 Laryngotracheal papilloma. (a) Multiple papillomas removed from the larynx of a child with hoarseness and respiratory distress consist of pale gray-white cauliflower-like growths. (b)

Papillary formations composed of nonkeratinized stratified squamous epithelium rest on a fibrovascular core. Minimal koilocytotic atypia is present (Reprinted from Isaacs [6]. © WB Saunders 1997)

17.7 Congenital Pulmonary Myofibroblastic Tumor

Congenital pulmonary myofibroblastic tumor is a spindle cell neoplasm unique to the neonate. The tumor has been variously called *bronchopulmonary fibrosarcoma*, *leiomyosarcoma*, *hamartoma*, and *mesenchymal tumor or malformation* [1, 2, 7, 24, 26–30]. Although pulmonary myofibroblastic tumor is rare, it is one of the leading congenital primary tumors of the lung during the first year of life [26–30]. Newborns with this neoplasm present with severe respiratory distress occurring soon after birth [27]. McGinnis et al. proposed the name for this tumor and suggested that it is histologically analogous to the renal congenital mesoblastic nephroma [29]. Despite its ominous histological appearance, it behaves in a benign fashion if adequately treated [26].

Pulmonary myofibroblastic tumor arises from either the bronchus or from the lung parenchyma. McGinnis et al. suggest that the neoplasm develops from the mesenchyme that surrounds primitive respiratory ducts [29] (Fig. 17.7). The tumors range in size from 3.5 to 6 cm. Grossly, they are firm, gray, yellow, or light tan with focal hemorrhage and cyst for-

mation. Histological examination reveals a cellular tumor with spindle-shaped cells forming interdigitating fascicles similar to those observed in the soft tissue congenital fibromatosis or fibrosarcoma. Central necrosis and dystrophic calcification may be present [26]. The mitotic rate varies from moderate to high. Benign entrapped bronchoalveolar elements are present.

Immunohistochemical and EM findings indicate a fibroblastic-myofibroblastic origin. The tumor cells are immunoreactive with vimentin; the muscle markers desmin and actin are focally positive. Tumor cells are nonreactive with neuron-specific enolase, S-100, leu-7, and α -1-antichymotrypsin [26, 28, 29].

EM shows spindle-shaped tumor cells displaying indented nuclei and infrequent nucleoli. The cytoplasm contains a prominent rough endoplasmic reticulum and intermediate filaments. Primitive cell junctions and extracellular deposits of collagen are present [27, 28]. Cells are noted with cytoplasmic actin filaments, dense bodies, and attachment plaques having features of myofibroblasts [26, 29]. The lesion is benign, although it is locally invasive. A favorable prognosis following complete surgical resection should be anticipated [2, 26, 27, 29].

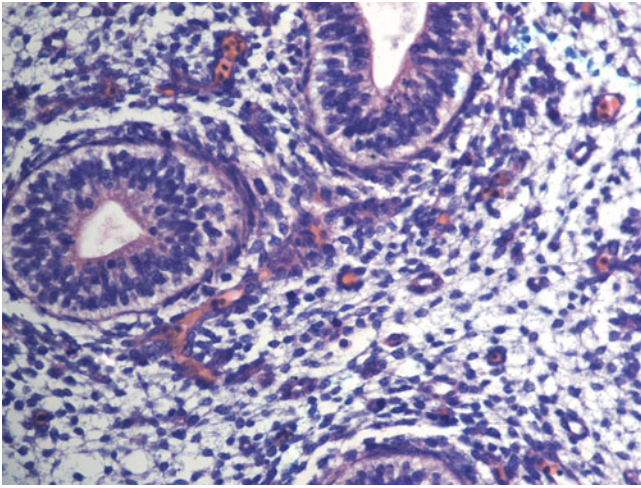


Fig. 17.7 Developing lung. Branches of the pulmonary tree are uniformly lined by tall columnar cells and widely separated by primitive mesenchyme containing tiny spindle-shaped cells. From a fetus of estimated 10–12 weeks gestation (Reprinted from Isaacs [7]. © Springer-Verlag, 2002)

17.8 Pleuropulmonary Blastoma

Pleuropulmonary blastoma (pulmonary blastoma of childhood) is a highly aggressive, malignant tumor of childhood distinct from pulmonary blastoma (carcinosarcoma) of adults [1, 7, 16, 17, 24, 31–38]. The former are considered malignant mesenchymal tumors rather than the adult biphasic neoplasms [24, 33]. First described by Barnard in 1952, only 4–7 % are found in infants and newborns [16–18, 36, 37]. There is a definite male predominance of almost 3–1. The malignancy arises *de novo* or from pulmonary cysts, especially *cystic adenomatoid malformation* [16, 17, 31–33].

The clinical findings are a nonproductive cough, fever, and chest pain suggestive of a respiratory infection [17]. Respiratory distress, abdominal pain, anorexia, lethargy, and weight loss are other signs in the infant. Imaging studies reveal opacification of part of an entire lung (“whiteout”), a large pleural-based mass with a mediastinal shift to the opposite side [7, 17] (Fig. 17.8a). Cysts may be present in the adjacent lung. The tumors are located in the lung, pleura, or in the mediastinum [17, 24, 34]. Prenatal sonography reveals a cyst or a multicystic mass at the periphery of the lung [38].

Pleuropulmonary blastomas tend to be large, some weighing over a kilogram, and having a multilobated appearance. They are located at the periphery of the lung occupying part or the entire lobe. Portions of visceral pleura may be attached to the tumor. The cut surfaces range from firm light gray to red alternating with pale tan gelatinous areas with varying degrees of necrosis, hemorrhage, and cyst formations [17, 24, 33–35] (Fig. 17.8b).

The tumor has a distinctive microscopic appearance varying from one area to the next. There are nests of small

undifferentiated blastemal cells with round or oval dark-staining nuclei, inconspicuous nucleoli, and scant cytoplasm (Fig. 17.8c, d). Nests of blastemal cells, similar to those found in Wilms’ tumor, are surrounded by pale areas of loosely arranged *spindle-shaped cells* and bizarre *multinucleated giant cells*. Both *intra-* and *extracytoplasmic globules* (PAS positive, diastase resistant) are noted (cf. hepatic embryonal sarcoma). Characteristically two or more different kinds of malignant mesenchymal components are present, that is, cells with myoblastic, chondroblastic, lipoblastic, and fibrohistiocytic differentiation [7, 24, 33–37]. The epithelial and mesothelial structures present are histologically benign and probably represent reactive entrapped elements rather than true neoplastic ones [24, 33, 34].

It may be difficult to distinguish between pleuropulmonary blastoma from embryonal rhabdomyosarcoma, especially from small, inadequate biopsy specimens [6, 7]. PNET of thoracopulmonary origin (Askin tumor) occurs in the lung and mediastinum and is one of the differential diagnosis [24]. Immunohistochemical studies show that tumor cells are immunoreactive with vimentin, desmin, α -1-antitrypsin, and α -1-chymotrypsin and focally positive for S-100 protein. The entrapped epithelial elements are epithelial membrane antigen and cytokeratin positive [17, 34–37].

By EM, the blastemal cells are primitive appearing with round to oval nuclei and scant cytoplasm, containing a few organelles. Spindle-shaped fibroblasts and myofibroblasts with a well-formed endoplasmic reticulum, actin-like filaments with focal condensations beneath the cytoplasmic membrane, and rhabdomyoblasts showing thick and thin filaments and Z-band formations are present. There are fibrohistiocytoid and histiocytoid cells with numerous lysosomes [17, 34–37].

17.9 Skeletal Muscle Tumors

There are well-documented examples of *benign striated muscle* occurring in the lungs of fetuses and newborns, in lungs with cystic adenomatoid malformation and extralobar pulmonary sequestration [2, 5, 6, 39–42]. The presence of striated muscle in the lungs, termed *rhabdomyomatous dysplasia* or *rhabdomyomatosis*, is accompanied by significant malformations of the heart and lungs [5, 40]. It may present as a solid tumorlike mass occupying one or more lobes [41, 42]. Microscopically, the dysplasia consists of many bundles of striated fibers arranged haphazardly in expanded alveolar septae.

Skeletal muscle fibers may show marked variation in differentiation and are desmin and actin immunoreactive [5, 41, 42].

Primary rhabdomyosarcoma of the lung has not been described very often [43]. In older literature, some examples of pleuropulmonary blastoma were diagnosed as rhabdomyosarcoma.

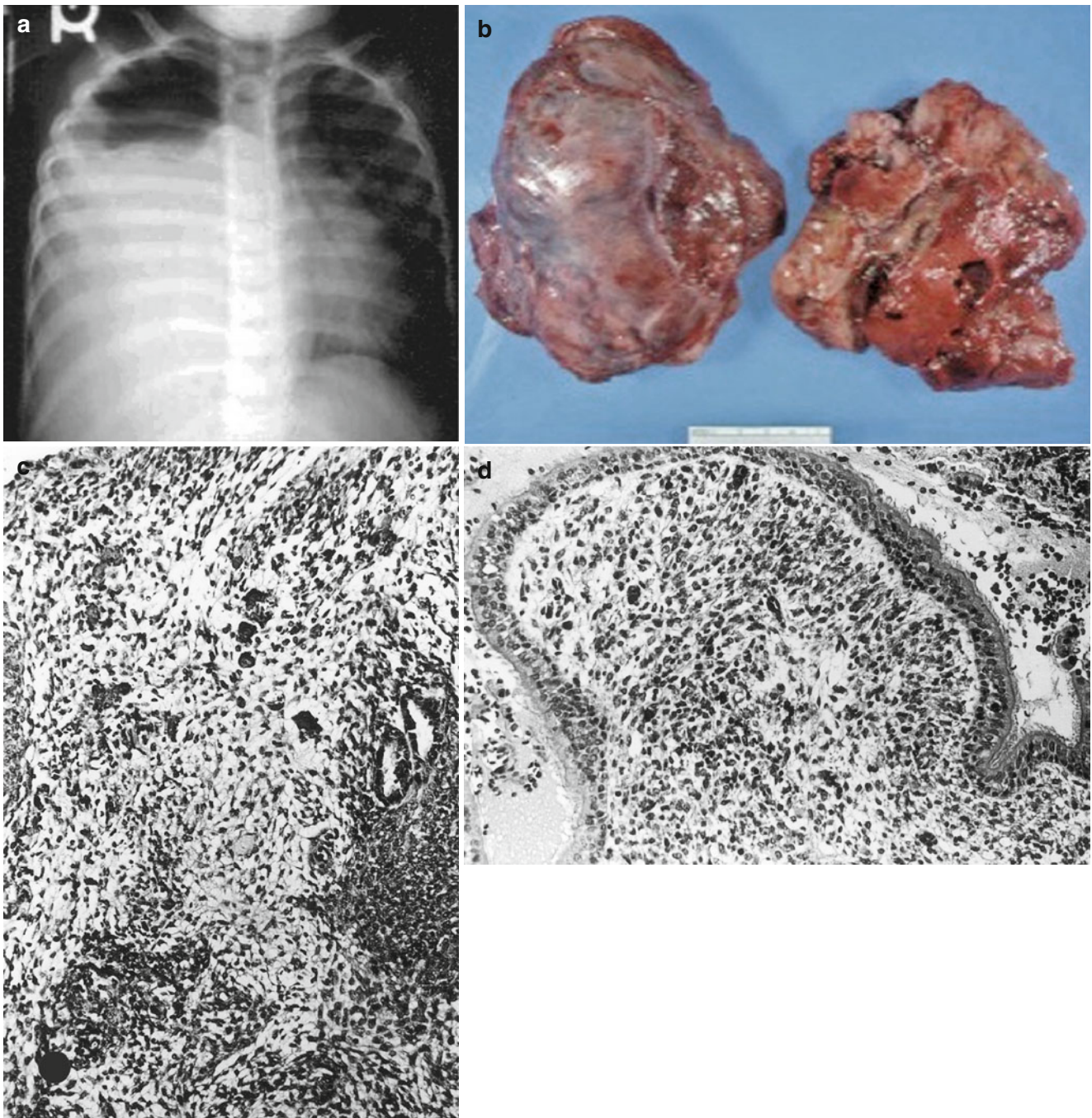


Fig. 17.8 Pleuropulmonary blastoma. Two-year-old female with progressive respiratory distress and low-grade fever. (a) Chest X-ray, pulmonary blastoma showing opacification of the right hemithorax (“whiteout”). (b) The tumor is light tan-gray, friable with extensive necrosis and hemorrhage. (c) Blastemal (darkly cellular) areas alternate with pale, myxoid

areas with tiny stellate and spindle-shaped cells. Small primitive-appearing bronchial-like structures are present at the right side of the photomicrograph. (d) Tumor growing beneath the respiratory mucosa assumes a polypoid or “botryoid” appearance similar to that of embryonal rhabdomyosarcoma (Reprinted from Isaacs [6]. © WB Saunders 1997)

17.10 Peripheral Neuroectodermal Tumor of Thoracopulmonary Origin

The small blue cell malignant tumor of thoracopulmonary origin (chest wall Ewing’s sarcoma, Askin tumor, PNET of chest wall and lung) is one of the small cell tumors of childhood associated with a rapidly progressive, downhill clinical

course and generally a poor outcome [1, 5, 7, 44–47]. Current views based on immunohistochemical, EM, and cytogenetic studies suggest that this tumor is probably the same entity as the extra-skeletal Ewing’s sarcoma and PNET of the soft tissues [44, 45]. A neural crest origin is proposed for these malignancies.

The *PNET of thoracopulmonary origin* occurs in two age peaks, one in late infancy and the other in adolescence [1]. The

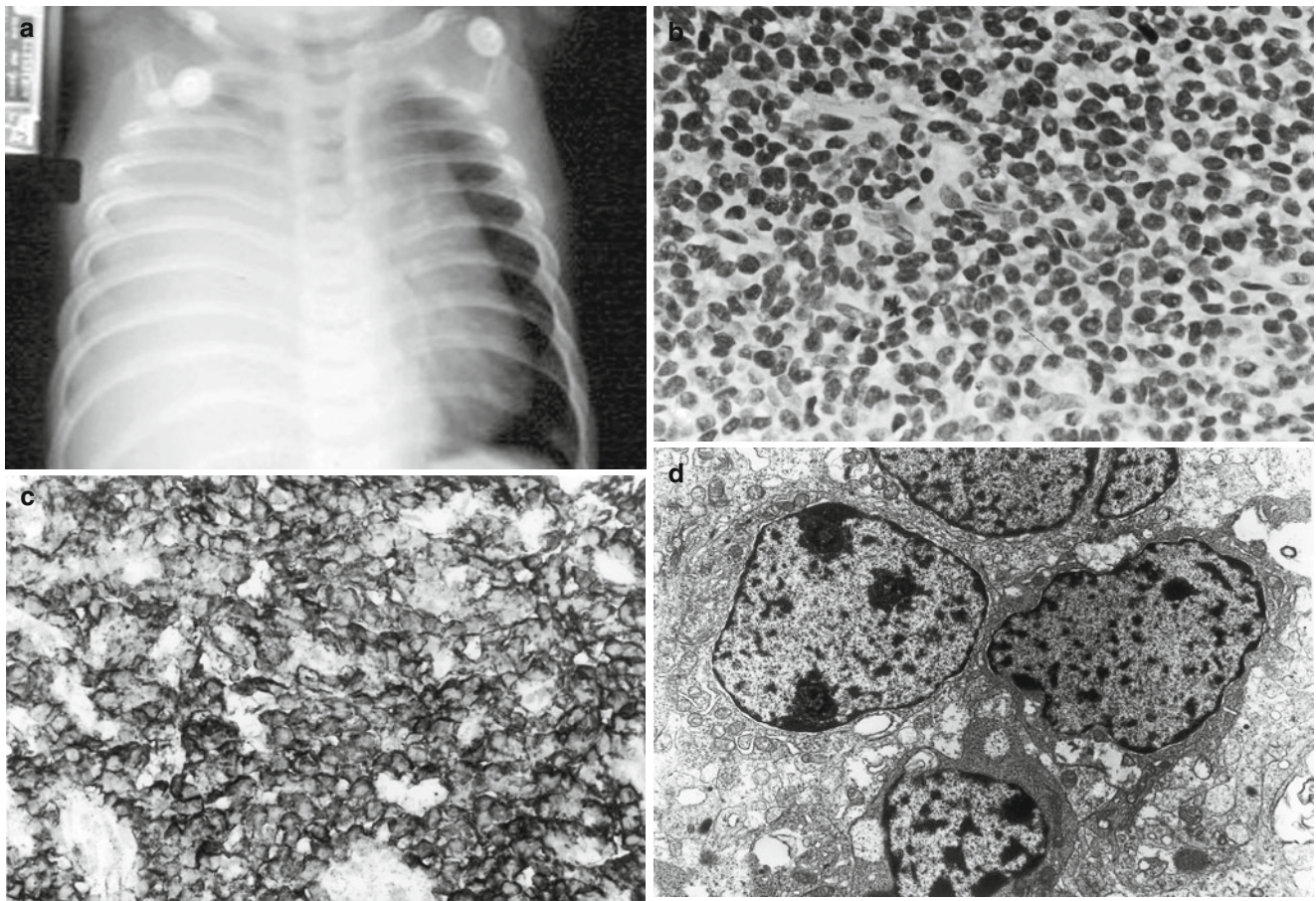


Fig. 17.9 Primitiv neuroectodermal tumor of thoracopulmonary origin. Six-month-old male with a chest wall mass. (a) Chest radiograph reveals consolidation of the right thorax by an infiltrative mass. (b) The biopsy shows a small cell malignant tumor forming nests of cells, which have round or oval nuclei, coarse or clumped chromatin, small nucleoli, and indistinct or scant cytoplasm. Several mitoses are present. (c) Tumor cells are diffusely immunoreactive with the Ewing's antibody

MIC2 (013), neuron-specific enolase, and neurofilament. They are weakly reactive with synaptophysin but unreactive with actin and desmin. (d) EM features consist of small primitive-appearing cells with sparse organelles. Well-defined cell junctions, neurosecretory granules, or neurofilaments are not present. (b) H&E. (c) MIC2 (013) immunoperoxidase. (d) EM $\times 10,000$ (Reprinted from Isaacs [7]. © Springer-Verlag, 2002)

patient with this malignancy presents with fever, chest pain, a palpable mass in the chest wall, and pleural effusion [1, 44, 46, 47]. It arises from the soft tissues of the chest wall, but because of its proximity, the lung and pleura are involved as well.

On gross inspection, the chest wall and adjacent lung are replaced by one or more pale gray tumor nodules measuring up to 10 cm in greatest diameter. The pale, gray, gelatinous cut surfaces show foci of necrosis, hemorrhage, and cyst formation [1]. Histologically, the tumor is highly cellular consisting of small round darkly staining cells with scant cytoplasm occasionally arranged in lobules (Fig. 17.9). *Pseudorosette formations* are noted in some. Neural differentiation is manifested on EM by the presence of neuritic processes, dense core granules, and neurotubules. Glycogen deposits are variably present. Neuron-specific enolase and more specifically the cell surface antigen HBA71 (Ewing's antibody 013) are diagnostically immunoreactive [7]. Chromosomal analysis from tissue culture material reveals a

characteristic *t(11;22) rearrangement* which will aid in confirming the diagnosis [7, 45, 46].

References

1. Dehner LP (1989) Tumors and tumor-like lesions of the lung and chest wall in childhood: clinical and pathologic review. In: Stocker JT (ed) Pediatric pulmonary disease. Hemisphere, Washington, D.C., p 207
2. Stocker JT (1992) The respiratory tract. In: Stocker JT, Dehner LP (eds) Pediatric pathology, vol 1. JB Lippincott, Philadelphia, p 505
3. Hartman GE, Schochat SJ (1983) Primary pulmonary neoplasms of childhood: a review. *Ann Thorac Surg* 36:108–119
4. Cohen MC, Kaschula RO (1992) Primary pulmonary tumors in childhood: a review of 31 years' experience and the literature. *Pediatr Pulmonol* 14:222–232
5. Isaacs H Jr (1997) Tumors. In: Gilbert-Barnes E (ed) Potter's pathology of the fetus and infant, vol 2. Mosby, St. Louis, pp 1242–1339

6. Isaacs H Jr (1997) Tumors of the lung. In: Tumors of the fetus and newborn, vol 35, Major problems in pathology. W.B. Saunders, Philadelphia, pp 344–356
7. Isaacs H Jr (2002) Lung tumors. In: Tumors of the fetus and infant: an atlas. Springer, New York, pp 387–406
8. Katzenstein A-LA, Askin FB (1990) Surgical pathology of non-neoplastic lung disease. In: Bennington JL (ed) Major problems in pathology, vol 13, 2nd edn. WB Saunders, Philadelphia
9. Conran RM, Stocker JT (1999) Extralobar sequestration with frequently associated congenital cystic adenomatoid malformation, type 2: report of 50 cases. *Pediatr Dev Pathol* 2:454–463
10. Hunter WS, Becroft DMO (1984) Congenital pulmonary lymphangiectasis associated with pleural effusions. *Arch Dis Child* 59:278–279
11. Wilson RH, Duncan A, Hume R et al (1985) Prenatal pleural effusion associated with congenital lymphangiectasis. *Prenat Diagn* 5: 73–76
12. Lehman TJ, Church JA, Isaacs H Jr (1989) Lymphomatoid granulomatosis in a 13-month-old infant. *J Rheumatol* 16:235–238
13. Hussong JW, Brown M, Perkins SJ et al (1999) Comparison of DNA ploidy, histologic, and immunohistochemical findings with clinical outcome in inflammatory myofibroblastic tumors. *Mod Pathol* 12:279–286
14. Matsubara O, Tan Liu NS, Kenney RM et al (1988) Inflammatory pseudotumor of the lung: progression from organizing pneumonia to fibrous histiocytoma or to plasma cell granuloma in 32 cases. *Hum Pathol* 19:807–814
15. Rosenberg HS, Stenback WA, Spjut HJ (1978) The fibromatoses of infancy and childhood. In: Rosenberg HS, Bolande RP (eds) Perspectives in pediatric pathology, vol 4. Year Book Medical Publishers, Chicago, pp 269–348
16. Holland-Moritz RM, Heyn RM (1984) Pulmonary blastoma associated with cystic lesions in children. *Med Pediatr Oncol* 12:85–88
17. Manivel JC, Priest JR, Watterston J et al (1988) Pleuropulmonary blastoma: the so-called pulmonary blastoma of childhood. *Cancer* 62:1516–1526
18. Kuller JA, Yankowitz J, Goldberg JD et al (1992) Outcome of antenatally diagnosed cystic adenomatoid malformations. *Am J Obstet Gynecol* 167:1038–1041
19. Cha I, Adzick NS, Harrison MR et al (1997) Fetal congenital cystic adenomatoid malformations of the lung: a clinicopathologic study of eleven cases. *Am J Surg Pathol* 21:537–544
20. Morotti RA, Cangiarella J, Gutierrez MC et al (1999) Congenital cystic adenomatoid malformation of the lung (CCAM): evaluation of the cellular components. *Hum Pathol* 30:618–625
21. Cohen SR, Geller KA, Selzer S et al (1980) Papilloma of the larynx and tracheobronchial bronchial tree in children. A retrospective study. *Ann Otol Rhinol Laryngol* 89:497–503
22. Mounts P, Kashima H (1984) Association of human papilloma virus subtype and clinical course in respiratory papillomatosis. *Laryngoscope* 94:28–33
23. Kramer SS, Wehunt WD, Stocker JT et al (1985) Pulmonary manifestations of juvenile laryngotracheal papillomatosis. *AJR Am J Roentgenol* 144:687–694
24. Colby TV, Koss MN, Travis WD (1995) Tumors of the lower respiratory tract. In: Atlas of tumor pathology, 3rd series, fascicle 13. Armed Forces Institute of Pathology, Washington, D.C.
25. Siegel SE, Cohen SR, Isaacs H et al (1979) Malignant transformation of tracheobronchial juvenile papillomatosis without prior radiotherapy. *Ann Otol Rhinol Laryngol* 88:192–197
26. Alobeid B, Beneck D, Sreekantaiah C et al (1997) Congenital pulmonary myofibroblastic tumor: a case report with cytogenetic analysis and review of the literature. *Am J Surg Pathol* 21:610–614
27. Jimenez JF, Uthman EO, Townsend JW et al (1986) Primary bronchopulmonary leiomyosarcoma in childhood. *Arch Pathol Lab Med* 110:348–351
28. Pettinato G, Manivel C, Saldana MJ et al (1989) Primary bronchopulmonary fibrosarcoma of childhood and adolescence. Reassessment of a low grade malignancy-clinicopathologic study of five cases and a review of the literature. *Hum Pathol* 20:463–471
29. McGinnis M, Jacobs G, El-Naggar A et al (1993) Congenital peribronchial myofibroblastic tumor (so-called “congenital leiomyosarcoma”). A distinct neonatal lung lesion associated with nonimmune hydrops fetalis. *Mod Pathol* 6:487–492
30. Isaacs H Jr (2008) Fetal hydrops associated with tumors. *Am J Perinatol* 25:43–68
31. Bove KE (1989) Sarcoma arising in pulmonary mesenchymal cystic hamartoma. *Pediatr Pathol* 9:785–792
32. Becroft DMO, Jagusch MF (1987) Pulmonary sarcomas arising in mesenchymal hamartomas. *Pediatr Pathol* 7:478
33. Dehner LP, Watterston J, Priest J (1995) Pleuropulmonary blastoma: a unique intrathoracic pulmonary neoplasm of childhood. In: Askin FB, Langston C, Rosenberg HS, Bernstein J (eds) Pulmonary disease, vol 18, Perspectives in pediatric pathology. Karger, Basel, p 214
34. Hachitanda Y, Aoyama C, Sato JK et al (1993) Pleuropulmonary blastoma in childhood: a tumor of divergent differentiation. *Am J Surg Pathol* 17:382–391
35. Priest JR, McDermott MB, Bhatia S et al (1997) Pleuropulmonary blastoma. A clinicopathologic study of 50 cases. *Cancer* 80:147–161
36. Ashworth TG (1983) Pulmonary blastoma, a true congenital neoplasm. *Histopathology* 7:585–594
37. Koss MN, Hochholzer L, O’Leary T (1991) Pulmonary blastomas. *Cancer* 67:2368–2381
38. Miniati DN, Chintagumpala M, Langston C et al (2006) Prenatal presentation and outcome of children with pleuropulmonary blastoma. *J Pediatr Surg* 41:66–71
39. Chen MF, Onerheim R, Wang NS et al (1991) Rhabdomyomatosis of newborn lung: a case report with immunohistochemical and electron microscopic characterization of striated muscle cells in the lung. *Pediatr Pathol* 11:123–129
40. Drut RM, Quijano G, Drut R et al (1988) Rhabdomyomatous dysplasia of the lung. *Pediatr Pathol* 8:385–390
41. Hardisson D, Garcia-Jimenez JA, Jimenez-Heffernan JA et al (1997) Rhabdomyomatosis of the newborn lung unassociated with other malformations. *Histopathology* 31:474–479
42. Ramaswamy A, Weyers I, Duda zippidy V et al (1998) A tumorous type of pulmonary rhabdomyomatous dysplasia. *Pathol Res Pract* 194:639–642
43. Allan BT, Day DL, Dehner LP (1987) Primary pulmonary rhabdomyosarcoma of the lung in children. Report of two cases presenting with spontaneous pneumothorax. *Cancer* 59: 1005–1011
44. Schmidt D, Harms D, Burdach S (1985) Malignant peripheral neuroectodermal tumours of childhood and adolescence. *Virchows Arch A Pathol Anat Histopathol* 406:351–365
45. Tsokos M (1992) Peripheral primitive neuroectodermal tumors: diagnosis, classification and prognosis. *Perspect Pediatr Pathol* 16:27–98
46. Kennedy JG, Frelinghuysen P, Hoang BH (2003) Ewing sarcoma: current concepts in diagnosis and treatment. *Curr Opin Pediatr* 15:53–57
47. Saenz NC, Hass DJ, Meyers P et al (2000) Pediatric chest wall Ewing’s sarcoma. *J Pediatr Surg* 35:550–555

18.1 Introduction

Primary tumors of bone occur infrequently during the first year of life. Few cases have been reported [1–12]. For example, in a series of 249 children with bone lesions less than 10 years of age, 16 were younger than 1 year of age [1]. Langerhans cell histiocytosis was the dominant neoplasm (ten cases); the skull was the site most frequently involved (Fig. 18.1). In addition, there were two

examples of chest wall hamartoma and one each of Ewing's sarcoma of the scapula, fibrous dysplasia of the turbinate, osteochondroma of the rib, and myofibromatosis of the mandible [1].

Symptoms of skeletal neoplasms usually are nonspecific, often leading to an erroneous diagnosis. Skeletal tumors may mimic benign conditions such as osteomyelitis or trauma [1]. Tumors and tumor-like conditions of bone in the fetus and infant are listed in Table 18.1.

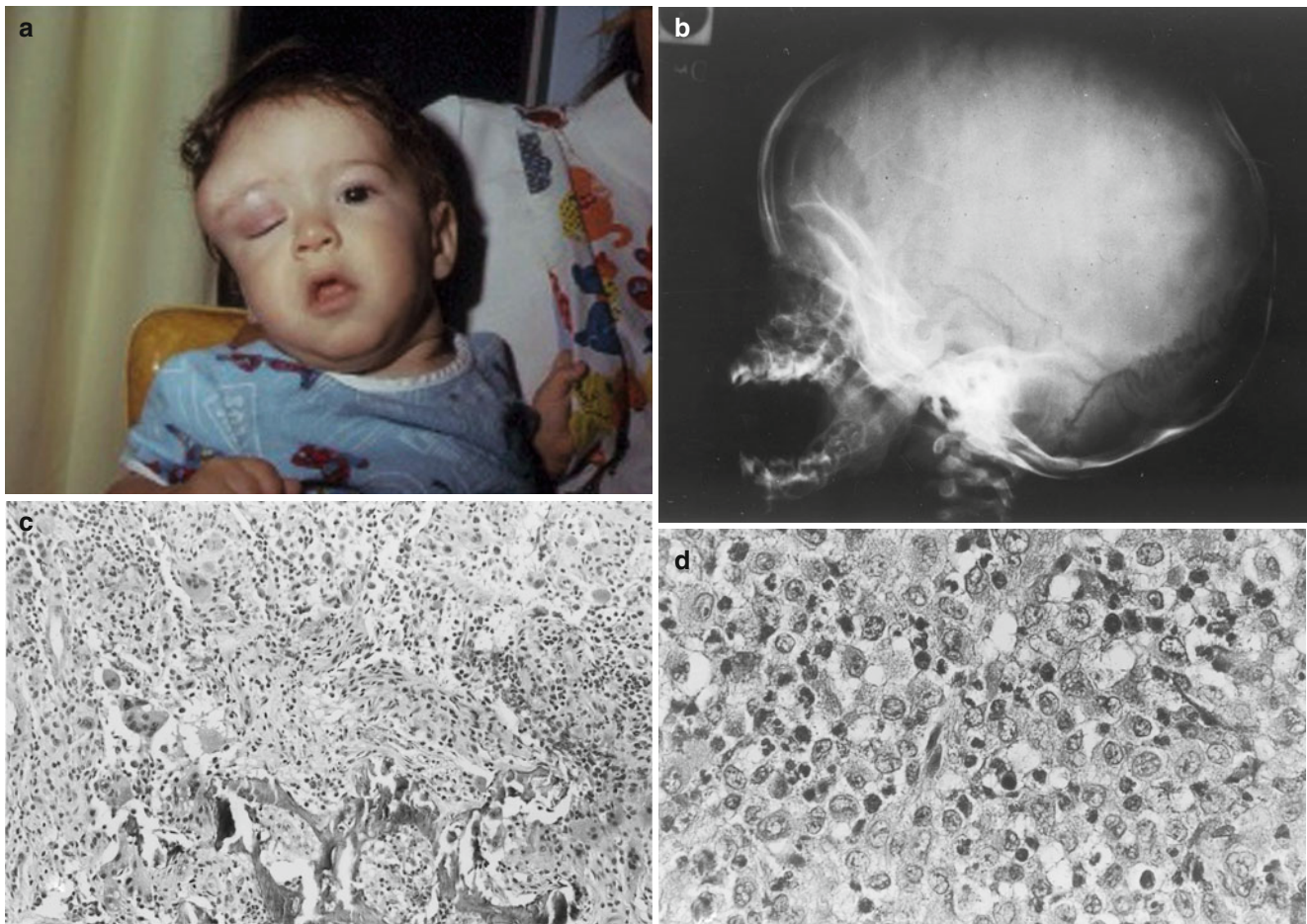


Fig. 18.1 Langerhans cell histiocytosis. (a) Seven-month-old male with painful swelling, 3 × 3 cm, over the right orbital ridge noted 1 month prior to biopsy. The skull is one of the bones most commonly affected by this disease. (b) Skull radiograph, lateral view, reveals a lytic defect in the right frontal bone. Characteristically no reaction is present along the advancing margins of the lesion. (c) Cranial bone is

replaced by a cellular infiltrate. (d) The infiltrate consists mostly of histiocytes with eosinophilic cytoplasm, occasionally vacuolated, and infolded nuclei and one or two small nucleoli. A few lymphocytes and neutrophils are present. S-100 is strongly positive within the histiocytes (Reprinted from Isaacs [11]. © WB Saunders 1997)

Table 18.1 Tumors and tumor-like conditions of bone in the fetus and infant

Chest wall hamartoma
Nasal chondromesenchymal hamartoma
Langerhans cell histiocytosis
Congenital myofibromatosis
Fibrous dysplasia
Osteofibrous dysplasia
Melanotic neuroectodermal tumor of infancy
Enchondroma (Ollier's disease)
Reparative giant cell granuloma
Juvenile xanthogranuloma
Osteochondromyxoma
Ewing's sarcoma
Osteosarcoma
Congenital fibrosarcoma
Chordoma
Osteolysis ("disappearing bone disease")

Reprinted from Isaacs [12]. © Springer-Verlag, 2002

18.2 Chest Wall Hamartoma

Chest wall hamartoma has been variously referred to as benign mesenchymoma, aneurysmal bone cyst, and cartilaginous hamartoma [8, 12–15]. It is a tumor-like condition of newborns and infants involving one or more adjacent ribs producing a mass and deformity of the chest wall [12, 15] (Fig. 18.2).

Hamartoma is defined as an *overgrowth of tissue(s) normally present at the site of origin*. The lesion has been detected prenatally by sonography [14]. When chest wall hamartomas are extensive, they bulge into the thoracic cavity and adjacent lung causing mediastinal shift and respiratory distress.

The involved rib is expanded, partially or totally replaced by a cystic lesion composed of cartilaginous, osseous, fibrous, and vascular elements (Figs. 18.2 and 18.3). Microscopically, the hamartoma resembles an *aneurysmal bone cyst* characterized by striking proliferation of hyaline cartilage in addition to bone, fibrous connective tissue, and blood vessels [12, 13] (Figs. 18.2 and 18.3). The lesion is best considered a malformation or hamartoma rather than a true neoplasm [12]. Conservative surgical excision is the treatment of choice [12–15]. However, several procedures may be required because of the extensive nature of some lesions [9]. Nasal chondromesenchymal hamartoma shares some histological features in common with chest wall hamartoma [16–18].

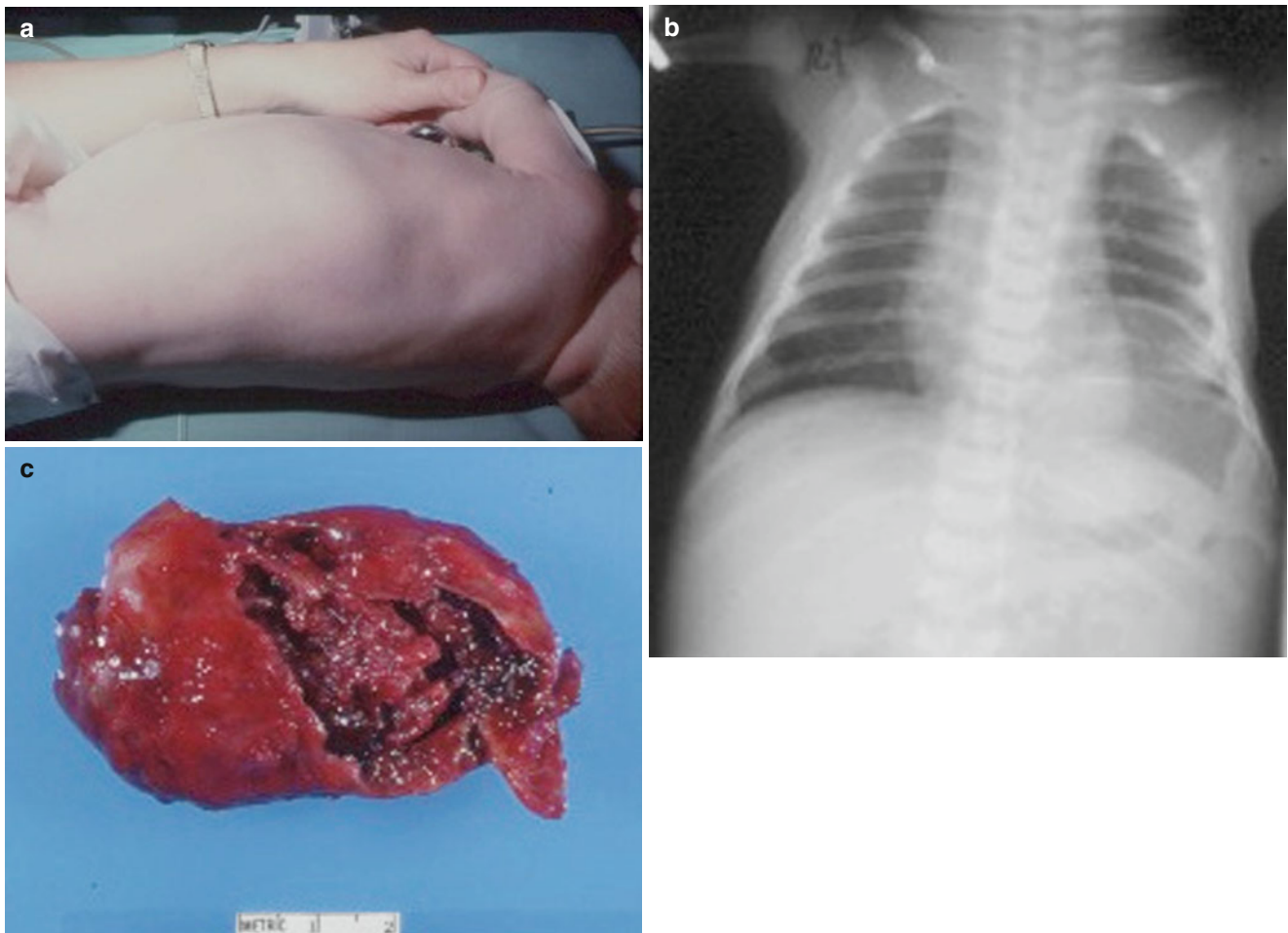


Fig. 18.2 Chest wall hamartoma. (a) One-month-old male with a bulge over the left chest wall since birth. (b) Cystic, expansile lesion involving the left eighth rib. (c) The soft, hemorrhagic contents of the markedly expanded rib are covered by a thin, “egg shell” layer of bone. (d) The

vascular component consists of irregular channels filled with blood separated by fibrovascular tissue containing osteoclasts. (e) Nodules of cartilage and spicules of partially decalcified bone are surrounded by vascular connective tissue (Reprinted from Isaacs [11]. © WB Saunders 1997)

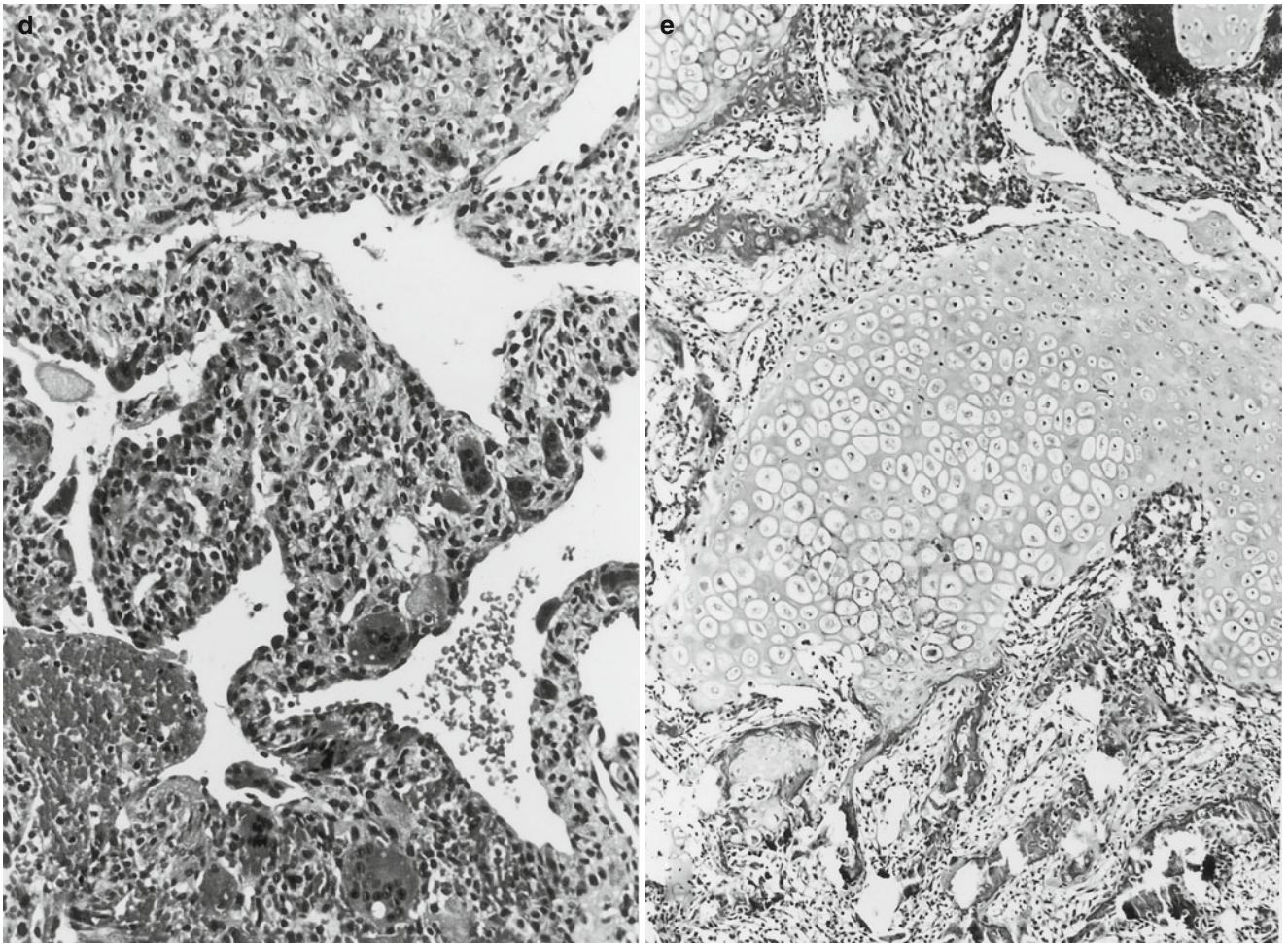


Fig. 18.2 (continued)

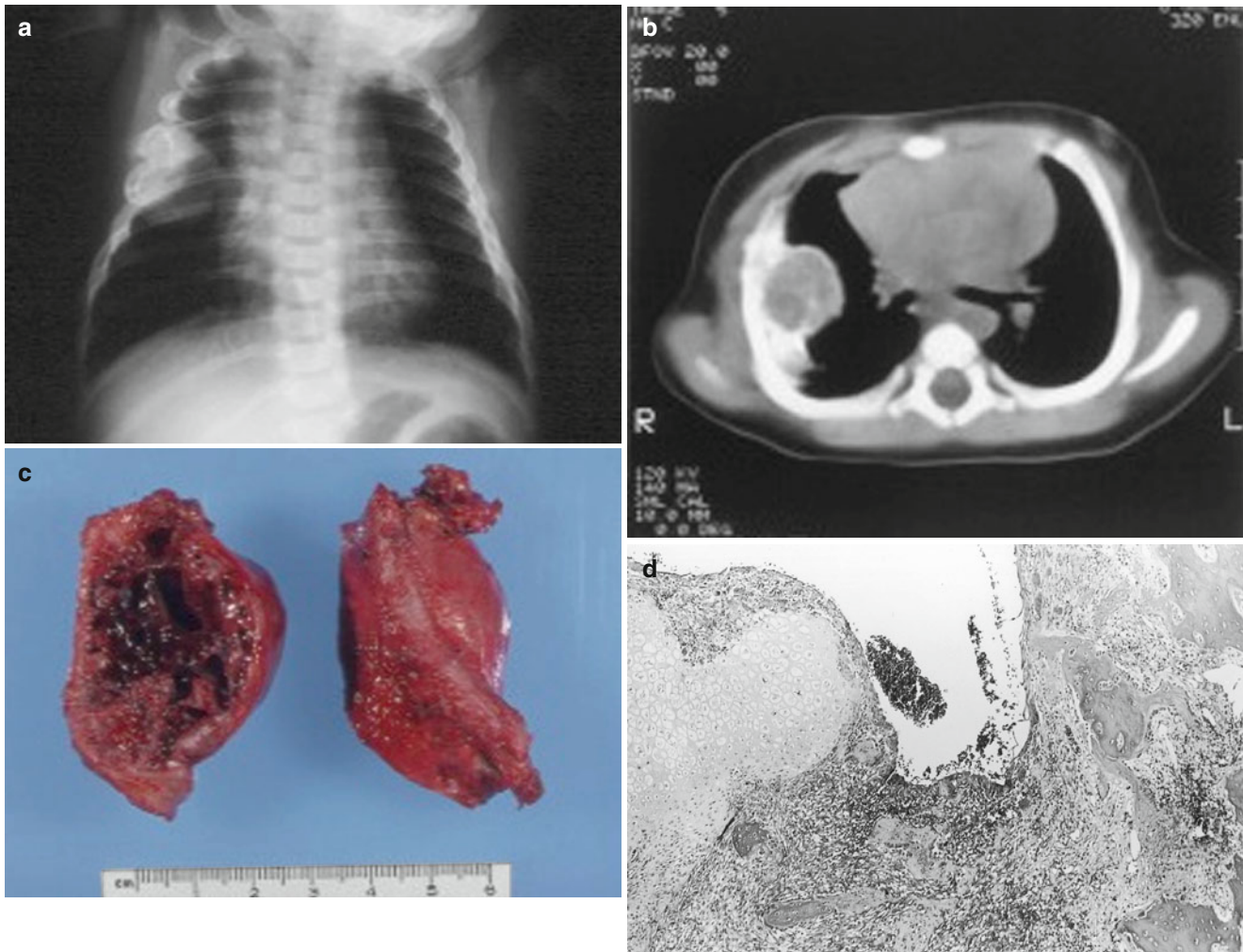


Fig. 18.3 Chest wall hamartoma. Five-month-old male with a chest mass. (a) A cystic, expansile lesion involves the right fourth rib. Scoliosis and a chest wall deformity present here can be serious complications of the hamartoma. (b) CT scan reveals a defect in the right chest wall and a cystic lesion bulging into the thoracic cavity. (c) The involved

rib is divided in half revealing an expansile, sponge-like mass occupying the rib reminiscent of an aneurysmal bone cyst. (d) Vascular, cartilaginous, and osseous components are illustrated (Reprinted from Isaacs [11]. © WB Saunders 1997)

18.3 Nasal Chondromesenchymal Hamartoma

Nasal chondromesenchymal hamartoma is the name applied by McDermott, Ponder, and Dehner to describe a tumor of the nasal passages and paranasal sinuses with a detectable mass in the nose [16]. The patients are usually 3 months of age or less at the time of diagnosis [16–18]. Imaging studies reveal a complex solid and cystic lesion occupying the nasal cavity with extension into the ethmoid sinus [16–18] (Fig. 18.4). Occasionally, intracranial and orbital involvement occurs [18].

Gross inspection reveals fragments of white, firm fibrous tissue containing nodules of bone and cartilage [12, 18]. The hamartoma displays a varied histological appearance

consisting of islands of osseous tissue, nodules of cartilage composed of both mature and immature (but not malignant looking) chondrocytes, a myxoid stroma with spindle-shaped fibroblastic cells, focal osteoclastic giant cells, and a vascular component resembling the aneurysmal bone cyst [11, 12, 16–18] (Fig. 18.4). Immunohistochemical studies reveal cartilage nodules with S-100 reactivity and mesenchymal spindle cells showing vimentin and variable actin reactivity [16]. The stromal spindle-shaped cells exhibit fibroblastic and myofibroblastic features by EM [17, 18].

Surgical excision is the treatment of choice [16]. Neither recurrence nor metastases have been reported. However, instances of residual, unresectable tumor are described in a few case reports [16, 18].

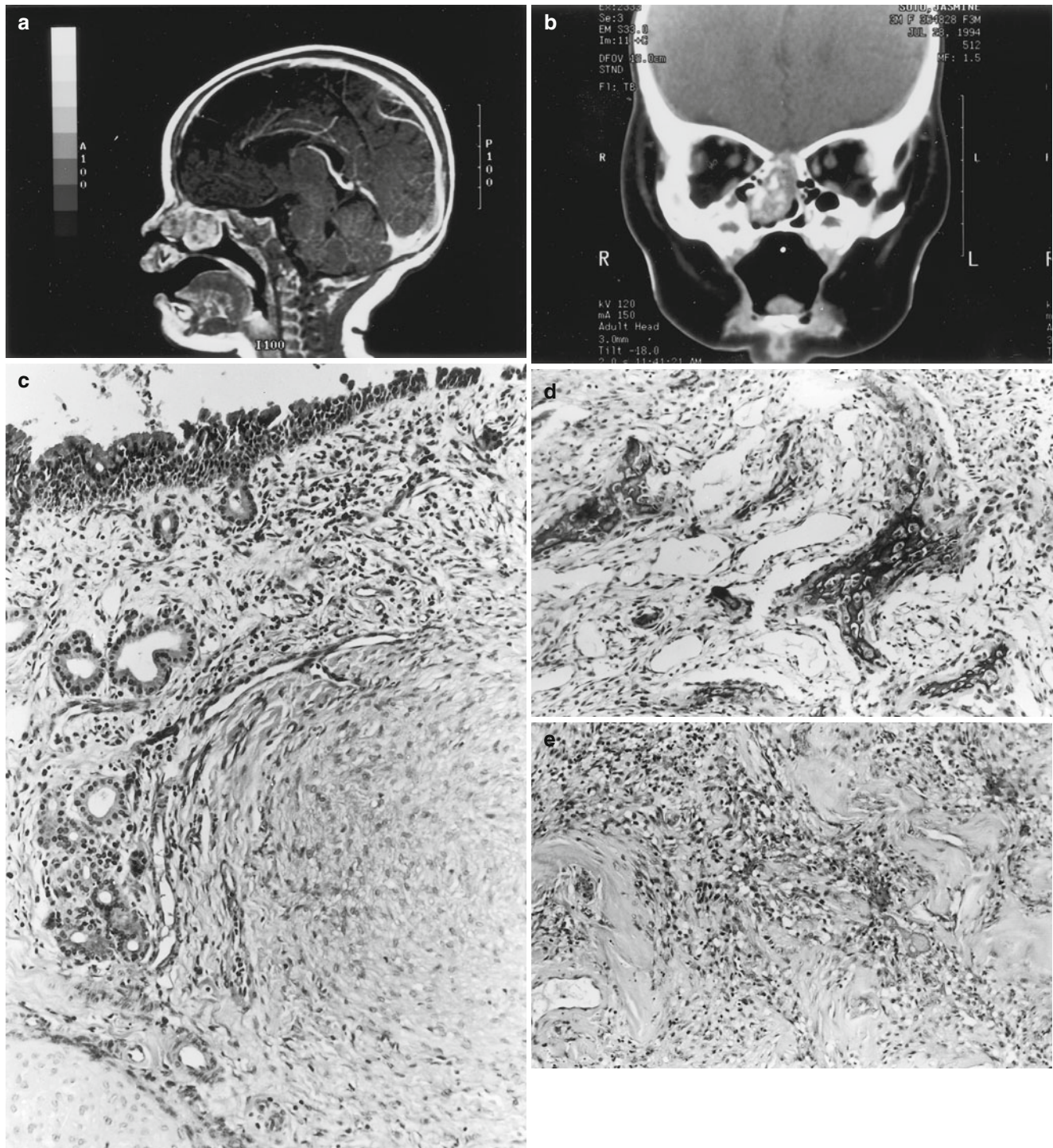


Fig. 18.4 Nasal chondromesenchymal hamartoma. Three-month-old female with a nasal mass. (a) MRI showing a mass displaying heterogeneous areas of high density situated within the nasal cavity beneath the cribriform plate. (b) CT scan demonstrating the mass within the right nasal cavity and adjacent paranasal sinuses. The lesion extends across the midline deviating the nasal septum and perforating the cribriform plate. (c) Chondroid nodules are present beneath metaplastic,

chronically inflamed respiratory mucosa. (d) Higher magnification reveals stroma composed of tiny round and spindle-shaped cells surrounding the hyaline cartilage component. (e) Reactive new bone formation, vascular channels, and cellular spindle cell stroma are present. The author would like to thank Louis Dehner, M.D., for reviewing the case and for providing us with the diagnosis (Reprinted from Isaacs [12]. © Springer-Verlag, 2002)

18.4 Fibrous Dysplasia of Bone

This condition has several variations. *Fibrous dysplasia* involves localized portions of one or more bones. It is regarded as a congenital developmental defect [2, 3, 10, 12]. Fibrous dysplasia may be present at birth, or not become evident until later in childhood [9].

The *monostotic* form (*only one bone involved*) usually affects children or young adults and is uncommon in infants. The bones most often involved are the rib, tibia, femur, mandible, and maxilla. The first sign may be a fracture or local swelling and tenderness. The child is often otherwise normal. Histologically, the marrow and osseous structures in sharply delineated areas are replaced by fibrous connective tissue and poorly formed, haphazardly arranged, immature bone having a “Chinese checker-like” appearance. Characteristically, the trabeculae lack normal osteoblastic activity [9, 10] (Fig. 18.5).

Polyostotic fibrous dysplasia is characterized by *lesions in many bones*, cutaneous cafe-au-lait spots, and sexual precocity (*the McCune-Albright syndrome*). Bone lesion manifestations of polyostotic fibrous dysplasia, for example, osteoporosis, may appear as early as 1 month of age [20]. Later in life, areas of flat bones are distended into tumor-like masses while the long bones are curved, shortened, and thickened. Serum calcium and phosphorus levels are normal, but *serum phosphatase* is abnormally elevated [9, 12, 20].

When associated with *Cushing's syndrome* and *adrenal nodular hyperplasia*, the *McCune-Albright syndrome* may become evident shortly after birth causing life-threatening metabolic problems and sudden, unexpected death if not corrected [20] (see Chap. 13).

18.5 Enchondromatosis (Ollier's Disease)

Although *enchondromatosis* is seldom recognized at birth, it may be identified as early as 6 months of age [9, 12] (Fig. 18.6a, b). The disease consists of multiple cartilaginous

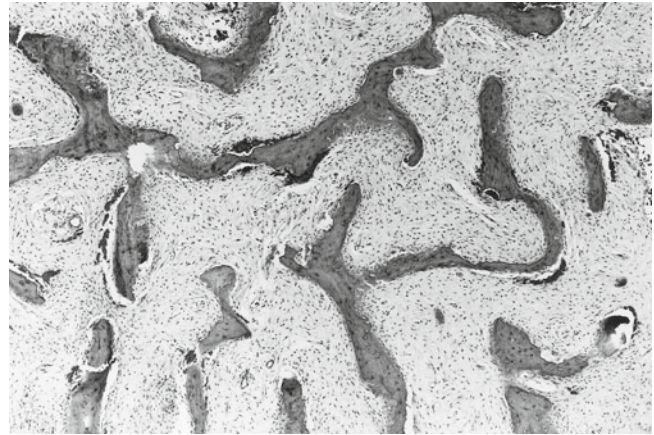


Fig. 18.5 Fibrous dysplasia. Irregularly shaped trabeculae of bone are situated in a moderately cellular, pale-staining fibrous stroma. There is little or no osteoblastic activity. Examination under polarized light reveals mostly immature woven bone (Reprinted from Isaacs [11]. © WB Saunders 1997)

tumors originating in the enchondral growth zone. The tumors grow with the remainder of the shaft and extend in a triangular fashion toward the diaphysis. Radiologically, they appear as rarefactions in the metaphysis and ends of the diaphysis, with expansion of the cortex around the tumor. Eventually, the disease is accompanied by severe shortening and bowing of the tumor-containing long bones and by distortion of the nearby joints. The tumors are usually unilateral and irregularly distributed. Histologically, they are lobulated with marked variation in cellularity, organization, calcification, and degeneration of cartilage (Fig. 18.7). In approximately a third of older cases, the enchondromas undergo malignant change into *chondrosarcoma* [10, 22].

Unless sarcomas develop, the prognosis is relatively good, although fractures or joint disability may be prominent. Some cases are complicated in later childhood by vascular anomalies, particularly angiomas, phlebectasis, or hemangiomas [9, 12]. When these findings are present, the condition is then known as the *Maffucci-Kast syndrome*.

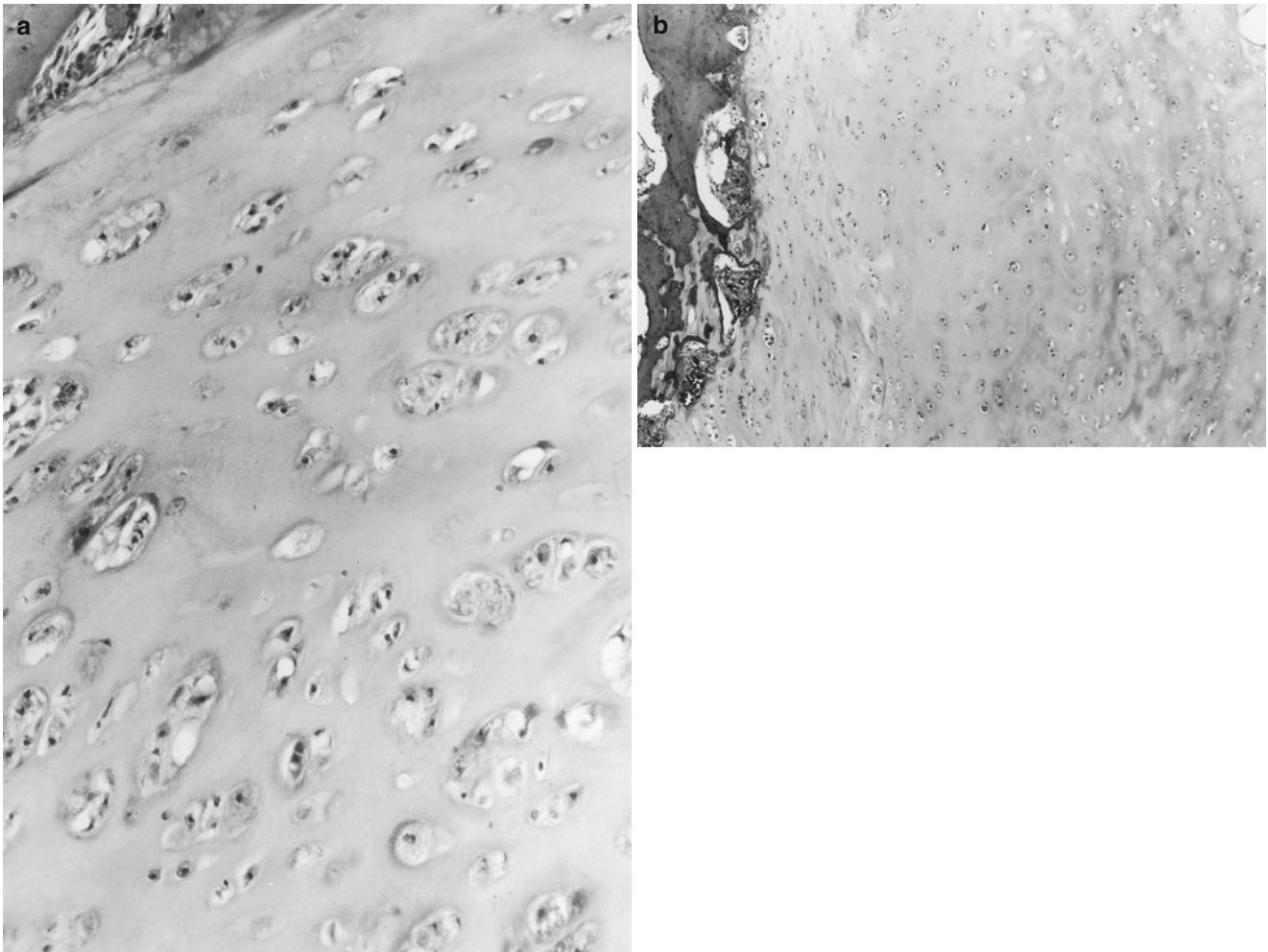


Fig. 18.6 Enchondromatosis (Ollier's disease). Child with Ollier's disease. **(a)** Tumor consists of one or more chondrocytes situated in large lacunae surrounded by abundant hyaline chondroid matrix. The tumor is hypercellular with large numbers of multinucleated

chondrocytes. **(b)** Normal bone from this patient is shown for comparison. (Courtesy of Rob Newbury, M.D., Department of Pathology, Children's Hospital of San Diego; Reprinted from Isaacs [12]. © Springer-Verlag, 2002)

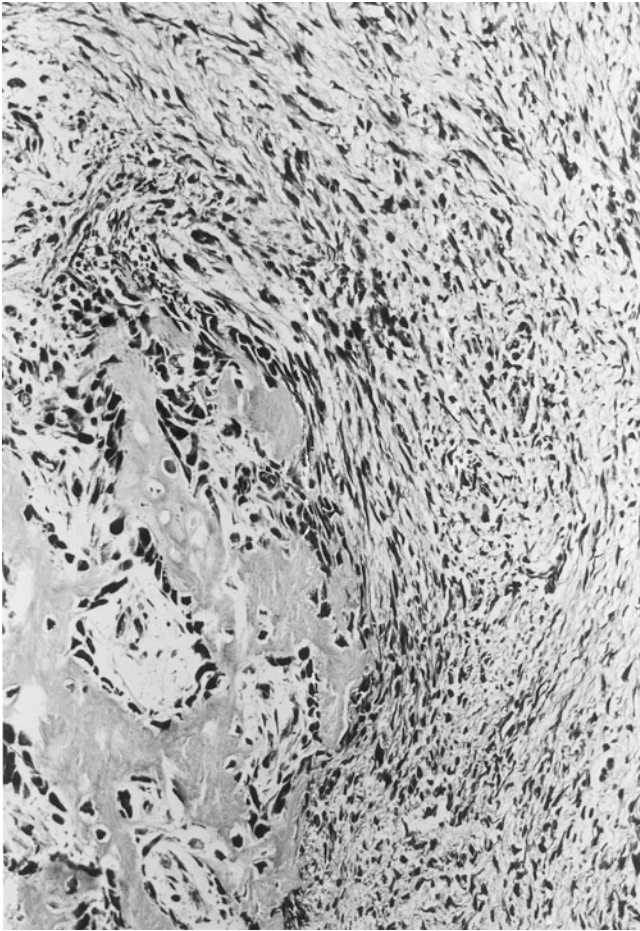


Fig. 18.7 Myofibromatosis. Three-week-old male with multiple subcutaneous nodules over the face, chest, arms, and in the bones. Biopsy of a jaw lesion shows an island of reactive bone surrounded by spindle-shaped myofibroblastic cells (Reprinted from Isaacs [12]. © Springer-Verlag, 2002)

18.6 Congenital Generalized Fibromatosis (Infantile Myofibromatosis)

This condition is discussed also in Chap. 4. Soft tissue fibrous tumors occasionally present predominantly as bone lesions, or they are limited entirely to the skeletal system [7, 21–27].

Some remain unnoticed until the infant presents with swelling or a pathological fracture. *Solitary myofibromatosis* of bone involving the craniofacial bones is described [7, 26]. The tumor causes prominent orbital bone destruction and proptosis mimicking a malignant neoplasm [26]. The radiologic features consist of a lytic lesion with a sclerotic rim involving most often the craniofacial bones, femur, tibia, vertebra, or rib [7, 24, 26, 27]. Microscopically, the lesion consists of bundles of spindle-shaped fibroblasts and myofibroblasts with central vascular spaces (Fig. 18.7). The light microscopic, immunohistochemical and EM features are similar to those of myofibromatosis of skin, soft tissue, and viscera [7, 23, 26, 27]. Conservative treatment is recommended since many bone lesions regress spontaneously [7, 24].

18.7 Congenital Fibrosarcoma

Although *congenital fibrosarcoma of the soft tissues* is relatively common, *primary osseous fibrosarcoma* is rare [9, 12, 28, 29]. Distinguishing congenital fibrosarcoma from fibromatosis of bone may be difficult such as with the soft tissue counterpart [12, 29]. Fibromatoses are less cellular and more fibrogenic in their histological appearance than fibrosarcomas [9, 24, 28]. Congenital fibrosarcoma is a highly cellular neoplasm composed of small spindle cells arranged in a whorling pattern with relatively little collagen. Nuclei are uniform displaying many mitotic figures [9, 28, 29]. The femur and humerus are the primary sites most often reported in infants [28, 29]. If the tumor is extensive, limb salvage or amputation may be required for cure.

18.8 Ewing's Sarcoma

Ewing's sarcoma (peripheral neuroectodermal tumor of bone, PNET) is unusual in infants. It is primarily a tumor of older children and adolescents occurring more often in girls than in boys during the first 3 years of life [1, 6, 10, 30–32]. Clinical findings in young patients with Ewing's sarcoma include pain and swelling of the affected part for several

weeks sometimes accompanied by fever and leukocytosis, suggesting the diagnosis of osteomyelitis. Pathological fracture may be the presenting sign [1, 12].

On plain films or CT scans, the tumor has a lytic, destructive, “moth-eaten” appearance frequently affecting a rib or flat bone with soft tissue extension (Fig. 18.8a). The diaphysis is the site of involvement in the long bones as in the humerus, tibia, or femur. A soft tissue mass and layers of periosteal new bone formation (“onion skin” appearance) are frequently present about the periphery. The main radiographic differential diagnosis of Ewing’s sarcoma in the infant includes osteomyelitis, Langerhans cell histiocytosis, and metastatic neuroblastoma and rhabdoid tumor [1, 12].

Tumor currettings or biopsy specimens tend to be very soft, mushy light gray with extensive necrosis. Some are almost liquid in consistency. Because of this, often a barely adequate biopsy sample is obtained for diagnosis.

Ewing’s sarcoma is a prime example of one of the small blue cell malignant tumors of childhood [9]. Microscopic examination reveals sheets or nests of small cells containing round or oval nuclei with a fine, diffuse chromatin pattern and tiny nucleoli (Fig. 18.8b). PAS stain for glycogen is positive in about half the cases. The cells are immunoreactive with vimentin and the cell surface antigen *HBA71* (*O13*, *CD99* Ewing’s antigen) and occasionally are focally positive for neuron-specific enolase and S-100 protein [10, 30] (Table 4.2). The skeletal muscle markers desmin and actin are not expressed. EM reveals primitive-appearing small

cells with a high nuclear to cytoplasmic ratio, sparse organelles, variable glycogen deposits, and rudimentary cell junctions (Fig. 18.8d). Occasionally, dense core granules and neurofilaments are identified.

Both Ewing’s sarcoma and *primitive neuroectodermal tumor* (PNET) of the soft tissues are thought to be histogenetically related, both presumably arising from the neural crest. They have a consistent cytogenetic abnormality, that is, a *translocation* $t(11;22)(q24;Q12)$ and similar histological findings [30, 31]. The Intergroup Ewing’s Sarcoma Study found that the dismal overall survival rate in patients less than 3 years of age was 56 % which is practically the same as the survival rates of the older children [30].

18.9 Miscellaneous Conditions

Melanotic neuroectodermal tumor is one of the entities that should be considered in differential diagnosis of a craniofacial mass in the fetus and infant [33, 34] (see Chap. 4). *Cranial fasciitis* is discussed also in Chap. 4. Other examples of bone tumors and tumor-like conditions occurring in the young include reparative giant cell granuloma [5], chordoma [4, 35–37], juvenile xanthogranuloma [38, 39], osteolysis (“disappearing bone disease”) [40], and osteochondromyxoma associated with lentiginos and other unusual findings [2]. See Chap. 8 for discussion of Langerhans cell histiocytosis.

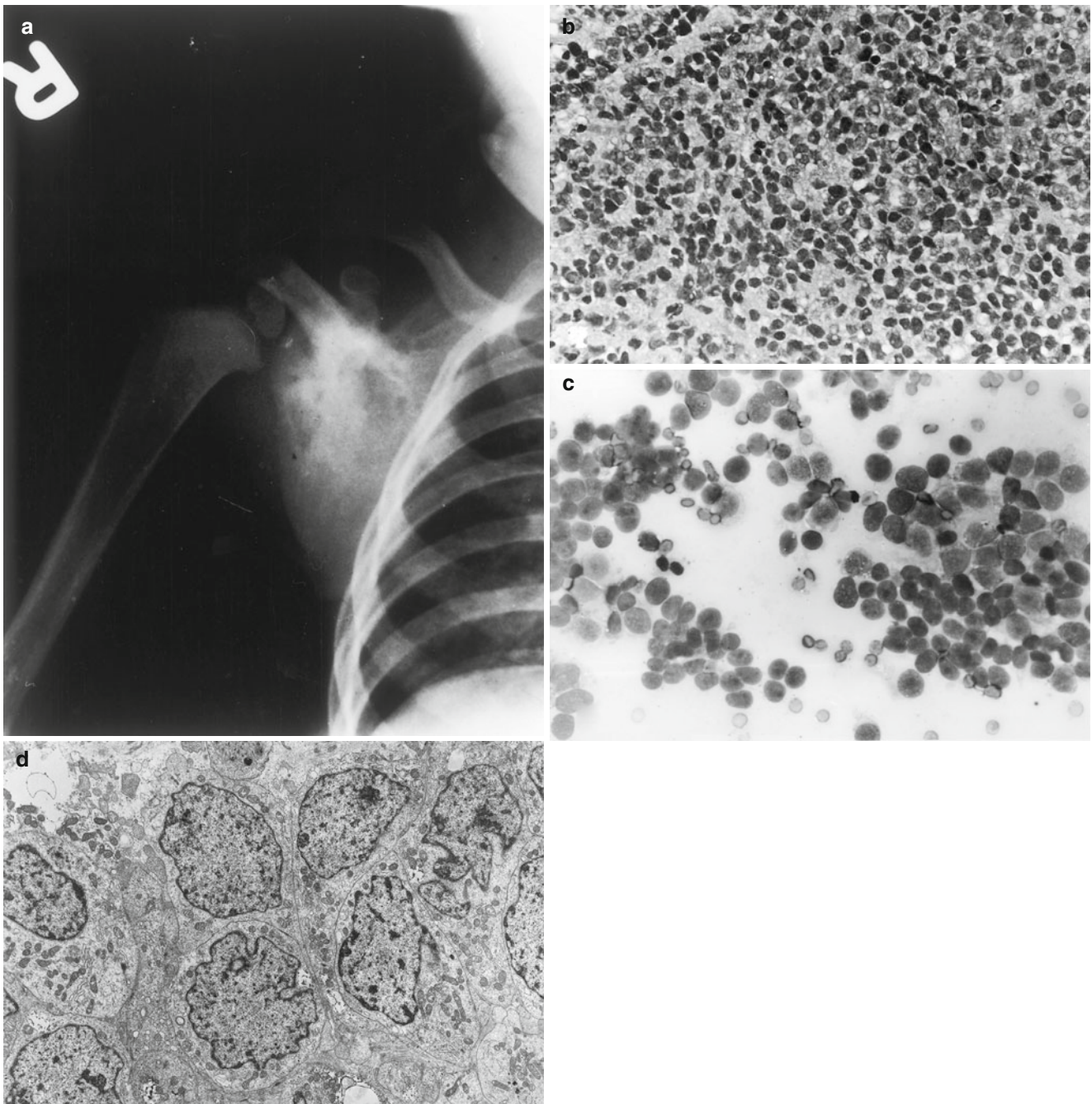


Fig. 18.8 Ewing's sarcoma. Nine-month-old female with pain, a mass in the right shoulder, and refusal to use the right upper extremity. **(a)** Radiograph depicts diffuse loss of the normal contour of the right scapula. The tumor shows mixed lytic and sclerotic areas and an adjacent soft tissue mass. **(b)** The tumor consists of nests of small cells containing round or oval nuclei with a fine, diffuse chromatin pattern and tiny nucleoli. The cytoplasm is scanty and indistinct. Immunoperoxidase studies revealed strong immunoreactivity for the Ewing's sarcoma anti-

gen 013, weakly reactive with NSE and vimentin; leukocyte common antigen, desmin, and actin were nonreactive. **(c)** Touch imprint smear shows scanty to practically absent cytoplasm. One or more tiny nucleoli are present. **(d)** Extensive foci of hemorrhage and necrosis are typically present. **(e)** EM features consist of small primitive cells with sparse organelles and poorly formed intercellular attachments (Reprinted from Isaacs [12]. © Springer-Verlag, 2002)

References

- Senac MO Jr, Isaacs H Jr, Gwinn JL (1986) Primary lesions of bone in the 1st decade of life: retrospective survey of biopsy results. *Radiology* 160:491–495
- Carney JA, Boccon-Gibod L, Jarka DE (2001) Osteochondromyxoma of bone. A congenital tumor associated with lentiginos and other unusual disorders. *Am J Surg Pathol* 25:164–176
- Anderson MJ, Townsend DR, Johnston JO et al (1993) Osteofibrous dysplasia in the newborn: report of a case. *J Bone Joint Surg Am* 75:265–267
- Coffin CM, Swanson PE, Wick MR (1993) Chordoma in childhood and adolescence. A clinicopathologic analysis of 12 cases. *Arch Pathol Lab Med* 117:927–933
- Cohen D, Granda-Ricart MC (1993) Giant cell reparative granuloma of the base of the skull in a 4-month-old infant- CT findings. *Pediatr Radiol* 23:319–320
- Hsieh HY, Hsiao CC, Chen WS et al (1998) Congenital Ewing's sarcoma of the humerus. *Br J Radiol* 71:1313–1316
- Inwards CY, Unni KK, Beabout JW et al (1991) Solitary congenital fibromatosis (infantile myofibromatosis) of bone. *Am J Surg Pathol* 15:935–941
- Cohen MC, Drut R, Garcia C et al (1992) Mesenchymal hamartoma of the chest wall: a cooperative study with review of the literature. *Pediatr Pathol* 12:525–534
- Isaacs H Jr (1997) Tumors. In: Gilbert-Barness E (ed) *Potter's pathology of the fetus and infant*, 2nd edn. Mosby, St. Louis, pp 1240–1339
- Rosenberg AE, Nielsen GP, Krishnasetty V, Rosenthal DI (2007) Disorders of the skeletal system including tumors. In: Gilbert-Barness E (ed) *Potter's pathology of the fetus and infant*, vol 2, 2nd edn. Mosby, Philadelphia, pp 1797–1897
- Isaacs H Jr (1997) Bone tumors. In: *Tumors of the fetus and newborn. Major problems in pathology*, vol 35. W.B. Saunders, Philadelphia, pp 357–364
- Isaacs H Jr (2002) Bone tumors. In: Isaacs H (ed) *Tumors of the fetus and infant: an atlas*. Springer, New York, pp 407–424
- McCarthy EF, Dorfman HD (1980) Vascular and cartilaginous hamartoma of the ribs in infancy with secondary aneurysmal bone cyst formation. *Am J Surg Pathol* 4:247–253
- Jung AL, Johnson DG, Condon VR et al (1994) Congenital chest wall mesenchymal hamartoma. *J Perinatol* 14:487–491
- Troum S, Dalton ML, Donner RS et al (1996) Multifocal mesenchymal hamartoma of the chest wall in infancy. *J Pediatr Surg* 31:713–715
- McDermott MB, Ponder TB, Dehner LP (1998) Nasal chondromesenchymal hamartoma. An upper respiratory tract analogue of the chest wall mesenchymal hamartoma. *Am J Surg Pathol* 22:425–433
- Hsueh C, Hsueh S, Gonzalez-Crussi F (2001) Nasal chondromesenchymal hamartoma in children. Report of 2 cases with review of the literature. *Arch Pathol Lab Med* 125:400–403
- Kato K, Ijiri R, Tanaka Y (1999) Nasal chondromesenchymal hamartoma of infancy: the first Japanese case report. *Pathol Int* 49:731–736
- Kirk JMW, Brain CE, Carson DJ et al (1999) Cushing's syndrome caused by nodular adrenal hyperplasia in children with McCune-Albright syndrome. *J Pediatr* 134:789–792
- Shenker A, Weinstein LS, Moran A et al (1993) Severe endocrine and nonendocrine manifestations of the McCune-Albright syndrome associated with activating mutations of stimulatory G protein Gs. *J Pediatr* 123:509–518
- Fechner RE, Mills SE (1991) Tumors of the bones and joints. Atlas of tumor pathology, 3rd series, Fascicle 8. Armed Forces Institute of Pathology, Washington, D.C.
- Chung EB, Enzinger FM (1981) Infantile myofibromatosis. *Cancer* 48:1807–1818
- Rosenberg HS, Stenback WA, Spjut HJ (1978) The fibromatoses of infancy and childhood. In: Rosenberg HS, Bolande RP (eds) *Perspectives in pediatric pathology*, vol 4. Year Book Medical Publishers, Chicago, pp 269–348
- Chan YF, Lau JHK, Tong CY (1989) Congenital generalized fibromatosis predominant osseous involvement in a Chinese newborn. *J Pediatr Orthop* 9:64–68
- Zeller B, Storm-Mathisen I, Smevik B et al (1997) Cure of infantile myofibromatosis with severe respiratory complications without antitumor therapy. *Eur J Pediatr* 156:841–844
- Shields CL, Husson M, Shields JA et al (1998) Solitary intraosseous infantile myofibroma of the orbital roof. *Arch Ophthalmol* 116:1528–1530
- Hasegawa M, Kida S, Yamashita T et al (1995) Multicentric infantile myofibromatosis in the cranium: case report. *Neurosurgery* 36:1200–1203
- Bernad L, Admella C, Lucaya J (1987) Infantile fibrosarcoma of femur. *Pediatr Pathol* 7:201–207
- Faure C, Gruner M, Boccon-Gibod L (1981) Case report 149. *Skeletal Radiol* 6:208–211
- Maygarden SJ, Askin FB, Siegel GP et al (1993) Ewing sarcoma of bone in infants and toddlers: a clinicopathologic report from the Intergroup Ewing's Study. *Cancer* 71:2109–2118
- Dehner LP (1994) Neuroepithelioma (primitive neuroectodermal tumor) and Ewing's sarcoma. At least a partial consensus. *Arch Pathol Lab Med* 118:606–607
- Navarro S, Cavazzana AO, Llombart-Bosch A (1994) Comparison of Ewing's sarcoma of bone and peripheral neuroepithelioma. An immunocytochemical and ultrastructural analysis of two primitive neuroectodermal neoplasms. *Arch Pathol Lab Med* 118:608–615
- Dehner LP (1973) Tumors of the mandible and maxilla in children. II. A study of 14 primary and secondary malignant tumors. *Cancer* 32:112–120
- Walsh JW, Strand RD (1982) Melanotic neuroectodermal tumor of the neurocranium in infancy. *Childs Brain* 9:329–346
- Matsumoto J, Towbin RB, Ball WS Jr (1989) Cranial chordomas in infancy and childhood. A report of two cases and review of the literature. *Pediatr Radiol* 20:28–32
- Oexle K, Dammann O, Bechmann B et al (1992) Intracranial chordoma in a neonate. *Eur J Pediatr* 151:336–338
- Probst EN, Zanella FE, Vortmeyer AO (1993) Congenital clivus chordoma. *AJNR Am J Neuroradiol* 14:537–579
- Eggl KD, Caro P, Quiogue T et al (1992) Juvenile xanthogranuloma: non-X histiocytosis with systemic involvement. *Pediatr Radiol* 22:374–376
- Isaacs H (2006) Fetal and neonatal histiocytoses. *Pediatr Blood Cancer* 47:123–129
- Kulenkampff HA, Richter GM, Hassee WE et al (1990) Massive pelvic osteolysis in the Gorham-Stout syndrome. *Int Orthop* 14:361–366

Index

A

Abdominal mass

- adrenocortical adenoma, 263, 265
 - CMN, 222, 224, 226, 227
 - ectomesenchymoma, 80, 81
 - embryonal sarcoma, 250, 251
 - follicular cyst of ovary, 32
 - gastric teratoma, 11
 - hepatoblastoma, 244, 246, 247, 249
 - hydronephrosis, 209, 211
 - JGCTs, 33
 - liver hemangioma, 238, 240
 - mesenchymal hamartoma, 241, 242
 - multicystic dysplastic kidney, 209, 212
 - multilocular cyst, 230–232
 - neuroblastoma, 112, 115, 117, 118
 - ossifying renal tumor of infancy, 233
 - pancreatic adenocarcinoma, 278
 - renal tumors, 209
 - retroperitoneal tumor, 12
 - Wilm's tumor, 216, 218, 219
- ACA. *See* Adrenocortical adenoma (ACA)
- ACC. *See* Adrenocortical carcinoma (ACC)
- ACH. *See* Adrenal cortical hyperplasia (ACH)
- Acute lymphocytic leukemia (ALL), 140
- morphological and cytochemical features of, 141
- Acute megakaryocytic leukemia (AMKL), 142
- diagnosis of, 141
 - translocation of, 135
- Acute monocytic leukemia, 141
- Acute myeloblastic leukemia, 141
- Acute myeloid leukemia (AML), 143
- morphological and cytochemical features of, 141
- Acute myelomonocytic leukemia, 141
- Acute nonlymphocytic leukemia (ANLL), 131
- Acute undifferentiated leukemia, 141
- Adipose tissue tumors, 74–75
- Adrenal cortical hyperplasia (ACH)
- congenital adrenal hyperplasia
 - cortisol secretion, 267
 - description, 267
 - 21-/11-hydroxylase deficiency, 267
 - neonatal screening study, 267
 - pathology, 268–269
 - salt wasting type, 268
 - sonography, 268
 - virilization, 267–268
 - Cushing's syndrome, 269
 - excess hormone secretion, 266
- Adrenal cysts, 270
- Adrenal cytomegaly, 269–270
- Adrenal neuroblastomas, 112, 116

- Adrenocortical adenoma (ACA), 264
- capsular and vascular invasion, 261
 - cell types, 261
 - Cushing's syndrome, 261–263
- Adrenocortical carcinoma (ACC), 265–266
- Adrenocortical tumors
- adrenal cysts, 270
 - adrenal cytomegaly, 269–270
 - adrenocortical adenoma, 261–264
 - adrenocortical carcinoma, 265–266
 - clinical findings
 - abdominal sonography, 260
 - computerized tomography, 260
 - histology, 261
 - hyperaldosteronism and feminizing signs, 260
 - hyperplasia, 266–269
 - incidence, 259–260
 - steroid biosynthetic pathways, 260
- ALL. *See* Acute lymphocytic leukemia (ALL)
- Alveolar rhabdomyosarcoma, 70, 73
- AMKL. *See* Acute megakaryocytic leukemia (AMKL)
- AML. *See* Acute myeloid leukemia (AML)
- Anaplastic astrocytoma, 170
- Angiomyolipoma, 253
- ANLL. *See* Acute nonlymphocytic leukemia (ANLL)
- Antenatal imaging diagnosis, 1
- Astrocytic retinal tumors, 204
- Astrocytoma
- anaplastic, 170
 - desmoplastic cerebral, 171
 - glioblastoma, 170, 171
 - histology, 168
 - optic glioma, 169
 - pilocytic, 168–169
 - subependymal giant cell astrocytomas, 170–172
 - WHO classification, 168, 169
- Atypical teratoid/rhabdoid tumor, 188

B

- Bean syndrome. *See* Blue rubber bleb nevus syndrome
- Becker's nevus, 95
- Bilateral retinoblastoma, 199–201
- Bilateral Wilms' tumors, 216, 220
- Blueberry muffin baby
- differential diagnosis, 88
 - neoplastic group, 102
 - neuroblastoma, 103, 104
 - nonneoplastic group, 102
 - rhabdomyosarcoma, 106
- Blue rubber bleb nevus syndrome, 93–94

- Bone tumor and tumor-like conditions
 chest wall hamartoma, 317–319
 congenital fibrosarcoma, 323
 congenital generalized fibromatosis, 323
 enchondromatosis, 321–323
 Ewing's sarcoma, 323–324, 326
 fibrous dysplasia, 321
 Langerhans cell histiocytosis, 315, 316
 melanotic neuroectodermal tumor, 324
 nasal chondromesenchymal hamartoma, 319–320
- Brain tumors
 astrocytoma (*see* Astrocytoma)
 atypical teratoid/rhabdoid tumor, 188
 choroid plexus carcinomas, 185
 choroid plexus papilloma, 182–184
 chromosomal abnormalities, 166
 craniopharyngioma, 187
 diencephalic syndrome, 165
 ependymoma, 180–182
 gangliocytoma, 178
 ganglioglioma, 178
 histological type and survival rate, 163, 164
 hydrocephalus, 165
 immunohistochemical methods, 165, 166
 incidence, 163
 infantile desmoplastic ganglioglioma, 178–179
 location and histological types, 165
 macrocephaly, 165
 medulloblastomas, 177
 medulloepithelioma, 188–189
 meningioma, 189
 nasal encephalocele, 192, 193
 neurofibromatosis, 164
 oligodendrogliomas, 186
 PNET, 172–176
 prognosis, 192
 signs and symptoms, 163
 teratoma, 166–168
 tuberous sclerosis, 164, 165
 vascular malformations, 189–191
- C**
- Capillary hemangioma
 lobular, 93
 sublingual gland, 293, 294
- Cardiac fibromas, 289
- Cardiac myxoma, 289
- Cardiac rhabdomyoma
 characteristic components, 285
 fetal arrhythmia and tuberous sclerosis, 285
 glycogen filled vacuoles, 285, 286
 spider cells, 285–287
 spontaneous regression, 285
- Cardiac tumors
 blood cysts, 291
 fibromas, 289
 fibrosarcoma, 291
 hamartoma, 283
 hemangiomas, 289
 incidence, 284
 juvenile xanthogranuloma, 291
 myxoma, 289
 neonatal conditions, 283
 oncocytic cardiomyopathy, 290
 rhabdoid tumor, 291
 rhabdomyoma (*see* Cardiac rhabdomyoma)
 rhabdomyosarcoma, 290
 teratoma, 287–289
 vascular tumors, 289
- CCAM. *See* Congenital cystic adenomatoid malformation (CCAM)
- CCSK. *See* Clear cell sarcoma of the kidney (CCSK)
- Cerebral PNET, 177
- Cervical neuroblastomas, 123, 125
- Chest wall hamartoma, 317–319
- Choriocarcinoma, 27, 28
- Choristomas, 299
- Choroid plexus carcinomas, 185
- Choroid plexus papilloma, 182–184
- Chromosomes
 association with childhood tumors, 3
 association with leukemia, 133–135
- Classical congenital mesoblastic nephroma, 224, 225
- Clear cell sarcoma of the kidney (CCSK), 229, 230
- CMN. *See* Congenital mesoblastic nephroma (CMN)
- Congenital adrenal hyperplasia (CAH)
 cortisol secretion, 267
 description, 267
 21-/11-hydroxylase deficiency, 267
 neonatal screening study, 267
 pathology, 268–269
 salt wasting type, 268
 sonography, 268
 virilization, 267–268
- Congenital cystic adenomatoid malformation (CCAM), 307–308
- Congenital fibrosarcoma, 323
- Congenital generalized fibromatosis, 323
- Congenital mesoblastic nephroma (CMN)
 cellular, 226, 227
 classical, 222
 diagnosis, 222
 physical examination, 222
 vs. Wilms' tumor, 222, 224
- Congenital neuroblastomas, 111, 117, 123
- CPDN. *See* Cystic partially differentiated nephroblastoma (CPDN)
- Cranial fasciitis, 62, 64
- Craniopharyngioma, 187
- Cushing's syndrome
 adrenal cortical adenoma, 261–263
 adrenal cortical hyperplasia, 269
 adrenocortical carcinoma, 265
- Cystadenoma, 277–278
- Cystic adenomatoid malformation, 301–303
- Cystic hygroma, 94
- Cystic partially differentiated nephroblastoma (CPDN), 230
- Cystic renal lesions, 230
- Cystic Wilms' tumors, 230
- D**
- Dendritic cell disorders, histiocytoses
 JXG, 155
 LCH, 151–155
- Desmoplastic cerebral astrocytoma, 171
- Diencephalic syndrome, 165
- Digital fibromatosis, 49, 53–54
- Disseminated neuroblastomas, 111, 113–114
- DNA cytometric analysis (DNA index), 121
- Down syndrome, 132, 133, 138, 142, 146
- Ductal adenocarcinoma, 278
- Dysgerminoma, 27

E

- Ectomesenchymoma, 80, 81
- Embryonal carcinoma, 26
- Embryonal epithelial hepatoblastoma, 245–250
- Embryonal rhabdomyosarcomas, 68–70, 72, 73, 250–252
- Embryonal sarcomas, 250–252
- Enchondromatosis, 321–323
- Endodermal sinus tumor. *See* Yolk sac tumor
- Ependymoma, 180–182
- Epidermal nevus, 94, 95
- Epignathus, 6, 9
- Erythroblastosis, 136, 137
- Ewing's sarcoma, 323–324, 326
- Eye tumors
 - astrocytic retinal tumors, 204
 - medulloepithelioma, 204
 - neurofibromatosis, 205
 - optic glioma, 206
 - orbital tumors, 206–207
 - retinoblastoma (*see* Retinoblastoma)

F

- Familial hemophagocytic lymphohistiocytosis, 155–157
- Familial neuroblastomas, 111
- Fetal hydrops, 1, 2, 44, 45, 111, 112, 165, 243, 249, 287, 289, 307, 308
- Fetus-in-fetu, 19–21
- Fibrohistiocytic tumors, 63–64
 - angiomatoid fibrous histiocytoma, 65–67
 - fibrous histiocytoma, 65
 - JXG, 65, 67, 71
- Fibromas, 35
- Fibromatosis, 307
 - of forearm, 48, 50
 - gross features, 47
 - lung tumors and tumor-like conditions, 307
 - of mediastinum and supraclavicular area, 48, 51
 - sampling error, 48
 - sites, 47
 - spindle cell neoplasms, 48
 - of sternum, 48, 52
 - surgical excision, 48
- Fibrosarcoma, 61–63
 - cytogenetics, 53
 - histology, 57, 58
 - immunoreactive, 58
 - metastases incidence, 59
 - recurrence rate, 53
 - treatment, 59, 60
- Fibrous connective tissue tumors, 46
 - cranial fasciitis, 62
 - digital fibromatosis, 49
 - fibromatosis, 47–48
 - fibrosarcoma, 61–63
 - cytogenetics, 53
 - histology, 57, 58
 - immunoreactive, 58
 - metastases incidence, 59
 - recurrence rate, 53
 - treatment, 59, 60
 - fibrous hamartoma, 52–53
 - Gardner fibroma, 48–49
 - giant-cell fibroblastoma, 53
 - granular cell tumor, 50–52
 - inflammatory myofibroblastic tumor, 62–63
 - myofibromatosis, 49–50
 - nodular (proliferative) fasciitis, 60–62, 64
 - torticollis, 49
- Fibrous dysplasia, 321
- Fibrous hamartoma, of infancy, 52–53, 60
- Focal nodular hyperplasia, 252–253
- Follicular ovarian cysts, 33

G

- Gangliocytoma, 178
- Ganglioglioma, 178
- Ganglioneuroma, 128
- Gangliorhabdomyosarcoma. *See* Ectomesenchymoma
- Gardner fibroma, 48–49
- GATA-6 transcription factors, 7
- Germ cell tumors, 252
 - choriocarcinoma, 27, 28
 - clinicopathological features, 5, 6
 - cytogenetics, 7
 - dysgerminoma, 27
 - embryonal carcinoma, 26
 - fetus-in-fetu, 19–21
 - gonadoblastoma, 24–26
 - origin, 5, 6
 - polyembryoma, 27
 - teratoma
 - clinical presentation, 13
 - definition, 7
 - epignathus, 6, 9
 - gastric, 6, 11
 - immature, 13, 14, 16–18
 - mature, 13–16
 - mediastinal, 6, 11
 - pharyngeal, 6, 9
 - prognosis, 21
 - retroperitoneal, 6, 12
 - sacrococcygeal teratoma, 6–8
 - survival rates, 21
 - thyrocervical, 6, 8
 - WHO classification, 5
 - yolk sac tumor, 22–24
- Giant-cell fibroblastoma, 53
- Giant congenital melanocytic nevi, 97–99
- Giant linear epidermal nevus, 94, 95
- Gingival granular cell tumor, 52, 59
- Glioblastoma, 170, 171
- Gonadoblastoma, 24–26
- Granular cell tumor, 50–52

H

- Hamartoma
 - Becker's nevus, 95
 - definition, 87
 - fibrous hamartoma, of infancy, 102
 - nevus lipomatosus, 96
 - smooth muscle, 96
- Hand-Schuller-Christian syndrome, 152
- Hashimoto-Pritzker syndrome, 152
- Hemangiomas
 - blue rubber bleb nevus syndrome, 93–94
 - capillary, 90–92
 - cavernous, 90, 92
 - focal, 238
 - of liver, 238–241

Hemangiomas (cont.)

- lymphangiomas, 94
 - multifocal, 238
 - pyogenic granuloma, 93
 - soft tissue tumors, 40–44
 - strawberry, 90, 92
 - tufted angioma, 94
- Hemolytic diseases, of newborn, 102, 111, 132, 135, 136, 138, 142, 146
- Hemophagocytic syndromes
- primary, 155–157
 - secondary, 157–158
 - terminology, 155
- Hepatoblastoma
- anaplastic epithelial pattern, 247
 - description, 244
 - embryonal epithelial, 245–250
 - histological classification of, 245, 246
 - mixed, 245, 247, 249
 - staging system for, 249, 250
 - teratoid, 249
- Hepatocellular carcinoma, 253, 254
- Hereditary retinoblastoma, 197
- Heterotopia, 299
- Histiocytoid cardiomyopathy, 290
- Histiocytoses
- acute monocytic leukemia, 159–160
 - definition, 149
 - dendritic cell disorders
 - JXG, 155
 - LCH, 151–155
 - fetal and infant disorder classification, 149
 - histiocyte features, 151
 - lysosomal storage disease, 149, 150
 - macrophage-related disorders
 - hemophagocytic syndromes, 155–158
 - sinus histiocytosis with massive lymphadenopathy, 158–159
 - malignant histiocytoses, 159
 - monophagocytic system, 150–151
 - pathogenesis, 149
- Hydronephrosis, 209, 211, 224, 230

I

- Infantile cerebral desmoplastic ganglioglioma, 179
- Infantile ganglioglioma, 178–179
- Infantile myofibromatosis, 55, 56, 58, 323
- Infantile polycystic disease, 213–214, 253, 256
- Infection-associated hemophagocytic (IAH) syndrome, 157–158
- Inflammatory myofibroblastic tumor, 62–63
- Inflammatory pseudotumor, 306, 307
- Intracranial teratomas, 166–168
- Intraocular retinoblastoma, 198
- Intrapericardial teratoma, 287, 288
- Islet cell adenoma, 276–277

J

- Juvenile granulosa cell tumor (JGCT)
- bilateral, 33, 34
 - description, 33
 - testicular and ovarian, 33, 34
- Juvenile xanthogranuloma (JXG), 64, 65, 67, 68, 71, 104–106, 155

K

- Kasabach-Merritt syndrome, 238, 240

L

- Langerhans cell histiocytosis (LCH)
- Birbeck granules, 152
 - bone tumor and tumor-like conditions, 315, 316
 - classification, 151
 - clinical findings, 151–152
 - disseminated, 104, 105
 - Hand-Schuller-Christian syndrome, 152
 - Hashimoto-Pritzker syndrome, 152
 - infiltration, 152
 - lymph node biopsy, 152, 154
 - pathology, 152
 - prognosis, 154–155
 - self healing, 152, 154
 - skin lesions, 104
- Laryngotracheal papilloma, 308, 309
- LCH. *See* Langerhans cell histiocytosis (LCH)
- Letterer-Siwe disease, 153
- Leukemia, 131
- chromosomal defects, 133–134
 - clinical features of, 132–133
 - congenital
 - differential diagnosis of, 135, 136
 - immunophenotypes and karyotypes in, 133, 134
 - petechiae and purpura, 132, 133
 - congenital defects and syndromes, 134–135
 - cutis, 102, 103
 - cytogenetic abnormalities, 135
 - description of, 131
 - diagnosis of, 139–142
 - differential diagnosis of, 135–139
 - French-American-British classification, 139–141
 - hematopoiesis, 131–132
 - incidence, 131
 - pathology, 142–146
 - prognosis, 146
- Leukemic infiltration of infant testis, 32, 33
- Leukocoria, 197, 198
- Lipoblastoma
- definition, 74
 - immunoperoxidase studies, 74
 - and lipoma, 74, 75
- Liver tumors
- classifications and tumorlike conditions, 237
 - focal nodular hyperplasia, 252–253
 - germ cell tumors, 252
 - hemangioma, 238–241
 - hepatic adenomas, 252
 - hepatoblastoma
 - anaplastic epithelial pattern, 247
 - Children's Oncology Group staging system for, 249, 250
 - description, 244
 - embryonal epithelial, 245–250
 - histological classification of, 245, 246
 - mixed, 245, 247, 249
 - teratoid, 249
 - hepatocellular carcinoma, 253, 254
 - infantile polycystic disease, 253, 256
 - liver cell adenoma, 252–253
 - mesenchymal hamartoma
 - description, 241–242
 - diagnosis, 242–244
 - pathogenesis of, 243
 - nodular regenerative hyperplasia, 253
 - primary sarcomas, 250–252

rhabdoid tumor, 253
 unilocular cyst, 253, 255
 Lobular capillary hemangioma, 93
 Lung tumors and tumor-like conditions
 CCAM, 307–308
 cystic adenomatoid malformation, 301–303
 fibromatosis, 307
 inflammatory pseudotumor, 306, 307
 laryngotracheal papilloma, 308, 309
 lymphomatoid granulomatosis, 301, 305
 pleuropulmonary blastoma, 310, 311
 PNET, 311–312
 pulmonary lymphangiectasis, 301, 304
 pulmonary myofibroblastic tumor, 309, 310
 rhabdomyomatous dysplasia, 310
 skeletal muscle tumors, 310
 vascular conditions, 307
 Lymphadenomegaly, 142
 Lymphangiomas, 94
 arteriovenous malformation, 45, 49
 cystic lymphangiomas, 44–47
 mediastinum, 45, 48
 size, 44
 Turner syndrome, 45
 Lymphomatoid granulomatosis, 301, 305

M

Macrophage-related disorders, histiocytoses
 hemophagocytic syndromes, 155–158
 sinus histiocytosis with massive lymphadenopathy, 158–159
 Macular stains, 90, 92
 Maffucci's syndrome, 321
 Malignant melanoma, 99, 100
 Mast cell disease, 106–108
 Maternal dystocia, 1
 McCune-Albright syndrome, 269
 Medulloblastomas, 177
 Medulloepithelioma, 188–189, 204
 Megakaryoblasts, 141–142
 Melanocytic nevi
 giant congenital melanocytic nevi, 97–99
 malignant melanoma, 99, 100
 neurocutaneous melanosis, 100–101
 pigmented nevi, 96, 97
 Melanotic neuroectodermal tumor, 80, 324
 Meningioma, 189
 Mesenchymal hamartoma
 description, 241–242
 diagnosis, 242–244
 pathogenesis of, 243
 Mitotic-karyorrhexis index (MKI), 121
 Mixed hepatoblastoma, 245, 247, 249
 Monophagocytic system, 150–151
 Mucoceles, 299
 Multicystic dysplastic kidney, 209, 212
 Multilocular cyst, of kidney, 230, 231
 Myofibromatosis, 49–50

N

Nasal chondromesenchymal hamartoma, 319–320
 Nasal encephalocele, 192, 193
 Nasopharyngeal dermoid, 6, 10
 Neonatal leukemia, 132, 135
 Nephroblastomatosis, 221–222

Nephrogenic rests, 221–222, 224
 Nesidioblastoma, 273, 276
 Nesidioblastosis, 273, 274
 Neuroblastomas, 102–104
 adrenal, 111, 112, 116, 122
 bone marrow smear, 122, 123
 cervical, 123, 125
 clinical manifestations, 111, 112
 congenital, 111, 117, 123
 cystic adrenal hemorrhage, 122, 126, 128
 diagnostic tests, 121
 disseminated, 111, 113–114
 familial, 111
 ganglioneuroma, 128
 genetic factors, 121–122
 hemorrhagic, 115
 histopathologic differential diagnosis, 122, 127
 incidence, 111
 International staging system, 112, 120
 malformation associated with, 111, 112
 neuroblastoma in situ, 126–128
 N-myc amplification, 122
 occurrence, 111
 pathology, 122
 posterior mediastinal, 119, 120
 prognostic indicators, 121
 spontaneous regression, 127
 stage 4S, 112
 survival rates, 129
 undifferentiated, 118, 122, 124
 Neurocutaneous melanosis, 100–101
 Neurocutaneous syndromes, 3, 94
 Neurofibromatosis, 205
 brain tumors, 164
 plexiform, 101
 Von Recklinghausen's disease, 101
 Nevocellular nevi. *See* Pigmented nevi
 Nevus flammeus, 92
 Nodular (proliferative) fasciitis, 60–62, 64
 Nodular regenerative hyperplasia, 253
 Non-germ-cell gonadal tumors, 31–35
 Nonhereditary retinoblastoma, 197
 Nonimmune fetal hydrops, 13, 41, 238, 244, 285

O

Oligodendrogliomas, 186
 Ollier's disease. *See* Enchondromatosis
 Oncocytic cardiomyopathy, 290
 Optic glioma, 206
 Orbital tumors, 206–207
 Organomegaly, 142
 Ossifying renal tumor of the kidney, 233
 Ovarian cysts, 31, 33

P

Pancreatic adenocarcinoma, 278
 Pancreatic tumors
 Beckwith-Wiedemann syndrome, 275, 276
 endocrine conditions
 islet cell adenoma, 276–277
 islet hypertrophy/hyperplasia, 273
 nesidioblastosis, 273, 274
 persistent hyperinsulinemic hypoglycemia of infancy, 275
 exocrine conditions

- Pancreatic tumors (*cont.*)
 adenocarcinoma, 278
 cystadenoma, 277–278
 pancreatoblastoma, 278–79
 lymphocytic infiltration, 280
 Pancreatoblastoma, 278–79
 Perinatal leukemia, 138
 Peripheral nervous system tumors
 neural crest, 76
 neurofibroma
 diffuse, 77
 neurofibromatosis, 77–78
 plexiform, 76, 77
 solitary type, 77
 Persistent hyperinsulinemic hypoglycemia of infancy, 275
 Phakomatoses. *See* Neurocutaneous syndromes
 Pigmented nevi, 96, 97
 Pilocytic astrocytoma, 168–169
 Pleomorphic adenoma, of nasopharynx, 296–298
 Pleuropulmonary blastoma, 310, 311
 Plexiform neurofibroma, 76, 77, 101, 204, 205, 293, 294
 PNET. *See* Primitive neuroectodermal tumor (PNET)
 Polyembryoma, 27
 Polyhydramnios, 1, 2, 13, 153, 166, 168, 187, 224
 Polyostotic fibrous dysplasia, 321
 Polyphenotypic small cell tumor, 82
 Port-wine stain, 92
 Primary hemophagocytic syndromes, 155–157
 Primitive neuroectodermal tumor (PNET)
 cerebral, 175, 176
 characterization, 172–173
 diagnosis, 173
 locations, 173
 medulloblastoma, 174
 prognosis, 173
 soft tissue tumors, 78–80
 thoracopulmonary origin, 311–312
 Prune belly syndrome, 209, 214–215
 Pulmonary lymphangiectasis, 301, 304
 Pulmonary myofibroblastic tumor, 309, 310
 Pyogenic granuloma. *See* Lobular capillary hemangioma
- Q**
 13q (del) syndrome, 198
- R**
 Reese-Ellsworth staging system, 198
 Renal tumors
 abdominal mass, 209
 CCSK, 229, 230
 classification, 209
 CMN, 222–224
 features of, 209, 210
 nephroblastomatosis, 221–222
 nephrogenic rests, 221–222, 224
 RTK, 228
 staging of, pediatric, 209, 216
 Renomegaly, 142
 Respiratory distress, 132
 Retinoblastoma
 bilateral, 199–201
 clinical presentation, 197–198
 cytogenetics, 197
 description, 197
 differential diagnosis, 198
 diffuse infiltrating form, 199
 endophytic/exophytic growth, 199
 with extensive necrosis and calcification, 202
 fleurettes, 202
 Flexner-Wintersteiner rosettes, 202, 203
 hereditary form, 197
 Homer-Wright rosettes, 202, 203
 immunohistochemical studies, 202
 intraocular, 198
 neuron-specific enolase, 202
 nonhereditary form, 197
 photoreceptor cell differentiation, 199
 prognosis, 203
 13q (del) syndrome, 198
 Reese-Ellsworth staging system, 198
 spontaneous regression, 198–199
 trilateral, 203–204
 Retinopathy of prematurity, 198, 199
 Rhabdoid tumors, 73, 107, 228, 253
 Rhabdomyoma, 72
 Rhabdomyomatous dysplasia, 310
 Rhabdomyosarcoma, 106–107
 alveolar, 70, 73
 clinical group stage system, 73
 cytogenetics, 72
 embryonal, 68–70, 72, 73
 prognosis, 73
 spindle-cell, 73
- S**
 Salivary gland anlage tumor, 296–298
 Salivary gland tumors
 cystic choristomas, 299
 gastric heterotopia, 299
 mucoceles, 299
 mucoepidermoid carcinoma, 296, 299
 neonatal salivary gland anlage tumor, 296–298
 sialoblastoma
 vs. congenital pleomorphic adenoma, 296
 facial/submandibular mass, 295
 histological features, 295
 immunohistochemical studies, 295
 recurrence, 295, 296
 sizes, 295
 Sebaceous nevus, 95, 96
 Secondary hemophagocytic lymphohistiocytosis. *See* Infection-associated hemophagocytic (IAH) syndrome
 Sertoli-Leydig cell tumor, 34–35
 Sex cord-stromal tumors, 33
 JGCT (*See* Juvenile granulosa cell tumor (JGCT))
 Sertoli-Leydig cell tumor, 34–35
 Sialoblastoma
 vs. congenital pleomorphic adenoma, 296
 facial/submandibular mass, 295
 histological features, 295
 immunohistochemical studies, 295
 recurrence, 295, 296
 sizes, 295
 Sinus histiocytosis with massive lymphadenopathy, 158–159
 Skeletal muscle tumors
 rhabdomyoma, 72
 rhabdomyosarcoma
 alveolar, 70, 73
 clinical group stage system, 73

- cytogenetics, 72
 - embryonal, 68–70, 72, 73
 - prognosis, 73
 - spindle-cell, 73
 - Skin tumors and tumor-like conditions
 - cutaneous metastases, in neonates, 102
 - epidermal birthmarks
 - Becker's nevus, 95
 - epidermal nevus, 94, 95
 - sebaceous nevus, 95, 96
 - hamartoma (*see* Hamartoma)
 - JXG, 104–106
 - LCH, 104
 - leukemia cutis, 102, 103
 - melanocytic nevi, 96–101
 - neuroblastoma, 102–104
 - neurofibromatosis
 - plexiform, 101
 - Von Recklinghausen's disease, 101
 - rhabdoid tumor, 107
 - rhabdomyosarcoma, 106–107
 - TSC
 - description, 101
 - digital fibromatosis, 102
 - fibrous hamartoma, of infancy, 102
 - papillomas, 102
 - skin manifestations, 87, 89
 - vascular conditions
 - hemangioma, 90–94
 - macular stains, 92
 - Sturge-Weber syndrome, 92–93
 - Soft tissue tumors
 - adipose tissue tumors, 74–75
 - ectomesenchymoma, 80, 81
 - features, 37, 38
 - fibrohistiocytic tumors, 63–64
 - angiomatoid fibrous histiocytoma, 65–67
 - fibrous histiocytoma, 65
 - JXG, 65, 67, 71
 - fibrous connective tissue tumors, 46
 - cranial fasciitis, 62
 - digital fibromatosis, 49
 - fibromatosis, 47–48
 - fibrosarcoma, 53–54, 57–63
 - fibrous hamartoma, 52–53
 - Gardner fibroma, 48–49
 - giant-cell fibroblastoma, 53
 - granular cell tumor, 50–52
 - inflammatory myofibroblastic tumor, 62–63
 - myofibromatosis, 49–50
 - nodular (proliferative) fasciitis, 60–62, 64
 - torticollis, 49
 - hemangiomas, 40–44
 - lymphangioma (*see* Lymphangiomas)
 - peripheral nervous system tumors, 76–78
 - PNET, 78–80
 - polyphenotypic small cell tumor, 82
 - rhabdoid tumor, 73
 - skeletal muscle tumors
 - rhabdomyoma, 72
 - rhabdomyosarcoma, 72–73
 - triton tumor, 80, 82
 - vascular malformations, 45–46
 - Spindle-cell rhabdomyosarcoma, 73
 - Spontaneous regression
 - cardiac rhabdomyoma, 285
 - neuroblastomas, 127
 - retinoblastoma, 198–199
 - Sturge-Weber syndrome, 92–93, 189–191
 - Subependymal giant cell astrocytomas, 170–172
- T**
- Teratoma
 - clinical presentation, 13
 - definition, 7
 - epignathus, 6, 9
 - gastric, 6, 11
 - immature, 13, 14, 16–18
 - mature, 13–16
 - mediastinal, 6, 11
 - pharyngeal, 6, 9
 - prognosis, 21
 - retroperitoneal, 6, 12
 - sacrococcygeal teratoma, 6–8
 - survival rates, 21
 - thyrocervical, 6, 8
 - Thecomas, 35
 - Torticollis, 49, 54–55
 - Touraine's syndrome, 100
 - Transient congenital leukemia, 138, 139
 - Transient myeloproliferative disorder, 138
 - Trilateral retinoblastoma, 203–204
 - Triton tumor, 80, 82
 - Tuberous sclerosis (TSC)
 - description, 101
 - digital fibromatosis, 102
 - fibrous hamartoma, of infancy, 102
 - papillomas, 102
 - skin manifestations, 87, 89
 - Tumors and tumor-like conditions. *See also* Brain tumors; Eye tumors
 - adrenocortical tumors
 - adrenal cysts, 270
 - adrenal cytomegaly, 269–270
 - adrenocortical adenoma, 261–264
 - adrenocortical carcinoma, 265–266
 - clinical findings, 260–261
 - hyperplasia, 266–269
 - incidence, 259–260
 - steroid biosynthetic pathways, 260
 - of bones
 - chest wall hamartoma, 317–319
 - congenital fibrosarcoma, 323
 - congenital generalized fibromatosis, 323
 - enchondromatosis, 321–323
 - Ewing's sarcoma, 323–324, 326
 - in fetus and infants, 315, 316
 - fibrous dysplasia, 321
 - Langerhans cell histiocytosis, 315, 316
 - melanotic neuroectodermal tumor, 324
 - nasal chondromesenchymal hamartoma, 319–320
 - cardiac tumors (*see* Cardiac tumors)
 - fetal and infant testis classification, 31
 - liver (*see* Liver tumors)
 - lung (*see* Lung tumors and tumor-like conditions)
 - neoplasms, 1, 3
 - of pancreas (*see* Pancreatic tumors)
 - salivary gland tumors (*see* Salivary gland tumors)
 - skin (*see* Skin tumors and tumor-like conditions)
 - soft tissue tumors (*see* Soft tissue tumors)
 - Turner syndrome, 45, 47, 112, 134

U

Undifferentiated neuroblastomas, 118, 122, 124
Unilocular cysts, of liver, 253, 255
Urticaria pigmentosa. *See* Mast cell disease

W

White pupillary reflex. *See* Leukocoria
Wilms' tumor (WT), 216, 218
 anaplastic features, 216, 221
 bilateral, 216, 220
 blastemal, 216, 219
 conditions associated with, 216, 217
 congenital, 216, 218
 cystic, 230
 epithelial, 216, 219
 fetal rhabdomyomatous, 216, 221

 histological patterns, 216
 karyotypic analyses, 216
 occurrence, 216
 pathology, 216
 stages of, 216

Wright-Giemsa stained smears, 123, 132, 141, 146

Y

Yolk sac tumor, 252
 description, 22
 histologic patterns, 22–23
 lung and liver metastases, 23, 24
 sacrococcygeal area, 22
 serum alpha-fetoprotein levels, 23
 of testis, 22–23